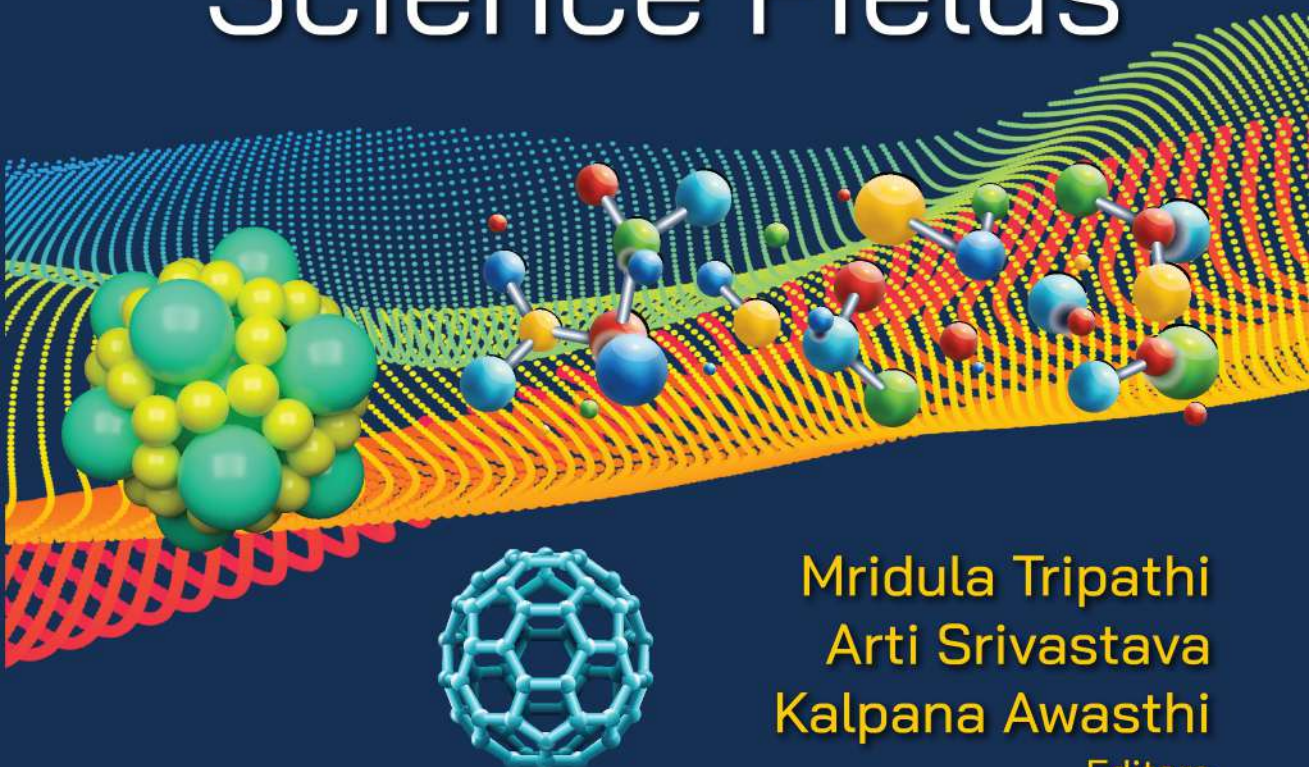


MATERIALS SCIENCE AND TECHNOLOGIES

Versatile Solicitations of Materials Science in Diverse Science Fields



Mridula Tripathi
Arti Srivastava
Kalpana Awasthi
Editors

NOVA
Complimentary Contributor Copy

Complimentary Contributor Copy

MATERIALS SCIENCE AND TECHNOLOGIES

VERSATILE SOLICITATIONS OF MATERIALS SCIENCE IN DIVERSE SCIENCE FIELDS

No part of this digital document may be reproduced, stored in a retrieval system or transmitted in any form or by any means. The publisher has taken reasonable care in the preparation of this digital document, but makes no expressed or implied warranty of any kind and assumes no responsibility for any errors or omissions. No liability is assumed for incidental or consequential damages in connection with or arising out of information contained herein. This digital document is sold with the clear understanding that the publisher is not engaged in rendering legal, medical, or any other professional services.

Complimentary Contributor Copy

MATERIALS SCIENCE AND TECHNOLOGIES

Additional books and e-books in this series can be found on Nova's website under the Series tab.

Complimentary Contributor Copy

MATERIALS SCIENCE AND TECHNOLOGIES

**VERSATILE SOLICITATIONS OF
MATERIALS SCIENCE IN DIVERSE
SCIENCE FIELDS**

**MRIDULA TRIPATHI
ARTI SRIVASTAVA
AND
KALPANA AWASTHI
EDITORS**



Complimentary Contributor Copy

CONTENTS

Preface		vii
Chapter 1	Societal Impact of Nanomaterials <i>Narendra Kumar Pandey and Priya Gupta</i>	1
Chapter 2	Nanomaterials: Synthesis, Properties, and Societal Applications <i>Meena Nemiwal, Ankita Dhillon and Dinesh Kumar</i>	17
Chapter 3	Role of Nanomaterial in the Health Sector <i>Devendra Singh, Deepmala Sharma and Vishnu Agarwal</i>	35
Chapter 4	Medicinal Importance of Inorganic Materials <i>Shraddha Shukla and A. P. Mishra</i>	51
Chapter 5	Impact of Polymeric Materials on Society and Complex Impedance Spectroscopy <i>A. L. Saroj</i>	61
Chapter 6	Carbon and Transition Metal Two Dimensional Quantum Dots: New Era of Material Science <i>Madhu Tiwari</i>	81
Chapter 7	Nanomaterials as Intrinsic Enzyme Mimetic Catalysts <i>Vinita</i>	99
Chapter 8	Graphene: A Revolutionary Exotic Material and Its Applications <i>Seema Awasthi, O.N. Srivastava, A. Rajanikanth and C. Bansal</i>	115
Chapter 9	Materials for Energy <i>R. K. Shukla and Amrit K. Mishra</i>	131

Chapter 10	AB ₅ -Type Metal Hydrides to Serve the Society as Energy Material: Development in Last Decade <i>Kuldeep Panwar and Sumita Srivastava</i>	139
Chapter 11	Carbon Based Nanomaterials for Energy Applications <i>Rajesh Kumar Dwivedi, Esha Dwivedi and Raghav Dwivedi</i>	155
Chapter 12	Functionalized Nanomaterials Based Efficient Photocatalyst for Renewable Energy and Sustainable Environment <i>Sunil Kumar and Pankaj Kumar Chaurasia</i>	173
Chapter 13	Functionalization of Carbon-Based Materials for the Electrochemical Sensing Applications <i>Mamta Yadav, Devesh Kumar Singh, Vellaichamy Ganesan and Ramasamy Ramaraj</i>	193
Chapter 14	Recent Development of Graphene Nanosheets Supported PT-Free Electrocatalysts in Field of Direct Methanol Fuel Cell <i>Rahul Awasthi and C. S. Sharma</i>	217
Chapter 15	Two-Dimensional (2D) Nanomaterials for Energy Harvesting <i>Thakur Prasad Yadav</i>	235
Chapter 16	Hybrid Materials and Their Applications <i>Arjita Srivastava, Pravin Kumar Singh, Akram Ali and Vishal Srivastava</i>	247
Chapter 17	ZrO ₂ Nanoparticle-Catalyzed One-Pot Multi-Component Synthesis of Bio-Active Organic Scaffolds <i>Subhash Banerjee</i>	257
Chapter 18	Bioremediation of Bauxite Residue Dumping Sites of Alumina Industry <i>Kumud Dubey and K. P. Dubey</i>	267
Chapter 19	Decontamination of Water with Metal Nanocomposites and Hybrid Nanomaterials <i>Vijay Pandey, Mahesh Kumar Gupta, Harendra Singh and P. K. Tandon</i>	283
Chapter 20	Nanoconjugates from Chitosan Hydrogel: A Novel Drug Delivery Tool <i>Tanvi Jain and P. K. Dutta</i>	299
About the Editors		313
Index		315

PREFACE

The beginning of the scientific research in nanomaterials had an obvious mix of hope and hype both but the spinning off the scientific knowledge in nanomaterials and their general purpose all pervasive applications for improving the quality of human life is weighing heavily in favor of hope for the society. Material science is an emerging field of science which continuous growth involves lot of areas of research field belongs to industry, government, academia, and research laboratories to share findings in the research and development of new materials of technological prominence. The materials that have been mostly used in this universe are Metal, Polymers, glass, Ceramic, synthetic fibres and Composite. This book consists of twenty chapters from well-reputed universities and institutes. Chapters of the book covers the area like nanomaterials in society, nanomaterials in medicine ultimate in health sectors, nanomaterials as Intrinsic Enzyme Mimetic Catalysts. Second portion of this book consists of application of materials/ nanomaterials for energy and its functionalization for particular applications like Carbon Based Nanomaterials for Energy Applications, and for electrochemical sensing, nanomaterials based efficient photocatalyst for renewable energy and sustainable environment. A chapter by chapter brief description are as follows:

In Chapter 1, Narendra Kumar Pandey and Priya Gupta have given an overview on the societal impact of nanomaterials and described about recent studies on the potency of nanoparticles as diagnostic or antiviral tools against corona viruses. The possibilities of effectively using nanomaterials as nanosensors are also presented.

Chapter 2 describes that the Nanomaterials and nanotechnology are emerging as potential candidate in manufacturing and production, developing novel and advanced materials for wide range of applications in various fields such as water treatment, catalysis, energy storage, sensors, nanomedicines and other environmental remediation.

Chapter 3 presents immense application of Nanomaterial in the healthcare sector, including drug development, therapeutics, bioimaging, medical devices, and diagnostic kits. The main reason behind using these nano-sized materials is its solubility because they have the potential of solubilizing at nanoscale due to its changing properties when attached to nanoparticles

Complimentary Contributor Copy

Chapter 4 reviewed significant insights into the advancement of future researches on biomaterials in view of medicinal uses and applications of inorganic materials and metal complexes have clinical and societal importance. Inorganic materials include metals, minerals, metalloenzymes, metal complexes and organometallic compounds which can be used as catalysts, pigments, coatings, surfactants, fuel, medicine etc.

The author A. L. Saroj discussed the principal and application of Complex impedance spectroscopy (CIS) or electrochemical impedance spectroscopy along with its application in studying the electrical transport properties and bulk properties of the materials like PEs/SPEs, amorphous materials and crystalline materials in chapter 5. In addition, the complex impedance spectroscopic measurement can provide the information about diffusion of charge carriers (diffusion coefficient), mobility of charges, ionic conductivity, dielectric properties, number density of charge carriers and electric modulus especially for solid polymer electrolyte films or PE films.

Madhu Tiwari has focuses about the synthesis, printing techniques and properties of carbon, transition metal 2D-QDs and their efficient application in photodetectors, batteries, supercapacitors and wastewater treatment in chapter 6

The chapter 7 highlights the advancement in the field of nanomaterials as artificial enzyme, named as “nanozymes” and their kinetic study, reaction mechanisms and various applications, from immunoassays, biosensing and catalysis.

Chapter 8 deals with the various synthesis methods, different characterization techniques, properties and applications of rapheme. This chapter focuses mainly on electrochemical exfoliation method for the production of rapheme through aqueous and non-aqueous route.

R.K. Shukla and Amrit K.Mishra have given their research output in chapter 9. They worked on the perovskite solar cell, now a day's which is the most efficient material for the energy harvesting material and perovskite is recoverable at a high value of humidity under the dark condition and under UVLED it is still recoverable up to RH 50%. So for industrialization, perovskite can sandwich with Si, which enhances the stability of the device

Chapter 10 Present the development in AB₅-type metal hydride to serve the society as energy material. Parent AB₅-type alloy (LaNi₅/MmNi₅) is needed to be tailored for improved hydrogenation properties.

The carbon-based nanomaterials are used as a substitute of traditional materials for different applications in several energy generation and storage systems which are presented in the chapter 11.

Chapter 12 article present a review on the current status of photoactive nanomaterial (Photocatalyst) used to clean the environment for sustainable development of society.

In chapter 13 the role of the functionalization of the carbon-based materials and their exploitation in electrochemical sensing have been discussed.

Chapter 14 describes the different synthesis method of GNS and recent progress of Pt-free GNS supported electrocatalysts in the field of DMFC.

Thakur Prasad Yadav and Kalpana Awasthi have reviewed the synthesis of Two-dimensional (2D) Nanomaterials for energy harvesting from production to storage in chapter 15.

Chapter 16 explore the basic concepts and applications of hybrid materials they have given details of Bio Nanocomposites, Mesoporous Hybrid Materials, Nanocomposite Based Gas Sensors, Sol Gel Derived Hybrid Materials, Nano Diamond Hybrid Materials and Carbon Nanotubes hybrid materials.

In book chapter 17, Dr Subhash Banerjee has explored applications of ZrO_2 NPs in the green synthesis of bioactive molecules via one-pot multi-component

Chapter 18 deals with the study of Bioremediation of Bauxite Residue Dumping Sites of Alumina Industry. Bioremediation through biomining/ bioleaching and nano particles is also discussed for reducing the environmental risk of red mud.

Chapter 19 describes the The present chapter focuses on metal nanocomposite and hybrid nanomaterials for the removal of heavy metals, inorganic anions, organic pollutants, and microorganisms from water including tap water, groundwater, and wastewater.

Chapter 20 explained the various nanoconjugates with enhanced antibacterial and effective drug release properties, some recent chitosan hydrogel based nanoconjugates, and some other nanocojugates dealing with drug delivery.

Dr. Mridula Tripathi
Dr. Arti Srivastava
Dr. Kalpana Awasthi

Complimentary Contributor Copy

Chapter 1

SOCIETAL IMPACT OF NANOMATERIALS

Narendra Kumar Pandey* and Priya Gupta

Department of Physics, University of Lucknow, Lucknow, India

ABSTRACT

The importance of nanomaterials has grown steadily in the interdisciplinary areas of research and development due to their exceptional characteristics such as improved catalysis and adsorption properties as well as high reactivity. Nanomaterials refer to materials whose constituents exist up to 100 nm (but not restricted to) in size or scale. With a wide range of applications available, nanomaterials have the potential to make a significant impact on society, specially to the field of biotechnology and medical tools and procedures.

Nanomaterials which carry specific chemical drugs, peptides, proteins and genes promise effective drug delivery to infected parts of the body. Nanomaterials have also contributed immensely to the advancement of sensor technology, water treatment, air purification, energy storage, cosmetics, electronics, and catalytic applications. The extraordinary properties of nanomaterials include their high resistance to oxidation, antibacterial activity, and high thermal conductivity, etc. This chapter mainly gives an overview of the present and future aspects of nanomaterials in various applications such as water and wastewater treatment, medical, nano sensors, etc.

One of the biggest challenges the world faces today is the COVID-19 pandemic due to SARS-CoV-2 virus. This chapter discusses the latest strategic developments in the human fight against the pandemic. Novel nanomaterials have been developed and nanotechnology applied to the creation of corona virus vaccines, improved protective masks, specific disinfectants, and innovative diagnostic methods. Nano-interferometric biosensors are being developed as point-of-use testing devices for COVID-19, gold nanoparticles are being used to

* Corresponding Author's Email: profnarendrapandey137@gmail.com.

make probes that attach to COVID-19 RNA and nanostructures are in the pipeline to deliver peptide molecules to COVID-19 virus molecules.

Keywords: nanomaterials, COVID-19, drug-delivery, nanoparticles, classification, characterization

1. INTRODUCTION

Various structures and materials with particles of very small dimensions, which exist in Nature or are synthetically developed, play a critical role in modern science and technology. Nanomaterials are materials whose particles range between 1 to 100 nm in size. They also include materials with external dimensions or surface structure or internal local structures in the nanoscale range. Since the internal structure of most materials around us can be modified to be at nano-scale, they also qualify as nanomaterials. Although some experts insist that nanotechnology refers to the measurement or visualization of particles that naturally exist on the scale of 1-100 nanometres, a consensus seems to be forming around the idea that control and restructuring of matter at the nanoscale should also be included in its purview.

A different approach for the term 'nanoparticle' was proposed in 2011 by the European Commission [1]. Nanomaterials usually constitute of a collection of particles with some degree of variance in their sizes, both larger and smaller than 100 nm. Many a time, microparticles and nanoparticles cannot be differentiated as they vary minutely in terms of their size. Hence it is reasonable to propose that the size distribution of such micro and nano dimensions should be taken into account while defining nanoparticles, using the mean size and the standard deviation of the size to categorize them more accurately. The sizes of nanoparticles are comparable to those of DNA, viruses, and proteins, while sizes of microparticles fall in the ranges of cells, organelles, and comparatively larger physiological structures.

Nanomaterials with exceptional properties have become indispensable for research in the field of science and technology. Their unique mechanical, chemical, electronic, thermal, and optical properties at nanoscale, that are drastically different from their properties at macroscale, are continuously attracting interest of scientific community toward them. Materials reduced to the nanoscale can show different properties compared to what they exhibit on a macroscale, enabling unique applications; opaque substances become transparent (copper); stable materials turn combustible (aluminium); insoluble materials become soluble (gold). The main challenge lies in the production of nanoscale materials on a large scale that has led to its synthesis and studies only at the laboratory scale. Commercial availability on nanomaterials is a challenge that the scientists are yet struggling with. Some of the materials commonly used for the synthesis of nanomaterials with their applications are outlined in Table 1.1.

Richard Feynman while delivering his lecture at the American Physical Society meeting at Caltech on December 29, 1959 said "There's plenty of room at the bottom."

He was referring to the world of nanotechnology. Feynman described a process by which the ability to manipulate individual atoms and molecules might be developed, using a set of precise tools to build and operate another proportionally smaller set, and so on, down to the needed scale. "I want to build a billion tiny factories, models of each other, which are manufacturing simultaneously. The principles of physics, as far as I can see, do not speak against the possibility of manoeuvring things atom by atom. It is not an attempt to violate any laws; it is something, in principle, that can be done; but in practice, it has not been done because we are too big" - Richard Feynman.

Table 1.1. Nanomaterials with their synthesis methods and applications [2]

Materials	Synthesis methods	Applications
Metals	Combustion method, chemical precipitation, sol-gel synthesis, laser ablation, pyrolysis, mechanochemical method etc.	Electromagnetic interference, wound dressings etc.
Metal Oxides	Combustion method, chemical precipitation, sol-gel synthesis, laser ablation, pyrolysis, mechanochemical method etc.	Humidity sensors, Gas sensors, Water and strain repellent textiles etc.
Carbonnanotubes	Chemical vapor deposition, carbon arc discharge, laser ablation	Antistatic materials, carbon nanotube enhanced plastic etc.
Carbon Fullerenes	Generated arc using two carbon electrodes in a neon or helium atmosphere	Lubricants, catalysts, targeted drug delivery, nano scale chemical sponges

In the course of this, he noted, scaling issues would arise from the changing magnitude of various physical phenomena: gravity would become less important, surface tension and Van der Waals attraction would become more important, etc. [3].

Tokyo Science University Professor Norio Taniguchi in a 1974 defined nanotechnology as encompassing a multitude of rapidly emerging technologies, based upon the scaling down of existing technologies to the next level of precision and miniaturization. Nano-technology, in a nut shell, mainly consists of the processing, separation, consolidation, and deformation of materials by one atom or by one molecule [4].

Nanotechnology, in its traditional sense, means building things from the bottom up, with atomic precision. As used today, the term nanotechnology usually refers to a broad collection of mostly disconnected (earlier) but now closely connected fields. Essentially, anything sufficiently small and interesting can be called nanotechnology. The nanomaterials field includes subfields which develop or study materials having unique properties arising from their nanoscale dimensions. Much of the fascination with nanotechnology stems from the quantum and surface phenomena that matter exhibits at the nanoscale. In the realm of sustainable development endeavour, a new term 'Green Nanotechnology' is being referred to quite frequently. Green

nanotechnology may be described as the development of clean and environment friendly technology, that can minimize potential environmental and human health risks associated with the manufacture and application of nanomaterial products. This associated nanotechnology should encourage replacement of existing products with novel nano-products that are more environment friendly in their lifecycle. So Green Nanotechnology includes reducing any harmful and hostile impact on the environment, human health and wellness. Green nanotechnology thus talks of enhancing sustainability and maintaining a pristine ecosystem. It proposes the development of products that benefit the environment and society directly or indirectly. Nanomaterials or their associated products have the potential to clean hazardous waste sites directly and in-situ. They can treat pollutants and help in cleaning up water from toxicants and other impurities. Nanotechnology has outstanding prospective applications in dealing with different health related issues including viruses, different environmental hazards, etc. which are considered to be a serious threat to the human life.

Application of nanotechnology could represent a new approach for the treatment or disinfection of viruses. The control of corona viruses is an increasing concern, of which, Middle East Respiratory Syndrome Corona Virus, Severe Acute Respiratory Syndrome Corona Virus and Severe Acute Respiratory Syndrome Coronavirus-2 are well known and dangerous examples. This chapter aims to provide an overview of recent studies on the potency of nanoparticles as diagnostic or antiviral tools against corona viruses. The possibilities of effectively using nanomaterials as nano sensors are also presented.

2. CARBON NANOTUBES: THE NEW REVOLUTIONARY MATERIAL

Carbon nanotubes (CNT) were discovered in 1991 by Sumioliijima. Any tube with nanoscale dimensions is a nanotube. But generally, carbon nanotubes are sheets of graphite rolled up to make a tube. Nanotubes exhibit varying electrical properties (depending on the way the graphite structure spirals around the tube, and other factors, such as doping), and can be superconducting, insulating, semiconducting or conducting (metallic).

One-dimensional nanotubes exhibit electrical conductivity as high as copper, thermal conductivity as high as diamond, strength 100 times greater than steel at one sixth the weight, and high resistance to failure. CNT exhibits extraordinary mechanical properties with the Young's modulus over 1 Tera Pascal and stiffness as high as diamond. The estimated tensile strength is 200 Giga Pascal. These properties are ideal for reinforced composites and nano-electromechanical systems (NEMS). Carbon Nanotube Transistors exploit the fact that nm-scale nanotubes are ready-made molecular wires and can be rendered into a conducting, semiconducting, or insulating state, which makes them valuable for future nano-computer design.

3. QUANTUM DOTS

Quantum dots are small devices that contain a tiny droplet of free electrons. They are fabricated in semiconductor materials and have typical dimensions between a few nanometres to microns. The size and shape of these structures and therefore the number of electrons they contain can be precisely controlled; a quantum dot can have anything from a single electron to a collection of several thousands. The physics of quantum dots shows many parallels with the behaviour of naturally occurring quantum systems in atomic and nuclear physics. As in an atom, the energy levels in a quantum dot become quantized due to the confinement of electrons. Unlike atoms however, quantum dots can be easily connected to electrodes and are therefore excellent tools to study atomic-like properties.

4. NANOTECHNOLOGY: THE GENERAL-PURPOSE TECHNOLOGY

Nanotechnology is also referred to as a general-purpose technology. When its potential is fully realized, nanotechnology will have significant impact on almost all kinds of industries and it will touch all areas of society. It will offer efficiently manufactured, durable, cleaner, safer, and smarter products for homes and industries both. The fields of medicine, agriculture, communications, transportation and industry all are up for significant changes. Nanotechnology is expected to revolutionize areas like semiconductors, pharmaceuticals and materials. The total societal impact of nanotechnology is expected to be much greater than the Silicon Valley revolution in silicon integrated circuits because it has applications in many more areas than electronics. Studies on nanomaterials and nanotechnology have in itself turned out to be a special branch that requires chemists, physicists, biologists, and engineers to work together in an integrated manner. This multidisciplinary nature presents a challenge for the scientific community and the R&D bodies of governments and industry and requires multidisciplinary and multi-institutional approach. The increasing pace of research and development in this field requires development of huge manpower. Hence, human resource development is a very important component of such advancement of national and international importance.

Nanomaterials in association with nanotechnology have the potential to significantly impact energy efficiency, storage and production. Solar energy is a renewable source of energy. Less than 1% of the energy used is produced from the Sun because it is difficult to transform the Sun's rays into electricity. Researchers world over are busy in fabricating nanomaterials for the purpose of developing efficient solar cells, fuel cells, and environment friendly batteries. The focal point in this area of developing nanomaterials for renewable energy is their storage, conversion and manufacturing in order to reduce the material and process cost. Solar cells are attractive candidates for clean and renewable power; with miniaturization, they might also serve as integrated power sources for nano electronic systems.

The use of nanostructures or nanostructured materials represents a general approach to reduce both cost and size and to improve efficiency in photovoltaics. Nanoparticles, nanorods and nanowires have been used to improve the charge collection efficiency in polymer-blend and dye-sensitized solar cells. The p-type/intrinsic/n-type (p-i-n) coaxial silicon nanowire solar cells yield a maximum power output of up to 200 pW per nanowire device and an apparent energy conversion efficiency of up to 3.4 per cent. Individual and interconnected silicon nanowire photovoltaic elements can serve as robust power sources to drive functional nano electronic sensors and logic gates [5-9]. Another example is the use of fuel cells powered by hydrogen, potentially using a catalyst consisting of carbon supported noble metal particles with diameters of 1–5 nm. Materials with small nanosized pores may be suitable for hydrogen storage.

Nanotechnology may also find applications in batteries, where the use of nanomaterials may enable batteries with higher energy content or super capacitors with a higher rate of recharging. Nanotechnology is used to provide improved performance coatings for photovoltaic (PV) and solar thermal panels. Hydrophobic and self-cleaning properties combine to create more efficient solar panels, especially during inclement weather. PV covered with nanotechnology coatings are said to stay cleaner for longer to ensure maximum energy efficiency is maintained [10].

Today nanomaterials are being developed and used in sensing technologies that may give warning signals in advance of the presence of toxic metals or gases or any other life-threatening substances. This not only saves lives but also acts as time monitoring device for safety against unknown and unforeseen perils, endangerments and other hazards. Novel nanomaterials are addressing health concerns and saving mankind from heart disease, lung cancer, and motor neuron diseases. Functionalized nanoparticles are able to form anionic oxidants bonding thereby allowing the detection of carcinogenic substances at very low concentrations. Polymer nanospheres have been developed to measure organic contaminants in very low concentrations.

In the twenty-first century, criminal investigation has reached a point where increased sophistication and precision is needed to ensure proper deliverance of justice. Due to this, there is involvement of many branches of sciences in crime detection. Lately, nanotechnology and taggant technology have found potential use in forensic science also [11].

4.1. Drug Delivery to Treat Tumour or Cancer (Without Using Radiotherapy & Chemotherapy)

The ultra-small size of nanoparticles endows them with special properties that are useful in oncology, mainly in the imaging process and drug delivery to the affected tissues or organs. Quantum dots (nanoparticles with quantum confinement properties, such as size-tunable light emission), when used in conjunction with MRI (magnetic resonance imaging), can produce exceptional images of tumour sites. These

nanoparticles are much brighter than organic dyes and only need one light source for excitation.

The property of nanomaterials such as large surface-area-to-volume ratio, allows many functional groups to be attached to a nanoparticle, which can seek out and bind to certain tumour cells. The ultra-small size of nanoparticles allows them to preferentially accumulate at tumour sites. This process is helped by the property of the tumour itself as tumours do not have an effective lymphatic drainage system. Researchers are continuing to look for more effective methods to target nanoparticles carrying therapeutic drugs directly at diseased cells. For example, scientists at MIT have demonstrated increased levels of drug delivery to tumours by using two types of nanoparticles. The first type of nanoparticle locates the cancer tumour and the second type of nanoparticle (carrying the therapeutic drugs) goes through the signal generated by the first type of nanoparticle. An alternative technique delivers chemotherapy drugs to cancer cells and also applies heat to the cell. DNA strands are attached to the gold nanorods. The DNA strands act as a scaffold, holding together the nanorod and the chemotherapy drug. When Infrared light illuminates the cancer tumour, the gold nanorod absorbs the infrared light, and turns it into heat. The absorption of heat releases the chemotherapy drug that destroys the cancer cells.

Researchers at North Carolina State University are developing a technique by which cardiac stem cells will be delivered to damaged heart tissue. They attach nanovesicles that are attracted to an injury to the stem cells to increase the amount of stem cells delivered to an injured tissue.

Researchers are improving dental implants by adding nanotubes to the surface of the implant material. They have demonstrated the ability to load the nanotubes with anti-inflammatory drugs that can be applied directly to the area around the implant. They have also shown that bone adheres better to titanium dioxide nanotubes than to the surface of standard titanium implants.

Researchers have developed nanoparticles that release insulin when glucose levels rise. The nanoparticles contain both insulin and an enzyme that dissolve in high levels of glucose. When the enzyme dissolves the insulin is released. In laboratory test these nanoparticles were able to control blood sugar levels for several days. Researchers are developing nanoparticles that can deliver drugs across the brain barrier to tackle neurological disorders. A method being developed to fight aging uses mesoporous nanoparticles with a coating that releases the contents of the nanoparticle when an enzyme found in aging cells is present [12].

4.2. Environmental Remediation

Nano-remediation is an emerging industry. During nano-remediation, a nanoparticle agent is brought into contact with the target contaminant under suitable conditions that allows a detoxifying or immobilizing reaction. This process typically involves a pump-and-treat process or in-situ application. Nano remediation thus uses

nanoparticles for environmental remediation. One such area where nano remediation has been most widely used is for groundwater treatment. For the past more than 20 years, nanoscale metallic iron (nZVI) has been investigated as a new tool for the treatment of contaminated water and soil. The technology is being commercially used in many countries worldwide, however it is yet to gain universal acceptance. The concerns over the long-term fate, transformation and eco-toxicity of nZVI in environmental systems and, a lack of comparable studies for different nZVI materials and deployment strategies are some of the reasons for the lack of universal acceptance of this technique [13].

4.2.1. Water Purification Technology

Thermonuclear Trap Technology (TTT) has the potential to clean all sources of water from any kind of pollutants and toxic contents. This is a patented nanotechnology. It uses a high pressure and temperature chamber to separate isotopes away from the water. Professor Vladimir Afanasiew, at the Moscow Nuclear Institution has developed this novel method. This technology is useful in cleaning the sea, river, lake and landfill waste waters. The method is capable of removing radioactive isotopes from sea water after Nuclear Power Stations catastrophes and cooling water plant towers. With this technology pharmacal rests can be removed as well as narcotics and tranquilizers. The bottom layers and sides at lake and rivers can be renewed after being cleaned. The machinery used for this purpose is very similar to that used in deep-sea mining. Removed waste items can be sorted by this process and can be re-used as raw material for other industrial production.

4.2.2. Disinfecting Water Through Nanotechnology

Water is our natural heritage, the miracle of our life. Unfortunately, about 35 percent of people in the developing world die from water-related problem. Currently, more than 1 billion people are at risk due to lack of clean water. To alleviate these problems and make pure drinking water available to common people, water purification technology requires new approaches for effective management and conservation of water resources. Nanotechnology has the potential to contribute to long-term water quality, availability and viability of water resources, through the use of advanced filtration materials that enable greater water reuse, recycling and desalinization. The existing techniques employed for the disinfection of water are either energy-intensive or have toxic by-products harmful to human health. Drinking water disinfection techniques effectively combine chemical, physical, biological, and engineering principles in one.

Recent advances strongly suggest that many of the current problems involving water quality can be addressed and potentially resolved using nano adsorbents, nano catalysts, bioactive nanoparticles, nanostructured catalytic membranes, and nanoparticle enhanced filtration [14]. Novel nanomaterials are being developed for the treatment of ground water, surface running water and waste water. Nanomaterials are helping in removing toxic metal ions, organic and inorganic toxicants, and harmful

microorganisms [15]. There are four classes of nanomaterials that are employed for water treatment and these are dendrimers, zeolites, carbonaceous nanomaterials, and metals containing nanoparticles. There are benefits of reducing the size of the metals (e.g., silver, copper, titanium, and cobalt) to the nanoscale such as contact efficiency, greater surface area, and better elution properties [16-17]. The nanomaterials-based technologies applied in water treatment consist of reverse osmosis (RO), nanofiltration and ultrafiltration membranes. Nanofiber filters, carbon nanotubes and many nanoparticles are emerging areas for water filtration [18]. The very high surface area to volume ratio of nanomaterials increases adsorption, desorption, dissolution and reactivity of contaminants [19]. Antimicrobial nanotechnology offers several nanomaterials that show strong antimicrobial properties like the photocatalytic production of reactive oxygen species that damage cell components and viruses. Synthetically fabricated nanometallic particles produce antimicrobial action called oligodynamic disinfection, which has the ability to inactivate microorganisms even at low concentrations. Commercial purification systems based on titanium oxide photocatalysis are also currently available in the market. Studies show that this technology can achieve complete inactivation of faecal coliforms in 15 minutes once activated by sunlight.

4.2.3. Getting Rid of Oil Spills

Oil spills are a perpetual problem. There are 10 to 15 thousand oil spills per year. Conventionally, oil spills are corrected through gelling, or deploying biological and dispersing agents. But these techniques have their limitations. They cannot retrieve the valuable and non-replaceable spilled oil. Nanowires have the capability to both clean up the oil spills faster and recover the lost oil as well to a great extent. These nanowires have the property of forming a mesh which has a greater absorption capacity, up to twenty times its weight, in hydrophobic liquids; while its water repellent coating rejects water. Potassium manganese oxide is very stable even at high temperatures. In this way, the oil can be boiled off the nanowires, and both the oil can be recovered and the nanowires can be reused [20]. In 2005, Hurricane Katrina damaged or destroyed more than thirty oil platforms and nine refineries. The Interface Science Corporation successfully launched an oil remediation and recovery application, which used water repelling nanowires to clean up the oil spilled by the damaged oil platforms and refineries.

4.2.4. Removing Plastics from Oceans

More than 50 million tons of plastics found in most disposable water bottles known as polyethylene terephthalate (PET) are produced globally each year leading to a huge environmental problem and dangerous to biodiversity. A team of Japanese scientists has found a species of bacteria that eats the type of plastic found in most disposable water bottles. The researchers reported that a community of *Ideonellasakaiensis* could break down a thin film of PET over the course of six weeks if the temperature were held at a steady 86 degrees. These nano-machines are able to decompose plastics

many times faster than bioengineered bacteria due their increased surface area. Also, the energy released from decomposing the plastic is used to fuel the nano-machines [21].

4.3. Monitoring and Control of Air Pollution

Air pollution is one of the world's most significant problems. Air pollution may be defined as the alteration in the natural composition of the atmosphere that is caused by the introduction of chemical, physical, or biological substances that are emitted from anthropogenic, geogenic, or biogenic sources. Poor air quality has an adverse impact on ecosystems (e.g., vegetation and living organisms) and on human health by possibly causing various types of diseases which can be fatal, such as cancer, respiratory, and cardiovascular diseases. The World Health Organization (WHO) in 2014 reported that around seven million people died in 2012 due to air pollution exposure [22, 23]. The loss of life expectancy globally “from air pollution surpasses that of HIV/AIDS, parasitic, vector-borne, and other infectious diseases by a large margin. Every year more than 10000 people die due to air pollution related to fossil fuels only.”

Air pollution can be remediated using nanotechnology in several ways. One is through the use of nano-catalysts with increased surface area for gaseous reactions. Catalysts work by speeding up chemical reactions that transform harmful vapours from cars and industrial plants into harmless gases. Catalysts currently in use include a nanofiber catalyst made of manganese oxide that removes volatile organic compounds from industrial smokestacks [24]. Other methods are still in development stage.

Another approach uses nanostructured membranes that have pores small enough to separate methane or carbon dioxide from exhaust [25]. John Zhu of the University of Queensland is researching carbon nanotubes (CNTs) for trapping greenhouse gas emissions caused by coal mining and power generation. CNTs can trap gases up to a hundred times faster than other methods, allowing integration into large-scale industrial plants and power stations. This new technology both processes and separates large volumes of gas effectively, unlike conventional membranes that can only do one or the other effectively. The substances filtered out still presented a problem for disposal, as removing waste from the air only to return it to the ground leaves no net benefits. In 2006, Japanese researchers found a way to collect the soot filtered out of diesel fuel emissions and recycle it into manufacturing material for CNTs [26]. The diesel soot is used to synthesize the single-walled CNT filter through laser vaporization so that essentially, the filtered waste becomes the filter.

4.4. Nano Sensors

Nano sensors in conjunction with polymers are used to screen food pathogens and chemicals during storage and transit processes in smart packaging. Additionally, smart

packaging confirms the integrity of the food package and authenticity of the food product. Nano-gas sensors, nano-smart dust can be used to detect environmental pollution. These sensors are composed of compact wireless sensors and transponders. Nano barcodes are also an efficient mechanism for detection of the quality of agricultural fields. An electrochemical glucose biosensor was nanofabricated by layer-by-layer self-assembly of polyelectrolyte for detection and quantification of glucose. Nano sensors can detect environmental changes, for example, temperature, humidity, and gas composition as well as metabolites from microbial growth and by-products from food degradation [27-31]. The types of nano sensors used for this purpose include array biosensors, carbon nanotube-based sensors, electronic tongue or nose, microfluidic devices, and nanoelectromechanical systems technology. Sensors based on nanomaterials (nano sensor), both chemical sensors (chemical nano sensors) and biosensors (nano biosensors), can be used online and combined into existing industrial process and distribution line or off-line as speedy, simple, and transportable, as well as disposable sensors for food contaminants.

4.5. COVID – 19 PANDEMIC and Nanomaterials

In early December 2019, an outbreak of coronavirus disease 2019 (COVID-19), caused by a novel severe acute respiratory syndrome corona virus 2 (SARS-CoV-2), occurred in Wuhan City, Hubei Province, China. On January 30, 2020 the World Health Organization declared the outbreak as a Public Health Emergency of International Concern. Today one of the biggest challenges the world faces is the COVID-19 pandemic due to SARS-CoV-2 virus. Corona viruses are enveloped positive-stranded RNA viruses that belong to the family *Coronaviridae* and the order *Nidovirales* [32]. Corona viruses, which are zoonotic in origin, can evolve into a strain that can infect human beings leading to fatal illness [33]. In general, corona viruses first replicate in epithelial cells of the respiratory and enteric cells, which leads to cytopathic changes [34].

Novel nanomaterials are being developed and nanotechnology applied to the creation of corona virus vaccines, improved protective masks, specific disinfectants, and improved diagnostic methods. Nano-interferometric biosensor are being developed as point of use testing device for COVID-19, gold nanoparticles are being used to make probes that attach to COVID-19 RNA and nanostructures are in the pipeline to deliver peptide molecules to COVID-19 virus molecules.

Researchers at the Queensland University of Technology have shown that a filter made with cellulose nanofibers can block virus size particles. These filters can be made at a very low cost and their mass production can be easily done. Researchers are using gold nanoparticles to make probes that attach to COVID-19 RNA. Researchers at the North-western University and MIT are working on using nanostructures to deliver peptide molecules to COVID-19 virus molecules. The peptide molecules are able to bond to the COVID-19 spike protein, therefore disabling the virus molecule. Researchers at the Catalan Institute of Nanoscience and Nanotechnology

are using a nano-interferometric biosensor to develop a point of use testing device for COVID-19. Sona Nanotech is developing a diagnostic test for COVID-19 using gold nanorods. The test is expected to provide results in about 5 to 15 minutes and not require laboratory analysis. Researchers at the Norwegian University of Science and Technology have developed a test for COVID-19 that doesn't require reagents (which are in limited supply). The test uses silica coated magnetic nanoparticles. RNA from the virus is attracted to the nanoparticles, which are then extracted from the sample with a magnetic field. Mammoth Biosciences has developed a test for COVID-19 using CRISPR diagnostic techniques which give results in 45 minutes without needing to send the sample to a lab. The first study published with this test reports accuracy similar to lab test results [37]. Today the fate of the world in the pandemic time depends on an international competition for a COVID-19 vaccine. Major companies ahead in race to save valuable human lives, who have developed vaccines are Zydus Cadila, Bharat Biotech, Serum Institute, Astra Zeneca, Novavax, Sanofi, Johnson & Johnson, Glaxo Smith Kline, Moderna, Pfizer and BioNTech. They have raced against time and launched their vaccines having varying degree of efficacies. Many more vaccines are in the pipeline. COVID-19 vaccines help our bodies develop immunity to the virus that causes COVID-19 without us falling sick. Different kinds of vaccines work in different ways to offer protection against infection. The common factor to all vaccines is that with all kinds of vaccines, the body is left with a supply of T-lymphocytes and B-lymphocytes that will have the memory as to how to fight that virus in the future. As a matter of fact, it typically takes a few weeks after vaccination for the body to produce T-lymphocytes and B-lymphocytes. Therefore, it is possible that a person could be infected with the corona virus that causes COVID-19 just before or just after vaccination. The person can therefore fall sick since the vaccine did not have sufficient time to provide protection. It may also be remembered that sometimes after vaccination, the process of building immunity can cause symptoms, such as fever, body ache or headache. These symptoms are normal and indicates that the body is building immunity.

CONCLUSION

As an innovative branch among emerging sciences, nanotechnology has the potential to completely revolutionize our lives. There exists a massive variety of nanomaterials today which possess a wide range of properties with the potential to be developed into endless applications. Emerging studies describing the manipulation of materials at their atomic level has paved way for the development of nanomaterials ranging in the sizes scaling 1–100 nanometres. Modification of the properties of materials on a molecular scale offers the prospect of upgrading their performance in various aspects of human lives.

Potential applications of nanomaterials in the future are limitless, with chances of producing significant advances in the fields of electronics, food, medicine, computing,

etc. The beginning of scientific research in nanomaterials had an obvious mix of hope and hype both but the spinning off of the scientific knowledge in nanomaterials and their general-purpose all-pervasive applications for improving the quality of human life is weighing heavily in favour of hope for the society. The field of nanomaterials has grown at tremendous speed during the last couple of years. However, while there are unlimited researches being undertaken on nanomaterials, limits due to the cost of nanomaterial manufacturing and applications exist; all in spite of the generous funding that nanotechnology projects have received. There has recently been an exponential increase in the number of studies concerning health-related nanomaterials, considering the various medical applications of nanomaterials that drive medical innovation. There is a need to analyse the effect of the cost factor on acceptability of health-related nanomaterials independently or in relation to material toxicity. It appears that from the materials studied, those used for cancer treatment applications are more expensive than the ones for drug delivery. The ability to evaluate cost implications improves the ability to undertake research mapping and develop opinions on nanomaterials that can drive innovation. Like electricity or computers, nanomaterials and nanotechnology will offer better products and greatly improved efficiency in almost every aspect of life. But as a general-purpose technology, it will be dual-use, it will have commercial uses and it will also have military uses-making far more powerful weapons and tools of surveillance and warfare. Thus, it represents not only wonderful benefits for humanity but also grave risks.

REFERENCES

- [1] Potocnik, J. 2011. Commission recommendation of 18 October 2011 on the definition of nanomaterial (Text with EEA relevance) (2011/696/EU). In: Commission, T. E. (ed.) *Official Journal of the European Union*.
- [2] Anbazhagan Mageswari, Ramachandran Srinivasan, Parthiban Subramanian, Nachimuthu Ramesh, and Kodiveri Muthukaliannan Gothandam. 2016. *Nanomaterials: Classification, Biological Synthesis and Characterization. Nanoscience in Food and Agriculture 3*. Edited by Shivendu Ranjan, Nandita Dasgupta and France Lichtfouse. 31-71. Switzerland: Springer International Publishing.
- [3] Feynman, Richard P. (1960). There's plenty of room at the bottom. *Engg. and Sci.* 23:22-36.
- [4] Taniguchi, N. (1974). On the Basic Concept of Nano-Technology. *Proceedings of International Conference on Production Engineering, Tokyo, Part II*. pp. 18-23.
- [5] Santos, J. P., Polichetti, C., Hontanon, E., Sayago, I., Aleixandre, M., Alfano, B., Miglicta, M., DiFrancia, C. and Lozano, J. (2018). Study of Graphene Based Nanosensors for the Detection of Nitrogen Dioxide. *Proceedings of the 12th Spanish Conference on Electron Devices (CDE), Salamanca*. pp. 1-4. doi: 10.1109/CDE.2018.8597167.

- [6] Lewis, N. S. (2007). Toward cost-effective solar energy use. *Science* 315:798–801.
- [7] Baxter, J. B. and Aydil, E. S. (2005). Nanowire-based dye-sensitized solar cells. *Appl. Phys. Lett.* 86:053114.
- [8] Luque, A., Marti, A. and Nozik, A. J. (2007). Solar cells based on quantum dots: multiple exciton generation and intermediate bands. *Mat. Res. Bull.* 32:236–241.
- [9] Tian, B., Zheng, X., Kempa, T. J., Fang, Y., Yu. N., Yu, G., Huang, J. and Lieber, C. M. (2007). Coaxial silicon nanowires as solar cells and nanoelectronic power sources. *Nature*. 449 (7164): 885–889. doi: 10.1038/nature06181.
- [10] Wikipedia. “*Green Nanotechnology*.” Last modified Sep. 2020. https://en.wikipedia.org/wiki/Green_nanotechnology.
- [11] Bhatt, P. V., Pandey, G. and Tharmavaram, M. (2020). Nanotechnology and taggant technology in forensic science. *Tech. in Forensic Sci.* 279-301.
- [12] *Understanding nano*. “Nanotechnology in Medical Diagnostics” <https://www.understandingnano.com/Nanotechnology-Medical-Diagnostics.html>.
- [13] Crane, R. A. and Scott, T. B. (2012). Nanoscale zero-valent iron: Future prospects for an emerging water treatment technology. *J. Hazard. Mat.* 211-212: 112–125.
- [14] Cloete, T. E., Kwaadsteniet, M., Botes, M. and López-Romero, J. M. (2010). *Nanotechnology in Water Treatment Applications*. Caister Academic Press. ISBN 978-1-904455-66-0.
- [15] Hanft, Susan. 2011. *Market Research Report Nanotechnology in Water Treatment*. USA: BCC Research.
- [16] Goyal, K., Amit, S., Johal, E. and Rath, G. (2011). Nanotechnology for water treatment. *Current Nanoscience*. 7 4: 640-654(15).
- [17] Street, A., Sustich, R., Duncan, J. and Savage, N. (2014). *Nanotechnology applications for clean water: solutions for improving water quality*. Oxford: Elsevier. pp. 286-322.
- [18] Kumar, J. K. and Pandit, A. B. (2012). *Drinking water disinfection techniques*. Boca raton, FL: CRC Press. p. 186.
- [19] Sharmaa, Y. C., Srivastava, V., Singh, V. K., Kaul, S. N. and Weng, C. H. (2009). Nano-adsorbents for the removal of metallic pollutants from water and wastewater. *Environ. Technol.* 30: 583–609.
- [20] Yunus, I. S., Harwin, Kurniawan, A., Adityawarman, D. and Indarto, A. (2012). Nanotech for Oil. *Env. Tech. Rev.* 1: 136–148.
- [21] Phys.org. *Newly Discovered bacteria can eat plastic bottles*. <https://phys.org/news/2016-03-newly-bacteria-plastic-bottles.html>.
- [22] Ibrahim, R.K., Hayyan, M., Al Saadi, M.A., Hayyan, A. and Ibrahim, S. (2016). Environmental application of nanotechnology: Air, soil, and water. *Env. Sci. and Poll. Res.* 23:13754–13788.
- [23] Bratovcic, A. (2019). Different applications of nanomaterials and their impact on the environment. *SSRG Int. J. Mat. Sci. Engg.* 5 1: 1-7. doi: 10.14445/23948884/IJMSE-V5I1P101.

- [24] *Understandingnano*. “Air Pollution and Nanotechnology”. <http://www.understandingnano.com/air.html> s.
- [25] Zhu, J., *School of Engineering*. (2007). Available at <http://www.uq.edu.au/research/index.html?page=68941&pid=68941>
- [26] Uchida, T., Ohashi, O., Kawamoto, H., Yoshimura, H., Kobayashi, K. Tanimura, M., Fujikawa, N., Nishimoto, T., Awata, K. and Tachibana, M. (2006). Synthesis of single-wall carbon nanotubes from diesel soot. *Jpn. J. Appl. Phys.* 45: 8027-8029.
- [27] Pandey, N. K., Roy, A., Tiwari, K., Mishra, A., Rai, A., Jayaswal, S., Rashmi, Madhvendra and Govindan, A. (2012). NO₂ sensing studies of WO₃ and Ag doped WO₃ prepared through sol-gel route. *IEEE Explore* p. 342-345..
- [28] Misra, S. K., Pandey, N. K., Shakya, V. and Roy, A. (2015). Application of undoped and Al₂O₃-doped ZnO nanomaterials as solid-state humidity sensor and its characterization studies. *IEEE Sensors Journal* 15:3582-3589.
- [29] Yadav, B. C., Pandey, N. K., Srivastava, A. K. and Sharma, P. (2007). Optical humidity sensors based on titania films fabricated by sol-gel and thermal evaporation. *J. Meas. Sci. Tech.* 18:260-264.
- [30] Rajput, V. and Pandey, N. K. (2017). Moisture sensing studies of CuO-ZnO nanocomposites. *Int. J. Appl. Ceramic Tech.*14:77–83.
- [31] Gupta, P., Maurya, S. Pandey, N. K. and Verma, V. (2020). Metal-oxide based ammonia gas sensors - A review. *Nanosci. Nanotech. Asia* Manuscript Number: BMS-NNA-2020-19 (In Press).
- [32] Wormser, G. P. and Aitken, C. Clinical virology 3rd Edition. *Clinical Infectious Diseases*, Edited by Richman, D. D., Whitley, R. J. and Hayden, F. G. 2010. DC: ASM Press. 50 12:1692. <https://doi.org/10.1086/652862>.
- [33] Su, S., Wong, G. and Shi, W. (2016). Epidemiology, genetic recombination, and pathogenesis of coronaviruses. *Trends Microbiol.* 24:490–502.
- [34] Fields, B. N., Knipe, D. M. and Howley, P. M. (2007). *Fields Virology*. 5th ed. Philadelphia: London: Wolters Kluwer Health/Lippincott Williams & Wilkins.
- [35] *Prevention & Treatment*. (2020). www.cdc.gov/coronavirus/2019-ncov/about/prevention-treatment.html.
- [36] *Developing MERS and SARS therapeutics and vaccines*. (2020). www.niaid.nih.gov/diseases-conditions/mers-sars-therapeutics-vaccines.
- [37] *Understandingnano*, “Nanotechnology vs. COVID-19”. <https://www.understandingnano.com/coronavirus-nanotechnology.html>.

Complimentary Contributor Copy

Chapter 2**NANOMATERIALS: SYNTHESIS, PROPERTIES,
AND SOCIETAL APPLICATIONS*****Meena Nemiwal¹, Ankita Dhillon² and Dinesh Kumar^{3,*}***¹Department of Chemistry, Malaviya National Institute of Technology,
Jaipur, INDIA²Department of Chemistry, Banasthali Vidyapith, Rajasthan, INDIA³School of Chemical Sciences, Central University of Gujarat, Gandhinagar, INDIA**ABSTRACT**

Nanomaterials are grained size substances ranging from a billionth of a meter (1–100 nm). They exhibit beneficial and extraordinary properties (high area to volume ratio) that endow it a top field of research globally. In this chapter, synthesis methods of nanomaterials and their basic properties such as electrical, optical, and mechanical are discussed in brief. The characterization of nanomaterials is carried out by high technologies such as scanning electron microscopy (SEM), transmission electron microscopy (TEM), and X-ray diffractions (XRD). Nanoparticles (NPs) can be classified based on their shape, size, and properties. The various types of nanoparticles (NPs) such as metal NPs, carbon-based NPs, semiconductor NPs, ceramics NPs, lipid-based NPs, and polymeric NPs. Herein, nanomaterials' applications in different fields of water treatment, catalysis, energy storage, sensors, and nanomedicine are discussed in detail with their harmful impact on the environment. Nanomaterials for environmental improvement are associated with solar cells to produce clean energy, sonochemical decolorization of dyes through nanocomposites and nanotechnological based coatings for exterior surface building. Currently, nanoscale materials are being extensively explored, and a key role is being provided in the service of society.

Keywords: nanomaterials, synthesis, properties, societal applications

* Corresponding Author's Email: dinesh.kumar@cug.ac.in.

1. INTRODUCTION

Nanomaterials (NMs) having dimensions ranging from 1 to 100 nm show tremendous applications in present modern society [1]. When a bulk reaches to the nanoscale, the properties like reactivity, electronic structure, thermal and mechanical properties change drastically [2]. Nanoparticles (NPs) exhibit unique properties such as high surface area, specific optical and electronic properties, good mechanical and thermal properties, etc. that make NPs a potential candidate for a wide variety of applications in the field of water treatment, nanomedicine, catalysis, sensors, and energy [3]. Bottom-up method and top-down method are the two approaches by which NPs have been synthesized. Generally, the top-down approach is exploited, but nowadays, the bottom-up approach is explored to avoid the wastage of the materials. Depending on the shape, size and precursors, NPs are of many types such as metal NPs (MNPs), carbon-based NPs, ceramics, polymeric, lipid, and semiconductor nanoparticles [4]. These NPs are characterized by using modern technologies like scanning electron microscopy (SEM), transmission electron microscopy (TEM), and X-ray diffraction (XRD), which provide information regarding morphology, size and crystallinity of NPs, respectively [5].

The present chapter gives an overview of NPs by discussing synthesis methods, properties, types, and characterization. Since NPs are significantly important in many fields, their applications are discussed in detail. The rapid production and use of nanomaterials (NMs) in construction, industrial processes, consumer products, and the medical field leads to increasing exposure to humans and the environment; thus its adverse effects are yet to be explored.

2. SYNTHESIS METHODS

Several methods can be used for the fabrication of NPs, but there are two categories i.e., Top-down approach and Bottom-up approach. Both approaches are further classified on the bases of reaction condition, operation, and basic principles used, as shown in Figure 1.

2.1. Top-Down

Top-down is destruction-based approach in which starting larger molecules are decomposed into smaller units and further transformed into appropriate NPs. The decomposition methods are mechanical milling, chemical etching, sputtering, laser ablation, and electro-explosion [6, 7]. In general, physical processes or a combination of chemical and physical processes is employed for the grinding or carving methods [8]. Guan et al. developed single layer nanosheets by exfoliating of transition metal dichalcogenides (TMDs) and graphite through the top-down approach. Protein and

bovine serum albumin (BSA) were used as exfoliating agents. They also acted as stabilizing agents, which prevented further aggregation of single layer for making them biocompatible in biomedical applications [9]. Although this approach is the most widely exploited in nanotechnology, but a lot of wastage of material is of major concern. Therefore, the combination of both top-down and bottom-up technologies are being used for the efficient production of nanoparticles [10].

2.2. Bottom-Up

The properties of bottom-up approach is a building up approach in which simpler substances are grown into suitable NPs [11]. Mainly reduction and sedimentation techniques are employed in green synthesis, sol-gel, biochemical, spinning, etc. [12]. Cai et al. employed sonochemical, chemical, and lithographic methods to produce graphene nanoribbons with excellent electronic properties that can be exploited to fabricate electronic devices at the nanoscale [13]. Nowadays, less expensive, eco-friendly and chemical free approach for the synthesis of NPs is of major concern, emphasizing the purity of the particles. Biogenic reduction is the chemical reduction in which extract of natural plant is being used in place of reducing agents. These biogenic reducing agents exhibit both stabilization and capping properties with good control on the shape and size of NPs [14]. Although the bottom-up approach is in its infancy, tremendous work is being done to explore this research approach.

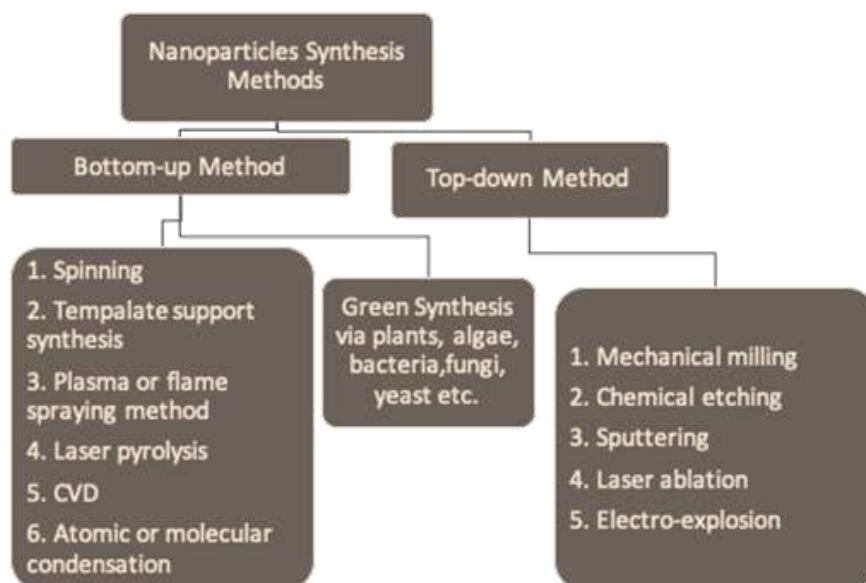


Figure 1. Synthetic methods for nanoparticles.

3. NANOPARTICLES

3.1. Magnetic Properties

Magnetic NPs have been successfully employed in environmental and medical fields, and this property is highly dependent on the nanoparticle's size. Excellent performances are shown by the particles smaller than 35 nm [15, 16]. For the single compound NPs, the number of magnetic atoms represents the magnetic moment values. For multicomponent NPs value of the magnetic moment depends on the number of lone pair of electrons calculated by valence shell electron pair repulsion (VSEPR) theory. In the case of pure metals, change in particle size hardly changes the lattice parameters of the metals, but in the case of metal oxides over the surface of metals, the particle size change alters the lattice parameters due to mismatches between the lattice parameters of the metals and metal oxides and causes interfacial stress at the surface. Synthesis methods and composition of nanostructure are also key factors that affect magnetization values [17]. Zhang et al. substituted Mn^{2+} in nickel-cobalt ferrite and studied the lattice constant and ferromagnetic behaviour of the resultant compound [18].

3.2. Optical

Semiconductor materials exploit the optical properties in several applications such as photocatalysts and photovoltaics, and this property is measured by Beer–Lambert law (basic light principle). Extensive research has been made to improve the adsorption of wavelengths for semiconductor NPs, which depends on the size, shape, distribution of size, and types of modification agents. Metal ion doping, the composition of nanostructure, and surface modification greatly affects the optical properties. Rahman et al. studied the optical properties of Nd-doped NiO through UV–Visible spectroscopy and observed the decrease in energy value owing to the electrons exchange between localized electrons of Nd^{3+} and the energy band of NiO [19, 20]. Basically, optical properties depend on reflectance and scattering phenomena that directly depends on the particles' size, with an increase in particle size and decrease in refractive index, the reflectance increases [21].

3.3. Thermal

NPs show a large surface area that makes them suitable for heat transfer directly on the surface of the material, and this property is better than their fluid form. Thermal properties of polymers have been improved by incorporating metal oxides, increasing the interaction of polymers with NPs [22]. In some cases, nanofillers with high intrinsic thermal properties are used for better performances [23].

3.4. Mechanical

NPs possess various mechanical properties in comparison to microparticles and bulk materials. NMs exhibits improved mechanical properties such as adhesion, hardness, elastic modulus, stress, and strain. Generally, inorganic compounds produce NPs with high mechanical properties and organic compounds produce NPs with low mechanical properties. Thus, inorganic material NPs are incorporated into the organic compounds-based NPs for better performance of mechanical properties. Rice husk ash (RHA)-SiO₂ NPs were incorporated with acrylic polyols and polyisocyanate, and improved mechanical properties were observed [24].

4. CHARACTERIZATION METHODS

4.1. Scanning Electron Microscopy (SEM)

Scanning electron microscopy (SEM) determines the morphology of the surface of NPs. SEM determines the back scattered electrons at high magnification, high resolution and observes good depth of focus. In SEM analysis, the electron beam of low energy (1–30 keV) is subjected to the sample and scattered electrons are detected. Liquid or solid SEM samples for analysis are placed on carbon or aluminium stubs, and bulk form can be used, and no need of cutting thin sections is required. Preparation of sample is easy for SEM compared to TEM analysis, and liquid samples can easily be dried even directly on the SEM stub. To photograph the image, a camera is also attached that can be easily processed on a computer. Energy and intensity of the emitted characteristic X-rays are analysed, which provides information of specific elements and their quantity.

4.2. Transmission Electron Microscopy (TEM)

Transmission electron microscopy (TEM) is one of the most important tools for analysing the nanoparticle structure. It provides information related to the morphology of shape and size of NPs along with analysis at an atomic level. There are two modes through which TEM analysis can be carried out, one Bright-field TEM, and another one is dark-field TEM. Bright-field mode is generally used in which directly transmitted electrons are analysed by capturing image. In dark-fields TEM, diffracted electrons are directly analysed at a specific set of crystal planes. In TEM analysis, first samples are dried and mounted on carbon coated copper grid and fast electrons are subjected that penetrate into various atomic planes which are diffracted like X-rays through the crystalline regions.

4.3. X–ray Diffractions (XRD)

XRD is an excellent technique for analysing the data like shape and width of the nanomaterial sample. Samples are prepared as compact flat or as a smear or taken in a capillary, and a beam of monochromatic X–ray is exposed, which is diffracted and noted at an angle (2θ) at the incident beam. XRD also provides information about crystallinity or amorphous content by studying the phase patterns of the peak widths. By comparing the analysis obtained for average particle size by TEM and XRD, nanoparticles' crystal structure can be understood. The important observation is X–ray coherence length that gives an idea for an average size of the crystalline domain of NPs.

5. TYPES OF NANOPARTICLES

NPs offer a great variety of materials derived from different precursors. Based on various size, shape, morphology, physical and chemical properties, NPs are divided into well–known classes given below.

5.1. Metal NPs

Metal NPs are derived from the metal precursors and show localized surface plasmon resonance (LSPR) characteristics and unique optoelectronic properties. Noble metals (Ag, Au, Cu) and alkali metals derived NPs show strong absorption bands in the visible region of electromagnetic spectrum [25]. AgNPs have been extensively synthesized and exploited for disinfection and colorimetric sensing of heavy metal ions [26]. Their advanced optoelectronic properties make them potential candidates in wide areas of research. Presently metal NPs are being doped with many metals and nonmetal NPs to obtain enhanced results in various fields such as electrocatalysis, photocatalysis, adsorption, and filtration [2]. Nowadays, green synthesis of metal NPs is emphasized by using plant extract and microorganisms [27].

5.2. Carbon–Based Nanoparticles

Carbon–based NPs are the good replacement of precise metal NPs and are cheap, abundant, and easy to synthesize, such as carbon nanotubes (CNTs) and fullerene. Carbon nanotubes have been extensively used for the adsorption of heavy metal ions from water [28]. Graphene, doped graphene and graphene composites have shown desired electrochemical performances for electrochemical energy storage densities and catalysis in chemical reactions [29].

5.3. Semiconductor NPs

Semiconductor materials exhibit properties between metals and nonmetals and have a wide band gap, which can be tuned for a wide variety of applications [30]. Many metals, nonmetals, metal–oxides, and graphene–based compounds possess semiconductor properties and are extensively modified as photocatalysts and electrocatalysts for water remediation and energy production and storage purpose. Amongst metal oxides, TiO₂ and ZnO NPs have been extensively used due to their suitable band gaps and abundance in nature [31]. TiO₂ have shown good results as photocatalysts for water splitting to produce hydrogen [32].

5.4. Ceramics NPs

Ceramic nanoparticles are polycrystalline, amorphous, dense, inorganic porous nonmetallic solids developed by heating and annealing processes. Ceramic NPs have a wide range of applications in photocatalysis, catalysis, imaging applications and dyes' degradation [33]. Ceramic nanofiber composites have been exploited for biomedical applications, such as regenerative medicines, drug delivery and tissue engineering due to tailorable mechanical property and porous architecture [34].

5.5. Polymeric NPs

Polymeric NPs are organic-based materials commonly known as polymer nanoparticles (PNP) and generally nanocapsules or nanospheres in shape [35]. These can be doped easily and open a wide range of applications in catalysis and energy storage and production [36]. Nowadays, organic polymers are being incorporated with inorganic nanoparticles to form polymeric nanocomposites, which show enhanced performances of mechanical, thermal, catalytic, rheological, electrical, and optical properties. However, particle aggregation is still a problem to solve [37].

5.6. Lipid Based NPs

Lipid NPs are spherical, having a diameter ranging from 10 to 100 nm and contain lipid in solid core and a matrix made of soluble lipophilic molecules. The external core of these NPs is stabilized by emulsifiers [38]. Lipid NPs are biocompatible, highly stable, and large–scale production is easy with cheap raw material that makes it interesting to be used for drug delivery. These are employed to deliver biopharmaceuticals such as genes, peptides, and proteins [39, 40].

6. APPLICATIONS

Nanomaterials and nanotechnology are emerging as a potential candidate in manufacturing and production, developing novel and advanced materials. Miniaturization of devices to very small elementary units has changed modern society drastically [41, 42]. There are explosive developments in exploiting the unique properties of nanoparticles for a wide range of applications in various fields such as water treatment, catalysis, energy storage, sensors, nanomedicines, and other environmental remediations.

6.1. Water Treatment

Nanoparticles exploitation for water and wastewater treatment have gained wide attention due to large specific area, very small size, strong adsorption capacity, and high reactivity [43, 44]. Extensive research has been reported to treat heavy metal ions, bacteria, organic pollutants and inorganic anions by using various types of nanoparticles [45]. Nowadays photodegradation of dyes in water by metal oxide nanoparticles has been attracted researchers widely [46]. TiO₂ NPs have been a highly studied material for dye degradation owing to its chemical stability, non-toxicity, high photoactivity, and commercial availability [47, 48]. During photodegradation of dyes, solar light is utilized to catalyse the process and highly active species ($\bullet\text{OH}$, $\bullet\text{O}_2^{2-}$) are produced, which oxidizes dyes into CO₂ and H₂O along with anions such as nitrates, phosphates, and chlorides [49]. Sharma et al. developed g-C₃N₄-TiO₂ nanocomposites by simple chemical method and employed for photodegradation of Rhodamine B dye under irradiation of visible light. The photocatalytic activity results showed enhanced performances if compared with the individual g-C₃N₄ and TiO₂ [50]. In summary, NPs have emerged as a potential tool for wastewater treatment, and it is important to investigate the technologies for large scale treatment and real water problems.

6.2. Catalysis

Catalysis is one of the major important applications of the NPs exhibited by materials like iron, aluminium, clays, titanium oxide and silica. Nanocatalysis has been emerging as a promising field of science owing to its high selectivity, sensitivity, and productivity [51]. This extraordinary catalytic high activity is attributed to the high surface-to-volume ratio, electronic effect, quantum size effect, and surface geometric effect [52]. Heterogeneous catalysts are environmentally friendly because the suspended metal nanoparticles in water can be separated easily and recovered very fast with high recyclability [53, 54]. The nanoparticles' catalytic properties are highly dependent on the size of the particles and tend to alter drastically with changes in size.

The use of catalyst is actually a green technology as a lower temperature is required for any transformation, and reagent-based waste is also reduced with high selectivity of the reaction. Unwanted side reactions and various useless products are obtained without catalyst. Many important products such as polymers, fibres, fine chemicals, medicines, fuels, lubricants and paints are not feasible in the absence of catalyst. Therefore, manufacturing protocols can be made more sustainable, green and economic by exploiting catalyst. Recently, carbon nanotubes tubes (CNTs) have attracted wide attention for partial oxidation of fuel cells, methane, and synthetic ammonia as photocatalysts [55].

6.3. Energy

Tremendous exploitation of fossil fuels as an energy resources has impacted the environment adversely and attracted researchers to search for easily available and low-cost renewable alternate. NPs have become a suitable candidate for this purpose due to their large surface area, catalytic nature, and optical properties. NPs have been exploited for generation of energy by electrochemical water splitting and photoelectrochemical (PEC) as a photocatalyst [56–58].

NPs have also shown remarkable results for energy generation by solar cells, reduction of CO₂ to fuel precursors, and piezoelectric generators [59–62]. Jiang et al. developed graphene nanosheets dispersed with Ni single atoms for efficient CO₂ reduction by electrocatalysis [63]. Owing to the good adsorbent property, NPs reserve energy by storage applications and have been investigated for H₂ and methane storage [64]. Recently, the conversion of mechanical energy into electrical energy by using nanogenerators is used to generate energy. Ding et al. exploited Formamidinium lead halide perovskite nanoparticles (FAPbBr₃ NPs) for piezoelectric applications and excellent results were obtained when combined with poly (vinylidene fluoride) (PVDF) polymer (FAPbBr₃ NPs @ PVDF) to form composite based piezoelectric. The resultant nanocomposite showed the outstanding output with a voltage of 30 V and current density of 6.2 $\mu\text{A cm}^{-2}$ for devices based on halide perovskite material [65].

6.4. Sensors

Nanomaterials have shown their remarkable applicability in the area of electrochemical sensing devices for environmental remediation, food safety, and medical diagnostics [66]. Electrochemical determination of some pollutants such as hydrazine(N₂H₄), ascorbic acid (AA), bisphenol A(BPA), malachite green (MG), nitrite (NO₂⁻), sulphite (SO₃²⁻), caffeine, etc. have been reported with good performances [67]. Recently, biosensors have been developed with high selectivity and sensitivity for sensing glucose, urea, cholesterol, etc. [68]. Carbon nanotubes (CNTs) have been successfully employed for the development of molecular detection such as

electrochemical detectors, gas sensors, small molecular detection, and chromatographic applications [69] [70]. Macroelectrodes are being modified by using nanomaterials and nanoparticles, which reduces limit of detection (LOD) and enhances selectivity and sensitivity of measurements [71]. In this context, Govindhan et al. developed hierarchical three-dimensional nickel and cobalt oxide nanomaterial to detect H₂ at high temperature with excellent sensitivity, selectivity and stability for many other gaseous mixtures also [72].

6.5. Nanomedicines

Revolutionary change in lifestyle, eating habits and increasing pollution have resulted in various types of diseases that are drug resistant, and the present medical aid cannot cure these diseases in all ways. Despite rapid technological advancements, the development of biocompatible, active, economical, and innovative drug substances, and the product is required [73]. Nowadays, nanomedicine has been extensively exploited in the pharmaceutical market [74]. Nanomedicine includes the use of engineered nanodevices and nanostructures for monitoring, repairing, constructing, and controlling biological systems of humans at the molecular level [75]. It consists of an exploitation of nanotechnology to diagnose, prevent and treat disease with understanding the molecular mechanism of a specific disease. With advancement, biogenic nanomedicine derived from natural sources such as plants and microorganisms have shown potential therapeutic use in the treatment of microbial infection, cancer, inflammation, etc. [76]. Nanomedicines exhibit unique chemicophysical properties (large surface area-to-mass ratio, very small size, high reactivity) and size resemblance to viruses, proteins, and bacteria, which make them suitable agents to replace conventional diagnosis and therapy methods. Nanomaterials used in nanomedicines are organic substances (polymers, dendrimers, liposomes, solid lipid nanoparticles), inorganic materials (metals, metal oxides, quantum dots, carbon nanotubes) [77–79]. In addition to this, hybrids of metals (Au, Ag, Pt) and metal oxides (Fe₃O₄) have shown remarkable progress for a variety of applications such as gene delivery, theragnostic, cell sorting, biosensing, catalysis, and bioseparation [80]. By virtue of passive intake, nanoparticles highly permeable and their retention is also high, due to which they stay more in cancer cells than in normal cells [81].

Metal nanoparticles (Ag, Au) have been extensively explored for their applications in medicine and biology by researchers owing to their controlled optical, geometrical, and surface chemical properties [82]. Treatment of liver cancer via magnetic fluid hyperthermia (MFH) has been investigated by using hydrophilic and surface functionalized superparamagnetic iron oxide nanoparticles (SPIOs) as nanomedicines [83].

CONCLUSION

Nanomaterials have found applications in almost all the fields in the present era, and this chapter represented a few of them in brief. It has been observed that NMs exhibit some specific properties of high surface-to-volume ratio, reactivity, excellent optical and magnetic properties, which make them a potential candidate to be exploited for applications in the field of nanomedicine, sensors, catalysis, environment, etc. Although there are lots of advantages of NMs, their unique characteristics are of big concern for analysing the toxicological and ecotoxicological properties.

ACKNOWLEDGMENTS

Dinesh Kumar is thankful to DST, New Delhi, for the financial support offered to this work (sanctioned vide project Sanction Order F. No. DST/TM/WTI/WIC/2K17/124. Meena Nemiwal is thankful to MNIT, Jaipur for providing research facility.

REFERENCES

- [1] Elahi, N., Kamali, M. & Baghersad, M. H. (2018). Recent biomedical applications of gold nanoparticles: A review. *Talanta*, 184, 537–556.
- [2] Khan, I., Saeed, K. & Khan, I. (2019). Nanoparticles: Properties, applications and toxicities. *Arabian J. of Chem.*, 12, 908–931.
- [3] Ealias, A. M. & Saravanakumar, M. P. (2017). A review on the classification, characterisation, synthesis of nanoparticles and their application. *IOP Conference Series: Materials Science and Engineering*, 263, 32019.
- [4] Ganesan, P. & Narayanasamy, D. (2017). Lipid nanoparticles: Different preparation techniques, characterization, hurdles, and strategies for the production of solid lipid nanoparticles and nanostructured lipid carriers for oral drug delivery. *Sust. Chem. Pharm.*, 6, 37–56.
- [5] Fahlepy, M. R., Wahyuni, Y., Andhika, M., Tiwow, V. A. & Subaer. (2019). Synthesis and characterization of nanoparticle hematite (A-Fe₂O₃) minerals from natural iron sand using co-precipitation method and its potential applications as extrinsic semiconductor materials type-n. *Mat. Sci. Forum*, 967, 259–266.
- [6] Basiuk, V. A. & Basiuk, E. V. (2015). Green processes for nanotechnology. *Inorg. to bioins. nanomat.*, 1–446.
- [7] Zhu, X., Pathakoti, K. & Hwang, H. M. (2019). Green synthesis of titanium dioxide and zinc oxide nanoparticles and their usage for antimicrobial applications and environmental remediation. *Green Synt. Charact. and App. of Nanopart.*, 223–263.

- [8] Yaya, A., Agyei–Tuffour, B., Dodoo–Arhin, D., Nyankson, E., Annan, E., Konadu, D. S. & Ewels, C. P. (2012). Layered nanomaterials– A review. *Global J.f Engg., Design and Tech.*, 2, 32–41.
- [9] Guan, G., Zhang, S., Liu, S., Cai, Y., Low, M., Teng, C. P. & Han, M. Y. (2015). Protein induces layer–by–layer exfoliation of transition metal dichalcogenides. *J. the Ameri. Chem. Soci.*, 137, 6152–6155.
- [10] Gerasopoulos, K., Pomerantseva, E., McCarthy, M., Brown, A., Wang, C., Culver, J. & Ghodssi, R. (2012). Hierarchical three–dimensional microbattery electrodes combining bottom–up self–assembly and top–down micromachining. *ACS Nano*, 6, 6422–6432.
- [11] Dowling, A., Cliff, R., Grobert, N., Hutton, D., Oliver, R., O’neill, O., et al. (2004). Nanoscience and nanotechnologies: opportunities and uncertainties. *London: Royal Soc. and Royal Acad. Engg.*, 46, 618–618.
- [12] Dhingra, R., Naidu, S., Upreti, G. & Sawhney, R. (2010). Sustainable nanotechnology: Through green methods and life–cycle thinking. *Sustainability*, 2, 3323–3338.
- [13] Cai, J., Ruffieux, P., Jaafar, R., Bieri, M., Braun, T., Blankenburg, S. & Fasel, R. (2010). Atomically precise bottom–up fabrication of graphene nanoribbons. *Nature*, 466, 470–473.
- [14] Hussain, I., Singh, N. B., Singh, A., Singh, H. & Singh, S. C. (2016). Green synthesis of nanoparticles and its potential application. *Biotech. Lett.*, 38, 545–560.
- [15] Lamouri, R., Mounkachi, O., Salmani, E., Hamedoun, M., Benyoussef, A. & Ez–Zahraouy, H. (2020). Size effect on the magnetic properties of CoFe₂O₄ nanoparticles: A Monte Carlo study. *Ceram. Int.*, 46, 8092–8096.
- [16] Shrimali, V. G., Gadani, K., Rajyaguru, B., Gohil, H., Chudasama, D. K., Dhruv, D., et al. (2020). Size dependent dielectric, magnetic, transport and magnetodielectric properties of BiFe_{0.98}Co_{0.02}O₃ nanoparticles. *J. of Alloys and Comp.*, 817, 152685.
- [17] Lakshmi prasanna, H. R., Jagadeesha Angadi, V., Rajesh Babu, B., Pasha, M., Manjunatha, K. & Matteppanavar, S. (2019). Effect of Pr³⁺–doping on the structural, elastic and magnetic properties of Mn–Zn ferrite nanoparticles prepared by solution combustion synthesis method. *Chem. Data Coll.*, 24, 100273.
- [18] Zhang, W., Sun, A., Pan, X., Han, Y., Zhao, X., Yu, L. & Suo, N. (2019). Structural, morphological and magnetic properties of Ni–Co ferrites by the Mn²⁺ ions substitution. *J. Mat. Sci. Mat. in Elect.*, 30, 18729–18743.
- [19] Rahman, M. A., Radhakrishnan, R. & Gopalakrishnan, R. (2018). Structural, optical, magnetic and antibacterial properties of Nd doped NiO nanoparticles prepared by co–precipitation method. *J. Alloys and Comp.*, 742, 421–429.
- [20] Pauly, N., Yubero, F., García–García, F. J. & Tougaard, S. (2016). Quantitative analysis of Ni 2p photoemission in NiO and Ni diluted in a SiO₂ matrix. *Surface Sci.*, 644, 46–52.

- [21] Mikhailov, M. M., Yuryev, S. A. & Lovitskiy, A. A. (2018). On the correlation between diffuse reflectance spectra and particle size of BaSO₄ powder under heating and modifying with SiO₂ nanoparticles. *Optical Mat.*, 85, 226–229.
- [22] Nomai, J. & Schlarb, A. K. (2019). Effects of nanoparticle size and concentration on optical, toughness, and thermal properties of polycarbonate. *J. Appl. Poly. Sci.*, 136, 47634.
- [23] Jeon, H. & Lee, K. (2019). Effect of gold nanoparticle morphology on thermal properties of polyimide nanocomposite films. *Coll. and Surf. A: Physicochem. and Engg. Aspects*, 579, 123651.
- [24] Bui, T. M. A., Nguyen, T. V., Nguyen, T. M., Hoang, T. H., Nguyen, T. T. H., Lai, T. H. & Nguyen–Tri, P. (2020). Investigation of crosslinking, mechanical properties and weathering stability of acrylic polyurethane coating reinforced by SiO₂ nanoparticles issued from rice husk ash. *Mat. Chem. Phys.*, 241, 122445.
- [25] Chen, L., Li, J. & Chen, L. (2014). Colorimetric detection of mercury species based on functionalized gold nanoparticles. *ACS Appl. Mat. Inter.*, 6, 15897–15904.
- [26] Maiti, S., Barman, G. & Konar Laha, J. (2016). Detection of heavy metals (Cu⁺², Hg⁺²) by biosynthesized silver nanoparticles. *Appl. Nanosci.*, 6, 529–538.
- [27] Rane, A. V., Kanny, K., Abitha, V. K. & Thomas, S. (2018). Methods for Synthesis of Nanoparticles and Fabrication of Nanocomposites. *Synthesis of Inorganic Nanomaterials*, edited by Sneha Mohan Bhagyaraj, Oluwafemi, and Sabu Thomas, 121–139, Elsevier Ltd.
- [28] Xu, J., Cao, Z., Zhang, Y., Yuan, Z., Lou, Z., Xu, X. & Wang, X. (2018). A review of functionalized carbon nanotubes and graphene for heavy metal adsorption from water: Preparation, application, and mechanism. *Chemosphere*, 195, 351–364.
- [29] Li, Q., Mahmood, N., Zhu, J., Hou, Y. & Sun, S. (2014). Graphene and its composites with nanoparticles for electrochemical energy applications. *Nano Today*, 9, 668–683.
- [30] Morales–García, Á., Macià Escatllar, A., Illas, F. & Bromley, S. T. (2019). Understanding the interplay between size, morphology and energy gap in photoactive TiO₂ nanoparticles. *Nanoscale*, 11, 9032–9041.
- [31] Guo, Q., Zhou, C., Ma, Z. & Yang, X. (2019). Fundamentals of TiO₂ Photocatalysis: Concepts, Mechanisms, and Challenges. *Adv. Mat.*, 31, 1901997.
- [32] Ni, M., Leung, M. K. H., Leung, D. Y. C. & Sumathy, K. (2007). A review and recent developments in photocatalytic water–splitting using TiO₂ for hydrogen production. *Renew. and Sust.e Energy Rev.*, 11, 401–425.
- [33] Thomas, S., Harshita, B. S. P., Mishra, P. & Talegaonkar, S. (2015). Ceramic nanoparticles: Fabrication methods and applications in drug delivery. *Current Pharm. Design*, 21, 6165–6188.
- [34] Lakshmi Priya, M., Rana, D. & Ramalingam, M. (2017). Ceramic nanofiber composites. *Nanofiber Composites for Biomedical Applications*, 33–54, edited by

- Murugan Ramalingam, Seeram Ramakrishna, Nanofiber Composites for Biomedical Applications, Woodhead Publishing.
- [35] Mansha, M., Khan, I., Ullah, N. & Qurashi, A. (2017). Synthesis, characterization and visible–light–driven photoelectrochemical hydrogen evolution reaction of carbazole–containing conjugated polymers. *Int. J. Hyd. Energy*, 42, 10952–10961.
- [36] Schwarz, D., Acharja, A., Ichangi, A., Lyu, P., Opanasenko, M. V., Goßler, F. R. & Bojdys, M. J. (2018). Fluorescent sulphur– and nitrogen–containing porous polymers with tuneable donor–acceptor domains for light–driven hydrogen evolution. *Chemistry – A Eur. J.*, 24, 11916–11921.
- [37] Kango, S., Kalia, S., Celli, A., Njuguna, J., Habibi, Y. & Kumar, R. (2013). Surface modification of inorganic nanoparticles for development of organic–inorganic nanocomposites – A review. *Prog. in Poly. Sci.*, 38, 1232–1261.
- [38] Rawat, M. K., Jain, A. & Singh, S. (2011). Studies on binary lipid matrix based solid lipid nanoparticles of repaglinide: *In vitro* and *in vivo* evaluation. *J. of Pharmac. Sci.*, 100, 2366–2378.
- [39] Lu, Y., Qi, J. & Wu, W. (2018). Lipid nanoparticles: *In vitro* and *in vivo* approaches in drug delivery and targeting. *Drug Targ. and Stimuli Sens. ve Drug Del. Sys.*, 749–783.
- [40] Kumar, R. & Sinha, V. R. (2016). Solid lipid nanoparticle: an efficient carrier for improved ocular permeation of voriconazole. *Drug Devel. and Indust. Pharmacy*, 42, 1956–1967.
- [41] Abdullaeva, Z. (2017). Nanomaterials in daily life: Compounds, synthesis, processing and commercialization. *Springer Cham.*, 1–149.
- [42] Gupta, R. & Xie, H. (2018). Nanoparticles in daily life: Applications, toxicity and regulations. *J. Env. Pathology, Tox. and Oncology*, 37, 209–230.
- [43] Zhang, Y., Wu, B., Xu, H., Liu, H., Wang, M., He, Y. & Pan, B. (2016). Nanomaterials–enabled water and wastewater treatment. *Nano Impac*, 3, 22–39.
- [44] Prathna, T. C., Sharma, S. K. & Kennedy, M. (2018). Nanoparticles in household level water treatment: An overview. *Sep. and Purif. Tech.*, 199, 260–270.
- [45] Xiong, C., Wang, W., Tan, F., Luo, F., Chen, J. & Qiao, X. (2015). Investigation on the efficiency and mechanism of Cd(II) and Pb(II) removal from aqueous solutions using MgO nanoparticles. *J. of Haz. Mat.*, 299, 664–674.
- [46] Abbas, K. K. & Al–Ghaban, A. M. H. A. (2019). Enhanced solar light photoreduction of innovative TiO₂ nanospherical shell by reduced graphene oxide for removal silver ions from aqueous media. *J. of Env. Chem. Engg.*, 7, 103168.
- [47] Dariani, R. S., Esmaeili, A., Mortezaali, A. & Dehghanpour, S. (2016). Photocatalytic reaction and degradation of methylene blue on TiO₂ nano–sized particles. *Optik*, 127, 7143–7154.
- [48] Azeez, F., Al–Hetlani, E., Arafa, M., Abdelmonem, Y., Nazeer, A. A., Amin, M. O. & Madkour, M. (2018). The effect of surface charge on photocatalytic degradation of methylene blue dye using chargeable titania nanoparticles. *Scient. Reports*, 8, 1–9.

- [49] Kheirabadi, M., Samadi, M., Asadian, E., Zhou, Y., Dong, C., Zhang, J. & Moshfegh, A. Z. (2019). Well-designed Ag/ZnO/3D graphene structure for dye removal: Adsorption, photocatalysis and physical separation capabilities. *J. of Coll. and Int. Sci.*, 537, 66–78.
- [50] Sharma, M., Vaidya, S. & Ganguli, A. K. (2017). Enhanced photocatalytic activity of g-C₃N₄-TiO₂ nanocomposites for degradation of Rhodamine B dye. *J. of Photochem. and Photobiol. A: Chemistry*, 335, 287–293.
- [51] Gauchot, V., Sutherland, D. R. & Lee, A. L. (2017). Dual gold and photoredox catalysed C–H activation of arenes for aryl–aryl cross couplings. *Chem. Sci.*, 8, 2885–2889.
- [52] Ojha, K., Saha, S., Dagar, P. & Ganguli, A. K. (2018). Nanocatalysts for hydrogen evolution reactions. *Phys. Chem. Chem. Phys.*, 20, 6777–6799.
- [53] Zhao, J. & Jin, R. (2018). Heterogeneous catalysis by gold and gold-based bimetal nanoclusters. *Nano Today*, 18, 86–102.
- [54] Karakalos, S., Xu, Y., Cheenicode Kabeer, F., Chen, W., Rodríguez-Reyes, J. C. F., Tkatchenko, A. & Friend, C. M. (2016). Noncovalent bonding controls selectivity in heterogeneous catalysis: Coupling reactions on gold. *J.I of the Amer. Chem. Society*, 138, 15243–15250.
- [55] Wang, W., Lv, F., Lei, B., Wan, S., Luo, M. & Guo, S. (2016). Tuning nanowires and nanotubes for efficient fuel-cell electrocatalysis. *Advanced Materials*, 28, 10117–10141.
- [56] Avasare, V., Zhang, Z., Avasare, D., Khan, I. & Qurashi, A. (2015). Room-temperature synthesis of TiO₂ nanospheres and their solar driven photoelectrochemical hydrogen production. *Int. J.I of Energy Res.*, 39, 1714–1719.
- [57] Vadakkekara, R., Illathvalappil, R. & Kurungot, S. (2018). Layered TiO₂ nanosheet-supported NiCo₂O₄ nanoparticles as bifunctional electrocatalyst for overall water splitting. *Chem Electro Chem*, 5, 4000–4007.
- [58] Wang, J., Wang, Z. & Zhu, Z. (2017). Synergetic effect of Ni(OH)₂ cocatalyst and CNT for high hydrogen generation on CdS quantum dot sensitized TiO₂ photocatalyst. *Appl. Catalysis B: Env.*, 204, 577–583.
- [59] Back, S., Yeom, M. S. & Jung, Y. (2015). Active sites of Au and Ag nanoparticle catalysts for CO₂ electroreduction to CO. *ACS Catalysis*, 5, 5089–5096.
- [60] Zhao, S., Jin, R. & Jin, R. (2018). Opportunities and challenges in CO₂ reduction by gold- and silver-based electrocatalysts: From bulk metals to nanoparticles and atomically precise nanoclusters. *ACS Energy Lett.*, 3, 452–462.
- [61] Pohanka, M. (2018). Overview of piezoelectric biosensors, immunosensors and DNA sensors and their applications. *Materials*, 11, 448.
- [62] Kumari, G., Zhang, X., Devasia, D., Heo, J. & Jain, P. K. (2018). Watching visible light-driven CO₂ reduction on a plasmonic nanoparticle catalyst. *ACS Nano.*, 12, 8330–8340.
- [63] Pohanka, M. (2018). Overview of piezoelectric biosensors, immunosensors and DNA sensors and their applications. *Materials*, 11, 448.

- [64] Jiang, K., Siahrostami, S., Zheng, T., Hu, Y., Hwang, S., Stavitski, E. & Wang, H. (2018). Isolated Ni single atoms in graphene nanosheets for high-performance CO₂ reduction. *Energy and Env. Sci.*, 11, 893–903.
- [65] Pyle, D. S., Gray, E. M. A. & Webb, C. J. (2016). Hydrogen storage in carbon nanostructures via spillover. *International Journal of Hydrogen Energy*, 41, 19098–19113.
- [66] Ding, R., Zhang, X., Chen, G., Wang, H., Kishor, R., Xiao, J. & Zheng, Y. (2017). High-performance piezoelectric nanogenerators composed of formamidinium lead halide perovskite nanoparticles and poly(vinylidene fluoride). *Nano Energy*, 37, 126–135.
- [67] Stephen Inbaraj, B. & Chen, B. H. (2016). Nanomaterial-based sensors for detection of foodborne bacterial pathogens and toxins as well as pork adulteration in meat products. *J. of Food and Drug Analy.*, 24, 15–28.
- [68] He, X., Deng, H. & Hwang, H. min. (2019). The current application of nanotechnology in food and agriculture. *J. of Food and Drug Analys.*, 27, 1–21.
- [69] Gualandi, I., Vlamidis, Y., Mazzei, L., Musella, E., Giorgetti, M., Christian, M. & Tonelli, D. (2019). Ni/Al Layered double hydroxide and carbon nanomaterial composites for glucose sensing. *ACS Applied Nano Mat.*, 2, 143–155.
- [70] Maity, D., Minitha, C. R. & Rajendra, R. K. (2019). Glucose oxidase immobilized amine terminated multiwall carbon nanotubes/reduced graphene oxide/polyaniline/gold nanoparticles modified screen-printed carbon electrode for highly sensitive amperometric glucose detection. *Mat. Sci. and Engg. C*, 105, 110075.
- [71] Mittal, M. & Kumar, A. (2014). Carbon nanotube (CNT) gas sensors for emissions from fossil fuel burning. *Sensors Actuators, B Chem.*, 203, 349–362.
- [72] Ahmad, R., Majhi, S. M., Zhang, X., Swager, T. M. & Salama, K. N. (2019). Recent progress and perspectives of gas sensors based on vertically oriented ZnO nanomaterials. *Adv. in Colloid and Int. Sci.*, 270, 1–27.
- [73] Govindhan, M., Sidhureddy, B. & Chen, A. (2018). High-temperature hydrogen gas sensor based on three-dimensional hierarchical-nanostructured nickel-cobalt oxide. *ACS Appl. Nano Mat.*, 1, 6005–6014.
- [74] Bhardwaj, V. & Nikkhah-Moshaie, R. (2017). Nanomedicine. *Advances in Personalized Nanotherapeutics*, edited by AjeetKaushik, Rahul Dev and JayantMadhavan Nair, 1–10, Springer International Publishing AG.
- [75] Soares, S., Sousa, J., Pais, A. & Vitorino, C. (2018). Nanomedicine: Principles, properties, and regulatory issues. *Front. Chem.*, 6, 360.
- [76] Morrow Jr, K. J., Bawa, R. & Wei, C. (2007). Recent advances in basic and clinical nanomedicine. *Med. Clinics of North America*, 91, 805–843.
- [77] Watkins, R., Wu, L., Zhang, C., Davis, R. M. & Xu, B. (2015). Natural product-based nanomedicine: recent advances and issues. *Int. J. of Nanomed.*, 10, 6055.
- [78] Alshehri, R., Ilyas, A. M., Hasan, A., Arnaout, A., Ahmed, F. & Memic, A. (2016). Carbon nanotubes in biomedical applications: factors, mechanisms, and remedies of toxicity: miniperspective. *J. of Med. Chem.*, 59, 8149–8167.

- [79] Dias, A. P., da Silva Santos, S., da Silva, J. V., Parise-Filho, R., Igne Ferreira, E., Seoud, O. El & Giarolla, J. (2020). Dendrimers in the context of nanomedicine. *Int. J. Pharm.*, 573, 118814.
- [80] Xue, Y. (2017). Carbon nanotubes for biomedical applications. *Micro and Nano Technologies*, edited by Huisheng Peng, Qingwen Li, Tao Chen, Industrial Applications of Carbon Nanotubes, 323-346, Elsevier.
- [81] Leung, K. C. F. & Xuan, S. (2016). Noble metal–iron oxide hybrid nanomaterials: Emerging applications. *Chemical Recor*, 16, 458–472.
- [82] Tammina, S. K., Mandal, B. K., Ranjan, S. & Dasgupta, N. (2017). Cytotoxicity study of Piper nigrum seed mediated synthesized SnO₂ nanoparticles towards colorectal (HCT116) and lung cancer (A549) cell lines. *J. of Photochem. and Photobiol. B: Biology*, 166, 158–168.
- [83] Dykman, L. & Khlebtsov, N. (2012). Gold nanoparticles in biomedical applications: Recent advances and perspectives. *Chem. Soci. Rev.*, 41, 2256–2282.
- [84] Kandasamy, G., Sudame, A., Luthra, T., Saini, K. & Maity, D. (2018). Functionalized hydrophilic superparamagnetic iron oxide nanoparticles for magnetic fluid hyperthermia application in liver cancer treatment. *ACS Omega*, 3, 3991–4005.

Complimentary Contributor Copy

Chapter 3

ROLE OF NANOMATERIAL IN THE HEALTH SECTOR

***Devendra Singh¹, Deepmala Sharma²
and Vishnu Agarwal^{1,*}***

¹Department of Biotechnology,

Motilal Nehru National Institute of Technology Allahabad, INDIA

²Department of Mathematics, National Institute of Technology Raipur, INDIA

ABSTRACT

Nanomaterials are used for many years, but in recent times nanomaterials is emerged as a big hope for low cost and better healthcare. Nanomaterials are currently used in different science branches, particularly in healthcare, for the prognosis and diagnosis of diseases and their related symptoms. They have unique electrical, chemical, mechanical behaviors and are widely used in pharmaceuticals for their sensitivity and precision. The nanomaterials which are used in health care diagnostics are either inorganic, hybrid, or organic nanomaterials. Inorganic nanomaterials, including quantum dots, metal oxides, and metallic nanoparticles, are commonly used in biosensor designing.

On the other hand, because of their unique characteristic hybrid nanomaterials are used for imaging purposes, and organic nanomaterials such as liposomes, carbon nanotubes, dendrimers, nanocrystals, and micelles nanoparticles are utilized as therapeutic agents. Other nanomaterial applications include remediation, environmental monitoring, cosmetics, construction of versatile devices, and medicine. The role of nanomaterials in the healthcare sector has been described in this chapter.

Keywords: nanomaterials, healthcare, sensitivity, diagnostics, cosmetics, medicines

* Corresponding Author's Email: vishnua@mnnit.ac.in.

1. INTRODUCTION

In recent times, nanotechnology-based applications are being continuously and widely used in the healthcare sector. The health care sector basically deals with three major constituents, including diagnostics, drugs, and medical devices for the patients to prevent mortality and morbidity. Nowadays, various nanomaterials with new potentials have been developed, discovered, and used in modern healthcare, focusing on diagnostics, health care devices, and therapeutics [1].

Due to their unusual behaviors (physical, optical, mechanical, chemical, and electrical) and nature, these nanomaterials are widely used in drugs and therapeutics purposes because of their higher sensitivity, preciseness, and sharp visible imaging of diseased cells. There are numerous nanoparticle-based health care devices, therapeutic and diagnostic kits that are developed and available in the market for the treatment of various diseases such as diabetes, asthma, cancer, allergy, and many more infections [2, 3]. Apart from its numerous advantages and application in the healthcare field, a rise in the voice was noted related to its possible toxicity based on different *in vitro* and *in vivo* experimental studies outcomes. In several research *in vivo* adverse effects like granulomas and inflammation in animals are reported, but till now, no proper research claiming toxicity of nanomaterials on a human being is reported [4,5]. Due to the growing human concerns, researchers have started focusing on nanomaterials specificity, efficacy with the least toxicity. At present, due to its higher application of these nanomaterials in drugs, health care devices, therapeutic and diagnostic kits, the discovery and development of new nanomaterials are kept increasing at a rapid pace [6].

In summary, nanomaterial has a wide application in the healthcare sector. Due to its expanding application, researchers are continuously developing and discovering new potential nanomaterials; in this chapter, an overview of nanomaterial's role in the healthcare sector emphasizes diagnostics kits, therapeutics, and medical devices.

2. NANOMATERIALS AND IT'S CHARACTERISTIC

Nanomaterials are nano-sized materials that may be found in nature (incidental) or human-engineered. Any nano-sized material within the range of 0–200 nm will be considered as a nanomaterial and can be used in the form of particles, tubes, fibers, or rods [7]. Due to their enormous potential, these nanomaterials are widely used in the healthcare sector and directly or indirectly interact with human cells. It has been reported that the property (chemical and physical) of nanomaterials differs from bulk material at nanoscale, and it was observed that an increase in ability to cross the tissue barrier would lead to new drug delivery and targeting systems [8]. Because of the difference in nanomaterials' physic-chemical properties from bulk materials, these nanomaterials require more attention for risk assessment before they are being used in healthcare devices [9].

Theoretically, these nanoparticles can be directly or indirectly used in the healthcare sector for the purpose of identifying and destroy even a single malignant cell, which will further take us nearer to the ultimate disease treatment and prevention. They are already effectively used in disease prognosis and diagnosis [10]. Another important factor that causes significant differences in nanomaterials characteristics is the quantum effect (because of the quantum confinement of delocalized electrons). As on the surface, the number of atoms of these nanoparticles is more than the bulk; nanoparticles show less binding energy, hence showing a lower melting point. The nanoparticle shape will play a vital role in deciding its properties [11, 12].

Synthetic nanostructures (artificial atoms) like quantum dots will depend upon the exploitation of quantum effects seen in nanoparticles. They are owing multiple unpaired electron spins from 100s of atoms and possess magnetic moments, showing their highest performance at 10 to 29 nm sizes due to super magnetism, making them suitable for contrast agents in MRI (magnetic resonance imaging) [13, 14]. Because of these features, nanomaterials are classified into several categories. On a chemical constitution basis, these nanomaterials can be mainly classified into organic nanomaterials (mainly consist of polymeric nanomaterials), inorganic nanomaterials (made up of constituents such as SiO₂, Au, Ag), and carbon allotrope-based nanomaterials (consisting of carbon atoms only). These nanoscale agents may provide more effective or more convenient routes of administration, extend the product life cycle, and ultimately reduce healthcare costs (Figure 1) [15].

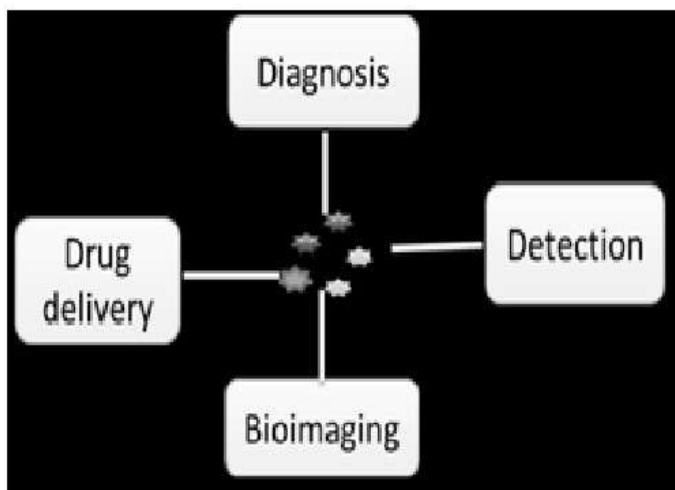


Figure 1. Role of nanomaterials in healthcare.

2.1. Organic Nanomaterials

It was found that inorganic nanoparticles generally have safety issues, such as toxicity due to heavy metal, and don't have quick clearance from the human body. Because of such concerns, organic systems are usually preferred. PNPs (polymer

nanoparticles) are commonly used for the purpose of cancer therapy and diagnostics because of their excellent photostability, biocompatibility, high extinction coefficients, and fluorescence intensity [16-18]. Through EPR (enhanced permeability and retention) effect, these PNPs can easily accumulate in the tumor region, cancer-targeting moieties such as aptamers will be altered by physical or chemical interaction onto the surface of nanoparticles, which gives functionalized PNPs having higher sensitivity, specificity, and selectivity for cancer therapy and diagnosis [19-24]. Still, some more *in vivo* studies will be performed to systematically investigate the effectiveness and safety of these novel PNPs before being used for clinical application.

2.2. Inorganic Nanomaterials

The inorganic nanomaterials possess some unique features, such as SPR (surface plasmon resonance) and GNPs (gold NPs) are generally selected to enhance the optical imaging on the basis of their scattering, fluorescence, absorption [25]. The stability of gold NPs covalently bond with thiolated ligands allows direct chemical modifications on their surfaces [26]. For stabilizing GNPs, ligands are specifically chosen for drug release and encapsulation to tissues [27, 28]. Still, in clinical application safety of GNPs yet remains doubtful, and more *in vivo* long-term toxicity information is required.

QDs (Quantum dots) have diameters <10 nm nanocrystals, which are semiconductor material and exhibit optical features such as luminescence and absorption [29]. Usually, quantum dots of numerous ingredients or shapes are excited by a single light source, which separately emits various wide range colors with minor spectral overlap, making them appropriate for multiple imaging processes [30, 31]. Due to their conductive properties, these quantum dots generate electrical waves, and patterns used in humans as an indicator activity. They are developed for disease screening tests and optics technology [32]. It can be conjugated with proteins, DNA, antibodies (a recognition molecule). Flexibility in emission peak and surface chemistry of quantum dots increases their application as nanocarriers or optical probes for the purpose of therapy, imaging, diagnostics, and drug [33]. Due to the toxicity of QD in the human body, silicon QD was preferred over cadmium QD. On the other side, due to its antimicrobial activity, silver nanoparticles have now been used in a variety of surgical devices, masks, and medical kits. There will be great benefits of using nanoparticles to suffer from CNS (central nervous system) diseases [34].

3. NANOMATERIALS AND DRUGS

In recent years, emphasis on nanomedicine formulations utilization opens new possibilities for diseased diagnosis and treatment. Now, these nanoparticles are specifically designed with surface characteristics and optimal size for the purpose of

improving the biodistribution of cancer drugs in the bloodstream [35]. Doped nanomaterial will have emerged as a promising therapy due to its electrochemical and optical properties, low resistance, high specific surface area, and high catalytic activity [36]. These doped nanomaterials will help in delivering the drugs to the specifically targeted HIV or cancer cells, alleviate allergy symptoms [37].

Nanomaterials are available in different shapes, sizes, and materials due to which it causes different effects on different systems of the body [38]. Some common nanomaterial use effects include the higher production of ROS (reactive oxygen species) and inflammatory responses [37]. For the purpose of increase the drug-tissue bioavailability, nanometer-sized carrier materials are being used [39]. For the first time in the year 1995, a nano-sized therapeutic formulation (Doxil) came into the market. This Doxil was introduced in the market for the purpose of the effective treatment for recurrent ovarian cancer and metastatic breast cancer [38, 40]. Other nanomaterial-based therapeutic formulation includes BIND-014, which accumulates only in tumor cells and not in healthy cells [41]. In the coming time, nanomedicine will have a huge impact on the health sector and personalized medicine development [42]. On the other side, there will be increasing concerns related to the potential toxicity effect on humans' health, which arises due to the unique chemical and physical properties of nanoparticles [38]. Due to their long half-life, crystalline structure, and metallic nature, it will make it possible that some of the nanoparticles will not be cleared from the human body and resides for some years, which may result in toxicity [38]. At present, efforts are made to make a balance between the toxicity and efficacy of therapeutic interventions by designing efficacious and safer nanomedicine [39].

4. NANOMATERIALS IN DIAGNOSIS AND IMAGING

In recent years, the nanomaterials properties were assessed. It was found that it has different advantages such as long fluorescence lifetime, deep and noninvasive tissue penetration, superior photostability, high signal to background ratio, and sharp visible emission lines in the bioimaging field.

These nanomaterials' advantages indicate that nanomaterials have great potential and can be used effectively in bioimaging and early-stage diagnosis of infection. Some imaging techniques where nanomaterials can be used are magnetic resonance imaging (MRI), optical imaging (OI), radionuclide imaging (RI), and ultrasound imaging (UI) are mention in Figure 2 [43].

Researchers are trying to develop a diagnostic sensor for detecting 3 to 5 cancer cells in a 1 ml blood sample. The diagnostic sensor uses carbon nanoparticles allotrope (graphene oxide) to which an antibody (with fluorescent markers) is attached [44]. So when attached to the cancer cells, the fluorescence confirms the cancer cell's presence. For the early detection of brain cancer, NMR technology, and magnetic nanoparticles are used. These magnetic nanoparticles are attached to the microvesicles (develop in brain cancer cells) in the bloodstream. Then they can be

easily detected in NMR imaging. This method can be easily used for brain cancer early detection.

Different studies have started replacing conventional gold beads with super-paramagnetic nanoparticles [45]. For Endoscopic imaging, a noncontact, fiber-optic-based surface-enhanced Raman spectroscopy device was developed. This developed device was inserted via a clinical endoscope and will provide real-time, multiplexed functional and structural information. By using this endoscope, endoscopists can be able to identify flat lesions that are usually missed and can also distinguish between the precancerous and normal tissues quickly [46, 47]. They have been shown to noninvasively monitor liver fibrosis and resolution without the need for invasive core biopsies, and they can also improve the early detection of cancer [47]. Nanomaterials are also used for theranostic application (lanthanide-doped hollow nanomaterials) [48].

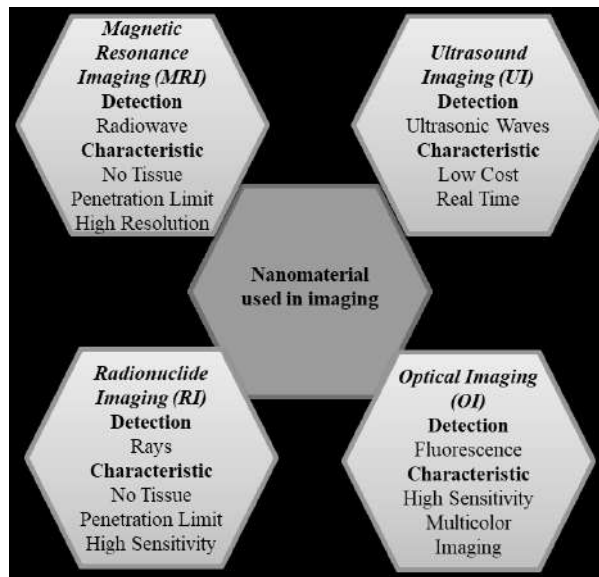


Figure 2. Main imaging highlights of nanomaterials.

5. APPLICATION IN IMAGING

5.1. Magnetic Resonance Imaging

MRI (Magnetic resonance imaging) is a non-invasive imaging technique. This imaging technique uses radiofrequency waves and a strong magnet to produce a clear image of high spatial resolution, specificity, and sensitivity of internal organs. These clear MRI images are obtained by the process of relaxation of magnetic spins and nuclei excitation [49]. The main notable benefit of the MRI technique is its high spatiotemporal resolution of level 25–100 μm and good tissue contrast and is also used for both functional as well as morphological assessments [50].

5.2. Ultrasound Imaging

Ultrasound, also known as ultrasonography, is among the most applied and commonly used imaging techniques. During the ultrasound imaging process, contrast agents such as colloidal suspensions, perfluorocarbon emulsions, and gas-filled microbubbles are generally used for perfusion imaging, lesion characterization, and enhancement. These contrast agents are usually made up of biodegradable and biocompatible materials. These materials possess good vascular circulation properties and *in vivo* study; they were found stable and safe, making them suitable for ultrasound imaging purposes. Ultrasound imaging's main benefit includes high safety, less expensive, easy availability for portable devices, and real-time imaging [51].

5.3. Radionuclide Imaging

Radionuclide imaging (RI) uses radioactive rays for detection and imaging. The two main types of RI modalities include PET (Positron emission tomography) and SPECT (Single Photon Emission Computed Tomography). Radionuclide imaging's main benefit includes low dose of radiotracers, no tissue penetration limitation, high sensitivity, and on the other side, it also has some limitations such as radiation risk and poor spatial resolution [52].

5.4. Optical Imaging

Optical imaging (OI) is an extensively used, non-invasive, and low-cost imaging technique. It is a challenging and important imaging technique used in the biomedical field because of its spatial resolutions and high temporal [53-55]. There are two important techniques in OI first one is BLI (bioluminescence imaging) and FLI (fluorescence imaging). These imaging techniques are used to evaluate the propagation of non-ionizing radiation and light photons through tissue. In humans, optical imaging uses a highly sensitive camera for the purpose of detecting fluorescence released from fluorophores [56]. Conventional fluorophores, commonly including inorganic/organic fluorophores, fluorescent transition metal complexes such as iron oxide, fluorescent proteins, and quantum dots, have been broadly used [57-59].

In a research study, it was found that lanthanide (Ln)-doped UCNPs (upconversion nanoparticles) vea remarkable benefit over conventional fluorophores, like non-photoblinking, low cytotoxicity, and high spatial resolution [60]. The main benefit of optical imaging includes high sensitivity, multicolor imaging, and on the other side, it also has some limitations such as low spatial resolution and poor tissue penetration (Table 1) [61-63].

6. APPLICATION IN COVID-19

These nanomaterials have been discovered and developed to prevent, diagnose, and treat different diseases. On the other side, for treating some common viral infections, nanocapsules, dendrimers, nanoparticles, micelles, and liposomes are currently used. For the purpose of detecting pathogens, such as viruses and bacteria, bionanosensors are commonly used [64]. Because these designed nanosensors will work at the nanoscale size, the nanoparticles will interact with spike proteins and disrupt the viral structure by electromagnetic radiation. Hence, leading to structural destruction, which in result, suppresses the ability of the pathogen (virus) and its genome to reproduce and replicate inside the host [65].

These nano-sized nanoparticles can be further altered for the purpose of targeting a specific or range of bacteria and viruses. Because of their small (nanoscale) size, these reformed nanoparticles can easily move in the body's bloodstream without disrupting any functions. Nanotechnology not only allows the early identification of circulating tumor cells, bacteria, and viruses but also for single-cell analysis [66]. Quite a few nanofillers have been designed and developed by different researchers, such as a Tribo E (triboelectricity electronic) mask, which can hold electric charges to block the entry of pathogens and don't require any external power supply. In another study, researchers have developed a charged nanofiber for capturing the airborne coronavirus (COVID-19 virus) of a mean size of approximately 100 nm [67]. Apart from the benefits of nano-filter-based masks, some possible disadvantages are that they cannot be reused and sterilized because they are specially made with the polymers on the other side; its disposal may cause an environmental problem.

Table 1. Nanoparticles with its imaging applications

Nanoparticles	Imaging application	Therapeutic
Iron oxide	MRI	PTT
Silica nanoparticles	Optical imaging and MRI	Drug delivery
Quantum dots	Optical imaging	PDT
Micelle	MRI, Optical, and radionuclide imaging	Drug delivery, PDT
Dendrimer	Optical imaging and MRI	Drug delivery

Where, PTT: Photothermal therapy, PDT: Photodynamic therapy, MRI: Magnetic resonance imaging

Interestingly the use of masks, which are made up of super-hydrophobic nanostructured surfaces, may serve as an alternative to the above problem. Synthesizing graphene using a low-cost laser technology makes it possible to make a superhydrophobic carbon sheet by controlling the different parameters during the processing step. Because this synthesized graphene is superhydrophobic, so it is self-cleaning and can be reused many times [68].

Nano-sized particles show excellent anti-viral properties, and these properties of nanoparticles have an important role in antiviral activities. The nanoparticle's properties are their surface area to volume ratio, tunable surface charge, and small particle size. Due to the smaller size, drug delivery to the infected regions becomes easy. Several nanoparticles, particularly silver nanoparticles, possess an intrinsic anti-viral characteristic. Moreover, these nanoparticles will form stable structures that will help in effective drug encapsulation and improve its delivery capabilities. On the other side, gold nanoparticles are designed to attach to different viruses like influenza or Ebola and destroy the virus structure by heating them with particular infrared wavelengths [69].

Recently, a team of German scientists successfully synthesized a nanoparticle that will attach to the spike proteins of the viruses, thus effectively inhibiting them from entering the host cells. Images taken showed that the nanoparticles would fully encapsulate the viruses and block the viruses from entering the host. These nano-sized nanoparticles may serve as a good candidate for further human trials [70].

7. TOXICITY ISSUE

Due to the increasing use of nanoparticles in the healthcare sector, these materials toxicity should be a topic of concern [71]. When focusing on nanoparticle toxicity, the analysis of material properties, charge, size, surface chemistry, and shape is important [72, 73]. In *in vivo* or *in vitro* studies, nanomaterials can agglomerate and may also chemically degrade, which makes it tough to relate nanoparticle toxicity to such a wide set of materials [74]. A comprehensive study for every type of nanoparticles, such as its biodistribution, systemic and local toxicity, and pharmacokinetics, will be essential in evaluating its overall toxicity. Though there is significant progress reported in the case of nanomaterials development and discovery for biomedical applications, but still study related to nanotoxicity is still lagging far behind [75]. Thus, there is an urgent need to develop and introduce efficient and rapid methods for identifying the toxicity of these nanomaterials.

8. CONCLUSION

Nanomaterial has an exceptionally high surface area and small size, due to which it has immense application in the healthcare sector, including drug development, therapeutics, bioimaging, medical devices, and diagnostic kits. The main reason behind using these nano-sized materials is their solubility because they have the potential of solubilizing at nanoscale due to their changing properties when attached to nanoparticles. On the other side, the fast, facile operational procedures and low-cost benefit of nanomaterial-based biosensors are going to overhaul the expensive conventional systems in the coming years. Apart from all these mentions facilitating

benefits, toxicity issues are matters of concern. Some important *in vivo* research should be performed to address its rising. In concise, these nanomaterials have huge applicability, and these practical applications have enormous potential.

ACKNOWLEDGMENTS

The authors gratefully acknowledge TEQIP for financial support.

REFERENCES

- [1] Niemeyer, C. M. (2001). Nanoparticles, proteins, and nucleic acids: Biotechnology meets materials science. *Angewandte Chemie*, 40, 4128–4158.
- [2] Ferrari, M. (2005). Cancer nanotechnology: Opportunities and challenges. *Nature Reviews. Cancer*, 5, 161–171.
- [3] Forrest, M. L. & Kwon, G. S. (2008). Clinical developments in drug delivery nanotechnology. *Adv. Drug Delivery Rev.*, 60, 861–862.
- [4] Shiohara, A., Hoshino, A., Hanaki, K., Suzuki, K. & Yamamoto, K. (2004). On the cytotoxicity caused by quantum dots. *Microbiol. Immunology*, 48, 669–675.
- [5] Zhang, L., Gu, F. X., Chan, J. M., Wang, A. Z., Langer, R. S. & Farokhzad, O. C. (2008). Nanoparticles in medicine: Therapeutic applications and developments. *Clinical Phar. Therap.*, 83, 761–769.
- [6] Juliano, R. L. (2012). The future of nanomedicine: Promises and limitations. *Sci. Public Policy*, 39, 99–104.
- [7] Davis, M. E., Chen, Z. G. & Shin, D. M. (2008). Nanoparticle therapeutics: An emerging treatment modality for cancer. *Nature Rev. Drug Discovery*, 7, 771–782.
- [8] Angeli, E., Buzio, R., Firpo, G., Magrassi, R., Mussi, V., Repetto, L. & Valbusa, U. (2008). Nanotechnology applications in medicine. *Tumori*, 94, 206–215.
- [9] Kustandi, T. S., Loh, W. W., Shen, L. & Low, H. Y. (2013). Reversible recovery of nanoimprinted polymer structures. *Langmuir*, 29, 10498–10504.
- [10] Deng, L., Ke, X., He, Z., Yang, D., Gong, H., Zhang, Y., Jing, X., Yao, J. & Chen, J. (2012). A MSLN-targeted multifunctional nanoimmunoliposome for MRI and targeting therapy in pancreatic cancer. *Int. J. of Nanomed.* 7, 5053–5065.
- [11] *Biosensors and nanotechnology-applications in health Care Diagnostics*. (2017). Z. Altintas (Ed.). Hoboken, NJ: John Wiley and Sons Press, ISBN 978-1-119-06501-2.
- [12] Roduner, E. (2006). Size matters: Why nanomaterials are different. *Chem. Society Rev.*, 35, 583–592.
- [13] Buzea, C., Pacheco, I. I. & Robbie, K. (2007). Nanomaterials and nanoparticles: Sources and toxicity. *Biointerphases*, 2, MR17–MR71.

- [14] Aljabali, A. A. A., Hussein, E., Aljumaili, O., Al Zoubi, M. A., Altrad, B., Albatayneh, K. & Abd Al-Razaq, M. A. (2018). Rapid Magnetic Nanobiosensor for the detection of *Serratia marcescens*. *IOP Conference Series: Materials Science and Engineering*, 305, 012005.
- [15] Rocha-Santos, T. A. P. (2014). Sensors and biosensors based on magnetic nanoparticles. *Trends in Anal. Chem.*, 62, 28–36.
- [16] Pecher, J. & Mecking, S. (2010). Nanoparticles of conjugated polymers. *Chem. Rev.*, 110, 6260–6279.
- [17] Yang, K., Xu, H., Cheng, L., Sun, C. Y., Wang, J. & Liu, Z. (2012). *In vitro* and *in vivo* near-infrared photothermal therapy of cancer using polypyrrole organic nanoparticles. *Adv. Mat.*, 24, 5586–5592.
- [18] Feng, G., Fang, Y., Liu, J., Geng, J., Ding, D. & Liu, B. (2017). Multifunctional conjugated polymer nanoparticles for image-guided photodynamic and photothermal therapy. *Small*, 13.
- [19] Luk, B. T. & Zhang, L. F. (2014). Current advances in polymer-based nanotheranostics for cancer treatment and diagnosis. *ACS Appl. Mat. Interf.*, 6, 21859–21873.
- [20] Tang, Z. H., He, C. L., Tian, H. Y., Ding, J. X., Hsiao, B. S., Chu, B. & Chen, X. (2016). Polymeric nanostructured materials for biomedical applications. *Prog. in Poly. Sci.*, 60, 86–128.
- [21] Liu, F. Y., He, X. X., Chen, H. D., Zhang, J. P., Zhang, H. M. & Wang, Z. X. (2015). Gram-scale synthesis of coordination polymer nanodots with renal clearance properties for cancer theranostic applications. *Nature Comm.*, 6, 8003.
- [22] Li, S., Wang, X., Hu, R., Chen, H., Li, M., Wang, J., Wang, Y., Liu, L., Lv, F., Liang, X. & Wang, S. (2016). Near-infrared (NIR)-absorbing conjugated polymer dots as highly effective photothermal materials for *in vivo* cancer therapy. *Chem. of Mat.*, 28, 8669–8675.
- [23] Li, Z. & Yang, Y. W. (2017). Creation and bioapplications of porous organic polymer materials. *J. of Mat. Chem. B*, 5, 9278–9290.
- [24] Lin, W. H., Zhang, W., Sun, T. T., Liu, S., Zhu, Y. & Xie, Z. G. (2017). Rational design of polymeric nanoparticles with tailorable biomedical functions for cancer Therapy. *ACS Appl. Mat. and Interf.*, 9, 29612–29622.
- [25] Wu, Y., Ali, M. R. K., Chen, K. C., Fang, N. & El-Sayed, M. A. (2019). Gold nanoparticles in biological optical imaging. *Nano Today*, 24, 120–140.
- [26] Boisselier, E., Salmon, L., Ruiz, J. & Astruc, D. (2008). How to very efficiently functionalize gold nanoparticles by “click” chemistry. *Chem. Comm.*, 30, 5788–5790.
- [27] Guo, J., Rahme, K., He, Y., Li, L. L., Holmes, J. D. & O’Driscoll, C. M. (2017). Gold nanoparticles enlighten the future of cancer theranostics. *Int. J. of Nanomed.* 12, 6131–6152.
- [28] Her, S., Jaffray, D. A. & Allen, C. (2017). Gold nanoparticles for applications in cancer radiotherapy: Mechanisms and recent advancements. *Adv. Drug Delivery Rev.*, 109, 84–101.

- [29] Xu, Y. H., Wang, X. X., Zhang, W. L., Lv, F. & Guo, S. J. (2018). Recent progress in two-dimensional inorganic quantum dots. *Chem. Society Rev.*, 47, 586–625.
- [30] Yong, K. T. (2012). Quantum dots for biophotonics. *Theranostics*, 2, 629–630.
- [31] Zhao, P., Xu, Q., Tao, J., Jin, Z. W., Pan, Y., Yu, C. M. & Yu, Z. (2018). Near infrared quantum dots in biomedical applications: Current status and future perspective. *Wiley Interdisciplinary Reviews. Nanomed. Nanobiotech.*, 10, e1483.
- [32] Bratschitsch, R. & Leitenstorfer, A. (2006). Quantum dots: Artificial atoms for quantum optics. *Nature Mat.*, 5, 855–856.
- [33] Bilan, R., Nabiev, I. & Sukhanova, A. (2016). Quantum dot-based nanotools for bioimaging, diagnostics, and drug delivery. *Chem. Bio. Chem*, 17, 2103–2114.
- [34] Biondi, M., Guarnieri, D., Yu, H., Belli, V. & Netti, P. A. (2013). Sub-100 nm biodegradable nanoparticles: *In vitro* release features and toxicity testing in 2D and 3D cell cultures. *Nanotechnology*, 24, 045101.
- [35] Cho, K., Wang, X., Nie, S., Chen, Z. G. & Shin, D. M. (2008). Therapeutic nanoparticles for drug delivery in cancer. *Clin. Cancer Res.*, 14, 1310–1316.
- [36] Ahmad, M. Z., Akhter, S., Rahman, Z., Akhter, S., Anwar, M., Mallik, N. & Ahmad, F. J. (2013). Nanometric gold in cancer nanotechnology: Current status and future prospect. *J. Phar. Pharm.*, 65, 634–651.
- [37] Syed, S., Zubair, A. & Frieri, M. (2013). Immune response to nanomaterials: Implications for medicine and literature review. *Current Allergy and Asthma Reports*, 13(1), 50–57.
- [38] Zhang, C. Y. & Hu, J. (2010). Single quantum dot-based nanosensor for multiple DNA detection. *Anal. Chem.*, 82, 1921–1927.
- [39] Jokilaakso, N., Salm, E., Chen, A., Millet, L., Guevara, C. D., Dorvel, B., Reddy, B., Jr, Karlstrom, A. E., Chen, Y., Ji, H., Chen, Y., Sooryakumar, R. & Bashir, R. (2013). Ultra-localized single cell electroporation using silicon nanowires. *Lab on a Chip*, 13, 336–339.
- [40] Barenholz, Y. (2012). Nanomedicine: Shake up the drug containers. *Nature Nanotec.*, 7, 483–484.
- [41] Zamboni, W. C., Torchilin, V., Patri, A. K., Hrkach, J., Stern, S., Lee, R., Nel, A., Panaro, N. J. & Grodzinski, P. (2012). Best practices in cancer nanotechnology: Perspective from NCI nanotechnology alliance. *Clinical Cancer Res.*, 18, 3229–3241.
- [42] Zheng, S., Li, X., Zhang, Y., Xie, Q., Wong, Y. S., Zheng, W. & Chen, T. (2012). PEG-nanolized ultrasmall selenium nanoparticles overcome drug resistance in hepatocellular carcinoma HepG2 cells through induction of mitochondria dysfunction. *Int. J. Nanomed.*, 7, 3939–3949.
- [43] Prabhu, P. & Patravale, V. (2012). The upcoming field of theranostic nanomedicine: An overview. *J. Biomed. Nanotech.*, 8, 859–882.
- [44] Lu, Y. J., Yang, H. W., Hung, S. C., Huang, C. Y., Li, S. M., Ma, C. C., Chen, P. Y., Tsai, H. C., Wei, K. C. & Chen, J. P. (2012). Improving thermal stability and

- efficacy of BCNU in treating glioma cells using PAA-functionalized graphene oxide. *Int. J. Nanomed.*, 7, 1737–1747.
- [45] Li, Z., Wu, X., Li, J., Yao, L., Sun, L., Shi, Y., Zhang, W., Lin, J., Liang, D. & Li, Y. (2012). Antitumor activity of celastrol nanoparticles in a xenograft retinoblastoma tumor model. *Int. J. Nanomed.* 7, 2389–2398.
- [46] Zavaleta, C. L., Garai, E., Liu, J. T., Sensarn, S., Mandella, M. J., Van de Sompel, D., Friedland, S., Van Dam, J., Contag, C. H. & Gambhir, S. S. (2013). A Raman-based endoscopic strategy for multiplexed molecular imaging. *Proceedings of the National Academy of Sciences of the United States of America*, 110(25), E2288–E2297.
- [47] Tobin, L. A., Xie, Y., Tsokos, M., Chung, S. I., Merz, A. A., Arnold, M. A., Li, G., Malech, H. L. & Kwong, K. F. (2013). Pegylated siRNA-loaded calcium phosphate nanoparticle-driven amplification of cancer cell internalization *in vivo*. *Biomaterials*, 34(12), 2980–2990.
- [48] Chiang, P. C., Deng, Y., Ubhayaka, S., La, H., Cui, Y., Chou, K. J., Ran, Y. & Wong, H. (2012). Novel nanoparticles formulation for cassette dosing via intravenous injection in rats for high throughput pharmacokinetic screening and potential applications. *J. Nanosci. Nanotech.*, 12, 7993–8000.
- [49] Zhang, Z., Nair, S. A. & McMurry, T. J. (2005). Gadolinium meets medicinal chemistry: MRI contrast agent development. *Current Med. Chemistry*, 12, 751–778.
- [50] Varadan, V. K., Chen, L. & Xie, J. (2008). Nanomedicine: Design and applications of magnetic nanomaterials. *Nanosensors and Nanosystems*. London, UK: Wiley.
- [51] Bloch, S. H., Dayton, P. A. & Ferrara, K. W. (2004). Targeted imaging using ultrasound contrast agents. Progress and opportunities for clinical and research applications. *IEEE Engineering in Medicine and Biology Magazine: The Quarterly Magazine of the Engineering in Medicine and Biology Society*, 23(5), 18–29.
- [52] Wagner, H. N., Szabo, Z. & Buchanan, J. W. (1995). *Principles of nuclear medicine* (2nd edition). Philadelphia, PA: W. B. Saunders.
- [53] Berezin, M. Y. & Achilefu, S. (2010). Fluorescence lifetime measurements and biological imaging. *Chem. Rev.*, 110, 2641–2684.
- [54] Kobayashi, H., Ogawa, M., Alford, R., Choyke, P. L. & Urano, Y. (2010). New strategies for fluorescent probe design in medical diagnostic imaging. *Chem. Rev.*, 110, 2620–2640.
- [55] Louie, A. (2010). Multimodality imaging probes: Design and challenges. *Chem. I Rev.*, 110, 3146–3195.
- [56] Rao, J., Dragulescu-Andrasi, A. & Yao, H. (2007). Fluorescence imaging *in vivo*: Recent advances. *Current Opinion in Biotech.*, 18, 17–25.
- [57] Lau, J. S., Lee, P. K., Tsang, K. H., Ng, C. H., Lam, Y. W., Cheng, S. H. & Lo, K. K. (2009). Luminescent cyclometalated iridium(III) polypyridine indole complexes--synthesis, photophysics, electrochemistry, protein-binding properties, cytotoxicity, and cellular uptake. *Inorg. Chem.*, 48, 708–718.

- [58] Malkani, N. & Schmid, J. A. (2011). Some secrets of fluorescent proteins: Distinct bleaching in various mouting fluids and photoactivation of cyan fluorescent proteins at YFP-excitation. *Nat Preceding*, 6, e18586.
- [59] Medintz, I. L., Uyeda, H. T., Goldman, E. R. & Mattoussi, H. (2005). Quantum dot bioconjugates for imaging, labelling and sensing. *Nature Mat.*, 4, 435–446.
- [60] Abdul Jalil, R. & Zhang, Y. (2008). Biocompatibility of silica coated NaYF(4) upconversion fluorescent nanocrystals. *Biomaterials*, 29, 4122–4128.
- [61] Xiong, L., Yang, T., Yang, Y., Xu, C. & Li, F. (2010). Long-term *in vivo* biodistribution imaging and toxicity of polyacrylic acid-coated upconversion nanophosphors. *Biomaterials*, 31, 7078–7085.
- [62] Park, Y. I., Kim, J. H., Lee, K. T., Jeon, K. S., Na, H. B., Yu, J. H., Kim, M. H., Lee, N., Choi, S. H., Baik, S. I., Kim, H., Park, S. P., Park, B. J., Kim, Y. W., Lee, S. H., Yoon, S. Y., Song, I. C., Moon, W. K., Suh, Y. D. & Hyeon, T. (2009). Nonblinking and nonbleaching upconverting nanoparticles as an optical imaging nanoprobe and T1 magnetic resonance imaging contrast agent. *Adv. Mat.*, 21, 4467–4471.
- [63] Sudhagar, S., Sathya, S., Pandian, K. & Lakshmi, B. S. (2011). Targeting and sensing cancer cells with ZnO Nanoprobes *in vitro*. *Biotech. Lett.*, 33, 1891–1896.
- [64] Mocan, T., Matea, C. T., Iancu, C., Agoston-Coldea, L., Mocan, L. & Orasan, R. (2016). Hypersensitivity and nanoparticles: Update and research trends. *Clujul Medical*, 89, 216–219.
- [65] Huang, W. C., Tsai, P. J. & Chen, Y. C. (2007). Functional gold nanoparticles as photothermal agents for selective-killing of pathogenic bacteria. *Nanomedicine*, 2, 777–787.
- [66] Zhou, H., Yang, D., Ivleva, N. P., Mircescu, N. E., Niessner, R. & Haisch, C. (2014). SERS detection of bacteria in water by *in situ* coating with Ag nanoparticles. *Anal. Chem.*, 86, 1525–1533.
- [67] Leung, W. W. F. & Sun, Q. (2020). Charged PVDF multilayer nanofiber filter in filtering simulated airborne novel coronavirus (COVID-19) using ambient nano-aerosols. *Separation and Purif. Tech.*, 245, 116887.
- [68] Zhong, H., Zhu, Z., Lin, J., Cheung, C. F., Lu, V. L., Yan, F., Chan, C. Y. & Li, G. (2020). Reusable and recyclable graphene masks with outstanding superhydrophobic and photothermal performances. *ACS Nano*, 14, 6213–6221.
- [69] Singh, L., Kruger, H. G., Maguire, G. E. M., Govender, T. & Parboosing, R. (2017). The role of nanotechnology in the treatment of viral infections. *Therap. Adv. Inf. Disease*, 4, 105–131.
- [70] Wen, A. M. & Steinmetz, N. F. (2016). Design of virus-based nanomaterials for medicine, biotechnology, and energy. *Chem. Society Rev.*, 45, 4074–4126.
- [71] Pan, Y., Neuss, S., Leifert, A., Fischler, M., Wen, F., Simon, U., Schmid, G., Brandau, W. & Jahnen-Dechent, W. (2007). Size-dependent cytotoxicity of gold nanoparticles. *Small*, 3, 1941–1949.

- [72] Simon, A., Thiebault, C., Reynaud, C., Gouget, B. & Carriere, M. (2006). Toxicity of oxide nanoparticles and carbon nanotubes on cultured pneumocytes: Impact of size, structure and surface charge. *Tox. Lett.*, 164, S222–S222.
- [73] Jiang, J. K., Oberdörster, G. & Biswas, P. (2009). Characterization of size, surface charge, and agglomeration state of nanoparticle dispersions for toxicological studies. *J.f Nanopart. Res.*, 11, 77–89.
- [74] Aillon, K. L., Xie, Y., El-Gendy, N., Berkland, C. J. & Forrest, M. L. (2009). Effects of nanomaterial physicochemical properties on *in vivo* toxicity. *Adv. Drug Delivery Rev.*, 61, 457–466.
- [75] Fischer, H. C. & Chan, W. C. W. (2007). Nanotoxicity: The growing need for *in vivo* study. *Current opinion in Biotech.*, 18, 565–571.

Complimentary Contributor Copy

Chapter 4

MEDICINAL IMPORTANCE OF INORGANIC MATERIALS

Shraddha Shukla* and A. P. Mishra

Department of Chemistry, Dr. Hari Singh Gour University,
Sagar, India

ABSTRACT

Science and technology have had a major impact on society, and their impact is growing in every aspect of life. Inorganic materials are required to keep the human body healthy because several critical biological functions in humans depend upon their presence, and their absence or scarcity may lead to diseases. Beginning with the plow, science has changed how we live and what we believe. To make life easier, science has given to human the chance to pursue societal concerns and to improve human living conditions. Science has grown enormously in past 3-4 decades, and now a lot of attention is being given on material science on one hand and on biology/medicine at the other, where chemical sciences have acquired a central place. In chemistry, researchers are focusing on synthesis of 'tailor made compounds' and structural studies in solid state as well as in solution, with an approach to go deeper into the concepts and applicability of nanomaterials and molecular biology/molecular medicines. The medicinal uses and applications of inorganic materials and metal complexes are of increasing clinical and societal importance. Inorganic materials include metals, minerals, metalloenzymes, metal complexes and organometallic compounds which can be used as catalysts, pigments, coatings, surfactants, fuel, medicine etc.

Keywords: inorganic material, Anticancer, Insulin mimetic and medicinal inorganic

* Corresponding Author's Email: shuklashraddha25@gmail.com.

1. INTRODUCTION

Inorganic materials play a significant role in our societies. Inorganic materials are being used in medicines for centuries. Metal ions are required for many critical functions in biology. Scarcity of some metal ions can lead to some diseases and cure society. In the prehistoric times, human has been using inorganic material and metals namely gold (Au), silver (Ag) and mercury (Hg) in the ionic states as copper (Cu) and iron (Fe) as in the nature. The first finding of metals must date back thousand years (Table-1). During the prehistoric and middle ages, 9 and 5 elements were found and used for social benefits. Discovery of metals and elements from nature increased in the 18th century, which further improved in the 19th century (Table-2) [1]. At the end of 19th century, radionuclides were explored from earth ores/minerals.

Table 1. Metal use in ancient age

Metals	Age	Area
Au & Ag	4000 B.C.	Chaldear
Pb	3800 B.C.	-
Cu & Sn	3500 B.C.	Bronze age
Fe	1500 B.C.	Iron age
Hg & As	350 B.C.	Ancient Greece
Zn	-	Ancient Romans

Table 2. Elements discovered from nature [1]

Age	Elements
17 th century	
Prehistoric age	Au, Ag, Hg, Pb, Sn, Cu, Fe, S, C
Middle age	Zn, As, Bi, Sb, P
18 th century	
The first half	Co, Ni, Pt
The latter half	Mn, W, Ti, Mo, Cr, U, Zr, Y, H, N, O, Cl, Te, Be
19 th century	
The first half	Mg, Pd, Os, Ce, Rh, Ir, Na, K, Ca, Sr, Ba, Li, Cd, Se, Si, Ta, Al, La, Th, V, Er, Tb, Nb, Ru, B, I, Br
The latter half	Rb, Ce, Tl, In, Ga, Yb, Sc, Sm, Ho, Tm, Gd, Ge, Pr, Nd, Dy, Po, Ra, Ac, F, He, Ne, Ar, Kr, Xe, Rn
20 th century	Eu, Lu, Pa, Hf, Re

The first finding of a bio-element from human urine was by a German alchemist Henning Brand (1639-1710), who discovered phosphorus (P) in 1669. This was a significant example of finding an element originated from living materials. Following the finding, several essential elements, vitamins, bio-molecules and hormones were

explored. In second half of 20th century a large number of metallo-biomolecules viz. metalloproteins and metalloenzymes, were studied. These studies became the strong basis of new sub-discipline: Inorganic Biochemistry; later different metallo-biomolecules were isolated from microorganisms, cultured cells, plants, animal and human organs and blood. The medicinal uses and applications of metals and other inorganic materials are increasing on clinical and biomedical aspects [2, 3].

Indian medicinal system- Ayurveda, is already having several reports on use of metallodrugs- '*Rasa Shastra*,' since the time of *Carak* and *Shrushat* (4th Century), in health sciences. Mostly nine metals and metalloids were used for rejuvenation, metabolic disorders and treatment for humans. AcharyaPrafulla Chandra Ray wrote about ancient Indian knowledge and wisdom in his book '*A Hindu Chemistry*' in 1908. Several principles of health sciences are still hidden in Indian wisdom and Granthas, which talks about very fine narrow line of life systems and equilibria based on organic-inorganic balances and imbalances.

Since 1965, transition metal complexes are in use as radiation therapeutic, diagnostic- imaging agents and as small molecule drugs. It is ironic to note that the first structure-activity relationship evolved by Ehrlich Paul in the first decade of 20th century (1908), evolved the development of the inorganic compound arsphenamine (salvarsan) for successful treatment of syphilis. Founder of chemotherapy Ehrlich, defined it as the use of drugs to injure an invading organism without injury to the host. Recent advances in chelation research have paved the way for targeting '*magic-bullets*' for chemotherapy, using different strategies and pharmacological manipulation to utilise metal complexes as drugs.

Peter Sadler noted some years ago, that most of the elements of periodic table upto and including bismuth have potential uses in design of new drugs and diagnostic agents. *James Cowan's* new molecules, called metal-coordination complexes, mimic the activity of natural enzymes that break apart DNA, RNA and proteins in the body. Metallic preparations can be toxic, but so can some organic molecules also be, used as drugs.

Reactivity of metal chelates can be modulated by modifying their redox potential, saturation level of coordination sphere, hydrophilicity and lipophilicity by changing the nature of ligands. In general, the synthesized metal complexes have higher biological activities comparative to free ligands. The increased inhibition activity of metal complexes can be explained on the basis of Tweedy's chelation theory [4]. In metal complexes, on chelation the polarity of metal ion is reduced to a greater extent due to overlapping of the ligand orbitals and partial sharing of the positive charge of the metal ions with donor ring. Further, it increases the delocalization of π - electrons over the whole chelate ring. The large ring size of attached two ligand moiety makes the complexes more lipophilic [5]. This increased lipophilicity enhances the penetration of the metal complexes into lipid membranes and block the metal binding sites in the enzymes [6]. Alfred Werner (1866-1919) proposed the "coordination theory" and a new concept of "metals and life" came into being with the finding of urease, which the first crystallized enzyme was obtained in 1926 and found to bind nickel (Ni) at the active

centre in 1975. Approximately thousands of metalloenzymes and metalloproteins are now analysed by scientist. With the progress and researches, the concept of essential trace elements in humans and animals has been established and health disorders due to deficiency of elements such as Fe, Zn, Cu, Se, Ca etc., in human. In mostly cases, the supplementation of these elements alleviated disorders in societal health. On the basis of this knowledge, wide varieties of metal containing medicines have been proposed and some of them have been clinically used since the 20th century as summarised in Table-3. Inorganic materials used as medicine and diagnostic care have been described here.

1.1. Antibiotic

Antibiotic like Bleomycin causes DNA strand scission through formation of an intermediate inorganic material like metal complexes requiring a metal ion cofactor such as copper or iron for the activity in the treatment of cancer. Antibiotic drugs of the tetracycline family are chelators of Ca²⁺ and Hg²⁺ ions.

1.2. Antimicrobial

Inorganic materials of Ni, Cu, Co, Ag, Zn and Hg have a long history of use as antibacterial and antifungal agents. The use of mercurochrome as a topical disinfectant is now discouraged. Silver sulfadiazine finds use for treatment of severe burns; the polymeric material slowly releases the antibacterial Ag ion. Silver nitrate is still used in many countries to prevent ophthalmic disease in newborn children. The mechanism of action these materials through slow release of the active metal ion inhibition of function in bacterial cell walls gives a rationale for the specificity of bacteriocidal action [7].

1.3. Antiviral

Polyoxometallates, for example, [NaW₂₁Sb₂₉O₈₆] [NH₄]₁₇ and K₁₂H₂[P₂W₁₂O₄₈]. 24H₂O exhibit antiviral activity. These transition metals (V, W, Mo) with oxygen to form a variety of cage-like structure. Being negative charged, these materials bind to positive charged patches of HIV gp120 blocking binding to lymphocyte CXCR₄ receptor. Some inorganic materials discovered that Ruthenium Polyaminocarboxylate (Ru-pac complexes) possess cysteine protease inhibition activity [8].

1.4. Anticancer

Two major drugs based on inorganic materials that have no known natural biological function, Pt (cisplatin) and Au (auranofin), are widely used for the treatment

of genitourinary and head and neck tumors and of rheumatoid arthritis, respectively. Cisplatin is cited for treatment of germ-cell cancers, gestational trophoblastic tumors, epithelial ovarian cancer, and small cell lung cancer as well as for palliation of bladder, cervical, nasopharyngeal, esophageal, and head and neck cancers. The use of cisplatin has rendered at least one cancer, testicular cancer, curable and is significant in treatment of ovarian and bladder cancers. A large number of Ru-based inorganic materials, including carboxylate-bridged di- and trinuclear complexes, exhibit antitumor activity in animal models. Platinum complexes are cytotoxic agents yet the paradigm in cancer chemotherapy has moved to a more targeted approach, with special emphasis on signalling pathways [9-11].

1.5. Neurological

The clinical value of Li has been recognized since 1949. Lithium carbonate is used in manic depressive psychoses for the treatment of recurrent mood change. Mood stability may only occur after months rather than weeks. Li(I) interferes with the biochemistry of Mg (II) which is of similar size. Li(I) acts as an uncompetitive inhibitor of inositol monophosphatase that hydrolyses inositol. Phosphate into inositol and phosphate. According to the 'inositol depletion' theory of bipolar disorder treatment, the therapeutic effect of lithium is to block inositol recycling via inositol monophosphatase inhibition, and thus reduce inositol levels in the cell [12, 13].

1.6. Anti-Inflammation

Inflammation, angiogenesis and remodelling are self limiting processes under normal healing conditions. Chronic inflammatory processes such as rheumatoid arthritis, Crohn's disease and psoriasis share these abnormal healing features. Thus, therapies that attenuate inflammatory angiogenesis and fibrotic processes are able to prevent progression and/or maintenance of chronic inflammatory conditions. Non-steroidal anti-inflammatory drugs (NSAIDs) are widely used for the treatment of pain, fever, and inflammation. Inorganic materials of vanadium complexes show moderate to very good anti-inflammatory activity [14].

1.7. Anti-Arthritics

There are four main drugs used in the treatment of early stages of rheumatoid arthritis: Auranofin, Myochrysine, Sodium bis(thiosulfate)gold, and Solganl. These are Au(I) complexes administered to rheumatoid arthritis patients via ingestion or injection. Inherent in acid-base chemistry of Au(I), the soft metal prefers soft bases, as seen in the interaction between Au-S. This bonding is relevant in the biological effects in the treatment of rheumatoid arthritis [15, 16].

1.8. Insulin Mimetic

During the past 25 years, ions of elements such as Se, Cr, Mn, Mo, W, V and Zn have been reported to exhibit insulin like effects. V proving to be one of the most efficient. The insulin-like antidiabetic effects of vanadium compounds were reported as long ago as 1899 and rediscovered about 80 years later, first in -vitro and later in in-vivo studies. Even simple inorganic vanadium salts in oxidation state IV or V (e.g., vanadyl sulfate or sodium vanadate) mimic most of the physiological effects of insulin, such as stimulation of the glucose uptake and metabolism in the fat cells, the enhancement of glycogenesis in the muscles and the liver, inhibition of the reformation of glucose (gluconeogenesis) from proteins or the stimulation of fatty acid formation in the adipocytes. The main advantage of these vanadium compounds relative to insulin is that they may be administered orally [17, 18].

1.9. Antiulcer

Bismuth compounds have been used for their antacid and astringent properties in a variety of gastrointestinal disorders. The effectiveness of bismuth is due to its bacteriocidal action against the Gram-negative bacterium, *Helicobacter pylori*. Usually, the bismuth preparations are obtained by mixing an inorganic salt with a sugar-like carrier. Commonly used agents are colloidal bismuth subcitrate (CBS), and bismuth subsalicylate (BSS). The mechanism of action is complex and includes inhibition of protein and cell wall synthesis, membrane function and ATP synthesis. The most notable salts are tripotassiumdicitratobismuth, bismuth salicylate, Pepto-Bismol (BSS), and De-Nol (CBS) [13].

Table 3. Medicinal applications of inorganic materials

Element	Compounds	Applications
Ag	Silver sulphadiazine	Antibacterial
Al	Al(OH) ₃ Silicate	Antacid Antidiarrhoeal
As	Salvarsan, Melarsen, Tryparsamide Arsphenamine Trisinol (Arsino trioxide)	Antimicrobial Syphilis Acute Promyeloicytic leukemia (APL)
Au	Gold(I) thiolates Auranofin Au(I) diphosphine complexes	Antitumor Rheumatoid arthritis Antiviral
B	Boric acid	Antifungal
Ba	Barium sulphate	X-ray contrast

Element	Compounds	Applications
Bi	Bismuth subsalicylate, colloidal bismuth citrate, ranitidine bismuth citrate	Antacid, antiulcer
Br	Sodium bromide	Sedative
Cr	Chromium complexes	Antidiabetic
Cu	Copper histidine complexes	Supplement for Menkes disease treatment
Co	Vitamin B12	Pernicious anaemia
Fe	Glycine sulphate Sodium nitroprusside Fe (III) desferrioxamine chelates	Iron deficiency-anaemia Vasodilator Antimicrobial
Ga	Ga(NO ₃) ₂	Hypercalcemia of malignancy
Gd	Gdmetallotexaphyrins	MRI contrast agent PDT, Radiopharmaceuticals
Ge	Ge-132	Bacteria, Cancers
Hg	Mercurochrome	Antiseptic
I	I ₂ Na ¹³¹ I	Antiseptic Diagnosis of Thyroid
Li	Li ₂ CO ₃	Manic depression
Lu	Lutetium complexes	PDT
La	Lanthanum carbonate	Chronic kidney disease
Mg	Sulphate, hydroxide	Antacid, laxative
Mn	Mn-SOD complexes	Superoxide scavengers, MRI contrast agent
Mo	Tetrathiomolybdate	Wilson disease
Pt	Dichlorodiammine	Antineoplastic disorders
Ru	Ru(III)complexes	Lung metastatic tumour
Os	Osmium tetroxide Osmium carbohydrate polymers	Fingerprint detection Antiarthritic
Sb	Pentostam, N-methylglucamineantimonate	Antileishmanial
Si	Al ₂ (OH) ₄ Si ₂ O ₅	Antidiarrhoeal
Se	Sulphate Ebselen: (2-phenyl-1,2-benzisoselenazol-3(2H)-one) Phenylaminoalkylselenide Selenazofurin Selenotifen	Antidandruff Synthetic antioxidant Antiinflammatory, Neuroprotective agent Antihypertensive Antineoplastic & antiviral Antiallergic
Sn	Tin (IV) ethyl etiopurpurin Fluorides	PDT Anticaries
Tc	^{99m} Tc (V) proyleneamineoxime	Diagnostic imaging
Ti	Titanocene dichloride,	Anticancer

Element	Compounds	Applications
	bis(β -diketonato)Ti(IV)	
W	Polyoxometallates	Anti-HIV
Zn	Polaprezinc Zinc complexes Zinc complexes Zinc-thioallixin-N-methyl Zinc-dithiocarbamate Zinc-acetate	Stomach ulcer Diabetes mellitus UV-induced dermatitis Metabolic syndromes Diabetes Wilson disease
Zr	Zr(IV) glycinate	Antiperspirant

CONCLUSION

This chapter summarized the advances on bioapplicable inorganic materials for human health benefits in particular and society at large. Inorganic materials have been used since antiquity and scientific research has further uplifted its potential for more medicinal application. The authors hope that the review presents significant insights into the advancement of future researches on biomaterials.

ACKNOWLEDGMENTS

The authors are thankful to Dr. Arti Srivastava, Guru Ghasidas University, Bilaspur (C.G.). Thanks, are also due to the Head, Department of Chemistry, Dr. Hari Singh Gour University, Sagar (M.P.).

REFERENCES

- [1] Farrell N. P. (1989). *Transition Metal Complexes as Drugs and Chemotherapeutic Agents*. James B. R. Ugo, R. Ed. Reidel-Kluwer Academic Press: Dordrecht. 11.
- [2] Farrell N. P. (1999). *The Uses of Inorganic Chemistry in Medicine*. The Royal Society of Chemistry: Cambridge.
- [3] Keppler B. (1993) *Metal Complexes in Cancer Chemotherapy*. VCH: Basel.
- [4] Tweedy B. G. (1964). Plant extracts with metal ions as potential antimicrobial agents. *Phytopathology* 55: 910-914.
- [5] Mazumeler U. K. and Gupta M. (2003). Synthesis, antitumour and antibacterial activity of some Ru(bpy)₂²⁺/4-substituted thiosemicarbazide complexes. *Indian J. Chem.* 42:313-317.

- [6] Vaghasia Y., Nair K., Soni M., Baluja S. and Chandra S. (2004). Synthesis, structural determination and antibacterial activity of compounds derived from vanillin and 4-aminoantipyrine. *J. Serb. Chem. Soc.* 69: 991-998.
- [7] Mishra A. P., Soni M. (2008). Synthesis, structural, and biological studies of some schiff bases and their metal complexes. *Metal-Based Drugs*. 10, Article ID 875410. doi: 10.1155/2008/875410.
- [8] Chouhan Z. H. (2006). Antibacterial and antifungal ferrocene incorporated dithiothione and dithioketone compounds. *Appl. Organomet. Chem.* 20, 112-116.
- [9] Jain S., Longia S., Ramnani VK. (2009). *People's Journal of Scientific Research*. 2(1), 37-40.
- [10] Clarke M. J. (2003). Ruthenium metallopharmaceuticals. *Coord. Chem. Rev.* 236 (1-2), 299-233.
- [11] Shukla S. Mishra A. P. (2013) Synthesis, Structure, and Anticancerous Properties of Silver Complexes. *J. of Chemistry*. Article ID 527123, 6 pages.
- [12] Birch N., Farrell N. (1999). *Biomedical Uses of Lithium*. The Royal Society of Chemistry: Cambridge. 11-21.
- [13] Reglinski J. (1998). *Chemistry of Arsenic, Antimony, and Bismuth*. Blackie Academic & Professional: London.
- [14] Shukla S. Mishra A. P. (2019) Metal complexes used as anti-inflammatory agents: Synthesis, characterization and anti-inflammatory action of VO(II)-complexes. *Arabian J. of Chemistry*. 12, 1715-1721.
- [15] Clinic M. (2016). Rheumatoid Arthritis. *Overview myoclinic. Org.*
- [16] Shaw C. F. (1999). Gold based therapeutic agents. *Chemical Reviews*. 99(9), 2589-2600.
- [17] Kiss T., Sakurai H. (2008). Biospeciation of antidiabetic VO(IV) complexes. *Coordination Chemistry Reviews*. 252, 1153-1162.
- [18] Shechter Y. (1990). Insulin-mimetic effects of vanadate: Possible implications for future treatment of diabetes. *Diabetes*. 39, 1-5.

Complimentary Contributor Copy

Chapter 5**IMPACT OF POLYMERIC MATERIALS ON SOCIETY
AND COMPLEX IMPEDANCE SPECTROSCOPY****A. L. Saroj***Department of Physics, Institute of Science,
Banaras Hindu University, Varanasi, UP, India**ABSTRACT**

This chapter deals with the deep insights about polymers and its potential applications for developing solid polymer electrolyte (SPE) based electrochemical (EC) devices like batteries, electrochemical capacitors, fuel cells, etc. Polymeric materials are very useful in modern society. The structure and properties of such materials can be modified chemically as well as physically. Polymeric materials are used to prepare several products and goods like rubber, polymer cloth made by synthetic fibers, polymer glass, nylon bearings, polymer bags, polymer paints, epoxy glue, Teflon/or polymer-coated cookware, and many more. These materials are all around us and we cannot imagine our daily life without polymers. Complex impedance spectroscopy (IS) or electrochemical impedance spectroscopy is a most versatile technique which can be used to study the electrical transport properties, dielectric properties and ion dynamics behaviour of the SPE and amorphous/semi-crystalline materials. In this chapter, the IS technique and its application to interpret the impedance data has been discussed in details with help of ion conducting bio-polymer electrolyte sample. By using this technique different parameters like electrical conductivity (ionic/electronic conductivity), activation energy, ac conductivity (frequency dependent conductivity), dielectric permittivity, electric modulus, loss tangent, mobility of charge carriers and total number of charge carrier density can be explored for conducting polymeric/amorphous systems. The data of complex IS is associated with translational motion of free

* Corresponding Author's Email: al.saroj@bhu.ac.in.

charge carriers via polymer segmental motion or orientation/re-orientation of polar groups attached with the backbone of polymer chains.

Keywords: polymers, polymer electrolytes, AC impedance spectroscopy, ionic conductivity, dielectric properties

1. INTRODUCTION

Polymeric materials are very useful in modern society. The structure and properties of such polymers/its derivatives can be modified chemically (by crosslinking of two polymers and by using additives) as well as physically (by polymer blending i.e., miscible/non-miscible). A polymer is a chemical compound consisting of repeated structural/basic units (monomer) joined end to end by a process called polymerization. The use of polymers/polymeric materials as a host, for the development of solid polymer electrolyte (PE) is one of the important applications. PE is a membrane/film composed of dissociated salts (cation+anion) in which the polymer (high molecular weight) network will acts as a host matrix for the conduction of free charge carriers or ions. Consideration of a polymer as a successful host should generally carry the following essential characteristics (i) Monomer should have at least one donor group (an atom with at least one lone pair of electrons) to form a co-ordinate bond with the free charge carriers (ii) Minimum bond rotation barrier for the ease of segmental motion of the polymer chains/segments. In recent years, PEs have other prospective applications in energy storage devices as well as green energy devices like electrochemical double layer capacitors or super capacitors, fuel cells, electrochromic display devices and electrochemical sensors [1, 2]. Complex impedance spectroscopy (CIS) is a very versatile tool to measure the electrical properties of dielectric/amorphous materials and their interfaces. By knowing the frequency dependent resistance i.e., impedance and phase one can study the ion dynamics behavior, dielectric properties and electric modulus of the ion/electron conducting solid polymer electrolytes [3, 4].

2. POLYMERS: AN OVERVIEW

The word polymer is derived from classical Greek words '*poly*'= *many* and '*mers*' =*parts* i.e., 'many parts' having high molecular weight $\sim 10^3$ - 10^6 g/mol. Polymeric materials are used to prepare several products and goods such as rubber, polymer cloth made by synthetic fibers, polymer glass, nylon bearings, polymer bags, polymer paints, epoxy glue, Teflon-coated cookware, and other things. Polymers are all around us like our DNA (a type of biopolymer) to polyethylene (plastic) and we cannot imagine our daily life without polymers. 'Polymers' or sometimes called 'macromolecules' is a large class of materials having many small molecules known as monomers and monomers are joined together in regular manner via chemical bonding (covalent

bonds) to form large polymeric chains [5, 6]. Polymeric materials have the unique physical properties such as flexibility and viscoelasticity. First synthetic polymer was produced in 1909 as Bakelite and later on several synthetic polymers like rayon was developed. The industrial development was started in 1919 with the new concept of polymer i.e., a material having high molecular weight and its compound were composed of long covalently bonded molecules (by Herman Staudinger). The idea regarding the modification of physical properties of polymers came into existence in eighteenth century when Thomas Hancock gave an idea to modify the physical structure of natural rubber by blending. By using the idea of cross-linking, Charles Goodyear modify the properties of natural rubber through vulcanization process with sulfur at 270-degree Fahrenheit and discovered the 'Tire' which is frequently used in vehicles. The development of today's polymer industry is based on the important discoveries made in nineteenth century concerning the modification of physical/chemical properties of natural polymers. Firstly, poly(methyl methacrylate) (PMMA) was commercially synthesized by John Crawford in 1932. The polyethylene was discovered by two scientists Eric Fawcett and Reginald Gibson in 1933. F. Crick and J. Watson proposed the double helix structure of the DNA which is also a type of biopolymer. Alan J. Heeger, Alan G. MacDiarmid and Hideki Shirakawa have been honored with the Nobel Prize in Chemistry in 2000 for their "discovery and development of conductive polymers" [7-9].

3. CLASSIFICATION OF POLYMERS

Polymers can be classified on the basis of (i) origin or source of availability (i.e., natural, synthetic and semi-synthetic polymers), (ii) structure of monomer (i.e., linear homopolymer, co-polymer) and (iii) polarity (i.e., polar and Non-polar polymers) as shown in Figure 1.

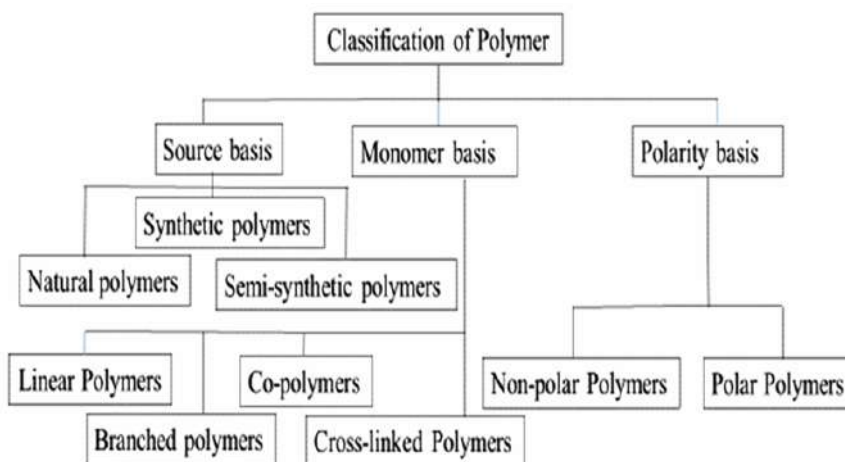


Figure 1. Classification of polymers.

3.1. Natural, Synthetic and Semi-Synthetic Polymers

Natural polymers are obtained from natural sources like plants and animals. These polymers are abundant in nature, non-toxic, renewable, biodegradable, cost effective and eco-friendly. Polysaccharides are the good examples of natural polymers. CS is more interactive with respect to chitin due to the presence of amino (NH_2) group at C-2 positions. The chemical properties of chitosan (CS) are as follows: (i) amino (NH_2) and hydroxyl (O-H) groups present with back bone, (ii) this is a linear polyamine (iii) it has chelating and complexing properties (iv) CS is enable to form hydrogen bonding with the additives (v) CS is insoluble in water and organic solvents but soluble in dilute aqueous acidic solution (vi) this is a cationic biopolymer with high charge density (one positive charge per glucosamine residue) (vii) film-forming ability (viii) this easily interacts with negatively charged molecules (flocculating agent) (ix) CS has bio-compatibility and anti-microbial properties [10]. Synthetic polymers are man-made polymers by chemical route. The first synthetic polymer was produced in 1909 as Bakelite and later on several synthetic polymers like rayon was developed. Polyethylene (plastic), nylon, poly(methylmethacrylate) (PMMA) and poly(ethylene oxide), PEO are the examples of synthetic polymers. Semi-synthetic polymers are very useful to develop polymer electrolyte films and these polymers are generally derived from naturally occurring polymers via chemical modification. Cellulose acetate, carboxymethyl cellulose (CMC), cellulose nitrate are the examples of such polymers. In order to prepare polymer electrolyte films one can prefer natural polymers, semi-synthetic polymers and in some context synthetic polymers. PEO is one of the best synthetic polymer and worldwide several research groups uses this polymer as a host material for the preparation of polymer electrolytes [11-13]. Nowadays, people are doing research on biopolymer-based materials. Bio-polymeric materials are cost effective, non-toxic, naturally abundant, renewable, eco-friendly and can be easily obtained from natural sources like cell walls, plants and animals [12, 14, 15].

3.2. Linear Polymers, Co-Polymers, Branched Polymers and Cross-Linked Polymers

When the polymer chain consists of only one type of monomers (homo-polymers) i.e., single monomer in repeating units, then such type of polymer is defined as linear polymer (Figure 2(a)). If the chains of polymer consists dissimilar monomers, the polymer is referred to as a co-polymer (Figure 2 (b)). Sometimes the branch chains having similar monomers or dissimilar monomers attached with the back bone of polymer such type of polymer is referred as branched polymer (Figure 2 (c)). When branching and some interactions between the side chains of polymer occur with other similar/dissimilar branch chains of different polymer then polymer network is defined as a cross-linked polymer (Figure 2 (d)). Some simple polymer chain structures like (a) linear polymer (b) co-polymer (c) branched polymer and (d) cross-linked polymer are

shown in Figure 2. The physical properties of a given polymer can be analyzed by knowing the chemical structure of monomer units. Linear polymers are one of the simplest types of polymer and these polymers are generally soluble in organic solvent. Whereas a co-polymer which is also a type of single polymer chain having two monomers of different kinds that may be in particular sequence/or not and also have the properties of the two respective homo-polymers.

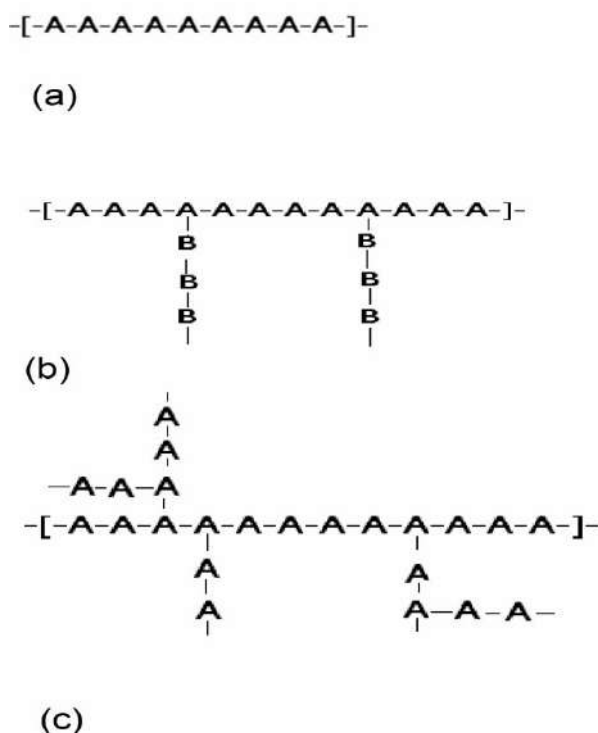


Figure 2. Schematic diagram of different types of polymer chain structures viz. (a) linear polymer (b) co-polymer (c) branched polymer and (d) cross-linked polymer.

Branched polymers can be obtained when there is a central polymer chains that has branching points to which different/or same polymer chains are attached whereas the cross-linked polymer is similar with the branched polymer except that some of the branched chains are covalently linked to other polymeric chains. The chemical interactions between the constituents of polymer is responsible for solubility of a particular polymer i.e., soluble/or insoluble in organic solvents viz. the cross-linked polymers are in-soluble in organic solvents.

3.3. Polar and Non-Polar Polymers

In polymeric materials generally, the molecules are joined together by a covalent bond and form a dipole due to presence of positively charged atom nuclei and negatively charged atom nuclei separated by a finite distance. However, in some cases

the molecules of a polymer are arranged in different ways and they may not share the electrons equally which make their one end more negatively charged than the other. Such type of polymers are said to be polar polymers and they have a permanent dipole moment even in absence of electric field. Electro-negativity may play a significant role in polar molecules and its value for common atoms is as follows: $F > O > Cl$ and $N > Br > C$ and H . The charge of polar polymers can be measured as negative or positive charge and such materials have some permanent dipole moment. Some examples of polar polymers are poly (vinyl) alcohol, PVA, poly (vinyl) pyrrolidone, PVP and poly(ethyleneoxide), PEO. These polymers have high polarity/proton acceptor molecules. Polymers like PVA and PVP has the hydroxyl (O-H) and pyrrole (C=O) functional groups, respectively and they are water-soluble, excellent dielectric, optical properties, high chemical stability and film forming availability. These materials are also useful for medical applications and food packaging applications and very well suited to form polymer blend with different polymers like PVA-PVP, PVA-starch and PVA-Chitosan [16, 17] polymer blends.

4. PHYSICAL AND CHEMICAL PROPERTIES OF POLYMERS

Generally, polymers have semi-crystalline phase i.e., some portion of polymer is crystalline and some portion is amorphous as depicted in Figure 3(b). The chain length and the cross-linking in between the segments enhanced the mechanical strength of the polymer network. The molecules of the polymer are enabled to interact with the side chains/segments of the polymer itself via hydrogen bonding and ionic bonding (weak interactions). The cross-linking between two polymers strengthens the polymer network. The high flexibility of polymer chains is possibly due to dipole-dipole interactions and Van der Waal (weak) interactions which results in low glass transition temperature (T_g) of a particular polymer. Some polymers like PEO, PVP, PMMA, PVA has the low T_g value which resulted as the high amorphousness near room temperature.

Polymer has well known temperature dependent physical properties and its phase changes with temperature (crystalline/semi-crystalline phase to amorphous phase/rubbery phase) and hence electrical (associated with segmental motion of polymer chains) and dielectric properties. At low temperatures (below glass transition temperature, T_g) polymer do not possess any segmental motion due to crystalline phase or hardness and segmental motion of polymer chains are almost frozen. As the temperature increases (moving towards T_g and above the T_g) the polymer network becomes flexible and enhanced the amorphous phase due to phase transformation from crystalline state to rubbery/molten state. Therefore, T_g is directly associated with the movement of polymer chains segment and hence dielectric relaxation behavior of the polymeric system. Glass transition temperature, T_g is a transitional temperature at which polymer segments start to move from the frozen state as shown in Figure 3(a). In order to prepare polymer electrolyte films, polymer should have the following properties such as (i) High Chemical Stability. (ii) Ease of synthesizing a variety of new

materials. (iii) Good mechanical strength as well as mechanical flexibility (iv) Film forming availability (v) Mouldability into different shapes and size.

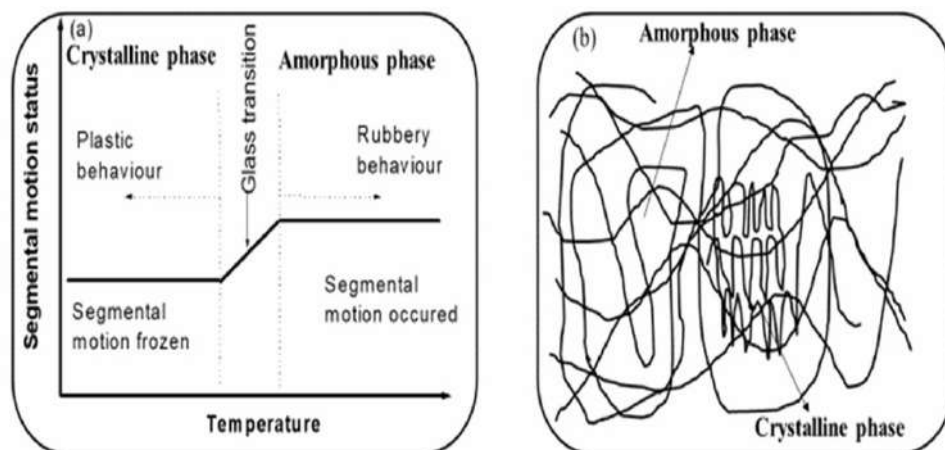


Figure 3. Schematic diagram of (a) effect of temperature on segmental motion of polymer chains and (b) amorphous and crystalline phase in semi-crystalline polymers.

5. COMPLEX IMPEDANCE SPECTROSCOPY (CIS)

The complex impedance spectroscopy or Electrochemical impedance spectroscopy (EIS) is a versatile and powerful tool for analysing the properties of a material as a bulk and its interface. The electrical impedance is usually measured by applying an ac signal/potential across the sample sandwiched in-between electrodes (spring loaded stainless steel/brass can be used as electrodes).

Let, $V(t) = V_0 \sin \omega t$ is applied voltage and the current induced is $I(t) = I_0 \sin(\omega t + \varphi)$, the complex impedance (Z^*) can be calculated by using the expression[3]:

$$Z^* = \frac{V(t)}{I(t)} = \frac{V_0}{I_0} e^{-j\varphi} = |Z| e^{j \cdot \arg(Z)} = Z' - j Z'' \quad (1)$$

where V_0 and I_0 are the voltage and the current amplitudes, respectively and $\omega = 2\pi f$ is the angular frequency; f is the test signal frequency, φ is the phase difference between $V(t)$ and $I(t)$, Z' is the real part of impedance and Z'' is the imaginary part of impedance.

In the presence of external electric field every dielectric material gets polarized and dielectric relaxation behavior of polymeric material is associated with polarization effect in the material and/or near the electrode-polymer interface [1, 3]. In the different range of frequencies, different types of polarization occurred which is associated with the relaxation/orientation or re-orientation of polymeric chains/side chains or functional

groups attached with the polymer back bone. The dielectric relaxation behavior can be analysed in terms of an electronic, ionic and dipolar polarizabilities (polarizability is defined as dipole moment per unit electric field). In all types of polarization phenomena, different relaxation time was observed and hence a dielectric spectroscopy i.e.. dielectric relaxation spectroscopy (DRS) is used to identify the dominating relaxation mechanism prevailing in the system in the particular frequency range.

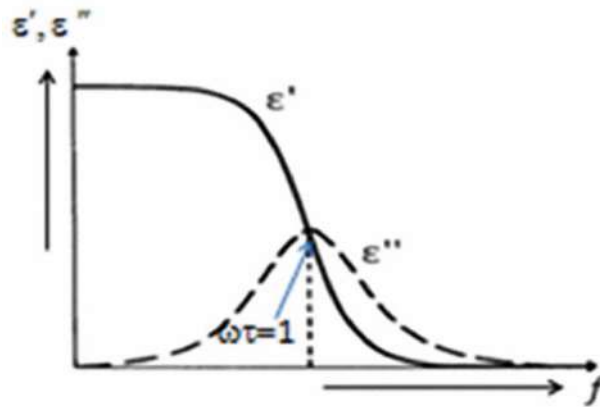


Figure 4. Schematic representation of dielectric permittivity (ϵ' and ϵ'') plotted as a function of frequency, f (Hz).

With help of DRS one can measure the complex dielectric permittivity, $\epsilon^*(\omega)$ expressed as:

$$\epsilon^*(\omega) = \epsilon' - j\epsilon'' \quad (2)$$

where ϵ' is dielectric constant associated with charge storage properties of the dielectric/polymeric material and ϵ'' is the dielectric loss which is a measure of energy losses. The real and imaginary parts of dielectric permittivity i.e., ϵ' and ϵ'' are calculated as follows;

$$\epsilon' = \frac{Z'}{(Z'^2 + Z''^2)\omega C} \text{ and } \epsilon'' = \frac{Z''}{(Z'^2 + Z''^2)\omega C} \quad (3)$$

where C is capacitance, ω ($=2\pi f$) is the angular frequency, Z' and Z'' are the real and imaginary parts of impedance estimated from impedance spectroscopic measurement. The ratio of loss factor (ϵ'') to dielectric constant (ϵ') is defined as loss tangent ($\tan\delta$) expressed as;

$$\tan \delta = \frac{\epsilon''}{\epsilon'} \quad (4)$$

The relaxation time (τ) is expressed as;

$$\tau = \frac{1}{2\pi f_r} \quad (5)$$

where f_r is the dielectric relaxation peak frequency estimated from Figure 4. Dielectric relaxation peak frequency, f_r (Hz) must satisfy the Arrhenius type behaviour expressed as;

$$f_r = f_0 \exp \frac{-E_a}{kT} \quad (6)$$

where f_0 is the pre-exponential factor, E_a is the activation energy in eV, k is Boltzmann constant and T is the temperature in K. The electric modulus analysis reveals the effect of electrode polarization and the conductivity relaxation mechanism can be analysed from the complex electric modulus spectra. The electric modulus M^* is defined as the reciprocal of complex relative permittivity, ϵ^* ;

$$M^* = \frac{1}{\epsilon^*} = M' + j M'' = \frac{\epsilon'}{(\epsilon'^2 + \epsilon''^2)} + j \frac{\epsilon''}{(\epsilon'^2 + \epsilon''^2)} \quad (7)$$

where M' is the real part and M'' is the imaginary part of the complex modulus M^* . The conductivity relaxation can be analysed from the complex electric modulus spectra.

6. POLYMER ELECTROLYTES

Polymer electrolyte (PE) was first introduced by Fenton and Wright in 1973, by complexing the alkali metal salts with polyethylene oxide (PEO) [18] whereas in 1979 its potential application was recognized by M. B. Armand [19]. Generally, polymer electrolyte is an ion conductors formed by the dissociation of alkali metal salt in suitable polymer network. In PE, polymer behaves like solvent and also provides conducting path/channel for the transportation of ions from one site to the other. Solid polymer electrolytes (SPEs) are mixed phase system i.e., crystalline phase (non-conducting), semi-crystalline (poorly conducting) and amorphous phase (conducting phase). In amorphous phase, more free volume is available and the polymer segment/chains have fast internal modes of bond rotations which produce faster segmental motion and hence higher conductivity. Liquid electrolytes have several limitations like leakage problem, bulky in shape and size, poor chemical stability and volatile in nature. Polymer electrolytes are an alternative of the liquid electrolytes with several advantages properties like high chemical stability, high energy density, good mechanical flexibility, proper electrode- electrolytes interface, ease of fabrication, mouldability and free from leakages.

For solid state electrochemical device applications point of view, the polymer electrolytes should have the following properties as follows: (i) High ionic conductivity $\sigma \sim 10^{-3} \text{ S cm}^{-1}$ at room temperature (ii) ionic transference number close to unity i.e., ~ 1 (iii) high thermal and chemical stability (iv) high electrochemical stability window and good mechanical strength (v) Compatibility with the electrode materials and proper electrode-electrolyte contact (vi) low activation energy [1, 3-5]. Figure 5 shows the some interesting properties of polymer electrolyte film.

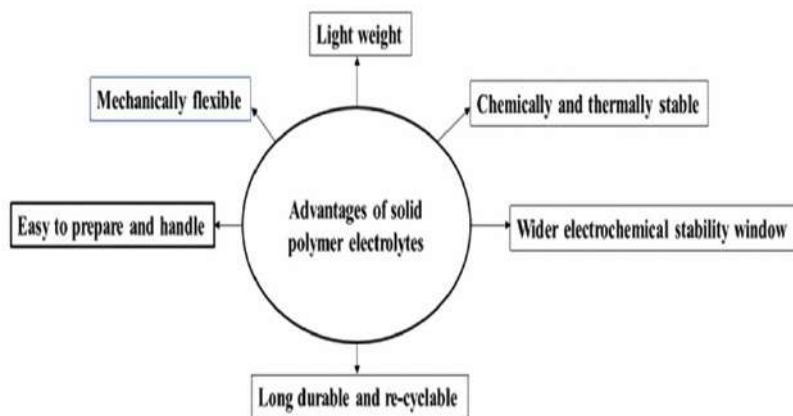


Figure 5. Some important properties of polymer electrolytes (PEs)/solid polymer electrolytes (SPEs).

7. APPLICATIONS OF SOLID POLYMER ELECTROLYTES (SPES)

Electrolyte is a key component (part) of any electrochemical device (EC). The important properties of polymer electrolytes like chemical stability, high energy density, long durability, leak proof, mechanical flexibility (for proper electrode-electrolyte contact) and electrochemical properties maximize the possibility of its applications in EC devices. These materials have different functions like (i) they can provide free charge carriers in the network (ii) behaves like adhesive and there is no need of any separator (to prevent short circuiting within the electrolyte) [18]. SPEs can be prepared by using polymer/polymer blend as host network and this network actually provides strong network and enhances the durability, safety related issues, minimizes the cost of the device and improves the performance of device [1-4]. The potential applications of SPE films are shown in Figure 6. In all the devices PE film provides free ions as well as behaves like separator (prohibited the internal short circuit). Several solid-state EC devices such as rechargeable batteries, electrochemical double layer capacitors, fuel cells (Figure 6) etc. can be developed by using solid polymer electrolytes.

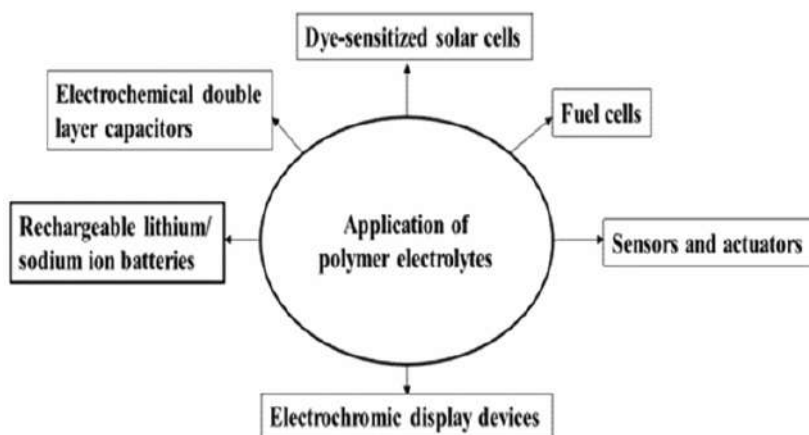


Figure 6. Potential applications of polymer electrolytes (PEs) in electrochemical (EC) devices.

8. PREPARATION OF POLYMER ELECTROLYTE FILMS

To prepare polymer electrolyte (PE) films one can use polymer/polymer blend/biopolymer as a host matrix and alkali metal salts based on lithium ion or sodium ion such as lithium tetra-fluoro borate (LiBF_4), lithium per chlorate (LiClO_4), methyl sulphate sodium salt (MeSO_4Na), sodium iodide (NaI), etc as an additives. Solution caste technique/hot press technique can be used for the preparation of solid polymer electrolyte films. The prepared polymer electrolytes based on above said materials have low room temperature ionic conductivity $\sim 10^{-5}$ - 10^{-6} S/cm due to poor amorphicity and less polymer chains flexibility [20, 21]. In order to enhance the room temperature ionic conductivity several approaches have been made and samples were optimised [22]. In this chapter, the PE films based on CS-PVP-PEG-NaI-IL were prepared using conventional solution casting method. The materials such as chitosan (CS), poly(vinyl) pyrrolidone (PVP), polyethylene glycol-200(PEG-200), Ionic liquid: 1-ethyl-3methylimidazolium methyl sulphate $[\text{EMIM}][\text{MeSO}_4]$ and salt NaI-sodium iodide have been used to prepare PE films.

9. IONIC LIQUID

Ionic liquids (ILs) are molten salts which are composed of weakly co-ordinated and self dissociated organic cations (bulky in size) and inorganic/organic anions. The chemical bonding between asymmetric organic cations and anions of IL is not so strong as compared to alkali metal ionic salts like NaI, NaCl, KCl, etc. Hence ILs has low lattice anergy and don't need any solvents for its dissociation into cations and anions. Generally, ILs remains its physical state as molten state at below 100°C called as room temperature ionic liquids (RTILs). By varying the size of cation and anion one can tailor the physical and chemical properties of IL. ILs have several important

properties like High ionic conductivity, high chemical stability, high electrochemical stability window, negligible vapour pressure, low melting temperature, etc [20-22]. But liquid nature of IL limits its performance in electrochemical devices like batteries, electrochemical capacitors, fuel cells, dye-sensitized solar cells. Therefore, in order to use the IL as electrolyte it should be trapped into a polymer/polymer blend/bio-polymer network.

10. IMPORTANT PROPERTIES OF POLYMER ELECTROLYTES

10.1. Ionic Conductivity Study

The polymeric film was cut into desired shape and sandwiched between two blocking electrodes of 1 cm² area for impedance spectroscopic measurements. The measurement of ionic conductivity from impedance spectroscopy of PE film was performed using HIOKI IM3536 LCR tester, Japan in the frequency range 4Hz to 1MHz. The dc conductivity, σ_{dc} of the sample can be calculated by using the expression:

$$\sigma_{dc} = \frac{t}{R_b \times A} \quad (8)$$

where 't' is thickness of the sample and 'A' is the electrode-electrolyte contact area. R_b is bulk resistance estimated from the intercept on the real impedance axis of the Nyquist plot (Figure 7). The ionic conductivity of the PE film was measured in the frequency range 4Hz to 8MHz with the applied bias voltage 100 mV. The Nyquist plot of prepared PE film at 30°C is shown in Figure 7.

The Cole-Cole plot shows the two well defined regions, namely high frequency region i.e., a semi-circular arc and inclination spike at low frequency region [23]. The bulk dc conductivity, σ_{dc} value was estimated from Cole-Cole plot and it is found to be $\sim 3.03 \times 10^{-4}$ S/cm at 30°C. Figure 7 (b) shows the temperature dependent dc conductivity prepared PE film. Here, at low temperature ($T \leq 60^\circ$) i.e., below T_g , the linear relationship between dc conductivity. The temperature dependent electrical conductivity can be explained by Arrhenius equation [24] as follows:

$$\sigma_{dc} = \sigma_0 \exp\left(\frac{-E_a}{k_B T}\right) \quad (9)$$

where σ_0 is pre-exponential factor, E_a is the activation energy and k_B is the Boltzmann constant. This equation signifies that the motion of ions is temperature dependent. In this region, an ion jumps to nearest vacant site, which causes the dc conductivity [25]. At higher temperature ($T \geq 60^\circ\text{C}$), the pattern of $\log \sigma_{dc}$ vs $1000/T$ is almost linear and also follows the Arrhenius type thermally activated process.

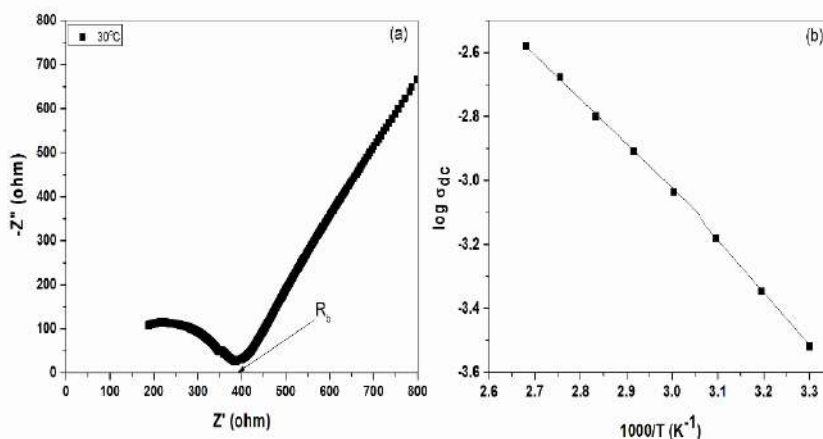


Figure 7. (a) The complex impedance plot (Cole-Cole plot) of IL based PE film at 30°C and (b) $\log \sigma_{dc}$ vs. $1000/T$ plot for prepared PE film.

10.2. AC Conductivity Study

The forward-backward co-related hopping of charge carriers gives rise to AC conductivity. Fig.8 shows the AC conductivity spectra at different temperature for the chitosan-based biopolymer blend electrolyte film.

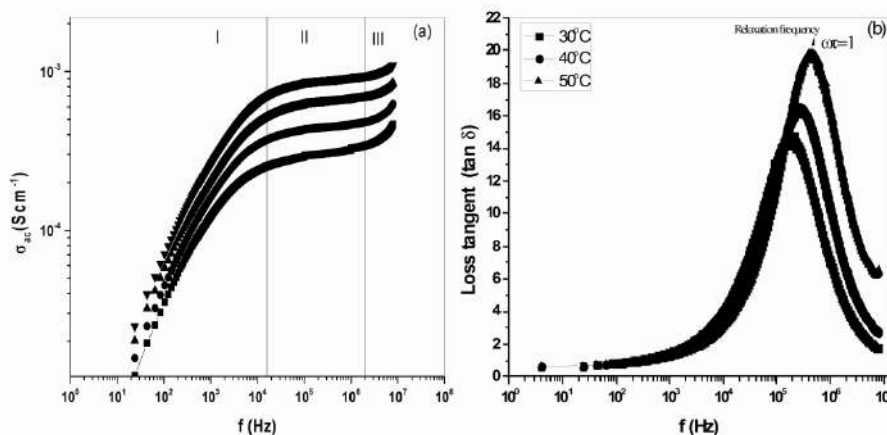


Figure 8. (a) AC conductivity spectra of prepared PE film at different temperatures (30-60°C) and (b) variation of loss tangent ($\tan \delta$) with frequency at different temperatures.

From Figure 8 it has been observed that the AC conductivity spectra consists of three regions; (i) low-frequency dispersive region, (ii) frequency-independent intermediate region and (iii) high-frequency dispersive region. The low-frequency dispersive region is due to electrode polarization effect at the blocking electrode-electrode interface. In this frequency region, conductivity decreases with decrease in frequency as more charge will accumulate near the electrode-electrolyte interface.

This accumulation decreases the free charge carriers and hence conductivity decreases. The mid frequency region is associated with free hopping of charge carriers with adjacent sites [26] which contribute to DC conductivity. In high frequency region, conductivity increases with increasing frequency due to capacitive effect. For the present system, conductivity versus frequency curve follows the Jonscher's power law, stated as:

$$\sigma(\omega) = \sigma_{dc} + A\omega^s \quad (10)$$

where, σ_{dc} , A , s , and ω are the dc conductivity, pre-exponential factor, fractional exponent and angular frequency, respectively. The frequency at which the conductivity starts following the power law is called the critical or hopping frequency ω_p . AC conductivity increases with increasing temperature. Also, the hopping frequency shift towards higher frequency with increasing temperature. The increase in the conductivity is due to:

1. Higher number of free charge carriers due to higher dissociation of salt and
2. Higher mobility of the hopping ions at higher temperature.

10.3. Dielectric Permittivity Study

Dielectric studies are required to understand the relaxation behaviour of polymer electrolytes. In polymer salt complexes, dielectric behaviour is a complicated property which is controlled by many factors such as (i) Change in polymer morphology due to addition of salt, (ii) Dielectric response of polymer backbone and side chains (normal mode and segmental mode), (iii) Coupling and/or decoupling of ion and segmental motion, and (iv) Ion relaxation arising from localized movement of ions, etc.

10.3.1. Dielectric Constant Analysis

Dielectric permittivity, ϵ is physical property of material which characterizes the degree of electrical polarization that a material experiences under the influence of an external electric field. It is also used to measure the energy stored in the material. It is defined as the ratio between the electric field (\vec{E}) within a material and corresponding electrical displacement vector, \vec{D} ;

$$\epsilon = \frac{\vec{D}}{\vec{E}} \quad (11)$$

It is also referred as the ability to hold an electrical charge. In polymer electrolyte, permittivity is a frequency dependent complex function as defined in Eq. (2).

The real part of permittivity corresponds to ordinary dielectric constant of material which measures the amount of elastic energy stored in the material during every cycle of applied alternating electric field. Higher value of ϵ' corresponds to better conductivity of material. Figure 9 (a) and (b) shows the dielectric constant (ϵ') and dielectric loss (ϵ'') as a function of frequency. Sharp increase is observed in ϵ' at lower frequency due to the electrode polarization and space charge effect [27]. The increase in dielectric permittivity (ϵ') in the low-frequency region is due to accumulation of more charge carriers at the electrode–electrolyte interface.

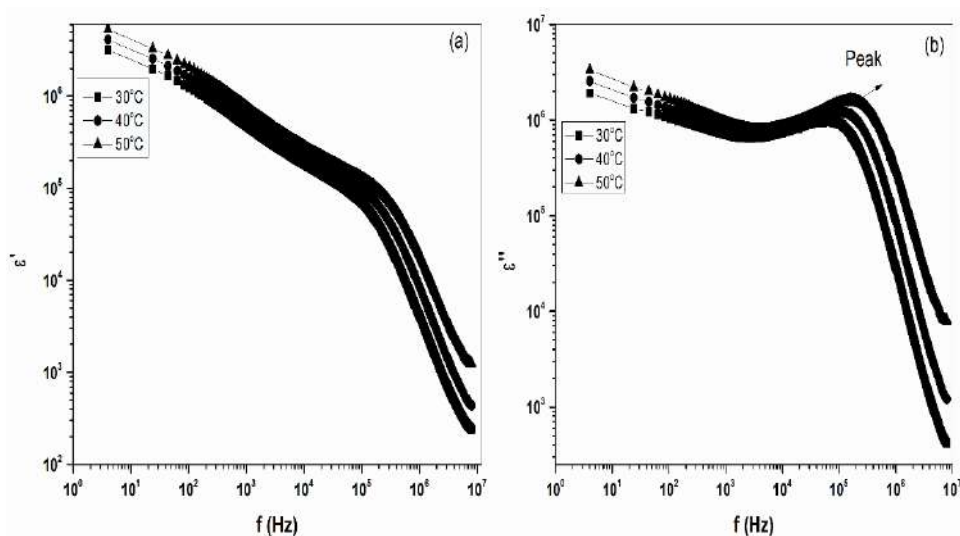


Figure 9. The variation of real and imaginary parts of electric permittivity, ϵ' and ϵ'' with the frequency (Hz) at different temperatures.

At high frequency, the accumulation of charge carriers decreases at the electrode–electrolyte interface due to the high periodic reversal of the electric field and hence the dielectric permittivity decreases. The dielectric permittivity increases with increase in temperature, which is due to an increase in the number of charge carriers resulting from the dissociation of ion aggregates [28].

10.3.2. Dielectric Loss Analysis

Energy dissipation arising from charge transport and electrode polarization effect can be measured from dielectric loss. Figure 9 (b) shows the dielectric loss (ϵ'') as a function of frequency at different temperatures from prepared polymer electrolyte. Dielectric loss is generally comprised of contributions from ionic transport and from charge polarization or a dipole. Accumulation of charges at the electrode–electrolyte interface can be regarded as a polarization of macro-dipoles and results in a peak in the dielectric loss spectra [29]. The loss peak is situated in the region where dc conductivity dominates, which confirms the contribution of ionic conduction to the dielectric loss peak. As the temperature increases the peak shift towards the high

frequency region which may be related to the flexibility of polymer chain and increase in charge carrier density at higher temperature.

10.4. Loss Tangent (Tan δ) Analysis

Dielectric loss tangent, $\tan\delta$ is a measure of ratio of electrical energy lost to electrical energy stored in the polymer electrolyte system due to external applied electric field. It can be formulated as the ratio of loss factor (ϵ'') of the permittivity to the dielectric constant (ϵ') defined by Eq. 5. It is a dimensionless quantity. The dielectric loss tangent as the function of frequency has been plotted in Figure 8(b). The $\tan\delta$ increases with increase in frequency and reaches its maximum value and further decreases with increase in frequency. This behaviour is due to the ion jump and dc conductivity loss of ion [30]. Also, as the temperature increases the peak of the curve shifted towards higher frequency side. The height of peak also increases with temperature. This is due to the fact that at higher temperature the charge carrier movement is easier and thus capable of relaxation at higher frequency [31]. The relaxation time, τ and frequency of peak (ω) is related as: $\omega\tau = 1$. Hence with the increase in temperature, the relaxation time decreases. From Figure 8(b), it has been observed that at lower frequency, when $\tan\delta$ increase, the ohmic component of current increases more sharply than its capacitive component. Also, at higher frequency, where $\tan\delta$ decreases, the capacitive component ($X_c = \frac{1}{\omega C}$) decreases due to very high frequency [32].

10.5. Electric Modulus Analysis

The complex electric modulus (M^*) formalism is frequently used when the relaxation behaviour is presumed due to the motion of ions or electron. Dielectric relaxation is due to the re-orientation process of dipoles in the polymer chain. The real and imaginary part can be obtained from impedance spectroscopy and are given as: $M^* = M' + jM''$, where the real part of electric modulus, $M' = \frac{\epsilon'}{\epsilon'^2 + \epsilon''^2}$ and the imaginary part of electric modulus: $M'' = \frac{\epsilon''}{\epsilon'^2 + \epsilon''^2}$ as already discussed in Eq. (7). The dependency of real part of electric modulus on frequency at different temperatures is shown in Figure 10 (a). We can see that M' is tending towards zero at low frequency and its value is higher at high frequency. The appearing of long tail in low frequency region is due to the large capacitance associated with the electrode [33]. The higher value of M' at higher frequencies is associated with relaxation processes. The value of M' decreases with increase in temperature. This shows that the conduction is due to the short-range mobility of charge carriers. Figure 10 (b) shows the variation of M'' with

frequency at different temperatures. The small value of M'' toward low frequency region indicates the migration of ion. Rising of the M'' value with frequency is related with long-range random hopping, and it passes through hidden peak where this long-term motion is restricted to caged motion at higher frequency [34]. As the temperature increases, long range motion of ions becomes more feasible. Ions have greater kinetic energy and hence greater chance to overcome lattice potential, and hence, long distance hopping can be observed even at higher frequency, resulting in M'' vs frequency curve peak shifting toward higher frequency.

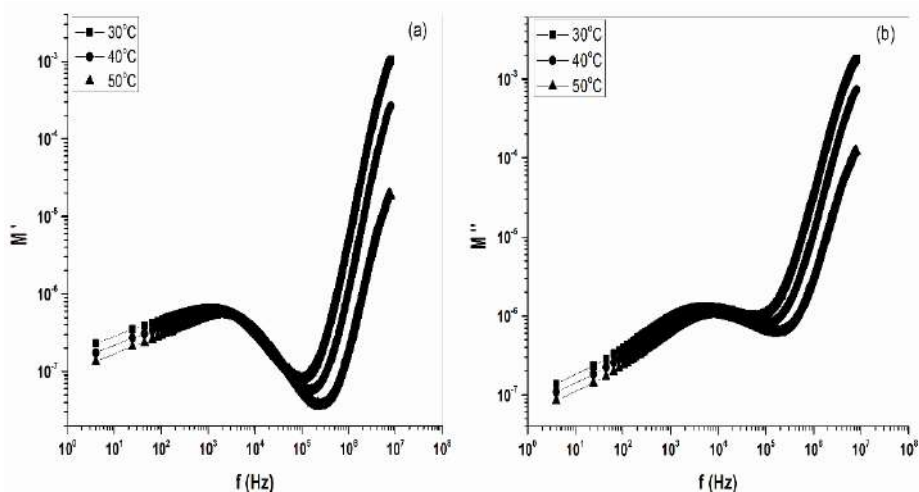


Figure 10. The variation of (a) real, M' and (b) imaginary, M'' parts of electric modulus with the applied frequency at different temperatures.

CONCLUSION

Polymeric materials are very useful for society and these materials can also be used as host matrix for the preparation of polymer electrolyte films. Worldwide many researches are involved to enhance the room temperature ionic conductivity, mechanical flexibility, chemical stability and compatibility with the electrodes. Complex impedance spectroscopy/ electrochemical impedance spectroscopy is a powerful tool to study the electrical transport properties of the different conducting materials like solid polymer electrolytes, amorphous materials. The electrochemical impedance spectroscopic measurement provides the information about diffusion of charge carriers (diffusion coefficient), mobility of charge carriers, ionic conductivity, dielectric properties, number density of charge carriers and electric modulus for conducting systems.

ACKNOWLEDGMENT

The author is thankful to Science and Engineering Research Board (SERB), India for financial assistance by the major research grant EEQ/2018/000862.

REFERENCES

- [1] Bruce, P. G. 1995. *Solid State Electrochemistry*. Cambridge University Press, Cambridge.
- [2] Gray, F. M. 1991. *Solid Polymer Electrolytes: Fundamentals and Technological Applications*, VCH, New York.
- [3] Gray, F. M. 1997. *Polymer Electrolytes. RSC Materials Monographs*, The Royal Society of Chemistry, Cambridge
- [4] Vincent, C. A. (1987). Polymer electrolytes. *Prog.Solid State Ch.* 17: 145–261.
- [5] Gowariker, V. R., Viswanathan, N. V. and Sreedhar, J. (2005). *Polymer Science*. New Age International.
- [6] Billmeyer, F. W. 1984. *Textbook of Polymer Science*. John Wiley & Sons.
- [7] https://en.wikipedia.org/wiki/Polymer_chemistry.
- [8] MacCallum, J. R., Vincent, C. A. 1987. *Polymer Electrolyte Review-I &II*. London: Elsevier.
- [9] Shirakawa, H. Nobel Prize in Chemistry 2000. Nobel Lecture Video and autobiography. *Nobele-Museum*. <http://www.nobel.se/chemistry/laureates/2000/index.html>.
- [10] Dutta, P. K., Dutta, J. and Tripathi, V. S. (2004). Chitin and chitosan: Chemistry, properties and applications. *J. Sci. Ind. Res.* 63: 20-31.
- [11] Itoh, T., Ichikawa, Y., Uno, T. Kubo, M. and Yamamoto, O. (2003). Composite polymer electrolytes based on poly (ethylene oxide), hyperbranched polymer, BaTiO₃ and LiN(CF₃SO₂)₂. *Solid State Ion.* 156: 393–399.
- [12] Jung, Y. C., Lee, S. M., Choi, J. H., Jang, S. S. and Kim, D. W. (2015). All Solid-State Lithium Batteries Assembled with Hybrid Solid Electrolytes. *J. Electrochem. Soc.* 162: A704–A710.
- [13] Sun, H. Y., Yakeda, Y., Imanishi, N., Yamamoto, O. and Sohn, H. J. (2000). Ferroelectric Materials as a Ceramic Filler in Solid Composite Polyethylene Oxide-Based Electrolytes. *J. Electrochem. Soc.* 147: 2462–2467.
- [14] Sudhakar, Y. N., Selvakumar, M. and Bhat, D. K. (2018). *Biopolymer electrolytes fundamental and application in energy storage*. Elsevier.
- [15] Winie, T., Arof, A. K. 2016. *Biopolymer Electrolytes for Energy Devices. Nanostructured polymer Membranes*. Scrivener Publishing LLC.2: 311–356.
- [16] Navaratnam, S., Ramesh, K., Ramesh, S., Sanusi, A., Basirun, W. J. and Arof, A.K. (2015). Transport Mechanism Studies of Chitosan Electrolyte Systems. *Electrochim. Acta.* 175: 68–73.

- [17] Bharati, D. C., Kumar, H. and Saroj, A. L. (2019). Chitosan-PEG-Nal based bio-polymer electrolytes: Structural, thermal and ion dynamics studies. *Mater. Res. Express*. 6: 12.
- [18] Fenton, D. E., Parker, J. M. and Wright, P. V. (1973). Complexes of alkali metal ions with poly (ethylene oxide). *Polymer* 14: 589.
- [19] Ramesh, S. and Lu, S. C. (2012). Enhancement of ionic conductivity and structural properties by 1-butyl-3-methylimidazolium trifluoromethanesulfonate ionic liquid in poly(vinylidene fluoride-hexafluoropropylene) – based polymer electrolytes. *J. Appl. Polym. Sci.* 126: 484-492.
- [20] Saroj, A. L., Singh, R. K. and Chandra, S. (2014). Thermal, vibrational, and dielectric studies on PVP/LiBF₄ + ionic liquid [EMIM][BF₄]-based polymer electrolyte films. *J. Phys. Chem. Solids*. 75: 849-857.
- [21] Saroj, A. L. and Singh, R. K. (2012). Thermal, dielectric and conductivity studies on PVA/Ionic liquid [EMIM][EtSO₄] based polymer electrolytes. *J. Phys. Chem. Solids*. 73: 162-168.
- [22] Saroj, A. L., Singh, R. K. and Chandra, S. (2013). Studies on polymer electrolyte poly(vinyl pyrrolidone (PVP) complexed with ionic liquid: Effect of complexation on thermal stability, conductivity and relaxation behaviour. *Mater. Sci. Eng. B*. 178: 231-238.
- [23] Selvasekarapandian, S., Baskaran, R. and Hema, M. (2005). Complex AC impedance, transference number and vibrational spectroscopy studies of proton conducting PVAc–NH₄SCN polymer electrolytes, *Phys. B Condens. Matter*. 357: 412–419.
- [24] Grossi, M. and Riccò, B. (2017). Electrical impedance spectroscopy (EIS) for biological analysis and food characterization: A review. *J. Sens. Sens. Syst.* 6(2): 303-325.
- [25] Rault, J. (2000). Origin of the Vogel-Fulcher-Tammann law in glass-forming materials: The α - β Bifurcation. *J. Non-Cryst. Solids*. 271: 177–217.
- [26] Mariappan, C. R. and Govindaraj, G. (2005). Conductivity and ion dynamic studies in the Na_{4.7+x}Ti_{1.3-x}(PO₄)_{3.3-x} (0≤x≤0.6) NASICON material. *Solid State Ion*. 176, 1311.
- [27] Shukla, N. and Thakur, A. K. (2011). Enhancement in electrical and stability properties of amorphous polymer blend nanocomposite electrolyte. *J. Non-Cryst. Solids*. 357:3689-3701.
- [28] Tripathi, S. K., Gupta, A. and Kumari, M. (2012). Studies on electrical conductivity and electrical behaviour of PVdF-HFP- PMMA-Nal polymer blend electrolyte. *Bull. Mater. Sci.* 35: 969-975.
- [29] Stephan, A. M., Kumar, T. P., Renganathan, T. G., Pitchumani, S., Thirunakaran, R. and Muniyandi, N. (2000). Ionic conductivity and FT-IR studies on plasticized PVC/PMMA blend polymer electrolytes. *J. Power Sources*. 89: 80-87.
- [30] Dave, G. and Kanchan, D. K. (2018). Dielectric relaxation and modulus studies of PEO-PAM blend-based sodium salt electrolyte system. *Indian J. Pure Appl. Phys.* 56: 978-988.

- [31] Koops, C. G. (1951). On the dispersion of resistivity and dielectric constant of some semiconductors at audio frequencies. *Phys. Rev.* 83: 121–124.
- [32] Louati, B., Hlel, F. and Guidara, K. (2009). Ac electrical properties and dielectric relaxation of the new mixed crystal $(\text{Na}_{0.8}\text{Ag}_{0.2})_2\text{PbP}_2\text{O}_7$. *J. Alloy. Compd.* 486: 299–303.
- [33] Khiar, A. S. A., Puteh, R. and Arof, A. K. (2006). Conductivity studies of a chitosan-based polymer electrolyte. *Physica B: Condensed Matter.* 373: 23-27.
- [34] Das, S. and Ghosh, A. (2015). Ionic conductivity and dielectric permittivity of PEO-LiClO₄ solid polymer electrolyte plasticized with propylene carbonate. *AIP Advances.* 5: 027125.

Chapter 6**CARBON AND TRANSITION METAL TWO
DIMENSIONAL QUANTUM DOTS: NEW ERA
OF MATERIAL SCIENCE*****Madhu Tiwari****Department of Chemistry, Kashi Naresh Government Post Graduate College,
Gyanpur, Uttar Pradesh, India**ABSTRACT**

Current advancement in the efficient quantum dots (QDs) development have offered new domain for the exploration of sensors, batteries, bio imaging, optoelectronic and electrochemical device fabrication due to their intriguing optical, electrical, electrochemical and catalytic properties. These intriguing properties have led them to their extraordinary success and have triggered their exploration. Although the research in the synthesis and evolution of their intriguing properties are in its initial stage and lots of challenges are still existing. The two-dimensional quantum dots (2D-QDs) derived from phosphorene, transition metal dichalcogenide (TMD) and graphene have been of significant interest among QDs for the last few years. Various literatures of graphene derived QDs are available but the transition metal derived QDs are continuously growing extensive interest in the scientific community as it fill up the key issue of easily oxidizable phosphorous-based QDs in air, thus the synthesis and fundamental property evolution of these emerging 2D-QDs need to be explored. Further the effective implementation of these 2D-QDs into the mentioned applications depends on the effectiveness of patterning or printing QDs from solutions onto the predetermined solid substrate locations. The frequently used techniques, includes bubble printing Langmuir-Blodgett printing, contact printing, ink-jet printing, microtransfer printing and have promising achievement of quite high-resolution patterning down to the single-QD level. This chapter focuses the synthesis, printing techniques and properties of carbon, transition metal 2D-QDs and their efficient application in

* Corresponding Author's Email: madhurchem@gmail.com.

photodetectors, batteries, supercapacitors and wastewater treatment. Additionally the 2D-QDs assembly to boost up the performance and to achieve the necessities of industrial scale production for various applications in the quantity, quality and productivity is investigated and highlighted.

Keywords: 2D hetero-structured QDs, transition metal dichalcogenide, properties, applications

1. INTRODUCTION

Quantum dots (QDs) are semiconductor nano-particles, with unique properties and interesting phenomena of size dependent emission wavelength, narrow emission peak and broad excitation range in which excitons are confined in all three spatial dimensions. Due to quantum confinement effects, QDs behaves like artificial atoms with controllable discrete energy levels. First QDs was fabricated by Louis E. Brus in the 80's and the exceptional properties of these distinctive nano-structures attracted much interest. Owing to the interesting properties of graphene and its great achievement, the exploration of other two dimensional materials has been triggered and encouraged such as phosphorene transition metal dichalcogenides (TMDs) and hexagonal boron nitride (hBN) derived from layered bulk crystals analogous to graphite. These classes of materials cover the applications in a widespread range including optoelectronics, electronics, catalysis, energy storage and sensors. However, the challenging concerns of the 2D materials e.g., low absorptivity and zero band gap have encouraged scientists to explore the structural modification to overcome the limitations. Conversion of 2D materials to 0D (i.e., lateral sizes reduction to <20 nm) results change in properties due to prominent edge effects and quantum confinement [1-3]. For instance, graphene quantum dots (GQDs) started fluorescing as the crystal boundary considerably modifies the electron distribution due to the decreased dimension of the crystal to nanometer scale. Many of their characteristics are tremendously superior to those of conventional semiconductor quantum dots, and thus have prompted to several potential applications in optical sensing, bioimaging, energy storage and conversion photovoltaics [4].

Recent investigation on GQDs unlocks a novel dimension and vitalizes the great anticipations about the prospective of two-dimensional quantum dots (2D-QDs). Amazingly, the introduction of these 2D-QDs into the mentioned applications depends on the effective printing or patterning QDs from solutions onto the prearranged positions of solid substrates. The main implemented techniques, including microtransfer printing, bubble printing, Langmuir-Blodgett printing contact printing and ink-jet printing have exposed tremendously high-resolution patterning down to the single-QD level [5-6]. Thus, acquiring heterostructured 2D-QDs and patterning them is important. Although the study of 2D-QDs is till at an initial stage and superior understanding relating to their properties instantly led to thorough exploration of basic and important properties, applications, which have still to be located. Many chapters

on the synthesis, properties and applications of QDs have been issued in current years but the comprehensive and relative studies on heterostructure 2D-QDs and their patterning are still missing. This chapter summarizes the synthesis and properties of 2D-QDs, mainly GQDs and TMD-QDs.

2. SYNTHESIS OF 2D-QDs

The synthesis of 2D-QDs is categorized into two parts: top-down and bottom-up approaches. For the top-down method, disintegration and exfoliation of low-cost, easily available bulk materials in harsh environments are directed to get QDs using physical, chemical or electrochemical methods. The bottom-up process uses atomic or molecular precursors for the QDs formation. Fascinating benefits of this process are larger atomic utilization, improved structural regulation and the governing factor of morphology and size.

2.1. Synthesis of Graphene Quantum Dots (GQDs)

2.1.1. Top Down Approach

2.1.1.1. Solvothermal or Hydrothermal

The solvothermal or hydrothermal synthesis method is nontoxic, cheap and environment friendly method for the synthesis of GQDs from bulk. Under high pressure, thermally reduced graphene oxide (RGO) sheets as precursor yields the formation of graphene quantum dots. These RGOs are exposed to oxidizing agents e.g., O_3 or HNO_3 to produce epoxy groups at the cleavage sites in the carbon lattice resulting in reduced size RGO and being 9.6 nm average diameter GQDs after the hydrothermal deoxidation with 5% yield (Figure 1).

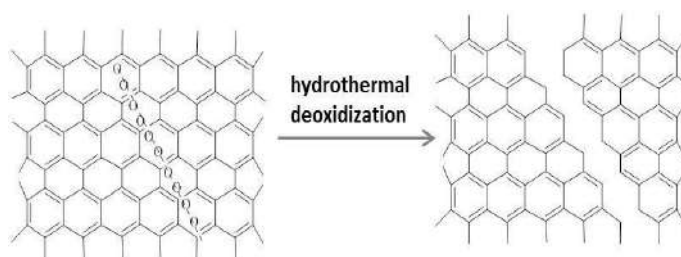


Figure 1. Schematics of GQD fabrication by top-down approach via Hydrothermal method.

2.1.1.2. Electrochemical Exfoliation

The electrochemical exfoliation (EC) process is a one-step process that always results in high yield GQDs by chemical vapor deposition (CVD) made graphene, RGO films, electrochemical cutting from carbon nanotubes (CNT), graphite rods. Here, the corrosion caused by hydroxyl and oxygen radicals obtained from the anodic oxidation

of H₂O function as electrochemical scissors originated at edge locations and accelerated at the defect locations to release GQDs [7].

2.1.1.3. Acid Etching

This process uses HNO₃ treatment to exfoliate GQDs from bulk. GODs are formed from acidic solution by negatively charged oxygenated groups, and adjust their properties by creating hydrophilic surfaces of GQD and increasing the defective sites. The greatly rich defective sites affect GQD surface area and improve its performance [8].

2.1.1.4. Ultrasonicated Exfoliation

This is environment friendly and cost effective method to make GQDs applying mechanical force and cutting a bulk precursor. GQDs can be prepared by cutting graphene sheets with an ultrasonic treatment after various purification steps with the help of a solvothermal process. Additionally, graphene sheets can be oxidized by ultrasonic treatment under acidic conditions. However, numerous steps comprise oxidation in acidic media and the microwave treatment or solvo–thermal required for this method to make uniform GQDs [9].

2.1.2. Bottomup Approach

2.1.2.1. Organic Precursor Carbonization

The process of carbonization involves condensing the organic moiety by heating them above their melting points, which stimulates the nucleation thus result the formation of GQDs (Figure 2) [10]. This method is easy, cheap, has the large-scale ability and lets the natural inheritance of heteroatoms from precursors.

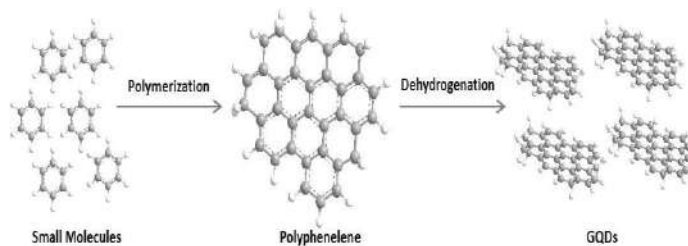


Figure 2. Schematics of GQD fabrication by bottom–up approaches via Carbonization.

2.1.2.2. Additional Approaches

The other remaining bottom-up methods as ruthenium-catalyzed cage opening of fullerene C₆₀ and chemical synthesis are also accomplished to formulate GQDs. Moreover, these methods need challenging conditions using complex steps and problems in getting rid of the aggregates formed by π – π interactions. Additionally, the oxidative condensation of aryl groups of polyphenylene dendritic precursors in a solution process started fusing graphene moieties with the final construction of GQDs [11].

2.2. Synthesis of Transition Metal Dichalcogenide Quantum Dots (TMD-QDs)

2.2.1. Top Down Approach

2.2.1.1. Potassium/Lithium Intercalation

K/Li intercalation based liquid exfoliation process is referred to be an efficient path to get large-scale manufacture of monolayer 2D-QDs. Taking advantage of the huge interlayer distance of TMD materials, much more than graphite, K and Li intercalation into its bulk are utilized to make MoS_2 and WS_2 QDs. This method composed of the whole cutting off round edges and defects by breaking down the 2D layered structure during reaction. Under ambient conditions, these TMD QDs are synthesized by Na^+ intercalation besides alkali metal intercalation due to the reaction medium restriction. Furthermore, Li intercalation based multistep liquid exfoliation from bulk 2H- MoS_2 powder are established to make monolayer MoS_2 -QDs [12]. These QDs size is largely decreased by two-step Li intercalation followed by exfoliation in water, vacuum drying, and again Li intercalation results 2-5 nm MoS_2 -QDs.

2.2.1.2. Ultrasonication Assisted Liquid Exfoliation

Liquid exfoliation lacking K or Li intercalation definitely produces a layer aggregation in suitable solvents, which is a serious issue of this process [13]. It has been overwhelmed by the modified liquid exfoliation technique and implemented to overcome this by bath sonication followed by ultrasonication as presented in Figure 3. The combination of the bulk MoS_2 cleavage into tiny particles by a bath sonication method with the help of hydrodynamic forces and breakdown of bulk layer into ultrathin sheets by ultrasonication results formation of 2 nm MoS_2 -QDs.

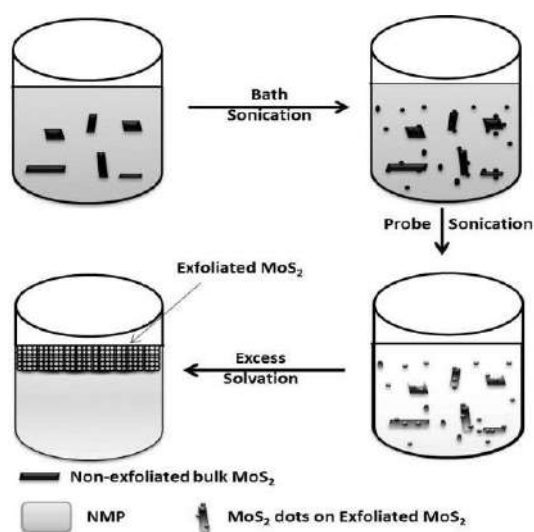


Figure 3. Schematics of TMD-QDs preparation by top-down approach *via* liquid exfoliation assisted ultrasonication.

2.2.1.3. Electro–Fenton

TMD-QDs are also produced by an electrochemical process on a large scale similarly to the exfoliation of GQDs. In general, the electro–Fenton reaction is a fascinating method as it is easy, cost–effective, and controlled process, which involves in situ hydrogen peroxide generation and the addition of ferrous ions addition permits increment of oxidation *via* the hydroxyl radicals generation tuned by the electrochemical process. This reaction occurs towards cathode side where the effect of radicals depends solely on the reaction time [14]. This method provides the controlled high yield consecutive development of 5 nm plane size uniform MoS₂-QDs.

2.2.2. Bottom up Approach

2.2.2.1. Solvothermal

This method uses small molecules to prepare QDs. Thiourea and ammonium molybdate are used as the capping agent in the presence of N-acetyl-L-cysteine as precursors of Mo and S to confine the hydrothermal growth of MoS₂-QDs. The optimum reaction time is necessary to get QDs in terms of avoiding overgrowth or nongrowth of MoS₂ following the decomposition of thiourea, nucleation and epitaxial growth thus providing single layer formation of 2.5 nm sized uniform MoS₂. Likewise precursors, variation and use of sodium molybdate, sodium molybdate, dibenzene disulfides and L-cysteine results a tunable size of QDs of 3.6 nm and 1.79 nm [15]. Furthermore, 2 to 7 nm tuned size of MoS₂ QDs can be obtained in oleylamine solvent in solvothermal reaction.

3. PROPERTIES OF 2D QDS

3.1. Properties of GQDs

Graphene segment exhibit quantum confinement effect due to infinite Bohr diameter existence of its excitons followed to nonzero bandgap and luminescence on excitation. This bandgap is tunable by altering the surface chemistry and size of GQDs. GQDs displays absorption between 270-390 nm due to $n-\pi^*$, 200 and 270 nm for the $\pi-\pi^*$ transition of C=O functional groups. These absorption features can be varied by the functionalizing GQDs, influencing the properties of PL [16]. The band gap depends on the size of GQD since the increase in size causes decrease in gap progressively. Thus, small sized GQDs release shorter wavelengths due to the quantum confinement effect by the bandgap opening. Although, the strong support from the theoretical study directly decide the size-dependent bandgap of the GQDs initiated by quantum confinement. Apart from the size-dependency, PL is intensely affected by additional aspects, including edge configurations, chemical groups, defects, geometry and heteroatom dopants. Furthermore, these aspects command the catalytic and electrochemical properties of GQDs due to the single-electron transfer. The abundant

edge sites and huge specific surface area present in GQDs proficiently improve its electron transfer. Excitingly, GQDs with oxygenated groups at the basal plane reduce electron transfer due to the disruption of the conducting sp^2 carbon network while edges oxygen groups provide the catalytic properties of GQD [17]. The GQDs catalytic properties are controlled by electron withdrawing groups, donating, heteroatom dopants and vacancy imperfections that serve as active sites. Highly abundant on earth with enormously low toxicity and solubility in several solvents are the key factors of GQDs.

3.2. Properties of TMD-QDS

TMD covers a vast range of physiochemical properties. TMD is single-layered and noncentrosymmetric material of general formula MX_2 where two hexagonal planes of chalcogen atoms (X) covalently sandwich the plane of transition metal atoms (M) with the formal oxidation states of -2 and $+4$ with chalcogen and metal, respectively. The single layered TMD has two types, followed by the arrangement of the chalcogen and metal in the X-M-X structure. Usually, octahedral or trigonal prismatic honeycomb motif referred to 1T metallic phase and 2H semiconductor phase is two polytypes present in TMD materials. The intraplane X-M-X bonds are ruptured to make QDs; monolayer MoS_2 -QDs are metallic since the unsaturated coordinate Mo atoms are at the edges. Therefore, the quantum confining effects open the TMD-QDs bandgap. The bandgap is also affected by dopants, functional groups and defects. The intense absorption at 277 nm is due to the optical transition between the density of state peaks in the conduction and valence bands. The multiple PL emission peaks with nanosecond lifetimes are detected in the blue-green region for WS_2 -QDs due to spin-valley couplings of improved quantum yield. The strong effect of functional groups as NAC on MoS_2 -QDs displays uncommon up-conversion PL with the most intense emission at 780 nm excitation wavelength [18]. Although, TMD-QDs and sheets have exciting charge storage capacity and electrocatalytic properties due to increased active sites caused by pseudo-capacitance behavior, easy intercalation process of foreign materials and quantum confinement.

4. APPLICATIONS

The distinctive properties of GQDs and TMD-QDs are highlighted in vast domain applications of water electrolysis, supercapacitors, energy, optoelectronics, photodetectors, batteries, and photocatalysis.

4.1. Water Electrolysis

Electrolysis of water produces hydrogen from the splitting of water because of the passage of electric current in an electrolyzer comprising three parts: a cathode, an electrolyte and an anode. When an external voltage is employed to the electrodes, water split into oxygen at the anode side and hydrogen at the cathode side (the thermodynamic voltage at 25°C is 1.23 V). Therefore, the water–decomposition reaction can be categorized into two main half–reactions: oxygen evolution reaction (OER) and hydrogen evolution reaction (HER) (Equations 1 and 2).



4.1.1. Hydrogen Evolution Reaction

It is the most investigated electrochemical reaction to store energy *via* hydrogen production to switch from traditional fossil fuels and is a potential solution for environmental and energy crises. Recently, nano TMDs of larger exposed active edge sites are proved to be one of the most competitive and potential candidates for HER. QDs of lesser diameter than 20 nm such as nanoflowers and nanosheets, exhibit higher conductivity, more edge sites and a larger specific surface area beneficial to the HER rather than other TMD structures. MoS₂–QDs are synthesized through precursor solution of 0.5 M thiourea and 10–30 mM ammonium molybdate by growing MoS₂ atomic layers using chemical bath deposition. Thereafter the MoS₂ layers are annealed for 1 h at 450 °C under Sulphur environment to increase the crystallinity of layers. The prepared MoS₂ layer display QD nature due to the nucleation growth of MoS₂ crystal. The Au/MoS₂-QD electrocatalyst shows exceptional performance, displaying a Tafel slope of 94 mV decade⁻¹ of exchange current density 0.191 mA cm⁻². MoS₂-QDs are synthesized electrochemically and the desired size of the QDs is achieved by tuning the applied DC voltage [19]. A homogeneous size range of 2.5–8 nm is achieved by altering the composition of the electrolyte. Thus, a MoS₂-QD developed *via* [BMIm]Cl–based 1 wt% aq electrolyte displays smaller Tafel slope 60 mV dec⁻¹ and lower onset potential 210 mV due to the more active edge sites in ultra-small MoS₂ nanoparticles of increased surface area. Now days TiO₂ nanotube arrays decorated MoS₂-QDs are fabricated by electro–deposition and they are the key photocatalyst that imparts to endorse photocatalytic activity on NIR irradiation [20]. The photocurrent density gets increased for the composite electrode rather than blank TiO₂, because the hole–electron pair gets separated from MoS₂-QD/TiO₂ nanotube arrays. The hole–electron pair originated from TiO₂ nanotubes in UV irradiation transfer the valence electrons to the conduction band and frequently transfer to MoS₂ *via* close interface for hydrogen evolution. Additionally, surface plasmon resonance (SPR) of MoS₂ is activated by visible light illumination; this SPR considerably increases the hole–electron creation and separation as shown in Figure 4. These improved photocatalytic activity of hetero–

structured 2D-QDs is credited due to enhanced light absorption to diminish the activation barrier with abundant active sites, consequently refining conductivity with increased charge transfer capacity and preferring band position to prohibit the recombination of hole-electron pairs.

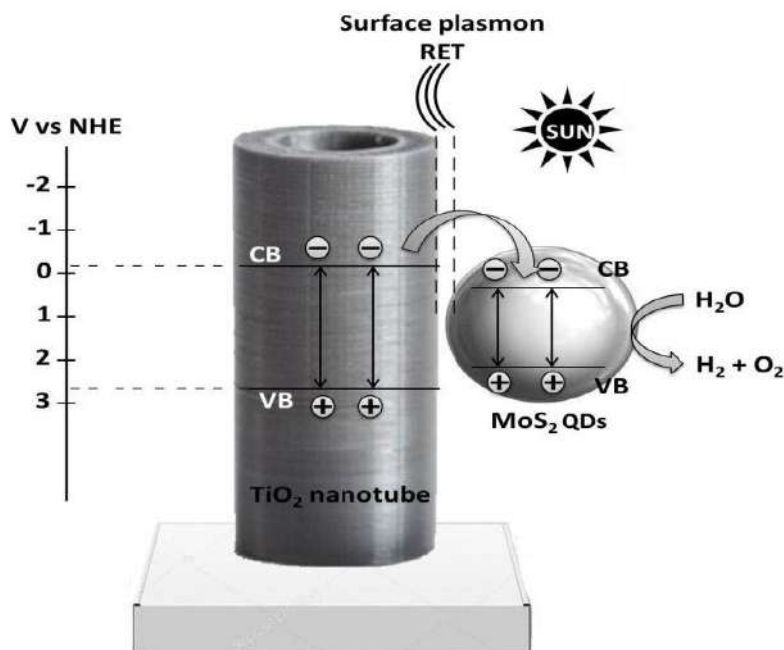


Figure 4. Schematics of energy band structure and photocurrent density vs time.

4.1.2. Oxygen Evolution Reaction

The OER is also crucial for metal–air batteries and fuel cells, and it involves a multistep oxidation of proton coupled with four electrons and poor durability, thereby limiting the power capability and energy efficiency of prototype devices. Ruthenium and Iridium catalysts provide a high rate OER process, but the high cost and scarcity of these limit their practical implementations. 2D-QDs based nanomaterials are preferred for efficiency for OER over their bulk counterparts. A single–step hydrothermal technique is used to prepare MoS₂-QDs for 24 h at 200 °C with a homogeneous size less than 5 nm and very low aggregation. The prepared materials reached lower onset over potential of 280 mV, and the remarkable increment in OER activity is due to lower charge transfer resistance, resulting in a lower Tafel slope [21]. Furthermore, single vacancy can generate active sites at the vertex and edge of QD with full Sulphur coverage, improving the OER performance. It extends the adsorption of reaction intermediates on the MoS₂ QDs influenced by CQDs, which inhibit the electrocatalytic activity.

4.2. Supercapacitor

The key features of an electrochemical capacitor are storage mechanisms and charge transfer. The utilization of ion absorption and desorption mechanisms is a double-layer capacitor or supercapacitor. GQDs are advantageous for application in electrochemical capacitors because of their fascinating properties e.g., high mobility, high surface area, good dispersion and high electrical conductivity in several solvents. GQD–HNT nanocomposite is fabricated to deliver enhanced charge storage sites, including fast charge transport for high performance in supercapacitors. 323 F/g specific capacitance at 5 mV s^{-1} rate is demonstrated for this composite because of good electron density, lower resistance capacitance and better electroactive sites. Relatively, the attained specific capacitance is higher than GQDs and established good stability in a vast range of current densities [22].

TMD–based substances fulfill the electrochemical requirement due to the high electrical conductivity and specific capacity. They also have low energy density and low stability due to the, non–effective contacts, active redox reactions and destruction of structure in the redox reactions. Although, integrating GQDs overcomes the existing limitations without any other issue. NiCo_2S_4 nanowires are prepared on GQDs/ NiCo_2S_4 and Ni foam arrays hydrothermally at $120\text{ }^\circ\text{C}$ for 6h. Electrochemical investigation of this composite nanostructure is executed in a potential range of -0.2 – 0.6 V at scan rate 10 mV s^{-1} . The higher specific capacitance compared to bare electrodes is endorsed to the introduction of GQDs and the exceptional hollow nanostructure. The increase in scan rate displays the voltammetric current and anodic with cathodic current decreases due to the diffusion of hydroxyl ions into hollow nanostructures. The galvanostatic charge-discharge experiments are accomplished in the voltage range of 0 – 0.46 V at different current densities discloses a specific capacitance of 678.22 F/g at current density of 0.2 A g^{-1} . Furthermore, the specific capacitance of GQDs/ NiCo_2S_4 enhance steadily after the initial 1000 cycles due to the complete activation of electrode. GQD is assembled on an inter–digital Au finger electrode electro–phoretically as an asymmetric and symmetric microsupercapacitor (Figure 5). The electrolyte is tuned to an ionic liquid from an aqueous solution and further upgraded upto seven times the energy density and power from 0.074 to $7.5\text{ }\mu\text{Whcm}^{-2}$. The ideal capacitor behavior and high reversibility are created from the electric double layer at diverse current densities at the interface of GQD film–electrolyte. This symmetric microsupercapacitor shows a fast power response, high-rate performance, and good cycling stability with 97.8% retention after 5000 cycles [23]. Moreover, sponge-like morphologies of MoS_2 display decent supercapacitive performance because of cation intercalation into the intra and interlayer, abundant active edges, and the redox reaction between various valence states of Mo.

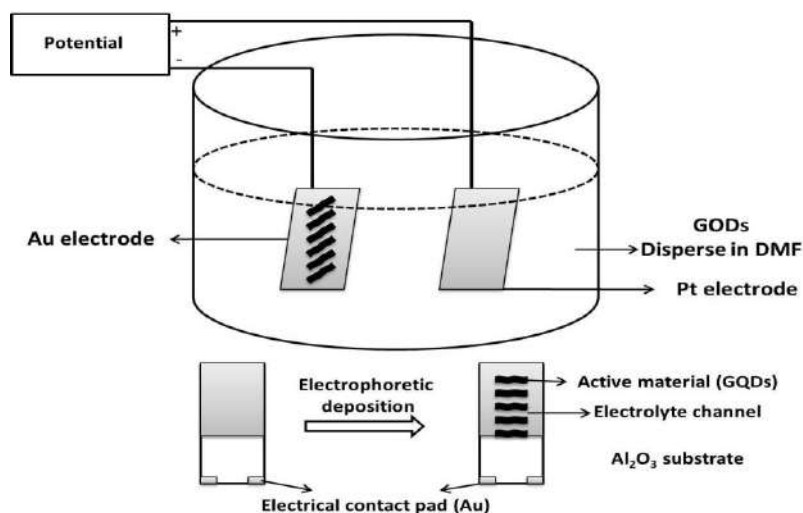


Figure 5. Electrophoretic deposition of GQDs on finger electrode for preparation of symmetric micro-supercapacitor.

4.3. Batteries

Increasing energy crises caused by ever-growing population and the extensive use of fossil fuels causes high levels of CO₂ and have driven efforts to search alternative renewable energy sources, peculiarly, nature harvested, which need storage through batteries. Thus, it is imperative to formulate long term stability, high efficiency, high energy density, long-term cycling life and low weight. To this end, Li/Na ion batteries (LIBs/NIBs) have auspicious vision due to their cost effective, long cycle life and high energy densities.

4.3.1. Lithium-Ion Battery

Transition metal and sulfides oxides can function as admirable reversible cathode materials and also graphite as anode material after the intrusion of rechargeable battery concept. As lithiated transition metal oxide emerged to utilize as cathode to make sure the safety concerns. The key reactions of LIBs are reversible Li-ion intercalation-de-intercalation cycles in two layered substrates. The delithiation of known cathode material in LIBs e.g., LiCoO₂ is restricted to 4.2 V certify a very prolonged shelf life and outstanding safety characteristics determined its significance compared to Li metal-based batteries. The basic mechanism of LIB are summarized, the first procedure is every time charging in the cell, namely, oxidation; delithiation of LiCoO₂ parallel to reduction and lithiation of graphite. Graphite with Li form LiC₆ through intercalating reversibly. The intercalation of Li into graphite takes place following first-order phase transition in stages such as LiC₂₄, LiC₂₇, and LiC₁₂. Thus, it is important to ensure excess Li source in cathode material to deliver Li ions and the charge needed to make the passivating surface films on graphite. This basic

mechanism is commendable to recognize the process in hybrid structures which utilize quantum dots.

The outstanding properties of 2D QDs can be employed to offset some faults of conventional electrode materials, e.g., slow Li^+ diffusion, low conductivity and poor stability. For instance, the exceptional properties of GQDs, including ease of functionalization and large surface area show a vital role in the increment of battery performance. VO_2 nanobelt arrays coated with GQDs is formulated (~ 2 nm) on 3D graphene as a potential cathode for LIBs and attained a 99% columbic efficiency, high specific capacity of 421 mA h g^{-1} at a $1/3$ C current density and good rate performances. Furthermore 94% retention at 60 C after 1500 cycles results in the increased stability rather than other VO_2 -based electrodes.

The distinctive nanostructure form it binder free, abolishing the practice of a conductive agent, current collector and diminishing the weight of full cell. Hierarchical TiO_2 is fabricated embedded with GQDs resulting exceptional rate capability and high specific capacity of $160.1 \text{ mA h g}^{-1}$ at 10 C after 500 cycles. Carbon-based sulphur-doped materials have appealed remarkable attention due to their rechargeable battery performance induced by sulfur doping. For instance, graphene doped MoS_2 as the anode consequences to a high reversible capacity of 1290 mA h g^{-1} [24]. Though MoS_2 is believed to be highly desirable active material in LIB but consist of limitation of aggregation and pulverization, substantial volume expansion of MoS_2 . Thus, the competition between the charge exciton and photogenerated exciton stimulated by charge transfer at the 0D/2D multilayer interface induces anomalous PL after the GQDs doping.

4.3.2. Sodium Ion Battery

However, LIBs have been believed a potential energy storage device, but the raw material and fabrication cost is one of the challenging concerns for grid-scale energy storage systems as well as the incapability to satisfy the enhanced requirement on energy storage. Furthermore, Li recycling can support the supply by 2040 with a recycling rate of 50-100% because of the shortage of facilities and advanced techniques. Now a day's less than 1% is being recycled. Research dedicated on rechargeable battery systems using Na as guest is enormously investigated due to its abundance to overcome the challenging concern. The ordinary electrochemical potential ($2.71 \text{ V vs. Na}^+/\text{Na}$) of Na results in low energy densities and power, which are attributed to its huge ionic size (1.02 \AA). Sodium ion battery (NIB) adopts similar mechanism as LIB, though, NIB has a dual intercalation system, capacities and mass of all components are evaluated to act as electrode. Lithium is more reducing than sodium (-3.04 V vs SHE compared to -2.71 V) and the gravimetric capacity is also more (3829 mAh g^{-1} compared to 1165 mAh g^{-1}). Thus LIB has higher operating voltages and energy density. Ultimately, the most abundant anodes of LIB (graphite) do not intercalate Na and is irreversible electrochemical method. Thus, graphene containing but non-graphitic, carbonaceous substances are assumed the "first-generation" anode for NIB. Furthermore, few non-carbonaceous transition metal

oxides are being studied currently because of high sodium insertion potentials. Theoretically, phosphorene is anticipated to be a potential material for NIBs with a large theoretical capacity of 865 mA h g^{-1} . Currently, a sandwiched phosphorene-graphene hybrid structure is fabricated as a cathode for NIB, which provides a high specific capacity of 2440 mA h g^{-1} at current density 0.05 A g^{-1} . Furthermore, QDs plays a crucial role in current work on developing novel active material due to its large Na^+ storage ability and large active surface area. A large yield product of CQDs (carbon quantum dots) and derivative 3D porous carbon frameworks (PCFs) is reported through calcining at $800 \text{ }^\circ\text{C}$ in an argon atmosphere, which acts as anode material for NIBs with an ultralong cycle life and extraordinary rate capability. Interestingly, the MoS_2 embedded LTO reveals the large capacity of 91 mA h g^{-1} at a rate of 5 C, and after 200 cycles; the superior capacity retention of 101 mA h g^{-1} at a rate of 2 C is attained [25]. The better cycling stability, capacity and rate capability of 2D QD/LTO-based anode material for NIBs cover the way to formulate low cost alternative storage systems and diminishes the mechanical stress caused by ion intercalation and enhances its cycling stability and capacity.

4.4. Photocatalysis

Photocatalysis is a process in which a chemical reaction is accelerated by catalyst in the presence of light. It has paid significant attention due to its implementation in renewable energy sources. The traditional colloidal semiconductor QDs normally suffer from large surface traps, which obstruct effective charge transfer and separation. Furthermore, the photocatalysts prepared from heavy metals are hazardous and toxic, and 2D-QDs are a substitutive and alternative photocatalytic material due to their tunable optical and catalytic properties, low toxicity and outstanding photochemical robustness. QDs bind to the surface of TiO_2 nanocomposites serve as photocatalysts and find out the methylene blue (MB) ability in visible-light irradiation. The photodegradation efficacy of this nanocomposite is 97% in 60 min especially for the rutile phase rather than the anatase phase of TiO_2 (31%). Usually, the anatase phase TiO_2 has more photodegradation ability. Though, the semiconductor absorbs energy equal to its bandgap to make electron-hole pairs in this composite under visible-light irradiation, and the energy is larger than that for anatase phase because of the upconversion effect of QDs (Figure 6). Further a 2D- WS_2/CD hybrid material is fabricated currently using microwave leading to enhanced photocatalytic activity, and it is tried in the photodegradation of organic pollutants. 12% of congo red (CR) dyes are degraded after 10 min in light illumination with a smaller initial concentration of catalysts (0.24 mg L^{-1}) [26]. The larger photocatalytic activity resulted from enhanced physisorption of CR molecules onto hybrid flakes and the bandgap modification caused by the carbon dots.

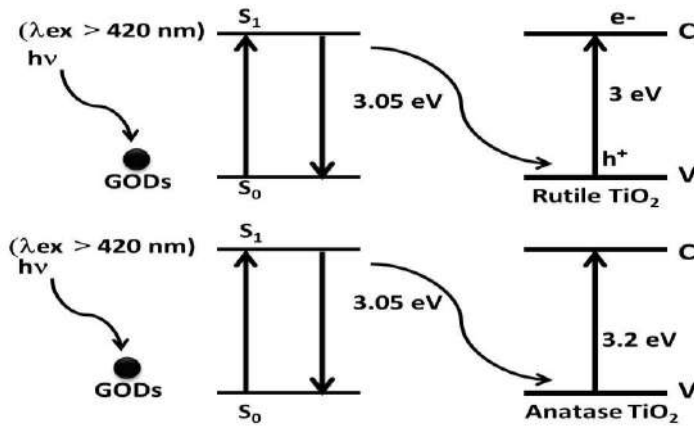


Figure 6. Schematic for photocatalytic process of rutile and anatase TiO_2/GQDs , rutile TiO_2 nanoparticles (NPs) and anatase TiO_2 -NPs.

4.5. Photodetector

The optoelectronic devices that assemble and use the photo-generated transporters in space exploration, real-time monitoring and national defense are called photodetector. Si-integrated photodevices are well investigated and ready to industry among various materials. The outstanding properties of optical materials with large luminescence and absorption mark them beneficial in optoelectronic devices. Carbon materials e.g., graphene QDs and carbon QDs, are intensively investigated due to the friendly compatibility and large environmental stability in order to avoid the instability and toxicity of colloidal QDs (PbS-QDs). Furthermore, the utilization of these 2D-QDs confirms the large stability and improved photoelectric performance. The massive conjugated system consisting delocalized π electrons imparts broadband emissions in graphene QD photodevices with the responsivity as high as 325 V/W. Another strategy to design graphene QDs photodevices is the sandwich assembly of graphene/GQDs/graphene. The broadband emission can be attained not only due to the π electrons. A negative photocurrent is shown during irradiation with different light due to the surface passivation of GQDs where electron-hole pairs generated photochemically cannot travel freely. GQDs composited with conventional materials e.g., P3HT, ZnO, silicon, of different dimensions are intensively investigated as an active material for photodetectors. GQDs doped with nitrogen display photoresponse in the UV to NIR range, usually known as the Tang-Lau method. Furthermore, these GQDs are also utilized to fabricate hybrid composites with other 2D materials. Thus hybrids of the nitrogen-doped graphene and monolayer WSe_2 QDs (N-GQDs) are suggested to attain high-performance photodetectors caused by the increased charge transfer and light absorption due to the built-in electrical field between WSe_2 and GQDs. Both WSe_2 and graphene are considered as the future potential material in optoelectronics. The photocurrent of $\text{WSe}_2/\text{N-GQDs}$ is significantly enhanced

compared to pure WSe_2 due to the Schottky barrier built in the interface, making feasible the efficient separation of holes and electrons. Furthermore, the graphene decorated MoS_2 -QDs are advantageous. The response time significantly shortens from 20 s down to 70 ms and the photocurrent also significantly increases. The work function of MoS_2 is larger than graphene results the construction of the Schottky barrier and the opposite polarity of graphene and MoS_2 provide increased built-in electrical field, which causes the fast separation and the reduction of recombination. If the decorating species altered to semiconducting QDs from metal-like QDs, it follows the modulation of the optical properties of TMD. The conduction band and minimum Fermi level of MoSe_2 -QDs are higher than MoS_2 , therefore the electrons of MoSe_2 tended to move downward to MoS_2 , bringing up the Fermi level of MoS_2 and causing the band structure modulation in the interface. The degree of modulation is correlated with the QD numbers. A latest investigation marked that MoS_2 could be a functional stage for several applications. Though the MoS_2 bandgap did not match the long wavelengths range, decoration with HgTe onto MoS_2 displays potential for high-performance IR detectors [27]. The hole-electron pairs are formed by photon excitation on light illumination, which produce to a photoinduced current. Additionally, this large responsivity is also credited to the large surface-to-volume ratio of hybrid MoS_2/InSe .

CONCLUSION

The zero-dimensional quantum-confined material consists of atomically ultra-thin 2D-layered structure whose physicochemical properties can be tuned in terms of defects, size, edge configuration, thickness and chemical functionalities. This also paves the path to disclose novel properties in combination with electronic, optical, electrochemical, catalytic and chemical ones. The distinctive optical properties of 2D-QDs are not usually present in the bulk counterparts, furnishing it an appealing material for a wider domain of applications. This chapter focuses optoelectronic and energy based application, though 2D-QDs are also a potential material in the field of electrochemical sensors, photodynamic therapy drug delivery, bioimaging and photovoltaics etc. The higher solubility, largely tunable PL, photostability and biocompatibility of GQDs are useful in the field of bioimaging. Additionally, their application is widen because of their exceptional properties of high selectivity, full-spectrum PL color and ease of surface functionalization. Though, emission and excitation at longer wavelengths are mainly preferred in deep tissue imaging. The domestic utilization of sea-water is not fit because of high salinity and the traditional techniques can only eliminate nutrient and organic matters effectively. Current investigation claims that MoS_2 monolayer can remove 88% of ions. Moreover, black phosphorous (BP) is enormously fascinating owing to its electronic and optical properties. BP QDs with a lateral size of 4.9 nm are exfoliated from bulk *via* solution method and scrutinized in memory devices. Phosphorene QDs occupy the gap between TMDs and graphene in terms of electrical properties though the easily

oxidative nature of phosphorous-based QDs which is the key issue. The 2D-QDs are more electro-active, further the mechanical stress due to ion intercalation leads to improve the cycling stability and specific capacity in NIBs or LIBs. This chapter unlocks a broad and thorough understanding and prompts further developments in the exciting and emerging field of synthesis, properties and application for optoelectronics and energy.

ACKNOWLEDGMENTS

Dr. MadhuTiwari is thankful to Dr. P. N. Dongre, Principal, K. N. Govt. P. G. College, Gyanpur and the faculty members of department of Chemistry for their support.

REFERENCES

- [1] Novoselov, K. S., Geim, A. K., Morozov, S. V., Jiang, D., Zhang, Y., Dubonos, S. V., Grigorieva, I. V. and Firsov, A. A.(2004). Electric field effect in atomically thin carbon films. *Science*, 306:666-669.
- [2] Liu, Y., Dong, X. and Chen, P. (2012). Biological and chemical sensors based on graphene materials. *Chem. Soc. Rev.*, 41: 2283-2307.
- [3] Wang, X., Sun, G., Routh, P., Kim, D. H., Huang, W. and Chen, P. (2014)., Heteroatom-doped graphene materials: syntheses, properties and applications, *Chem. Soc. Rev.*, 43: 7067-7098.
- [4] Xu, M., Liang, T., Shi, M. and Chen, H. (2013). Graphene-like two-dimensional materials. *Chem. Rev.*, 113: 3766-3798.
- [5] Tan, C. and Zhang, H. (2015). Two-dimensional transition metal dichalcogenidenanosheet-based composites.*Chem. Soc. Rev.*, 44: 2713-2731.
- [6] Pan, D., Guo, L., Zhang, J., Xi, C., Xue, Q., Huang, H., Li, J., Zhang, Z., Yu, W. and Chen, Z. (2012). Cutting sp^2 clusters in graphene sheets into colloidal graphene quantum dots with strong green fluorescence. *J. Mater. Chem.*, 22: 3314-3318.
- [7] Tan, X., Li, Y., Li, X., Zhou, S., Fan, L. and Yang, S. (2015). Electrochemical synthesis of small-sized red fluorescent graphene quantum dots as a bioimaging platform. *Chem. Commun.*, 51: 2544-2546.
- [8] Qiao, Z. A., Wang, Y., Gao, Y., Li, H., Dai, T., Liu, Y. and Huo, Q. (2010). Commercially activated carbon as the source for producing multicolor photoluminescent carbon dots by chemical oxidation. *Chem. Commun.*, 46: 8812-8814.

- [9] Zhuo, S., Shao, M. and Lee, S. T. (2012). Upconversion and downconversion fluorescent graphene quantum dots: ultrasonic preparation and photocatalysis, *ACS Nano*, 6, 1059-1064.
- [10] Shen, J., Zhu, Y., Yang, X. and Li, C. (2012), Graphene quantum dots: emergent nanolights for bioimaging, sensors, catalysis and photovoltaic devices, *Chem. Commun.*, 48: 3686-3699.
- [11] Yan, X., Cui, X. and Li, L. S. (2010). Synthesis of large, stable colloidal graphene quantum dots with tunable size. *J. Am. Chem. Soc.*, 132: 5944-5945.
- [12] Ha, H. D., Han, D. J., Choi, J. S., Park, M. and Seo, T. S. (2014). Dual role of blue luminescent MoS₂ quantum dots in fluorescence resonance energy transfer phenomenon. *Small*, 10: 3858-3862.
- [13] Gopalakrishnan, D., Damien, D. and Shaijumon, M. M. (2014). MoS₂ quantum dot-interspersed exfoliated MoS₂ nanosheets. *ACS Nano*, 8: 5297-5303.
- [14] Li, B. L., Chen, L. X., Zou, H. L., Lei, J. L., Luo, H. Q. and Li, N. B. (2014). Electrochemically induced Fenton reaction of few-layer MoS₂ nanosheets: preparation of luminescent quantum dots via a transition of nanoporous morphology. *Nanoscale*, 6: 9831-9838.
- [15] Huang, H., Du, C., Shi, H., Feng, X., Li, J., Tan, Y. and Song, W. (2015). Water-soluble monolayer molybdenum disulfide quantum dots with upconversion fluorescence. *Part. Part. Syst. Charact.*, 32: 72-79.
- [16] Sk, M. A., Ananthanarayanan, A., Huang, L., Lim, K. H. and Chen, P. (2014). Revealing the tunable photoluminescence properties of graphene quantum dots. *J. Mater. Chem. C*, 2: 6954-6960.
- [17] Sun, H., Zhao, A., Gao, N., Li, K., Ren, J. and Qu, X. (2015). Deciphering a nanocarbon-based artificial peroxidase: chemical identification of the catalytically active and substrate-binding sites on graphene quantum dots. *Angew. Chem. Int. Ed.*, 54: 7176-7180.
- [18] Loh, G., Pandey, R., Yap, Y. K. and Karna, S. P. (2015), MoS₂ quantum dot: effects of passivation, additional layer, and h-BN substrate on its stability and electronic properties. *J. Phys. Chem. C*, 119: 1565-1574.
- [19] Vikraman, D., Akbar, K., Hussain, S., Yoo, G., Jang, J. Y., Chun, S. H., Jung, J. and Hui, J. P. (2017). Direct synthesis of thickness-tunable MoS₂ quantum dot thin layers: optical, structural and electrical properties and their application to hydrogen evolution. *Nano Energy*, 35: 101-114.
- [20] Wang, Q., Huang, J., Sun, H., Ng, Y. H., Zhang, K. Q. and Lai, Y. (2018). MoS₂ quantum dots@ TiO₂ nanotube Arrays: an extended-spectrum-driven photocatalyst for solar hydrogen evolution. *Chem Sus Chem*, 11: 1708-1721.
- [21] Mohanty, B., Ghorbani-Asl, M., Kretschmer, S., Ghosh, A., Guha, P., Panda, S. K., Jena, B., Krasheninnikov, A. V. and Jena, B. K. (2018). MoS₂ quantum dots as efficient catalyst materials for the oxygen evolution reaction. *ACS Catal.*, 8: 1683-1689.
- [22] Ganganboina, A. B., DuttaChowdhury, A. and Doong, R. (2017). New avenue for appendage of graphene quantum dots on halloysite nanotubes as anode

- materials for high performance supercapacitors. *ACS Sustain. Chem. Eng.*, 5: 4930-4940.
- [23] Liu, W. W., Feng, Y. Q., Yan, X. B., Chen, J. T. and Xue, Q. J. (2013). Superior micro-supercapacitors based on graphene quantum dots. *Adv. Funct. Mater.*, 23: 4111-4122.
- [24] Zhang, W., Xu, T., Liu, Z., Wu, N. L. and Wei, M. (2018), Hierarchical TiO₂-x imbedded with graphene quantum dots for high-performance lithium storage., *Chem. Commun.*, 54: 1413-1416.
- [25] Xu, G., Yang, L., Wei, X., Ding, J., Zhong, J. and Chu, P. K. (2016), MoS₂-Quantum-Dot-Interspersed Li₄Ti₅O₁₂nanosheets with enhanced performance for Li-and Na-ion Batteries., *Adv. Funct. Mater.*, 26: 3349-3358.
- [26] Zhuo, S., Shao, M. and Lee, S. T. (2012). Upconversion and downconversion fluorescent graphene quantum dots: ultrasonic preparation and photocatalysis. *ACS Nano*, 6: 1059-1064.
- [27] Nguyen, D. A., Oh, H. M., Duong, N. T., Bang, S., Yoon, S. J. and Jeong, M. S. (2018). Highly enhanced photoresponsivity of a monolayer WSe₂photodetector with nitrogendopedgraphene quantum dots. *ACS Appl. Mater. Interfaces*, 10: 10322-10329.

Chapter 7**NANOMATERIALS AS INTRINSIC ENZYME
MIMETIC CATALYSTS*****Vinita****Department of Chemistry, Deen Dayal Upadhyaya Gorakhpur University,
Gorakhpur, UP, India**ABSTRACT**

In recent decades, a variety of nanomaterials have been attracted considerable attention due to their intrinsic enzyme-like catalytic activities (nanozymes). Significant advancements have been made owing to huge development in nano research and unique properties of the nanomaterials. Nanozymes are now a good relevant alternative to natural enzymes due to their facile synthesis, extraordinary catalytic activity, low cost, high stability and, selectivity in the large range of applications with outstanding advances in biotechnology, nanotechnology, computational design and catalysis science. Different types of nanomaterials such as metal nanoparticles, carbon nanotubes metal chalcogenides, metal oxides, quantum dots, halogen compounds, nanocomposites, and nano-size metal–organic frameworks (MOFs) have been abundantly explored for enzyme mimicking. This chapter discusses the recent advancements made in the design of enzyme-like properties of these various nanozymes. It also includes different types of reaction mechanisms and various parameters influence catalytic activity of nanozymes. Then, it concludes numerous methods to calibrate the nanozymes activity and selectivity. Finally, a comparative study between nanozymes and natural enzymes are outlined. Current challenges and future scope for promoting nanozyme research as a novel platform for the design of affordable, sustainable, safe, and reliable therapeutics are also suggested.

Keywords: nanozymes, enzyme mimetic, nanomaterials, biosensing, nanotechnology, catalyst

* Corresponding Author's Email: vinitavermabhu@gmail.com.

1. INTRODUCTION

Nature is the best architect and the main source of inspiration throughout. Naturally motivated plans or adaptation from nature and an endeavor to incorporate such thoughts into better solutions for sustainable living and technological issues is generally known as “biomimetics” or, “biomimicry.” In general, biomimetics normally refers to “mimicking biology or nature.” The “biomimetics” term is coined by Otto Schmitt [1] which is derived from the Greek word ‘biomimesis.’ In any case, “biomimetics” unveiled its first appearance in 1974 in Webster's dictionary and is characterized as “the investigation of the arrangement, structure, or capacity of organically delivered substances and materials (as enzymes) and biological systems and process (photosynthesis or protein synthesis) particularly to synthesizing comparable products by artificial methods which mimic to natural products.” So, biomimetics in the research field is multidisciplinary, drawing from numerous zones of science, including, yet not restricted to, catalysis, chemistry, molecular biology, material science, nanotechnology, physiology, designing, biosensing, immunology, environmental science, and food technology.

Natural enzymes, the majority of which are proteins, are linear chains of amino acids that can self-assemble by multivalent interactions to create a three-dimensional structure, a factor responsible for the specificity of enzymes. Natural enzymes play an important role in the several biological processes in the organism, are dazzling biocatalysts that show high catalytic activity with high selectivity and specificity under comparatively mild conditions (pressure, pH, and temperature) [2, 3]. Despite of this, on introduction to compound denaturants, inhibitors, or moderately harsh environmental conditions, the catalyst structures denature leading less stability to the structure, which thus lost their catalytic activity. Moreover, the high expense in synthesis, storage, and purifications of natural enzymes also restricts their wide innovative applications. Thus, the quest for alternative materials that can accomplish the greater part of the previously mentioned challenges has resulted to the introduction of synthesized or artificial enzymes [4–10]. Firstly, the term artificial enzymes was used by “Ronald Breslow” for the enzyme mimetics [11] which are very exciting and crucial area of biomimic chemistry, points to simulate general and important concepts of natural enzyme applying substitute materials [12,13]. In the course of recent many years, analysts have set up artificial enzymes as exceptionally steady, simple, efficient, high-performance, stable and minimal effort options in contrast to natural enzymes in a wide scope of uses. Metal complexes, Cyclodextrins, supramolecules, polymers, porphyrins and biomolecules like proteins, catalytic antibodies and nucleic acids were widely investigated to mimic natural enzymes by different techniques [11-27]. Until this point, noteworthy advancement has been made in the field of artificial enzymes and a few monographs and various brilliant audits have been distributed.

As of late, some nanomaterials, for example, gold nanoparticles, rare earth metal nanoparticles fullerene derivatives, ferromagnetic nanoparticles, inorganic metal nanoparticles, and carbon structures-based nanozyme have been found to display

unforeseen catalyst - like activity. From that point forward, significant advances have been made around there because of the huge advancement in nano-research and the interesting characteristics of nanomaterials [28-41]. Nanomaterials as an artificial enzyme (nanozyme) have discovered a wide range of applications in various fields, including immunoassays, biosensing, disease diagnostics and treatment, neuroprotection, contamination evacuation, and stem cell growth. The "nanozymes" term was at first authored by Scrimin, Pasquato and, associates to depict their gold clusters with remarkable ribonuclease-like activity [32]. Here, we embrace the term and extend it to nanomaterials with an enzyme like catalytic activity. Even though the advancement and accomplishments of exemplary artificial enzymes have been completely investigated [42, 43].

To highlight the advancement of nanozyme research, this chapter deals with different biomimetic nanomaterials, their reaction mechanism, enzyme kinetics and, various applications. Various ways to deal with the tune the catalytic activities of nanozymes are discussed. We additionally compare nanozymes with other catalytically active materials, (for example, natural enzymes, other artificial enzymes and organic catalysts, quantum dots). At last, we discuss the current challenges confronting nanozyme technologies and future headings to understand their incredible potential.

2. NANOMATERIALS TO MIMIC NATURAL ENZYMES

Until this time, various types of nanomaterials have been designed to develop nanozyme system. As per the distinctive catalysts composition and active sites of the enzyme mimic process, nanomaterials utilized in intrinsic enzyme mimics can be of different types. In this part, we will provide a profound introduction to the primary enzyme - like properties and enzyme mimicking systems develop strategies of these types of nanomaterials that are utilized in the natural enzyme (peroxidases, catalases, SOD, oxidase) mimicking applications.

2.1. Metal-Based Nanomaterials as Nanozymes

Metal-based nanomaterials can be promising candidates for enzyme mimetics, as shown by various ongoing reports [44-51]. Over the previous years, various metal-based nanomaterials for example Pt, Au, and Ag have been widely examined with a characteristic enzyme-like activity and fascinating in enormous research interests. Due to their shape and size relevant physiochemical properties, incredible efforts have been made in the development of metal nanomaterial based biomimicking assay for various applications.

2.1.1. Gold Nanomaterials

Citrate coated gold nanoparticles (AuNPs) have been broadly analyzed for various applications, like, biomedical applications, owing to easy synthesis and functionalization techniques that have been created. These nanomaterials have also been explored for their high catalytic activity. Moreover, it was all the striking and surprising when Rossi and associates indicated that citrate capped gold nanoparticles catalyzed the oxidation of glucose with oxygen [53-55]. The reaction mechanism was fundamentally the same as the reaction catalyzed by the glucose oxidase and proposed that gold nanoparticles could act as a mimic for glucose oxidase. In recent research, gold nanomaterials, for example, gold nanoclusters and nanoparticles have been accounted for remarkable enzyme-like activity [56-57] after a natural oxidase mimicking catalytic activity from citrate capped gold nanoparticles reported in 2004 [58]. What's more, various attempts have been made to use AuNPs or gold nanoclusters supported on a different system as catalysts in chemical reactions [59]. The gold nanozyme based catalysis likewise followed Michaelis–Menten enzyme kinetics, and the outcomes indicated that the native enzyme was multiple times more dynamic than the nanozyme.

2.1.2. Silver Nanomaterials

Some of the reports show that silver nanoparticles (AgNPs), exhibit enzyme - like catalytic activity and are further used in colorimetric and visual glucose detection techniques [60]. The joining of AgNPs into chitosan polymers could significantly build the uncovered surface region and avoid the aggregation of silver nanoparticles. Concerning nanoclusters, practically all explores were centered around nucleic acid stabilized Ag nanoclusters which were originated from the fluorescence character of DNA and Ag nanoclusters for a long duration. A few researchers developed a cluster based sensor for delicate and quick detection of H₂O₂ by utilizing the hydrogen peroxide and silver nanowire [61-63].

2.1.3. Platinum Nanomaterials

Platinum nanoparticles are additionally very good catalysts and have enzyme like catalytic activity [65-67]. Exceptionally steady uniform platinum nanoparticles with a size of 1-2 nm were synthesized by utilizing apoferritin (Ft@apo) as a nucleation substrate nanoparticles showed high stability and both catalase and peroxidase like activities dependent on temperature and pH. The research study from Nie's demonstrated that the catalase-like activity was increased by enhancing temperature and pH while the peroxidase-like activity had an extreme value at mildly acidic conditions and physiological temperature [68]. The catalytic activity was depends on Platinum content, with large Platinum content having greater activity. The catalytic activity of platinum nanomaterials was decreased when the nanoparticles agglomerates because of the reduction in surface area [69].

2.1.4. Noble Metal-Based Nanoalloys

In Contrast alone with metal nanomaterials, metal-based nanoalloys ordinarily show more effective properties and functions. Because of the electronic effect and synergistic effect between the two materials, nanoalloys exhibit an enhanced catalytic activity [70, 71]. These results inspire researchers to investigate the potential for enzyme mimics through utilizing composite nanostructures, for example, Ag@M (where, M = Pd, Pt and Au) combination nanostructures and Au@M (where, M = Pd, Bi and Pt) alloy nanomaterials. Various kinds of combination nanostructures demonstrated diverse natural enzymes like activity, which acquainted another effective path to regulate the catalytic activity separated from shape and size.

2.1.5. Metal Chalcogenide Nanostructures

Metal chalcogenide nanomaterials like MoS₂, CuS, FeS, WS₂, MnSe, and FeSe are developing as a significant class of metal-based nanomaterials in enzyme mimics applications because of their outstanding electronic properties, cost - effective and simple preparation. For instance, sheet-like FeS nanomaterials has been showing a smaller bandgap than FeO, which is favorable for electron movement through the active center of Fe²⁺ or Fe³⁺. Simultaneously, the greater specific surface area achieved from its novel nanostructure additionally supplies FeS an enhanced enzyme - like catalytic activity [72]. CuS nanostructures were additionally investigated peroxidase-like activity by preparing an inward superstructure [73]. This study extends the application of chalcogenide nanomaterials in numerous fields, like clinical diagnosis, biosensing and environmental monitoring. In this manner, Cu nanocrystals, CuS nanoparticles, decorated over Cu nanoclusters, and polyaniline nanowires were also showed peroxidase-like activity [74-76].

2.2. Carbon-Based Nanomaterials

In recent research carbon-based nanostructures have much attention because of their electronic, optical, thermal, physical, and chemical properties [77]. Their properties are mainly dependent on the synergistic effects and structure with different other materials [78]. A large portion of the carbon-based nanomaterials is rich in oxygenated functional groups like hydroxyl, carboxyl, epoxide, ketone, etc, which may also plays a significant role in their enzyme - like catalytic activity [79]. The revelation of the peroxidase-like activity from carbonic nanostructures, including graphene and its subordinates, carbon nanotubes [80], carbon dots [81, 82], and graphene quantum dots [83] have broadened the scope of biomimetic research.

2.3. Other Nanomaterials

Moreover the previously mentioned nanostructures, other recently created nanomaterials, for example, Iron oxide-based nanomaterials [84,85], fullerene

subordinates [86], metal-organic frameworks (MOFs) [87-89], nano-organized layered double hydroxide (LDH) [90], cobalt oxide [91] and so on additionally show incredible potential for enzyme mimics applications. For instance, MOFs have been drawing in expanding consideration because of their unique structures which consists metal with connecting organic ligands. A tremendous assortment of metal ions and organic ligands provide coordination networks with various structures, porosity and topologies. Profiting from their high surface area, high thermal stability, and stable nanoscale porosity, MOFs have been effectively utilized in various fields: drug delivery, catalytic carrier, bioimaging, gas separation, sensing, etc. Due to their uniform cavities which can produce a high density of biocatalysis active sites, previous reports on enzyme mimics of metal-organic frameworks generally centered around the biocatalysis active centers [92]. In recent time, there has been a fast development in research publications related to natural catalytic activity-dependent on LDHs materials including CoAl-LDHs, CoFe-LDHs [93], nanohybrids [94], NiCo LDHs [95], and NiAl-LDHs [96]. Different easy engineered procedures of LDHs and their derived nanocomposites have been created to satisfy specific requirements for various applications in this field.

3. STRATEGIES TO ENHANCE SUBSTRATE SPECIFICITY OF NANOZYMES

It is notable that natural enzymes induce high catalytic activity as well as substrate specificity. Even though nanozymes display great catalytic activity, their substrate selectivity is very poor. For most oxidase and peroxidase mimics, nanozymes can catalyze the oxidation of TMB substrate, yet additionally different substrates. Accordingly, the main challenge is to design nanozymes with superb substrate specificity. To enhance the substrate specificity of nanozymes, it is essential to present substrate binding sites through the chemical change technique [97, 98].

The catalytic efficiency i.e., K_{cat}/K_m is used for comparative study for substrate specificity execution, indicating favorable specificity with the adsorbed substrate. Monolayer coated metal nanostructures can enhance the enzymatic catalytic activity of nanozymes [99, 100].

4. CATALYTIC MECHANISM

As referenced, nanozymes exhibit tunable catalytic efficiency to enzyme mimic. Since, poor substrate specificity and less catalytic activity confine their practical applications. To additionally improve the catalytic activity of nanozymes, it is a significant issue to investigate an enzyme-like catalytic reaction mechanism to plan and manufacture more proficient enzyme mimics. To investigate the catalytic reaction mechanism of nanozymes, we ought to explain the reaction process and binding

mechanism with the substrates, active catalytic sites, active intermediates, and electron transfer including the catalysts and substrates.

4.1. Catalytic Reaction Process

Normally, a ping-pong reaction mechanism is used to depict the catalytic process of nanozymes [101]. The enzyme kinetic factors determined from the Michaelis–Menten equation and curve are comparable with natural enzymes.

4.2. Active Intermediates

Various active intermediates can be recognized for various types of the catalytic processes. For example, in the peroxidase-like responses, it is commonly viewed as that the production of OH radical intermediates by catalyzing hydrogen peroxide contributes to the catalytic activity [102].

4.3. Active Sites

The active sites in the enzymes decide their catalytic activity range. For natural enzyme HRP, the iron metal in the heme assumes the key function in the peroxidase catalytic activity [103]. Metal ions typically act as an active center or site similar to natural enzymes for the enzyme catalysis. For example, Fe_3O_4 nanoparticles have both ferric and ferrous particles; notwithstanding, it has been demonstrated that ferrous particles are the main active sites for high peroxidase-like activity [104]. Similarly, CeO_2 nanoparticles as SOD mirrors show brilliant catalytic activity attributable to the redox coupling somewhere in the range of Ce^{3+} and Ce^{4+} . [105] However, for carbon-nanomaterial-based nanozymes without any metal ions, there ought to be sure special functional groups act as the active sites. Graphene quantum dots are the active sites for the peroxidase mimicking process.

4.4. Electron Transfer

Electron transfer generally takes place between the substrate and catalysts in the process of enzyme catalysis. As an illustration, to understand the peroxidase-like catalytic activity toward the oxidation reaction of TMB, it is commonly perceived that the LUMO of hydrogen peroxide received electrons from the nonbonding orbital of TMB substrate [106]. However, the greater energy of LUMO of hydrogen peroxide restricts such electron movement from the nonbonding orbital of TMB substrate.

5. VARIOUS PARAMETERS INFLUENCE THE CATALYTIC ACTIVITY OF NANOZYMES

Nanozymes impersonate the catalytic activity of natural enzymes have increased a potential exploration due to natural enzymes experiences some limitations like denaturation, loss of catalytic activity in harsh environmental conditions. A wide number of nanoparticles show an intrinsic enzyme mimetic activity like that existed in normal peroxidases. However, nanomaterials are normally chemically and biologically stable. There are few parameters, like temperature, pH, and concentration of nanomaterials can widely affects the catalytic activity of nanozymes.

CONCLUSION

This chapter highlights the ongoing advancement in the field of nanomaterials as artificial enzymes, named "nanozymes." As examined, however, the zone of nanozymes is still in its infancy, it has developed significantly as an aspect of the artificial enzyme area. As enzyme mimics, nanozymes exhibit some advantages over natural enzymes. Since most of the enzymes lost catalytic activity under harsh condition, and can be easily denatured by changes in environmental conditions. With the advancement of nanomaterials as artificial enzymes, the materials like nanozymes have attracted in an incredible potential as an alternative of natural enzymes, due to their favorable advantageous, for example, high stability, easy synthesis, cost-effective, and high catalytic activity. Therefore, various nanozymes with natural enzyme-like catalytic activity have been effectively reported. In this area, the research highly dynamic, as proven by the quickly developing number of publications. The easy preparation of these nanozymes may additionally outfit their application. Based on the unique properties of the developed nanozymes, the design a platform for detection of several analytes by various techniques. Due to its high sensitivity and simple operation, it was normal that the nanozymes may hold extraordinary responses in the field of science and technology. Likely use of nanozymes in chemical and clinical devices may be considered as a substitute for natural compounds. Since these prepared compounds have been demonstrated to have high catalytic activity, they can be considered as a decent decision for a single system or in the mix with safe materials for the recognition of a wide scope of compounds and diseases. Although, nanozymes have some limitations, like less bioavailability and multi-substrate activities, which limits their synthetic and medical applications. Novel nanotechnology procedures, including micelles and liposomes, are promising to address these limitations. Future advancements in nanozyme innovation will prompt another rush of novel biocatalysts for vast applications by overcoming the previously mentioned and other possible difficulties.

REFERENCES

- [1] Schmitt, O. H. (1969). Some Interesting and Useful Biomimetic Transform, *Proceedings of Third Internatioanl Biophysics Congress*, Boston, MA, USA, 29 p.p. 297.
- [2] Garcia-Viloca, M.; Gao, J.; Karplus, M.; Truhlar, D. G. (2004) How enzymes work: Analysis by modern rate theory and computer simulations. *Science* 303: 186–195.
- [3] Wolfenden, R. and Snider, M. J. (2001). The depth of chemical time and the power of enzymes as catalysts. *Acc. Chem. Res.* 34: 938–945.
- [4] Hennrich, N. and Cramer, F. (1965). Inclusion compounds. XVIII.1 the catalysis of the fission of pyrophosphates by cyclodextrin. A model reaction for the mechanism of enzymes. *J. Am. Chem. Soc.* 87: 1121–1126.
- [5] Breslow, R. and Overman, L. E. (1970). Artificial enzyme combining a metal catalytic group and a hydrophobic binding cavity. *J. Am. Chem. Soc.* 92: 1075–1077.
- [6] Klotz, I. M. Royer, G. P. and Scarpa, I. S. (1971). Synthetic derivatives of polyethyleneimine with enzyme-like catalytic activity (synzymes). *Proc. Natl. Acad. Sci. USA*, 68, 263–264.
- [7] Yoshihisa, Y. Zhao, Q. L. Hassan, M. A. Wei, Z. L. Furuichi, M. Miyamoto, Y. Kondo, and Shimizu, T. (2011) SOD/catalase mimetic platinum nanoparticles inhibit heat-induced apoptosis in human lymphoma U937 and HH cells. *Free Rad. Res.* 45: 326–335.
- [8] Gao, L. Zhuang, J. Nie, L. Zhang, J. Zhang, Y., Gu, N. Wang, T. Feng, J. Yang, D. Perrett, S. et al. (2007). Intrinsic peroxidase-like activity of ferromagnetic nanoparticles. *Nat. Nanotech.* 2: 577–583.
- [9] Bhabak, K. P. and Mugesh, G. (2010). Functional mimics of glutathione peroxidase: bioinspired synthetic antioxidants. *Acc. Chem. Res.* 43, 1408–1419.
- [10] Friedle, S. Reisner, E. and Lippard, S. J. (2010). Current challenges of modeling diiron enzyme active sites for dioxygen activation by biomimetic synthetic complexes. *Chem. Soc. Rev.* 39: 2768–2779.
- [11] Breslow, R. and Overman, L. E., (1970). Artificial enzyme combining a metal catalytic group and a hydrophobic binding cavity. *J. Am. Chem. Soc.* 92: 1075–1077.
- [12] Kirby, A. J. and Hollfelder, F. *Enzyme models to model enzymes*, Royal Society of Chemistry, Cambridge, 2009.
- [13] Breslow, R. *Artificial enzymes*, Wiley-VCH, Weinheim, 2005.
- [14] Aiba, Y. Sumaoka, J. and Komiyama, M. (2011). Artificial DNA cutters for DNA manipulation and genome engineering. *Chem. Soc. Rev.* 40: 5657–5668.
- [15] Bonarlaw R. P. and Sanders, J. K. M. (1995). Polyol Recognition by a Steroid-Capped Porphyrin, Enhancement and Modulation of Misfit Guest Binding by Added Water or Methanol. *J. Am. Chem. Soc.* 117: 259–271.

- [16] Royer, G. P. and Klotz, I. M. (1969). Enhanced rates due to apolar interactions between polymer and substrate. *J. Am. Chem. Soc.* 91:5885–5886.
- [17] Zhang, X. Xu, H. P. Dong, Z. Y. Wang, Y. P. Liu J. Q. and Shen, J. C.(2004). Highly Efficient Dendrimer-Based Mimic of Glutathione Peroxidase. *J. Am. Chem. Soc.* 126: 10556–10557.
- [18] Cram D. J. and J. M. (1974). Host-Guest Chemistry. *Cram, Sci.* 183: 803–809.
- [19] Lehn, J. M. and Sirlin, C. J. (1978). *Chem. Soc., Chem. Commun.* 949–951.
- [20] Dong, Z. Y. Wang, Y. G. Yin, Y. Z. and Liu, J. Q. (2011). Supramolecular enzyme mimics by self-assembly. *Curr. Opin. Colloid Interface Sci.* 16: 451–458.
- [21] Wulff, G. and Sarhan, A. (1972). Practice and Synthesize Molecularly Imprinted Polymers for Separating Target Neuro-protective Compounds from TCM with Less Pollution. *Angew. Chem., Int. Ed. Engl.* 11: 341–342.
- [22] Takagish T. and I. M. Klotz, (1972). Macromolecule-small molecule interactions; introduction of additional binding sites in polyethyleneimine by disulfide cross-linkages, *Biopolymers*, 11, 483–491.
- [23] Pan T. and Uhlenbeck, O. C. (1992). *In vitro* selection of RNAs that undergo autolytic cleavage with lead (2+). *Biochemistry* 31: 3887–3895.
- [24] Breaker R. R. and Joyce, G. F. (1994). A DNA enzyme that cleaves RNA. *Chem. Biol.* 1: 223–229.
- [25] Tramontano, A. Janda, K. D. and Lerner, R. A. (1986). Catalytic antibodies. *Science* 234: 1566–1570.
- [26] Pollack, S. J. Jacobs J. W. and Schultz, P. G. (1986). Selective chemical catalysis by an antibody. *Science* 234: 1570–1573.
- [27] Lu, Y. Yeung, N. Sieracki N. and Marshall, N. M. (2009). Design of functional metalloproteins., *Nature* 460: 855–862.
- [28] Dugan, L Gabrielsen, J. K Yu,. S. P. Lin T. S. and Choi, D. W. (1996). Buckminsterfullerenol free radical scavengers reduce excitotoxic and apoptotic death of cultured cortical neurons. *Neurobiol. Dis.* 3: 129–135.
- [29] Dugan, L. L. Turetsky, Du, D. M. C. Lobner, D. Wheeler, M. Almlı, C. R. Shen, C. K. F. Luh, T. Y. Choi D. W. and Lin, T. S. (1997) Carboxyfullerenes as neuroprotective agents, *Proc. Natl. Acad. Sci. USA* 94, 9434–9439.
- [30] Pasquato, L. Rancan, F. Scrimin, P. Mancin F. and Frigeri, C. (2000). N-Methylimidazole-functionalized gold nanoparticles as catalysts for cleavage of a carboxylic acid ester. *Chem. Commun.* 2253–2254.
- [31] Ali, S. S. Hardt, J. I. Quick, K. L. Kim-Han, J. S. Erlanger, B. F. Huang, T. T. Epstein C. J. and Dugan, L. L. (2004). A biologically effective fullerene (C60) derivative with superoxide dismutase mimetic properties. *Free Radical Biol. Med.* 37: 1191–1202.
- [32] Manea, F. Houillon, F. B. Pasquato L. and Scrimin, P. (2004). Nanozymes: Gold-Nanoparticle-Based Transphosphorylation Catalysts. *Angew. Chem., Int. Ed.* 43: 6165–6169.
- [33] Comotti, M. Della Pina, Matarrese C. R. and Rossi, M. (2004). The Catalytic Activity of “Naked” Gold Particles. *Angew. Chem., Int. Ed.* 43: 5812–5815.

- [34] Tarnuzzer, R. W. Colon, J. Patil S. and Seal, S. (2005). Vacancy engineered ceria nanostructures for protection from radiation-induced cellular damage, *Nano Lett.*, 5, 2573–2577.
- [35] Beltrame, P. Comotti, M. Della C. Pina and Rossi, M. (2006). Aerobic oxidation of glucose: II. Catalysis by colloidal gold. *Appl. Catal., A* 297: 1–7.
- [36] Chen, J. P. Patil, S. Seal S. and McGinnis, J. F. (2006). Rare earth nanoparticles prevent retinal degeneration induced by intracellular peroxides. *Nat. Nanotechnol.* 1: 142–150.
- [37] Gao, L. Z. Zhuang, J. Nie, L. Zhang, J. B. Zhang, Y. Gu, N. Wang, T. H. Feng, J. Yang, D. L. Perrett S. and Yan, X. (2007). Intrinsic peroxidase-like activity of ferromagnetic nanoparticles. *Nat. Nanotechnol.* 2: 577–583.
- [38] Wei H. and Wang, E. (2008). Fe₃O₄ Magnetic Nanoparticles as Peroxidase Mimetics and Their Applications in H₂O₂ and Glucose Detection. *Anal. Chem.* 80: 2250–2254.
- [39] Natalio, F. Andre, R. Hartog, A. F. Stoll, B. Jochum, K. P. Wever, R. and Tremel, W. (2012). Vanadium pentoxide nanoparticles mimic vanadium haloperoxidases and thwart biofilm formation. *Nat. Nanotechnol.* 7: 530–535.
- [40] Fan, K. L. Cao, C. Q. Pan, Y. X. Lu, D. Yang, D. L. Feng, J. Song, L. N. Liang M. M. and Yan, X. Y. (2012). Magnetoferritin nanoparticles for targeting and visualizing tumour tissues. *Nat. Nanotechnol.* 7: 459–464.
- [41] Wang, Z. L. Liu, H. Y. Yang, S. H. Wang, T. Liu C. and Cao, Y. C. (2012). Nanoparticle-based artificial RNA silencing machinery for antiviral therapy. *Proc. Natl. Acad. Sci. USA.* 109: 12387–12392.
- [42] Vinita, Nirala, N. R. Prakash, R., (2018). One step synthesis of AuNPs@MoS₂-QDs composite as a robust peroxidase-mimetic for instant unaided eye detection of glucose inserum, saliva and tear. *Sensors and Actuators B* 263: 109–119.
- [43] Wei, H. and Wang, E. (2012). Nanomaterials with enzyme-like characteristics (nanozymes): next-generation artificial enzymes (II). *Chem. Soc. Rev.* doi: 10.1039/c3cs35486e.
- [44] He, W. W. Liu, Y. Yuan, J. S. Yin J. J., Wu, X. C. Hu, X. Zhang, N. K. Liu, J. B. Chen, C. Y. Ji Y. L. and Guo, Y. T. (2011). Au@Pt nanostructures as oxidase and peroxidase mimetics for use in immunoassays. *Biomaterials* 32: 1139–1147.
- [45] Fan, J. Yin, J. J. Ning, B. Wu, X. C. Hu, Y. Ferrari, M. Anderson, G. J. Wei, J. Y. Zhao Y. L. and Nie, G. J. (2011). Direct evidence for catalase and peroxidase activities of ferritin–platinum nanoparticles. *Biomaterials* 32: 1611–1618.
- [46] Liu, J. B. Hu, X. N. Hou, S. Wen, T. Liu, W. Q. Zhu, X. Yin J. J. and Wu, X. C. (2012). Au@ Pt core/shell nanorods with peroxidase-and ascorbate oxidase-like activities for improved detection of glucose. *Sens. Actuators B* 166–167: 708–714.

- [47] Wang, X. X. Wu, Q. Shan Z. and Huang, Q. M. (2011). BSA-stabilized Au clusters as peroxidase mimetics for use in xanthine detection. *Biosens. Bioelectron.* 26: 3614–3619.
- [48] Wang, S. Chen, W. Liu, A. L. Hong, L. Deng H. H. and Lin, X. H. (2012) Comparison of the peroxidase-like activity of unmodified, amino-modified, and citrate-capped gold nanoparticles. *Chem. Phys. Chem*, 13: 1199–1204.
- [49] He, W. W. Wu, X. C. Liu, J. B. Hu, X. N. Zhang, K. Hou, S. A. Zhou W. Y. and Xie, S. S. (2010). Design of AgM bimetallic alloy nanostructures (M = Au, Pd, Pt) with tunable morphology and peroxidase-like activity. *Chem. Mater.* 22: 2988–2994.
- [50] Jv, Y. Li B. X. and Cao, R. (2010). Positively-charged gold nanoparticles as peroxidase mimic and their application in hydrogen peroxide and glucose detection. *Chem. Commun.* 46: 8017–8019.
- [51] Lien, C. W. Huang C. C. and Chang, H. T. (2012). Peroxidase-mimic bismuth–gold nanoparticles for determining the activity of thrombin and drug screening. *Chem. Commun.* 48: 7952–7954.
- [52] Wang, S. Chen, W. Liu, A. L. Hong, L. Deng, H. H. Lin, X. H. (2012). Comparison of the peroxidase-like activity of unmodified, amino-modified, and citrate-capped gold nanoparticles, *Chem Phys Chem*, 13, 1199-1204.
- [53] Beltrame, P. Comotti, Della Pina M. C. and Rossi, M. (2006). Aerobic oxidation of glucose: II. Catalysis by colloidal gold. *Appl. Catal. A* 297: 1–7.
- [54] Beltrame, P. Comotti, M. Della Pina C. and Rossi, M. (2004). Aerobic oxidation of glucose I. enzymatic catalysis. *J. Catal.* 228: 282–287.
- [55] Garg, B. Bisht, T. and Lin, Y. C. (2015). Graphene-based nanomaterials as efficient peroxidase mimetic catalysts for biosensing applications: An overview. *Molecules* 20: 14155-14190.
- [56] Lin, Y. Ren, J. and Qu, X. (2014). Nano-gold as artificial enzymes: hidden talents. *Adv. Mater.* 264:200-4217.
- [57] Landon, P. Collier, P. J. Papworth, A. J. Kiely, C. J. and Hutchings, G. J. (2002), Direct formation of hydrogen peroxide from H₂/O₂ using a gold catalyst., *Chem. Commun.* 2058-2059.
- [58] Comotti, M. Della Pina, C. Matarrese, R. and Rossi, M. (2004). The catalytic activity of “naked” gold particles. *Angew. Chem. Int. Ed.* 43: 5812-5815.
- [59] Rousseau, S. Marie, O. Bazin, P. Daturi, M. Verdier, S. and Harlé, V. (2010). Investigation of methanol oxidation over Au/catalysts using operando IR spectroscopy: Determination of the active sites, intermediate/spectator species and reaction. *J. Am. Chem. Soc.* 132: 10832-10841.
- [60] Jiang, H. Chen, Z. Cao, H. And Huang, Y. (2012). Peroxidase-like activity of chitosan stabilized silver nanoparticles for visual and colorimetric detection of glucose. *Analyst* 137: 5560-5564.
- [61] Obliosca, J. M. Liu, C. Yeh, H. C. (2013). Fluorescent silver nanoclusters as DNA probes. *Nanoscale* 5: 8443-8461.

- [62] Sharma, J. Rocha, R. C. Phipps, M. L. Yeh, H. C. Balatsky, K. A. Vu, D. M. et al., (2012). A DNA-templated fluorescent silver nanocluster with enhanced stability. *Nanoscale* 4: 4107-4110.
- [63] Zhang, L. and Wang, E. (2014). Metal nanoclusters: new fluorescent probes for sensors and bioimaging. *Nano Today* 9: 132-157.
- [64] Zhang, L. Zhu, J. Guo, S. Li, T. Li, J. and Wang, E. (2013). Photoinduced electron transfer of DNA/Ag nanoclusters modulated by G-quadruplex/hemin complex for the construction of versatile biosensors. *J. Am. Chem. Soc.* 135: 2403-2406.
- [65] Ma, M. Zhang, Y. And Gu, N. (2011). Peroxidase-like catalytic activity of cubic Pt nanocrystals. *Colloids Surf. A* 373: 6-10.
- [66] Fan, J. Yin, J. J. Ning, B. Wu, X. Hu, Y. Ferrari, M. et al., (2011). Direct evidence for catalase and peroxidase activities of ferritin–platinum nanoparticles, *Biomaterials* 32 1611-1618.
- [67] Song, Y., X. Xia, X. Wu, P. Wang, L. Qin, *Angew. Chem. Int. Ed.* 126 (2014). 12659-12663.
- [68] Fan, J. Yin, J. J. Ning, B. Wu, X. C. Hu, Y. Ferrari, M. Anderson, G. J. Wei, J. Y. Zhao Y. L. and Nie, G. J. (2011). Integration of Platinum Nanoparticles with a Volumetric Bar-Chart Chip for Biomarker Assays, *Biomaterials*, 32, 1611–1618.
- [69] Ma, M. Zhang Y. and Cu, N. (2011). Peroxidase-like catalytic activity of cubic Pt nanocrystals, *Colloids Surf., A*, 373, 6–10.
- [70] Ferrando, R. Jellinek, J. and Johnston, R. L. (2008). Nanoalloys: from theory to applications of alloy clusters and nanoparticles. *Chem. Rev.* 108: 845-910.
- [71] He, W. Wu, X. Liu, J. Hu, X. Zhang, K. Hou, S. et al., (2010). Design of AgM bimetallic alloy nanostructures (M= Au, Pd, Pt) with tunable morphology and peroxidase-like activity. *Chem Mater.* 22: 2988-2994.
- [72] Dai, Z. Liu, S. Bao, J. and Ju, H. (2009). Nanostructured FeS as a mimic peroxidase for biocatalysis and biosensing. *Chem. Eur. J.* 15: 4321-4326.
- [73] He, W. Jia, H. Li, X. Lei, Y. Li, J. Zhao, H. et al., (2012). Understanding the formation of CuS concave superstructures with peroxidase-like activity. *Nanoscale* 4: 3501-3506.
- [74] Dutta, A. K. Das, S. Samanta, S. Samanta, P. K. Adhikary, B. and Biswas, P. (2013). CuS nanoparticles as a mimic peroxidase for colorimetric estimation of human blood glucose level., *Talanta* 107: 361-367.
- [75] Hu, L. Yuan, Y. Zhang, L. Zhao, J. Majeed, S. And Xu, G. (2013). Copper nanoclusters as peroxidase mimetics and their applications to H₂O₂ and glucose detection. *Anal. Chim. Acta.* 762: 83-86.
- [76] Lu, X. F. Bian, X. J. Li, Z. C. Chao, D. M. and Wang, C. (2013). A facile strategy to decorate Cu₉S₅ nanocrystals on polyaniline nanowires and their synergetic catalytic properties. *Sci. Rep.* 3: 2955.
- [77] He, W. Wamer, W. Xia, Q. Yin, J. J. and Fu, P. P. (2014). Enzyme-like activity of nanomaterials. *J Environ. Sci. Health C* 32: 186-211.

- [78] Jariwala, D. Sangwan, V. K. Lauhon, L. J. Marks, T. J. and Hersam, M. C. (2013) Carbon nanomaterials for electronics, optoelectronics, photovoltaics, and sensing. *Chem. Soc. Rev.* 42: 2824-2860.
- [79] Wang, X. Guo, W. Hu, Y. Wu, J. and Wei, H. (2016). *Nanozymes: next wave of artificial enzymes*, Springer.
- [80] Song, Y., Wang, X., Zhao, C., Qu, K., Ren, J. and Qu, X. (2010). *Chem. Eur. J.* 16: 3617-3621.
- [81] Shi, W. Wang, Q. Long, Y. Cheng, Z. Chen, S. Zheng, H. et al., (2011) Label-free colorimetric detection of single nucleotide polymorphism by using single-walled carbon nanotube intrinsic peroxidase-like activity. *Chem. Commun.* 47: 6695-6697.
- [82] Wang, X. Qu, K. Xu, B. Ren, J. and Qu, X. (2011) multicolor luminescent carbon nanoparticles: synthesis, supramolecular assembly with porphyrin, intrinsic peroxidase-like catalytic activity and applications. *Nano. Res.* 4: 908-920.
- [83] Sun, H. Zhao, A. Gao, N. Li, K. Ren, J. and Qu, X. (2015). Deciphering a nanocarbon-based artificial peroxidase: chemical identification of the catalytically active and substrate-binding sites on graphene quantum dots, *Angew. Chem. Int. Ed.* 54: 7176-7180.
- [84] Natalio, F. Andre, R. Hartog, A. F. Stoll, B. Jochum, K. P. Wever, R. and Tremel, W. (2012). Vanadium pentoxide nanoparticles mimic vanadium haloperoxidases and thwart biofilm formation. *Nat. Nanotechnol.* 7: 530–535.
- [85] Fan, K. L. Cao, C. Q. Pan, Y. X. Lu, D. Yang, D. L. Feng, J. Song, L. N. Liang M. M. and Yan, X. Y. (2012). Magnetoferritin nanoparticles for targeting and visualizing tumour tissues. *Nat. Nanotechnol.* 7: 459–464.
- [86] Li, R. Zhen, M. Guan, M. Chen, D. Zhang, G. Ge, J. et al., (2013) A novel glucose colorimetric sensor based on intrinsic peroxidase-like activity of C₆₀-carboxyfullerenes. *Biosens. Bioelectron.* 47: 502-507.
- [87] Feng, D. Gu, Z. Y. Li, J. R. Jiang, H. L. Wei, Z. And Zhou, H. C. (2012). Zirconium-metalloporphyrin PCN-222: mesoporous metal–organic frameworks with ultrahigh stability as biomimetic catalysts. *Angew. Chem. Int. Ed.* 124: 10453-10456.
- [88] Yang, F., S. Hu, Y. Zhang, X. Cai, Y. Huang, F. Wang, et al., (2012). *Adv. Mater.* 24: 5205-5211.
- [89] Zhang, J. W. Zhang, H. T. Du, Z. Y. Wang, X. Yu, S. H. And Jiang, H. L. (2014) Water-stable metal–organic frameworks with intrinsic peroxidase-like catalytic activity as a colorimetric biosensing platform. *Chem. Commun.* 50: 1092-1094.
- [90] Zhang, Y. Tian, J. Liu, S. Wang, L. Qin, X. Lu, W. et al., (2012). Novel application of CoFe layered double hydroxide nanoplates for colorimetric detection of H₂O₂ and glucose. *Analyst* 137: 1325-1328.
- [91] Yin, J. F. Cao H. Q. and Lu, Y. X. (2012). Meglumine catalyzed expeditious four-component domino protocol for synthesis of pyrazolopyranopyrimidines in aqueous medium. *J. Mater. Chem.* 22:527–534.

- [92] Gascon, J. Aktay, U. Hernandez-Alonso, M. D. Van Klink, G. P. and Kapteijn, F. (2009). Amino-based metal-organic frameworks as stable, highly active basic catalysts *J. Catal.* 261: 75-87.
- [93] Li, C. Wei, M. Evans, D. G. and Duan, X. (2014). Layered double hydroxide-based nanomaterials as highly efficient catalysts and adsorbents. *Small* 10: 4469-4486.
- [94] Chen, L. Sun, K. Li, P. Fan, X. Sun, J. and Ai, S. (2013). DNA-enhanced peroxidase-like activity of layered double hydroxide nanosheets and applications in H₂O₂ and glucose sensing. *Nanoscale* 5: 10982-10988.
- [95] Su, L. Yu, X. Cai, Y. Kang, P. Qin, W. Dong, W. et al., (2017). *Anal. Chim. Acta.* 987: 98-104.
- [96] Guo, Y. Liu, X. Wang, X. Iqbal, A. Yang, C. Liu, W. et al., (2015). Carbon dot/NiAl-layered double hydroxide hybrid material: facile synthesis, intrinsic peroxidase-like catalytic activity and its application. *RSC Adv.* 5: 95495-95503.
- [97] Zhang, Y. W. Tian, J. Q. Liu, S. Wang, L. Qin, X. Y. Lu, W. B. Chang, G. H. Luo, Y. L. Asiri, A. M. Al-Youbi A. O. and Sun, X. P. (2012). Novel application of CoFe layered double hydroxide nanoplates for colorimetric detection of H₂O₂ and glucose. *Analyst*, 137: 1325–1328.
- [98] Deng, L. Guo, S. J. Liu, Z. J. Zhou, M. Li, D. Liu, L. Li, G. P. Wang E. K. and Dong, S. J. (2010). To boost c-type cytochrome wire efficiency of electrogenic bacteria with Fe₃O₄/Au nanocomposites. *Chem. Commun.* 46: 7172–7174.
- [99] Jv, Y. Li B. X. and Cao, R. (2010). Positively-charged gold nanoparticles as peroxidase mimic and their application in hydrogen peroxide and glucose detection. *Chem. Commun.* 46, 8017–8019.
- [100] Luo, W. Li, Y. S. Yuan, J. Zhu, L. H. Liu, Z. D. Tang and H. Q. And Liu, S. S. (2010). Ultrasensitive fluorometric determination of hydrogen peroxide and glucose by using multiferroic. BiFeO₃ nanoparticles as a catalyst. *Talanta* 81: 901–907.
- [101] Sun, H. Zhou, Y. Ren J. and Qu, X. (2018). Carbon nanozymes: enzymatic properties, catalytic mechanism, and applications. *Angew. Chem. Int. Ed.* 57: 9224–9237.
- [102] Wang, Q. Wei, H. Zhang, Z. Wang, E. and Dong, S. (2018). Nanozyme: an emerging alternative to natural enzyme for biosensing and immunoassay. *Trends Anal. Chem.* 105: 218–224.
- [103] Henriksen, A. Smith A. T. and Gajhede, M. (1999). The structures of the horseradish peroxidase C-ferulic acid complex and the ternary complex with cyanide suggest how peroxidases oxidize small phenolic substrates. *J. Biol. Chem.* 274: 35005–35011.
- [104] Gao, L. Zhuang, J. Nie, L. Zhang, J. Zhang, Y. Gu, N. Wang, T. Feng, J. Yang, D. Pettett S. and Yan, X. (2007). Intrinsic peroxidase-like activity of ferromagnetic nanoparticles. *Nat. Nanotechnol.* 2: 577–583.

- [105] Naganuma, T. (2017). Shape design of cerium oxide nanoparticles for enhancement of enzyme mimetic activity in therapeutic applications. *Nano Res.* 10: 199–217.
- [106] Yuan, F. Zhao, H. Zang, H. Ye F. and Quan, X. (2016). Three-dimensional graphene supported bimetallic nanocomposites with DNA regulated-flexibly switchable peroxidase-like activity. *ACS Appl. Mater. Interf.* 8: 9855–9864.

Chapter 8**GRAPHENE: A REVOLUTIONARY EXOTIC MATERIAL
AND ITS APPLICATIONS**

***Seema Awasthi^{1,*}, O.N. Srivastava², A. Rajanikanth¹
and C. Bansal¹***

¹School of Physics, University of Hyderabad, Hyderabad, INDIA

²Department of Physics, Banaras Hindu University, Varanasi, INDIA

ABSTRACT

Materials science involves understanding of materials behavior based on their macro/microstructures. Nanoscience has emerged as one of the exciting area of materials science and has created an impact on almost every field of science and technology. Particles at the nanoscale length exhibit exotic physico-chemical properties as compared to their bulk counterparts. Carbon is the most studied material in nanoscience due to its versatility in being found in 0D, 1D, 2D and 3D structures. Graphene, a 2D honeycomb lattice of carbon atoms attracted the attention of scientists from all over the world after its discovery in 2004. This exotic form of carbon has versatile properties and manifold applications. It has also provided a whole new branch of materials known as two dimensional layered materials, which exhibits similar and superior properties and applications when combined with/without graphene. The present chapter deals with various synthesis methods, properties and applications of graphene. This chapter focuses mainly on electrochemical exfoliation method for the production of graphene through aqueous and non-aqueous route, since it is a promising bulk method for producing graphene from graphite and can produce single and multilayer graphene in less time. A summary of important characterization methods for graphene will also be discussed. Applications of graphene in many areas of materials science will also be discussed, due to which it has created huge impact on research and current societal development. Exfoliation of layers of graphene from bulk graphite has given a lead to exfoliate various other stable layered materials besides graphite.

* Corresponding Author's Email: sasp2111@gmail.com.

These types of new exotic materials other than graphene and their hybrid structure with graphene will also be discussed briefly.

Keywords: graphene, synthesis, applications, materials science, nanoscience, layered materials

1. INTRODUCTION

Materials science continues to occupy a central place in our lives through the design and creation of new materials and improve our quality of life over a period of time with the discovery of new materials [1]. One of the recent and most exciting branches of materials science is the area of nanoscience and technology, in which we study the behavior of materials at nanometer scale. Nanoscience requires the precise knowledge of material structures/microstructures at nanoscale, and is an interdisciplinary branch of materials science. It has potential to create a huge societal impact now a day. It has been identified as one of the most critical technologies that would shape the future of the humans in 21st century. The nanostructured materials may be metals [2], alloys and intermetallics [3], as well as ceramics [4]. They can be created in zero dimension (0D), one dimension (1D), two dimensions (2D) and three dimensions (3D). These nanomaterials show different superior properties in comparison with their bulk counterparts. H. Gleiter [5] has summarized basic physical concepts and microstructural features of equilibrium and non-equilibrium nanostructured materials. Due to their superior properties, various nanomaterials show a range of applications in diverse fields [6, 7]. In vast variety of nanomaterials available today, carbon nanomaterials are one of the most studied systems. Carbon is the most abundant element of earth; it exists in a vast number of organic compounds. Carbon atoms can bond in many diverse ways, giving rise to various allotropes such as graphite and diamond in macroscopic form and fullerenes, carbon nanotubes and graphene in microscopic form [8, 9].

2. GRAPHENE

After the discovery of graphene in 2004 [10], research groups from worldwide could not take their eyes off from its fascinating properties and soon it became a rapidly rising star on the horizon of materials science and condensed-matter physics. These discoveries also lead to the 2010 Nobel Prize in physics to AK Geim and KS Novoselov. Graphene is an infinite 2D layer of sp^2 hybridized carbon atoms on a hexagonal lattice, which is one of the five 2D Bravais lattices. It is the basic building block of fullerenes, nanotubes and graphite. It can be wrapped into zero dimensional fullerenes, rolled into one dimensional carbon nanotubes and by piling up graphene layers in an ordered way one can form 3-dimensional graphite. There are other

pseudo-2D sp^2 hybridized carbon structures, such as bi-, tri- and few-layers graphene. Few layer graphene has 3-10 layers of such 2D sheets [9]. Graphene exhibits many useful properties. In a 2D carbon system for graphene, three carbon electrons in four hybridized bonding levels ($2s^2p_x^12p_y^12p_z^1$) form strong in-plane sp^2 bond consisting of a honeycomb structure and a fourth electron known as π electron spreads out over top or bottom of the layer. These π electrons play an important role in coupling interaction of multilayered graphene. The two dimensionally spread C=C resonance structure and the hybridized electron confined in graphene planes are directly related to graphene's unique characteristics such as ballistic electron conduction, high thermal conduction and high mechanical strength [11]. The unique properties of graphene includes electronics properties-it has high electron mobility $\sim 10000 \text{ cm}^2\text{V}^{-1}\text{s}^{-1}$ [12], it can sustain current up to six orders of magnitude higher than copper, mechanical properties- graphene is the strongest materials ever known with a Young's modulus of 1 TPa and intrinsic strength 130 GPa [13], thermal properties-graphene has excellent thermal conductivity of $5000 \text{ Wm}^{-1}\text{K}^{-1}$, ~ 25 times greater than silicon [14], graphene has the highest surface area of $2630 \text{ m}^2\text{g}^{-1}$, that makes it an excellent support to attach chemical groups or other nanomaterials and increased adsorption capacity and hence enhanced chemical properties [15].

2.1. Applications of Graphene

Graphene sheets have been shown to be very promising for many potential applications e.g., high performance in nanoelectronics, as a transparent conductor, in photonics, in optoelectronics [16] and in composites [17]. Different types of graphene lead to a variety of applications in various fields such as electronics, life sciences, medical science, and chemical sciences. These outstanding applications of graphene change many things presently and are continuing to do so. Scientists all over the world are continuously researching the new possibilities in application of graphene. Some of the graphene applications are described below.

2.1.1. Nanoelectronics

The compelling demand for higher performance and lower power consumption in electronic systems is the main driving force of the electronics industry's quest for devices and architectures based on new materials [18]. The thinness, mechanical strength and flexibility, high current carrying capacity ($\sim 10^9 \text{ A/cm}^2$) and very high carrier mobility is making graphene extremely appealing for application in electronics, specifically regarding its exploitation as a channel material in field effect transistors (FETs) and as a potential alternative for silicon-based devices [16]. However, being a zero gap semiconductor, graphene cannot be directly utilized in FET applications. For transistor applications, graphenenanoribbons in the form of a quasi-one dimensional structure, with narrow widths and atomically smooth edges may be useful. They are

predicted to have band gaps useful for room temperature FET applications with excellent switching speed and high carrier mobility [19].

2.1.2. Composites Materials with Graphene as Reinforcing Agent

To achieve specific properties and cost effectiveness and to fully exploit nanomaterial properties making combination of nanoparticles of various dimensionalities with polymers or other base materials is gaining special attention now a days. In all the systems of matrix materials, polymers are most studied matrix materials for this purpose. Due to unique physical properties of graphene, the most immediate application of graphene is its integration in polymer composites materials. Polymer-graphene composites show superior mechanical, thermal gas barrier, electrical and flame retardant properties compared to neat polymers [20]. However, interfacial bonding between the filler and matrix material plays a crucial role in property enhancement of the final product. For this purpose, graphene oxide which bears hydroxyl, carbonyl and carboxyl group on its surface interacts with side chains of the polymer and gives rise to strong interfacial bonding thereby improving various properties [19].

2.1.3. Self-Healing Materials

Self-healing materials are intelligent materials capable of feeling external stimulus to repair them-selves after damage and restore their intrinsic properties, thus can extend lifespan, improve, security, save cost and achieve sustainable development. Graphene based self-healing materials have enhanced mechanical properties, electrical and thermal conductivities, responsive to external stimuli, healing efficiency and energy conversion efficiency compared with conventional materials [21]. These materials have applications in biological systems, flexible electronic devices [22], coating, self-cleaning absorbents, and biomimetic materials [21].

2.1.4. Supercapacitors

Supercapacitors/electrochemical capacitors/ultra-capacitors, are supposed to be promising candidates for alternative energy storage devices because of their high rate capability, pulse power supply, long cycle life, simple principle, and low maintenance cost. Due to extraordinarily high electrical conductivity and large surface area, graphene based materials exhibit great potential for application in supercapacitors [23]. Table 1 describes many other important properties of graphenenanosheets and their applications related to those properties.

2.2. Synthesis of Graphene

The real life applications of graphene and also for other futuristic aspects, it is very essential to produce graphene in a cost effective, defect free and in less time consuming way. There are many synthesis methods to prepare graphene and its

derivatives through physical/chemical methods which are broadly categorized into top down and bottom up approaches. The abundantly available graphite is made of stacked layers of graphene sheets. These sheets are held together by van der Waals forces. By means of exfoliation/cleavage/chemical energy, one can break or loosen these bonds and separate individual graphene sheets. There are various methods for producing graphene.

Table 1. The important properties of graphene nanosheets and related applications

S.No.	Properties	Description	Related applications
1.	Electrical Properties	Electron mobility-10000 to 50000 $\text{cm}^2\text{V}^{-1}\text{s}^{-1}$	Electronic devices[7,22], supercapacitors [23], Li-ion Battery [24], energy[25]
2.	Mechanical Properties	Young's modulus-1TPa, Intrinsic strength-130 Gpa	Actuators [21], tissue engineering [26]
3.	Thermal Properties	Thermal conductivity-5000 $\text{Wm}^{-1}\text{K}^{-1}$	Thermal interface materials [27]
4.	Chemical Properties	Support for anchoring various chemical functionalities or with molecules	environmental sensors[28]
5.	Optical Properties	Transparency ~97%	photo detectors [29]
6.	Magnetic properties	long spin diffusion length (~ 4 μm) at room temperature	Spintronics [30]
Other properties			
7.	Reinforcing agent	Due to extraordinary electrical, thermal, mechanical properties	Composites with metal [31] and polymer [17,20, 21], electromagnetic interference shielding [32]
8.	Catalyst	Graphene can be used as catalysts materials	[33]
9.	Asbullet proof materials		[34]

2.2.1. Micromechanical Cleavage of Highly Oriented Pyrolytic Graphite (HOPG)

The scotch tape technique is the first ever method to obtain graphene from graphite [10]. The as- obtained graphene prepared in this way is of very high quality and contains negligible amount of defects, however the yield is very poor. It involves

the repeated peeling of graphite layers with the help of scotch tape, after peeling the layers are deposited on silicon wafer and studied for further characterizations. This type of graphene contains negligible or very less amount of defects and were used to study the various properties of graphene.

2.2.2. Arc Discharge Method

It is one of the oldest methods to synthesize carbon nanomaterials. It was first used for fullerenes synthesis in 1990 by Krastchmer and Hoffman [35]. For the synthesis of graphene, the set up consists of pure graphite rods as cathode and anode electrodes fitted in a water cooled reactor, in inert atmosphere. Current in discharge is of the order of 100-150A. The commonly used inert gases are hydrogen, ammonia, argon, argon-hydrogen mixture, helium and helium-hydrogen. At the end of the arc discharge process, black color soot deposited on cathode and on chamber walls is collected for further characterization and applications. Awasthi et al. did a study of various argon gas pressures to synthesize single walled carbon nanotubes from arc discharge method [36].

2.2.3. Chemical Vapor Deposition

Chemical vapor deposition (CVD) is one the most popular method for the synthesis of graphene of high quality and large area graphene. Chemical vapor deposition is a technique of thin film deposition on substrates from vapor species through chemical reaction. One of the highly popular techniques of graphene growth is thermal decomposition of Si on the (0001) surface plane of single crystal of 6H-SiC [37]. The graphitic structure formation requires 2500°C without catalysts, which is too high. So the introduction of catalysts is required to lower the energy barriers. Catalysts also provide support for the graphitic structure formation. Copper and Nickel are most common catalyst support for the formation of graphene [38].

2.2.4. Physical Exfoliation of Graphite

This method of ball milling is generally used to reduce the size of bulk material in nano forms. It consists of a milling chamber whose inside walls are made of anticorrosion material such as rubber/polymer lining and manganese steel. The balls are made of stainless steel, ceramics or rubber. It is the process of splitting a layered material into atomically thin sheets. Graphite layers can be exfoliated by ball milling a mixture of graphite and chemically inert water soluble inorganic salts. Some researchers produced graphene sheets by wet ball milling of graphite in melamine [39]. This technique is known as wet ball mill and gained recent interest in large scale production of graphene from graphite in different medium.

2.2.5. Chemical/Thermal Exfoliation of Graphite Oxide

Graphite oxide (GO) is a compound of carbon, oxygen and hydrogen in variable ratios. GO obtained by treating graphite with strong oxidizers. Thermally reduced graphene from GO, produced from graphite using various chemical oxidation routes,

has attracted considerable attention because of its high yield and lowering the cost. However thermal reduction of GO is a complex multistep phenomenon, and can also significantly affect the graphene lattice and introduce a number of defects because in chemical reduction, individual GO sheets are chemically reduced by a strong chemical base. Hummer's method involves treatment of graphite with potassium permanganate and sulfuric acid [40]. GO possess layer structure like graphite with increased/irregular spacing. Reduced graphene oxide (rGO) is a single layer of graphite oxide which has been obtained by complete exfoliation of graphite oxide after removing the various functional groups present on graphite oxide lattice by reducing it in presence of strong reducing agents, or by simple sonication.

2.2.6. Solvent Assisted Exfoliation

Liquid phase exfoliation gained vast attention in the synthesis of graphitic materials recently because of its reduced cost and simple experimentation procedures. With the help of ultrasonication some draw backs e.g., high temperature, pressure and long reactions were made easy whereby graphite can be directly exfoliated to graphene layers. In this method, graphite is being dispersed in a liquid medium containing a suitable ionic liquid by sonication. A suitable surfactant can be added in order to prevent restacking of graphene sheets in the solutions. The word suitable refers to those surfactants or solvents which have comparable surface energy along with that of graphite. SDBS, NMP are some common surfactant used for the purpose. Lotya et al. exfoliated graphite in water surfactant solutions and produced suspended graphene. Transmission electron microscopy showed the dispersed phase to consist of small graphitic flakes. More than 40% of these flakes had <5 layers with ~3% of flakes consisted of monolayers [41].

2.3. Electrochemical Exfoliation of Graphite

Various synthesis methods described above produce different types of graphene and their derivatives in terms of their structure and properties, which can be used in various types of applications according to their utility. However, these methods have their own set of advantages and disadvantages. They can be time consuming, use of high temperature requires more power consumption, strong acid treatment affects the honeycomb lattice, disrupts the sp^2 bonding and can affect various properties of graphene. By using electrochemical method, one can obtain desired graphene flakes in minutes under suitable experimental conditions. Recently electrochemical methods have been demonstrated by a number of research groups to produce graphene flakes in milligram and gram quantities. There is still a need to develop a method in which we can tune the structure of graphene just by choosing raw materials, and also can vary

number of layers in graphene by making simple modification in the process. The added advantage with any of the other synthesis methods should also include its cost effectiveness and environmental friendly nature. A simple electrochemical set up avoids sophisticated instrumentation/handling, and can be finished even in minutes to hrs and gives better yield/quality of the end product. The electrochemical exfoliation of graphite has recently gained sufficient attention due to its ease of process, cost effectiveness; green and environmental friendly nature and it can be operated under ambient conditions. There are also some reviews available in which the authors elaborated studies about the synthesis of graphene sheets through electrochemical exfoliation method which have been done in past years [42, 43]. The typical experimental set up for electrochemical exfoliation consists of an electrochemical cell which comprises of solvent with supporting electrolyte, electrodes, and a dc power supply or a potentiostat. The selection of suitable solvent and electrolyte is an important and tedious task as the end product structure quality yield depends on it. The solvent should be able to dissolve high concentration of electrolyte, it should be stable during oxidation/reduction reaction in the electrochemical cell, and the electrolyte should be chemically and electrochemically inert in the experiment [44]. The experimental arrangement for the electrochemical set up can be divided in two types, (i) two electrode system, in which one positive and one negative electrode are immersed in a suitable electrolyte and connected through a power supply. (ii) Three electrodes system in which a WE, CE and RE are immersed in an electrolyte solution and connected through a power supply. The WE is the electrode where exfoliation reaction takes place. WE carries out the electrochemical event of interest e.g., exfoliation in the case of graphene synthesis. The types of WE can be varied from experiment to experiment. The purpose of counter electrode is to complete the electrical circuit. Current is recorded as electron flows between the WE and CE. The reference electrode is used as a reference point against which the potential of other electrodes can be measured in an electrochemical cell. Some commonly used RE are saturated calomel electrode (SCE), standard hydrogen electrode (SHE), and the AgCl/Ag electrode [44]. For the production of graphene sheets through electrochemical exfoliation contains following experimental arrangements- (i) a graphite working electrode (commonly used graphite electrode are, natural graphite fill rods, sheets or highly oriented pyrolytic graphite (HOPG)), (ii) a standard RE, depending upon the electrolyte, (iii) A CE (can be platinum wire, foil, or sometimes graphite rods to increase the yield), (iv) An aqueous or non-aqueous electrolyte, (v) DC power supply or a potentiostat. The schematic set up for the above system shown in Figure 1 (a). Figure 1 (b) shows the reaction vessel after the complete exfoliation of graphite electrode. The processes involved in exfoliation experiment are anodic oxidation and cathodic oxidation, in non-aqueous solvents and in aqueous acidic electrolytes [42].

When the electrochemical exfoliation is performed under suitable electrolyte and operational conditions, intercalation of cations/anions from the electrolyte into graphite electrode results in the structural expansion of graphite layers. The WE/graphite electrodes swells and corrodes after complete intercalation, a black precipitate gradually appears at the bottom of the reaction vessel, which can be collected by filtering. After washing several times to completely remove the contaminated species due to electrolyte it is taken for further characterization and applications. One disadvantage of graphene flakes synthesized by this method is that the graphene sheets often re-aggregate. This problem can be overcome by adding surfactants either in the electrolyte while performing the electrochemical reaction or after the completion of reaction during cleaning and ultra-sonication process. Several research groups have synthesized graphene from graphite through electrochemical exfoliation in different electrolyte medium [45-47].

Su et al. [45] prepared high quality and large area graphene sheets by electrochemical exfoliation of natural graphite flakes in sulphuric acid as electrolyte medium. Hui-Lin Guo and co-workers synthesized high quality GNS in large quantity via electrochemical reduction of exfoliated graphite oxide precursor at cathodic potentials [48]. Singh et al. have produced high quality GNS from pencil by electrochemical exfoliation in ionic liquid medium by following non-aqueous route [49]. We have synthesized graphene nanosheets (GNS) through commercially available pencil lead, these GNS were used to prepare composites with polyaniline on ITO coated PET substrate. Table 2 shows the various efforts on synthesis of graphene through electrochemical exfoliation of graphite.

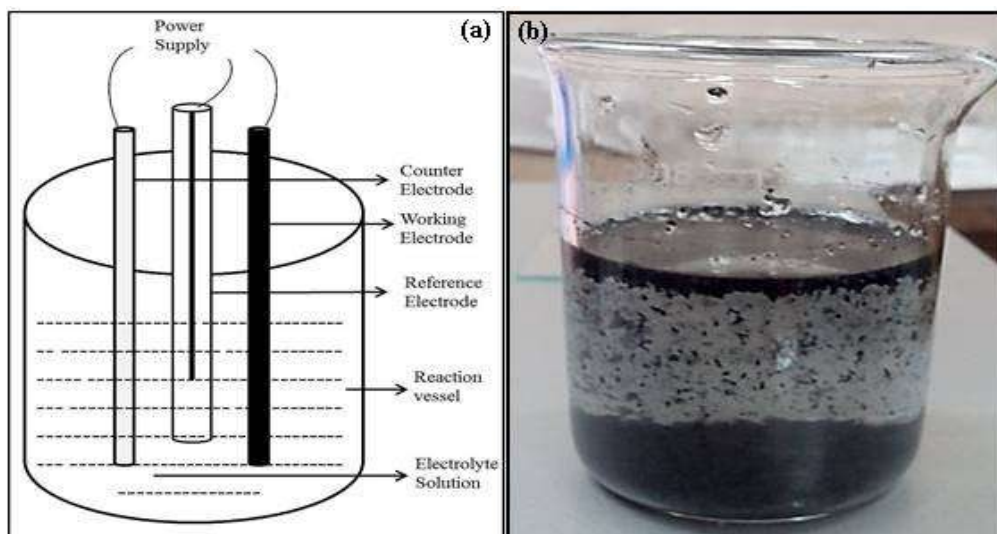


Figure 1. (a) Schematic diagram of electrochemical exfoliation set up, (b) Reaction vessel after the complete exfoliation of graphite electrode.

3. CHARACTERIZATION

In order to exploit the unique properties of any materials, characterizing the synthesized materials is of crucial importance. Morphology, texture, surface chemistry, and other properties of graphene, are important to study their suitable applications according to their structure and properties.

Scanning electron microscopy is a powerful technique which permits the characterization of materials and surfaces on a local scale. Recently transmission electron microscopy has achieved a unique distinction, for the characterization of different nano-structured materials. Both these techniques are used to study the surface morphology, number of layers, thickness, and extent of defect, vacancy and dislocations. Figure 2(a-f) shows the scanning electron microscope images of pencil graphite and as-synthesized GNS from 8V to 12V, respectively [50].

I-V characteristics of the GNS-PANI composite device shows a decrease in band gap of PANI from 2.8 eV to 6.9 meV at 15 wt% loading of GNS in PANI SEM and Raman spectroscopy show good dispersion of GNS and interfacial interaction with the GNS-PANI composite by a significant shift in the G peak at 15 wt% GNS-PANI, further confirming the formation of the composite at 15 wt% [50].

Table 2. Methodology used for synthesis of graphene via electrochemical route

S.N.	Working electrode (WE)	Counter electrode (CE)	Reference electrode (RE)	Electrolyte	Properties of end product
1	HOPG	--	Ag/AgCl	0.1 mol/L Na ₂ SO ₄ (aq.)	Tri layer graphene [52]
2	Graphite rod	Graphite rod	--	10mL IL ² and 10mL IL ³	1.1nm thick flakes [53]
3	Graphite plate	Pt foil	Saturated calomel electrode (SCE)	96% H ₂ SO ₄	Few layer graphene [54]
4	Graphite rod	Platinum foil	Platinum wire	0.1M SDS	High quality monolayers 1.0nm thick [49]
5	Pencil	Pt spiral	Pt	10mL IL ¹	Monolayers 0.8 and 1.3nm thick [55]

HOPG- Highly oriented pyrolytic graphite

IL¹-triethylsulfonium bis (trifluoromethylsulfonyl) imide ionic liquid

IL²-1-octyl-3-methyl-imidazolium hexafluorophosphate

IL³-1-methyl-3-butylimidazolium tetrafluoroborate

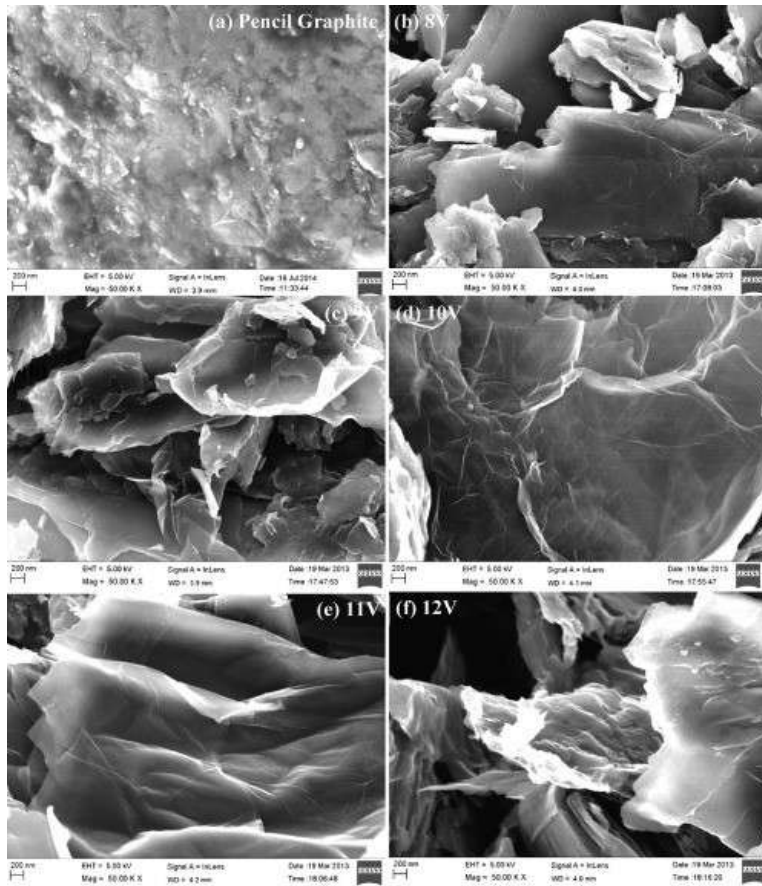


Figure 2. Scanning electron microscopic images of (a) pencil graphene, and exfoliated GNS at different voltages (b) 8 V, (c) 9 V, (d) 10 V, (e) 11 V, and (f) 12 V. (Awasthi et al. [50], with permission from Elsevier).

In the continuation of various efforts for the synthesis of graphene from graphite, we have also synthesized bi layer graphene in non-aqueous electrolyte. The transmission electron micrographs of graphene prepared in this way is shown in Figure 3 (a-c). Figure 3 (a) shows a crumpled graphene sheet, while in Figure 3 (b) a transparent, large area graphene sheet is visible. Figure 3 (c) shows the high resolution TEM image of bilayer graphene, marked by arrows. The work is in progress and the further results will be discussed and described.

AFM is used to measure thickness, surface roughness and size distribution of graphene sheets in the sample. X ray diffraction is one of the most prominent techniques used for unraveling the structure as well as the phase of the materials in bulk and in thin film forms. XRD is used to identify crystallinity, atomic arrangement and crystal size of as-synthesized graphene. Raman spectroscopy possesses many advantages for materials characterization. The development of Raman spectroscopy has made it possible to look at very small quantities of materials and it is nondestructive technique

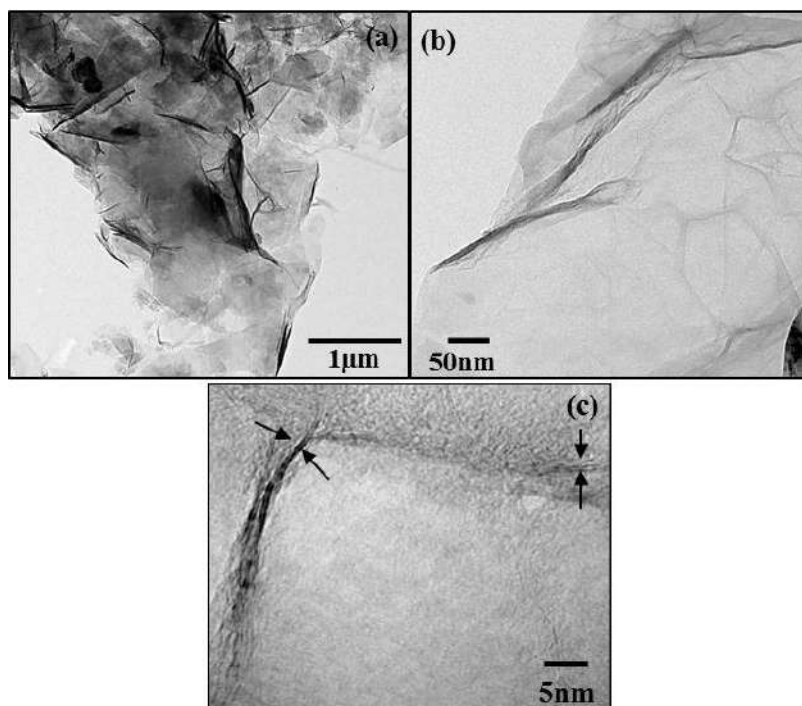


Figure 3. (a-c) Transmission electron micrographs of graphene sheets synthesized by electrochemical exfoliation of graphite in non-aqueous solvents.

Raman spectroscopy is particularly well suited to molecular morphology characterization of carbon materials. Graphene and other carbon nanomaterials have unique Raman spectra, making it an essential analytical technique for graphene characterization [55]. Fourier transform infrared spectroscopy (FTIR) is a powerful tool for identifying types of chemical bonds in a molecule by producing an infrared absorption spectrum that is like a molecular fingerprint. The peak at 1559 cm^{-1} in FTIR spectrum is due to C=C bond present in the ring structure [36]. It also gives the information about the various functional groups on graphene surface. XPS is another important technique to analyze the relative amount of carbon oxygen and other groups in graphene materials. BET surface area analysis is an advanced technique employed to determine the specific surface area and pore size distribution of graphene and its derivatives [56].

CONCLUSION

Two dimensional graphene has attracted lots of attention worldwide due to its excellent properties which is being used for the development of many useful applications from nano-electronics to energy storage. Preparation of high quality graphene materials in a cost effective manner and on the desired scale is essential for many applications. Graphene has also given us a new branch of 2D layered materials.

The determination of the unique features offered by graphene and other 2D materials is of critical importance in the design and development of truly novel constructs of enhanced or previously unattainable functionality.

ACKNOWLEDGMENTS

Authors are acknowledged to DST, DRDO, DAE and UGC for funding. One of the authors SeemaAwasthi is thankful to Dr DS Kothari PDF fellowship scheme of UGC for funding award letter no-F.4-2/2006 (BSR)/13-769/2012 (BSR) and CSIR-SRA (13(9008-A)/2018-Pool).

REFERENCES

- [1] Salavagione, H.J., Martínez, G. & Ellis, G. (2011). Graphene-based polymer nanocomposites. In *Physics and Applications of Graphene – Experiments*, Edited by Sergey Mikhailov, 169-192. Croatia: *InTechJanezaTrdine*, 9, 51000 Rijeka, Croatia.
- [2] Kumar, K.H., Venkates, N., Bhowmik, H. & Kuila, A. (2018). Metallic nanoparticle: A review. *Biomed. J. Sci. & Tech. Res.*, 4, 3765-3775.
- [3] Blaber, M.G., Arnold, M.D. & Ford, M.J. (2010). A review of the optical properties of alloys and intermetallics for plasmonics. *J. Phys.: Cond. Matter*, 22, 143201-143216.
- [4] Thomas, S.C., Harshita, Mishra P.K. & Talegaonkar, S. (2015). Ceramic nanoparticles: Fabrication methods and applications in drug delivery. *Current Pharmac. Design*, 21, 6165-6188.
- [5] Gleiter, H. (2000). Nanostructured materials: Basic concepts and microstructure. *Acta Materelia*, 48, 1-29.
- [6] Sharma, V.P., Sharma, U., Chattopadhyay, M. & Shukla, V.N. (2018). Advance applications of nanomaterials: A review. *Materials today proceedings*, 5(2), 6376-6380.
- [7] Kolahalam, L.A., Viswanath, I.V.K., Diwakar, B.S., Govindh, B., Reddy, V. & Murthy, Y.L.N. (2019). Review on nanomaterials: Synthesis and applications. *Mat.today proceedings*, 18, 2182-2190.
- [8] Terrones, M. (2003). Science and technology of the twenty-first century: synthesis, properties and applications of carbon nanotubes. *Annu. Rev. Mater. Res.*, 33, 419–501.
- [9] Geim, A.K. & Novoselov, K.S. (2007). The rise of graphene. *Nature Materials*, 6, 183-191.
- [10] Novoselov, K.S., Geim, A.K., Morozov, S.V., Jiang, D., Zhang, Y., Dubonos, S.V., Grigorieva, I.V. & Firsov, A.A. (2004). Electric field effect in atomically thin carbon films. *Science*, 306, 666-669.

- [11] Seung, H.H. (2011). Thermal reduction of graphene oxide. In *Physics and Applications of Graphene – Experiments*, Edited by Sergey Mikhailov, 73-90. Croatia: InTechJanezaTrdine, 9, 51000 Rijeka, Croatia.
- [12] Bolotin, K.I., Sikes, K.J., Jiang, Z., Klima, M., Fudenberg, G., Hone, J., Kim, P. & Stormer, H.L. (2008). Ultrahigh electron mobility in suspended graphene. *Solid State Commun.*, 146, 351-355.
- [13] Lee, C., Wei, X., Kysar, J.W. & Hone, J. (2008). Measurement of the elastic properties and intrinsic strength of monolayer graphene. *Science*, 321, 385-388.
- [14] Balandin, A. A., Ghosh, S., Bao, W., Calizo, I., Teweldebrhan, D., Miao, F. & Lau, C.N. (2008). Superior thermal conductivity of single-layer graphene. *Nano. Lett.*, 8, 902-907.
- [15] Kuila, T., Bose, S., Mishra, A. K., Khanra, P., Kim, N. H. & Lee, J. H. (2012). Chemical functionalization of graphene and its applications: *Prog. Mater. Sci.*, 57, 1061-1105.
- [16] Avouris, P. & Dimitrakopoulos, C. (2012). Graphene: Synthesis and applications. *Materials Today*, 15, 86-97.
- [17] Itapu, B.M. & Jayatissa, A.H. (2018). A review in graphene/polymer composites. *Chem. Sci. Int. J.*, 23, 1-16.
- [18] Fiori, G., Bonaccorso, F., Lannaccone, G., Palacios, T., Neumaier, D., Seabaugh, A., Banerjee, S.K. & Colombo, L. (2014). Electronics based on two-dimensional materials. *Nature Nanotech.*, 9, 768-779.
- [19] Tahy, K., Xing, H. & Jena, D. (2013). Graphenenanoribbonfets for digital electronics: Experiment and modeling. *Int. J. Circ. Theor. Appl.*, 41, 603–607.
- [20] Govindaraj, P., Fox, B., Aitchison, A. & Hameed, N. (2019). A review on graphene polymer nanocomposites in harsh operating conditions. *Ind. Eng. Chem. Res.*, 58 (37), 17106–17129.
- [21] Li, G., Xiao, P., Hou, S. & Huang, Y. (2019). Graphenebased self-healing materials. *Carbon*, 146, 371-387.
- [22] Wu, S., Li, J., Zhang, G., Yao, Y., Li, G., Sun, R., et al. (2017). Ultrafast self-healing nanocomposites via infrared laser and its application in flexible electronics. *ACS Appl. Mater. Interfaces*, 9, 3040-3049.
- [23] Huang, Y., Liang, J. & Chen, Y. (2012). An overview of the applications of graphene-based materials in supercapacitors. *Small*, 8, 1-30.
- [24] Wang, G., Shen, X., Yao, J. & Park, J. (2009). Graphenenanosheets for enhanced lithium storage in lithium ion batteries. *Carbon*, 47, 2049-2053.
- [25] Zhu, J., Yang, D., Yin, Z., Yan, Q. & Zhang, H. (2014). Energy applications graphene and graphene-based materials for energy storage applications. *Small*, 10, 3480-3498.
- [26] Shin, S.R., et al. (2016). Graphene-based materials for tissue engineering. *Adv. Drug Delivery Rev.*, 105, 255-274.
- [27] Shahil, K. M. F. & Balandin, A. A. (2012). Graphene–multilayer graphenenanocomposites as highly efficient thermal interface materials. *Nano Lett.*, 12, 861–867.

- [28] Novikov, S., Lebedeva, N., Satrapinski, A., Walden, J., Davydov, V. & Lebedev, A. (2016). Graphenebased sensor for environmental monitoring of NO₂. *Sensors and Actuators B: Chem.*, 236, 1054-1060.
- [29] Liu, M, Yin, X., Ulin-Avila, E., Geng, B., Zentgraf, T., Ju, L., Wang, F. & Zhang, X. (2011). A graphene-based broadband optical modulator. *Nature*, 474, 64-67.
- [30] Han, W., Kawakami, R.K., Gmitra, M. & Fabian, J. (2014). Graphenespintronics. *Nature Nanotech.*, 9, 794-807.
- [31] Kumar, H.G.P. & Xavior, M.A. (2014). Graphenereinforced metal matrix composite (grmmc): A review, *ProcediaEngg.*, 97, 1033-1040.
- [32] Jan, R., Saboor, A., Khan, A.N. & Ahmad, I. (2017). Estimating EMI shielding effectiveness of graphene-polymer composites at elevated temperatures. *Mat. Res. Express*, 4, 085605-085613.
- [33] Huang, C., Li, C. & Shi, G. (2012). Graphenebased catalysts. *Energy Environ. Sci.*, 5, 8848-8868.
- [34] Lee, J. H., Loya, P.E., Lou, J. & Thomas, E. L. (2014). Dynamic mechanical behavior of multilayer graphene via supersonic projectile penetration. *Science*, 346, 1092-1096.
- [35] Krätschmer, W., Lamb, L. D., Fostiropoulos, K. & Huffman, D. R. (1990). C₆₀: A new form of carbon, *Nature*, 347, 354-358.
- [36] Awasthi, S., Awasthi, K. & Srivastava, O. N. (2018). Formation of single-walled carbon nanotube buckybooks, graphenenanosheets and metal decorated graphene. *J. Nano Res.*, 53, 37-53.
- [37] Berger, C., Song, Z., Li, T., Li, X., Ogbazghi, A.Y., Feng, R., Dai, Z., et al. (2004). Ultrathin epitaxial graphite: 2d electron gas properties and a route toward graphene-based nanoelectronics. *J. Phys. Chem. B*, 108, 19912-19916.
- [38] Mattevi, C., Kima, H. & Chhowalla, M. (2011). A review of chemical vapor deposition of graphene on copper. *J. Mater. Chem.*, 21, 3324-3334.
- [39] León, V., Quintana, M., Antonia Herrero, M., Fierro, L.G.J., da la Hoz, A., Prato, M. & Vázquez, E. (2011). Few-layer graphenes from ball-milling of graphite with melamine. *Chem. Commun.*, 47, 10936-10938.
- [40] Hummers, W.S. & Offeman, R.E. (1958). Preparation of graphitic oxide. *J. Am. Chem. Soc.*, 80, 1339-1339.
- [41] Lotya, M., Hernandez, Y., King, P.J., et al. (2009). Liquid phase production of graphene by exfoliation of graphite in surfactant/water solutions. *J. Am. Chem. Soc.*, 131, 3611-3620.
- [42] Low, C.T.J., Walsh, F.C., Chakrabarti, M.H., Hashim, M.A. & Hussain, M.A. (2013). Electrochemical approaches to the production of graphene flakes and their potential applications. *Carbon*, 54, 1-21.
- [43] Liu, F., Wang, C., Sui, X., Riaz, M.A., Xu, M., Wei, L. & Chen, Y. (2019). Synthesis of graphene materials by electrochemical exfoliation: recent progress and future potential. *Carbon Energy*, 1, 173-199.

- [44] Elgrishi, N., Rountree, K.J., McCarthy, B.D., Rountree, E.S., Eisenhart, T.T. & Dempsey, J.L. (2018). A practical beginner's guide to cyclic voltammetry. *J. Chem. Educ.*, 95, 197-206.
- [45] Su, C. Y., Lu, A. Y., Xu, Y., Chen, F. R., Khlobystov, A. N. & Li, L. J. (2011). High-quality thin graphene films from fast electrochemical exfoliation. *ACS Nano*, 5, 2332–2339.
- [46] Kuila, T., Khanra, P., Kim, N.H., Lim, J.K. & Lee, J.H. (2013). Effects of sodium hydroxide on the yield and electrochemical performance of sulfonated poly(ether-ether-ketone) functionalized graphene. *J. Mater. Chem. A*, 1, 9294-9302.
- [47] Wang, G., Wang, B., Park, J., Wang, Y., Sun, B. & Yao, J. (2009). Highly efficient and large-scale synthesis of graphene by electrolytic exfoliation. *Carbon*, 47, 3242–3246.
- [48] Guo, H.L., Wang, X.F., Qian, Q.Y., Wang, F.B. & Xia, X.H. (2009). A green approach to the synthesis of graphene nanosheets. *ACS Nano*, 3, 2653-2659.
- [49] Singh, V.V., Gupta, G., Batra, A., Nigam, A.K., et al. (2012). Greener electrochemical synthesis of high quality graphene nanosheets directly from pencil and its spr sensing application. *Adv. Func. Mater.*, 22, 2352-2362.
- [50] Awasthi, S., Gopinathan, P.S., Rajanikanth, A. & Bansal, C. (2018). Current voltage characteristics of electrochemically synthesized multi-layer graphene with polyaniline. *J. Sci. Adv. Mat. Devices*, 3, 37-43.
- [51] Qi, B., He, L., Bo, X., Yang, H. & Guo, L. (2011). Electrochemical preparation of free-standing few-layer graphene through oxidation–reduction cycling. *Chem. Eng. J*, 171, 340-344.
- [52] Liu, N., Luo, F., Wu, H., Liu, Y., Zhang, C. & Chen, J. (2008). One-step ionic liquid-assisted electrochemical synthesis of ionic-liquid functionalized graphene sheets directly from graphite. *Adv. Funct. Mater.*, 18, 1518-1525.
- [53] Sima, M., Enculescu, I. & Sima, A. (2011). Preparation of graphene and its application in dye-sensitized solar cells. *Adv. Mater.*, 5, 414-418.
- [54] Alanyalioglu, M., Segura, J.J., Oro-Sole, J. & Casan-Pastor, N. (2012). The synthesis of graphene sheets with controlled thickness and order using surfactant-assisted electrochemical processes. *Carbon*, 50, 142-152.
- [55] Dresselhaus, M. S., Jorio, A., Hofmann, M., Dresselhaus, G. & Saito, R. (2010). Perspectives on carbon nanotubes and graphene raman spectroscopy. *Nano Lett.*, 10, 751-758.
- [56] Mohan, V. B., Jayaraman, K. & Bhattacharyya, D. (2020). Brunauer–Emmett–Teller (BET) specific surface area analysis of different graphene materials: A comparison to their structural regularity and electrical properties. *Solid State Commun.*, 320, 114004-114017.
- [57] Lin, Z., McCreary, A., Briggs, N., Subramanian, S., Zhang, K., et al. (2016). 2D materials advances: from large scale synthesis and controlled heterostructures to improve characterization techniques, defects and applications. *2D Materials*, 3, 042001-042039.

Chapter 9**MATERIALS FOR ENERGY*****R. K. Shukla* and Amrit K. Mishra***

Department of Physics, University of Lucknow, Lucknow, India

ABSTRACT

Solar energy is one of the best sources of the energy generator device for the next generation. We have a lot of energy transformation sources on the earth for the energy requirement of a human being like coal, petroleum, fossil fuel, compressed natural gas, liquid petroleum gas, biogas, etc. In which solar cell is the best for us because of the environmental free energy generator source? Now a day's Perovskite solar cells have flying enhancement in the efficiency which is very important for the photovoltaic industry but perovskite degradation is a major problem for viable and sustainable commercialization. We discussed degradation of perovskite due to moisture, oxygen, light and heat. Perovskite material has emerged as an attractive strategy to efficiently convert light into electricity. We are using organic-inorganic-halide $\text{CH}_3\text{NH}_3\text{PbI}_3$ as a heart of solar cells with the device structure: FTO/Compact TiO_2 /Mesoporous TiO_2 /Perovskite/Spiro-MeOTAD/Au.

Keywords: perovskite solar cell, fossil fuel, diffusion length, energy band gap, efficiency

1. INTRODUCTION

Now a day's requirement of energy for the human being is increasing due to the continuous growth of the world population and the development of new energy consumed technology. We have limited energy generation sources on the earth, many of energy sources create pollution like burning of petrol or diesel kerosene oil, coal,

* Corresponding Author's Email: rajeshkumarshukla_100@yahoo.co.in.

etc. generate a huge amount of the carbon-dioxide (CO_2), carbon mono-oxide (CO), which is not environment-friendly resources because it creates global warming on the earth and harmful for the Ozone (O_3) layer. So we need to focus on environmentally friendly resources like wind energy consumption, biogas enhancement, solar cell, etc. The generation of electrical energy by solar cells is a very effective area of research and technology, which can solve the worldwide energy consumption problem. Solar energy generation is an environment-friendly methodology for the researcher, scientists and professor's to do great achievements in this area. A modern solar cell is an electronic device of semiconductor material; it converts a fraction of the energy contained in sunlight directly into electrical energy at the voltage and current levels determined by the properties of semiconductors, solar cell design and fabrication techniques, and incident light. A background covering such areas is needed to gain a understanding of how solar cells work and to be in a position to design and build energy conversion systems using solar cells: the nature of solar radiation; semiconductor physics; quantum mechanics; energy storage techniques; optics; heat flow in solids; nature of elemental compound, single crystal, polycrystalline and amorphous semiconductors; semiconductor device. Manufacturing techniques; and economics of energy flow. It is not physically possible to cover all these areas in-depth, in a single work. In writing this chapter, we have attempted to create a survey text. This chapter explores several important background areas and then outlines the principle of operation of solar cells considering their design and construction. A solar cell is performed in the general sense and for some specific examples [1, 2]. These examples select semiconductor, junction types, and optical orientation and fabrication techniques and then describe solar cell design and areas of future research and development, in both general and specific fashion. The 1.51 eV energy bandgap is in the perovskite material which is great for power conversion efficiency. We are studying the degradation of perovskite solar cell device in the presence of UV light and white light, for a clear understanding of degradation we are measuring I-V characteristics and dielectric properties under various conditions. The schematic energy level diagram shows that electron-hole transport in the tuneable energy band of the intermediate layer of the device. Due to high light absorption, photovoltaic and diffusion length properties of perovskite is the most appropriate material for solar cell application. Organometallic perovskite solar cells have shown great promising for next-generation thin-film solar cells. Solar cell devices made of organometallic halide perovskite material have reached an efficiency of more than 21%. Perovskite materials are the most appropriate for energy harvesting technology; we are using perovskite materials as the heart of solar cells because perovskite material has good photovoltaic properties. The absorption of light and diffusion length is also a major factor to select material for energy harvesting. The direct bandgap of the perovskite $\text{CH}_3\text{NH}_3\text{PbI}_3$ material is 1.55 eV which is good for the power conversion efficiency of the solar cells. Perovskite material has a high absorption coefficient, high mobility of electron ($7.5 \text{ cm}^2 \text{ v}^{-1} \text{ s}^{-1}$), and holes ($12.5\text{-}65 \text{ cm}^2 \text{ v}^{-1} \text{ s}^{-1}$), long carrier diffusion length (100 nm to $1 \text{ }\mu\text{m}$), and large grain size. Due to the large grain size of the perovskite material hysteresis

effect reduces. In this work, we are analyzing a complete perovskite solar cell with the device structure: FTO/c-TiO₂/Mesoporous TiO₂/perovskite/spiroMeOTAD/Au. Where FTO stands for fluorine-doped tin oxide, c-TiO₂ stands for compact TiO₂ (work as a hole blocking layer), mesoporousTiO₂ (size of the grain 5-40 μm), perovskite works as a heart of the solar cells, spiroMeOTAD works as a hole transporting layer and finally Au is used for the electrode of the typical solar cell's.

This chapter is a comprehensive (and concise) survey of the elements. This creates an “energy crisis.” It is dedicated to showing limited Nature for discussion of currently used energy sources and various “non-conventional” energy sources proposed for the future: Biological, wind, wave and solar. It has three points as its main objective. To create: (1) that our traditional energy sources will be exhausted nothing in the distant future, (2) that solar power is capable managing humanity's energy needs for foresight future, and (3) that photovoltaic energy conversion is a major candidate treat mankind with its essential energy.

1.1. What Is a Solar cell?

The device which converts photonic energy into electrical energy generation based on photovoltaic effect is known as a solar cell. The conversion of optical energy into electrical energy is a physical and chemical phenomenon. A solar cell generates energy because the I-V curve exists in the fourth coordinate product of I*V gives a negative value which is negative power that means power generation.

The operation of the solar cell is based on the three main parts.

- Light absorption by the photovoltaic material and generate electrons and holes or excitons.
- Opposite types of charge carrier's separation.
- Separate charge carrier's extraction to an external circuit by applying external voltage.

1.2. Types of Solar cell

Solar cell is different types such as Amorphous silicon solar cell (a-Si), Biohybrid solar cell, Cadmium telluride solar cell (CdTe), Concentrated PV Cell (CVP and HCVP), Copper indium gallium selenide solar cells, Crystalline silicon solar cell, Float-zone silicon, A dye-sensitized solar cell (DSSC), Gallium arsenide germanium solar cell (GaAs), Hybrid solar cell, Luminescent solar concentrator cell (LSC), Micromorph (tandem-cell using a-Si/μc-Si), A Monocrystalline solar cell (mono-Si), A multi-junction solar cell (MJ), Nanocrystal solar cell, An organic solar cell (OPV), Perovskite solar cell, Photo-electro-chemical cell (PEC), Plasmonic solar cell, A polycrystalline solar cell (multi-Si), Quantum dot solar cell, Solid-state solar cell, A thin-film solar cell

(TFSC), Wafer solar cell, or wafer-based solar cell crystalline, Non concentrated heterogeneous PV cell.

In all types of the solar cell, I have worked on the perovskite solar cell now a day's which is frequently used in the energy harvesting materials for Solar cell applications. The typical perovskite solar cells [3-7] made of three parts, light absorber (converting incidents photon to electron and holes), charge carrier collector materials (capturing the carriers - electrons and holes: TiO_2 , ZnO , Spiro-MeOTAD), and metal contacts (transferring the carriers to the circuit Ag, Au). The perovskite material has high charge-carrier mobility, high carrier diffusion length (it means that the light generated electrons and holes can move large enough distances to be extracted as current, instead of losing their energy as heat with the cell), high values of open-circuit voltage ($V_{oc} = 0.6-1.1$ volt) typically obtained and $\text{CH}_3\text{NH}_3\text{PbI}_3$ is a semiconducting pigment with a direct bandgap of 1.55 eV with absorption coefficient as high as $10^4-10^5 \text{ cm}^{-1}$, good light absorber in the whole visible solar emission spectrum, the weak binding energy of excitons produced by light absorption around 0.03 eV (most of the excitons dissociate rapidly into electrons and holes at room temperature and recombination time hundreds of nanoseconds. We are using perovskite ($\text{CH}_3\text{NH}_3\text{PbI}_3$) as the heart of a solar cell which works as a photovoltaic material [8]. The energy band gap of $\text{CH}_3\text{NH}_3\text{PbI}_3$ is 1.55 eV which is suitable for energy harvesting in the visible region, with the help of bandgap engineering, we are selecting materials for the fabrication of a perovskite solar cell device. We are selecting layers as FTO/c- TiO_2 /M- TiO_2 /Perovskite/Spiro-MeOTAD [9]. Where c- TiO_2 stands for the compact layer, the M- TiO_2 layer stands for mesoporous, which is used as the hole blocking layer and the Spiro-MeOTAD layer is used as hole transporting material. The total average thickness of typical perovskite solar cells is 1.1 μm - 1.5 μm with the individual layer thickness are glass (200 nm), FTO (400 nm), TiO_2 (30-90 nm), perovskite (250-450 nm), HTM (150-250 nm) and Au (60-120 nm) [10].

2. MATERIAL AND METHODS

The solar cell fabrication technique is done by a spin coating method. The schematic diagram of the fabricated Perovskite solar cell is shown in Figure 1. We are using patterned fluorine-doped tin oxide substrates (FTO) etched by Zn metal powder and dilute hydrochloric acid. The cleaning of etched FTO is done by sequential sonication technique into the soap solution, deionized water, and isopropanol for 15 min each. And next, coat TiO_2 (hole blocking layer) on it by using spin coating method with 5000 rpm for 45 sec and heated at 450°C for 25 minutes, which is prepared by the mixture of 0.5 ml Ti (IV) isopropoxide (Sigma Aldrich), 7.25 ml of ethanol and 75 microliters of concentrated HCl. A TiO_2 Mesoporous layer is made by using a dilute solution of Dyesol 18 N-RT paste (1:3.5 w/w in ethanol) at 4000 rpm for 30 seconds and heated at 500°C for 30 minutes and the film thickness to be formed 360 nm. For the perovskite deposition, TiO_2 films were transformed into the glove box. The

perovskite layer was deposited and after that First, we take 2M TiCl_4 (1 ml) in 100 ml D. I. water and put TiO_2 film's into the solution and heat at 80°C in the oven. After that, the film is wash with water, ethanol and dry Ar gas, and then heated at 500°C for 30 minutes and again we take 1M PbI_2 (462 mg) solution in DMF (1 ml) and steering at 40°C up-to dissolve, after that spin-coated at 6000 rpm for 5 sec. Heated for 25 min at 70°C on a hot plate, drop into MAI (8 mg/ml) in isopropanol after that dip the PbI_2 film into the above solution for 15 min, and then washed with isopropanol and then heated at 70°C for 15 min and the deposition of Spiro-MeOTAD Layer Deposition. First, we take 100 ml of Spiro-MeOTAD in 1 ml chlorobenzene 28.5 microliters of TBP (Tursary butyl pyridine) + Li salt solution (17.5 microliters) using spin coater at 4000 rpm for 30 sec and finally gold deposition on Spiro-MeOTAD layer by the thermal evaporator [11-13].

3. RESULTS AND DISCUSSION

In the perovskite solar cell stability is still challenging so for the clear understanding of the degradation of $\text{CH}_3\text{NH}_3\text{PbI}_3$ material has been studied by the I-V hysteresis [14] at a different level of humidity under the UV light and dark condition. In Figure 2, we can observe that under UVLED at RH 17% perovskite shows good diode behavior when humidity decrease by the O_2 flow in the chamber in which device testing has been recorded.

Now again if we increase humidity by sending humid O_2 into the chamber humidity level increases up to RH 50%, so we found there is degradation occurs in the device because of perovskite solar cell loses diode behavior and there is a shifting of I-V hysteresis that is called electric field degradation.

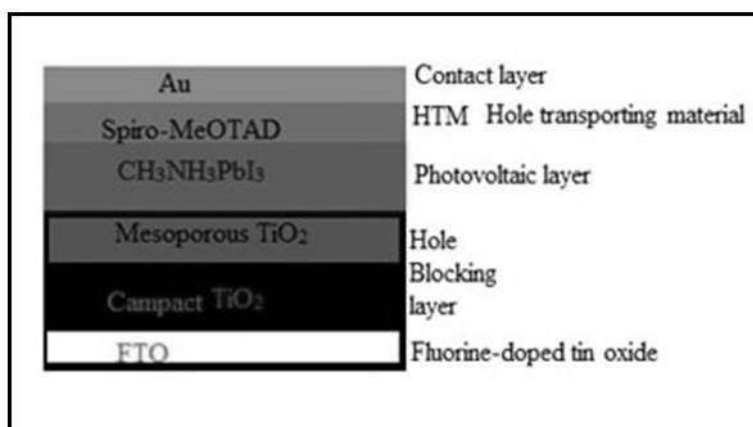


Figure 1. The schematic diagram of the fabricated Perovskite solar cell.

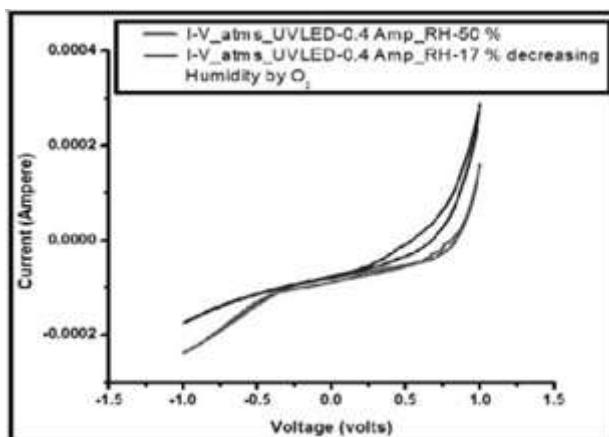


Figure 2. I-V characteristics of the under the UVLED at the different levels of the humidity.

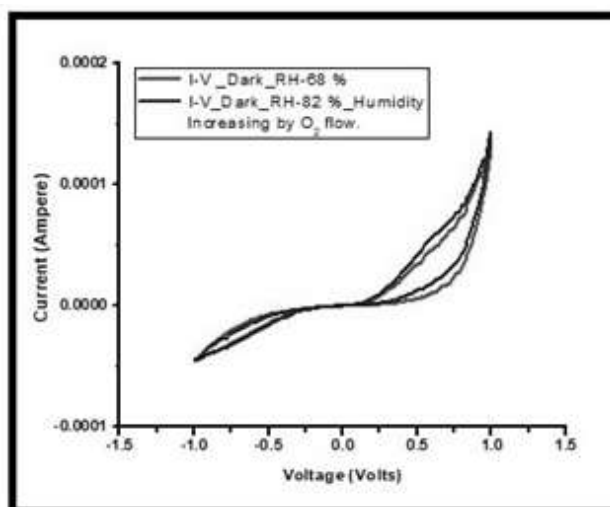
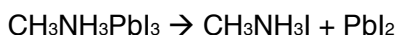


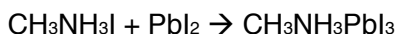
Figure 3. I-V characteristics of the under the dark condition at the different levels of the humidity.

So we conclude that for UVLED perovskite solar cell is still recoverable up to RH 50% because if we further decrease humidity by sending dry O_2 into the setup chamber, I-V hysteresis shifted to the original hysteresis at RH 17%. Figure 3 shows I-V hysteresis of the perovskite solar cell at the different level of humidity under the dark condition we found that diode behavior of the device at RH 68% and RH 82% are still existing which indicate that in the dark condition perovskite material stability exist up to the high level of humidity. That means degradation in the $CH_3NH_3PbI_3$ occurs due to the UV light as well as humidity. So degradation [15] and recovery of the perovskite material can be express by using a chemical equation which is given below.

Perovskite material Degradation chemical equation



Perovskite material recovery chemical equation



CONCLUSION

In this chapter, we have explained the importance of solar energy enhancement for the 21st Century. With the help of solar energy, we can solve the global energy consumption problem. We are working on the perovskite solar cell, now a day's which is the most efficient material for the energy harvesting material. We found that perovskite is good for the energy harvesting device but it is degradable. So the degradation study has been studied with I-V hysteresis under UVLED and dark condition. We found that perovskite is recoverable at a high value of humidity under the dark condition and under UVLED it is still recoverable up to RH 50%. So for industrialization, we can sandwich perovskite with Si, which enhances the stability of the device.

REFERENCES

- [1] Dong, D., Wang, Z. and Liao, L. (2020). Durable strategies for perovskite photovoltaics. *APL Materials* 8:100703.
- [2] Lorena, P., Zhang, H., Markina, A., Yuan, J., Hosseini, S. M., Wolff, C. M., Zuo, G., Stolterfoht, M., Zou, Y., Gao, F., Andrienko, D., Shoaee, S. and Neher, D. (2020). Barrier less free charge generation in the high-performance PM6:Y6 bulk heterojunction non-fullerene solar cell. *Adv. Mater.* 1906763.
- [3] Kojima, A., Teshima, K., Shirai, Y. and Miyasaka, T. (2009). Organometal halide perovskites as visible-light sensitizers for photovoltaic cells. *J. Am. Chem. Soc.* 131: 6050-6051.
- [4] Kim, H. S. (2013). High efficiency solid-state sensitized solar cell-based on submicrometer rutile TiO₂ nanorod and CH₃NH₃PbI₃ perovskite sensitizer. *Nano Lett.* 13: 2412-2417.
- [5] Heo, J. H. (2013). Efficient inorganic-organic hybrid heterojunction solar cells containing perovskite compound and polymeric hole conductors. *Nature Photon* 7: 486-491.
- [6] Burschka, J. (2013). Sequential deposition as a route to high-performance perovskite sensitized solar cells. *Nature* 499: 316-319.
- [7] Ball, J. M., Lee, M. M., Hay, A. and Snaith, H. J. (2013). Low-temperature processed meso-super structured to thin-film perovskite solar cells. *Energy Environ. Sci.* 6: 1739-1743.

- [8] Ju, Y., Park, S. Y., Han, H. S. and Jung, H. S. C. (2019). Point defect-reduced colloidal SnO_2 electron transport layer for stable and almost hysteresis-free perovskite solar cells. *RCS Adv. Sol.* 9:7334.
- [9] Xin, L., Junyou, Y., Qinghui, J., Weijing, C., Dan, Z., Zhiwei Z. and Jiwu, X. (2017). Synergistic effect to high-performance perovskite solar cells with reduced hysteresis and improved stability by the introduction of Na-treated TiO_2 and spraying-deposited CuI as transport layers. *ACS Appl. Mater. Interfaces* 9:47, 41354-41362.
- [10] Narge, Y., Aghoobi, N., Fabio, M., Lucio, C. and Aldo, D. C. (2017). High-efficiency perovskite solar cell based on poly (3-hexylthiophene): influence of molecular weight and mesoscopic scaffold layer. *Chem. Sus. Chem.* 10: 3854-3860.
- [11] Chen, C., Kang, H., Hsiao, S., Yang, P., Chiang, K. and Lin, H. (2014). Efficient and uniform planar type perovskite solar cells by simple sequential vacuum deposition. *Adv. Mater.* 1:201402461.
- [12] Mishra, A. K. and Shukla, R. K. (2020). Fabrication and characterization of perovskite ($\text{CH}_3\text{NH}_3\text{PbI}_3$) solar cells. *SN Applied Sciences* 2: 321.
- [13] Mishra, A. K. and Shukla, R. K. (2020). Effect of humidity in the perovskite solar cell. *Material Today: Proceeding* 29: 836-838.
- [14] Hui-Seon, K., In-Hyuk, J., Namyoung, A., Mansoo, C., Antonio, G., Juan, B. and Nam-Gyu, P. (2015). Control of I-V hysteresis in $\text{CH}_3\text{NH}_3\text{PbI}_3$ perovskite solar cell. *J. Phys. Chem. Lett.* 6:22, 4633-4639.
- [15] Dunfield, S. P., Bliss, L., Zhang, F., Luther, J. M., Zhu, K., Hest, M. F. A. M., Reese, M. O. and Berry, J. J. (2020). From defects to degradation: a mechanistic understanding of degradation in perovskite solar cell devices and modules. *Adv. Energy Mater.* 1904054.

Chapter 10**AB₅-TYPE METAL HYDRIDES
TO SERVE THE SOCIETY AS ENERGY MATERIAL:
DEVELOPMENT IN LAST DECADE*****Kuldeep Panwar¹ and Sumita Srivastava^{2,*}***¹Department of Physics, Pt. L.M.S.Government Post Graduate College,
Rishikesh, India²SBC Government Degree College, Pokhri Quili, Tehri Garhwal, India**ABSTRACT**

For safe storage with higher density, solid hydrogen storage modes are preferred over gaseous and liquid modes. Solid state materials have range of variety, available for hydrogen storage; like metal hydride, alanates, borohydrides and carbon based materials such as, fullerenes, graphene, carbon nanotubules, etc. Metal hydrides can be further categorized into AB₅, AB₂/A₂B and AB types. Metal hydrides have large applications as stationary storage of hydrogen, fuel bed for vehicles in transportation sector, Nickel-metal hydride battery, heat engine, heat pump, compressor, separator for purification of hydrogen and many more. A metal hydride is characterized by hydrogenation properties of hydrogen storage capacity, activation process, p-c isotherms, operating temperature-pressure, heat of formation, kinetics and cyclic stability. Therefore, to cater the need of a particular application, specific metal hydride is developed with well define hydrogenation characteristics. Present communication deals with the development in AB₅-type metal hydride to serve the society as energy material. The parent AB₅-type alloy has certain fix hydrogenation properties, which are not satisfactory for all the application point of view. Therefore the parent AB₅-type alloy (LaNi₅/MmNi₅) is needed to be tailored for improved hydrogenation properties. For tailoring, either another element is substituted at the site of 'A' or/and 'B' or a different synthesis route is followed. In present chapter, various types of modifications done in the

* Corresponding Author's Email: sumita_uki1@rediffmail.com.

parent AB₅-type alloy to develop more applicable version of energy materials are discussed by focusing on their properties and applications studied recently in last decade.

Keywords: metal hydrides, AB₅-type, synthesis, substitution, hydrogenation properties, applications

1. INTRODUCTION

Development is a key factor in economy of any country. It affects human lifestyle with ease of work related to habitation, communication and production. Every aspect of the development is directly based on energy consumption. Among various non-conventional renewable energy options, Hydrogen energy has efficiency to cater long term energy demand of clean energy. Hydrogen is produced from water and after combustion it again converts into the water. Hence, it is completely non-polluting. The major source of hydrogen, that is water, covers 75% of earth, hence abundant availability. Cost comparison of hydrogen with other renewable energy sources is clear that even though the popularity of solar energy is high, the energy conversion efficiency is less than 30% and its overall energy power is very low compared to hydrogen energy [1]. Among various options of non-conventional energy sources, hydrogen energy can fulfill the demand of clean energy for long time.

Hence, hydrogen plays an important role for future energy market with suitable properties and compatibility with nature. To harness hydrogen energy in real practical life, one has to focus on some technical aspects related to the hydrogen as:

1. First is the production of hydrogen from its core element at low cost with high efficiency. So cost effective production may present the hydrogen as future fuel.
2. Second is the storage of hydrogen in safe and high density mode, so that society can use it efficiently in practical life.

The technologies for the storage of fossil fuel as petroleum, natural gas, LPG have been stabilized; but for hydrogen, yet not well-defined storage technology has been described. Generally gaseous storage mode using heavy cylinders are in practice, which requires large volume for storage. This type of storage has weight penalty and also risky due to being compressed at high pressure. Hence the storage of hydrogen in cylinders is not viable. The other process is to liquefy hydrogen that is storage in liquid mode. But the technology used to store hydrogen in liquid form is cryogenics, which is very complex. Hydrogen in liquid form needs cryogenic compression at -240 degree centigrade under very high pressure of 69 mega Pascal, which is stored in fiber reinforced Kevlar cylinder. The liquid hydrogen has advantage of volumetric high density in comparison to gaseous storage. So it is viable for specific use. This type of liquefaction is very expensive [2]. One more drawback is the ortho-para conversion,

which affects the economics of transoceanic shipping of hydrogen in liquid form in tankers. It critically affects the shipping economics of liquid hydrogen by decreasing loading limit at higher ortho concentration and also minimizes the total supply chain cost [3].

The solid state storage of hydrogen in special materials (solid) is a new idea. The solid state storage mode has higher energy density in comparison to gaseous and liquid mode [4]. Solid state storage modes are stable and technically advantageous over liquid and gaseous storage. The density of hydrogen per unit volume is greater in solid storage. It is also safe and reliable for every sector with indefinite storage and released capacity.

Thus solid state hydrogen storage mode is technically and economically perfect for storage system. Some solid storage modes are metal hydrides, carbon nanotubes, fullerenes, graphene, active carbon, alanates, borohydrides, glass micro spheres and zeolites.

Many applications like Ni-MH cells, transport vehicles, heat pumps etc are using solid state hydrogen storage technology due to its advantage over liquid and gaseous storage on the level of volumetric efficiency [6]. Metal hydrides are primarily characterized by its wt% hydrogen storage capacity, operating temperature and pressure. A comparison of various storage modes of hydrogen in terms of energy density is shown in Table 1.1.

Table 1.1. Energy density of different storage modes of hydrogen

Hydrogen storage types and densities [4].		
	Kg H ₂ /kg	Kg H ₂ /m ³
Bulk storage (10 ² to 10 ⁴ m ³ geometric volume)		
Underground storage		5-10
Pressurized gas storage (above ground)	0.01-0.014	2-16
Metal hydride	0.013-0.015	50-55
Liquid hydrogen	~1	65-69
Stationary storage in small amount (1 to 100 m ³ geometric volume)		
Pressurized gas cylinder	0.012	~15
Metal hydride	0.012-0.014	50-53
Liquid hydrogen tank	0.15-0.50	~65
Storage in vehicle tanks (0.1 to 0.5 m ³ geometric volume)		
Pressurized gas cylinder	0.05	15
Metal hydride	0.02	55
Liquid hydrogen tank	0.09-0.13	50-60

2. AB₅-TYPE HYDROGEN STORAGE MATERIALS

Among major three options of hydrogen storage, i.e., gaseous, liquid and solid, the most promising storage mode is solid state hydrogen storage mode. Metal hydrides represent one class of hydrogen storage material, which store hydrogen in solid mode.

There are many other material classes also to store hydrogen in solid mode. A large number of studies and experimental works have been done to synthesize low-cost metal hydrides with low absorption/desorption temperatures, high gravimetric and volumetric hydrogen storage densities and good resistance to oxidation. Alloys must have the properties of good reversibility, cyclic efficiency, rapid kinetics and reactivity together with moderate thermodynamic stability [7]. Metal hydrides can be categorized into many types as, AB_5 , AB_2/A_2B and AB . Among all these, AB_5 -type metal hydride is known for its easy activation and ambient operating condition. Here only recent studies on AB_5 -type metal hydride will be presented.

2.1. Synthesis Process

In last decade a new synthesis technique, namely ball-milling/mechanical alloying has come forward together with conventional arc/induction melting. Several reports are available on preparing alloy with mechanical alloying route to tailor the hydrogenation properties of alloys prepared through conventional means.

The mechanical alloying of a $La_{0.25}Ce_{0.52}Nd_{0.17}Pr_{0.06}-Ni-Sn$ mixture was studied by X-ray diffraction, Scanning Electron Microscopy, Energy Dispersive Spectroscopy and Differential Scanning Calorimetry by Hurtado et al. [8]. Four stages were identified and characterized. Initial stage was observed at integrated milling times (t_m) between 0 and 30 h, dominated by fracture of the larger particles. Intermediate stage was observed between 30 and 50 h having both fracture and cold welding process. At this stage, compositional changes were detected due to solid–solid reaction. Ni and Sn particles were alloyed in the larger particles of $La_{0.25}Ce_{0.52}Nd_{0.17}Pr_{0.06}$. The Final stage was observed between 50 and 70 h with the cycle of fracture and cold welding. At final stage steady state was reached and no further changes in chemical composition were observed. At completion stage, only refinement was observed and $La_{0.25}Ce_{0.52}Nd_{0.17}Pr_{0.06}Ni_{4.7}Sn_{0.3}$ intermetallic was obtained.

Nano-structured $LaNi_5$ hydrogen storage material was prepared through ball-milling. It was analyzed using differential scanning calorimetry (DSC) and x-ray photoelectron spectroscopy (XPS) [9]. DSC results indicated a partial elimination of defects at 500°C in a more efficient way for the short-time ball-milled powders compared to the long-time ball-milled ones. XPS results showed almost no change in the core-level electronic structure for La and Ni of $LaNi_5$ in the bulk and the nano-structured forms. Structural studies suggested that the reduced unit-cell volume and the enhanced atomic disorder in the nano-structured $LaNi_5$ caused a larger energy barrier for the hydrogen sorption reactions of the long-time ball milled samples.

In another work, $LaNi_5$ was obtained from raw materials by low energy mechanical alloying. Annealing improved the hydriding properties of as-milled intermetallic. Pressure-composition isotherms showed flat plateaus when annealing temperature was 600°C, which is at least 300°C lower than the synthesis and annealing temperature of standard equilibrium methods. Thus low energy mechanical alloying

with annealing at low temperature reduced the number of intermediate stages needed for fabrication of the intermetallic. Hydriding properties of this recycled material were studied in the temperature range of 25–90°C. From these results, Talaganis et al. [10] proposed a one-stage hydrogen thermal compression scheme working between 25°C (absorption) and 90°C (desorption) with a compression ratio of 2.5 and a useful capacity of 1.0 mass %.

MmNi_{5-x}Al_x intermetallics (Mm = mischmetal = La_{0.25}Ce_{0.52}Nd_{0.17}Pr_{0.06}) with $x = 0.5$ and 1, were synthesized by low energy reactive alloying [11]. The optimization was correlated to the structural parameters obtained on the structure. From these results, an improvement on the milling time-annealing process was proposed.

2.2. Substitutions in Parent AB₅ Alloy

AB₅-type storage alloys are easily activated at ambient temperature condition. Because of this property, it is widely used in research work for future hydrogen storage concepts. Vast researches have been done on hydrogenation behavior of AB₅-type alloys with the varieties of substitution done in this alloy. The representative alloy among AB₅-type hydrogen storage materials corresponds to LaNi₅. Another cost effective version namely MmNi₅ (Mm = misch metal, a mixture of rare earth elements) has also good properties for transport technologies due to its ability to react with hydrogen at moderate pressures and temperatures. As already discussed in earlier section, that each metal hydride is characterized by specific hydrogenation properties, like activation behavior, absorption-desorption plateau pressure, hydrogen storage capacity, operating temperature, kinetics, heat of formation and cyclic stability. Hence to deploy the same alloy in every application is not possible. Every application needs an alloy with a particular set of properties. For this, parent alloys LaNi₅ and MmNi₅ need to be tailored. Tailoring can be done by substitution of suitable element at 'A' or/and 'B' site of parent alloy. Tailoring can also be achieved by choosing different synthesis route. Many investigations have been done to study new materials in this context to improve the hydrogenation behavior of parent LaNi₅ and MmNi₅ alloy. Some of them are being discussed here.

Crystal structure, activation performance, hydrogen absorption/desorption properties and cycle life were investigated to examine the effect of non-stoichiometry on these properties for the La(Ni_{3.8}Al_{1.0}Mn_{0.2})_x ($x = 0.94, 0.96, 0.98, 1.0$) hydrogen storage alloys [12]. In LaNi_{3.8}Al_{1.2-x}Mn_x ($x = 0.2, 0.4, 0.6$) hydrogen storage alloys, effects of the Mn substitution on microstructures and hydrogen absorption/desorption properties were explored [13]. The pressure-composition (PC) isotherms and absorption kinetics were measured using the volumetric method in $433 \text{ K} \leq T \leq 473 \text{ K}$ temperature range. XRD analyses showed that, the lattice parameter 'a' was decreased, 'c' increased and the unit cell volume 'V' reduced with the increase of the Mn content in the LaNi_{3.8}Al_{1.2-x}Mn_x alloys. It was found that the hydrogen storage capacity was enhanced and the absorption/desorption plateau pressure was increased

with the increase in Mn content. With the Mn content x and the lattice parameter a , the absorption/desorption plateau pressure of the alloys was linearly changed, while the increase of c/a ratio, linearly increased the hydrogen storage capacity. The slope factor S_f was closely correlated with the strain of the lattice in the alloys.

The plateau pressure of hydride forming materials (such as metal hydrides) depends markedly on the operating temperature following the Van't Hoff relationships. It is necessary to select hydrogen storage materials by considering the thermal environment of the hydride tank for practical applications. The thermodynamic properties (absorption-desorption plateau pressure) of metal hydrides can be tailored to some extent by substituting with foreign metals on different crystallographic sites. In this work, Ngameni et al. reported on the hydriding kinetics of substituted AB_5 compounds [14]. Isotherms have been measured at different temperatures on $La_xNd_{1-x}Ni_5$ ($x \approx 0.2$) and $La_xCe_{1-x}Ni_5$ ($x \approx 0.3$) compounds. Use of such substituted compounds for application in auxiliary power units was discussed. Srivastava et al. [15] investigated on synthesis, characterization and hydrogenation behavior of the $MmNi_5$ -type hydrogen storage alloys $Mm_{0.9}Ca_{0.1}Ni_{4.9-x}Fe_xAl_{0.1}$ ($x = 0, 0.1, 0.2$ and 0.3). All the alloys were synthesized by radio frequency induction melting following the composite pellet route. The hydrogenation behavior is monitored by means of activation curves, absorption-desorption pressure-composition isotherms, hysteresis factors and desorption kinetic curves. The substitution of iron at the place of nickel in the alloys $Mm_{0.9}Ca_{0.1}Ni_{4.9-x}Fe_xAl_{0.1}$ ($x = 0, 0.1, 0.2$ and 0.3) gave an increase in the hydrogen storage capacity as 1.82, 1.90, 2.2 and 1.95 wt% corresponding to $x = 0, 0.1, 0.2$ and 0.3 respectively.

Li et al. [16] have investigated the effect of long-term hydrogen absorption/desorption cycling up to 3500 cycles on the hydrogen storage properties of $LaNi_{3.8}Al_{1.0}Mn_{0.2}$ alloy. In another work the effect of partial substitution of Ce by La in $Ce_{1-x}La_xNi_3Cr_2$ ($x = 0.2, 0.4, 0.6, 0.8, 1$) hydrogen storage alloy has been systematically investigated, synthesized by arc melting method [17]. A systematic study was performed on the effect of the iron content on the structural and electrochemical characteristics of the $La_{0.78}Ce_{0.22}Ni_{3.73}Mn_{0.30}Al_{0.17}Fe_xCo_{0.8-x}$ ($x = 0, 0.2, 0.5, 0.8$) hydrogen storage alloys in the temperature range of $20-60^\circ C$ [18]. The discharge capacity and high rate dischargeability deteriorates with increase in Fe content and temperature. The difference among the four alloys almost disappears with increase in temperature. It was shown that the dissolution of Ni, Mn and Al can be suppressed significantly in virtue of the sacrifice of Fe content, leading to a good relative anti-corrosion ability of high-Fe alloy, and consequently, excellent cycling stability, charge retention and other high-temperature performance was obtained.

Multi-substituted $LaNi_5$ alloys prepared by annealing, activating, and cycling were investigated systematically using synchrotron radiation X-ray diffraction (XRD), extended X-ray absorption fine structure spectroscopy (EXAFS), and X-ray photoelectron spectroscopy to clarify the evolution of the structural properties of the alloys [19]. Chumphongphan et al. [20] have investigated the substitution of Al and Mo for Ni in $CaNi_5$, to find its effect on structural and hydrogen storage properties of $CaNi_5$

[20]. The substitution increases the unit cell volume of CaNi₅ phase, reduces the hydrogen storage capacity and lowers the plateau pressure. Whereas, Mo substitution slows down the hydrogen sorption kinetics, Al substitution improves the hydrogen sorption kinetics and cyclic stability.

PCT characteristics of some Ti, Mm (Mish metal) and La based hydrides have been studied and the ΔH and ΔS have been estimated. It was shown that the reaction enthalpies during hydriding and dehydriding processes were function of hydrogen storage capacity and was represented as polynomial equation of degree of the order 3 [21]. In a separate study dynamic volumetric measurements on the interaction of LaNi_{5-x}Sn_x and H₂ have been performed, which resulted in the decrease in reaction pressure from 250 to 8 kPa with increase in Sn concentration from 0 to 0.5 at the temperature of 300 K [22].

Paschoalino et al. investigated the reaction of BH₄ oxidation on La-Ni based hydrogen storage system (LaNi_{4.7}Sn_{0.2}Cu_{0.1}) and showed that during the alloy discharge in presence of BH₄⁻ continuous hydriding takes place [23].

In another work the hydrogen sorption isotherms for two AB₅-type alloys (LaNi₅ and LaNi_{4.5}Co_{0.5}) were measured using gravimetric techniques and nonlinear regression was performed to fit model on experimental data [24].

A model was proposed to predict the topography of the gas absorbed molecules and to fit on hydrogen adsorption isotherm of LaNi_{4.75}Fe_{0.25} alloy at 303K and 313K having strong correlation with experimental curves. It was found that density of hydrogen receptor site, number of molecule per site and hydrogen adsorption energy affect the adsorption process [25].

Matysik et al. [26] have found that Mendeleev number M and chemical scale affects the binary metal hydride stability. The metal hydrides with only one hydrogen atom (H=1) and M from 0 to 21 exhibit adequate stability for practical applications and large variations in stability is noted for M from 53 to 102. It was reported that in gas phase hydrogen absorption and electrochemical performance of La₂(Ni, Co, Mg, M)₁₀ (Mg modified LaNi₅-based alloy), Al doping increases the hydrogen concentration, while Co substitution decreases the hydrogen concentration slightly [27]. Blanco et al. [28] studied the reaction kinetics of LaNi_{5-x}Sn_x alloys with H₂ for range of composition, temperatures and pressures and compared their experimental data with four different kinetic expressions.

Sharma and Kumar [29] worked on the effect of narrow and wide temperature range on thermodynamic properties of La-based metal hydrides LaNi_{5-x}Al_x (x=0.3 and 0.4) and it was observed that ΔH depends on the experimental temperature range.

It was shown that introduction of Sn in LaNi_{5-x}Sn_x alloys suppresses the formation of defects and improves the cycling resistance. Higher stability has been noted for the Sn-containing alloy [30]. It was also observed that stationary state comes after 10 cycles for Sn containing alloy (LaNi_{4.73}Sn_{0.27}) and in the presence of H₂-Co mixture absorption kinetics is stronger at lower temperatures [31]. H₂ trapping mechanism at metal vacancies was studied by Xing et al. [32] and they have found that hydrogen prefers those vacancies which are coupled with high pre-existing charge interstitials.

At maximum hydrogen capacity dominant charge donors changes from nearest neighbor to next nearest neighbor. Other study reports on the static and dynamic PC-isotherm of $MmNi_{5-x}Al_x$ ($x=0, 0.3, 0.5$ and 0.8) hydrides and demonstrate that the increase of Al content increases the heat of formation (enthalpy) but decreases the value of plateau pressure and maximum hydrogen storage capacity. For this simulation of PCIs the Zhou's and Smoothed model was used [33].

Series of $SmNi_{5-x}Al_x$ ($x=0.25, 0.5, 0.75, 1, 1.5, 2, 2.5$) hydrogen systems were prepared through melting corresponding to stoichiometric mixtures of samarium, nickel and aluminum in an arc furnace under argon and it was found that the hexagonal structure of $P6/mmm$ space group was retained for all considered values of x [34].

Anik et al. [35] synthesized the AB_5 -type La-Ni-Co alloys $La(Ni_{1-x}Co_x)_5$ ($x=0, 0.1, 0.2, 0.3$) by electro-deoxydation method by sintering on $1200^\circ C$ for 2 hours. For the formation of $LaNi_5$ the main La-Ni-Co phase was La_2NiO_4 . Al substitution at Ni in AB_5 -type $La_{0.78}Ce_{0.22}Ni_{3.95-x}Co_{0.65}Mn_{0.3}Si_{0.1}Al_x$ ($x=0-0.4$) alloys shows improvement in anti-corrosion ability at higher temperature. It also creates excellent cyclic stability and storage property. The self-sacrifice of Al has started the process of suppression of dissociation of La, Ce, Ni, Co, Mn and Si [36]. Palladium nanospheres and fluorinated layer as new surface structure (net mosaic) has enhanced the H_2 capacity and absorption rate of $LaNi_{4.25}Al_{0.75}$ alloy by resistance against poisoning of the alloy [37].

The reversibility reaction and activation of the AB_5 -type metal hydride, non-iron $LaNi_{3.55}Mn_{0.4}Al_{0.3}Co_{0.75}$ and iron containing $LaNi_{3.55}Mn_{0.4}Al_{0.3}Co_{0.2}Fe_{0.55}$ alloys were studied and better properties were observed for iron free alloy rather than iron containing alloy [38].

A practical method was developed to calculate the enthalpy and entropy changes in hydrogenation and dehydrogenation processes using $LaNi_{3.8}Al_{1.2-x}Mn_xH$ ($x=0.2, 0.4, 0.6$) hydrides and showed that all phonon vibrations contribute to vibrational enthalpies, whereas vibrational entropies are mainly dominated by low-frequency phonon vibrations [39].

Highly dispersed $LaNi_5$ nanoparticles on carbon (nano $LaNi_5/C$) were synthesized through a precipitation-reduction method. Carbon-supported $LaNi_5$ nanoparticles have much smaller particle size ($26\pm 8nm$) as compared to unsupported $LaNi_5$ nanoparticles ($214\pm 75nm$) (nano $LaNi_5$) prepared by the same method and bulk $LaNi_5$ ($35\pm 17\mu m$). It has been found that in $LaNi_5$ particle size reduction significantly altered the hydrogen storage properties. It has also enhanced the kinetics and the stabilization of hydride phase [40]. In the family of AB_5 -type hydrides the parent alloy corresponds to $LaNi_5$ [41]. Investigations on a set of $MmNi_{5-x}Al_x$ materials exploring different concentration of Ni and Al content ($x=0.15, 0.20, 0.25$), resulted in specific working conditions of these materials for possible employment in transportation [42]. Al improves the cyclic stability of alloys and it has been found that $LaNi_5$ lattice structure is stabilized with Al of larger atomic radius [43]. Al has been found to reduce subsequently the absorption/desorption pressure, it is seen that Bi substitution decreases the hydrogen storage capacity of $LaNi_5$ [44].

Multi-element LaNi₅ phase of La-Ni-Fe-V-Mn alloys have been studied by kunce et al. [45]. After hydrogen absorption by hydride particle, volume expansion of the order of 25% takes place. In this process, inter particle friction is main opposition character when particles tries to accommodate container geometry. When the particle size is correlated to flowability, it is found that flowability of LaNi₅ is more dependent on degree of activation of samples rather than hydrogen absorption state [46]. In the study of Al substitution in CeNi₅ (CeNi_{5-x}Al_x) the largest amount of hydrogen concentration has been found for the composition of CeNi₄Al [47].

A monolayer model treated by statistical physics by means of the grand canonical ensemble has been developed, describing P-C-T isotherms for absorption of hydrogen by LaNi_{3.6}Mn_{0.3}Al_{0.4}Co_{0.7} alloy [48]. This model presented a high correlation with the experimental results. Hydrogen storage capacity was analyzed by considering hydrogen absorption test rig depending on some reactor design parameters. These reactor design parameters are; metal hydride particle size, inlet radius of the tank, hydrogen inlet pressure, having fins at the tank, coolant temperature, general convective heat transfer coefficient and wall thickness of the tank [49]. COMSOL Multiphysics 5.1 software was used with specified design parameters of the hydrogen storage system to obtain some approaches in the large scale. Three different metal hydrides MmNi_{4.6}Al_{0.4}, LaNi_{4.75}Al_{0.25} and LaNi₅ were selected to study above parameters. Some parameters like amount of the hydrogen mass stored in the tank, the time durations with variations in the equilibrium pressure and temperature distribution inside the tank of the system were optimized.

Modification of compounds like LaNi₅ towards ternary compositions changes alloy hydrogen storage properties and influence the resistance to hydrogen contamination. Thermodynamic properties of ternary alloys LaNi_{4.75}M_{0.25} were investigated with ab initio methods and synthesized in order to select the composition with hydrogen sorption properties not worse than LaNi₅ [50]. The specific volume change, surface segregation energy and change of the hydride formation enthalpy were calculated for 34 elements (M: Al, Ag, Au, B, Bi, Ca, Cd, Cr, Cu, Fe, Ge, Ga, In, Ir, K, Mg, Mo, Mn, Nb, Pb, Pd, Pt, Rh, Ru, Sb, Sn, Ti, V, W, Y, Zn, Zr) substituting Ni. Five ternary compounds were synthesized and analyzed with respect to crystal structure and hydrogen sorption properties. Compounds like LaNi_{4.75}Ag_{0.25} and LaNi_{4.75}Pb_{0.25} showed favorable stability and H₂ sorption thermodynamics. The substituting elements segregating toward the surface were expected to be catalytically active for hydrogen contamination gasses.

Hydrogen storage within a metal hydride involves exothermic reaction during hydrogen absorption and endothermic processes for desorption. After repeated absorption processes, the thermal conductivity of the powdered metal hydride is extremely low compared to its bulk phase. Low heat conduction through the metal hydride powder makes the hydrogen charging slow; thus, appropriate thermal management is necessary to achieve the fast charging time with the maximum energy density. A thermal design of a portable hydrogen storage system with volume of 300-mL have been proposed by Kim et al. through balancing the internal and external

thermal resistances [51]. They employed a copper-mesh structure inside the vessel for enhancing the effective thermal conductivity of metal hydride powder (i.e., reducing the internal thermal resistance). On the other hand, a compact fan was used by them for enhancing the forced convection heat transfer from the vessel (i.e., reducing the external thermal resistance). The proposed thermal design was confirmed by actual hydrogen-charging experiments that showed 73.5% reduction of the charging time.

3. PROPERTIES OF MATERIALS FOR APPLICATIONS

When the hydrogen to the metal (H/M) ratio is high for any hydride it is said to have high hydrogen storage capacity. A low desorption temperature (near the room temperature) is desirable so that hydrogen can be easily recovered when needed. Another important criterion is the heat of dissolution which is sufficient even in the case of volatile hydrides. When metal hydride is used as an energy hydration media, the decomposition heat must be supplied from the waste heat of the converter with which it is coupled. The relative importance of other properties depends to some extent on the specific application. For example, in stationary storage application, weight is not an important parameter, whereas light weight hydrides are suitable for automotive hydrogen fuel storage applications (energy carriers). However, optimizing all these properties simultaneously is a difficult task.

In order to serve as a practical energy or hydrogen storage medium, a metal hydride must satisfy a number of criteria

- High hydrogen carrying(storage) capacity
- Low temperature of dissociation (<100°C)
- High kinetics of hydrogen uptake and discharge
- Low heats of formation and decomposition
- Abundant availability at low cost of alloy
- Low hysteresis
- Light weight
- Flat and extended plateau pressure isotherms
- Stable towards oxygen and moisture (poisoning resistance)
- Reversibility of reaction
- Ease of activation
- Safety
- Physical stability
- Thermal conductivity etc.

4. SPECIFIC APPLICATIONS OF HYDROGEN STORAGE MATERIALS

The purpose of this section is to provide a comprehensive list of the actual and potential applications of intermetallic hydrides. The versatility of intermetallic has led to an extraordinary diversity of potential applications. This ranges from H₂ storage containers and H₂ compressors, which use low-grade heat, to advance thermodynamic and thermo chemical devices that are already commercially available. The applications cover the time span from the present-day industrial hydrogen sector to the proposed future “hydrogen economy” where H₂ will serve as a synthetic fuel and energy carrier. In this section, an attempt is made to broadly underline the spectrum of specific intermetallic hydride application. The applications of metal hydrides are in various engineering sectors such as Ni-MH cell, thermal systems, actuation and sensing, processing, semiconductors, biomimetics and biomedical etc. Metal hydrides are more effective in neutron moderation when it is compared to conventional ones in nuclear power plants [52].

The reaction of gaseous H₂ and a metal alloy forming a metal hydride (including the back-reaction) can be employed in various technical applications:

- Hydrogen storage (stationary, mobile, portable)
 - (A) Static storage units
 - (B) Fuel for motor vehicles
- Hydrogen purification and separation
- Hydrogen separation from gas mixtures (e.g., H₂-CH₄)
- Thermo chemical devices:
 - Hydrogen compressors, Thermoboosters, Heat storage, Heat pumps, Thermochemico-mechanical actuators
- Electrochemical applications (e.g., battery electrodes)
- Electronic applications (e.g., sensors)
- Optical applications (e.g., switchable mirrors)
- Isotope separation
- Hydrogen getters
- Hydrogen compression
- Heat storage
- Heat pumps and refrigerators
 - (A) Mechanically operated
 - (B) Thermal driven, temperature gradient
 - (C) Thermally driven refrigerators
- Heat engine
- Temperature sensor and actuator
- Liquid hydrogen applications
- Catalyst
- Batteries and electrochemical catalyst

CONCLUSION

In conclusion it can be said that AB₅-type alloys are promising hydrogen storage material, which can be used for many applications. Many researches have been performed on AB₅-type alloys to tailor the properties with respect to the parent alloy for deployment as better candidate for application point of view. The technique of mechanical alloying or milling through ball-mill, results in the synthesis of nano-structured alloy with different hydrogenation properties. The annealing of as-synthesized nano-structured alloy may further improve the hydrogenation characteristics of as-milled alloy. The time of ball-milling has direct effect on the microstructure of the as-milled alloy. On the other hand, comparatively more studies have been performed on the substitution of other elements at 'A' and/or 'B' sites of parent AB₅ alloy. The substitution at 'B' site is more common in comparison to 'A' site. The most common substitution at 'A' site in parent LaNi₅ alloy is Ce, Ca, and use of Mm instead of La. There is more choice of substitution at 'B' site with a single, double or multi-element substitution. The common elements are Al, Mn, Co, Fe, Sn, Si, Mo etc. Each element is responsible for different role in the alloy. Whereas, Al decreases the plateau pressure and storage capacity, Fe increases the same. Fe, Mn and Co improves the stability of alloy in electrochemical reaction. Si and Sn are known to enhance the cyclic stability. Nowadays, the use of multi-element composition is more common for optimizing the hydrogenation characteristics. Thus, multi-element composition of AB₅ alloy may serve better to the society as energy material with suitability in many applications.

ACKNOWLEDGMENTS

Authors are grateful to Prof. O.N. Srivastava (BHU, INDIA) and Prof. I.P. Jain (Rajasthan University, INDIA) for helpful discussions.

REFERENCES

- [1] Mohan, V., VijayaBhaskar, S.Y. and Sharma, P. (2007). Bio hydrogen production from chemical waste water treatment in bio film configured reactor operated in periodic discontinuous batch mode by selective enriched anaerobic mixed. *Water Res.* 41:2652–2664.
- [2] Pottier, J.D. and Blondin, E. 1994. Mass storage of hydrogen. In *Hydrogen Energy System: Production and Utilization of Hydrogen and Future Aspects*. edited by Yürüm, Y., 167–179. Netherland: Springer.

- [3] You, H., Ahn, J., Jeong, S. and Chang, D. (2018). Effect of ortho-para conversion on economics of liquid hydrogen tanker with pressure cargo tanks. *J. of Ships and Offshore Stru.* 13:79–85.
- [4] Libowitz, G. (1994). Metallic hydrides; fundamental properties and applications. *J. Phys. Chem. Solids.* 55(12):1461–1470.
- [5] Chambers, A., Park, C., Baker, R.T.K. and Rodriguez, N.M. (1998). Hydrogen storage in graphite nanofibers. *J. Phys. Chem. B.* 102 (22):4253–4256.
- [6] Colbe, J.B.V. and Ramón Ares, J. (2019). Application of hydrides in hydrogen storage and compression: Achievements, outlook and perspectives. *Int. J. Hydrogen Energy.* 44: 7780–7808.
- [7] Rusman, N.A.A. and Dahari, M. (2016). A review on the current progress of metal hydrides material for solid-state hydrogen storage applications. *Int. J. Hydrogen Energy.* 41:12108–12126.
- [8] Ceron-Hurtado, N.M. and Esquivel, M.R. (2010). Stages of mechanical alloying during the synthesis of Sn-containing AB₅-based intermetallics. *Int. J. Hydrogen Energy.* 35: 6057–6062.
- [9] Joseph, B., Schiavo, B., Staiti, G.D. and Sekhar, B.R. (2011). An experimental investigation on the poor hydrogen sorption properties of nano-structured LaNi₅ prepared by ball-milling. *Int. J. Hydrogen Energy.* 36: 7914–7919.
- [10] Talaganis, B.A., Esquivel, M.R. and Meyer, G. (2011). Improvement of as-milled properties of mechanically alloyed LaNi₅ and application to hydrogen thermal compression. *Int. J. Hydrogen Energy.* 36:11961–11968.
- [11] Obregon, S.A., Andrade-Gamboa, J.J. and Esquivel, M.R. (2012). Synthesis of Al-containing MmNi₅ by mechanical alloying: Milling stages, structure parameters and thermal annealing. *Int. J. Hydrogen Energy.* 37:14972–14977.
- [12] Li, S.L., Wang, P., Chen, W., Luo, G., Chen, D.M. and Yang, K. (2010). Effect of non-stoichiometry on hydrogen storage properties of La(Ni_{3.8}Al_{1.0}Mn_{0.2})_x alloys. *Int. J. Hydrogen Energy.* 35:3537–3545.
- [13] Li, S.L., Wang, P., Chen, W., Luo, G., Han, X.B., Chen, D.M. and Yang, K. (2010). Study on hydrogen storage properties of LaNi_{3.8}Al_{1.2-x}Mn_x alloys. *Int. J. Hydrogen Energy.* 35:12391–12397.
- [14] Ngameni, R., Mbemba, N., Grigoriev, S.A. and Millet, P. (2011). Comparative analysis of the hydriding kinetics of LaNi₅, La_{0.8}Nd_{0.2}Ni₅ and La_{0.7}Ce_{0.3}Ni₅ compounds. *Int. J. Hydrogen Energy.* 36:4178–4184.
- [15] Srivastava, S. and Upadhyaya, R.K. (2011). Investigations of AB₅-type hydrogen storage materials with enhanced hydrogen storage capacity. *Int. J. Hydrogen Energy.* 36:7114–7121.
- [16] Li, S.L., Chen, W., Luo, G., Han, X.B., Chen, D.M., Yang, K. and Chen, W.P. (2012). Effect of hydrogen absorption/desorption cycling on hydrogen storage properties of a LaNi_{3.8}Al_{1.0}Mn_{0.2} alloy. *Int. J. Hydrogen Energy.* 37:3268–3275.
- [17] Jain, R.K., Jain, A. and Jain, I.P. (2012). Effect of La-content on the hydrogenation properties of the Ce_{1-x}La_xNi₃Cr₂ (x=0.2, 0.4, 0.6, 0.8, 1) alloys. *Int. J. Hydrogen Energy.* 37:3683–3688.

- [18] Chao, D., Zhong, C., Ma, Z., Yang, F., Wu, Y., Zhu, D., Wu, C. and Chen, Y. (2012). Improvement in high-temperature performance of Co-free high-Fe AB₅-type hydrogen storage alloys. *Int. J. Hydrogen Energy*. 37: 12375–12383.
- [19] Wan, C., Yan, H., Ju, X., Wanga, Y., Huang, M., Kong, F. and Xiong, W. (2012). Investigation of modification of hydrogenation and structure properties of multi-substituted LaNi₅ alloys. *Int. J. Hydrogen Energy*. 37:113234–13242.
- [20] Chumphongphan, S., Paskevicius, M., Sheppard, D.A. and Buckley, C.E. (2013). Effect of Al and Mo substitution on the structural and hydrogen storage properties of CaNi₅. *Int. J. Hydrogen Energy*. 38:2318–2324.
- [21] Selvam, P.K., Muthukumar, P., Linder, M., Mertz, R. and Kulenovic, R. (2013). Measurement of thermochemical properties of some metal hydrides – Titanium (Ti), misch metal (Mm) and lanthanum (La) based alloys. *Int. J. Hydrogen Energy*. 38: 5288–5301.
- [22] Borzone, E.M., Baruj, A., Blanco, M.V. and Meyer, G.O. (2013). Dynamic measurements of hydrogen reaction with LaNi_{5-x}Sn_x alloys. *Int. J. Hydrogen Energy*. 38:7335–7343.
- [23] Paschoalino, W.J. and Ticianelli, E.A. (2013). An investigation of the borohydride oxidation reaction on La–Ni-based hydrogen storage alloys. *Int. J. Hydrogen Energy*, 38:7344–7352.
- [24] Falahati, H. and Barz, D.P.J. (2013). Evaluation of hydrogen sorption models for AB₅-type metal alloys by employing a gravimetric technique. *Int. J. Hydrogen Energy*. 38:8838–8851.
- [25] Yahia, M.B., Knani, S., Dhaou, H., Hachicha, M.A., Jemni, A., Lamine, A.B. (2013). Modeling and interpretations by the statistical physics formalism of hydrogen adsorption isotherm on LaNi_{4.75}Fe_{0.25}. *Int. J. Hydrogen Energy*. 38:11536–11542.
- [26] Matysik, P., Czujko, T. and Varin, R.A. (2014). The application of Pettifor structure maps to binary metal hydrides. *Int. J. Hydrogen Energy*. 39:398–405.
- [27] Drulis, H., Hackemer, A., Głuchowski, P., Giza, K., Adamczyk, L. and Bala, H. (2014). Gas phase hydrogen absorption and electrochemical performance of La₂(Ni,Co,Mg,M)₁₀ based alloys. *Int. J. Hydrogen Energy*. 39:2423–2429.
- [28] Blanco, M.V., Borzone, E.M., Baruj, A. and Meyer, G.O. (2014). Hydrogen sorption kinetics of La–Ni–Sn storage alloys. *Int. J. Hydrogen Energy*. 39:5858–5867.
- [29] Sharma, V.K. and Kumar, E.A. (2014). Effect of measurement parameters on thermodynamic properties of La-based metal hydrides. *Int. J. Hydrogen Energy*. 39: 5888–5898.
- [30] Borzone, E.M., Blanco, M.V., Baruj A and Meyer GO. (2014). Stability of LaNi_{5-x}Sn_x cycled in hydrogen. *Int. J. Hydrogen Energy*. 39:8791–8796.
- [31] Borzone, E.M., Blanco, M.V., Meyer, G.O., Baruj, A. (2014). Cycling performance and hydriding kinetics of LaNi₅ and LaNi_{4.73}Sn_{0.27} alloys in the presence of CO. *Int. J. Hydrogen Energy*. 39:10517–10524.

- [32] Xing, W., Chen, X.Q., Xie, Q., Lu, G., Li, D. and Li, Y. (2014). Unified mechanism for hydrogen trapping at metal vacancies. *Int. J. Hydrogen Energy*. 39:11321–11327.
- [33] Sharma, V.K., Kumar, E.A., Maiya, M.P. and Murthy, S.S. (2014). Experimental and theoretical studies on static and dynamic pressure–concentration isotherms of MmNi_{5-x}Al_x (x=0, 0.3, 0.5 and 0.8) hydrides. *Int. J. Hydrogen Energy*. 39:18940–18951.
- [34] Biliškov, N., Miletić, G.I., Drašner, A. and Prezelj, K. (2015). Structural and hydrogen sorption properties of SmNi_{5-x}Al_x system – An experimental and theoretical study. *Int. J. Hydrogen Energy*. 40:8548–8561.
- [35] Anik, M., Hatirnaz, N.B., and Aybar A.B. (2016). Molten salt synthesis of La(Ni_{1-x}Co_x)₅ (x=0, 0.1, 0.2, 0.3) type hydrogen storage alloys. *Int. J. Hydrogen Energy*. 41:361–368.
- [36] Zhou, W., Ma, Z., Wu, C., Zhu, D., Huang, L. and Chen, Y. (2016). The mechanism of suppressing capacity degradation of high-Al AB₅-type hydrogen storage alloys at 60°C. *Int. J. Hydrogen Energy*. 41:1801–1810.
- [37] Zhao, B., Liu, L., Ye, Y., Hu, S., Wu, D. and Zhang, P. (2016). Enhanced hydrogen capacity and absorption rate of LaNi_{4.25}Al_{0.75} alloy in impure hydrogen by a combined approach of fluorination and palladium deposition. *Int. J. Hydrogen Energy*. 41:3465–3469.
- [38] Kaabi, A., Khaldi, C., Lamloumi, J. (2016). Thermodynamic and kinetic parameters and high rate discharge-ability of the AB₅-type metal hydride anode. *Int. J. Hydrogen Energy*. 41:9914–9923.
- [39] Liu, G., Chen, D., Wang, Y. and Yang, K. (2016). First-principles calculations of crystal and electronic structures and thermodynamic stabilities of La–Ni–H, La–Ni–Al–H and La–Ni–Al–Mn–H hydrogen storage compounds. *Int. J. Hydrogen Energy*. 41:12194–12204.
- [40] Liu, W. and Aguey-Zinsou, K.F. (2016). Synthesis of highly dispersed nanosized LaNi₅ on carbon: Revisiting particle size effects on hydrogen storage properties. *Int. J. Hydrogen Energy*. 41:14429–14436.
- [41] Chibani, A. and Bougriou, C. (2017). Effect of the tank geometry on the storage and destocking of hydrogen on metal hydride (LaNi₅-H₂). *Int. J. Hydrogen Energy*. 42: 23035–23044.
- [42] Molinas, B., Pontarollo, A., Scapin, M., Peretti, H., Melnichuk, M., Corso, H., Aurora, A., Gattia, D.M. and Montone, A. (2016). The optimization of MmNi_{5-x}Al_x hydrogen storage alloy for sea or lagoon navigation and transportation. *Int. J. Hydrogen Energy*. 41:14484–14490.
- [43] Liu, J., Li, K., Cheng, H., Yan, K., Wang, Y., Liu, Y., Jin, H. and Zheng, Z. (2017). New insights into the hydrogen storage performance degradation and Al functioning mechanism of LaNi_{5-x}Al_x alloys. *Int. J. Hydrogen Energy*. 42:24904–24914.
- [44] Yilmaz, F., Ergen, S., Hong, S.J. and Uzun, O. (2018). Effect of Bismuth on hydrogen storage properties of melt-spun LaNi_{4.7-x}Al_{0.3}Bi_x (x = 0.0, 0.1, 0.2, 0.3) ribbons. *Int. J. Hydrogen Energy*. 43:20243–20251.

- [45] Kuncce, I., Polański, M. and Czujko, T. (2017). Microstructures and hydrogen storage properties of La-Ni-Fe-V-Mn alloys. *Int. J. Hydrogen Energy*. 42:27154–27164.
- [46] Melnichuk, M., Cuscueta, D.J. and Silin, N. (2017). LaNi₅ hydride powder flowability as a function of activation and hydrogen content. *Int. J. Hydrogen Energy*. 42:15799–15807.
- [47] Yamagishi, R., Kojima, T., Kameoka, S., Okuyama, D., Sato, T.J., Nishimura, C. and Tsai, A.P. (2017). Creating the hydrogen absorption capability of CeNi₅ through the addition of Al. *Int. J. Hydrogen Energy*. 42:21832–21840.
- [48] Briki, C., Bouzid, M., Dhaou, M.H., Jemni, A. and Lamine, A.B. (2018). Experimental and theoretical study of hydrogen absorption by LaNi_{3.6}Mn_{0.3}Al_{0.4}Co_{0.7} alloy using statistical physics modeling. *Int. J. Hydrogen Energy*. 43:9722–9732.
- [49] Elmas, U., Bedir, F. and Kayfeci, M. (2018). Computational analysis of hydrogen storage capacity using process parameters for three different metal hydride materials. *Int. J. Hydrogen Energy*. 43:10741–10754.
- [50] Łodziana, Z., Dębski, A., Cios, G. and Budziak, A. (2019). Ternary LaNi_{4.75}Mo_{0.25} hydrogen storage alloys: Surface segregation, hydrogen sorption and thermodynamic stability. *Int. J. Hydrogen Energy*. 44:1760–1773.
- [51] Kim, J.B., Han, G., Kwon, Y., Bae, J. Cho, E.A., Cho, S.B. and Lee, B.J. (2020). Thermal design of a hydrogen storage system using La(Ce)Ni₅. *Int. J. Hydrogen Energy*. 45:8742–8749.
- [52] Bhuiya, M.M.H., Kumar, A. and Ki, K.J. (2015). Metal hydrides in engineering systems, processes, and devices: A review of non-storage applications. *Int. J. Hydrogen Energy*. 40:2231–2247.

Chapter 11

**CARBON BASED NANOMATERIALS
FOR ENERGY APPLICATIONS**

***Rajesh Kumar Dwivedi^{1,*}, Esha Dwivedi²
and Raghav Dwivedi³***

¹Department of Physics, Christ Church College, Kanpur (UP), India

²Department of Biochemical Engineering, H. B. T. U., Kanpur (UP), India

³Department of Electronics and Communication Engineering, PSIT,
Kanpur (UP), India

ABSTRACT

The carbon-based nanomaterials are getting profound attention these days due to their key role in providing a foundation for addressing many fundamental challenges such as energy security, global warming, human health, environment etc. due to their outstanding physical, chemical, thermal and electronic properties. The carbon allotropes including fullerenes, activated carbon, carbon nanotubes and graphene constitute a new class of nanomaterials whose properties differ significantly from other forms of carbon as graphite and diamond. The outstanding physical and electronic characteristics of these materials make them suitable candidates for a wide range of applications, such as supercapacitors, high-energy batteries, efficient solar cells and room temperature hydrogen-storage. Due to recent developments in its use in energy harvesting and storage systems, graphene and its derivatives are attracting increasing interest from both the scientific community and industries due to their superior electrical and thermal conductivity, transparency, rigidity, high charge carrier stability, interesting transport phenomena and a large electrochemical window. The possible use of carbon-based nanomaterials as a substitute of traditional materials for different

* Corresponding Author's Email: rkdwivedi1963@gmail.com.

applications in several energy generation and storage systems are presented in this chapter.

Keywords: carbon based nanomaterials, fullerenes, supercapacitors, solar cell, graphene, activated carbon

1. INTRODUCTION

Because of an unprecedented population growth and rapid technological development along with the limited supply of fossil fuels (coal, oil and natural gas), the world is struggling for an energy crisis ahead [1, 2]. The need to meet the tremendous demand for energy in future has led to growing research interests in the use of renewable and clean energy sources. Carbon is one of the most plentiful and indispensable resource found on earth. Carbon-based graphite, charcoal and carbon black material are used in writing, drawing and painting since long times. These materials are also suggested as an excellent tool in alternative source of energy harvesting and storage applications due to the presence of their diverse allotropes forming from amorphous carbon, graphite and diamond to newly discovered and synthesized conjugated materials specifically fullerenes, activated carbon, carbon nanotubes (CNT), graphene and graphene oxide (GO) having exceptional properties and ease of processing [3-5]. Carbon based nanomaterials (CBN's) are getting an increased remarkable attention these days from both the scientific community and industry for their unique combination of chemical, physical, thermal, optical, mechanical and electronic properties such as excellent heat conductivity, superb electrical conductivity, better chemical stability, advanced optical properties, outstanding mechanical strength, tunable porosity and a high surface area to volume ratio etc. Each member of carbon family with distinct dimensionalities such as 0D fullerenes and carbon nano-dots, 1D carbon nanotubes (CNT) and graphene nano-ribbons, 2D graphene and graphene oxides, and 3D nano-diamonds have been found to exhibit inimitable characteristics. Today, they are widely being used for several scientific and technological applications in a variety of areas such as electronics, optoelectronics, biomedical field, pharmaceutical industry, cosmetic industry, energy and environment etc. [6-9] The global demand for clean energy is predicted to get double by 2050, drawing our serious attention to double the energy supply ahead of us [10]. Because of their incredible properties, CBN's are believed to be most suitable and promising energy storage materials to solve the energy crisis ahead of time. Excellent carbon-based electrode materials for electrochemical supercapacitors are known to provide high specific surface area with the wide pore size distribution on it. They also attribute to an exciting combination of their excellent properties including their wider availability, inexpensive, non-toxic behavior, excellent thermal and electrical conductivity, magical chemical and thermal stability etc. [11, 12]. There is also tremendous interest worldwide in the possible use of CNT's in hydrogen-storage

these days because these materials are capable of storing large quantities of hydrogen under ideal conditions required for emerging vehicles powered by fuel cells [13, 14]. Many researchers have employed fullerenes and single walled CNT's hybrid assembly combinations for energy conversion devices because of their specific electrical and electronic properties and relatively high surface area to volume ratio [15, 16]. Due to the easiness of accepting and transporting high mobility electrons by spherical shaped fullerene molecule, they are founding an important role in improving power conversion efficiency of organic photovoltaic devices [17, 18].

CNT's outstanding physical and electronic properties have made them excellent candidates in a wide range of applications including the manufacturing of cathode ray lighting elements, flat panel displays, microelectrode fabrication, high-energy batteries, and room temperature H₂ storage etc. [13] Due to the recent developments in its use in energy harvesting and storage systems, graphene has recently attracted increasing interest from both the scientific community and industry [19, 20]. Graphene exhibits a high electrical and thermal conductivity, superior transparency, rigidity, high mobility of the charge carriers, interesting transport phenomena such as the fractional quantum Hall effect and a large electrochemical window [21, 22]. For its applications in energy storage and generation systems, these features have made graphene especially advantageous. Graphene is also used to manufacture small-scale gas sensors for monitoring the environment [23, 24]. This chapter will present the peculiar properties of various CBN's such as fullerenes, activated carbon, carbon nanotubes, graphene and its derivatives, together with their specific applications, especially electrochemical storage.

2. CARBON ALLOTROPIES

Carbon allotropies are materials of particular interest in various scientific and technological applications. These days, conjugated carbon-based nanomaterials, especially fullerenes, activated carbon, carbon nanotubes, graphene and its derivatives, are gaining traction for various applications in energy generation and storage devices. Figure 1.1 shows the structures of some of the selected allotropes of carbon. The following is a description of these nanostructured CBN's:

2.1. Fullerenes/Buckyball

The first fullerene discovered by Harold W. Kroto and Richard E. Smalley [25] in 1985 has provided exciting insights into carbon nanostructures based research. It is an architecture built from sp^2 carbon atoms based on simple geometrical principles having fascinating physical and chemical properties. The well known fullerenes available these days include C₆₀, C₇₀, C₇₆ and C₈₄, however the most popular in fullerene family is C₆₀ which consists of 60 carbon atoms consisting of 12 pentagonal and two

hexagonal faces structure [26]. These are spherical molecules and the only known allotrope of carbon soluble in various organic solvents at room temperature.

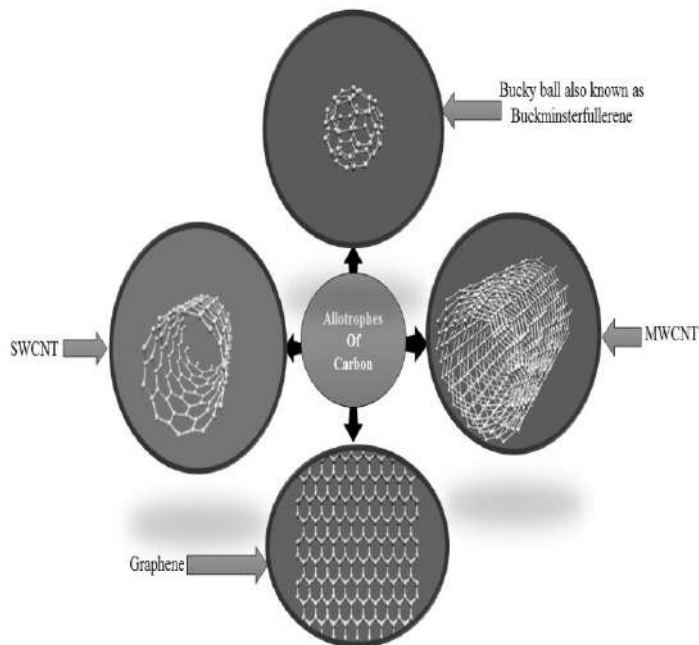


Figure 1.1. Structure of Some Selected Allotropies of Carbon.

Buckminster fullerenes or Buckyballs are composed of carbon of varying size and have the peculiar characteristics which are required in fabricating electrodes for batteries and supercapacitors. Cylindrical fullerenes referred as buckytubes or nanotubes also have an incredibly high surface area, strong electrical and thermal conductivity and linear geometry which make the electrolyte very open to their surface. Buckytubes have been shown to have the highest reversible potential for use in lithium-ion batteries (LIB's) [27, 28]. In addition, buckytubes are proving to be outstanding materials for making supercapacitors electrodes and fuel cell components [29, 30]. Very high tensile strength and toughness characteristics exhibited by buckytubes may be promising for its use as durable hybrid composite components in fuel cells deployed in transport applications [31, 32].

2.2. Carbon Nanotubes

Since the discovery of carbon nanotubes in 1991 by Sumio Iijima [7], they are attracting very promising interest in several scientific and technological applications due to their unique properties. It has a tubular structure in which every carbon atom is connected with three other surrounding carbon atoms. CNT's are known to exist in three different ways as armchair, zigzag and chiral depending upon the way of folding of graphene sheet into a tube. They can be thought of as a seamless closed ended

coaxial hollow cylinders made up of rolling a single or multiple graphene sheets known as single walled nanotubes (SWNT's) or multiple-walled nanotubes (MWNT's) respectively. MWNT's are essentially an arrangement of several concentric cylinders made up of carbon atoms with an outer diameter lying in the range 5-30 nm, length in the range 0.1-10 μm and intertube distance of about 0.34 nm order [33]. The extremely high electrical and thermal conductivity, large length to diameter ratio and greater field enhancement factor at scanning tunnelling microscope probe tip surface makes CNT's ideal for fabricating electron field emitters, solar cells, lithium ion batteries, hydrogen-storage cells, transistors, and cathode ray tubes etc. [34-36]. CNT's are reported to possess a very high tensile strength of 200 GPa and a high mechanical strength with Young's modulus around 1000 GPa [37]. CNT's are found as potential materials for gas sensors due to their high structural porosity and specific surface area. It has been reported that CNT's are very sensitive to various gases such as N_2 , O_2 , CO , CO_2 , NH_3 and CH_4 and volatile organic compounds [38, 39]. The adsorption of these gaseous molecules either donates or accepts electrons from CNT's giving rise to the change in its electrical properties.

2.3. Activated Carbon (AC)

Activated carbon, also called activated charcoal, is also a very useful carbonaceous material which can be distinguished from elemental carbon by the oxidation of carbon atoms found on its outer and inner surface [40]. It is being used since long for the purification of water, gas, gold, metal extraction, sewage treatment, gas masks and respirators, compressed air filters and medicines. AC is a type of carbon known for its high degree of porosity, a tunable surface that contains functional groups and a very high adsorption or chemical reaction surface region. The porous structure of AC differs from graphite as it consists of randomly positioned layers of carbon planes which are formed during its activation [41]. AC is known since long time in the form of powder, granules, pellets, cloths and felts [42]. However, AC in the form of nano-fibers is gaining a great momentum due to its high specific surface area enhancing its adsorption ability. Their pore characteristics including its total pore, micropore and mesopore volume offer several added advantages for applications. The pore size distribution can be modified by several activation procedures such as chemical, physical or both and/or using proper precursors.

AC finds several unique advantageous properties for their use in energy applications such as the requirement of constrained space in electrode materials and its great porosity for supercapacitors and solid-state hydrogen-storage [43, 44]. Its abundance, high porosity, better chemical and thermal stability, ease of processability and low structure density are the few desirable properties to exploit it for various energy harvesting applications. They are still very popularly being used for demanding potential energy applications in the fabrication of supercapacitors, Li-ion batteries and hydrogen-storage materials [44-46].

2.4. Graphene and Its Derivatives

Graphene is also a form of carbon offering potential to utilize carbon atoms in its structure to give rise to outstanding properties. This peculiar carbon allotrope was discovered by Andre Geim and Konstantin Novoselov in 2004 and they were awarded the Nobel Prize in Physics in 2010 for this fascinating discovery. It is attracting growing interest since its inception from both scientific community and industries due to the recent advancements that have led this material as a most explored carbon allotrope. Graphene is exciting and promising youngest carbon allotropic form and made up of a thin 2D planar sheet of sp^2 bonded carbon atoms. It is produced either as a single sheet of graphene or small stacks of multilayer highly crystalline graphene sheets called platelets. Both of these structures have remarkable properties such as large specific surface area, zero bandgap structure, band tuning ability, high optical transmittance, superior stiffness, high strength, outstanding thermal and electrical conductivity, electronic transport properties, chemical and thermal inertness [48]. Therefore, it fulfills the necessary requirements of its use not only as supercapacitor electrode material but also other alternate energy storage and generation devices such as solar cells, flexible displays, batteries and hydrogen-storage and gas sensors. Amongst all carbon allotropes available today, graphene is the thinnest and strongest material of the carbon family today. It is also claimed to be the mother of all CBN's due to its most amazing properties. Due to its maximum stretchability, graphene has the potential of easily converting into 0D fullerenes, 1D CNT's and 3D graphite and considered as a fundamental building block of all dimensional carbon materials. The relatively higher ion and electron mobility for transport and fast response timings exhibited by graphene than activated carbons makes it very attractive candidates for developing supercapacitors electrodes with attractive combinations of high power and high energy densities. The electrons in a graphene sheet behave as massless particles like light photons. It also opens its use in various exciting electric/electronics/optoelectronics applications such as development of ultrafast computers, replacement of silicon chip, electro-optic devices, infrared detectors, high electron mobility transistors, flexible electromechanical actuators and display devices [48, 49]. Graphene derivatives such as oxidized graphene, hydrogenated graphene, graphone, graphyne, graphdiyne, fluorographene, functionalized graphene nanocomposites, various non-metal, metal, polymer, organic molecules, and semiconductor doped graphene's are also gaining sharp attention as novel materials to meet out growing global challenges in terms of energy storage devices and also environmental pollutants sensing applications [50, 51].

Recently another ring shaped allotrope of carbon consisting of 18 carbon atoms joined by alternating single and triple bonds (Cyclo[18]carbon or C_{18}) has also been discovered which is the smallest electron acceptor from a range of donor molecules [52, 53]. The high reactivity of this cyclocarbon may be useful to create other carbon rich materials for their potential uses in electronics and energy storage devices of the future.

3. CARBON NANOMATERIALS OF ENERGY STORAGE AND GENERATION

The various uses of CBN's for energy storage and generation devices are as following:

3.1. CBN's in Fabrication of Supercapacitors Electrodes

A supercapacitor is an energy storing device whose storage capacity lies between that of a rechargeable battery and electrolytic capacitor [54]. They, also known as electrochemical capacitors or ultracapacitors, are becoming very popular these days because of their simple principle of operation, fast charging and long cycle life along with their wider use in consumer electronics, memory backup systems, industrial power and energy management [55, 56]. Supercapacitors can be described to be made up of two electrodes soaked in an electrolyte separated by an ultrathin insulator film between them. The structure of a typical supercapacitor is shown in Figure 2. The electrodes employed in traditional supercapacitors are normally made up of AC. When the electrodes are charged, the electrolyte ions move towards the electrodes and formation of electric double layers on it takes place. The potential difference across the electrodes is adjusted just above the threshold value for the electrochemical reactions to start and give rise to the formation of electric double layers on the electrode surface. The major drawback of AC is the presence of inaccessible micropores on its surface which can lower its electrochemical performance [57].

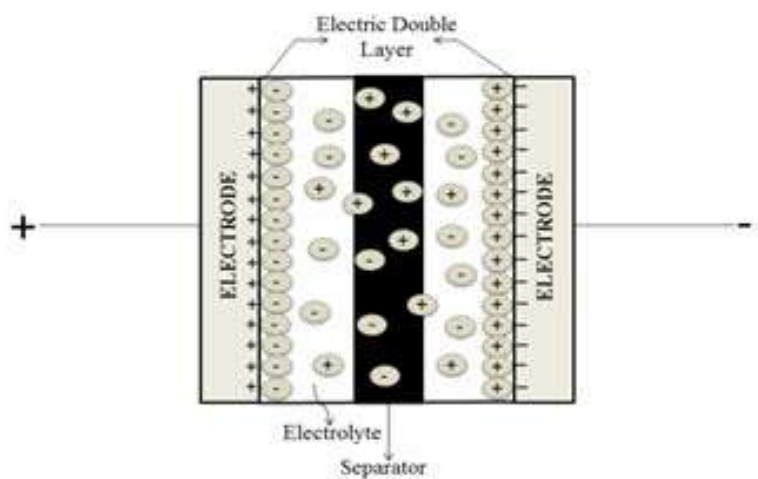


Figure 2. The Structure of a Typical Supercapacitor.

Therefore, it is essential to develop the right material for supercapacitor electrode to supplement uninterrupted energy. The most important factors dictating the selection of CBN's for supercapacitors electrodes are its high surface area with well interconnected pore structures and controlled pore size matching with the ions of electrolyte used. The supercapacitors are an attractive alternate energy storage solution for high power applications as a replacement of batteries. The supercapacitor can be charged in three different ways: (i) the formation of electrochemical double layer on the electrodes (ii) the pseudo capacitance formed by fast and reversible surface redox process and (iii) hybrid electrochemical capacitance resulting both from electrochemical double layer and redox reaction to store the charges.

The major advantage of replacing rechargeable batteries by supercapacitors in various electronic applications is its high-power capacity, fast charging rates at high power density, everlasting perpetual life [58]. The supercapacitors suffer from the problem of relatively low energy density. Increasing its energy density is an exigent issue and a major hindrance to elaborate its marketability. CNT's has the potential to provide solution to this problem because of very their outstanding electrical and thermal conductivity and high surface area. The active surface area in CNT's mostly lies outside of the nanotubes along with the interstitial spaces between them [59]. SWNT's are currently very expensive for commercial applications because of its poor solubility in most of the common solvents and therefore its processability is cumbersome and expensive. The additional dispersive agents added to process it limit the performance of the electrodes made up of CNT's. Thin graphene sheets are emerging as promising materials for supercapacitors, photovoltaic devices, hydrogen-storage and LIB's and flexible electronics. Single graphene sheets as well platelets have remarkable properties both for energy harvesting and storage devices [60]. Graphene based supercapacitors store energy by nanoscopic charge separation between the electrode and electrolyte [61]. They are capable of storing much more energy as compared to conventional dielectric capacitors. Like CNT's, graphene also suffer from the same processing difficulty as the additives are requires keeping its individual form aggregating in the solution.

Supercapacitors have also been prepared through screen printing on various substrates such as cloths, plastics and papers etc. thereby facilitating the possibility of fabricating flexible electronic devices [62, 63]. These printed solid-state supercapacitors have a great potential for storing energy in several energy harvesting applications. Supercapacitors electrodes made from graphene-based aerogel have been developed recently using 3D-printing technique [64]. AC's derived from packaging waste have been used for fabricating a 3D printed supercapacitor for the first time [65]. Supercapacitors made from screen printed AC/Ag hybrid electrode material are reported to exhibit its better performance that AC based supercapacitors [66]. It is believed that these supercapacitors could be recharged so quickly than that of LIB's making them as suitable alternative for powering electric vehicles.

Supercapacitors are proving to be superior alternative to batteries in terms of long-term operation and the cyclability requirement of an energy storage device.

3.2. Carbon Based Photovoltaic Devices

Because of the potential to tackle both the safe energy and clean environment issues, photovoltaics has come up as an emerging applications area of CBN's in the recent years. Organic photovoltaics (OPV'S) and perovskite thin films solar cells are attracting great attention due to their light weight, elasticity and economical production. The outstanding mechanical flexibility, chemical stability and elemental abundance of these carbon nanomaterials offer a unique opportunity for exploiting them in various photovoltaic applications [67, 68]. The fullerenes being the first carbon nanostructures isolated experimentally are relatively less utilized than CNT's and graphene derivatives as photoactive components in solar cells. However, it is proving to be most effective electron acceptor and transport materials in organic photovoltaic devices.

Graphene-based solar cells being produced today are not very different from the traditional inorganic/silicon solar cells except that some of the constituents of the cell are substituted with graphene, graphene derivatives or graphene nano-composites. The operational efficiency of these solar cells can be enhanced by either using number of graphene platelets or a doped functionalized graphene-based materials. Gold particles doped of graphene layers have been reported to improve the efficiency of the solar cell drastically [69]. Graphene based solar cells are found to be so elastic that they are capable of bending relatively much more than pure indium tin oxide electrodes-based devices [70]. Both graphene and CNT's hybridized with quantum dots have been exploited for fabricating functional solar cells in which fast electron transfer from quantum dot to graphene takes place. Multi junction solar cells, also known as tandem solar cells have been studied theoretically to reach much higher solar energy conversion efficiency as compared with single solar cell [70]. Graphene films exhibiting very high optical transparency and low resistance along with its excellent electrical, outstanding mechanical and thermal properties are used as transparent window electrodes in inorganic solar cells and help in electron-hole separation and transport. Various multilayer electrodes using graphene doped with gold, copper and PMMA in various compositions have been fabricated to yield very significant outstanding results. Graphene oxide nanoribbons, copper neutralized graphene, graphene-CdS based hybrid material etc. have also shown promising options in heterojunction solar cells. Graphene nanostructures have also been exploited for size-dependent bandgap and large optical absorption in graphene Schottky junction GaAs solar cells [71]. There seems to be tremendous progress into CBN's being utilized for various photovoltaic applications especially graphene-based solar cells.

3.3. Carbon Based Nanomaterials for Li-ion Batteries

Li-ion batteries are excellent power devices being used in all modern portable electronic devices. Among all rechargeable battery systems available at present, LIB's offer attractive properties such as superior and highest energy density to weight ratio, long lifespan, low pollution and superior performance over its other battery counterparts as lead-acid, Ni-Cd and nickel-metal hydride battery systems. The electrochemical performance of a LIB's is determined by the properties of its cathode, anode and electrolyte. A LIB normally contains a cathode made of lithiated transition metal oxide, anode of silicon and LiPF_6 as an electrolyte in carbonate based organic solvents. Silicon has been reported to suffer from huge volumetric changes during the lithiation and delithiation processes. Fulfilling the societal expectation and demand for inexpensive, long lasting, lighter, and thinner Li-ion battery have necessitated advanced research for exploring materials with better properties for both the electrodes and electrolyte. Efforts are being made continuously to improve its performance by exploiting various electrodes and electrolyte materials to upgrade battery capacity, cycle life, charge discharge rates and highest degree of safety. Carbon based electrodes are very promising candidates as anodes for LIB's due to their excellent conductivity, good endurance, high current collection efficiency, charge/discharge at high power, biocompatibility and low cost.

The fullerenes offer a significant potential to achieve a high degree of lithium intercalation. It has been reported in the literature that the most stable form of fullerenes C_{60} and C_{70} can be hydrogenated via different methods. Hydrogenated fullerenes particularly C_{70}H_x has been found as an excellent anode material for LIB's [72]. Nitrogen doped fullerenes and its derivatives have also been studied for its potential use as anode for LIB's and cathode catalysts for hydrogen fuel cells [73]. CNT's are also proving to be an attractive and promising anode materials for LIB's due to their unique outstanding properties. In order to accommodate most of the volumetric changes in semiconducting silicon anode, to make anode most robust and improving high charge/discharge rates of Li-ion battery, conductive additives as CNT's are utilized. The low density of carbon atom and its typical structure allows the imbedding of Li-ion not only inside the tube but also between the gap. It has been found that the conjugation of silicon with CNT's improves the performance of the battery drastically [74]. The potential suitability of MWNT's have also been studied as anode materials in LIB's using different combinations of Li, Co, Ni, Mn and Fe cathode materials.

The graphene LIB's are quickly emerging more favorable than their carbon predecessors due to the increased electrode density, faster cycle time with improved batteries lifespan. The energy storage capacity of LIB's can be significantly increased with anode made from folded graphene. Graphene is used in these batteries to enhance cathode conductor performance. The 2D graphene sheet and platelets exhibit very interesting properties including its excellent electrical and thermal conductivity, high flexibility, high strength and especially low weight. Just like LIB's, graphene batteries have also been developed using two conductive plates coated with

graphene immersed in an electrolyte solution. These solid-state batteries are capable of storing much more energy, supporting very high currents and super fast recharge than that of LIB's. 3D printed graphene batteries using graphene ink have also been developed. Thus, graphene battery seems to be the first choice of meeting energy demand crisis ahead and battery of the future [75].

3.4. Hydrogen-Storage in Carbon Based Nanomaterials

Hydrogen being the simplest and most abundant element in the universe has the potential to meet the energy demands as an efficient alternative fuel with growing futuristic needs ahead. Due to its ability to possess high specific energy and regenerative nature, it is an eco friendly and clean energy carrier. There are many ways to store hydrogen in different materials; however, the most economical and safest way is via its absorption or adsorption or both on solid materials surface. The estimation of hydrogen-storage in materials is mainly governed by two parameters the gravimetric density (GD) and volumetric density (VD). Being light and compact is an essential and necessary requirement for a hydrogen-storage device. Several CBN's like AC, fullerenes, CNT's, AC fibers, carbon nano-fibers, carbon nano-horns and graphene have been examined for their hydrogen-storage capacity in the literature [76, 77]. Two important processes namely physisorption and chemisorption are responsible for the storage of hydrogen in the CBN's. Carbon materials as compared to various metal hydrides used for hydrogen-storage offers several advantages such as its low atomic mass and micro-porous behavior. The adsorption of hydrogen molecules at its surface takes place mainly by Van der Waals forces. The hydrogen intake capacities of CNT's depend on its structure, geometry, structural defects, operating pressure, temperature, pre-treatments and doping. Both SWNT and MWNT's have been investigated extensively for their hydrogen-storage capacities. Their hydrogen-storage capability has been found to be highly dependent on both temperature and pressure. CNT's have also been exploited with other hydrogen-storage material as hybrid materials for hydrogen-storage. Metal nanoparticles (Pd, Ni) decorated MWNT's has been found to enhance its hydrogen-storage capacity due to spill over mechanism of metal nanoparticles around CNT's [76]. Functionalization of CNT's by adding atoms and molecules is reported to result in higher hydrogen-storage capacity [77]. CNT's are essentially termed as one of the promising nanostructures for storing hydrogen both on its inner and outer surfaces.

Graphene's are also becoming very popular for their promising applications in efficient hydrogen-storage due to its exceptionally large surface area, porous nature, lightweight, inexpensive, robust, and chemically stable and ease of chemical functionalization. Several theoretical studies have depicted graphene as a promising material for hydrogen-storage both in terms of gravimetric and volumetric densities. It has been reported for a single graphene sheet to have hydrogen uptake capacity of 8.3% on both surfaces with chemisorption. Both the strain and curvature in graphene

sheets have been found to influence its adsorption capacity. Researchers have reported decorated graphene for hydrogen-storage [78]. Layer spaced graphene sheets have also been reported to uptake large quantities of hydrogen [79] in the interlayer spacing as well as on the exposed surfaces. Hydrogen binding energy on graphene surface is found to dependent on graphene curvature [80]. Functionalized graphene is chemically modified graphene attaching various functional groups like hydroxyl, carboxyl, carbonyl containing oxygen, nitrogen, sulphur, phosphorus, boron etc. on its surface [81-83]. The increased surface area helps in accumulating or promoting adsorption of more number of hydrogen molecules in the inner layers. It is expected that metal hydride and graphene hybrid materials may lead some drastic improvement in their hydrogen-storage capacity.

CONCLUSION

CBN's represent very attractive materials in many energy harvesting and storage applications due to their abundance along with its excellent chemical, thermal, electrical and mechanical properties and possibility of tailoring its structure to meet the requirements of specific applications. High-performance carbon-based supercapacitors and hydrogen-based fuel cells are coming up as a promising electrochemical system for potential energy and power storage applications as alternative solutions of efficient and clean energy. Hydrogen-storage ability of CBN's is attributed to its high surface area, pore size, volume and its distribution. Graphene presents several new and exciting features for magical energy storage devices such as smaller supercapacitors, completely flexible and even rollable energy storage devices, transparent batteries and fast charging devices. Despite the tremendous growth in research on exploiting the CBN's for different energy generation and storage, much more attention is required to reduce the cost of graphene-based devices for both hydrogen-storage and graphene-based batteries. Today, the greatest potential and need is to develop and define an effective carbonaceous material that could provide substantially higher capacity in LIB's systems than the carbon materials currently used and replace them with efficient graphene-based batteries. A very exciting and increasingly evolving area of the future is graphene-based photovoltaics.

REFERENCES

- [1] Kaberger T (2018). Progress of renewable electricity replacing fossil fuels, *Global Energy Inter.* 1: 48-52.
- [2] Gielen D, Boshell F, Saygin D, Bazilian MD, Wagner N and Gorini R (2019), The role of renewable energy in the global energy transformation, *Energy Strategy Reviews* 24, 38-50.

- [3] Delgado JL et al. (2009), Fullerene dimers (C₆₀/C₇₀) for energy harvesting, *Chemistry A European Journal*, 15 (48), 13474-482.
- [4] Mondal K et al. (2019), Carbon nanostructures for energy and sensing applications, *Hindawi J. Nanotechnology*, 1454327, 1-3.
- [5] Gogotsi Y. (2015), Not just graphene: The wonderful world of carbon and related nanomaterials, *MRS Bulletin* 40, 1110–1121.
- [6] Wang H, Liang X, Wang J, Jiao S and Xue D (2020), Multifunctional inorganic nanomaterials for energy applications, *Nanoscale* 12, 14-42.
- [7] Iijima S. (1991), Helical microtubules of graphitic carbon, *Nature*, 354, 56-58.
- [8] Giubileo F, Bartolomeo AD, Lemmo L, Luongo G and Urban F. (2018), Field emission from carbon nanostructures, *Applied Sciences* 8, 526-47.
- [9] Saito S and Tomita I (2020), Topological carbon allotropes: Knotted molecules, carbon-nanochain, chainmails, and Hopfene, *Materials Research Express* 7, 056301, 1-19.
- [10] Shrestha P. (2020), Global energy use projected to nearly double by 2050, *Energy Live news*, www.energylivenews.com.
- [11] Justino da Silva R et al. (2020), Supercapacitors based on (carbon nanostructure)/PEDOT/(eggshell membrane) electrodes, *J. Electroanalytical Chemistry*, 856, 113658, 1-9.
- [12] Yu Z, Tetard L, Zhai L and Thomas J (2015), Supercapacitor electrode materials: nanostructures from 0 to 3 dimensions, *Energy and Environmental Science* 8, 702-30.
- [13] Mohan M, Sharma VK, Kumar EA and Gayathri V (2019), Hydrogen-storage in carbon materials- A review, *Energy Storage* 1, 1-74.
- [14] Zhao T et al. (2017), Hydrogen-storage capacity of single-walled carbon nanotube prepared by a modified arc discharge, *Fuller. Nanotubes Carbon Nanostruct.* 25, 355-358.
- [15] Shen Y and Nakanishi T (2014), Fullerene assemblies towards photo-energy conversions, *Physical Chemistry Chemical Physics* 16, 7199-7204.
- [16] Durbin DJ, Allan NL and Jugroot CM (2016), Molecular hydrogen-storage in fullerenes-A dispersion corrected density functional theory, *Inter. J. Hydrogen Energy*, 41, 13116-130.
- [17] Zhang J, Tan HS and Yan H (2018), Material insights and challenges for non-fullerene organic solar cells based on small molecular acceptors, *Nature Energy* 3, 720-731.
- [18] Speller EM et al. (2019). From fullerene to non-fullerene acceptors: prospects and challenges in the stability of organic solar cells, *Journal of Materials Chemistry A*, 41, 2019, 23361-77.
- [19] Ye M, Zhang Z, Zhao Y and Qu L (2018), Graphene platforms for smart energy generation and storage, *Joule* 2, 245-268.
- [20] Xuan Y et al. (2020), Graphene/semiconductor heterostructure wireless energy harvester through hot electron excitation, *AAAS Research*, 3850389, 1-8.

- [21] Novoselov KS et al. (2007), Room-temperature quantum Hall effect in graphene, *Science* 315 (5817), 1379-1379.
- [22] Bolotin KI, Ghahari F and Kim P (2009), Observation of the fractional quantum Hall effect in graphene *Nature* 462, 196-199.
- [23] Buckley DJ et al. (2020), Frontiers of graphene and 2D material-based gas sensors for environmental monitoring, *2D Materials* 7, 032002.
- [24] Demon SZN et al. (2020), Graphene-based materials in gas sensor applications: A Review, *Sensors and Materials* 32, 759-777.
- [25] Kroto HW et al. (1985), C₆₀: Buckminsterfullerene, *Nature* 318, 162-163.
- [26] Nimibofa A, Newton EA, Cyprain AY and Donbebe W (2018), Fullerenes: Synthesis and applications, *J. Materials Science Res.* 7 (3), 22-36.
- [27] Teprovich Jr. JA et al. (2019), Hydrogenated C60 as High-Capacity Stable Anode Materials for Li Ion Batteries, *ACS Appl. Energy Mater.* 2, 6453-60.
- [28] Changsheng S et al. (2017), Functionalized fullerenes for highly efficient lithium ion storage: Structure-property-performance correlation with energy implications, *Nano Energy* 40, 1-29.
- [29] Bairi P et al. (2019), Mesoporous carbon cubes derived from fullerene crystals as a high rate performance electrode material for supercapacitors, *J. of Mater. Chem. A* 2013, 1-3.
- [30] Bae J. (2018), Recent advances on multi-dimensional nanocarbons for supercapacitors: A review, *Journal of Electrochemical Science and Technology* 9 (4), 251-259.
- [31] Rambabu G, Bhat SD and Figueiredo FML. (2019), Carbon nanocomposite membrane electrolytes for direct methanol fuel cells—A concise review, *Nanomaterials* 9, 1292, 1-30.
- [32] Kulvelis YV et al. (2020), Composite proton-conducting membranes with nanodiamonds, *Fullerenes, Nanotubes and Carbon Nanostructures* 28, 140-146.
- [33] Ebbesen TW and Ajayan PM (1992), Large-scale synthesis of carbon nanotubes, *Nature* 358, 220.
- [34] Zhu W et al. (1999), Large current density from carbon nanotube field emitters, *Applied Physics Letters* 75, 873.
- [35] Gao B et al. (1999), Electrochemical intercalation of single-walled carbon nanotubes with lithium, *Chemical Physics Letters* 307, 153-57.
- [36] Venkataraman A, Amadi EV, Chen Y and Papdopoulos C (2019), Carbon nanotube assembly and integration for applications, *Nanoscale Res. Lett.* 14 (220), 1-47.
- [37] Yakobson BI and Avouris P, Mechanical properties of carbon nanotubes, in Dresselhaus MS, Dresselhaus G and Avouris P (Eds.): *Carbon Nanotubes: Synthesis, structure, properties and applications*, 2001, Springer, 287-327.
- [38] Zaporotskova IV, Boroznina NP, Parrkhomenko YN and Kozhitov LV (2016), Carbon nanotubes: Sensor properties. A review, *Modern Electronic Materials* 2 (4), 2016, 95-105.

- [39] Varghese OK et al. (2001), Gas sensing characteristics of multi-wall carbon nanotubes, *Sensors and Actuators (B)* 81, 2001, 32-41.
- [40] Mattson JS and Mark HB, *Activated carbon*, Marcel Dekker, (1971), New York.
- [41] Kwiatkowski JF (Ed), *Activated carbon: Classifications, properties and applications*, 2011, Nova Science Publishers, Incorporated, 125-168.
- [42] Al-Qodah Z and Shawabkah R (2009), Production and characterization of granular activated carbon from activated sludge, *Braz. J. Chem. Eng.* 26 (1), 2009, 127-36.
- [43] Herde ZD, Dharmasena R, Draper GL, Sumansekera G and Satyavolu J. (2018), Production of high surface area activated carbon for energy storage applications, *AIP Conference Proceedings* 1992 (1), 020004-1-020004-5.
- [44] Sevilla M and Mokaya R (2014), Energy storage applications of activated carbons: Supercapacitors and hydrogen-storage, *Energy and Environmental Science* 7, 1250, 1-31.
- [45] Javaid A. (2017), *Activated carbon fiber for energy storage*, *Activated Carbon Fiber and Textiles*, 281-303, doi.org/10.1016/B978-0-08-100660-3.00011-0.
- [46] Ghorbani H, Tavanai H and Morshed M (2014), Fabrication of activated carbon nanoparticles from PAN precursor, *J. Analytical and Appl. Pyrolysis* 110, 12-17.
- [47] Lu G, Yu K, Wen Z and Chen J (2013), Semiconducting graphene: Converting graphene from semimetal to semiconductor, *Nanoscale* 5, 1353-68.
- [48] Meng X (2019), Recent progress of graphene as cathode materials in lithium ion batteries, *IOP Conf. Series: Earth and Environmental Science* 300, 042039, 1-10.
- [49] Tozzini V and Pellegrini V (2013), Prospects for hydrogen-storage in graphene, *Physical Chemistry Chemical Physics*, 15, 80-89.
- [50] Dideikin A and Vul AY. (2019), Graphene oxide and derivatives: The place in graphene family, *Frontiers in Phys.* 6, 149, 1-23.
- [51] Tahir AA et al. (2016), The application of graphene and its derivatives in energy conversion, storage, environmental and bio-sensing devices, *The Chemical Record*, 16 (3), 1591-1634.
- [52] Stasyuk AJ, Stasyuk OA, Sola M and Voityuk AA (2020), Cyclo[18]carbon: the smallest all-carbon electron acceptor, *Chemical Communications* 56, 352-355.
- [53] Kaiser K et al. (2019), An sp-hybridized molecular carbon allotrope, cyclo[18]carbon, *Science* 365, 1299-1301.
- [54] Raza W et al. (2018), Recent advancements in supercapacitor technology, *Nano Energy* 52, 441-73.
- [55] Libich J et al. (2018), Supercapacitors: Properties and applications, *J. Energy Storage* 17, 224-227.
- [56] Prasad GG et al. (2019), Supercapacitor technology and its applications: a review, *IOP Conference Series: Materials Science and Engineering* 561, 012105, 1-12.

- [57] Lee HM, An KH, Park SJ and Kim BJ (2019), Mesopore-Rich activated carbons for electrical double-layer capacitors by optimal activation condition, *Nanomaterials* 9, 608, 1-13.
- [58] Gidwani M, Bagwani A and Rohra N (2014), Supercapacitors: The near future of batteries, *International J. Engineering Inventions* 4, 22-27.
- [59] Aval LF, Ghoranneviss M and Pour GB (2018), High performance supercapacitors based on the carbon nanotubes, graphene and graphite nanoparticles electrodes, *Heliyon* 4 (11), e00862.
- [60] Bai L et al. (2020), Graphene for energy storage and conversion: Synthesis and Interdisciplinary Applications, *Electrochemical Energy Reviews* 3, 395-430.
- [61] Ke Q and Wang J (2016), Graphene-based materials for supercapacitor electrodes – A review, *J. of Materiomics* 2 (1), 37-54.
- [62] Wei D et al. (2011), Properties of graphene inks stabilized by different functional groups, *Nanotechnology* 22, 245702.
- [63] Zhang Y, Wang Y, Cheng T, Yao LQ, Li X, Lai WY and Huang W (2019), Printed supercapacitors: materials, printing and applications, *Chemical Society Reviews* 48, 3229, 1-36.
- [64] Mao J, Iocozzia, Huang J, Meng K, Lai Y and Lin Z (2018), Graphene aerogels for efficient energy storage and conversion, *Energy and Environmental Science* 11, 772-799.
- [65] Idress M et al. (2020), 3D printed supercapacitor using porous carbon derived from packaging waste, *Additive Manufacturing* 36, 101525.
- [66] Alam A, Saeed G and Lim S (2020), Screen-printed activated carbon/silver nanocomposite electrode material for a high performance supercapacitor, *Materials Lett.* 273, 127933.
- [67] Zhang Z, Wei L and Li Y (2015), Carbon nanomaterials for photovoltaic process, *Nano Energy* 15, 490-522.
- [68] Bernardi M et al. (2012), Nanocarbon-based photovoltaics, *ACS Nano* 6, 8896-8903.
- [69] Umeyama T and Imahori H. (2019), Isomer Effects of Fullerene Derivatives on Organic Photovoltaics and Perovskite Solar Cells, *Acc. Chem. Res.* 52, 2046-55.
- [70] *Using graphene based solar cells for solar applications*, 2017, www.azonano.com.
- [71] Luceno-Sanchez, Diez-Pascual AM and Capilla RP. (2019), Materials for photovoltaics: State of art and recent developments, *Int. J. Molecular Sciences* 20, 976, 1-42.
- [72] Pistoia G (ed), *Lithium-Ion Batteries: Advances and Applications*, 2014, Elsevier Publisher.
- [73] Teprovich Jr. JA et al. (2019), Hydrogenated C60 as high-capacity stable anode materials for Li ion batteries, *ACS Appl. Energy Mater.* 2(9), 6453- 6460.
- [74] Ikonen T et al. (2020), Conjugation with carbon nanotubes improves the performance of mesoporous silicon as Li-ion battery anode, *Scientific Reports* 10, 5589, 1-9.

- [75] Al-Saedi S, Haider AJ, Naje AN and Bassil N. (2020), Improvement of Li-ion batteries energy storage by graphene additive, *Energy Reports* 6 (3), 64-71.
- [76] Han M et al. (2015), The enhanced hydrogen-storage of micro-nanostructured hybrids of $Mg(BH_4)_2$ carbon nanotubes, *Nanoscale* 7, 18305-311.
- [77] Ernould B et al. (2017), Electroactive polymer/carbon nanotubes hybrid materials for energy storage synthesized via a “grafting to” approach, *RSC Advances* 7, 17301-310.
- [78] Jin Z et al. (2011), Nano-engineered spacing in graphene sheets for hydrogen-storage, *Chem. of Mats.* 23 (4), 923-25.
- [79] Cocchi C, Prezzi D, Ruini A, Caldas MJ and Molinari E. (2012), Optical Excitations and Field Enhancement in Short Graphene Nanoribbons, *J. Phys. Chem. C* 116, 17328-335.
- [80] Goler S et al. (2013), Influence of graphene curvature on hydrogen adsorption: Towards hydrogen-storage device, *J. Phys. Chem. C* 117 (12), 11506-513.
- [81] Jain V and Kandasubramanian B. (2019), Functionalized graphene materials for hydrogen-storage, *J. Mater. Sci.* 55 (1), 1-39.
- [82] Ionita M (2017), Graphene and functionalized graphene: Extraordinary prospects for nanobiocomposite materials, *Composite Part B: Engineering* 12, 34-57.
- [83] Dehghanzad B et al. (2016), Synthesis and characterization of graphene and functionalized graphene via chemical and thermal treatment methods, *RSC Advances* 6, 2016, 3578-85.

Complimentary Contributor Copy

Chapter 12

**FUNCTIONALIZED NANOMATERIALS
BASED EFFICIENT PHOTOCATALYST
FOR RENEWABLE ENERGY
AND SUSTAINABLE ENVIRONMENT**

Sunil Kumar^{1,2,*}

and Pankaj Kumar Chaurasia³

¹Department of Chemistry, L.N.T. College
(A Constituent Unit of B.R.A.Bihar University) Muzaffarpur,
Bihar, India

²Department of Chemistry, R.B.B.M. College
(A Constituent Unit of B.R.A. Bihar University) Muzaffarpur,
Bihar, India

³PG Department of Chemistry, L.S. College
(A Constituent Unit of B.R.A. Bihar University) Muzaffarpur,
Bihar, India

ABSTRACT

Pollutants present in water are increasingly becoming an important public health issue. Photocatalytic efficiency depends on the number of active sites present on the surface of nanomaterials. Nanomaterials act as efficient adsorbent as well as effective photocatalyst because of surface conduction phenomenon. Functionalization promotes charge separation within nanomaterials. The future sustainable development of society relies on alternative energy sources that are renewable and environmentally friendly. The property of materials depends on size

* Corresponding Author's Email: sunilchemIntc@gmail.com.

and dimensions. Size of nanomaterials lies in the range of 1-100 nm. It can be designed as electrode (anode and cathode) for device fabrication. Quantum confinement displays the suitability of nanomaterials. Society requires energy for various activities along with industrial growth. Conductive group can improve the charge transport properties of nanomaterials. The present chapter is a review on the current status of photoactive nanomaterials (Photocatalyst) used in such environmental technologies. Removal of contaminants from polluted water has become a major environmental concern. The nanomaterial's surface has strong affinity to adsorb the heavy metals. Nanomaterials can be functionalized or grafted with functional groups that can target specific molecules of interest (pollutants) for efficient remediation. High surface-volume ratio makes nanomaterials useful in various sectors. Nanomaterials can convert solar energy into electrical energy and photocatalytic degradation causes production of chemical energy and electrical energy. The photo degradation efficiency depends on the interaction between the pollutant and the catalytic surface.

Keywords: nanomaterials, surface functionalization, active sites, quantum confinement, solar energy, photo activity, adsorption capacity, redox activity, photo degradation

1. INTRODUCTION

Solar light as an inexpensive, non-polluting, abundant and clean energy source is undoubtedly a strategy that will aid in reducing our fossil fuel dependency as well as reducing anthropogenic CO₂ emissions, leading to sustainability of social life on the earth. Highly efficient adsorbents exhibit fast kinetics and better adsorption capacity [1]. TiO₂ works as efficient photocatalyst to remove environmental pollution and to generate H₂ from water under sunlight irradiation [2]. Nanomaterials present enhanced reactivity and thus, better effectiveness when compared to their bulkier counterparts due to their higher surface-to-volume ratio [3]. Charge diffusion length and charge separation within nanomaterials are major factors which decide efficiency of the photo electrode. Degradation is defined as the gradual decomposition of substances (pollutants) into other substances and dye degradation is detected easily by the decolourisation of the natural dye color. Photo-generated charge carriers may recombine during the migration process, leading to the decrease of the photocatalytic activity [4]. The effective photocatalysts for pollutant's degradation require appropriate band gap, strong oxidative ability and high stability in water solution system. The functionalized nanoparticles (NPs) have good physical properties, anti-corrosion, and anti-agglomeration [5]. NPs can be coated with organic (monomer and polymer) and inorganic (metal and oxides) layers [6, 7]. Among the metals, gold and silica are well explored to be coated on NPs to induce high stability and conductive environment for subsequent functionalization. The functionalization always works as chemical and physical filter for suspended particulates over the surface of particle [8]. The introduction of doping is to control the type and concentration of the charge carriers

[9]. With the application of nanomaterials, photovoltaic solar cells are increasing their efficiency while reducing the production costs of electricity and manufacturing [10]. Combining silver nanowires, titanium dioxide nanoparticles and a polymer that absorbs infrared light to make a solar cell that is about 70% transparent to visible light, is allowing it to be used in windows. Energy storage devices composed of nanomaterials provide a large specific surface area. Large surface area is good for the accessibility of electrolyte, which is beneficial to the fast charge/discharge for Li-ion batteries. Semiconductor nanoparticles applied in a low temperature printing process results in low cost solar cells. Quantum dots (1-10 nm) are attractive for solar cell applications due to their ability to enhance light absorption via multiple energy levels and extend the absorption edge *into* the infrared range [11]. Using light absorbing nanowires embedded in a flexible polymer film is another method being developed to produce low cost flexible solar panels. The quantum efficiency of a photo catalyst is also affected by the transfer rate of photo generated electrons and holes [12]. Lack of environmental sustainability is a vital and growing problem due to the issues like climate change, pollution, and disturbances associated with biodiversity. Therefore, clean energy and environmental applications often demand the development of novel nanomaterials that can provide shortest reaction pathways for the enhancement of reaction kinetics [13]. Understanding the physicochemical, structural, microstructural, surface, and interface properties of nanomaterials is vital for achieving the required efficiency, cycle life, and sustainability in various technological applications [1, 7]. Nanomaterials with specific size and shape such as nanotubes, nanofibers/nanowires, nanocones, nanocomposites, nanorods, nanoislands, nanoparticles, nanospheres, and nanoshells to provide unique properties can be synthesized by tuning the process conditions [14, 15]. Nanomaterials having high surface-to-volume ratio, cover a variety of shapes of nanoparticles, nanorods, nonporous framework, and so on. One can also easily tune the optical and charge transfer properties by changing the size of semiconductor nanomaterials [11, 16]. The chemical properties such as catalytic activity can also be remarkably changed with increased surface atoms of nanocatalysts [17]. The major objective of this special issue is to bring out the salient research paradigms of nanomaterials and their potential impacts on clean energy generation, storage, utilization, waste heat recovery, environmental detoxification, and disinfection and advocate the process sustainability [18]. Nano metal oxides (TiO_2 , Fe_2O_3 , and ZnO) are very strong decoloring agents used for photo catalytic degradation of organic pollutants. It plays an effective role in the treatment of waste water effluents [19]. These promising applications of metal oxides characterized as charge transport in electronic structure stimulate its light absorption properties and make it possible to be utilized as photo catalyst as well as sensor [20]. Photon energy greater than the band gap, excites the catalyst and generates electrons and holes. Organic pollutants get adsorbed on the catalyst surface via lattice oxygen at the surface [21]. Electrocatalysis is a phenomenon by which redox reaction is governed at the interface of solar cell. Nano materials exhibited its role as electron hole pair separator and maintain the device reversibility, cycle life and efficiency. Many metals

are essential nutrients in trace amounts, but become significant threats to environmental and human health at high concentrations. Heavy metals [Hg(II), Pb(II), Cr(VI), Cd(II), and As(III)/(V)] are non-biodegradable and can accumulate in the environment and living organisms [19]. Oxidation and reduction play significant roles in the interactions between heavy metal ions and functionalized carbon-based [22] nanomaterials with redox capacity, especially during the removal of Cr(VI) and As(III). Au NPs-Al₂O₃ composite adsorbent is used for Hg removal from drinking water. A high loading capacity of 4.065 g/g Au NPs can be obtained, and this good performance was attributed to Au-Hg amalgam and the formation of amorphous Hg layer over the Au NP surface. Methylene Blue (MB) is a heterocyclic aromatic compound and hazardous in nature [23]. The composite with carbon materials favors the separation of the photo-generated electron-hole pairs by the formation of heterojunctions at the carbon/metal oxide interface, promoting faster photocatalytic reaction rates. The presence of oxygen surface groups on carbon nanotube (CNT) can act as anchoring sites for TiO₂ and favor the dispersion of CNT. The harmful effect of the existence of this dye in waste water may cover the burns effect of eye, nausea, vomiting and diarrhea, and etc. It may be poisonous if it is inhaled and in contact with skin. Therefore, society requires clean, green and renewable energy. The green environment provides pure oxygen and reduces pollutions. Thus, nanomaterials are core area of research and development. The recombination of the electrons and the holes must be prevented as far as possible if a photo catalyzed reaction want to be favored [24]. Photo-degradation system proceeds through photogenerated electrons which could react with electron acceptors (O₂) existed in the system [25]. Porous materials offer an enlarged active interface during the catalytic process due to their large surface area. Conjugated microporous polymers (CMP) NPs exhibited high stability during the photo degradation reaction [26]. Thus, in the presence of air or oxygen, irradiated semiconductor nanoparticles are capable of destroying many organic contaminants. Therefore, the need to construct sustainable adsorbents that are economical and offer both high removal rates and high adsorption capacities is urgent to the present scenario. Thus, nanomaterials have a capacity to clean the environment for sustainable development of society.

2. NANO SIZE DEPENDENT SELECTIVE ADSORBENT AND ITS PHOTOCATALYTIC INTEGRATION

Catalysts play a very important role in the chemical industries. Photocatalytic activity directly depends on the structure of the catalyst. Reaction rate or activity of catalyst depends on the ease by which the catalyst is creating electron-hole pair. Larger surface area contains higher number of active sites increasing the probability of reaction to take place. Nanoparticle *catalysts* can be easily separated and recycled. The catalytic activity is expressed as a function of number of active sites, size and porous diameter. Nano-catalysts improve the selectivity of the reactions by allowing

reaction at a lower temperature, reducing the occurrence of side reactions, higher recycling rates and recovery of energy consumption. Renewable energy development requires highly efficient nanostructured materials. Surface absorption enhances the catalytic efficiency. Catalysis can be controlled by tuning the optical and charge transfer properties with size of semiconductor nanomaterials. Photocatalyst acts as redox active center. Photocatalytic reactions are due to utilization of conduction band electron or valence band hole of a photo catalyst. Light harvesting depends on size of particle of photocatalyst. The efficient charge separation can increase the life time of the charge carrier and inhibit the recombination of electron-hole pairs which will enhance the efficiency of the interfacial charge transfer and stability to adsorbed substrates, and thus increase the number of carriers adsorbed by contaminant [18]. High fraction of coordinated unsaturated surface sites promotes rapid degradation.

3. CHARGE SEPARATION: INTERFACIAL MECHANISM AND CRITERIA OF PHOTOCATALYTIC ACTIVITY

Photocatalytic process requires photon energy for photoexcitation which is dependent on the optical gap of the photocatalyst. Photocatalysis involves the absorption of light by the nanomaterials and generation of electron-hole pairs in the CB and VB. The second step involves the charge separation and migration of charge carriers to the surface. Photoexcited electrons react with O_2 molecule to form superoxide anion that participates in the redox reaction involved in the degradation of the pollutants [27]. The major criterion for the photocatalytic degradation of organic compound is that the redox potential of the $OH^-/OH\cdot$ ($OH^- = OH\cdot + e^-$; $E^\circ = -2.8V$) couple lies within the band gap of the semiconductor. Hydroxyl radical that comes from the oxidation of adsorbed water or adsorbed OH^- is the primary oxidant that can degrade pollutants. The photogenerated electrons on the surface of adsorbent can react with dissolved oxygen in water to form oxidizing $O_2^{\cdot-}$ superoxide radical anion [$E^\circ (O_2/O_2^{\cdot-}) = 0.33V$]. The presence of oxygen can prevent the re-combination of hole-electron pairs [28]. In the degradation of organic compounds, the final products of the reaction among others are CO_2 and H_2O . Superoxide radical anion is the main radical responsible for the degradation of organic pollutant and their mineralization [29]. It is very important to strengthen the interfacial interaction between Carbon dots or polymer dots and TiO_2 (Ti-O-C). The strong interaction can accelerate the electron transfer on the interface, hence improve the photocatalytic activity [12]. Figure 1 indicates schematic generation of photoexcited electrons and free radicals which can interact with pollutants to degrade into simple and nontoxic molecules [30].

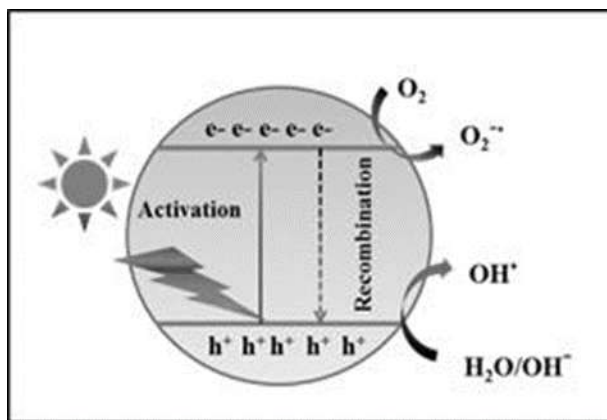


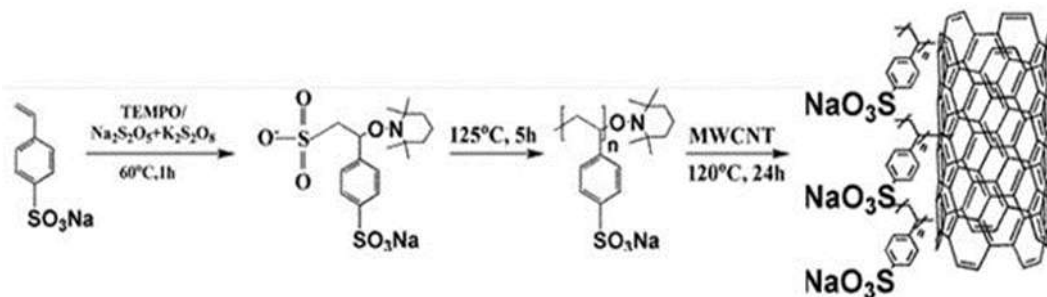
Figure 1. Charge separation and free radical generation under light irradiation. Adopted from ref. [30].

4. SURFACE FUNCTIONALIZATION AND ENGINEERING OF NANOMATERIALS

Surface functionalization essentially involves attaching functional groups onto nanoparticles surface [6]. Surface stabilizer improves the efficiency and capacity causing enhancement of degradation rate of contaminants. Polar groups improve the wettability of the material with water. Doping or chemical functionalization has proven to be effective in tuning the electronic band structure and optical band gap of the photo electrode materials, and thus, their photo activities. Carbon-based nanomaterials have great potential for use in water treatment, and should be designed to obtain suitable structures and properties. Carbon nanoparticle has good relative stability in both acidic and basic media, high specific surface area and good electric conductivity. Good conductivity and short diffusion length can be obtained within material through functionalization. The grafting strategy provides chemical anchoring between polymer chains and multi-walled carbon nanotubes (MWCNTs), with the extra advantage of favoring charge transfer and collection due the intimate contact between the two materials [31, 32]. The oxygen content can influence the adsorption capacity of CNTs. The edge/basal plane can be functionalized with $-NH_2$ and $-COOH$. Multi-wall carbon nanotube can be functionalized with water soluble ionic styrene based polymer. Photo degradation efficiency can be improved through appropriate functional group or charge [33]. Functionalized nanomaterial exhibited different physical properties i.e., electrical conductivity, surface morphology and charge transport properties [6]. The water-soluble conjugated polyelectrolyte greatly enhances the photocatalytic performance over that of their non-dissolved precursor conjugated polymer.

Scheme 1 represents Poly (styrene-4-sodiumsulfonate) (PSSNa) grafted CNTs which can be used as counter electrode to drive photocatalysis during illumination of

dye sensitized solar cell. Ionic group promotes the kinetics of interfacial charge transport with well-defined charge separation within photosensitizer [34].



Scheme 1. Poly (styrene-4-sodiumsulfonate) (PSSNa) grafted multiwall carbon nanotube MWCNT (MWCNT-g-PSSNa). Copyright permission from ref. [34].

5. ROLE OF ELECTRON TRAP, CHROMOPHORES AND FUNCTIONAL GROUP OVER SURFACE OF NANOMATERIALS

Photo degradation efficiency is directly related to stability of photogenerated electron over trapping sites present on the adsorbent. The properties of nanomaterials are not only size dependent, but also structure dependent [35]. The surfaces of carbon nanomaterials always contain some functional groups, which play an important role in the adsorption process. Thus, many studies have been performed to further increase the abundance of pre-existing functional groups (such as COOH and OH) or graft other functional groups (such as NH₂ and SH) onto the surface of carbon nanomaterials as a way to enhance their adsorptive capacities. Iron oxide NPs have commonly been used to remove aqueous As (arsenic) with an adsorptive capacity for mixed Fe₃O₄ and Fe₂O₃ of 5.99 mg g⁻¹. Because this capacity was a bit low, carbon materials with oxygen-containing groups were then induced to support the iron oxides and improve their adsorptive capacity. The maximum adsorptive capacities of As(III) and As(V) by the CNTs-base iron oxides were 24.05 mgg⁻¹ and 47.41 mgg⁻¹, respectively. Graphene oxide obtained from the oxidation and exfoliation of graphite contains functional groups, such as -COOH, -CO and -OH, which can be utilized as the anchoring sites to bind metal cations by both electrostatic and/or coordinated interactions. The adsorption capacity of graphene depends on the nature of the adsorption sites (e.g., presence of defects and surface oxygenated groups) and pore structure of the graphene aggregates, as well as the pH of the aquatic environments. Binding capacity depends on nature of chromospheres. The chromospheres may be electron withdrawing or electron donating. The surface electron density of nanomaterial can be altered through proper functionalization.

6. LIGHT HARVESTING CAPACITY AND PHOTO DEGRADATION OF DYES FROM WASTEWATER

Dye extracted from wastewater can be deposited over nanomaterials and same can be used as light harvesting materials. The light harvesting capacity depends on the chemical structure, composition and concentration of dye. The nature of side chain or group affects the adsorption capacity over nanomaterials. The light adsorption efficiency enhances with polar group present on the surface of dye. The dyes containing more sulfonic substituents are less reactive in the photocatalytic process, while hydroxyl group intensifies the electron resonance in molecule and the degradation rate of dye. As CNTs (carbon nanotubes) are carbonaceous nanomaterials, the adsorption mechanism between the chemical functional group of dyes and the CNT adsorbent is expected to be influenced by hydrophobic effects, π - π bonds, and hydrogen bonds, covalent and electrostatic interactions [21]. The dyes adsorbed over nanomaterials, can be used as photo sensitizer in solar device. On other hand, adsorbed dye can be degraded photo catalytically over the surface of TiO_2 nanomaterials. Methylene blue dye can be degraded in the presence of TiO_2 photocatalyst. Figure 2a indicates structure of methylene blue dye [23]. The presence of the more powerful electron withdrawing sulfonic group on a dye molecule makes it less sensitive to oxidation (degradation). Photocatalytic degradation rate of monoazo dyes is higher than that of dyes with anthraquinone structure. Ti nanomaterials such as TiO_2 and TiO_2 thin films have been used for degradation of atrazine and organochlorine pesticides. The high surface area assures the high adsorption of organic pollutants on the surface of graphene-based nanomaterials. Furthermore, the high dispersion of metal oxides on graphene nano sheets and graphene as electron transfer channels makes the degradation process to occur efficiently on these graphene-based nanomaterials. Chatterjee et al. [1] explored a multi carboxylate organic ligand, 1, 2, 4, 5-Benzenetetracarboxylic acid (BTCA) for surface functionalization of Fe_3O_4 nanoparticles for fast and selective adsorption of industrial pollutant Congo red dye.

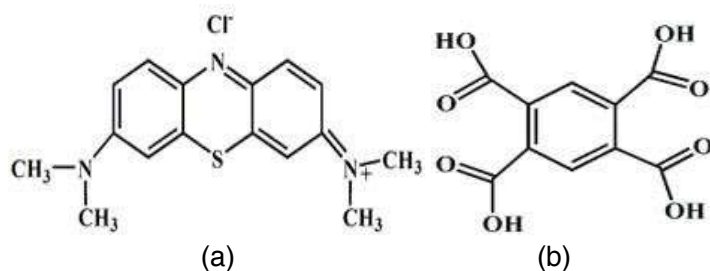


Figure 2. (a) Structure of methylene blue (ionic dye). (b) Structure of 1, 2, 4, 5-Benzenetetracarboxylic acid (BTCA). Copyright permission from ref. [1] and [23].

BTCA group, containing four carboxylate groups at 1, 2, 4 and 5- positions of the benzene ring as functionalization agent, is expected to significantly improve the adsorption capacity for selective dyes with better recyclability as strong anchorage through multiple chelation leading better recyclability. The BTCA functionalized Fe_3O_4 exhibited high adsorption capacity (630mg/g) for congo red dye. Figure 2b depicts the structure of BTCA [1]. The photocatalytic reaction often occurs at the surface of nanomaterials. Surface group can attract target material through H-bonding and enhances the rate of degradation.

7. PHOTOINDUCED CHARGE RETENTION CAPACITY AND MECHANISM OF PHOTO CATALYTIC DEGRADATION

The efficiency of photocatalytic degradation is closely affected by the band structure of the semiconducting nanomaterials. Functionalization can alter the band structure of native nanoparticle and thus, promote photoexcited electron towards target reaction surface sites. Photoexcitation threshold energy is reduced and thus, enhances the solar energy conversion capability. Semiconductor nanomaterial absorbs greater energy than its band gap energy which leads to the excitation of electrons from the valence band to the conduction band, subsequently producing electrons and holes. The valence band holes react with the water molecules and hydroxide ions to form hydroxyl radicals whereas the electron reacts with oxygen molecules and form superoxide radicals. These free radicals are powerful oxidizers of organic dye (Methylene blue) which can attack organic dyes and degrade them into CO_2 and H_2O . pH plays an important role in the photo catalytic study, as it controls the reactions during the degradation of dyes or organic compounds and beside this generation of hydroxyl radicals also depends on the pH of the solution. The introduction of tailored pyridinic functionalities as N-containing edge-type group over CNT mimics generates effective photocatalysts for the oxygen reduction reaction (ORR) in an alkaline environment [14]. Figure 3(a) demonstrates that the adsorbed dye over the surface of photocatalyst works as photosensitizer [2].

Under the illumination of light, dye undergoes photoexcitation result in injection of excited electron into CB of photocatalyst leaving behind a hole in the HOMO. The excited and injected electron is scavenged by oxygen molecule. Thus, dye obtains a cation radical and same time photocatalyst excites its valence electron leaving behind a hole which oxidizes hydroxyl anion leading to production of reactive free radicals. The free radicals can interact with radical state of cationic dye and degrade it. Figure 3(b) depicts schematic degradation of Congo red dye [11]. Alshehri et al. [11] demonstrated that the photo degradation efficiency depends on the dye concentration. The maximum efficiency for dye (Congo red) degradation was observed at a pH of 4 with 15 mg Fe nanoparticles. A degradation rate of 96.1% was achieved at a dye concentration of 1×10^{-5} M at room temperature (30°C).

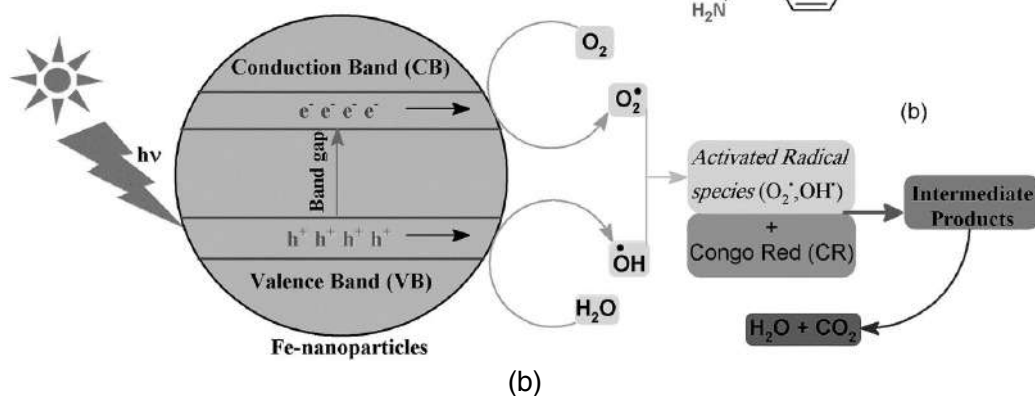
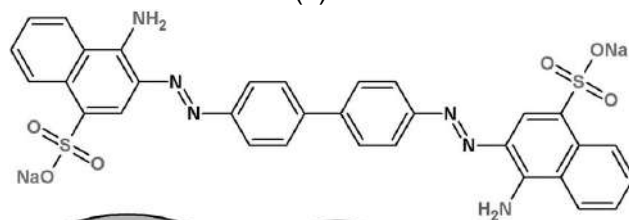
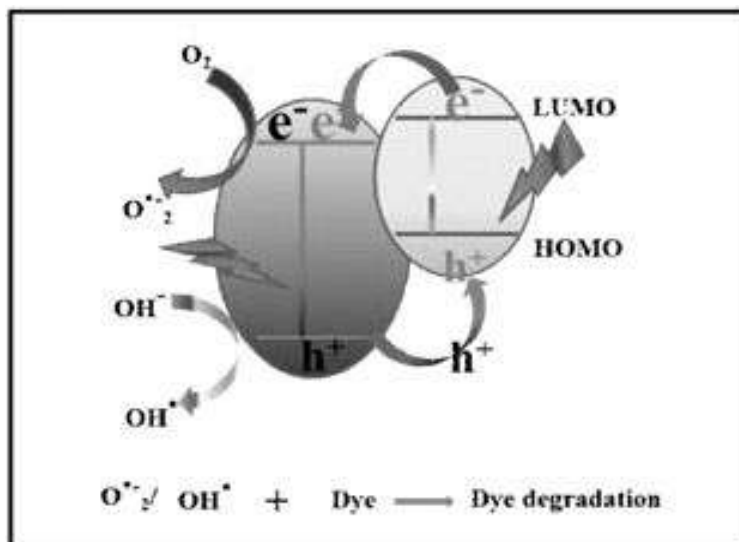


Figure 3. (a) Adsorption, photosensitization and degradation (decolourisation) of dye over the surface of nanomaterials. (b) Structure of Congo red and scheme of the photocatalytic mechanism of the Fe nanoparticles under UV light irradiation. Copyright permission from ref. [2, 11].

8. ROLE OF QUANTUM CONFINEMENT WITHIN NANOMATERIALS AS A PHOTOVOLTAIC ENHANCEMENT

The energy transfers play a fundamental role in energy conversions and energy harvesting. Photo catalyst immobilizes the photosensitizer through adsorption phenomenon. Photosensitizer injects its photoexcited electron into conduction band of

photocatalyst. Quantum confinement adjusts the energy levels of nanomaterials. Interfacial charge transport is due to energy difference. Narrow band gap colloidal quantum dots (CQDs) can create multiple excitons when a single photon having energy much higher than its band gap is absorbed by the CQDs. At the same time, by changing the size of the CQDs one can realize tuning its absorption spectra. The CQDs can be functionalized with conductive carbon nanotube to enhance absorption profile [7] and can be used as photo active layer. The surface functionalized single wall carbon nanotube (SWCNT) can be used as p-type dopants [36] for photo active layer. The presence of oxygen functionalities can cause the band gap to vary according to the degree of oxidation. GO is a p-doped semiconductor, because electron-withdrawing oxygen functionalities reduce electron density on graphene. Perovskite incorporated with TiO₂ nanoparticle/nanotube-based solar cells harvest more sunlight with the content of the nanotubes and thus, enhanced the carrier charge generation and conduction. However, a large amount of TiO₂ nanotubes did not result in improved energy conversion efficiency because of high levels of recombination and low electron density in the active layer [37]. The optimal content of TiO₂ nanotubes in TNNs was 9 wt%, resulting in 0.886 V of open circuit potential (V_{oc}) 25.5 mA/cm² of photocurrent density (J_{sc}) 67.9% of fill factor (FF) and 15.335% of photovoltaic conversion efficiency (PCE) More interestingly, TiO₂/Nanotube containing cells showed a substantial increase in J_{sc} , from 23.9 mA/cm² without nanotubes to 25.5 mA/cm² with 9 wt % nanotubes. The oxygen containing functional groups on CNTs can enhance the electro-catalytic activity for the reduction of the redox electrolyte. Thus, solar energy conversion can be facilitated through proper choice of electrocatalyst and its integration. Figure 4(a) shows schematic diagram for photo voltaic device [34]. MWCNT-g-PSSNa grafted nanostructure was employed as thin film counter electrode for dye sensitized solar cell and electro catalytic activity towards electrolyte was sensitized. The TiO₂ nanoparticle acts as photocatalyst for dye sensitized solar cell. Solar energy can be converted into electrical energy and chemical energy. Photocatalytic degradation involves conversion of solar energy into chemical energy as well as electrical energy through interfacial redox reaction over the surface of nanomaterials. The water-soluble polyelectrolyte grafted MWCNT based counter electrode in DSSCs achieved 7.03% efficiency, which was slightly lower than that (8.3%) of the reference platinated tin doped fluorine oxide (Pt/FTO) cell. The composite structure is attributed to rapid electron transfer at the counter electrode caused by π - π conjugation between the MWCNTs and PSSNa. Functionalization can enhance the number of CNT sites that interact with electrolyte. Photosensitization involves interfacial transfer of photoexcited electron towards photocatalyst leading to the conversion of solar energy into electrical energy. Functionalized photocatalyst plays an effective role as charge separator over the activated surface of photosensitizer.

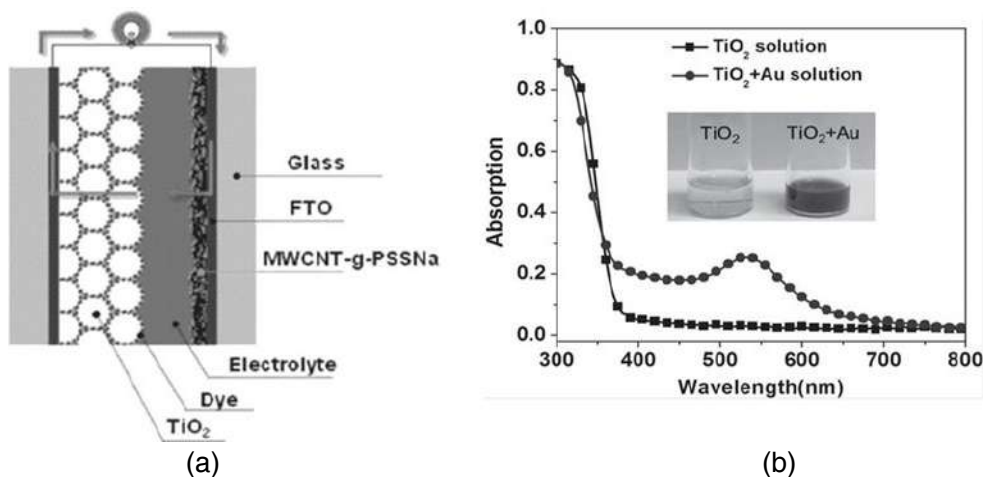


Figure 4. (a) Schematic diagram of dye-sensitized solar cell with MWCNT-g-PSSNa as counter electrode (electro-catalyst). (b) Absorption of TiO_2 and Au NP- TiO_2 composite solutions (plasmonic enhancement). Copyright permission from ref. [34, 38].

9. PLASMONIC INFLUENCE FOR EXTRACTION OF PHOTO EXCITED ELECTRON

TiO_2 nanoparticle acts as electron transport layer. UV-generated electrons in TiO_2 were reported to fill the electron traps with enhanced photoconductivity [38]. Here, the transferred plasmonically excited electrons from Au NPs to TiO_2 can achieve trap filling in the TiO_2 layer, leading to reduced effective extraction barrier, decreased resistance and charge recombination, which can enhance the electron extraction [38]. Figure 4(b) shows UV – visible spectra of gold nanoparticle functionalized titanium dioxide (Au NP- TiO_2) composite can be photoexcited at a plasmonic wavelength (560–600 nm) far longer than the originally necessary UV light (<400 nm) for non functionalized TiO_2 [38]. The experimental and theoretical results show that the improved charge extraction in TiO_2 under plasmonic wavelength illumination is attributed to the enhanced charge injection of plasmonically excited electrons from metal NPs into TiO_2 .

10. FACTORS INFLUENCING PHOTOCATALYSIS

10.1. Influence of Doped and Cross Linked/Grafted Nanostructures

Doping increases surface defects on the surface of photocatalyst and hence, enhances the kinetics of photocatalytic activity. The degradation rate can be enhanced by reducing the electron hole recombination rate, preventing the particle agglomeration and increasing the adsorption capacity. Intermolecular charge transfer can be realized by physically doping nanocarbon materials with electron acceptor(s)

or donor(s). A polar dopant is required to enhance the electron attraction forces for complete electrons–holes separation [24]. Due to fast charge conduction, carbon nanomaterials exhibited efficient redox activity for organic pollutants. Photocatalytic activity can be improved by doping or cross linking of carbon nanostructures. This facilitates smooth electrical conduction and reduces the chance of recombination leading to enhancement of solar energy conversion. The photo generated electrons are scavenged due to synergistic effect of doped or cross linked surface. Nitrogen doped nanostructures improve photocatalysis by facilitating charge separation between photogenerated electrons and holes. Doping material works as co-adsorbent. π -conjugated structures create fast electron transfer and promote the separation of electron–hole pairs on the photocatalyst surface. Cross linking can reduce the unwanted defects on the surface, thereby increases the chance of light absorption. Enhanced pollutant adsorption on the surface of carbon nanostructures is an additional advantage, which accelerates the photocatalytic degradation of adsorbed pollutants [39]. Doping improves adsorption or retention capacity of photocatalyst. Carbon nanotube serves both an adsorbent and a visible light photocatalyst. It can act as effective electron transfer unit on account of its high electron storage capacity and high electrical conductivity. Doping stabilizes the charge separation by trapping electrons, thereby hindering electron hole recombination by tailoring the band gap and sensitization density. The excess doping may act as a recombination center, or cover the active sites on the adsorbents and thereby, reduce the efficiency of charge separation. Therefore, it is a balance between the active trapping sites and trapped parts favoring the inhibition of the recombination of electron–hole pairs leading to enhancement of separation capacity for efficient interfacial charge transfer. Ge et al. [25] reported that 1.0wt% Ag/g-C₃N₄ shows the highest H₂ evolution rate of 10.105 molh⁻¹, which is about 11.7 folds higher than that of pure g-C₃N₄. Omer et al. [18] developed ZnO sensitized nitrogen doped CQDs for photocatalytic degradation of methylene blue and observed that the nanocomposites of ZnO-CDs enhanced the photo degradation efficiency (95% for 100 min) comparing to the pure ZnO in the UV region (365 nm). The high efficiency is probably due to the role of CDs which stabilizes photo excited electron. Sampaio et al. [39] prepared N-CNT/ZnO for degradation of phenol. Highest photocatalytic activity was observed for the composite prepared with N-doped carbon nanotubes (N-CNT), with k_{app} (apparent rate constant) = 0.260 min⁻¹ and a 100% phenol degradation achieved in 20 min. Nitrogen doping can induce the generation of free electrons on the carbon materials surface that can be transferred from its surface to adsorbed oxygen. Li et al. [40] developed cross-linked g-C₃N₃/rGO nanostructures with enhanced visible light harvesting capacity for the degradation of 4-nitrophenol. The photocatalytic degradation efficiency depends on the band structure and valence band edge potential of photocatalyst. The oxidation power of VB (photocatalyst) varies with narrowing the band gap as a function of r-GO. The r-GO collects the photo generated electrons, thereby reducing the chance of recombination. The best photocatalytic activity of g-C₃N₄/r-GO-2.5% was observed due to positive shifting of VB potential and enhanced degradation capacity [40].

10.2. Effect of Coating and Capping Over the Surface of Nanoparticle

The photocatalytic degradation involves an electron transfer process coupled with a redox reaction. Organic and inorganic materials coated surface can extend their light absorption in the visible region and their stability against photo-corrosion. Such materials could emerge as excellent photocatalysts for the elimination of pollutants from aqueous media using solar energy [29]. Coating prevents structural and surface degradation of photocatalyst and improves the life time of active sites. Surface capping can reduce the photocatalytic activity due to development of screen on the surface of nanoparticle and thus, delaying the photocatalytic reaction. However, the polymeric capping shells allow the photocatalyst nanoparticles to diffuse in water and make effective contact with dye molecules. Capping improves the absorbency of nanoparticle. The degradation efficiency can be calculated from following equation.

$$\text{Degradation (\%)} = \frac{C_0 - C}{C_0} \times 100 = \frac{A_0 - A}{A_0} \times 100$$

The rate constant of the dye decolourisation reaction was determined using the Langmuir–Hinshelwood equation:

$$\text{Degradation rate constant (k}_{\text{obs}}) = \frac{2.303}{t} \log_{10} \frac{A_0}{A}$$

Where A_0 , A , and C_0 , C are the absorbance and concentration of pollutant when the reaction time is 0 and t and k_{obs} is the apparent reaction rate constant.

Capped nanoparticle exhibited greater photocatalytic activity as compared to uncapped nanoparticle [41]. Electron affinity is a major parameter for photocatalytic degradation of reactive textile dyes as the ionic nature or the presence of lone pair electrons in the polymeric chain backbone acts as chelating agent to stabilize the nanoparticles [42]. Bonding of capping agents to nanoparticles is necessary to provide chemical passivation that prevent from agglomeration and improve the surface states and stability. Soltani et al. [41] synthesized polyvinyl pyrrolidone (PVP)-capped ZnS and CdS nanoparticles for photo degradation of Methylene blue. The physical mixture of 20% PVP-ZnS with PVP-CdS nanoparticle exhibited 81% photo degradation efficiency of methylene blue after 360 min.

10.3. Synergistic Influence of Porosity, Conducting Polymer and Metal Nanoparticle

The amalgamation of semiconducting metal nanoparticle into conjugated polymer can complement the spectral absorption range of the polymers as well as facilitates enhanced charge separation due to interfacial interaction. Ghosh et al. [15, 43] demonstrated that the Au/PEDOT nanohybrids exhibits 13-fold enhancements in

photocurrent compared to Poly (3, 4-ethylenedioxythiophene (PEDOT) nanofibers under visible light. The photo-induced electron transfer from PEDOT nanofibers to Au NPs at the hybrid interface may occur via a continuous extension of conjugation from polymeric moiety due to closer proximity of the Au NPs which enhance the charge separation. The polymeric hybrid materials having porous structures favor the dispersion of the nanophotocatalysts and the percolation of water [44]. Porous structures can enhance the interaction between polymeric nanomaterials and water molecules and promote the charge transfer in different dimension. Podasca et al. [45] prepared a composite film containing ZnO (6–13 nm)-Ag (2–6 nm) NPs and about 3% polypyrrole exhibited a maximum degradation efficiency of 99% for Rhodamine B within 120 min with rate constant $k = 2.96 \times 10^{-2} \text{ min}^{-1}$ under visible light irradiation. Feizpoor et al. [3] developed a ternary system of photocatalyst $\text{TiO}_2/\text{CDs}/(\text{polyaniline}) \text{ PANi}(20\%)$ for the degradation of Rhodamine B and degradation rate was found to be $481 \times 10^{-4} \text{ min}^{-1}$ which is significantly 36.5 fold higher than TiO_2 alone. The improved efficiency is due to reduced recombination loss at the interface. Yang et al. [46] developed a novel photocatalyst (1% PPy/Ag- TiO_2) for the decomposition of gaseous acetone under visible light irradiation. PPyAg- TiO_2 exhibited much higher photocatalytic activity and its rate constant (k) value was 0.087 min^{-1} which was 9.66, times greater than that of TiO_2 activity.

10.4. Effect of π – Conjugation, Side Chain and Chain Length Over Photocatalytic Redox Reaction

Photocatalytic redox reaction proceeds through effective charge transport from photocatalyst. The conjugation extends visible light gathering and side substituent works as carrier transfer bridge [47]. The π -conjugation along the polymer backbone enables them with unique photogenerated charge carrier separation and transport properties, which is critical to trigger photo redox reactions [48]. Photogenerated electrons and holes are utilized for the reduction and oxidation of water. Oxygen and water are prime source of highly reactive free radicals. Photoexcited electron can be stabilized by tuning the energy gap of photocatalyst [49]. The energy level alignments of the polymer photocatalyst and the redox potential of water must be well matched. Hydrophilic side chain pulls water for interfacial contact with polymer backbone. Planar unit (fluorine and pyrene) can be introduced into polymer chain to extend conjugation degree and charge transfer efficiency. The electron push–pull interaction in the donor-acceptor type polymer backbone could facilitate charge separation in the photocatalytic process. Side-chains aid the degree of polymer swelling and also extend the (charge separation) photo excited electron lifetime.

CONCLUSION

Native nanomaterials play important role due to size dependent properties. The functionalized nanoparticle has enhanced activity because it has more active sites over the surface of functional group. The functionalization of the material surface includes grafting of well-defined molecules to change the surface reactivity towards specific chemical species. Functionalized nanomaterials exhibited good storage capacity. Nanomaterials ignite its scope to enhance the photo physical process. The selective tuning and active functional group enhances the activity and efficiency of nanomaterials. The solar cells, adsorption and degradation for the toxic pollutants from large volumes of aqueous solutions are covered through novel nanomaterials. Functionalizing material with specific chemicals responsible for targeting contaminant molecules of interest can aid in enhancing the selectivity and efficiency of the material.

ACKNOWLEDGMENTS

The author (Sunil Kumar) strongly acknowledges B.R.A. Bihar University, Muzaffarpur for kind cooperation to publish the work. I also would like to thanks higher education department, Govt. of Bihar, Patna for recognizing me as an assistant Professor (Chemistry) for the service of higher education and research development. Dr. PK Chaurasia is thankful to PG Department of Chemistry, L.S. College, Muzaffarpur for any necessary help during the preparation of this chapter.

CONFLICTS OF INTEREST

The authors have declared no conflicts of financial interest.

REFERENCES

- [1] Chatterjee, S., Guha, N., Krishnan, S., Singh, A. K., Mathur, P. and Rai, D. K. (2020). Selective and Recyclable Congo Red Dye Adsorption by Spherical Fe₃O₄ Nanoparticles Functionalized with 1,2,4,5-Benzenetetracarboxylic Acid. *Sci. Rep.* 10: 1–11.
- [2] Shinde, D. R., Tambade, P. S., Chaskar, M. G. and Gadave, K. M. (2017). Photocatalytic degradation of dyes in water by analytical reagent grades ZnO, TiO₂ and SnO₂: A comparative study. *Drink. Water Eng. Sci.* 10: 109–117.
- [3] Feizpoor, S., Habibi-Yangjeh, A. and Yubuta, K. (2018). Integration of carbon dots and polyaniline with TiO₂ nanoparticles: Substantially enhanced

- photocatalytic activity to removal various pollutants under visible light. *J. Photochem. Photobiol. A Chem.* 367: 94-104.
- [4] Wang, L., Cai, M., Sun, W., He, L., & Zhang, X. (2018). Promoting Charge Separation in Semiconductor Nanocrystal Superstructures for Enhanced Photocatalytic Activity. *Adv. Mater. Interfaces.* 5: 1701694.
- [5] Zhao, Y. S., Fu, H., Peng, A., Ma, Y., Xiao, D. and Yao, J. (2008). Low-Dimensional Nanomaterials Based on Small Organic Molecules: Preparation and Optoelectronic Properties. *Adv. Mat.*, 20: 2859–2876.
- [6] Tuci, G., Zafferoni, C., Rossin, A., Milella, A., Luconi, L., Innocenti, M., et al. (2014). Chemically functionalized carbon nanotubes with pyridine groups as easily tunable N-decorated nanomaterials for the oxygen reduction reaction in alkaline medium. *Chem. Mater.* 26: 3460–3470.
- [7] Ni, T., Yan, J., Jiang, Y., Zou, F., Zhang, L., Yang, D. et al. (2014). Enhancement of the power conversion efficiency of polymer solar cells by functionalized single-walled carbon nanotubes decorated with CdSe/ZnS core-shell colloidal quantum dots. *J. Mater. Sci.* 49: 2571–2577.
- [8] Ipe, B. I., Yoosaf, K. and Thomas, K. G. (2006). Functionalized gold nanoparticles as phosphorescent nanomaterials and sensors. *J. Am. Chem. Soc.* 128: 1907–1913.
- [9] Q. Tang, Z. Zhou and Z. Chen, (2013). Graphene-related nanomaterials: Tuning properties by functionalization. *Nanoscale.* 5: 4541–4583.
- [10] Abdin, Z., Alim, M. A., Saidur, R., Islam, M. R., Rashmi, W., Mekhilef, S. and Wadi, A. (2013). Solar energy harvesting with the application of nanotechnology. *Renew. Sustain. Energy Rev.* 26: 837–852.
- [11] Alshehri, A., Malik, M. A., Khan, Z., Al-Thabaiti, S. A. and Hasan, N. (2017). Biofabrication of Fe nanoparticles in aqueous extract of Hibiscus sabdariffa with enhanced photocatalytic activities. *RSC Adv.* 7: 25149–25159.
- [12] Li, G., Wang, F., Liu, P., Chen, Z., Lei, P., Xu, Z., et al. (2018). Polymer dots grafted TiO₂ nanohybrids as high performance visible light photocatalysts. *Chemosphere* 197: 526–534.
- [13] Xu, J., Cao, Z., Zhang, Y., Yuan, Z., Lou, Z., Xu, X. and Wang, X. (2018). A review of functionalized carbon nanotubes and graphene for heavy metal adsorption from water: Preparation, application, and mechanism. *Chemosphere* 195: 351–364.
- [14] Georgakilas, V., Tiwari, J. N., Kemp, K. C., Perman, J. A., Bourlinos, A. B., Kim, K. S. and Zboril, R. (2016) . Noncovalent Functionalization of Graphene and Graphene Oxide for Energy Materials, Biosensing, Catalytic, and Biomedical Applications. *Chem. Rev.* 116: 5464–5519.
- [15] Ghosh, S., Mallik, A. K. and Basu, R. N. (2018). Enhanced photocatalytic activity and photoresponse of poly(3,4-ethylenedioxythiophene) nanofibers decorated with gold nanoparticle under visible light. *Sol. Energ.* 159: 548–560.

- [16] Gong, X., Liu, G., Li, Y., Yu, D. Y. W. and Teoh, W. Y. (2016) Functionalized-graphene composites: Fabrication and applications in sustainable energy and environment. *Chem. Mater.* 28: 8082–8118.
- [17] Haga, M. A., Kobayashi, K. and Terada, K. (2007). Fabrication and functions of surface nanomaterials based on multilayered or nanoarrayed assembly of metal complexes. *Chemistry Reviews*, 251: 2688–2701.
- [18] Omer, K. M., Mohammad, N. N., Baban, S. O. and Hassan, A. Q. (2018) Carbon nanodots as efficient photosensitizers to enhance visible-light driven photocatalytic activity. *J. Photochem. Photobiol. A Che.* 364: 53–58.
- [19] Ghasemzadeh, G., Momenpour, M., Omid, F., Hosseini, M. R., Ahani, M. and Barzegari, A. (2014). Applications of nanomaterials in water treatment and environmental remediation. *Front. Environ. Sci. Eng.* 8: 471–482.
- [20] Yang, H. Y., Rho, W. Y., Lee, S. K., Kim, S. H. and Hahn, Y. B. (2019). TiO₂ nanoparticles/nanotubes for efficient light harvesting in perovskite solar cells. *Nanomaterials* 9: 326.
- [21] Tan, K. B., Vakili, M., Horri, B. A., Poh, P. E., Abdullah, A. Z. and Salamatinia, B. (2015). Adsorption of dyes by nanomaterials: Recent developments and adsorption mechanisms. *Sep. Purif. Technol* 150: 229–242.
- [22] Toma, F. M., Sartorel, A., Iurlo, M., Carraro, M., Rapino, S., Hooper-Burkhardt, L. and Bonchio, M. (2011). Tailored functionalization of carbon nanotubes for electrocatalytic water splitting and sustainable energy applications. *Chem.Sus.Chem.* 4: 1447–1451.
- [23] Isai, K. A. and Shrivastava, V. S. (2019). Photocatalytic degradation of methylene blue using ZnO and 2%Fe–ZnO semiconductor nanomaterials synthesized by sol–gel method: a comparative study. *SN Appl. Sci.* 1: 1247.
- [24] Barakat, N. A. M., Nassar, M. M., Farrag, T. E. and Mahmoud, M. S. (2014). Effective photodegradation of methomyl pesticide in concentrated solutions by novel enhancement of the photocatalytic activity of TiO₂ using CdSO₄ nanoparticles. *Environ. Sci. Pollut Res.* 21: 1425–1435.
- [25] Ge, L., Han, C., Liu, J. and Li, Y. (2011) . Enhanced visible light photocatalytic activity of novel polymeric g-C₃N₄ loaded with Ag nanoparticles. *Appl. Catal. A Gen.* 409–410: 215–222.
- [26] Ma, B. C., Ghasimi, S., Landfester, K., Vilela, F. and Zhang, K. A. (2015). Conjugated microporous polymer nanoparticles with enhanced dispersibility and water compatibility for photocatalytic applications. *J. Mater. Chem. A* 3: 16064–16071.
- [27] Martins, N. C., Ângelo, J., Girão, A. V., Trindade, T., Andrade, L. and Mendes, A. (2016). N-doped carbon quantum dots/TiO₂ composite with improved photocatalytic activity. *Appl. Catal. B Environ.* 193: 67–74.
- [28] Chirita, M., Grozescu, I., Taubert, L., Radulescu, H. and Princz, E. (2009). Fe₂O₃ – Nanoparticles, Physical Properties and Their Photochemical And Photoelectrochemical Applications. *Chem Bull. Politeh. Univ Timsisoara* 54: 1–8.

- [29] Soltani, N., Saion, E., Yunus, W. M. M., Erfani, M., Navasery, M., Bahmanrokh, G. and Rezaee, K. (2014). Enhancement of visible light photocatalytic activity of ZnS and CdS nanoparticles based on organic and inorganic coating. *Appl. Surf. Sci.*, 290: 440–447.
- [30] Khataee, A. R. and Kasiri, M. B. (2010). Photocatalytic degradation of organic dyes in the presence of nanostructured titanium dioxide: Influence of the chemical structure of dyes. *J. Mol. Catal. A Chem.* 328: 8–26.
- [31] Zhang, C., Zhao, Y. S. and Yao, J. (2011). Organic composite nanomaterials: Energy transfers and tunable luminescent behaviors. *New J. Chem.* 35: 973–978.
- [32] Abousalman-Rezvani, Z., Eskandari, P., Roghani-Mamaqani, H. and Salami-Kalajahi, M. (2020). Functionalization of carbon nanotubes by combination of controlled radical polymerization and “grafting to” method. *Adv. Colloid Interface Sci.* 278: (102126).
- [33] Hu, Z., Zhang, X., Yin, Q., Liu, X., Jiang, X. F., Chen, Z., et al. (2019). Highly efficient photocatalytic hydrogen evolution from water-soluble conjugated polyelectrolytes. *Nano Energy* 60: 775–783.
- [34] Han, J., Kim, H., Kim, D. Y., Jo, S. M. and Jang, S. Y. (2010). Water-soluble polyelectrolyte-grafted multiwalled carbon nanotube thin films for efficient counter electrode of dye-sensitized solar cells. *ACS Nano* 4: 3503–3509.
- [35] Rao, K. V., Datta, K. K. R., Eswaramoorthy, M. and George, S. J. (2011). Light-Harvesting Hybrid Hydrogels : Energy-Transfer-Induced Amplified Fluorescence in Noncovalently Assembled Chromophore – *Organoclay Composites* 16: 1179–1184.
- [36] Miletić, T., Pavoni, E., Trifiletti, V., Rizzo, A., Listorti, A., Colella, S. et al. (2016). Covalently Functionalized SWCNTs as Tailored p-Type Dopants for Perovskite Solar Cells. *ACS Appl. Mater. Interfaces* 8: 27966–27973.
- [37] Zhao, H., Wu, Q., Hou, J., Cao, H., Jing, Q., Wu, R. and Liu, Z. (2017). Enhanced light harvesting and electron collection in quantum dot sensitized solar cells by TiO₂ passivation on ZnO nanorod arrays. *Sci. China Mater.* 60: 239–250.
- [38] Zhang, D., Choy, W. C., Xie, F., Sha, W. E., Li, X., Ding, B., et al. (2013) Plasmonic electrically functionalized TiO₂ for high-performance organic solar cells. *Adv. Funct. Mater.*, 23: 4255–4261.
- [39] Sampaio, M. J., Bacsá, R. R., Benyounes, A., Axet, R., Serp, P., Silva, C. G., et al. (2015) Synergistic effect between carbon nanomaterials and ZnO for photocatalytic water decontamination. *J. Catal.* 331: 172–180.
- [40] Li, Y., Zhang, H., Liu, P., Wang, D., Li, Y. et al. Zhao, H. (2013). Cross-linked g-C₃N₄/rGO nanocomposites with tunable band structure and enhanced visible light photocatalytic activity. *Small* 9 (2013) 3336–3344.
- [41] Soltani, N., Saion, E., Yunus, W. M. M., Navasery, M., Bahmanrokh, G., Erfani, M., et al., (2013). Photocatalytic degradation of methylene blue under visible light using PVP-capped ZnS and CdS nanoparticle., *Sol. Energy* 97: 147–154.

- [42] Sarkar, S., Ponce, N. T., Banerjee, A., Bandopadhyay, R., Rajendran, S. and Lichtfouse, E. (2020). Green polymeric nanomaterials for the photocatalytic degradation of dyes: a review, *Environ. Chem. Lett.* 1–12.
- [43] Ghosh, S., Kouame, N. A., Remita, S., Ramos, L., Goubard, F., Aubert, P. H. et al. (2015). Visible-light active conducting polymer nanostructures with superior photocatalytic activity. *Sci. Rep.* 5: 1–9.
- [44] Teixeira, S., Martins, P. M., Lanceros-Méndez, S., Kühn, K. et al. (2016). Reusability of photocatalytic TiO₂ and ZnO nanoparticles immobilized in poly(vinylidene difluoride)-co-trifluoroethylene. *Appl. Surf. Sci.* 384: 497–504.
- [45] Podasca, V. E., Buruiana, T. and Buruiana, E. C. (2019). Photocatalytic degradation of Rhodamine B dye by polymeric films containing ZnO, Ag nanoparticles and polypyrrole. *J. Photochem. Photobiol. A Chem.* 371: 188–195.
- [46] Yang, Y., Wen, J., Wei, J., Xiong, R., Shi, J. and Pan, C. (2013). Polypyrrole-decorated Ag-TiO₂ nanofibers exhibiting enhanced photocatalytic activity under visible-light illumination. *ACS Appl. Mater. Interfaces* 5: 6201–6207.
- [47] Zhou, C., Zeng, G., Huang, D., Luo, Y., Cheng, M., Liu, Y., et al. (2020). Distorted polymeric carbon nitride via carriers transfer bridges with superior photocatalytic activity for organic pollutants oxidation and hydrogen production under visible light. *J. Hazard. Mater.* 386: 121947.
- [48] Diao, R., Ye, H., Yang, Z., Zhang, S., Kong, K. and Hua, J. (2019). Significant improvement of photocatalytic hydrogen evolution of diketopyrrolopyrrole-based donor-acceptor conjugated polymers through side-chain engineering. *Polym. Chem.* 10: 6473–6480.
- [49] Kumar, S., Maurya, I. C., Prakash, O., Srivastava, P., Das, S., & Maiti, P. (2018). Functionalized thermoplastic polyurethane as hole conductor for quantum dot-sensitized solar cell. *ACS Applied Energy Materials.* 1(9): 4641-4650.

Chapter 13**FUNCTIONALIZATION OF CARBON-BASED
MATERIALS FOR THE ELECTROCHEMICAL
SENSING APPLICATIONS**

***Mamta Yadav¹, Devesh Kumar Singh¹,
Vellaichamy Ganesan^{1,*} and Ramasamy Ramaraj²***

¹Department of Chemistry, Institute of Science,
Banaras Hindu University, Varanasi, India

²Department of Physical Chemistry, Centre for Photoelectrochemistry,
School of Chemistry, Madurai Kamaraj University, Madurai, India

ABSTRACT

Carbon-based materials are group of materials in which carbon forms covalent bonds with other carbon atoms or with other elements (metal or non-metal) that leads to the formation of variety of materials. Carbon-based materials when coated on electrode surfaces, lead to the enhancement of electroactive surface area, electron transport properties, and promote adsorption of molecules which are advantageous for the electrochemical sensors. Depending on their hybridization (sp, sp², and sp³) and geometrical structure (0D, 1D, 2D, and 3D), carbon-based materials exist in multiforms like carbon nanodiamonds, fullerenes, graphene, carbon nanotubes, carbon nanodots, and carbon nanofibers. The functionalization of carbon-based materials is another important factor for selective sensing which leads to the change in the surface chemistry that optimizes the interaction of the carbon surface with the exterior domain. Numerous recent electrochemical sensors have been reported on the functionalization of carbon-based materials. Mesoporous carbon nitride (MCN) is another emerging class of carbon material having exchangeable N-H groups which makes it a potential material for sensing applications. The suitability of carbon materials (including MCN) in sensors is

* Corresponding Author's Email: velganes@yaho.com; velgan@bhu.ac.in.

further supported by their biocompatibility, high stability, tunable electronic structure, and cost-effective synthesis. In addition to the above advantages, carbon materials are liable for easy chemical modification through heteroatom doping or adsorption of metal and/or organic species for analyte sensing. In this chapter, the role of the functionalization of carbon-based materials and their exploitation in electrochemical sensing will be clarified.

Keywords: carbon-based materials, covalent functionalization, non-covalent functionalization, electrochemical sensor

1. INTRODUCTION

Electrochemical sensors are economical, sensitive, simple to construct, and easy to operate [1]. The changes in electrochemical parameters that occur at the electrode interface have been utilized for the detection of chemical and biological target analytes. It is well-known that the electrode material is the key to the construction of effective sensing platforms to detect various target analytes. Recent advancements in the field of nanoscience and nanotechnology made significant improvements in the development of electrode materials and subsequent fabrication of electrochemical sensors [1]. Carbon nanomaterials have set down their feet in scientific research with the first investigation of fullerene in the mid-eighties [2, 3]. Since then, worldwide research in this field has exponentially increased for a variety of applications. Carbon-based materials have revolutionized the field of electrochemical sensing due to their wide potential window, low cost, favorable electron transfer kinetics, and high chemical stability [2, 3]. They exhibit a large surface-to-volume ratio and high specific surface area. The characteristics of nanomaterials depend upon their size, shape, dimension, and composition which can be tuned by altering any of these factors [2]. Nonaka et al. have changed the dimensionality of 2D graphene into 3D crumpled graphene and decorated it with manganese ferrite resulting in the MnFe_2O_4 material. They have utilized an aerosol-assisted capillary compression process to synthesize MnFe_2O_4 and used the material for the electrochemical sensing of hydrogen peroxide [4]. Similarly, there have been various methods to modify the surface of carbon-based materials which may add specific properties to detect specific analytes. Indeed, carbon-based materials show heterogeneity in their morphology and physicochemical properties. In this chapter, a broad overview of carbon-based materials (mainly nanodiamonds (NDs), fullerenes, graphene, carbon nanotubes (CNTs), and carbon nitrides) and the effect of their functionalization on the fabrication of electrochemical sensors are considered [5]. Functionalization strategies are broadly classified into two ways, covalent or non-covalent functionalization.

Apart from NDs, other materials have an extended network of sp^2 hybridized carbon. Fullerenes have a high degree of curvature due to which they have strained C-C bonds which can be released by covalent functionalization [5]. Graphene has 2D layered structure, stacked over one another by strong van der Waals interaction. Its

functionalization requires harsh conditions while non-covalent functionalization requires simple equilibration as it mainly exploits π - π interactions [5]. CNTs have less curvature as compared to fullerenes and the covalent functionalization can be achieved by mild acid treatments while non-covalent functionalization requires simple equilibration or sometimes rigorous ultrasonication [5]. In the case of carbon nitride, non-covalent functionalization is more common than covalent functionalization. Non-covalent functionalization includes surface adsorption of active species [6]. In this chapter, various functionalization techniques used for carbon-based materials and their importance in the areas of electroanalysis and electrochemical sensing are covered.

2. CARBON-BASED MATERIALS

Carbon is present everywhere and it can form single or multiple (double or triple) covalent bonds with other carbon atoms or other elements resulting in a vast variety of materials [2, 7]. The carbon-based materials may exist in the form of NDs, fullerenes, graphene, CNTs, carbon nanodots, carbon nanofibers, carbon nitride, and many more depending upon their hybridization (sp , sp^2 , and sp^3) and dimension (0D, 1D, 2D, and 3D) [8].

2.1. Nanodiamonds (NDs)

Diamonds are the hardest known material where the carbons are sp^3 hybridized [9]. The nanoscopic version of diamonds, also known as nanodiamonds (NDs) are enriched with the properties of diamonds and nanomaterials [9] which were discovered in the USSR during the detonation of carbon-based explosives in the 1960s [9, 10]. Apart from the detonation, NDs can also be synthesized by chemical vapor deposition (CVD), high-pressure high-temperature, hydrothermal, and electrochemical methods [9-11]. The synthetic route determines the shape, size, and surface chemistry of the resulting NDs [8, 9]. NDs have a large surface area with a particle size around 4 nm and possess sp^3 core diamond structure and sp^2 surface carbon ending with functional groups like carboxylic acid, acid anhydride, epoxide, and hydroxyl groups [8, 9, 12] which can be utilized for further functionalization [12]. Functionalization can increase the surface area and detection limit that can be harnessed in the field of electrochemical sensing [12]. The macroscopic (hydrophilicity and colloidal stability) and microscopic (reactivity) properties of NDs can be regulated by controlling the functionalization of the NDs surface [13]. They exhibit excellent hardness, thermal conductivity, and least toxicity [2]. Due to the rich surface chemistry of the NDs, they can be grafted with a variety of molecules and the resulting material can be exploited in biomedicine, drug delivery, sensor development, and energy storage [12]. Grafting

of the NDs surface has been utilized advantageously in the field of electrochemical sensing towards the detection of glucose [14, 15] catechol [16], urea [17], etc. [12, 18].

2.2. Fullerene

Fullerenes are 0D carbon-based materials discovered in 1985 [2, 7, 19]. They possess a hollow spherical structure composed of carbon clusters (C_n , $n > 20$) and the most common is C_{60} [2]. C_{60} is a highly symmetrical spherical molecule with 60 carbon atoms covalently bonded to other carbon atoms with sp^2 hybridization. It is composed of 12 pentagons and 20 hexagons with a diameter of 0.7 nm [2, 7]. C_{60} can be easily grafted for electrochemical applications exploiting their rich π electron hollow carbon structure with a fast electron-accepting ability to accelerate the electron transfer [20]. Fullerenes have been attracted by the researchers for the modification of the electrode surface due to their chemical stability, metallic impurity-free nature, and reliable electrocatalytic response [21]. Fullerene itself was used for the electrode modification and successfully utilized for the determination of carbamazepine by Kalanur et al. [22]. A suspension of fullerene was coated onto a glassy carbon electrode surface and after drying the fullerene was electrochemically reduced and used for the carbamazepine determination [22]. Due to their efficient encapsulating properties through van der Waals and other interactions, they are widely employed in drug delivery [7]. The functionalization (like $-OH$, $-COOH$, $-OCH_3$) of the fullerenes enhances their solubility in the polar solvents and paves the way for further functionalization [23] and consecutively improves its applicability in the electrochemical, medical, and pharmaceutical fields [7].

2.3. Graphene

Graphene is a 2D thinnest and strongest material, composed of single-layered sp^2 carbons arranged in a honeycomb-like structure [2]. Graphene is considered as the basic unit for other carbon allotropes, for example, when the graphene sheets are wrapped up they form 0D fullerene, when they are rolled up they form 1D CNTs, and when they are stacked together they form 3D graphite [2]. Graphene was first investigated by a theoretical physicist, Wallace in 1947 [2] and later explored by Geim and Novoselove in 2004. Graphene has exceptional mechanical, thermal, physical, and chemical properties and finds immense applications in the field of sensors, supercapacitors, biotechnology, batteries, etc. Large surface area and high charge mobility in the layers of graphene make this material extremely important in the field of sensors [2]. Pristine graphene has exceptional electrical conductivity, however, has poor solubility in the aqueous medium and therefore it has been modified to graphene oxide (GO) and reduced graphene oxide (rGO) [19]. GO is the oxygen counterpart of

a single-layer graphene sheet. The basal plane of GO has hydroxyl and epoxy groups whereas the carboxyl group is present at the edges [8]. These oxygen-containing functional groups provide hydrophilicity to the graphene layers and increase their dispersion in water. Concurrently, such functionalization inhibits the electrical conductivity. To regain its electrical conductivity, GO is generally reduced again to synthesize rGO [19]. Suspension of GO is stable for a longer time which is exploited in the preparation of nanocomposites by combining them with biomolecules, nanoparticles, and polymers [7]. Graphene is considered to be a very promising material in the fabrication of sensors and biosensors since its 2D structure facilitates the immobilization of molecules and nanoparticles [7, 24]. Functionalized GO has been used for the electrochemical sensing of various biomolecules like methylmalonic acid [25], dopamine [26], hydrogen peroxide [27], and many more [28, 29].

2.4. Carbon Nanotubes (CNTs)

CNTs are one of the allotropic modifications of carbon, composed of a concentrically rolled-up structure of graphene sheets in a tubular shape with a high degree of aspect ratio [8]. These are 1D nanostructured materials solely made up of sp^2 carbon atoms with variable length, diameter, and layers [30, 31]. Depending upon the number of layers, CNTs can be classified into two classes, single-walled carbon nanotubes (SWCNTs) (if only one sheet is rolled up to form the tube) and multi-walled carbon nanotubes (MWCNTs) (formed when more than one sheet are concentrically arranged) [2]. SWCNTs possess a diameter of 1-3 nm and a few μm of length, while MWCNTs possess a diameter of 5-25 nm and a length around 10 μm . Due to their extraordinary and fascinating properties like high conductivity, mechanical strength, chemical, thermal, and structural stability, they have been widely used [2] in electrochemical sensing applications. CNTs are extensively employed in those applications owing to their large surface area resulting in the high adsorption capacity and significant change in the reactivity upon coupling with an analyte [8]. The main techniques for the synthesis of CNTs are chemical vapor deposition (CVD) and the laser ablation method [7]. The poor dispersion of CNTs is the biggest barrier for their wider applications and therefore, functionalization of CNTs becomes important to increase their dispersibility and to decrease their agglomeration caused due to van der Waals interaction [8]. Functionalization (covalent or non-covalent) modifies the interaction of CNTs with other entities [31] and improves their utility in the field of sensing. Functionalized CNTs have been used in the electrochemical sensors for a variety of analytes like uric acid, peroxide, o-nitrophenol [34], p-nitrophenol [32], glucose [33], and many more [34-38].

2.5. Carbon Nitride

Graphitic carbon nitrides are fascinating 2D materials having an economic synthetic route, tunable band structure, and surprisingly-high thermal and chemical stabilities [39]. These materials are unreactive towards common organic solvents, water, and moderately strong acids and bases. The high durability of carbon nitride materials is the result of strong van der Waals forces between the adjacent layers [39]. Physicochemical properties of carbon nitride can be altered easily by varying the precursors with different nitrogen contents and choosing different synthetic routes. Several exiting reports using carbon nitride materials have been reported in the field of chemical sensors and biosensors. Having a bandgap in the semiconducting region (2.7 eV), carbon nitrides have great potential to harvest sunlight and the majority of the reports on carbon nitride include photochemical applications [40]. Carbon nitrides and functionalized carbon nitrides are used for the target analyte determination with the aid of fluorescence, chemiluminescence, electrochemiluminescence, photoelectrochemical, and electrochemical techniques [40, 41]. Electrochemical sensors based on carbon nitrides are relatively less explored. In spite of the significant number of findings using carbon nitride materials, carbon nitrides still face some limitations due to their low surface area. In order to increase the specific surface area of the carbon nitride, Vinu et al., for the first time introduced porosity into it [41]. Porous carbon nitrides with high specific surface area show enhanced response towards electrochemical applications. Porosity may increase the electrochemical response in several ways, for example, porous materials may provide sufficient space for the homogeneous distribution of the adsorbed materials which decreases the chances of aggregation and provides better exposure of active sites to the analyte. Pores provide more convenient charge transfer and increase the loading amount of the active catalyst. The functionalization of carbon nitride has been extensively explored by several groups [39-42]. In this case also, the functionalization may be broadly classified into two parts, covalent and non-covalent functionalizations.

3. FUNCTIONALIZATION EFFECT ON ELECTROCHEMICAL SENSING

The functionalization process is an important step to tailor the carbon-based materials' surface according to the needs. One of the important features of functionalization is the change in surface chemistry, enabling the interaction of different species at the molecular level [8]. The main drawback of using carbon-based materials is their dispersibility in a polar solvent. The van der Waals interaction leads to agglomeration of the carbon-based materials, due to which the functionalization becomes very important. Surface functionalization enables us to graft the surface by well-defined molecules or materials that lead to its use in the specific area of interest [8]. It also enhances the electrochemical property which can be advantageously exploited in the field of sensing, supercapacitors, fuel cells, etc. [8]. The recently

described functionalization of individual carbon materials (NDs, fullerenes, graphene, CNTs, and carbon nitride) and the advantages of functionalization are discussed below. Figure 1 shows different functional groups derived/introduced on the carbon materials and target analytes successfully determined using the functionalized carbon materials.

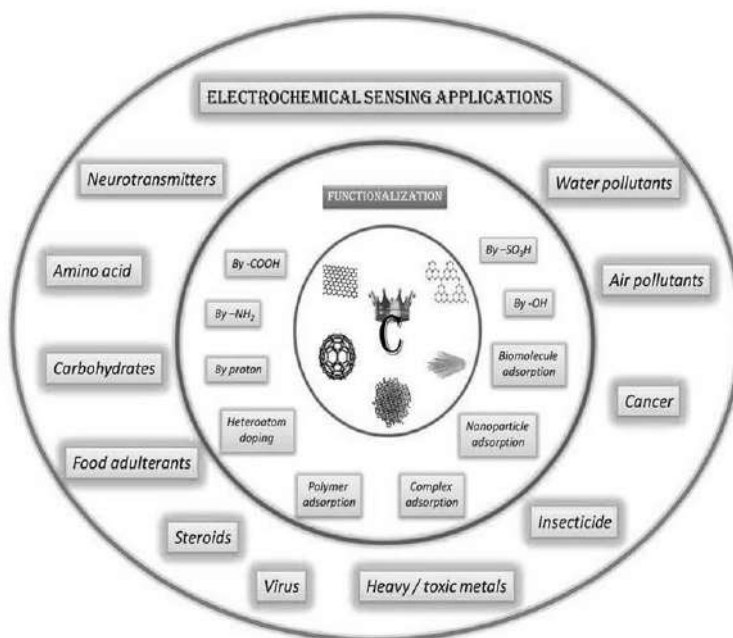


Figure 1. Functional groups derived/introduced on the carbon materials and target analytes successfully determined using the functionalized carbon materials.

3.1. Covalent Functionalization

As the name suggests, covalent functionalizations involve the surface tailoring through the covalent bonding of a specific molecule with the carbon present at the surface of carbon nanomaterials. During the functionalization, certain sp^2 hybridized carbons are changed to sp^3 [2, 42] hybridized carbons. Covalent integration of molecules on the NDs surface is mainly used for drug delivery purposes [8]. It includes the surface functionalization *via* hydroxyl, carboxyl, or amine groups [8]. Basiuk et al. [43] have prepared amine-functionalized NDs utilizing a solvent-free approach. For this, they thermally activated the carboxyl groups present on the surface of NDs. They have prepared a variety of amine-functionalized NDs by the same procedure using different amines like 1,12-diaminododecane, 1,5-diaminonaphthalene, poly(ethylene glycol) diamine, and polyethylenimine. Covalently modified NDs for the fabrication of an electrochemical biosensor has been reported by Camargo et al. [16]. They coupled the surface of NDs with potato starch, and then the composite was covalently modified

using tyrosinase enzyme for the detection of catechol [16]. Similarly, a urea biosensor has been developed by functionalizing NDs by polyaniline and adhering urease enzyme on its surface using ethyl(dimethylaminopropyl) carbodiimide (EDC) and *N*-hydroxysuccinimide. EDC helps to form the amide bond between the amine group of the composite and the carboxylic group of the urease enzyme [17]. Figure 2 shows the fabrication of the electrode surface using NDs and its application in urea sensing [17]. Electro-polymerization has been utilized to graft the surface of NDs with L-aspartic acid to make an efficient sensor for the quantitative assay of L-ascorbic acid [12]. The main problem associated with covalent functionalization is the decrease in enzyme activity [15].

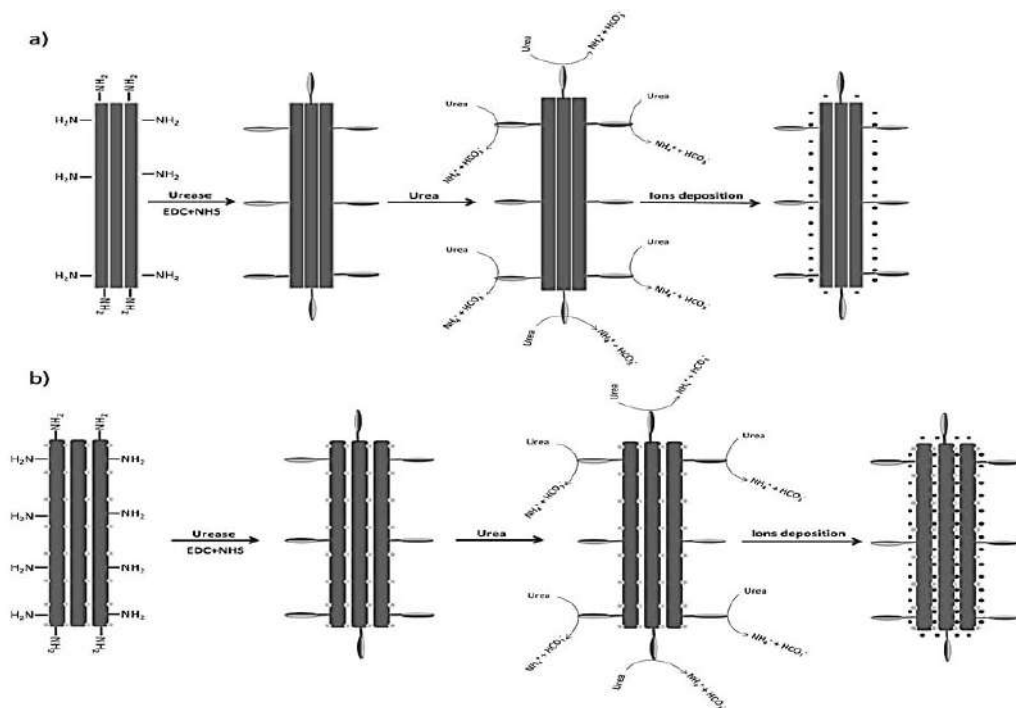


Figure 2. Schematic representation of step-wise functionalization polyaniline (a) and polyaniline-graphitized nanodiamond composite (b). This figure is reproduced with permission from reference [17].

Another class of carbon that can be utilized for sensing applications is fullerene. The first functionalization of fullerene was achieved with cyclodextrin to increase its dispersibility in water and was utilized to generate reactive oxygen species [8]. Treatment of fullerene with strong acid at elevated temperature leads to the inclusion of carboxyl and hydroxyl groups making the surface hydrophilic [8]. Zhou et al. demonstrated the covalent grafting of fullerene with ordered mesoporous carbon (OMC-C₆₀) for the electrochemical oxidation of the reduced form of nicotinamide adenine dinucleotide (NADH) [44]. The amperometry response and calibration curve for the determination of NADH are shown in Figure 3. A non-enzymatic electrochemical sensor was prepared for the determination of peroxide and nitrite by functionalizing the

fullerene surface with Zn-porphyrin using the flexible methylene linkage [45]. This sensor provided high sensitivity and high stability towards the target analytes determination [45]. Fullerene was further used for the functionalization of other carbon materials like CNTs (reported by Mazloum-Ardakani et al. [46]) and the resulting materials were used for the sensing of a neurotransmitter precursor, levodopa together with acetaminophen.

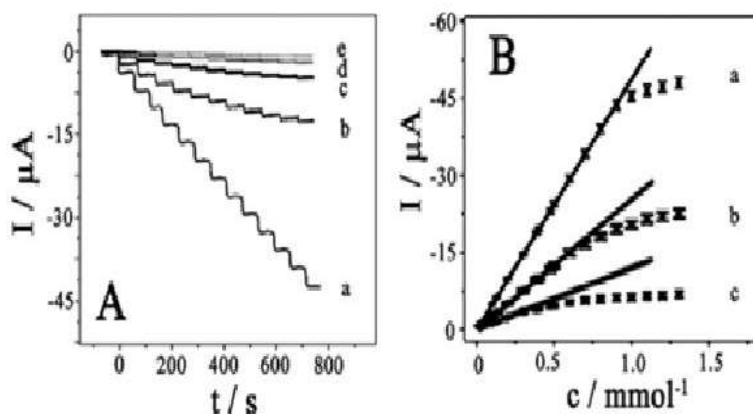


Figure 3. Amperometric response (A) for the glassy carbon electrodes modified with OMC-C₆₀ (a), ordered mesoporous carbon (b), CNTs (c), and C₆₀ (d), and bare glassy carbon (e) with the addition of 0.1 mM NADH and the calibration curves (B) for the determination of NADH. This figure is reproduced with permission from reference [44].

Graphene was chemically oxidized *via* Hummer's method that enables further functionalization. Electrochemical sensing of lead was done using GO-imi-(CH₂)₂-NH₂ material which was prepared by covalently grafting GO surface by imidazolium molecule and further functionalizing it with 2-chloroethyl amine hydrochloride, which introduces amine group that leads to high sensitive lead determination [29]. The scheme for the synthesis of Ni-doped FeS₂ on rGO (Ni-FeS₂/rGO) is shown in Figure 4 which is used for the sensing of hydrogen peroxide [27]. In another study, the Hummers method was used to synthesize GO which was then simultaneously subjected to its reduction and TiO₂ nanoparticles growth at its layers. This nanocomposite was used for the preparation of an electrochemical sensor which is very sensitive and demonstrates a low detection limit for the determination of rifampicin [28].

CNTs can be purified by treating them with strong acids. This process removes the amorphous carbon and also results in the acid functionalization of CNTs [8, 31]. During the acid treatment, CNTs undergo oxidation and [8, 31] this process opens up the tube ends and functionalize mostly with carboxylic acid groups [31]. These carboxylic groups can further be reacted with thionyl chloride (SOCl₂) and amine (for example, alkyl-aryl amine 4-dodecyl-aniline [31], octadecylamine [31], and ethylenediamine [47]) to synthesize amine-functionalized CNTs. Quantification of polyphenols was done by covalently grafting the CNTs by polytyrosine. This functionalization was

achieved by treating the oxidized SWCNTs with thionyl chloride followed by the covalent attachment of poly-L-tyrosine [34]. The obtained SWCNTs-Polytyr was then coated on the surface of a glassy carbon electrode and used for the determination of gallic acid [34].

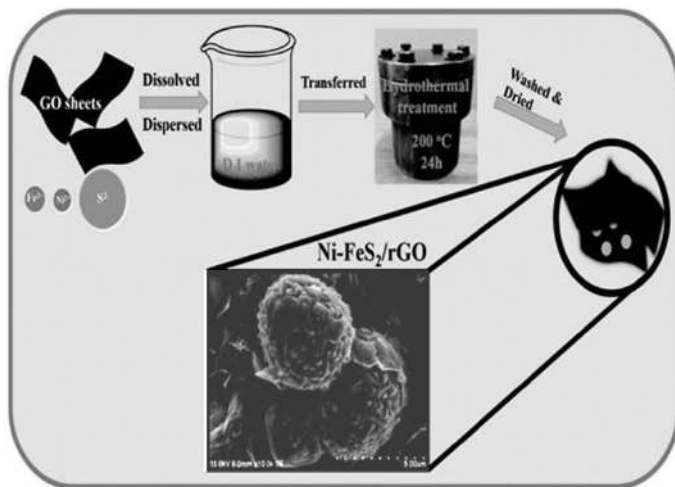


Figure 4. The synthetic route for the preparation of Ni-FeS₂/rGO. This figure is reproduced with permission from reference [27].

Another sensor was prepared by Pang et al. [32] in which the surface of pre-treated MWCNTs was functionalized with amine using 3-(aminopropyl)triethoxysilane. This amine-MWCNTs was further allowed to react with ferrocene carboxylic acid using N-hydroxysuccinimide and 1-ethyl-3-(3-dimethylamino propyl) carbodiimide. This treatment resulted in the ferrocene functionalized MWCNTs (Fc-MWNTs), which was utilized for the determination of *o*- and *p*-nitrophenols. The whole process is shown schematically in Figure 5 [32]. Simultaneous determination of guanine, adenine, and 8-hydroxy-2'-deoxyguanosine was done by Gutierrez et al. [35] in which SWCNTs surface was covalently grafted with lysine.

Covalent functionalization of carbon nitride involves the creation of a covalent bond among the carbon nitride and foreign species. The position of foreign species could be in the sheet plane or at the sheet surface. Herein, certain important varieties of functionalization and their effect on the behavior of carbon nitride are covered. Protonation of carbon nitride surface is one of the convenient approaches for surface modification. Protonation provides significant changes in properties, more active substitution sites, and enhanced redox properties. Several research groups used proton functionalization of the carbon nitride and reported motivating sensing properties [40]. Capilli et al. described an interesting approach to modify carbon nitride by amine functionalization [48]. Wang et al. [49] reported carboxyl functionalized graphitic carbon nitride for sensing carcinoembryonic antigen *via*. photoelectrochemical approach. Lv et al. demonstrated the use of hydroxyl functionalized graphitic carbon nitride for the [50] detection of copper, where the

hydroxyl group plays a vital role in the detection process [50]. Rajkumar et al. [51] have synthesized sulfur-doped graphitic carbon nitride nanosheets (S-GCN) as a metal-free catalyst for the electrochemical determination of 4-nitrophenol. The synthetic route and key results are schematically shown in Figure 6 [51]. Carbon nitrides doped with metal and nonmetals (other than C and N) are also explored extensively for electrochemical sensing.

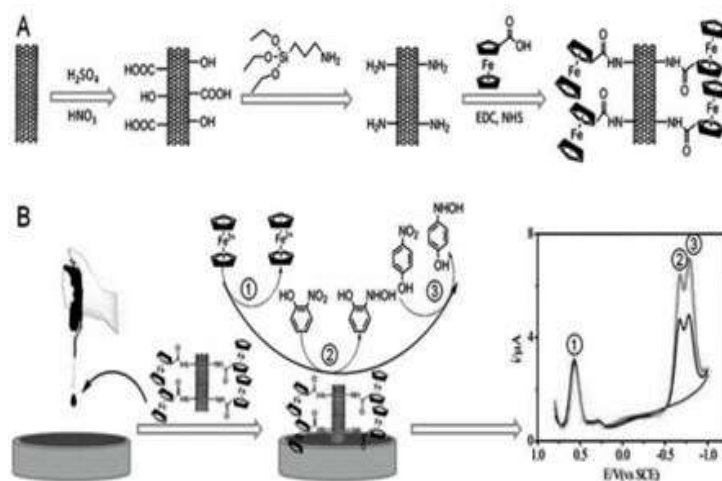


Figure 5. Schematic synthetic route for the preparation of Fc-MWNTs (A) and the fabrication of Fc-MWNTs coated glassy carbon electrode (B) with typical responses. This figure is reproduced with permission from reference [32].

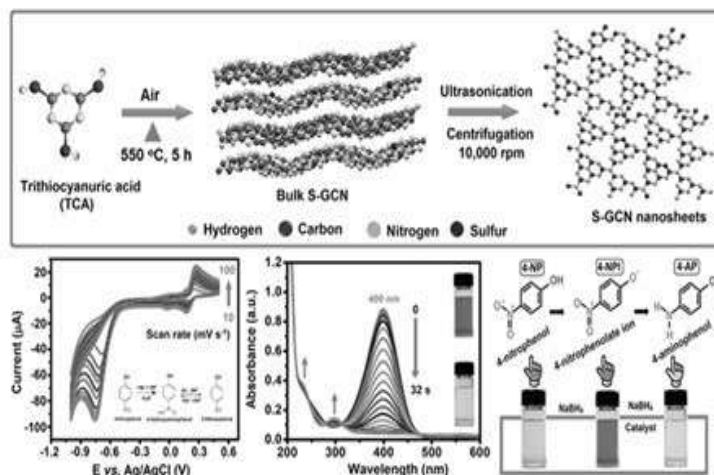


Figure 6. Schematic presentation showing the synthesis of S-GCN and its use in the sensing of 4-nitrophenol. This figure is reproduced with permission from reference [51].

3.2. Non-Covalent Functionalization

Non-covalent functionalization involves π - π interaction, van der Waals interaction, and hydrogen bonding [42]. Non-covalent functionalization can be achieved by a simple approach [13, 42]. The non-covalent functionalization of NDs was achieved by grafting neoglycoproteins on the surface of the NDs and exploited for the hepatocytes sensing *via* carbohydrate receptors [52]. Non-covalent functionalization of NDs with macrocyclic molecules like porphyrin has been achieved by sonicating the mixture of NDs and tetrakis(p-carboxyphenyl)porphyrin in acetonitrile for 2 h [53]. Supramolecular assembly of fullerene with porphyrin has been demonstrated as an efficient material for certain photoinduced electron transfer reactions. A composite based on the non-covalent interaction of fullerene with porphyrin-diazocine-porphyrin was prepared by Zhang et al. for the dopamine assay [54]. Graphene has a 2D extended conjugation suitable for non-covalent functionalization. One of the non-covalent functionalizations of graphene with gold nanoparticles is achieved using polyoxyethylene sorbitol anhydride monolaurate (TWEEN 20). Lu et al. initially functionalized the GO surface by sonicating it with TWEEN 20 for 30 min. The resulting composite material (TWEEN/GO) was re-dispersed in auric chloride solution containing NaOH. A mild shaking of the mixture yielded graphene grafted with gold nanoparticles. This material was used for the determination of hydrazine and 4-nitrophenol [55]. Pyrene functionalized molecules have the advantages of π - π stacking onto graphene surfaces. Han et al. synthesized non-covalently functionalized graphene with pyrene and exploited it for the determination of Concanavalin A [56].

There are various reports available regarding the non-covalent functionalization of CNTs with π - π interaction without disrupting the conjugation of the side walls. For such functionalization, CNTs are simply equilibrated with the particular species for a certain period to get it adsorbed on the surface (usually through π - π interaction). Using a similar procedure, substituted cobalt porphyrin complex immobilized CNTs were reported which rely on the π - π interaction between the porphyrin moiety and CNTs. The stable catalytic response exhibited by the material can be advantageously utilized in fuel cell applications [30]. Functionalized CNTs play a vital role in the preparation of selective electrochemical sensors for specific analytes. Zhu and group have reported non-covalently functionalized SWCNTs with β -cyclodextrin bridged by 3,4,9,10-perylene tetracarboxylic acid for the selective determination of 9-anthracenecarboxylic acid which is widely used in the fields of dyes and insecticides [57]. Similarly, a peroxide sensor has been prepared by non-covalently grafting the surface of oxidized CNTs by cytochrome c. Mixing the acid-treated MWCNTs with cytochrome c followed by sonication for 5 min and subsequent centrifugation yielded the required material. The obtained material has been successfully employed to detect peroxide [58]. In a similar procedure, Gutierrez et al. has fabricated an electrochemical sensor for the ultrasensitive detection of uric acid. In this case, MWCNTs were mixed with poly-L-argininehydrochloride and sonicated for 5 min to get MWCNTs-Polyarg dispersion,

which was centrifuged, collected, and dried. This composite was coated on the surface of a glassy carbon electrode to obtain an electrochemical sensor for uric acid [59].

Table 1. Some recent reports of carbon-based materials on electrochemical sensing

S. No.	Key carbon material	Type of Functionalization and nature of the interaction	Electrode/material	Analyte sensed	Ref.
1	NDs	Covalent, Azure A electrochemically grafted on NDs	AA/DNDs/SPAuE	NADH	64
2	NDs and carbon nanofibers	Non-covalent, electropolymerized composite	AOx/P(L-Asp)/ND-CNF/GCE	L-ascorbic acid	65
3	NDs	-	NDs-GCE	Hydroquinone and catechol	66
4	NDs	-	NDs-GCE	Pyrazinamide	67
5	NDs	Non-covalent composite	GCE/WS ₂ /DNPs	Sunset yellow and quinoline yellow	68
6	NDs	-	NDs-SPE	Dopamine and uric acid	69
7	Fullerene	Covalent, composite	ERC ₆₀ NRs-Ph-NH-GCE	Ethylparaben	70
8	Fullerene	Non-covalent, electrochemically prepared composite	CuNPs-NiNPs@reduced-fullerene-C ₆₀	Vitamin D ₃	71
9	Fullerene	Non-covalent, Electropolymerized composite	CE-Fullerene-PPy-PPyCOOH	Dopamine	72
10	Fullerene	Non-covalent, electrochemically prepared composite	AC ₆₀ /PdNPs modified SPE	Dopamine	73
11	Fullerene	Non-covalent, composite	Pt/C ₆₀ /PGE	Catechol and hydroquinone	74
12	Fullerene and nitrogen-doped graphene oxide	Non-covalent, composite	Au-C ₆₀ /NGS	Mycobacterium tuberculosis IS6110 fragment	75
13	Graphene	-	Graphene-GCE	Hydroquinone and catechol	66
14	Graphene oxide	Non-covalent, composite	SnS ₂ /GO/ β -CD modified SPE	Melatonin	76
15	Graphene oxide	Non-covalent, composite	TiO ₂ /ErGO	Allura Red	77
16	Graphene	Covalent and Non-covalent, composite	COx/GONPs/PG electrode	Cytochrome C	78
17	Graphene	Covalent and Non-covalent, composite	Gr/MOF-GCE	Arsenic(III)	79
18	Graphene	Covalent and Non-covalent, composite	MoS ₂ -TiO ₂ /rGO/SPE	Paracetamol	80
19	MWCNTs	Non-covalent, composite	ZnO/MWCNTs/GC	Epinephrin	81
20	MWCNTs	Covalent and Non-covalent, composite	AuNBP/MWCNTs	Dopamine	82

Table 1. (Continued)

S. No.	Key carbon material	Type of Functionalization and nature of the interaction	Electrode/material	Analyte sensed	Ref.
21	CNTs	Covalent and Non-covalent, composite	GIF-65@ CNTs/GCE	Ascorbic acid	83
22	SWCNTs	Non-covalent, Electropolymerization	dimericquinoidbicine/SWNTs-modified GC electrode	Hydroxylamine	84
23	Carbon nitride	Non-covalent, composite	Carbon nitride /graphite nanocomposite	Oxalic acid	-63
24	Carbon nitride	Non-covalent, composite	g-C ₃ N ₄ /PANI/CdO	Epinephrine, paracetamol, mefenamic acid, and ciprofloxacin	85
25	Carbon nitride	Covalent, composite	Na ₂ O-g-C ₃ N ₄	Hydrogen peroxide sensing	86
26	Carbon nitride	Non-covalent, composite	Cu ₂ O/g-C ₃ N ₄	8-hydroxy-2'-deoxyguanosine sensing	87

AA/DNDs/SPAUE = Azure A chloride modified detonation nanodiamonds screen printed gold electrodes; AOx/P(L-Asp)/NDs-CNF/GCE = ascorbate oxidase immobilized onto poly(L-aspartic acid) film fabricated on carbon nanofiber and nanodiamonds modified glassy carbon electrode; NDs-GCE = Nanodiamonds modified glassy carbon electrode; GCE/WS₂/DNPs = Tungsten disulphide-diamond nanoparticles modified glassy carbon electrode; NDs-SPE = nanodiamonds screen printed electrode; ERC₆₀NRs-Ph-NH-GCE = electrochemically reduced fullerene nanorod modified glassy carbon electrode; CuNPs-NiNPs@reduced-fullerene-C₆₀ = copper-nickel bimetallic nanoparticles nanocomposite at reduced fullerene modified glassy carbon electrode; CE-Fullerene-PPy-PPyCOOH = carbon screen printed fullerene-pyrrole-pyrrole-3-carboxylic acid electrode; AC₆₀/PdNPs modified SPE = Palladium nanoparticles decorated on activated fullerene modified screen printed carbon electrode; Pt/C₆₀/PGE = platinum nanoparticles and fullerene pyrolytic graphite electrode; Au-C₆₀/NGS = gold and C₆₀ nanoparticles decorated nitrogen-doped graphene sheet; SnS₂/GO/ β -CD modified SPE = tin disulfide nanoflakes, graphene oxide, and β -cyclodextrin ternary nanocomposite decorated on the screen-printed electrode; TiO₂/ErGO = Titania/electro-reduced graphene oxide; COx/GONPs/Pg = cytochrome c oxidase and graphene oxide nanoparticles modified pencil graphite; Gr/MOF-GCE = graphene oxide and zinc based metal-organic framework modified glassy carbon electrode; MoS₂-TiO₂/rGO/SPE = molybdenum disulphide, titanium dioxide, and reduced graphene oxide (rGO) nanocomposite modified screen printed electrode; ZnO/MWCNTs/GC = zinc oxide nanoparticle and multi-walled carbon nanotubes modified glassy carbon electrode; AuNBP/MWCNTs = gold nanobipyramidandmulti-walled carbon nanotube; GIF-65@ CNTs/GCE = metal-organic frameworks@ carbon nanotubes; S-g-C₃N₄= sulfur doped graphitic carbon nitride; Na-CN-300= sodium doped graphitic carbon nitride; g-C₃N₄/Fe₃O₄= graphitic carbon nitride iron oxide composite; g-C₃N₄/PANI/CdO= nanocomposites of graphitic carbon nitride, polyaniline and cadmium oxide; NiS/S-g-C₃N₄= Nickel sulfide-incorporated sulfur-doped graphitic carbon nitride; Na₂O-g-C₃N₄= sodium and oxygen co-doped graphitic carbon nitride; Cu₂O/g-C₃N₄= cuprous oxide supported on graphitic carbon nitride nanosheets.

Many interesting surface modifications are reported for graphitic carbon nitride and a few are exemplified in this section. Metal complex adsorption on the carbon nitride surface is a simple and convenient approach for non-covalent functionalization, though other methods are also available. Nitrogen present in the carbon nitride sheets provides strong interaction between the metal center and the sheet, preventing demetallation and providing extra stability to the adsorbed species [6].

Ethylenediaminetetraacetic acid incorporated carbon nitride was used for the detection of ultra-trace amounts of lead (Pb (II)) in water samples [60]. Copper phthalocyanine modified carbon nitride as a photoelectrochemical sensor for the determination of dopamine in blood samples is also reported recently [61]. Zhang et al. reported a composite of GO and carbon nitride for the simultaneous determination of ascorbic acid, dopamine, and uric acid [62]. Alizadeh et al. reported nanocomposites of carbon nitride with graphite for the sensitive determination of oxalic acid in biological samples [63]. Several other recent reports on the carbon-based materials modified electrodes and their applications in the field of electrochemical sensing are summarized in Table 1.

CONCLUSION

The main focus of this chapter is the functionalization of a variety of carbon-based materials and their importance in the field of electrochemical sensing. The functionalization of the carbon-based material is of immense importance because of their hydrophobicity and agglomerative behavior. It is focused mainly on NDs, fullerenes, graphene, CNTs, and carbon nitrides due to their vast use in the field of sensing. In this chapter, it is shown that the tailoring of the surface of the carbon-based materials imparts certain additional properties to the resulting materials that can be utilized for the selective and efficient sensing of specific analytes. The functionalization can be achieved *via* covalent and non-covalent routes. The latter one includes mainly the π - π interaction (between the carbon material and the adhering molecule) and van der Waals interaction while the former route has the covalent linkage between the carbon material and the adhering molecule. These functionalized materials are used as electrode materials to increase the selectivity and sensitivity of the resulting electrochemical sensors.

REFERENCES

- [1] Zhu, C., Yang, G., Li, H., Du, D. and Lin, Y. (2015). Electrochemical sensors and biosensors based on nanomaterials and nanostructures. *Anal. Chem.*, 87, 230–249.
- [2] Kour, R., Arya, S., Young, S. J., Gupta, V., Bandhoria, P. and Khosla A. (2020). Recent advances in carbon nanomaterials as electrochemical biosensors. *J. Electrochem. Soc.*, 167, 037555 (1-24).
- [3] Garrido, M., Gualandi, L., Noja, S. D., Filippini, G., Bosi, S. and Prato, M. (2020). Synthesis and applications of amino-functionalized carbon nanomaterials. *Chem. Commun.*, <https://doi.org/10.1039/D0CC05316C>.
- [4] Nonaka, L. H., Almeida, T. S. D., Aquino, C. B., Domingues, S. H., Salvatierra, R. V. and Souza V. H. R. (2020). Crumpled graphene decorated with manganese

- ferrite nanoparticles for hydrogen peroxide sensing and electrochemical supercapacitors. *ACS Appl. Nano Mater.*, 3, 4859–4869.
- [5] Rao, C. N. R., Ghosh, A. and Gomathi, A. (2011). Functionalization and solubilization of carbon and inorganic nanostructures. *Comprehensive Nanoscience and Technology*, 3, 445-490.
- [6] Singh, D. K., Ganesan, V., Yadav, D. K. and Yadav, M. (2020). Metal (Mn, Fe, Co, Ni, Cu, and Zn) phthalocyanine-immobilized mesoporous carbon nitride materials as durable electrode modifiers for the oxygen reduction reaction. *Langmuir*, 36, 12202-12212.
- [7] Siqueira Jr, J. R. and Oliveira Jr, O.N., 2017. Carbon-based nanomaterials. In *Nanostructures*, 233-249. William Andrew Publishing.
- [8] Speranza, G. (2019). The role of functionalization in the applications of carbon materials: An Overview. *C-Journal of Carbon Research*, 5, 84.
- [9] Chauhan, S., Jain, N. and Nagaich, U. (2020). Nanodiamonds with powerful ability for drug delivery and biomedical applications: Recent updates on in vivo study and patents. *J. Pharm. Anal.*, 10, 1-12.
- [10] Mochalin, V. N., Shenderova, O., Ho, D. and Gogotsi, Y. (2012). The properties and applications of nanodiamonds. *Nat. Nanotechnol.*, 7, 11-23.
- [11] Ho, D., Wang, C. H. K. and Chow, E. K. H. (2015). Nanodiamonds: The intersection of nanotechnology, drug development, and personalized medicine. *Sci. Adv.*, 1, e1500439.
- [12] Kaçar, C. and Erden, P. E. (2020). An amperometric biosensor based on poly(L-aspartic acid), nanodiamond particles, carbon nanofiber, and ascorbate oxidase–modified glassy carbon electrode for the determination of L-ascorbic acid. *Anal. Bioanal. Chem.* 412, 5315–5327.
- [13] Reina, G., Zhao, L., Bianco, A. and Komatsu, N. (2019). Chemical functionalization of nanodiamonds: opportunities and challenges ahead. *Angew. Chem. Int. Ed.*, 131, 18084-18095.
- [14] Shahrokhiana, S. and Ghalkhani, M. (2010). Glassy carbon electrodes modified with a film of nanodiamond–graphite/chitosan: Application to the highly sensitive electrochemical determination of Azathioprine. *Electrochim. Acta* 55, 3621–3627.
- [15] Komathi, S., Gopalan, A. I., Muthuchamy, N. and Lee, K. P. (2017). Polyanilinenanoflowers grafted onto nanodiamonds via a soft template-guided secondary nucleation process for high performance glucose sensing. *RSC Adv.*, 7, 15342-15351.
- [16] Camargo, J. R., Baccarin, M., Raymundo-Pereira, P. A., Campos, A. M., Oliveira, G. G., Fatibello-Filho, O., Oliveira Jr, O. N. and Janegitz, B. C. (2018). Electrochemical biosensor made with tyrosinase immobilized in a matrix of nanodiamonds and potato starch for detecting phenolic compounds. *Anal. Chim. Acta*, 1034, 137-143.
- [17] Kumar, V., Mahajan, R., Kaur, I. and Kim, K. H. (2017). Simple and mediator-free urea sensing based on engineered nanodiamonds with polyanilinenanofibers synthesized in situ. *ACS Appl. Mater. Interfaces*, 9, 16813–16823.

- [18] Shahrokhian, S. and Ghalkhani, M. (2010). Glassy carbon electrodes modified with a film of nanodiamond–graphite/chitosan: Application to the highly sensitive electrochemical determination of Azathioprine. *Electrochim. Acta* 55, 3621–3627.
- [19] Patel, K. D., Singh, R. K. and Kim, H. W. (2019). Carbon-based nanomaterials as an emerging platform for theranostics. *Mater. Horiz.* 6, 434-469.
- [20] Yanez-Sedeno, P., Campuzano, S. and Pingarron, J. M. (2017). *Fullerenes in Electrochemical Catalytic and Affinity Biosensing: A Review. C.*, 3, 21 (1-17).
- [21] Mazloum-Ardakani, M. and Khoshroo, A. (2014). High performance electrochemical sensor based on fullerene-functionalized carbon nanotubes/ionic liquid: Determination of some catecholamines. *Electrochem. Commun.*, 42, 9–12.
- [22] Kalanur, S. S., Jaldappagari, S. and Balakrishnan, S. (2011). Enhanced electrochemical response of carbamazepine at a nano-structured sensing film of fullerene-C₆₀ and its analytical applications. *ElectrochimActa*, 56, 5295–5301.
- [23] Tagmatarchis, N. and Prato, M. (2005). Carbon-based materials: From fullerene nanostructures to functionalized carbon nanotubes. *Pure Appl. Chem.*, 77, 1675-1684.
- [24] Yadav, M., Ganesan, V., Gupta, R., Yadav, D. K. and Sonkar, P. K. (2019). Cobalt oxide nanocrystals anchored on graphene sheets for electrochemical determination of chloramphenicol. *Microchem. J.*, 146, 881–887.
- [25] Deepa, J. R., Anirudhan, T. S., Soman, G. and Sekhar V. C. (2020). Electrochemical sensing of methylmalonic acid based on molecularly imprinted polymer modified with graphene oxide and gold nanoparticles. *Microchem. J.*, 159, 105489 (1-13).
- [26] Li, J., Shen, H., Yu, S., Zhang, G., Ren, C., Hua, X. and Yang, Z. (2020). Synthesis of a manganese dioxide nanorod anchored graphene oxide composite for highly sensitive electrochemical sensing of dopamine. *Analyst*, 145, 3283-3288.
- [27] Kumar, S., Tsai, C. H. and Fu Y. P. (2020). Multifunctional Ni-doped iron pyrite/reduced graphene oxide composite as an efficient counter electrode for DSSCs and a non-enzymatic hydrogen peroxide electrochemical sensor. *Dalton Trans.*, 49, 8516-8527.
- [28] Reddy, Y. V. M., Sravani, B., Łuczak, T., Mallikarjuna, K. and Madhavi, G. (2021). An ultra-sensitive rifampicin electrochemical sensor based on titanium nanoparticles (TiO₂) anchored reduced graphene oxide modified glassy carbon electrode. *Colloids Surf.*, 608, 125533 (1-7).
- [29] Eshlaghi, M. A., Kowsari, E., Ehsani, A., Akbari-Adergani, B. and Hekmati, M. (2020). Functionalized graphene oxide GO-[imi-(CH₂)₂-NH₂] as a high efficient material for electrochemical sensing of lead: Synthesis surface and electrochemical characterization. *J. Electroanal. Chem.*, 858, 113784 (1-14).
- [30] Sonkar, P. K., Prakash, K., Yadav, M., Ganesan, V., Sankar, M., Gupta, R. and Yadav, D. K. (2017). Co(II)-porphyrin-decorated carbon nanotubes as catalysts

- for oxygen reduction reactions: an approach for fuel cell improvement. *J. Mater. Chem. A*, 5, 6263-6276.
- [31] Sinnott, S. B. (2002). Chemical functionalization of carbon nanotubes. *J. Nanosci. Nanotech.*, 2, 113-123.
- [32] Pang, S. and Kan, X. (2019). Reliable detection of o-nitrophenol and p-nitrophenol based on carbon nanotubes covalently functionalized with ferrocene as an inner reference. *New J. Chem.*, 43, 10517-10522.
- [33] Sonkar, P. K., Ganesan, V., John, S. A., Yadav, D. K. and Gupta, R. (2016). Non-enzymatic electrochemical sensing platform based on metal complex immobilized carbon nanotubes for glucose determination. *RSC Adv.*, 6, 107094-107103.
- [34] Eguilaz, M., Gutierrez, A., Gutierrez, F., González-Domínguez, J. M., Anson-Casaos, A., Hernandez-Ferrer, J., Ferreyra, N. F., Martinez, M. T. and Rivas, G. (2016). Covalent functionalization of single-walled carbon nanotubes with polytyrosine: Characterization and analytical applications for the sensitive quantification of polyphenols. *Anal. Chim. Acta*, 909, 51-59.
- [35] Gutiérrez, A., Gutierrez, F. A., Eguílaz, M., González-Domínguez, J. M., Hernández-Ferrer, J., Anson-Casaos, A., Martínez, M. T. and Rivas, G. A. (2016). Electrochemical sensing of guanine, adenine and 8-hydroxy-2'-deoxyguanosine at glassy carbon modified with single-walled carbon nanotubes covalently functionalized with lysine. *RSC Adv.*, 6, 13469-13477.
- [36] Yadav, M., Ganesan, V., Maiti, B., Gupta, R., Sonkar, P. K., Yadav, D. K. and Walcarius, A. (2019). Sensitive determination of acetaminophen in the presence of dopamine and pyridoxine facilitated by their extent of interaction with single-walled carbon nanotubes. *Electroanalysis*, 31, 2472-2479.
- [37] Sonkar, P. K., Ganesan, V., Gupta, S. K. S., Yadav, D. K., Gupta, R. and Yadav, M. (2017). Highly dispersed multiwalled carbon nanotubes coupled manganese salen nanostructure for simultaneous electrochemical sensing of vitamin B₂ and B₆. *J. Electroanal. Chem.*, 807, 235-243.
- [38] Sonkar, P. K., Ganesan, V., Yadav, D. K. and Gupta, R. (2016). Dual electrocatalytic behavior of oxovanadium (IV) salen immobilized carbon materials towards cysteine oxidation and cystine reduction: graphene versus single walled carbon nanotubes. *ChemistrySelect*, 1, 6726-6734.
- [39] Malik, R., Tomer, V. K., Chaudhary, V., Dahiya, M. S., Sharma, A., Nehra, S. P., Duhand, S. and Kailasam, K. (2017). An excellent humidity sensor based on In-SnO₂ loaded mesoporous graphitic carbon nitride. *J. Mater. Chem. A*, 5, 14134-14143.
- [40] Ma, T. Y., Tang, Y., Dai, S. and Qiao S. Z. (2014). Proton-functionalized two-dimensional graphitic carbon nitride nanosheet: an excellent metal-/label-free biosensing platform. *Small*, 10, 2382-2389.
- [41] Vinu, A., Ariga, K., Mori, T., Nakanishi, T., Hishita, S., Golberg, D. and Bando, Y. (2005). Preparation and characterization of well-ordered hexagonal mesoporous carbon nitride. *Adv. Mater.* 17, 1648-1652.

- [42] Nezakati, T., Tan, A. and Seifalian, A. M. 2015. Different functionalization methods of carbon-based nanomaterials. In *Chemical Functionalization of Carbon Nanomaterials: Chemistry and Applications*, edited by Vijay Kumar Thakur and ManjuKumari Thakur, doi: 10.1201/b18724-4. CRC Press.
- [43] Basiuk, E. V., Santamaría-Bonfil, A., Meza-Laguna, V., Gromovoy, T. Y., Alvares-Zauco, E., Contreras-Torres, F. F., Rizo, J., Zavala, G. and Basiuk, V. A. (2013). Solvent-free covalent functionalization of nanodiamond with amines. *Appl. Surf. Sci.*, 275, 324-334.
- [44] Zhou, M., Guo, J., Guo, L. P. and Bai, J. (2008). Electrochemical sensing platform based on the highly ordered mesoporous carbon-fullerene system. *Anal. Chem.* 80, 4642-4650.
- [45] Wu, H., Fan, S., Jin, X., Zhang, H., Chen, H., Dai, Z. and Zou, X. (2014). Construction of a zinc porphyrin-fullerene-derivative based nonenzymatic electrochemical sensor for sensitive sensing of hydrogen peroxide and nitrite. *Anal. Chem.* 86, 6285-6290.
- [46] Mazloum-Ardakani, M., Ahmadi, S. H., Mahmoudabadi, Z. S. and Khoshroo, A. (2016). Nano composite system based on fullerene-functionalized carbon nanotubes for simultaneous determination of levodopa and acetaminophen. *Measurement*, 91, 162-167.
- [47] Chidawanyika, W. and Nyokong, T. (2010). Characterization of amine-functionalized single-walled carbon nanotube-low symmetry phthalocyanine conjugates. *Carbon*, 48, 2831-2838.
- [48] Capilli, G., Cavallera, S., Anfossi, L. Giovannoli, C., Minella, M., Baggiani, C., and Minero, C. (2019). Amine-rich carbon nitride nanoparticles: Synthesis, covalent functionalization with proteins and application in a fluorescence quenching assay. *Nano Res.* 12, 1862–1870.
- [49] Wang, H., Wang, Y., Zhang, Y., Wang, Q., Ren, X., Wu, D. and Wei, Q. (2016) Photoelectrochemical immunosensor for detection of carcinoembryonic antigen based on 2D TiO₂ nanosheets and carboxylated graphitic carbon nitride. *Sci Rep* 6, 27385 (1-7).
- [50] Lv, H., Teng, Z., Wang, C. and Wang, G. (2017). Ultra-high sensitive voltammetric sensor modified by largely oxygenous functionalized ultrathin carbon nitride nanosheets for detection of Cu (II). *Sens. Actuators B Chem.*, 242, 897-903.
- [51] Rajkumar, C., Veerakumar, P., Chen, S. M., Thirumalraj, B. and Lin, K. C. (2018). Ultrathin sulfur-doped graphitic carbon nitride nanosheets as metal-free catalyst for electrochemical sensing and catalytic removal of 4-nitrophenol. *ACS Sustain. Chem. Eng.*, 6, 16021–16031.
- [52] Chang, B. M., Lin, H. H., Su, L. J., Lin, W. D., Lin, R. J., Tzeng, Y. K., Lee, R. T., Lee, Y. C., Yu, A. L. and Chang, H. C. (2013). Highly fluorescent nanodiamonds protein-functionalized for cell labeling and targeting. *Adv. Funct. Mater.* 23, 5737-5745.

- [53] Ohtani, M., Kamat, P. V. and Fukuzumi, S. (2010). Supramolecular donor-acceptor assemblies composed of carbon nanodiamond and porphyrin for photoinduced electron transfer and photocurrent generation. *J. Mater. Chem.*, 20, 582–587.
- [54] Zhang, M. and Li, J. (2020). Preparation of porphyrin derivatives and C₆₀ supramolecular assemblies as a sensor for detection of dopamine. *Dyes. Pigm.* 173, 107966 (1-7).
- [55] Lu, W., Ning, R., Qin, X., Zhang, Y., Chang, G., Liu, S., Luo, Y. and Sun, X. (2011). Synthesis of Au nanoparticles decorated graphene oxide nanosheets: Noncovalent functionalization by TWEEN 20 in situ reduction of aqueous chloroaurate ions for hydrazine detection and catalytic reduction of 4-nitrophenol. *J. Hazard. Mater.*, 197, 320-326.
- [56] Han, Y., Li, H., Jafri, S. H. M., Ossipov, D., Hilborn, J. and Leifer, K. (2020). Optimization and analysis of pyrene-maltose functionalized graphene surfaces for Con A detection. *Appl. Surf. Sci.*, 510, 145409 (1-6).
- [57] Zhu, G., Zhang, X., Gai, P., Zhang, X. and Chen, J. (2012). β -Cyclodextrin non-covalently functionalized single-walled carbon nanotubes bridged by 3,4,9,10-perylene tetracarboxylic acid for ultrasensitive electrochemical sensing of 9-anthracenecarboxylic acid. *Nanoscale*, 4, 5703.
- [58] Eguílaz, M., Gutiérrez, A. and Rivas, G. (2016). Non-covalent functionalization of multi-walled carbon nanotubes with cytochrome c: Enhanced direct electron transfer and analytical applications. *Sensor Actuat. B-Chem.*, 225, 74–80.
- [59] Gutiérrez, A., Gutierrez, F., Eguílaz, M., Parrado, C. and Rivas, G. A. (2018). Non-Covalent functionalization of multi-wall carbon nanotubes with polyarginine: characterization and analytical applications for uric acid quantification. *Electroanalysis*, 30, 1416-1424.
- [60] Teng, Z. Lv H., Wang, L., Liu, L., Wang, C. and Wang, G. (2016). Voltammetric sensor modified by EDTA-immobilized graphene-like carbon nitride nanosheets: preparation, characterization and selective determination of ultra-trace Pb (II) in water samples. *Electrochim. Acta*, 212, 722-733.
- [61] Zhao, L., Ji, J., Shen, Y., Wu, K., Zhao, T., Yang, H., Lv, Y., Liu, S. and Zhang, Y. (2019). Exfoliation and sensitization of 2D carbon nitride for photoelectrochemical biosensing under red light. *Chem. Eur. J.*, 25, 15680-15686.
- [62] Zhang, L., Liu, C., Wang, Q., Wang, X. and Wang, S. (2020). Electrochemical sensor based on an electrode modified with porous graphitic carbon nitride nanosheets (C₃N₄) embedded in graphene oxide for simultaneous determination of ascorbic acid, dopamine and uric acid. *Microchim. Acta*, 187, 10.1007/s00604-019-4081-6.
- [63] Alizadeh, T., Nayeri, S. and Hamidi, N. (2019). Graphitic carbon nitride (g-C₃N₄)/graphite nanocomposite as an extraordinarily sensitive sensor for sub-micromolar detection of oxalic acid in biological samples. *RSC Adv.*, 9, 13096-13103.

- [64] Revenga-Parra, M., Villa-Manso, A. M., Briones, M., Mateo-Martí, E., Martínez-Periñán, E., Lorenzo, E. and Pariente, F. (2020). Bioelectrocatalytic platforms based on chemically modified nanodiamonds by diazonium salt chemistry. *Electrochim. Acta*, 357, 136876 (1-11).
- [65] Kaçar C. and Erden, P. E. (2020). An amperometric biosensor based on poly(L-aspartic acid), nanodiamond particles, carbon nanofiber, and ascorbate oxidase–modified glassy carbon electrode for the determination of L-ascorbic acid. *Anal. Bioanal. Chem.*, 412, 5315-5327.
- [66] Jiang, L., Santiago, I. and Foord, J. (2018). Nanocarbon and nanodiamond for high performance phenolics sensing. *Commun. Chem.*, 1, 1-9.
- [67] Simioni, N. B., Silva, T. A., Oliveira, G. G. and Fatibello-Filho, O. (2017). A nanodiamond-based electrochemical sensor for the determination of pyrazinamide antibiotic. *Sensor Actuat. B-Chem.*, 250, 315-323.
- [68] Blanco, E., Hristova, L., Martínez-Moro, R., Vázquez, L., Ellis, G. J., Sánchez, L., delPozo, M., Petit-Domínguez, M. D., Casero, E. and Quintana, C. (2020). A 2D tungsten disulphide/diamond nanoparticles hybrid for an electrochemical sensor development towards the simultaneous determination of sunset yellow and quinoline yellow. *Sensor Actuat. B-Chem.*, 324, 128731.
- [69] Baccarin, M., Rowley-Neale, S. J., Cavalheiro, É. T., Smith, G. C. and Banks, C. E. (2019). Nanodiamond based surface modified screen-printed electrodes for the simultaneous voltammetric determination of dopamine and uric acid. *Microchim. Acta*, 186, 200.
- [70] Rather, J. A., Al Harthi, A. J., Khudaish, E. A., Qurashi, A., Munam, A. and Kannan, P. (2016). An electrochemical sensor based on fullerene nanorods for the detection of paraben, an endocrine disruptor. *Anal. Methods*, 8, 5690-5700.
- [71] Anusha, T., Bhavani, K. S., Kumar, J. S. and Brahman, P. K. (2020). Designing and fabrication of electrochemical nanosensor employing fullerene-C₆₀ and bimetallic nanoparticles composite film for the detection of vitamin D₃ in blood samples. *Diam. Relat. Mater.*, 104, 107761 (1-10).
- [72] Uygun, E., H. D. and Demir, M. N. (2020). A novel fullerene-pyrrole-pyrrole-3-carboxylic acid nanocomposite modified molecularly imprinted impedimetric sensor for dopamine determination in urine. *Electroanalysis*, doi: 10.1002/elan.202060023.
- [73] Palanisamy, S., Thirumalraj, B., Chen, S. M., Ali, M. A. and Al-Hemaid, F. M., (2015). Palladium nanoparticles decorated on activated fullerene modified screen printed carbon electrode for enhanced electrochemical sensing of dopamine. *J. Colloid. Interf. Sci.*, 448, 251–256.
- [74] Zhu, Y., Huai, S., Jiao, J., Xu, Q., Wu, H. and Zhang, H. (2020). Fullerene and platinum composite-based electrochemical sensor for the selective determination of catechol and hydroquinone. *J. Electroanal. Chem.*, 878, 114726 (1-8).
- [75] Bai, L., Chen, Y., Liu, X., Zhou, J., Cao, J., Hou, L. and Guo, S. (2019). Ultrasensitive electrochemical detection of Mycobacterium tuberculosis IS6110

- fragment using gold nanoparticles decorated fullerene nanoparticles/nitrogen-doped graphene nanosheet as signal tags. *Anal. Chim. Acta*, 1080, 75-83.
- [76] Liu, X., Sakthivel, R., Chen, Y. C., Chang, N., Dhawan, U., Li, Y., Zhao, G., Lin, C. and Chung, R. J. (2020). Tin disulfide-graphene oxide- β -cyclodextrin mediated electro-oxidation of melatonin hormone: an efficient platform for electrochemical sensing. *J. Mater. Chem. B*, 8, 7539-7547.
- [77] Li, G., Wu, J., Jin, H., Xia, Y., Liu, J., He, Q. and Chen, D. (2020). Titania/Electro-Reduced Graphene Oxide Nanohybrid as an Efficient Electrochemical Sensor for the Determination of Allura Red. *Nanomaterials*, 10, 307.
- [78] Batra, B., Sangwan, S., Ahlawat, J. and Sharma, M. (2020). Electrochemical sensing of cytochrome c using graphene oxide nanoparticles as platform. *Int. J. Biol. Macromol.*, doi.org/10.1016/j.ijbiomac.2020.09.203.
- [79] Baghayeri, M., Ghanei-Motlagh, M., Tayebee, R., Fayazi, M. and Narenji, F. (2020). Application of graphene/zinc-based metal-organic framework nanocomposite for electrochemical sensing of As(III) in water resources. *Anal. Chim. Acta*, 1099, 60-67.
- [80] Demir, N., Atacan, K., Ozmen, M. and Bas, S. Z. (2020). Design of a new electrochemical sensing system based on MoS₂-TiO₂/reduced graphene oxide nanocomposite for paracetamol detection. *New J. Chem.*, 44, 11759-11767.
- [81] Shaikshavali, P., Reddy, T. M., Gopal, T. V., Venkataprasad, G., Kotakadi, V. S., Palakollu, V. N. and Karpoornath, R. (2020). A simple sonochemical assisted synthesis of nanocomposite (ZnO/MWCNTs) for electrochemical sensing of Epinephrine in human serum and pharmaceutical formulation. *Colloids Surf.*, 584, 124038 (1-10).
- [82] Cheng, J., Wang, X., Nie, T., Yin, L., Wang, S., Zhao, Y., Wu, H. and Mei, H. (2020). A novel electrochemical sensing platform for detection of dopamine based on gold nanobipyramid/multi-walled carbon nanotube hybrids. *Anal. Bioanal. Chem.*, 412, 2433-2441.
- [83] Li, Y., Ye, W., Cui, Y., Li, B., Yang, Y. and Qian, G. (2020). A metal-organic frameworks@ carbon nanotubes based electrochemical sensor for highly sensitive and selective determination of ascorbic acid. *J. Mol. Struct.*, 1209, 127986 (1-7).
- [84] Xi, W., Zhai, J., Zhang, Y., Tian, L. and Zhang, Z. (2020). Integrating brucine with carbon nanotubes toward electrochemical sensing of hydroxylamine. *Microchim. Acta*, 187, 343 (1-9).
- [85] Bonyadi, S., Ghanbari, K. and Ghiasi, M. (2020). All-electrochemical synthesis of a three-dimensional mesoporous polymeric g-C₃N₄/PANI/CdO nanocomposite and its application as a novel sensor for the simultaneous determination of epinephrine, paracetamol, mefenamic acid, and ciprofloxacin. *New J. Chem.*, 44, 3412-3424.
- [86] Mohammad, A., Khan, M. E., Yoon, T. and Choa, M. H. (2020). Na,O-co-doped-graphitic-carbon nitride (Na,O-g-C₃N₄) for nonenzymatic electrochemical sensing of hydrogen peroxide. *Appl. Surf. Sci.* 525, doi: 10.1016/j.apsusc.2020.146353.

- [87] Rajaji, U., Selvi, S. V., Chen, S. M., Chinnapaiyan, S., Chen, T. W. and Govindasamy, M. (2020). A nanocomposite consisting of cuprous oxide supported on graphitic carbon nitride nanosheets for non-enzymatic electrochemical sensing of 8-hydroxy-2'-deoxyguanosine. *Mikrochim Acta*, 187, 459.

Complimentary Contributor Copy

Chapter 14**RECENT DEVELOPMENT OF GRAPHENE
NANOSHEETS SUPPORTED PT-FREE
ELECTROCATALYSTS IN FIELD OF DIRECT
METHANOL FUEL CELL****Rahul Awasthi^{1,*} and C. S. Sharma²**¹Department of Chemistry, S. R. A. P. College, Barachakia,
EastChamparan, Bihar,, INDIA²Chemist in UPRVUNL, Anpara, Sonebhadra, Uttar Pradesh, INDIA**ABSTRACT**

The fuel cells and water electrolyzers are two main technologies which can resolve currently energy and environmental pollution issues. Fuel cell as advanced technology has thoroughly and widely studies in recent past as per its advantage over other parallel technologies like solar cell, battery, etc. Among different kind of fuel cell direct methanol fuel cell (DMFC) is most promising due to lower operational temperature, less hazards emission, higher energy conversion efficiency and easy transport of liquid fuels. In DMFC two electrode reaction takes place, one is electro-oxidation of methanol at anode and the other is reduction of oxygen at the cathode. However, DMFC is facing many technical issue such as, platinum (Pt) used as electrocatalyst which is costly and easily deactivated by intermediate species formed during methanol electro-oxidation and methanol crossover from anodic to cathodic compartment which reduces efficiency of DMFC, sluggish kinetics of oxygen reduction reaction at cathode. In order to reduce the cost and improve the performance of DMFC, Pt free electrocatalyst supported on novel material graphene nanosheet (GNS) has been widely used. GNS has gained attention due to its excellent flexibility, high surface area and

* Corresponding Author's Email: awasthi.r07@gmail.com.

superior electrical and mechanical properties. The present chapter describes the different synthesis method of GNS and recent progress of Pt-free GNS supported electrocatalysts in the field of DMFC.

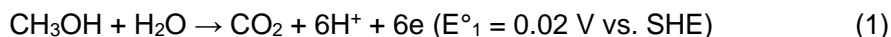
Keywords: graphene nanosheet, direct methanol fuel cell, methanol oxidation reaction, electrocatalyst, oxygen reduction reaction

1. INTRODUCTION

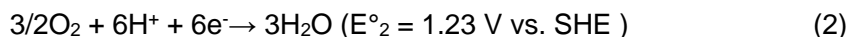
Due to gradual increase in the energy demand around the world, the continued depletion of fossil fuels and rise of greenhouse gases, energy engineers encourage to focus on the renewable energy to reduce the energy crisis and reduce harmful greenhouse gases such as SO_x, NO_x and carbon dioxide. Among the renewable resources, fuel cell can provide alternative and greener energy with almost zero emissions [1]. A fuel cell is a device that converts the chemical energy of a fuel (hydrogen, natural gases, methanol, ethanol, gasoline, etc.) and an oxidant (air or oxygen) into electric energy. Among different kinds of fuel cells, polymer electrolyte membrane fuel cells (PEMFCs) and direct alcohol fuel cells (DAFCs) particularly direct methanol fuel cells (DMFCs) are most promising [2, 3]. DMFCs are akin to PEMFCs with the main difference being that DMFCs oxidize methanol on the anode to produce protons while PEMFCs oxidize hydrogen to produce protons. In DMFCs, methanol aqueous solution is fed to the anode compartment, wherein methanol is oxidized to produce CO₂ releasing simultaneously proton and electron [2, 3]. Both proton and electron are transported to the cathode, the former through the electrolyte and latter through an external circuit. At the cathode, oxygen reacts with proton and electron producing water. In DMFCs, there is no need of reforming of methanol; it can be directly fed to the cell. A block diagram of a single fuel cell is shown in Figure 1.

The reaction occurs in DMFCs are as follows:

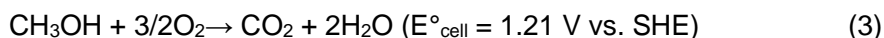
Anode reaction:



Cathode reaction:



Overall cell reaction:



The theoretical potentials of both the cells (DMFCs and PEMFCs) are nearly equal and looking at logistical issues, DMFCs appears to have many advantages over

hydrogen fed- PEMFCs and lithium ion batteries. The theoretical specific energy density of methanol (≈ 20 MJ/kg) is an order of magnitude higher than lithium ion battery systems (≈ 2 MJ/kg) [3, 4] and DMFCs are in early stages of commercialization for applications that compete with lithium ion batteries. Methanol has a significantly lower energy density than hydrogen based on mass, but the volumetric energy density of methanol is higher than that of gaseous hydrogen [3, 4]. Since, methanol is a liquid it can be easily transported, stored in lightweight plastic tanks, whereas hydrogen is a gas so, it has to be kept in high-pressure cylinders or hydride beds. This gives DMFC systems an even larger advantage when the storage efficiency of the fuel (kg of fuel/total kg of storage system + fuel) is also considered in the calculation[5].

Methanol is mainly produced from natural gas feed stock and consequently, its use leads to high greenhouse gas emission. It is also fairly abundant in supply. If DMFCs could provide performance high enough to be considered for vehicular transportation, the cost of converting existing infrastructure to distribute methanol would be significantly lower than trying to build a system to store and distribute hydrogen gas. Thus, on paper it would seem like DMFCs are the natural choice over PEMFCs. DMFCs not only provide clean energy but also offer good commercial viability (e.g., Ballard and Smart Fuel Cells) [2]. A large number of successful applications of DMFCs like passenger vehicles, generators, chargers and other portable and hand held devices including mobile phones and laptops are currently commercially available [6]. World famous companies such as Nippon electric company (NEC), Toshiba, Hitachi, Samsung and Motorola have developed and demonstrated the use of mobile phones and laptop powered by a DMFCs.

However, successful commercialization of DMFCs could not be made so far. This is because of the following major difficulties in the process of commercialization.

- Pt is used as an electrocatalyst both for methanol electrooxidation and oxygen reduction reaction (ORR) which is costly and has limited abundance in nature
- Pt is poisoned by intermediate species, particularly CO, formed during the methanol oxidation reaction (MOR)
- Methanol crossover from the anodic compartment through membrane to the cathodic compartment. In presence of methanol in the cathodic compartment, the Pt cathode gets depolarized during the cell operation.

To reduce the cost and improve efficiency of DMFCs the research work are mainly being carried out in the following directions:

- Preparation of Pt and Pt-based alloys/composites in highly dispersed form on high surface area carbon support.

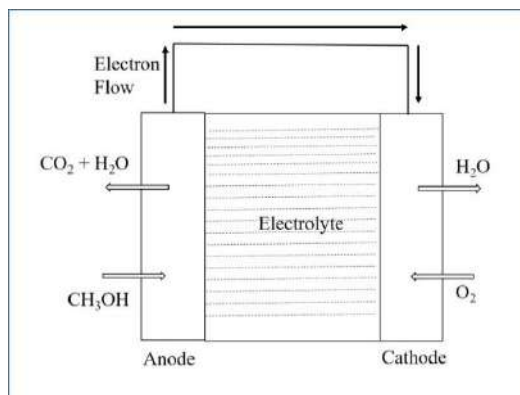


Figure 1. Block diagram of a fuel cell.

- Development of low cost and efficient Pt free anode catalysts which are more tolerant to CO poisoning.
- Development of methanol tolerant cathode materials.

Recently, the increased interests are shown towards the use of GNS as catalyst support material for electrochemical devices because it is low cost and has considerably higher specific surface area as well as conductivity in comparison to other carbon supports. GNS is an allotrope of carbon, whose structure is one-atom-thick planar sheets of sp² bonded carbon atoms that are densely packed in a 2D honeycomb crystal lattice. It possess high specific surface area (~ 2630 m²g⁻¹) [7], excellent electronic mobility (~2,50,000 cm²V⁻¹s⁻¹) [7], exceptional thermal conductivity (~5,000 Wm⁻¹K⁻¹) [7] super mechanical properties with theoretical Young's modulus of 1TPa [7], which enable it a promising material for use in electrochemical devices, such as fuel cells [8-10], supercapacitors [10-13], batteries [12-13], sensors [14-15], etc. In this chapter Pt free GNS supported electrocatalysts for direct methanol fuel cells have been discussed.

2. USE OF GNS BASED ELECTROCATALYSTS IN DIRECT METHANOL FUEL CELLS

2.1. For Methanol Electrooxidation

Three paths are known for the methanol oxidation in DMFCs: (i) the complete oxidation through CO₂ pathway, (ii) the complete oxidation through formaldehyde pathway and (iii) the complete oxidation through formic acid pathways [16]. These mechanisms are schematically represented in Figure 2.

To increase the overall efficiency significantly, it is to favor the complete oxidation of methanol to CO₂ (avoiding the formation of aldehyde and formic acid).

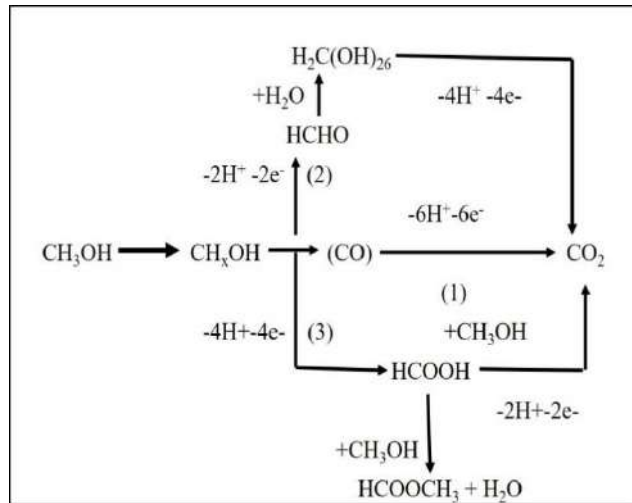
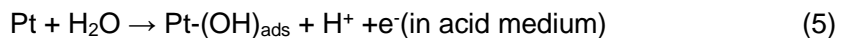
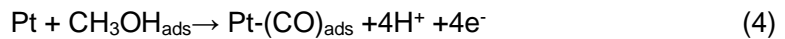
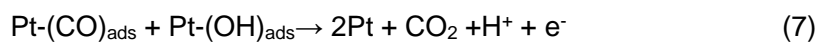


Figure 2. Schematic representation of mechanisms for methanol oxidation.

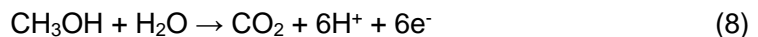
A complete methanol electrooxidation is a 6e^- process and main steps involved in MOR are as follow:



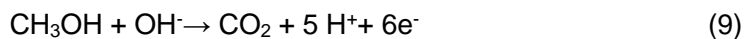
or



Over all reaction



or



Irreversible adsorption of methanol occurs in the range of 0.05-0.50 V vs. S.H.E. and CO_{ads} species are responsible for poisoning of the electrode [17]. The removal of CO_{ads} from the electrode surface requires the presence of atomic oxygen derived from dissociation of water (low pH) or OH^- (high pH). Surface oxides on Pt electrode begin to be formed at potential of 0.7 V vs. S.H.E., which is too high for an efficient performance of the cell and hence sluggish kinetics for MOR.

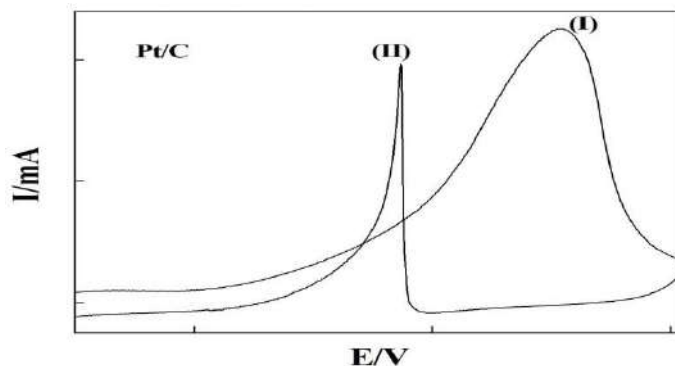


Figure 3. Cyclic Voltammogram (CV) of electro-oxidation of methanol of Pt/C catalyst.

In particular, till now no known anode catalyst based on platinum has demonstrated the capacity to produce acceptable power densities in either of DMFCs. Notable efforts are therefore being carried out to design new catalytic structures for DMFC anodes that do not contain platinum or contain tiny amounts of this rare metal and, most of all, are able to oxidize primary and secondary alcohols with fast kinetics and tolerable deactivation. Within this context, Pd is emerging as an attractive replacement for Pt in DMFCs. Pd is more abundant in nature and less expensive than Pt but cost-associated issues are not the main driving force behind the increasing interest in Pd, the real attraction for Pd-based electrocatalysts is originated by the fact that, unlike Pt-based electrocatalysts, they can be highly active for the oxidation of a large variety of substrates in alkaline environment wherein non-noble metals are sufficiently stable for electrochemical applications. The electrocatalytic activity of catalysts are compared by recording cyclic voltammograms (CVs). Typical CV of Pt/C catalyst are shown in Figure 3. The two oxidation peaks observed respectively in the positive (I) and the negative (II) going scans are the characteristic of the methanol electrooxidation. It is observed that on the positive going scan, the oxidation current increases progressively with potential, attains optimum and declines rapidly thereafter. The decrease in current has been attributed to the formation the Pd(II) oxide surface film as a result of oxidation of Pd, which strongly inhibits the methanol oxidation. The previously formed Pd (II) oxide under anodic condition gets reduced to active Pd metal under cathodic condition and the methanol oxidation starts again [8, 9]. The catalyst with higher current at lower potential in forward scan is better for MOR.

In literature Pd supported on GNS has been reported. For example, Ng et al. [18] synthesized Pd-guanine-GNS nanocomposite (Pd/rGOG) by one-pot microwave assisted method and reported that as-synthesized Pd/rGOG exhibits significant enhanced MOR (183% improvement), good durability, and higher stability in alkaline medium than its counterpart without guanine. Kumar et al. [19] synthesized Pd₂₀-xAu/Nitrogen dope GNS (NG180) (x wt% = 0, 5, 10 and 15) by simple hydrothermal one-pot polyol method, involving simultaneous reduction of both Pd and Au. Investigation have shown that among these catalyst Pd₁₀Au₁₀/NG180 catalyst has highest peak current density for MOR and is 1.5 times highly efficient compared to

Pd₂₀/NG180 with an enhanced shift in the onset potential by 140 mV to lower overpotentials. Yang et al. [20] prepared ultrafine Pd NPs immobilized on 3D boron and nitrogen-codoped GNS aerogels (Pd/BNGNS) via a self-assembly process and found that as prepared catalyst exhibits large electrochemical active surface areas, high peak current densities, and reliable long-term stability toward methanol oxidation reactions, which are apparently superior to those of conventional Pd/carbon black (Pd/C) and Pd/undoped GNS (Pd/G) catalysts. Hsieh et al. [21] synthesized bimetallic PdRh nanoparticles with different atomic ratios on GNS and investigated as electrocatalyst for the MOR in alkaline medium. They reported the synergetic effect for better catalytic activity of catalyst and catalyst with a Pd:Rh ratio of 3:1 displayed the best performance. Zhang et al. [22] prepared Pd nanoparticles (NPs) supported on N and S dual-doped GNS (NS-GNS) by incorporation of N and S atoms into GNS by a thermal treatment, followed by the controlled growth of Pd NPs by a solvothermal method and reported that Pd/NS-GNS hybrid exhibits outstanding electrocatalytic performance toward methanol electrooxidation than those of Pd/Vulcan XC-72R and Pd/undoped GNS catalysts under similar condition. Kiyani et al. [23] prepared Pd-Co/nitrogen doped GNS by polyol reduction method and found that Pd-Co/NGNS has better electrocatalytic activity than Pd/NGNS toward MOR in alkaline media and is more stable than commercial Pt/C for MOR. Yang et al. [24] prepared Pd/PdO nanoparticles supported on porous GNS (PGNS) by a gas-liquid interfacial plasma method using Pd(NO₃)₂ · 2H₂O as precursor. Result have shown that as prepared catalyst shows better activity than that on oxidation carbon nanotubes support for methanol oxidation. In addition, catalysts show better electrochemical stability than that of commercial Pd/C catalyst. Enhance catalytic activity of Pd by combination with second metal are explain by synergistic effect in which methanol adsorbed on the Pd active site and OH species adsorbed on the second metal which helps in the removal of poisonous intermediate species formed during methanol oxidation reaction. Further the presence of functional group on the surface of GNS help in removal of poisonous species and on doping with N, S atom further increases defect on GNS which further improve its electron transfer property.

Pd free GNS supported catalysts also reported in literature. Sarwar [1] prepared Ni-Co/GNS (Ni:Co, molar ratio = 1:1, 2:1, 4:1) by solution phase synthesis and reported that the increasing concentration of nickel nanoparticles enhanced electro-catalytic activity towards methanol electrooxidation in alkaline medium and Ni:Co with 4:1 molar ratio supported on GNS shows better activity among these catalyst. Sarkar et al. [10] prepared Ni nanoparticles supported on polypyrrole-GNS (Ni/PPy/GNS) nanocomposite by simply mixing PPy/GNS and NiCl₂·6H₂O at pH 10.5 and their electro-catalytic activity was investigated by cyclic voltammetry and chronoamperometry in 1M methanol in alkaline medium. As prepared nanocomposite showed higher anodic current density and lower onset potential for methanol electrooxidation. The improved electrocatalytic activity of prepared catalyst has been attributed to the synergistic effect of Ni nanoparticles, GNS and PPy. Narayanan and Bernaudshaw [25] prepared GNS supported NiCo₂O₄ (NiCo₂O₄/GNS) hybrid material

by hydrothermal synthesis followed by calcination and reported their catalytic activity towards methanol electrooxidation in alkaline medium. As prepared catalyst showed greater electrocatalytic activity during methanol oxidation which was 3.11 folds higher than the commercial Pt/C. This electrode also maintained its remarkable catalytic stability even after consecutive 500 cycles, which was ~50 times higher than that of the commercial Pt/C. Formation of mixed-valence cations of Ni^{2+} and Co^{3+} from the octahedral sites and high electron-transfer conductivity of GNS is attributed to the enhancement in electrocatalytic activity. Sheikh-Mohseni and co-worker [26] prepared electrochemically Ni–Co nanoparticles on GNS carbon paste electrode (Ni–Co/GNS/CPE), and investigated as electro-catalyst for methanol oxidation in alkaline medium. Result have shown that the presence of Ni–Co/GNS in the structure of electrocatalyst greatly enhance the electrocatalytic oxidation of methanol. The anodic peak potential of methanol oxidation was decreased to 0.65 V vs. saturated calomel electrode and also its current is greatly enhanced. Kang et al. [27] prepared Rh supported on GNS (Rh/GNS) by a one-pot hydrothermal approach and reported that as compared to the commercial Pt/C catalyst, the prepared catalyst shows excellent MOR activity in alkaline media and 3.6-times mass activity. Also, the Rh/GNS also showed better tolerance against CO poisoning species.

2.2. Oxygen Reduction Reaction

The oxygen electrode is highly irreversible in aqueous electrolyte and takes place at a high positive potential ($E^\circ=1.23$ V vs. SHE) in acid medium. At this potential, most of the metal electrodes will undergo dissolution, only noble metals and their alloys are stable. Both noble and non-noble metal based electrocatalysts have been investigated for ORR. As ORR proceeds via both $4e^-$ as well as $2e^-$ pathway as shown in Figure 4.

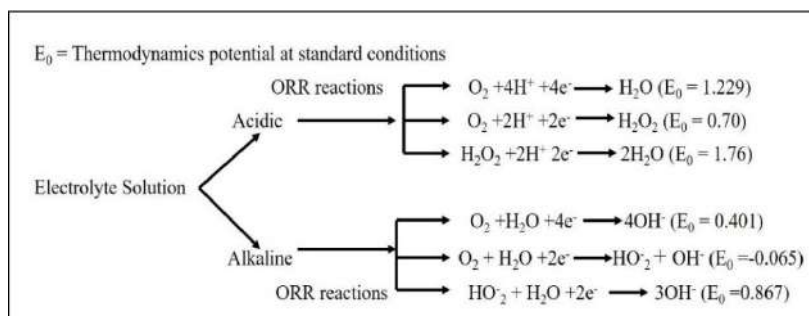
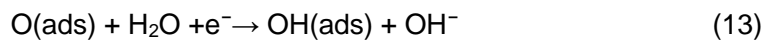
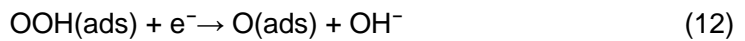
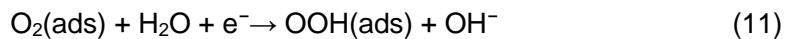


Figure 4. Schematic representation of oxygen reduction reaction in acid as well as alkaline medium.

In general, ORR occurs mainly through two pathways in which one is the 4-electron reduction of O_2 to H_2O in acidic media or OH^- in basic media whereas the other is the 2-electron reduction of O_2 to H_2O_2 in acidic media or HO_2^- in basic media. The

thermodynamic reaction potentials for each pathway are listed in Figure 4. As for kinetic ORR sequences, these are more complex and involve many intermediate and elementary steps (electron transfer or chemical reactions) that are dependent on the nature of the catalyst and electrolyte. In alkaline electrolytes, ORR can occur through associative or dissociative mechanisms [28, 29]. For the associative mechanism in alkaline media, ORR begins with the associative adsorption of O₂ and the overall reaction mechanism can be summarized as follows (*represents a surface free site on the catalyst):



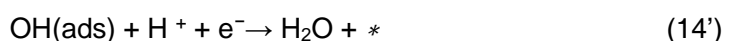
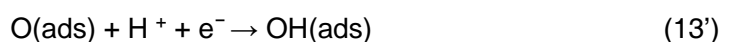
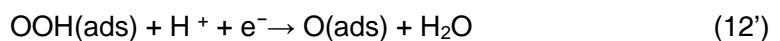
Here, four electrons in total are accepted by O₂, resulting in 4 OH⁻ ions being produced to complete a 4-electron ORR. Alternatively, if OOH(ads) accepts an electron, desorption may occur in which peroxide ions are formed and leave the catalytic site, resulting in the termination of the reaction chain and 2-electron ORR as represented in the following equation:



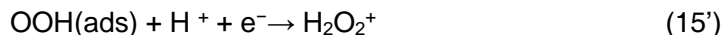
As for the dissociative mechanism in alkaline media, this reaction is simpler in which instead of going through Reactions (10) to (12), O₂ adsorbed on free sites directly dissociates into two O(ads), also consuming four electrons and completing a 4-electron ORR as represented in the following equations



As for acidic electrolytes, a similar reaction mechanism occurs in which in the presence of protons, the reaction route will change to:



Here, four protons and four electrons are consumed and O_2 is completely reduced into two H_2O . In addition, Reaction (15) will also change to reaction (15):



And based on these mechanisms, it is clear that the improvement of kinetics and the reduction in overpotentials for ORR in both acidic and alkaline media involve avoiding the production of H_2O_2 or HO_2^- for more efficient 4-electron pathways. And as mentioned above, suitable electrocatalysts can effectively influence reaction mechanisms and guide ORR through more efficient pathways.

Linear Sweep Voltammetry (LSV) carried out to measure the ORR in O_2 saturated acidic or alkaline medium. As oxygen has lower solubility in water, which further reduced by the addition of acid or alkali, so most of the analysis carried out in 0.1 M KOH (0.5 M acid). KOH preferred over NaOH due to its high specific conductance. The LSV graph (Figure 5) shows three distinct region viz. kinetic control (>0.950 V vs. RHE), mixed kinetic diffusion control (0.950–0.80 vs. RHE) and diffusion control regions (<0.80 V vs. RHE). Mixed region is taken for evaluation of the kinetic information. At more negative potentials (<0.80 V), the mass transport-limited current becomes significant where a dependence of disk current density (j) upon rotation rate is observed. With increasing the rotation rate, the limiting current increased due to an increase in the oxygen diffusion rate from bulk to the electrode surface. The kinetic study for ORR has been made by Rotating disc electrode (RDE) analysis recorded at different rotations, the graph thus obtained shown in Figure 6 (i).

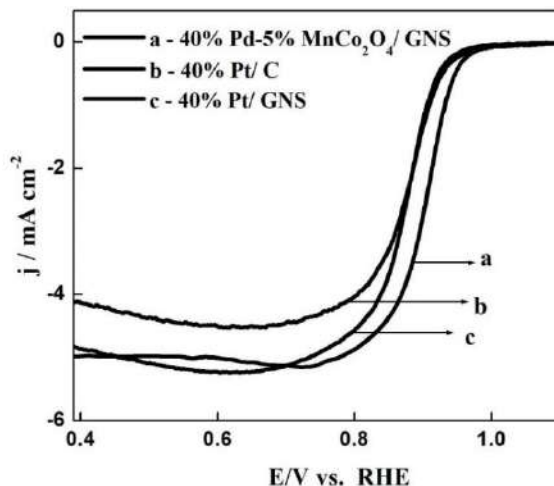


Figure 5. ORR graph for different composites in Linear sweep voltammograms in O_2 -saturated 1 M KOH; scan rate = 2 mV s^{-1} ; rotation = 1600 rpm and at 25°C .

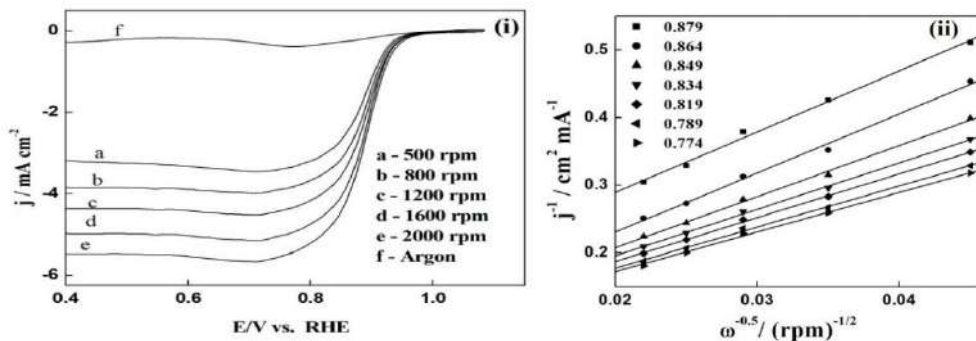


Figure 6. Linear sweep voltammograms of Pd-5wt%MnCo₂O₄/GNS at varying rotations in O₂-saturated 1 M KOH; scan rate = 2 mV s⁻¹; catalyst loading = 0.60 (i.e., Pd = 0.24) mg cm⁻² (i) and at 25°C. and corresponding K-L plot (1/j versus 1/ω^{1/2}) plots at constant potentials (ii).

In mixed region, the disk current density (*j*) measured at a potential that is the contribution of both processes, diffusion and kinetic- controlled ones. The three current densities, the observed (or disk) (*j*), kinetic (*j_k*) and mass transport (mainly diffusion) (*j_d*) follow the Koutecky–Levich (K-L) equation as follows [30]:

$$\frac{1}{j} = \frac{1}{j_k} + \frac{1}{j_d} \quad (17)$$

$$\frac{1}{j} = \frac{1}{j_k} + \frac{1}{BW^{1/2}} \quad (18)$$

Where ω is the electrode rotation in revolutions per minute (rpm) and *B* is the Levich constant given by

$$\frac{1}{B} = \frac{1}{0.2nFC_{O_2}D_{O_2}^{2/3}\nu^{-1/6}} \quad (19)$$

Where *j*, is the measured current density, *j_k* and *j_d* are the kinetic and diffusional current densities, ω is the angular velocity, *n* is transferred electron number, *F* is the Faraday constant (96,485 C mol⁻¹), *C_{O₂}* is the bulk concentration of O₂, ν is the kinematic viscosity of the electrolyte, and *D_{O₂}* is diffusion coefficient of O₂.

Thus, *B*-value can be estimated theoretically using the standard data and it can also be determined by constructing linear K-L plot (*j*⁻¹ vs. $\omega^{1/2}$) at varying potentials (Figure 6 (ii)) and measuring their slope consequently, the number of electron transferred per O₂ molecule reduced can be found.

To construct the Tafel plot, the kinetic current was determined using the relation,

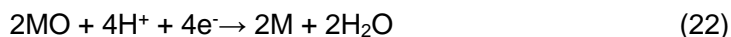
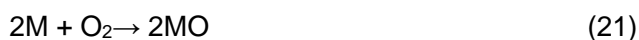
$$j_k = \frac{j_d \cdot j}{j_d - j} \quad (20)$$

The j_k values were noted at varying potentials and at a constant electrode rotation, 1600 rpm. $j_d/(j_d - j)$ is the mass-transport correction term. j_d value was noted from the LSV curve determined at 1600 rpm for each hybrid catalyst.

As attempt have been made to look after the Pt free electrode materials with efficient electrocatalytic activity, so brief overview of some composites developed in recent past for ORR catalyst mentioned here.

2.2.1. Pd and Pd Based Hybrid Materials

It has been found that in acidic media, Pd has a superior ORR activity than any other noble metals, except for Pt, but Pd is more sensitive to anion adsorption than Pt due to stronger interaction between the Pd surface and anion (Cl^- , ClO_4^- , SO_4^{2-} , etc.) [31, 32]. While in alkaline media Pd exhibits higher ORR activity than in acidic solution due to decrease in the anion poisoning effect in alkaline solution. Several studies have shown that the ORR activity of Pd/C in alkaline solution is comparable to that of Pt/C [31, 32]. On Pd the ORR takes place in the same manner as on Pt however, it has lesser ORR activity and poorer stability than Pt, particularly at high cathodic potentials [33]. To improve the activity and stability, a number of alloys of Pd with transition metals such as Co, Ni, Fe, Cu, Ag, Mo, etc. have been prepared and investigated. According to Fernandez et al. [34], the ORR on bimetallic electrocatalysts proceeds through a mechanism wherein one metal breaks the O-O bond of molecular oxygen and the other one acts to reduce the resulting adsorbed atomic oxygen as given below:



Incorporation of more active metals (eg. Co) into Pd simplifies the dissociative adsorption of O_2 forming adsorbed oxygen atoms (Oads). The latter (Oads) atoms then migrate from the Co site to Pd site where the electroreduction reaction occurs with less polarization. Liu et al. [35] investigated the impact of GNS substrate-Pd nanoparticle interaction on the O, OH, and OOH adsorption that is directly related to the electrocatalytic performance of these composites for ORR by first principles based calculations. Doping the single vacancy GNS with B or N will tune the average d-band center and also the activity of the composite toward O, OH, and OOH adsorption. The adsorption energies of O, OH, and OOH is reduced from -4.78 , -4.38 , and -1.56 eV on the freestanding Pd13 nanoparticle to -4.57 , -2.66 , and -1.39 eV on Pd13/single vacancy GNS composites, showing that the defective GNS substrate will not only stabilize the Pd NPs but also reduce the adsorption energies of the O-containing

species to the Pd particle, and so as the poisoning of the ORR active sites. Carrera-Cerritos et al. [36] synthesized Pd supported on GNS by polyol reduction method. Pd nanocatalyst displayed the enhanced ORR activity when supported on GNS in comparison to carbon black. The ORR activity followed the order Pt/C>Pt/GNS>Pd/GNS>Pd/C. In the case of Pd, the Tafel slopes were 65 mV/decade and 71 mV/decade at higher potentials. Fuel cell performance in the case Pd/GNS was 2.2 times higher than that with Pd/C in presence of 1M CH₃OH fed to the anode. It has been observed that the Pd-Fe-Mo catalyst optimized with 7.5:1.5:1.0 atomic ratio and 500 °C of the annealing temperature shows 32.18 mA mg⁻¹ PGM (PGM: platinum group metal) of the kinetic current density at 0.9 V for ORR, which is comparable to that of commercial Pt/C catalyst [37]. The current density is demoted to 6.20 mA mg⁻¹ PGM after 3000 cycling of cyclic voltammetry, nevertheless it is greatly enhanced value compared to other non-platinum catalysts. In actual application to PEMFCs, the 20% Pd-Fe-Mo catalyst dispersed on carbon exhibited a high performance of 506 mA cm⁻² at 0.6 V. The results suggested that the Pd-Fe-Mo catalyst can be a good candidate for non-platinum ORR catalysts. Singh et al. [38] find that Pd-Co/GNS catalyst as methanol tolerant cathode materials for ORR in 0.5 M H₂SO₄ at 25°C. on comparison with corresponding MWCNT supported composites it is found that GNS shows better activity for ORR. The GNS supported Spinel oxides, cobaltites (Co₃O₄, MnCo₂O₄ and NiCo₂O₄) and manganites (Mn₃O₄, CoMn₂O₄, FeMn₂O₄ and CuMn₂O₄) substituted Pd based catalysts showed appreciable ORR activity as well as stability in 0.1 M KOH, specially 40wt%Pd-5wt%MnCo₂O₄/GNS [9,30].

2.2.2. Transition Metal Mixed Oxide-Based Composites

Liang et al. [39] synthesized the catalytic activity of Co₃O₄ nanoparticles supported on GNS towards ORR and OER in an alkaline solution (KOH). The ORR activity was observed to enhance on nitrogen doping of GNS and that the Co₃O₄/N-GNS electrode the similar ORR activity similar to Pt but superior stability. Physical mixtures of Co₃O₄ and GNS, free Co₃O₄ nanoparticle (size ~ 4-8 nm) or GNS exhibited very poor ORR activities while Co₃O₄/N-GNS showed enhanced activity with the onset potential of ~0.88 V vs. RHE and the Tafel slope of 42 mV/decade (in 0.1M KOH). The RRDE study indicated only ~ 6% yield of HO₂⁻ and 4 - electron pathway mechanism. The results showed the synergistic effect of Co₃O₄ and GNS in the hybrid on the ORR reactivity. Durability test (10000-25000 sec.) showed little decay in the ORR activity in the case of Co₃O₄/N-GNS while that Pt/C (50 wt% Pt on Vulcan XC72) and Pd/C (10 wt%Pd on activated carbon) underwent respectively 30% and 20% decay in the ORR activity. In 1M KOH, Co₃O₄/N-GNS produced the lowest Tafel slope of 37 mV/decade among the spinel oxide ever reported. Such a low Tafel slope for ORR on spinel oxides are scarce in literature.

Liang et al. [40] studied GNS supported composites MnCo₂O₄/N-GNS and Co₃O₄/N-GNS by two steps solvothermal method and investigated their catalytic activity toward both ORR and OER in 1M KOH. The ORR onset and peak potentials for MnCo₂O₄/N-GNS and Co₃O₄/N-GNS were 0.95 & 0.88 and 0.93 & 0.86 V vs. RHE

respectively. While in the case of 20wt%Pt/C peak potential is on 0.90 V vs. RHE. The RRDE study exhibited 4 e- path for ORR with Tafel slope of 36 mV/decade on MnCo₂O₄/GNS. The stability test for 20000 sec showed only 3.5% decay in current density in the case of MnCo₂O₄/N-GNS while it was 25% and 33% in case of binary physical mixtures of MnCo₂O₄ with N-GNS and Pt/C. BET measurements showed that Mn doping increases the electrochemically active surface area of the hybrid. Tetragonal spinel showed lower intrinsic ORR activity than the cubic phase. Wu et al. [41] reported Fe₃O₄ supported on N-doped GNS aerogel (Fe₃O₄/N-GAs) as efficient electrocatalysts for the ORR in 0.1M KOH. As compared to carbon supported oxide (Fe₃O₄/N-CB), Fe₃O₄/N-GAs exhibited a more positive onset potential (-0.19V vs. Ag/AgCl), higher cathodic current density (-2.56 mA/cm²), lower H₂O₂ yield, and higher electron transfer number (3.72-3.95). The durability test showed ~79.3% current retention in the case of Fe₃O₄/N-GAs while only ~61.0% current retention in the case of Pt/C. The higher ORR activity of Fe₃O₄/N-GAs can be attributed to the effect of macropores on the diffusion rate of the electrolyte.

2.2.3. Transition Metal Macrocycles

Transition metal macrocycles (TMMC) are another type of fuel cell catalyst which have been extensively investigated as a potential substitute of Pt for ORR catalysis. The molecules of TMMC are having square planar structure with the metal ion symmetrically surrounded by 4N atoms. These N atoms are from each member of ring systems, which in turn are connected by C atoms (Porphyrins) or N atoms (Phthalocyanins). It is noteworthy that these TMMC are inert to MOR, while show reasonable activity and remarkable selectivity towards ORR. They can catalyze a direct 4e- reduction of O₂ to H₂O [42]. One of the major drawbacks of this kind of catalysts is their low stability in acidic medium however, heat treatment considerably improves the ORR activity and stability.

3. CONCLUSION

As an alternative of conventional energy resources fuel cell stands as a one of the best sustainable option. Among the different types of fuel cell, DMFCs are heavily researched fuel cells, due to their excellent features, such as high energy density, easy fuel storage and ambient operating conditions. Pt-based alloys and composites dispersed on high surface area carbon materials are considered as the best catalysts for electrocatalysis of both the reactions (MOR & ORR). However, Pt is pretty costly and its electrode surface is poisoned by the methanol oxidation intermediate, i.e., CO molecule. The latter chemical species in fact, gets adsorbed at the active Pt sites and, thereby, reduces the rate of adsorption and hence the oxidation of methanol molecule. Further, the use of Pt as the cathode material also adversely affecting the cell efficiency because of methanol crossover. GNS is a recently discovered 2D one atom thick planar sheet of sp²-bonded carbon atoms possesses high surface area (~ 2630

m^2g^{-1}) and high electronic conductivity ($\sim 15000 \text{ cm}^2\text{V}^{-1}\text{s}^{-1}$). GNS is considered as very potential support material to obtain better dispersion and enhanced electrocatalytic properties of fuel cell catalysts. So, from discussion of the present chapter, it can be concluded in nutshell that Pt-free GNS supported various metals and transition metal oxides provided an alternate and efficient electrode materials that would not only reduce the cost but also help in commercializing this environment friendly technology.

REFERENCES

- [1] Sarwar, E., Noor, T., Iqbal, N., Mehmood, Y., Ahmed, S. & Mehek, R. (2018). Effect of Co-Ni ratio in graphene based bimetallic electro-catalyst for methanol oxidation. *Fuel Cell*, 18, 189-194.
- [2] Sharma, S. & Pollet, B. G. (2012). Support materials for PEMFC and DMFC electrocatalysts—A review. *J. Power Sources*, 208, 96–119.
- [3] Garcia, B. L. & Weidner, J. W. (2007). Review of direct fuel cell. *Mod. Aspect. Electrochem.*, 40, 229-284.
- [4] Dillon, S. R., Srinivasan, S., Aricò, A. S. & Antonucci, V. (2004). International activities in DMFC R&D: status of technologies and potential applications, *J. Power Sources*, 127, 112-126.
- [5] Lanninie, J. & Dicks, A. (2003). *Fuel Cell Systems Explained*, 2nd ed. John Wiley & Sons Inc., Hoboken, N. J.
- [6] Gencoglu, M. T. & Ural, Z. (2009). Design of a PEM fuel cell for residential application. *Int. J. Hydrogen Energy*, 34, 5242-5248.
- [7] Krishnan, S., Singh, E., Singh, P., Meyyappan, M. & Nalwa, H. (2019). A review on graphene-based nanocomposites for electrochemical and fluorescent biosensors. *RSC Adv.*, 9, 8778-8881.
- [8] Awasthi, R. & Singh, R. N. (2013). Graphene-supported Pd-Ru nanoparticles with superior methanol electrooxidation activity. *Carbon*, 51, 282-289.
- [9] Sharma, C. S., Awasthi, R., Singh, R. N. & Sinha, A.S.K. (2014). Graphene-manganite-Pd hybrids as highly active and stable electrocatalysts for methanol oxidation and oxygen reduction. *Electrochim. Acta*, 136, 166–175.
- [10] Sarkar, C., Nath, N., Bhuyan, S. & Dolui, S. K. (2019). Multifunctional ternary nanocomposites of Ni/polypyrrole/reduced graphene oxide as supercapacitor and electrocatalyst in methanol oxidation. *Chemistry Select*, 4, 2529-2537.
- [11] Yang, Z., Tian, J., Yin, Z., Cui, C., Qian, W. & Wei, F. (2019). Carbon nanotube- and graphene-based nanomaterials and applications in high-voltage supercapacitor: A review. *Carbon*, 141, 467-480.
- [12] Mahmood, N., Zhang, C., Yin, H. & Hou, Y. (2014). Graphene-based nanocomposites for energy storage and conversion in lithium batteries, supercapacitors and fuel cells. *J. Mater. Chem. A*, 2, 15-32.

- [13] Hou, J., Shao, Y., Ellis, M. W., Moore, R. B. & Yi, B. (2011). Graphene-based electrochemical energy conversion and storage: Fuel cells, supercapacitors and lithium ion batteries. *Phys. Chem. Chem. Phys.*, 13, 15384-15402.
- [14] Yavari, F. & Koratkar, N. (2012). Graphene-Based Chemical Sensors, *J. Phys. Chem. Lett.*, 13, 1746–1753.
- [15] Shao, Y., Wang, J., Wu, H., Liu, J., Aksay, I. & Lin, Y. (2010). Graphene based electrochemical sensors and biosensors: A Review. *Electroanal.*, 22, 1027–1036.
- [16] Bagotzky, V., Vassiliev, Y. B. & Khazova, O. (1977). Generalized scheme of chemisorption, electrooxidation and electroreduction of simple organic compounds on platinum group metals, *J. Electroanal. Chem. Interf. Electrochem.*, 81, 229-238.
- [17] Lamy, C., Rousseau, S., Belgsir, E.M., Coutanceau, C. & L'eger, J. M. (2004). Recent progress in the direct ethanol fuel cell: development of new platinum–tin electrocatalysts. *Electrochim. Acta*, 49, 3901-3908.
- [18] Ng, J. C., Tan, C. Y., Ong, B. H., Matsuda, A., Basirun, W. J., Tan, W. K., Singh, R. & Yap, B. K. (2019). Novel palladium-guanine-reduced graphene oxide nanocomposite as efficient electrocatalyst for methanol oxidation reaction. *Mater. Res. Bull.*, 112, 213-220.
- [19] Kumar, V.S., Kumari, S., Goud, K. Y., Satyanarayana, M. & Gobi, K. V. (2020). One-pot synthesis of Pd₂₀-xAux nanoparticles embedded in nitrogen doped graphene as high performance electrocatalyst toward methanol oxidation. *Int. J. Hydrogen Energy*, 45, 1018-1029.
- [20] Yang, Y., Huang, H., Shen, B., Jin, L., Jiang, Q., Yanga, L. & He, H. (2020). Anchoring nanosized Pd on three-dimensional boron- and nitrogen-codoped graphene aerogels as a highly active multifunctional electrocatalyst for formic acid and methanol oxidation reactions, *Inorg. Chem. Front.*, 7, 700-708.
- [21] Hsieh, C. T., Yu, P. Y., Tzou, D. Y., Hsu, J. P. & Chiu, Y. R. (2016). Bimetallic Pd–Rh nanoparticles onto reduced graphene oxide nanosheets as electrocatalysts for methanol oxidation. *J. Electroanal. Chem.*, 761, 28-36.
- [22] Zhang, X., Zhu, J., Tiwary, C. S., Ma, Z., Huang, H., Zhang, J., Lu, Z., Huang, W. & Wu, Y. (2016). Palladium nanoparticles supported on nitrogen and sulfur dual-doped graphene as highly active electrocatalysts for formic acid and methanol oxidation. *ACS Appl. Mater. Interfaces*, 8, 10858-10865.
- [23] Kiyani, R., Rowshanzamir, S. & Parnian, M. J. (2016). Nitrogen doped graphene supported palladium-cobalt as a promising catalyst for methanol oxidation reaction: synthesis, characterization and electrocatalytic performance. *Energy*, 113, 1162-1173.
- [24] Yang, F., Wang, C., Dong, S., Chi, C., Jia, X., Zhang, L. & Li, Y. Plasma synthesis of Pd/PdO supported on porous graphene as electrocatalyst for methanol oxidation. *Mater. Lett.*, 174, 192–196.

- [25] Narayanan, N. & Neppolian, B. (2020). Reduced Graphene Oxide supported NiCo₂O₄ nano-rods: An efficient, stable and cost-effective electrocatalyst for methanol oxidation reaction. *Chem. Cat. Chem.*, 12, 771-780.
- [26] Sheikh-Mohseni, M. A., Hassanzadeh, V. & Habibi, B. (2019). Reduced graphene oxide supported bimetallic Ni–Co nanoparticles composite as an electrocatalyst for oxidation of methanol. *Solid State Sci.*, 98, 106022-106029.
- [27] Kang, Y., Xue, Q., Jin, P., Jiang, J., Zeng, J. & Chen, Y. (2017). Rhodium nanosheets–reduced graphene oxide hybrids: A highly active platinum alternative electrocatalyst for the methanol oxidation reaction in alkaline media. *ACS Sustain. Chem. Eng.*, 5, 10156-10162.
- [28] Chen, X., Yu, L. & Wang, S. (2017). Highly active and stable single iron site confined in graphene nanosheets for oxygen reduction reaction. *Nano Energy*, 32, 353–358.
- [29] Yu, L., Pan, X. & Cao, X. (2011). Oxygen reduction reaction mechanism on nitrogen-doped graphene: a density functional theory study. *J. Catal.*, 282, 183–190.
- [30] Sharma, C. S., Awasthi, R., Singh, R. N. & Sinha, A. S. K. (2013). Graphene–cobaltite–Pd hybrid materials for use as efficient bifunctional electrocatalysts in alkaline direct methanol fuel cells. *Phys. Chem. Chem. Phys.*, 15, 20333-20344.
- [31] Climent, V., Marković, N. & Ross, P. (2000). Kinetics of oxygen reduction on an epitaxial film of palladium on Pt (111). *J. Phys. Chem. B*, 104, 3116-3120.
- [32] Arenz, M., Schmidt, T., Wandelt, K., Ross, P. & Markovic, N. (2003). The oxygen reduction reaction on thin palladium films supported on a Pt (111) electrode. *J. Phys. Chem. B*, 7, 9813-9819.
- [33] Shao, M. (2011). Palladium-based electrocatalysts for hydrogen oxidation and oxygen reduction reactions. *J. Power Source*, 196, 2433-2444.
- [34] Fernández, J. L., Walsh, D. A. & Bard, A. J. (2005). Thermodynamic guidelines for the design of bimetallic catalysts for oxygen electroreduction and rapid screening by scanning electrochemical microscopy. M– Co (M: Pd, Ag, Au). *J. Am. Chem. Soc.*, 127, 357-365.
- [35] Liu, X., Li, L., Meng, C. & Han, Y. (2012). Palladium nanoparticles/defective graphene composites as oxygen reduction electrocatalysts: a first-principles study. *J. Phys. Chem. C*, 116, 2710-2719.
- [36] Carrera-Cerritos, R., Baglio, V., Aricò, A., Ledesma-García, J., Sgroi, M. & Pullini, D. (2014). Improved Pd electro-catalysis for oxygen reduction reaction in direct methanol fuel cell by reduced graphene oxide. *Applied Catalysis B: Environmental.*, 144, 554-560.
- [37] Lee, Y., Jang, J., Lee, J. G., Jeon, O. S., Kim, H. S. & Hwang, H. J. (2016). Optimization of the Pd-Fe-Mo catalysts for oxygen reduction reaction in proton-exchange membrane fuel cells. *Electrochimica Acta*, 220, 29-35.
- [38] Singh, R. N. & Sharma, C. S. (2012). Preparation of bimetallic Pd-Co nanoparticles on graphene support for use as methanol tolerant oxygen reduction electrocatalysts. *Eng. Technol. Appl. Sci. Res.*, 2, 295-301.

- [39] Liang, Y., Li, Y., Wang, H., Zhou, J., Wang, J. & Regier, T. (2011). Co_3O_4 nanocrystals on graphene as a synergistic catalyst for oxygen reduction reaction. *Nat. Mater.*, 10, 780-786.
- [40] Liang, Y., Wang, H., Zhou, J., Li, Y., Wang, J. & Regier, T. (2012). Covalent hybrid of spinel manganese–cobalt oxide and graphene as advanced oxygen reduction electrocatalysts. *J. Am. Chem. Soc.*, 34, 3517-3523.
- [41] Wu, Z. S., Yang, S., Sun, Y., Parvez, K., Feng, X. & Müllen, K. (2012). 3D nitrogen-doped graphene aerogel-supported Fe_3O_4 nanoparticles as efficient electrocatalysts for the oxygen reduction reaction. *J. Am. Chem. Soc.*, 134, 9082-9085.
- [42] Wang, Y. & Balbuena, P. B. (2005). Design of oxygen reduction bimetallic catalysts: ab-initio-derived thermodynamic guidelines. *J. Phys. Chem. B*, 109, 18902-18906.

Chapter 15

TWO-DIMENSIONAL (2D) NANOMATERIALS FOR ENERGY HARVESTING

Thakur Prasad Yadav*

Hydrogen Energy Centre, Department of Physics,
Institute of Science, Banaras Hindu University, Varanasi, India

ABSTRACT

The development of a clean, renewable and sustainable energy production is the main demand of the society nowadays. The issue of the production and application of renewable and clean energy can be solved by using advanced materials technology. The two-dimensional (2D) nanomaterials are gaining enormous attention for utilisation in energy harvesting applications because of their unique and tunable properties such as high flexibility, high active surface area, and extraordinary mechanical properties using low cost synthesis processes. The variety of 2D nanomaterials such as transition metal carbide nanosheets, transition metal dichalcogenides, nanosheets, black-phosphorus nanosheets, 2D nitrides, 2D carbonitrides, layered double hydroxides, metal-organic framework nanosheets, 2D alloys, 2D quasicrystals, and other 2D nanomaterials have been investigated in the area of energy harvesting extensively over the last decade. In this chapter, the synthesis of 2D materials for energy harvesting from production to storage has been summarized.

Keywords: nanomaterials, 2D nanomaterials, energy harvesting, hydrogen energy

* Corresponding Author's E-mail: yadavtp@gmail.com.

1. INTRODUCTION

Over the past two decades nanomaterials have attracted major attention due to their fascinating properties and wide range of potential applications [1-3]. Nanomaterials are typically defined as materials that have at least one dimension in the range of 1-100 nm [4]. There are two categories of nanomaterials: organic (mostly carbon allotropes) and inorganic nanomaterials (iron, silver, gold, boron nitride nanosheets, molybdenum disulphide, and tungsten disulphide) [5]. The nanomaterials have completely different properties than the bulk parent materials; these properties include high surface area, conductivity, mechanical strength, and transparency [6-8]. Nanotechnology is expanding in academic research as well as moving into industry in recent years and subsequently has very high multifunctional demands [9,10]. Versatility is essential for real practical application of materials and nanomaterials are versatile materials with properties such as elasticity, transparency, and high conductivity, which are often required simultaneously [11]. Nanomaterials can meet such demands and have the potential to stimulate new technologies for today and tomorrow. Nanoscience and technology is a multidisciplinary field, encompassing physics, chemistry, engineering, and biology. With the discovery of nanomaterials with zero-dimensional caged carbon molecule, the buckminsterfullerene (fullerene with the chemical formula C_{60}) in 1985 and the one-dimensional single-walled carbon nanotube in 1991, nanotechnology attracted a great deal of attention [12-15]. In 2004, a new low dimensional nanomaterial was discovered with a single sheet of carbon atoms called graphene and it was the first two-dimensional monolayer crystal [16]. Graphene is rich in exceptional physical and chemical properties, offering potential for fundamental research and exciting applications [17-19]. Just after six years of the discovery of graphene, in 2010 Andre Geim and Kostya Novoselov were awarded the Nobel Prize in physics for innovative experiments regarding the 2D nanomaterial. There is no doubt that the nanomaterial age is upon us, but how soon these materials will meet the consumer market will depend upon scalable and reliable ways to prepare these 2D nanomaterials of high quality. The 2D nanomaterials can be synthesized by different methods; however liquid phase exfoliation of layered crystals in solvents offers a way to produce billions of these nanosheets, in a small volume of solvent [20-22]. It will also allow cost-effective processing option that offers a multitude of advantages like spray-deposition or straightforward composite formation, and this preparation technique has also recently been deemed universal. It was shown that ultrasonication in specific solvents can be extended to a range of inorganic layered crystals, each with its own diverse, exotic properties. The motivation of this chapter was to explore and understand synthesis processes of 2D nanomaterials specifically so that more applications of these materials can be realised for energy applications.

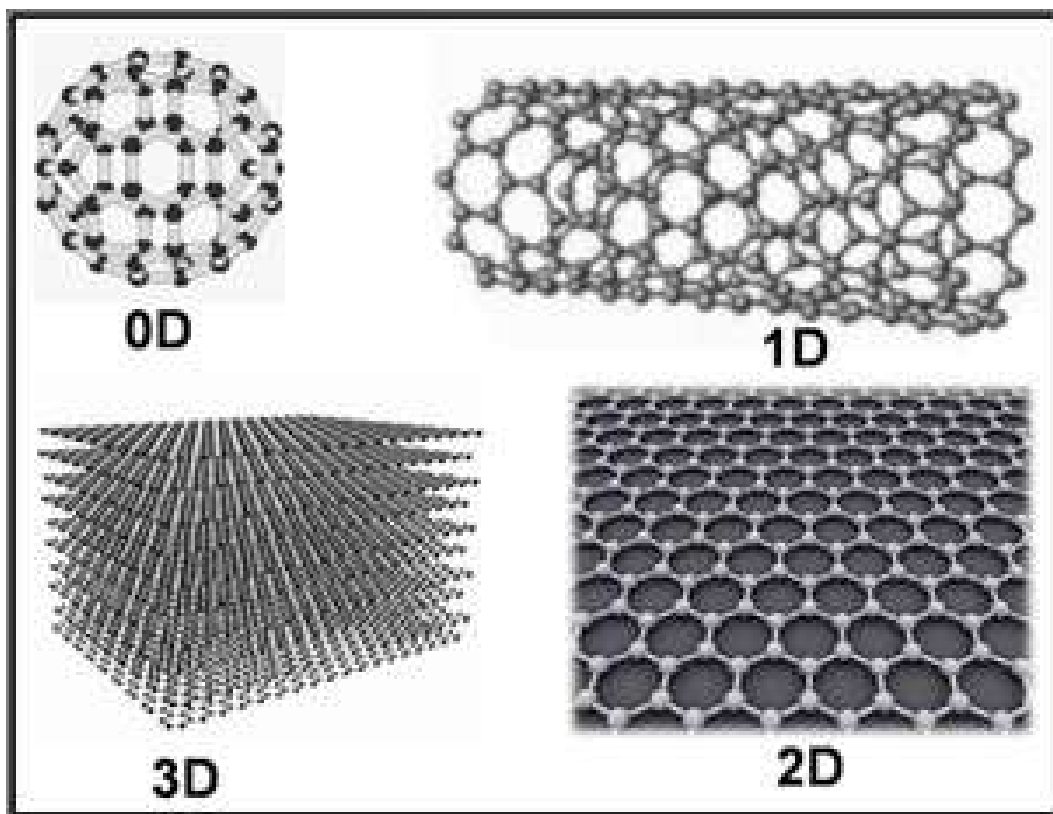


Figure 1. The schematic diagram of 0D, 1D, 2D and 3D materials.

2. NANOSTRUCTURES

When the size or dimension of a material is continuously reduced from a large or macroscopic size (3D), such as a metre or a centimetre, to a very small size, the properties remain the same at first, and then small changes begin to occur, until finally when the size drops to nm range, dramatic changes in properties can occur [23]. If one dimension is reduced to the nano range while the other two dimensions remain large, then we obtain a structure known as 2D nanomaterials. If two dimensions are so reduced and one remains large, the resulting structure is referred to as a quantum wire (1D). The extreme case of this process of size reduction in which all three dimensions reach the low nanometer range is called a quantum dot (0D). The word quantum is associated with these three types of nanostructures because the changes in properties arise from the quantum-mechanical nature of physics in the domain of the ultrasmall [24]. The schematic diagram of 0D, 1D, 2D and 3D materials have been shown in Figure 1. One approach to the preparation of a nanostructure, called the bottom-up approach, is to collect, consolidate, and fashion individual atoms and molecules into the structure. This came out by a sequence of chemical reactions controlled by catalysts, for example, in biology, catalysts called enzymes assemble amino acids to

construct living tissue that forms and supports the organs of the body. The opposite approach in the preparation of nanostructures is called the top-down method, which starts with a large-scale object or pattern and gradually reduces its dimension or dimensions e.g., lithography technique which shines radiation through a template on to a surface coated with a radiation-sensitive resist; the resist is then removed and the surface is chemically treated to produce the nanostructure.

3. SYNTHESIS OF TWO DIMENSIONAL MATERIALS

Since 400 Common Era, people have been harnessing properties of layered materials. Layered materials are those crystals which form strong in-plane chemical bonds but weak out-of-plane van der Waals interaction. These kinds of materials can allow people to exfoliate into so-called nanosheets which are less than one nanometre thick. When one dimension is of nanorange, while the other two are large, then this is 2-D nanostructure.

Exfoliation is the process that changes the pristine bulky materials to nano-scale thin sheets. After exfoliation, the nanosheets will not retain all the original properties of the pristine bulky crystal. However, some new properties will occur that are very different from the bulky one, which make the nanosheets so unique for applications. There are many kinds of layered materials as shown in Figure 2. One of the simplest and most common is the graphene and hexagonal boron nitride. Transition metal halides such as TiCl_2 , transition metal oxides such as MoO_3 , TiO_2 and metal double hydroxides such as $\text{Mg}_6\text{Al}_2(\text{OH})_{16}$ also represent diverse layered structures, clays, layered silicates and other layered minerals are the members of the layered materials family [25]. Nowadays, some of the most popular layered materials are the transition metal dichalcogenides, such as, MoS_2 , WS_2 [26]. After graphene, Transition metal dichalcogenides have attracted many research interests due to their unique electrochemical and mechanical properties [27]. After exfoliation, the accessible surface area of the material will dramatically increase, so it can be used as surface-active or catalytic chemical. Recently, another effect of exfoliation has been reported that the band gap of the transition metal dichalcogenide will change after the exfoliation, this allows electronic response to be chosen as well [28].

As for the exfoliation of layered materials, graphite was exfoliated by mechanical force such as scotch tape method [16]. These mechanical forces can obtain high quality graphene which has outstanding properties; however, low yield and production rate limited their applications. After some great research works, people developed some exfoliation methods that were done in the solution which can give us large quantities of high-quality and sizable few-layer or monolayer materials [20]. The earliest liquid-phase method of exfoliation is the chemical oxidation of graphite. Natural graphite was treated with oxidizers such as sulphuric acid and potassium permanganate. This oxidation will add hydroxyl and epoxide groups to the basal plane of graphite which makes the graphite become hydrophilic. Then water intercalation or

ultrasonication can be used to yield large scale monolayer graphene oxide which is stable in solution. Afterwards the thin graphene oxide can be easily reduced chemically in the liquid-phase, but will no longer be stable and aggregates unless polymer or surfactant stabilizers are present. However, although graphene oxide can be reduced to graphene easily, the structural defects will remain and will lower the quality which will narrow its applications [29].

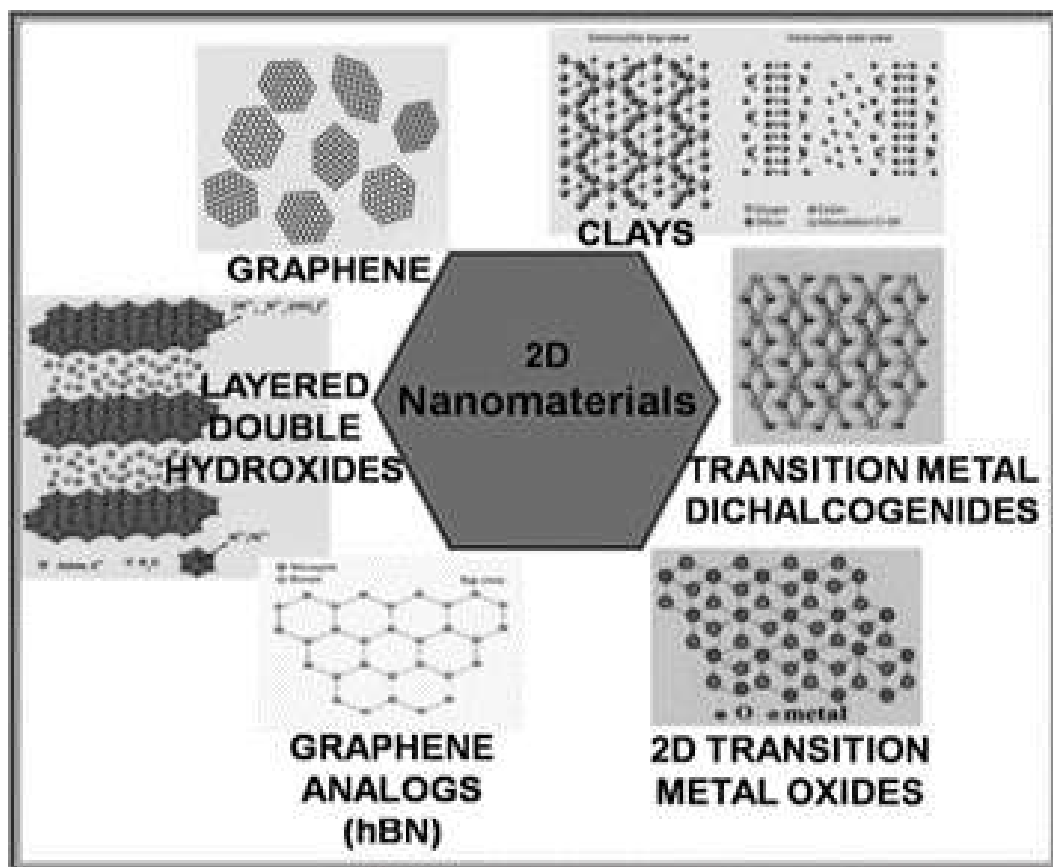


Figure 2. Different kinds of layered materials.

Recently, a new method has been developed as to exfoliate layered materials using ultrasonic waves in solvent. These kinds of powerful ultrasonic beams can generate cavitation bubbles that can collapse into high-energy jets which can break the van der Waals interaction between the layers of the materials so as to produce single layer materials. Graphite, hexagonal boron nitride, transition metal dichalcogenides and some of transition metal oxides can be exfoliated by this method. On the other hand, due to the power of the ultrasonic waves, the size of single layer flakes is relatively small and cannot be controlled [30].

Another liquid-phase method of exfoliation of layered materials is called intercalation. Because of the weak van der Waals interaction between the layers, layered materials can strongly absorb the small molecules into the space between

layers. This introduced another method of exfoliation of layered materials called intercalation, which has been widely applied in the exfoliation of graphite and transition metal dichalcogenides [31]. The intercalation of molecules will enlarge the space between sheets and weaken the interlayer adhesion so as to reduce the energy of exfoliation. Some intercalation species such as IBr can transfer the charge to the layers resulting in the reduction of interlayer binding. Further treatment such as low-power ultrasonication or thermal shock will be applied to exfoliate the intercalated layered materials. Intercalation can give high quality materials, but has some drawbacks such as sensitivity to the ambient conditions. For the transition metal oxides and clays, ion exchange has become a developed method of exfoliation [31]. Since these kinds of layered materials contain some exchangeable interlayer of cationic ions. Those ions can be exchanged for protons by soaking in acidic solutions. The protons can be exchanged for bulk organic ions leading to substantial swelling. Then low-power ultrasonication is applied to exfoliate the materials into nanosheets [33]. Among the methods that have been developed to exfoliate layered material, liquid phase exfoliation is most common [34].

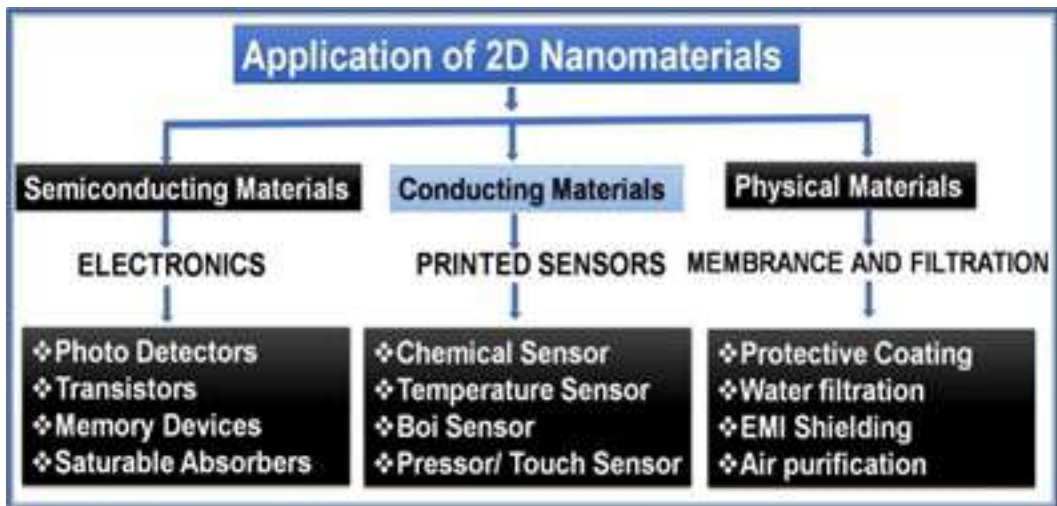


Figure 3. The different possible applications of 2D nanomaterials.

4. APPLICATIONS OF 2D NANOMATERIAL

Graphene is extensively used in fabricating sensors, solar cells, flexible electronics, electrically conductive composites, and also as thermal management material in electronic circuits. Moreover, the high surface area of graphene is also relevant for various applications such as catalysis, oil absorption, electrodes for supercapacitors, and batteries, energy storage applications. Graphene is also used as nanofiller in polymer to make polymer nanocomposite. The incorporation of graphene (with very low filler content) makes the insulating polymer to electrically conductive

nanocomposite. The direct band gap of MoS₂ nanosheets can be potentially used in transistors, light-emitting diodes, solar cells, and field-effect transistors (FET), ultra-high strength nanocomposites. WS₂ is a potential semiconducting material for solar energy conversion and also extensively used as electrode in lithium batteries, shock absorbers, and hydrogen storage. The hBN is an electrical insulator and is widely used material for gate dielectrics in capacitors. The different possible applications of 2D nanomaterials have been illustrated in Figure 3.

5. 2D MATERIALS FOR ENERGY (HYDROGEN) PRODUCTION AND STORAGE

Hydrogen generation using water provides the possibility towards low cost harnessing of renewable energy. However, suitable electrode materials are required. The Pt-based catalysts are a great promise for clean and sustainable energy production through efficient electrocatalyst towards hydrogen evolution reaction (HER) with low overpotential. In this processes, hydrogen can be generated from water through electrochemical splitting at the cathode, while oxygen is evolved at the anode in the oxygen evolution reaction (OER). The HER is one of the most important reactions in the electrochemistry which involves the process of protons from the electrolyte solution combining with the electrons at the electrode to form hydrogen, *i.e.*, fuel of the future. The Gibbs free energy of the atomic hydrogen adsorbed on the catalyst materials (ΔG_H) should be close to zero for good HER according to the theoretical calculations [35]. In general, the 2D nanomaterials have active sites with high surface area; therefore 2D nanomaterials are expected as a promising electrode material for HER. In the case of 2D MoS₂ nanomaterials, ΔG_H is only +0.08 eV and shows high performance HER activity [36]. In the case of 2D WS₂ nanomaterials, the edge length with high surface-to-volume ratio reveals the active site for high performance HER [37]. As a result of the rapid developments achieved in their synthesis, the mono and few-layer 2D nanomaterials, especially, the 2D transition metal dichalcogenide nanomaterials (MoS₂, WS₂, MoSe₂, WSe₂, MoTe₂) and their analogues have been widely investigated as HER electrocatalysts of high performance [38].

Most of the 2D nanomaterials including graphene work as catalysts for improving the hydrogen storage properties, like absorption-desorption kinetics, storage capacity, and the thermodynamics of the several hydrogen storage materials [39]. The 2D nanomaterials are also very useful materials to improve the cyclic stability, through obstruction of the hydrogen storage material agglomeration after several cycles of absorption-desorption. It should be remembered that 2D nanomaterials have several excellent properties, such as high mechanical strength, large surface area, zero band gaps, ballistic conduction, etc., which make them prominent candidates as templates along with effective catalytic action. There are some studies which explore the templated effect of the 2D nanomaterials so that the agglomeration of metal based

catalysts can be avoided [17]. In a recent study, the role of few-layer graphene nanosheets on enhancing the hydrogen sorption properties of MgH_2 has been demonstrated [40]. The another type of 2D material (MXene) has shown a higher hydrogen adsorption capacity up to 8.6 wt% and this material can fulfill the gravimetric hydrogen storage target as set by the United States Department of Energy (U.S. DOE) in 2015. Hydrogen storage performance was also estimated in several 2D materials and their composites.

CONCLUSION

Moving on from the bulk, the 2D nanomaterials have become a new class of nanomaterials for emerging applications. Extensive progress has been made in the research area of 2D nanomaterials, from the fundamental studies to the development of next generation technology in the past decade. This great stride has transformed the unique role of dimensionality in determining the intrinsic properties as well as the wide potential applications of nanomaterials in the area of energy harvesting. In this chapter, we summarized the recent progress in the area of 2D materials for potential application of energy harvesting. The extraordinary properties, due to monolayer structural uniqueness, have been explored for a variety of applications. Extensive exploration in the field of 2D nanomaterials also brings new challenges in the area of synthesis, production yield, quality production and production rate. The physical, chemical, and electronic properties of 2D nanomaterials are highly dependent on their structural features and suitable for energy harvesting application.

ACKNOWLEDGMENT

The author is grateful for stimulating discussions with Professor V.S. Subrahmanyam and for a critical reading of the manuscript. I would also like to thank Dr. Kalpana Awasthi (KNPG College, Bhadohi) for critical comments and constructive suggestions for useful experiments in the area of 2D nanomaterials. I would like to dedicate this article in the memory of my beloved and respected teacher and Ph.D. supervisor (Prof. O.N. Srivastava) who passed away due to COVID-19 ailment.

REFERENCES

- [1] Manandhar, K.D., Yadav, T.P., Prajapati, V.K., Basukala, O., Aganja, R.P., Dude, A., Shrivastav, O.N. and Sundar S. (2014). Nanonization increases the antileishmanial efficacy of amphotericin B: an ex vivo approach. *Infectious diseases and nanomedicine* II, 77-91.

- [2] Qu, L.L., Wang, N., Zhu, G., Yadav, T.P., Shuai, X., Bao, Yang, G., Li, D. and Li, H. (2018). Facile fabrication of ternary TiO₂-gold nanoparticle-graphene oxide nanocomposites for recyclable surface enhanced Raman scattering. *Talanta* 186: 265-271.
- [3] Lai, B., Singh, S.C., Bindra, J.K., Saraj, C.S., Shukla, A., Yadav, T.P., Wu, W., McGill, S.A., Dalal, N.S., Srivastava, A. and Guo C. (2019). Hydrogen evolution reaction from bare and surface-functionalized few-layered MoS₂ nanosheets in acidic and alkaline electrolytes. *Mat. Today Chemistry* 14: 100207.
- [4] Yadav, T.P., Yadav, R.M. and Singh, D.P. (2012). Mechanical milling: a top-down approach for the synthesis of nanomaterials and nanocomposites. *Nanosci. Nanotech.* 2: 22-48.
- [5] Awasthi, K., Kumar, R., Raghubanshi, H., Awasthi, S., Pandey, R., Singh, D., Yadav, T.P. and Srivastava, O.N. (2011). Synthesis of nano-carbon (nanotubes, nanofibres, graphene) materials. *Bull. Mat. Sci.* 34: 607-724.
- [6] Shahi, R.R., Yadav, T.P., Shaz, M.A., Srivastava, O.N. and Smaalen, S van (2011). Effect of processing parameter on hydrogen storage characteristics of as quenched Ti₄₅Zr₃₈Ni₁₇ quasicrystalline alloys, *Int. J. Hyd. Energy* 36: 592-599.
- [7] Singh, A. K., Pal, P., Gupta, V., Yadav, T. P., Gupta, V. and Singh, S. P. (2018). Green synthesis, characterization and antimicrobial activity of zinc oxide quantum dots using *Ecliptaalba*. *Mat. Chem. and Phys.* 203: 40-48.
- [8] Yadav, T.P., Singh, D., Tiwari, R.S. and Srivastava, O.N. (2012). Enhanced microhardness of mechanically activated carbon-quasicrystal composite. *Mat. Lett.* 80: 5-8.
- [9] Mishra, S.S., Yadav, T.P., Mukhopadhyay, N.K. and Srivastava O.N. (2020). Synthesis of fine skeletal structure on Al-Cu-Co decagonal quasicrystals for hydrogen production through steam reforming of methanol. *Intl. J. of Hyd. Energy* 45: 24491-24501.
- [10] Mishra, S.S., Yadav, T.P., Singh, S.P., Singh, A.K., Shaz, M.A., Mukhopadhyay, N.K. and Srivastava, O.N. (2020). Evolution of porous structure on Al-Cu-Fe quasicrystalline alloy surface and its catalytic activities. *J. Alloys and Comp.* 834: 155162.
- [11] Singh, S. P., Ansari, M. I., Pandey, B., Srivastava, J. K., Yadav, T. P., Rani, H., Parveen, A., Mala, J. and Singh, A. K. (2020). Recent Trends and Advancement Toward Phyto-mediated Fabrication of Noble Metallic Nanomaterials: Focus on Silver, Gold, Platinum, and Palladium. *Nano.and Env. Biotech.* 87-105.
- [12] Kroto, H. W., Heath, J. R., O'Brien, S. C., Curl, R. F. and Smalley, R.E. (1985). C₆₀: Buckminsterfullerene. *Nature* 318:162-163.
- [13] Iijima, S. (1991). Helical microtubules of graphitic carbon. *Nature* 354: 56-58.
- [14] Ebbesen, T.W. and Ajayan, P.M. (1992). Large-scale synthesis of carbon nanotubes. *Nature* 358: 220-222.
- [15] Ajayan, P.M. (1999) Nanotubes from carbon, *Chemical reviews* 99 (7), 1787-1800.

- [16] Novoselov, K. S., Geim, A. K., Morozov, S. V., Jiang, D., Zhang, Y., Dubonos, S. V., Grigorieva, I. V. and Firsov, A. A. (2004). Electric field effect in atomically thin carbon films. *Science* 306: 666–669.
- [17] Verma, S. K. Bhatnagar, A., Shukla, V., Soni, P.K., Pandey, A. P., Yadav, T. P. and Srivastava, O.N. (2020). Multiple improvements of hydrogen sorption and their mechanism for MgH₂ catalyzed through TiH₂@ Gr. *Int. J. of Hyd. Energy* 45:19516-19530.
- [18] Qu, L., Zhu, G., Ji, J., Yadav, T.P., Chen, Y., Yang, G., Xu, H. and Li H. (2018). Recyclable visible light-driven O-g-C₃N₄/graphene oxide/N-carbon nanotube membrane for efficient removal of organic pollutants. *ACS App. Mat. & Int.* 10: 42427-42435.
- [19] Qu, L., Wang, N., Xu, H., Wang, W., Liu, Y., Kuo, L., Yadav, T. P., Wu, J., Joyner, J., Song, Y., Li, H., Lou, J., Vajtai, R. and Ajayan, P. M. (2017). Gold nanoparticles and g-C₃N₄-intercalated graphene oxide membrane for recyclable surface enhanced raman scattering. *Adv. Funct. Mat.* 27: 1701714.
- [20] Yadav, T. P., Woellner, C. F., Sharifi, T., Sinha, S. K., Qu, L-L, Apte, A., Mukhopadhyay, N. K., Srivastava, O. N., Vajtai, R., Galvão, D. S., Tiwary, C. S. and Ajayan, P. M. (2020). Extraction of two-dimensional aluminum alloys from decagonal quasicrystals. *ACS Nano* 14: 7435–7443.
- [21] Yadav, T. P., Shirodkar, S. N., Lertcumfu, N., Radhakrishnan, S., Sayed, F. N., Malviya, K. D., Costin, G., Vajtai, R., Yakobson, B. I., Tiwary, C. S. and Ajayan, P.M. (2018). Chromiteen: A new 2D oxide magnetic material from natural ore. *Adv. Mat. Int.* 5: 1800549.
- [22] Yadav, T. P., Woellner, C. F., Sinha, S. K., Sharifi, T., Apte, A., Mukhopadhyay, N. K., Srivastava, O. N., Vajtai, R., Galvao, D. S., Tiwary C.S. and Ajayan, P.M. (2018). Liquid exfoliation of icosahedral quasicrystals. *Adv. Funct. Mat.* 28:1801181.
- [23] Manandhar, K. D., Yadav, T. P., Prajapati, V. K., Kumar, S., Rai, M., Dube, A., Srivastava, O. N. and Sundar S. (2008). Antileishmanial activity of nano-amphotericin B deoxycholate. *J. Antimicro.Chemother.* 62:, 376-380.
- [24] Sudo, S., Kokado, K. and Sada K. (2017). Quantum size effect and catalytic activity of nanosized single-crystalline spherical β -Ga₂O₃ particles by thermal annealing of liquid metal nanoparticles. *RSC Adv.* 7: 678-683.
- [25] Tan, C., Cao, X., Wu, X-J, He, Q., Yang, J., Zhang, X., Chen, J., Zhao, W., Han, S., Nam, G-H, Sindoro, and Zhang, H. (2017). Recent advances in ultrathin two-dimensional nanomaterials. *Chem. Rev.* 117: 6225–6331.
- [26] Gong, Y., Lin, J., Wang, X., Shi, G., Lei, S., Lin, Z., Zou, X., Ye, G., Vajtai, R., Yakobson, B. I., Terrones, H., Terrones, M., Tay, B. K., Lou, J., Pantelides, S.T., Liu, Z., Zhou, W. and Ajayan, P.M. (2014). Vertical and in-plane heterostructures from WS₂/MoS₂ monolayers. *Nature Materials* 13: 1135-1142.
- [27] Du, Z., Yang, S., Li, S., Lou, J., Zhang, S., Wang, S., Li, B., Gong, Y., Song, L. Zou, X. and Ajayan, P. M. (2020). Conversion of non-van der Waals solids to 2D transition-metal chalcogenides. *Nature* 577: 492-496.

- [28] Yang, F., Song, P., Ruan, M. and Xu, W. (2019). Recent progress in two-dimensional nanomaterials: Synthesis, engineering, and applications. *FlatChem* 18: 100133.
- [29] Awasthi, S., Awasthi, K. and Srivastava, O. N. (2018). Formation of Single-walled carbon nanotube buckybooks, graphenenanosheets and metal decorated graphene. *J. of Nano Res.* 53: 37-53.
- [30] Smith, R.J., King, P.J., Lotya, M., Wirtz, C., Khan, U., De, S., O'Neill, A., Duesberg, G.S., Grunlan, J.C., Moriarty, G., Chen, J., Wang, J., Minett, A.I., Nicolosi, V. and Coleman J.N. (2011). Large-scale exfoliation of inorganic layered compounds in aqueous surfactant solutions. *Adv. Mater.* 23 : 3944–3948.
- [31] Coleman, J. N., Lotya, M., O'Neill, A., Bergin, S. D., King, P. J., Khan, U., Young, K., Gaucher, A., De, S., Smith, R. J., Shvets, I. V., Arora, S. K., Stanton, G., Kim, H-Y, Lee, K., Kim, G. T., Duesberg, G. S., et al., (2011). Two-dimensional nanosheets produced by liquid exfoliation of layered materials. *Science* 331: 568-571.
- [32] Nicolosi, V., Chhowalla, M., Kanatzidis, M.G., Strano, M.S. and Coleman, J.N. (2013). Liquid exfoliation of layered materials. *Science* 340: 1226419.
- [33] Das, S., Tama, A. M., Dutta, S., Ali, M. S. And Basith, M. A. (2019). Facile high-yield synthesis of MoS₂ nanosheets with enhanced photocatalytic performance using ultrasound driven exfoliation technique. *Mat. Res. Exp.* 12: 125079.
- [34] Li, L., Zhou, M., Jin, L., Liu, L., Mo, Y., Li, X., Mo, Z., Liu, Z., You, S. and Zhu, H. (2019). Research progress of the liquid-phase exfoliation and stable dispersion mechanism and method of graphene. *Front. Mater.* 6: 325.
- [35] Velický, N. and Toth, P. S. (2017) From two-dimensional materials to their heterostructures: An electrochemist's perspective. *Applied Materials Today* 8: 68-103.
- [36] Jaramillo, T. F., Jørgensen, K. P., Bonde, J., Nielsen, J. H., Horch, S. and Chorkendorff, I. (2007). Identification of active edge sites for electrochemical H₂ evolution from MoS₂ nanocatalysts. *Science* 317: 100-102.
- [37] Balasubramanyam, S., Shirazi, M., Bloodgood, M. A., Wu, L., Verheijen, M. A., Vandalon, V., Kessels, W. M. M., Hofmann, J. P. and Bol, A.A. (2019). Edge-site nanoengineering of WS₂ by low-temperature plasma-enhanced atomic layer deposition for electrocatalytic hydrogen evolution. *Chem. Mater.* 31: 5104–5115.
- [38] Liang, T., Cai, Y., Chen, H. and Xu, M. (2019). *Two-dimensional transition metal dichalcogenides: An overview Book Title: Two dimensional transition metal dichalcogenides*. Switzerland: Springer Nature. pp 1-27.
- [39] Jain, V. and Kandasubramanian, B. (2019). Functionalized graphene materials for hydrogen storage. *J.I. of Mat. Sci.* 55: 1865–1903.
- [40] Liu, G., Wang, Y., Jiao, L. and Yuan, H. (2014). Understanding the role of few-layer graphenenanosheets in enhancing the hydrogen sorption kinetics of magnesium hydride. *ACS Appl. Mater. Interfaces* 6:11038–11046.

Complimentary Contributor Copy

Chapter 16**HYBRID MATERIALS AND THEIR APPLICATIONS**

***Arjita Srivastava, Pravin Kumar Singh, Akram Ali
and Vishal Srivastava****

Department of Chemistry,

CMP Degree College University of Allahabad, Prayagraj, India

ABSTRACT

Hybrid materials have become one of the fastest growing new material classes at the edge of technological innovations. These are products which are composed of two or more different types of components in one polymeric matrix. Recently, hybrid materials have been receiving increased attention by researchers due to their unique properties and superior performance compared to that of conventional inorganic and organic polymeric flocculants. The field of hybrid organic-inorganic materials has reached a stage of perfection that is beginning to materialize as extraordinary new developments. Unique possibilities to generate novel material properties by synergetic combination of inorganic and organic components on the molecular scale makes this materials class interesting for application oriented research of chemists, physicists, and materials scientists. These materials have been used in a wide variety of applications, including energy-storage, electrocatalysis, harnessing of electrochromic and photoelectrochromic properties, application in display devices, photovoltaics, and novel energy-conversion systems. The enhanced recognition and control of the chemistry, processing and microstructure of these versatile nanocomposite systems announces a new landscape of opportunities in in the context of increasingly complex chemistry and materials.

Keywords: hybrid materials, nanocomposites, energy storage, electrochemsitry

* Corresponding Author's Email: vishalgreenchem@gmail.com.

1. INTRODUCTION

The study of hybrid organic-inorganic materials is a recent but very fruitful and productive endeavour. In addition to the early interest in structural hybrid materials, many recent efforts have been done on the design of functional hybrid materials which harness the chemical activity of their components. Hybrid materials represent one of the fastest growing new material classes at the edge of technological innovations. Unique possibilities to create novel material properties by synergetic combination of inorganic and organic components on the molecular scale makes this materials class interesting for application-oriented research of chemists, physicists, and materials scientists. Hybrid organic-inorganic materials in general represent the natural interface between two worlds of chemistry each with very significant contributions to the field of materials science, and each with characteristic properties that result in distinct advantages and limitations. An ancient material, which is the old dye Maya blue, closer to the term hybrid material, is a mixture of a clay mineral and the organic dye indigo that exhibits remarkable high stability which indigo alone does not [1, 2]. This material old dye Maya blue is often mentioned when it comes to the beginning of the history of hybrid materials [3].

Hybrid materials [4] have also been developed in recent years for the coagulation and flocculation purposes for solid-liquid separation in waste water treatment including sludge dewatering for industries such as pulp and paper processing, pharmaceutical, cosmetics, food, mineral processing, metal working, textile and so on [5-7]. Hybrid materials exhibit superior performance than that of individual components [8, 9] due to the synergetic effect of hybrid components in one material. Furthermore, it is also evident that it is beneficial to combine different materials on the macroscopic scale. In materials science, sometimes macroscopic composites are already described as hybrid materials [10]. Therefore, hybrid materials can be considered as artificial systems developed in chemistry and materials science laboratories. In this chapter an attempt has been made to explore the basic concepts and applications of hybrid materials.

2. APPLICATIONS

Hybrid organic-inorganic materials can be functionalized in a number of ways and therefore have found numerous applications in various fields. One of the most common applications is their use as coating materials, particularly in the electronic industry [11]. Optimum functionalizations have been employed to obtain scratch resistance as a primary characteristic in such materials [12-14]. Some of the properties of hybrid materials such as high degree of transparency and mechanical flexibility define their uses in optoelectronic devices [15]. The widespread applications of hybrid materials in integrated circuit systems are already well known. Some of the specific types of such hybrid materials and their applications are as follows:

2.1. Bio Nanocomposites

These biohybrid materials are combinations of inorganic solids and natural polymers and exhibit a variety of functional properties for different applications. One of the primary aims of researchers in this field has been to mimic the amazing characteristics of naturally occurring nanocomposites. Specific types of bio nanocomposites have found numerous applications in tissue regeneration, bone repair, facilitation of cell proliferation and drug delivery [16-18]. Another field full of possibilities is the replacement of petroleum derived synthetic polymers with biopolymers [19-20]. Since these hybrid materials are easily decomposed by microorganisms, they are sustainable for the environment and they also find potential applications in food industry, agriculture, as biomedicine and bioplastics. The introduction of specific functional groups can cause these materials to exhibit excellent catalytic actions as well [21-22].

2.2. Mesoporous Hybrid Materials

Specific functionalizations of thin films of mesoporous silica phases have widespread technical applications [23-24]. There have been successful efforts to create solid state acids that could be alternatives to heterogeneous acid catalysts [25]. Similar functionalizations have been employed for the synthesis of mesoporous silica materials based heterogeneous base catalysts [26]. Mesoporous silica based hybrids have found extensive applications as oxidative catalysts, chiral catalysts, which involve functionalization with alkaloids, amino alcohols, etc. [27-28]. In a study reported by Motorina et al., [29], a SBA-15 phase functionalized with a cinchona derivative was employed for the asymmetric Sharpless dihydroxylation of olefins and excellent enantioselectivities were obtained.

Since the pore size of mesoporous silica hybrid materials is suitable for accommodation of small enzymes and proteins, they have also been applied for enzyme immobilization and biocatalysts. In an excellent study, amino- and carboxy-functionalized SBA-15 phases were used for immobilization of enzyme organophosphorus hydrolase by Lei et al., [30]. The authors were able to achieve double the activity of immobilized enzyme compared to that in the free state.

2.3. Nanocomposite Based Gas Sensors

Organic-Inorganic hybrid materials are extensively in use as smart materials for gas sensing [31]. Other than gas sensors, specifically functionalized nanocomposites have been in use as microwave absorbers, shielding materials, polarizers, etc. [32-33]. Efforts are being made by several research groups for proper tailoring of structural modifications of these nanocomposites to make them ideal candidates for gas

adsorption and detection. Suitably designed nanocomposites have been utilized for detection of VOCs, H₂, CO, CO₂, NH₃, etc. A PANI-MWCNT hybrid nanocomposite was prepared by Li et al., [34] for sensing of hydrocarbon vapors. For detection of NH₃ and HCl, a fabricated carbon nanofiber hybrid material was prepared by Jang et al., [35]. For H₂S gas sensing, PPy/ γ -Fe₂O₃ nanocomposites were prepared by Geng et al., [36]. Apart from gas detection, various different kinds of nanostructures have also been utilized for humidity measurements [37].

2.4. Applications in Coagulation of Waste Water

Amongst all types of hybrid materials, organic-inorganic hybrids have been most extensively used for waste water coagulation and flocculation purposes. Some specific examples such as PDMDAAC has been found very effective in waste water treatment since it can effectively remove pollutants from waste water and can reduce the amount of CHCl₃ formed during treatment of waste water [38-39].

2.5. Sol Gel Derived Hybrid Materials

These class of hybrid materials have many applications as sensors, storage media, insulators and catalysts [40-41]. Magnetic hybrid nanocomposite materials are widely being used for various different applications. One of the most emerging area of interest in this field is the designing of multi-component bio-active materials by incorporation of polysaccharides as biopolymers in nanocomposite synthesis. Various kinds of composite materials have been synthesized using Gum acacia [42], Chitosan [43], Chitin [44], Carageenan [45], Alginate [46], Cellulose [47] etc.

2.6. Nano Diamond Hybrid Materials

Diamond based bioactive hybrid scaffolds can be used for cartilage tissue engineering and for other applications in biomedicine [48]. Nanodiamonds have already been in use as polishing systems, lubricants, grinding, electroplating, magnetic recordings, coatings and catalysts. In some studies, by the covalent rare-earth complex functionalization of nanodiamonds, luminescent hybrid materials have been prepared [49].

2.7. Carbon Nanotubes

Carbon nanotubes are extremely popular among material scientists and have been utilized for a range of different purposes such as field emitters, quantum wires, organic

synthesis catalysts, photocatalysts, diodes, filed emission displays, supercapacitors, electrodes, biosensors and many more [50-51]. The unique properties of carbon nanotubes make them an excellent choice for many applications in different areas. Recently, studies have been going on for improvement in the energy storage properties of carbon nanotube hybrid materials by specific functionalization, specially association with oxides. Jin et al., reported a supercapacitor based on carbon nanotube supported MnO_2 [52]. Similarly, Zhao et al., [53] have synthesized a supercapacitor based CNT supported Fe_2O_3 . CNTs have also been used as an alternative to graphite anode in lithium-ion batteries to improve their performance [54]. The CNT supported oxides have been used for electroanalysis purposes as well and thus find uses in electrochemical sensors [55].

CONCLUSION

Organic-inorganic hybrid materials continue to be one of the most attractive materials since they combine the advantageous characteristics, variability and other property profiles of both organic and inorganic components. Although the general idea behind the synthesis of such hybrids is the enhancing of material properties, sometimes the results are highly exciting with the inclusion of some new characteristic in the hybrid. These materials are a huge topic of interest not only in the research field, but for several industrial applications as well. During the course of last few years, research on advanced methods of synthesis for hybrid materials has been garnering a lot of attention and is highly promising. Continued interest in this field will open up a plethora of applications of hybrid materials in various different areas such as mechanics, environment, medicine, targeted drug delivery, organic reactions, coatings, catalysts, sensors, waste water treatment, etc. Extensive amount of attention is also being paid on the structural control methods and nanostructured hybrids have become a widely researched concept.

REFERENCES

- [1] Van, O. H. (1966). Maya blue: A clay-organic pigment? *Science* 154: 645-646.
- [2] Jose-Yacaman, M., Rendon, L., Arenas, J. and Puche, M. C. S. (1996). Maya blue paint: An ancient nanostructured material. *Science*, 273: 223-225.
- [3] Gomez-Romero, P. and Sanchez, C. (2005). Hybrid materials. Functional properties. From maya blue to 21st century materials. *New J. Chem.* 29: 57-58.
- [4] Moussas, P. A. and Zouboulis, A. I. (2009). A new inorganic-organic composite coagulant, consisting of polyferric sulphate (PFS) and polyacrylamide (PAA), *Water Res.* 43: 3511-3524.

- [5] Zou, J., Zhu, H., Wang, F., Sui, H. and Fan, J. (2011). Preparation of a new inorganic-organic composite flocculant used in solid-liquid separation for waste drilling fluid, *Chem. Eng. J* 171: 350-356.
- [6] Lee, K. E., Teng, T. T., Morad, N., Poh, B. T. and Hong, Y. F. (2010). Flocculation of kaolin in water using novel calcium chloride-polyacrylamide (CaCl₂-PAM) hybrid polymer, *Sep. Purif. Technol.* 75: 346-351.
- [7] Lee, K. E., Teng, T. T., Morad, N., Poh, B. T. and Mahalingam, M. (2011). Flocculation activity of novel ferric chloride-polyacrylamide (FeCl₃-PAM) hybrid polymer, *Desalination* 266: 108-113.
- [8] Tang, H. and Shi, B. (2002). The characteristics of composite flocculants synthesized with inorganic polyaluminium and organic polymers, chemical water and wastewater treatment VII, in: H. H. Hahn, E. Hoffmann, (Eds.), *Proceedings of the 10th Gothenburg Symposium 2002*, Gothenburg, pp. 17-28.
- [9] Yang, W. Y., Qian, J. W. and Shen, Z. Q. (2004). A novel flocculant of Al(OH)₃-polyacrylamide ionic hybrid, *J. Colloid Interf. Sci.* 273, 400-405.
- [10] Ashby, M. F. and Brechet, Y. J. M. (2003). Designing hybrid materials. *Acta Mater.* 51: 5801-5821.
- [11] Haas, K. H., Amberg-Schwab, S., Rose, K. (1999). Functionalized coating materials based on inorganic-organic polymers. *Thin Solid Films* 351: 198-203.
- [12] Wu, G., Wang, J., Shen, J., Yang, T., Zhang, Q., Zhou, B., Deng, Z., Bin, F., Zhou, D., Zhang, F. (2000). Properties of sol-gel derived scratch-resistant nanoporous silica films by a mixed atmosphere treatment. *J. Non-Cryst. Solids*, 275, 169-174.
- [13] Toselli, M., Marini, M., Fabbri, P., Messori, M., Pilati, F. (2007). Sol-gel derived hybrid coatings for the improvement of scratch resistance of polyethylene. *J. Sol-Gel Sci. Technol.* 43: 73-83.
- [14] Textor, T., Mahltig, B. (2010). A sol-gel based surface treatment for preparation of water repellent antistatic textiles. *Appl. Surf. Sci.* 256: 1668-1674.
- [15] Houbertz, R., Domann, G., Cronauer, C., Schmitt, A., Martin, H., Park, J. U., Frohlich, L., Buestrich, R., Popall, M., Streppel, U., et al., (2003). Inorganic-organic hybrid materials for application in optical devices. *Thin Solid Films.* 442: 194-200.
- [16] Darder, M., Aranda, P., Ruiz-Hitzky, E. (2007). Bionanocomposites: A New Concept of Ecological, Bioinspired, and Functional Hybrid Materials. *Adv. Mater.* 19: 1309-1319.
- [17] Shin, H., Jo, S. and Mikos, A. G. (2003). Biomimetic materials for tissue engineering. *Biomaterials*, 24, 4353-4364.
- [18] Palin, E., Liu, H. and Webster, T. J. (2005). Mimicking the nanofeatures of bone increases bone-forming cell adhesion and proliferation. *Nanotechnology* 16: 1828-1835.
- [19] Pandey, J. K., Kumar, A. P., Misra, M., Mohanty, A. K., Drzal, L. T. and Singh, R. P. (2005). Recent advances in biodegradable nanocomposites. *J. Nanosci. Nanotechnol.* 5: 497-526.

- [20] Pandey, J. K. and Singh, R. P. (2005). Green Nanocomposites from Renewable Resources: Effect of Plasticizer on the Structure and Material Properties of Clay-filled Starch. *Starch* 57: 8-15.
- [21] Darder, M., López-Blanco, M., Aranda, P., Leroux, F. and Ruiz-Hitzky, E. (2005). Bio-Nanocomposites Based on Layered Double Hydroxides. *Chem. Mater.* 17: 1969-1977.
- [22] Forano, C., Vial, S. and Mousty, C. (2006). Nanohybrid Enzymes - Layered Double Hydroxides: Potential Applications. *Curr. Nanosci.* 2: 283-294.
- [23] Hoffmann, F., Cornelius, M., Morell, J. and Froba, M. (2006). Silica-based mesoporous organic-inorganic hybrid materials. *Angew. Chem. Int. Ed.* 45: 3216-3251.
- [24] Liu, N., Assink, R. A. and Brinker, C. J. (2003). Synthesis and characterization of highly ordered mesoporous thin films with -COOH terminated pore surfaces. *Chem. Commun.* 370-371.
- [25] Das, D., Lee, J. F. and Cheng, S. (2001). Sulfonic acid functionalized mesoporous MCM-41 silica as a convenient catalyst for Bisphenol-A synthesis. *Chem. Commun.* 2178-2179.
- [26] Weitkamp, J., Hunger, M. and Rymas, U. (2001). Base catalysis on microporous and mesoporous materials: recent progress and perspectives. *Microporous Mesoporous Mater.* 48: 255-270.
- [27] Lee, H. M., Kim, S. W., Hyeon, T. and Kim, B. M. (2001). Asymmetric dihydroxylation using heterogenized cinchona alkaloid ligands on mesoporous silica. *Tetrahedron: Asymmetry* 12: 1537-1541.
- [28] Whang, M. S., Kwon, Y. K. and Kim, G. J. (2002). MCM-41 Supported Chiral Amino Alcohols as Enantioselective Catalysts for the Reduction of Ketones. *J. Ind. Eng. Chem.* 8: 262-267.
- [29] Motorina, I. and Crudden, C. M. (2001). Asymmetric Dihydroxylation of Olefins Using Cinchona Alkaloids on Highly Ordered Inorganic Supports. *Org. Lett.* 3: 2325-2328.
- [30] Lei, C., Shin, Y., Liu, J. and Ackerman, E. J. (2002). Entrapping Enzyme in a Functionalized Nanoporous Support. *J. Am. Chem. Soc.* 124: 11242-11243.
- [31] Kaushik, A., Kumar, R., Arya, S. K., Nair, M., Malhotra, B. D. and Bhanshali, S. (2015). Organic-Inorganic Hybrid Nanocomposite-Based Gas Sensors for Environmental Monitoring. *Chem. Rev.* 115: 4571-4606.
- [32] Carotenuto, G., Nicolais, L., Martorana, B., Perlo, P. (2005). *Metal-Polymer Nanocomposite Synthesis: Novel ex-situ and in-situ Approaches in Metal-Polymer Nanocomposites*; John Wiley & Sons, Inc.: New York, 2005; pp 155-181.
- [33] Mitzi, D. B. (2001). Thin-Film Deposition of Organic-Inorganic Hybrid Materials. *Chem. Mater.* 13: 3283-3298.
- [34] Li, W., Kim, D. (2011). Polyaniline/Multiwall Carbon Nanotube Nanocomposite for Detecting Aromatic Hydrocarbon Vapors. *J. Mater. Sci.* 46: 1857-1861.

- [35] Jang, J., Bae, J. (2007). Carbon Nanofiber/Polypyrrole Nanocable as Toxic Gas Sensor. *Sens. Actuators B* 122: 7-13.
- [36] Geng, L., Wang, S., Zhao, Y., Li, P., Zhang, S., Huang, W., Wu, S. (2006). Study of the Primary Sensitivity of Polypyrrole/r-Fe₂O₃ to Toxic Gases. *Mater. Chem. Phys.* 99: 15-19.
- [37] Lee, C. Y., Lee, G. B. (2005). Humidity Sensors: A Review. *Sens. Lett.* 3: 1-15.
- [38] Lee, K. E., Morad, N., Teng, T. T., and Poh, B. T. (2012). Development, characterization and the application of hybrid materials in coagulation/flocculation of wastewater: A review. *Chemical Engineering Journal*. 203: 370-386.
- [39] Tian, B., Ge, X., Pan, G., Fan, B. and Zhaokun, L. (2006). Adsorption and flocculation behaviors of polydiallyldimethylammonium (PDADMA) salts: influence of counterion, *Int. J. Miner. Process.* 79: 209-216.
- [40] Pandey, S. and Mishra, S. B. (2011). Sol-gel derived organic-inorganic hybrid materials: Synthesis, characterizations and applications. *J Sol-Gel Sci Technol.* 59: 73-94.
- [41] Sepahvand, R., Adeli, M., Astinchap, B. and Kabiri, R. (2008). New nanocomposites containing metal nanoparticles, carbon nanotube and polymer. *J Nanoparticle Res.* 10:1309-1318.
- [42] Tiwari, A., Mishra, A. P., Dhakate, S. R., Khan, R. and Shukla, S. K. (2007). Synthesis of electrically active biopolymer-SiO₂ nanocomposite aerogel. *Mater Lett.* 61: 4587-4590.
- [43] Kato, M., Saruwatari, H., Sakai-Kato, K. and Toy'o'oka, T. (2004). Silica sol-gel/organic hybrid material for protein encapsulated column of capillary electrochromatography. *J Chromatogr A* 1044: 267-270.
- [44] Shchipunov, Y. A., Karpenko, T. Y., Krekoten, A. V. and Postnova, I. V. (2005). Gelling of otherwise nongelable polysaccharides. *J Colloid Interface Sci.* 287: 373-378.
- [45] Shchipunov, Y. A. (2003). *J Colloid Interface Sci.*, 268, 68-76.
- [46] Xu, S. W., Lu, Y., Li, J., Jiang, Z. Y. and Wu, H. (2006). Efficient Conversion of CO₂ to Methanol Catalyzed by Three Dehydrogenases Co-encapsulated in an Alginate-Silica (ALG-SiO₂) Hybrid Gel. *Ind Eng Chem Res.* 45: 4567-4573.
- [47] Mo, Z., Zhao, Z., Chen, H. and Niu, G. (2008). *FuheCailiaoXuebao/ActaMateriaeCompositaeSinica* 25: 24-28.
- [48] Aversa, R., Petrescu, R. V. V., Apicella, A. and Pstrescu, F. I. T. (2017). Nano-Diamond Hybrid Materials for Structural Biomedical Application. *Am. J. Biochem. Biotech.* 13: 34-41.
- [49] Zhang, D., Zhao, Q., Zang, J., Lu, Y. J., Dong, L. and Shan, C. X. (2018). Luminescent hybrid materials based on nanodiamonds. *Carbon* 127: 170-176.
- [50] Zhang, W. D., Xu, B. and Jiang, L. C. (2010). Functional hybrid materials based on carbon nanotubes and metal oxides. *J. Mater. Chem.* 20: 638-6391.

- [51] Ho, Y. M., Zheng, W. T., Li, Y. A., Liu, J. W. and Qi, J. L. (2008). Field Emission Properties of Hybrid Carbon Nanotube–ZnO Nanoparticles. *J. Phys. Chem. C* 112: 17702-17708.
- [52] Jin, X., Zhou, W., Zhang, S. and Chen, G. Z. (2007). Nanoscale Microelectrochemical Cells on Carbon Nanotubes. *Small* 3: 1513-1517.
- [53] Zhao, X., Johnston, C. and Grant, P. S. (2009). A novel hybrid supercapacitor with a carbon nanotube cathode and an iron oxide/carbon nanotube composite anode. *J. Mater. Chem.* 19: 8755-8760.
- [54] Moriguchi, I., Hidaka, R., Yamada, H., Kudo, T., Murakami, H. and Nakashima, N. (2006). A Mesoporous Nanocomposite of TiO₂ and Carbon Nanotubes as a High Rate Li-Intercalation Electrode Material. *Adv. Mater.* 18: 69-73.
- [55] McAuely, C. B., Wildgoose, G. G., Compton, R. G., Shao, L. D. and Green, M. L. H. (2008). Copper oxide nanoparticle impurities are responsible for the electroanalytical detection of glucose seen using multiwalled carbon nanotubes. *Sens. Actuators B* 132: 356-360.

Complimentary Contributor Copy

Chapter 17**ZrO₂ NANOPARTICLE-CATALYZED
ONE-POT MULTI-COMPONENT SYNTHESIS
OF BIO-ACTIVE ORGANIC SCAFFOLDS*****Subhash Banerjee****Department of Chemistry, Guru Ghasidas Vishwavidyalaya,
Bilaspur, Chhattisgarh, India**ABSTRACT**

Synthesis of novel bio-active heterocyclic molecules has attracted considerable attention due to their potential pharmaceutical and medicinal applications. Traditionally, these molecules have been synthesized by multi-step procedure using toxic and expensive catalysts and reagents. Moreover, tedious purification of reaction products in each step, use of volatile and hazardous organic solvents and lower isolated yields are the major limitations of the reported methods. Very recently, metal oxide nanoparticles (NPs) have been widely applied as catalysts in organic synthesis because of their dual Lewis acid and Lewis base nature and red-ox properties on the surface. Among others, ZrO₂ NPs have fascinated much attention in material science due to their specific optical and electrical properties. These nano-materials have also found applications in organic transformations. In this book chapter, applications of ZrO₂ NPs in the synthesis leading to construction of bioactive molecules have been discussed.

Keywords: heterocyclic molecules, nanomaterials, metal oxide nanoparticles**1. INTRODUCTION**

Recently, heterogeneous nano-catalysis have attracted much interest due to their unique properties of large and reactive surface areas, capable of tuning selectivity of

* Corresponding Author's Email: ocsb2006@gmail.com.

product formation, ability to perform the reaction under milder conditions. In addition to these, simple isolation of the particles after the reaction and reuse of the materials after reactions another major advantage of nanocatalysis [1]. The nanomaterials have offered advantages of both homogeneous and heterogeneous catalysis due to their small sizes, high reactivity and recyclability [2].

Among other nanoparticles, metal oxide nanoparticles (NPs) have been widely applied as catalysts because of their dual Lewis acid and Lewis base nature and red-ox properties on the surface [3]. Among other metal oxide nanoparticles, zirconia is a very important ceramic material. This material has been applied in several technologies, for examples, fuel cell electrolytes [4], high-performance transformation-toughened structural engineering ceramic [5], catalysts [6], buffer layers for superconductor growth [7], oxygen sensor [8], damage resistant optical coatings [9], and gate dielectric [10]. Structurally, zirconia is present mainly three different crystalline forms, namely, cubic, tetragonal, and monoclinic polymorphs. Several methods have been investigated reported for the synthesis of zirconia nanoparticles, which include the sol-gel process [11], spray pyrolysis [12], mechanochemical processing [13], salt-assisted aerosol decompositions [14], carbon nanotube templated method [15], and emulsion precipitation [16].

Nanostructured ZrO_2 materials have found wide applications [17] in the material science due to their unique and interesting optical and electrical properties. This is due to their high band gap of $\sim 5\text{eV}$. In catalysis, ZrO_2 NPs were mostly used as the solid support [17-18] or as photocatalysts [19-20].

On the other hand, over past decades, development of protocols for the one-pot multi-component reactions (MCRs) has attracted considerable attention in the context of green chemistry. The MCR permits rapid access to combinatorial libraries of complex biologically active scaffolds [21]. The one-pot MCR protocol offers several advantages over multi-step protocol such as higher isolated yields of desired final products, minimize use of solvents in purification, cost effect, selective formation of products and environmentally benign protocol. In this chapter, green synthesis of biomolecules using reusable ZrO_2 nanoparticles via one-pot multi-component approach has been discussed.

2. APPLICATIONS OF ZrO_2 NANOPARTICLES IN SYNTHESIS BIOACTIVE ORGANIC SCAFFOLDS

Traditionally, ZrO_2 nanoparticles have been used as a support for active catalysts. However, these particles have also shown dual Lewis acid and Lewis base properties due to presence of Zr^{4+} and surface hydroxyl groups. Thus, behave as solid acid-base catalyst. Recently, ZrO_2 nanoparticles were applied as active catalyst for the useful organic synthesis. In the next section, applications of ZrO_2 NPs in multicomponent organic reactions leading to synthesis of biomolecules have been discussed.

2.1. Synthesis of Benzylpyrazolyl Coumarin Derivatives

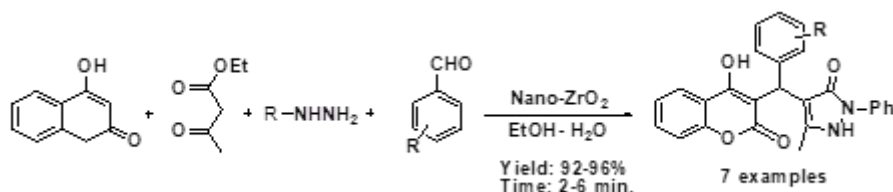
3-Benzylsubstituted 4-hydroxycoumarin derivatives have been found in many natural products and exhibit various biological activities such as warfarin, phenprocoumene, coumatetralyl, carbochromen, bromadiolone offering antibacterial, anti-HIV [22], antiviral [23], anticoagulant [24], antioxidant [25] and anticancer activities [26]. Thus, integrated biological properties can be obtained from a single nucleus which contains 3-benzylsubstituted coumarin and pyrazolone moieties. As a consequence, synthesis of molecular scaffolds comprising both the moieties will be beneficial from the biological point of view.

Banerjee and co-workers [27] have been developed an efficient and green one-pot multi-component protocol for the synthesis of benzylpyrazolyl coumarin derivatives by the reactions of ethyl acetoacetate, phenyl hydrazine, benzaldehyde, 4-hydroxycoumarin using tetragonal ZrO₂ nanoparticles as a reusable catalyst. The reactions were performed in aqueous ethanol under refluxing conditions (Scheme 1). The tetragonal ZrO₂ NPs were found to be more active compared to monoclinic ZrO₂ nanoparticles. This could possibly be due to the higher Lewis acidic properties of tetragonal ZrO₂ NPs. Later on, the *in-silico* binding affinity of benzylpyrazolyl coumarin derivatives to cyclooxygenase-II has been demonstrated [28].

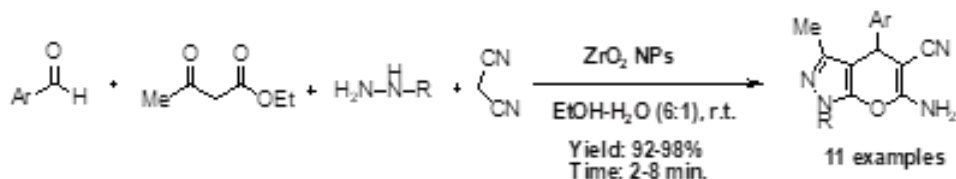
2.2. Synthesis of pyrano[2,3-c]pyrazole Derivatives

On the other hand, synthesis of pyrano[2,3-c]pyrazole derivatives are important as these molecules have potential applications in pharmaceuticals and several methods have been reported in the literature for the synthesis of above molecules [29]. However, most of the reported methods used acidic and basic catalysts and are not reusable.

To overcome the limitations of reported methods, Banerjee and his group have developed a facile one-pot multicomponent protocol [27] for the synthesis of biologically active pyrano[2,3-c]-pyrazole derivatives at room temperature using ZrO₂ NPs as reusable catalyst (Scheme 2). The authors have prepared both tetragonal and monoclinic ZrO₂ NPs by sol-gel method and tetragonal ZrO₂ found to be more reactive than monoclinic one. The catalyst, nano-ZrO₂ was recovered after the reactions and recycled for the subsequent runs.



Scheme 1.

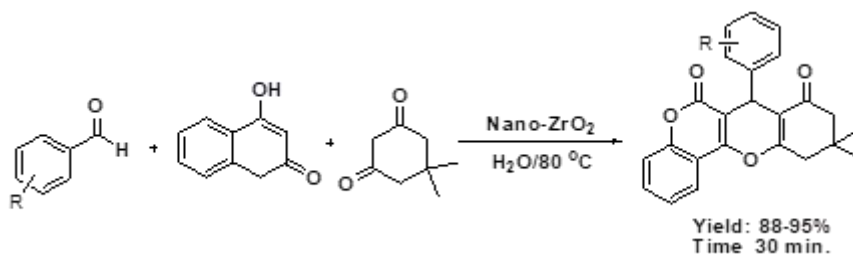


Scheme 2.

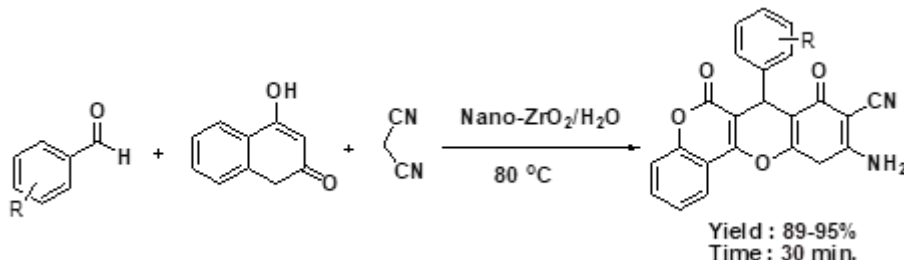
2.3. Synthesis of Bioactive Chromene Derivatives

Banerjee et al., [30] have synthesized 2-aminochromene, dihydropyrano[3,2-c]chromene, and chromeno[4,3-b]chromene by the reactions of aryl aldehydes, dimedone, 4-hydroxycoumarin in the presence of catalytic amount of fluorescent tetragonal ZrO_2 nanoparticles. All the reactions were fast (35-55 min.) high yielding (89-95%) and reactions were performed at 80 °C in aqueous medium (Scheme 3).

On the other hand, when a mixture of dimedone, aromatic aldehydes, and 4-hydroxy coumarin was treated with t- ZrO_2 nanoparticles in water at 80 °C, dihydropyrano[3,2-c] chromene derivatives were obtained in excellent yields within short reaction time (30 min.) [30] (Scheme 4).



Scheme 3.



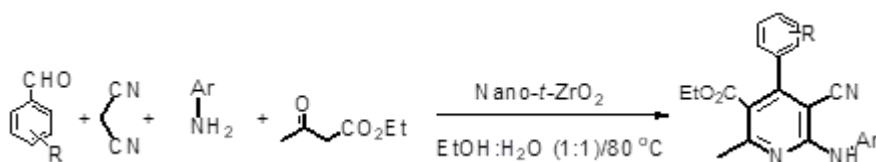
Scheme 4.

2.4. Synthesis of Highly Substituted Pyridine Derivatives

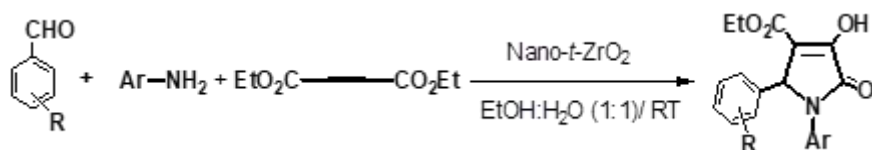
Banerjee and his group [31] have reported a facile synthetic protocol to synthesize a number of ethyl 5-cyano-2-methyl-4-aryl-6-(arylamino)nicotinate by the four component reactions of aromatic aldehydes, malonitrile, aromatic amines and ethyl acetoacetate using tetragonal nano-ZrO₂ as reusable catalyst (Scheme 5). They have studied the stability and recyclability of the catalyst. The ZrO₂ nanoparticles were stable during reaction and apparently no leaching of Zr-content was observed. The ZrO₂ nanoparticles were reused for eight times. The morphology and crystalline nature of the catalyst remained same even after 8th cycles.

2.5. Synthesis of Bio-Active 2-Pyrolidinone Derivatives

The bio-active, 2-pyrolidinone moieties namely, ethyl 4-hydroxy-2-(4-nitroaryl)-5-oxo-1-aryl-2,5-dihydro-1*H*-pyrrole-3-carboxylate derivatives have also been synthesized by Banerjee et al., using tetragonal nano-ZrO₂ as catalyst at room temperature (Scheme 6) [31].



Scheme 5.



Scheme 6.

2.6. Synthesis of pyrido[d]pyrimidine Derivatives

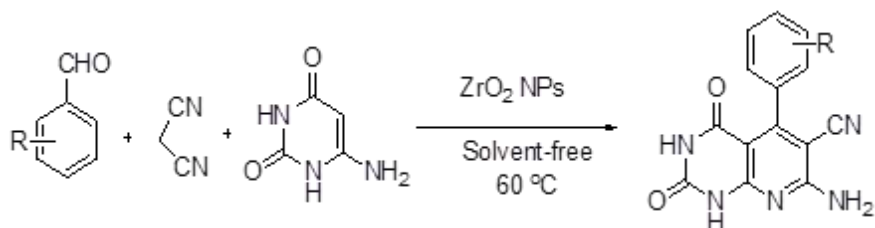
Abdolmohammadi et al., [32] have reported synthesis of pyrido[d]pyrimidine derivatives by the reactions of aromatic aldehydes, malonitrile, 4/6-aminouracil using ZrO₂ NPs under solvent free conditions. The higher isolated yields (86-97%), shorter reaction time (2 h) and solvent-free reaction conditions are the major advantages of the protocol (Scheme 7).

2.7. Synthesis of BOC-ester Derivatives

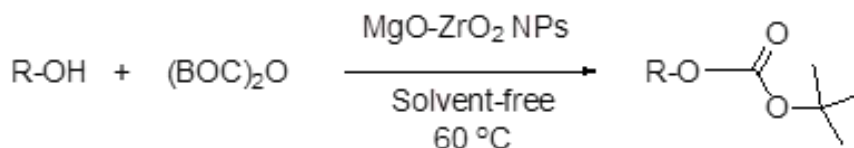
Gawande et al., [33] have prepared MgO-ZrO₂ NPs for the protection of alcohols (aliphatic and aromatic) and phenols under solvent free conditions. The protocol was very simple, efficient and green in nature (Scheme 8).

2.8. Synthesis of pyrano[1,2-a]triazole-1,3-dione Derivatives

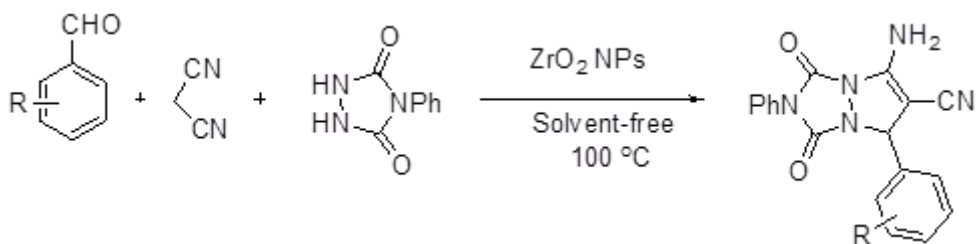
Anaraki-Ardakani and Heidari-Rakati [34] have used ZrO₂ NPs for the one-pot green synthesis of pyrano[1,2-a]triazole-1,3-dione derivatives by the reactions of aromatic aldehydes, malonitrile and 4-phenylurazole (Scheme 9).



Scheme 7.



Scheme 8.



Scheme 9.

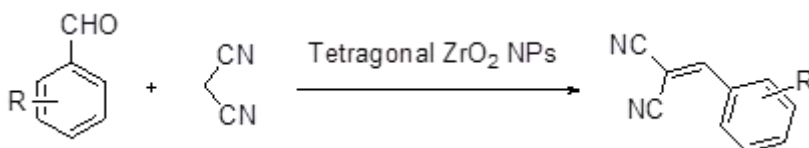
2.9. Knoevenagel Condensation Reaction

Makooti et al., [35] have prepared pure non-monoclinic zirconia nanoparticles by hydrolytic thermal decomposition of zirconyl chloride octahydrate in presence of oleylamine and oleic acid. The pure tetragonal ZrO₂ NPs were used for the

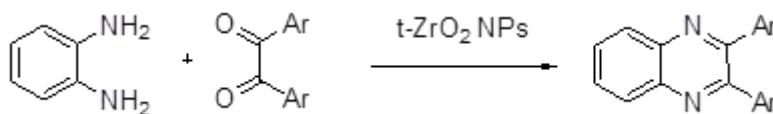
Knoevenagel condensation reactions between aromatic aldehydes and malonitrile (Scheme 10).

2.10. Synthesis of Heterocyclic Compounds via Condensation Reaction

Jafarpur et al., [36] have demonstrated synthesis of 20-40 nm sized ZrO₂ NPs by sol-gel method (polymerizing-complexing) and applied as reusable catalyst for the condensation reactions of 1,2-diamines with dicarbonyl compounds leading to the synthesis of heterocyclic compounds (Scheme 11).



Scheme 10.



Scheme 11.

CONCLUSION

In conclusion, in the chapter, details applications of ZrO₂ NPs in the synthesis of bio-active molecular scaffolds have been presented. The tetragonal ZrO₂ NPs were found to be more active compared to monoclinic NPs. This is due to higher Lewis acidic properties of tetragonal ZrO₂ NPs. Moreover, these NPs were very stable in the reactions and reused for many times without change in catalytic performance. Finally, this chapter will be beneficial for the material scientist as well as synthetic organic chemists.

ACKNOWLEDGMENT

We are pleased to acknowledge Chhattisgarh Council of Science & Technology (CCOST), Raipur, Chhattisgarh (ENDT No 2096/CCOST/MRP/2017) and Department of Chemistry, Guru Ghasidas Vishwavidyalaya.

REFERENCES

- [1] Astruc, D. (2008). Transition metal nanoparticles in catalysis: From Historical Background to the State of the Art. *Nanopart. Catalysis* 1-48.
- [2] Gawande, M., Branco, P. and Varma, R. S. (2013). Nano-magnetite (Fe_3O_4) as a support for recyclable catalysts in the development of sustainable methodologies. *Chem. Soc. Rev.* 42: 3371.
- [3] Bell, A. (2003). The impact of nanoscience on heterogeneous catalysis. *Science* 299: 1688.
- [4] Badwal, S. P. S. Yttria (1990). Tetragonal zirconia polycrystalline electrolytes for solid state electrochemical cells. *Appl. Phys.* A50: 449.
- [5] Garvie, R. C., Hannink, R. H. and Pascoe, R. T. (1975). Formation characterization and rheological properties of zirconia and ceria-stabilized zirconia. *Nature* 258: 703.
- [6] Haw, J. F., Zhang, J., Shimizu, K., Venkatraman, T. N., Luigi, D. P., Song, W., Barich, D. H. and Nicholas, J. B. (2000). NMR and theoretical study of acidity probes on sulfated zirconia catalysts. *J. Am. Chem. Soc.* 122: 12561.
- [7] Phillips, J. M. (1996). Substrate selection for high temperature superconducting thin films. *J. Appl. Phys.* 79: 1829.
- [8] León, C., Lucía, M. L. and Santamaría, J. (1997). Correlated ion hopping in single-crystal yttria-stabilized zirconia. *Phys. Rev. B* 55: 882.
- [9] Mansour, N., Mansour, K., Stryland, E. W. V. and Soileau, M. J. (1990). Diffusion of color centers generated by two photon absorption at 532 nm in cubic zirconia. *J. Appl. Phys.* 67: 1475.
- [10] Wilk, G. D., Wallace, R. M. and Anthony, J. M. (2001). High- κ gate dielectrics: Current status and materials properties considerations. *J. Appl. Phys.* 89: 5243.
- [11] Moon, Y. T., Park, H. K., Kim, D. K. and Kim, C. H. (1995). Preparation of monodisperse ZrO_2 by the microwave heating of zirconyl chloride solutions. *J. Am. Ceram. Soc.*, 78: 2690.
- [12] Stichert, W. and Schüth, F. (1998). Influence of crystallite size on the properties of zirconia. *Chem. Mater.* 10, 2020.
- [13] McCormick, P. G., Tsuzuki, T., Robinson, J. S. and Ding, J. (2001). Nanopowders synthesized by mechanochemical processing. *Adv. Mater.* 13: 1008.
- [14] Xia, B., Lenggoro, I. W. and Okuyama, K. (2001). Novel route to nanoparticle synthesis by salt assisted aerosol decomposition. *Adv. Mater.* 13: 1579.
- [15] Rao, C. N. R., Satishkumar, B. C. and Govindaraj, A. (1997). Zirconia nanotubes. *Chem. Commun.* 1581-1582.
- [16] Woudenberg, F. C. M., Sager, W. F. C., Sibelt, N. G. M. and Verweij, H. (2001) Dense nanostructured ZrO_2 coatings at low temperatures via modified emulsion precipitation. *Adv. Mater.* 13:514.
- [17] Ardiyanti, A. R., Gutierrez, A., Honkela, M. L., Krause, A. O. I. and Heeres, H. J. (2011). Hydrotreatment of wood-based pyrolysis oil using zirconia-supported mono- and bimetallic (Pt, Pd, Rh) catalysts. *Appl. Catal. A*, 407: 56.

- [18] Guerrero, S., Araya, P. and Wolf, E. E. (2006). Methane combustion over Pd/Al₂O₃ catalyst: Effects of chlorine ions and water on catalytic activity. *Appl. Catal.*, A298: 243.
- [19] Chen, X., Wang, X. and Fu, X. (2009). Hierarchical macro/mesoporous TiO₂/SiO₂ and TiO₂/ZrO₂ nanocomposites for environmental photocatalysis. *Energy Environ. Sci.* 2: 872.
- [20] Zheng, H., Liu, K., Cao, H. and Zhang, X. (2009). L-Lysine-assisted synthesis of ZrO₂ nanocrystals and their application in photocatalysis. *J. Phys. Chem. C.* 113: 18259.
- [21] Samai, S. Nandi, G. C., Kumar, R., Singh, M. S. (2009). Multicomponent one-pot solvent-free synthesis of functionalized unsymmetrical dihydro-1H-indeno[1,2-b]pyridines. *Tetrahedron Lett.* 50: 7096.
- [22] Hesse, S. and Kirsch, G. A (2002). Rapid access to coumarin derivatives (using Vilsmeier-Haack and Suzuki cross-coupling reactions). *Tetrahedron Lett.* 43: 1213.
- [23] Lee, B. H., Clothier, M. F., Dutton, F. E., Conder, G. A. and Johnson, S. S. (1998). Anthelmintic β -hydroxyketoamides (BKAs). *Bioorg. Med. Chem. Lett.* 8: 3317.
- [24] Jung, J. C., Jung, Y. J. and Park, O. S. (2001). A convenient one-pot synthesis of 4-Hydroxycoumarin, 4-Hydroxythiocoumarin and 4-Hydroxyquinolin-2(1h)-One. *Synth. Commun.* 31: 1195.
- [25] Melagraki, G., A. Afantitis, O. Igglessi-Markopoulou, A. Detsi, M. Koufaki, C. Kontogiorgis, D. J. and Hadjipavlou-Litina (2009). Synthesis and evaluation of the antioxidant and anti-inflammatory activity of novel coumarin-3-aminoamides and their alpha-lipoic acid adducts. *Eur. J. Med. Chem.* 44: 3020.
- [26] Jung, J. C., Lee, J. H., Oh, S., Lee, J. G. and Park, O. S. (2004). Synthesis and antitumor activity of 4-hydroxycoumarin derivatives. *Bioorg. Med. Chem. Lett.*, 14: 5527.
- [27] Saha, A., Payra, S. and Banerjee, S. (2015). One-pot multicomponent synthesis of highly functionalized bio-active pyrano[2,3-c]pyrazole and benzylpyrazolylcoumarin derivatives using ZrO₂ nanoparticles as a reusable catalyst. *Green Chem.* 17: 2859-2866.
- [28] Saha, A., Payra, S., Verma, S. K., Mandal, M., Thareja, S. and Banerjee, S. (2015). In-silico binding affinity to cyclooxygenase-II and green synthesis of benzylpyrazolyl coumarin derivatives. *RSC Adv.* 5: 100978-100983.
- [29] Wang, J. L., Liu, D., Zheng, Z. J., Shan, S., Han, X., Srinivasula, S. M., Croce, C. M., Alnemri, E. S. and Huang, Z. (2009). Structure-based discovery of an organic compound that binds Bcl-2 protein and induces apoptosis of tumor cells. *Proc. Natl. Acad. Sci. U.S.A.* 97, 7124.
- [30] Saha, A., Payra, S. and Banerjee, S. (2015). On water synthesis of pyran-chromenes via a multi-component reactions catalyzed by fluorescent t-ZrO₂ nanoparticles. *RSC Adv.* 5: 101664.

- [31] Saha, A., Payra, S. and Banerjee, S. (2016). In-water facile synthesis of poly-substituted 6-Arylamino pyridines and 2-Pyrrolidone derivatives using tetragonal nano-ZrO₂ as reusable catalyst. *RSC Adv.* 6: 101953-101959.
- [32] Abdolmohammadi, S. and Balalaie, S. (2012). A clean procedure for synthesis of Pyrido[d]Pyrimidine derivatives under solvent-free conditions catalyzed by ZrO₂nanoparticles. *Comb. Chem. High Throughput Screen.* 15: 395-399.
- [33] Gawande, M. B., Shelke, S. N., Branco, P. S., Rathi, A. and Pandey, R. K. (2012). Mixed metal MgO–ZrO₂ nanoparticle catalyzed OtertBoc protection of alcohols and phenols under solvent free conditions. *Appl. Organometallic Chem.* 26: 395-400.
- [34] Anaraki-Ardakani, H. and Heidari-Rakati, T. (2016). Zirconium oxide nanoparticles as an efficient catalyst for three-component synthesis of Pyrazolo[1,2-A][1,2,4]Triazole-1,3-Diones derivatives. *Orient. J. Chem.* 32: 1625-1629.
- [35] Malakooti, R., Mahmoudi, H., Hosseinabadi, R., Petrovb, S. and Miglioric, A. (2013). Facile synthesis of pure non-monoclinic zirconia nanoparticles and their catalytic activity investigations for Knoevenagel condensation. *RSC Adv.* 3: 22353.
- [36] Jaarpour, M., Rezapour, E., Ghahramaninezhad, M. and Rezaeifard, A. (2014). A novel protocol for selective synthesis of monoclinic zirconia nanoparticles as a heterogeneous catalyst for condensation of 1,2-diamines with 1,2-dicarbonyl compounds. *New J. Chem.* 38: 676.

Chapter 18**BIOREMEDIATION OF BAUXITE RESIDUE DUMPING
SITES OF ALUMINA INDUSTRY*****Kumud Dubey^{1,*} and K. P. Dubey²***¹Forestry Research Centre for Eco-Rehabilitation, Prayagraj, INDIA²Principal Chief Conservator of Forest (I/C Project), Environment,
Forest & Climate Change Department, Lucknow, INDIA**ABSTRACT**

Bauxite residue (Red mud) is an industrial waste byproduct of Alumina industry. It is very toxic and highly alkaline in nature and contains heavy metal oxides and variety of minor trace elements. Its disposal is the paramount environmental issue in Alumina refining processes and responsible for contamination of nearby forest soil, difficult to establish vegetation on red mud dumping sites. The bioremediation of Red Mud only seems to be a realistically convenient and suitable way for environmentally safe disposal of this toxic alkaline industrial waste residue. In an Indian Council of Forestry Research and Education, Dehradun sponsored research project, the bioremediation of red mud was carried out through *Cyanobacteria* and other bio-amendments. For study, M/s Hindalco Industries Ltd. (HINDALCo), India, was selected for study as it is the only Aluminium production industry functioning in Sonbhadra, Uttar Pradesh. Red Mud sample was analyzed for its physico-chemical characteristics. For Bioremediation studies, four Cyanobacteria species viz. *Oscillatoria sp.*, *Lyngbya sp.*, *Phormidium sp.* and *Microcystis sp.* were selected. These four Cyanobacteria species were subsequently cultured and propagated on liquid Blue Green Algae culturing medium BG-11 with different amendements of Red mud. Based on these, the physical growth of these Cyanobacteria in Red mud amended medium and their effect on physico-chemical characteristics of red mud, the promising cyanobacterial species were selected for bioremediation. Bioremediation through

* Corresponding Author's Email: dkumud@yahoo.com.

biomining/bioleaching and nano particles is also discussed for reducing the environmental risk of red mud.

Keywords: bioremediation, cyanobacteria, reclamation, nanotechnology, bauxite residue

1. INTRODUCTION

To meet the ever-growing demand of materials, the natural resources are being exploited to the fullest extent. As a result of which there is depletion of these valuable resources as well as accumulation of different types of wastes. Bauxite Residue, also known as Red Mud, is one such waste produced during alumina extraction from bauxite ore with concentrated NaOH at elevated temperature in the Bayer's process. Red mud composition varies depending on raw material composition [1].

Aluminium is the most abundantly available metal and the third most plentiful element (8%) of the earth. The economic ore of Aluminium is bauxite, $\text{Al}_2\text{O}_3 \cdot x\text{H}_2\text{O}$, which is always associated with silica, iron oxide; titanium dioxide and few others minor and traces impurities [2]. To produce primary Aluminium, the Aluminium compounds in the bauxite are first dissolved chemically, using caustic soda, in alumina refinery using the Bayer process. This produces Aluminium oxide and a waste product Bauxite Residue (Red mud), which is a slurry containing natural substances originally present in the Bauxite - i.e., the ore residues with a residual amount of alkali and left over from the process. The high concentration of iron compounds gives the waste product its characteristic red colour. The amount of red mud produced depends on the Aluminium content of the bauxite. Bauxite ores with a high Aluminium content result in lower ore residues than bauxite ores with a lower Aluminium content. Red mud is highly alkaline in nature and contains oxides and salts of six major oxides of Fe, Al, Ti, Si, Na, Ca, and a variety of minor trace elements. Red mud is then disposed of at a special holding site. By maximizing the separation of the caustic soda from the ore residues, one achieves the optimal conditions for disposal. Around 1.5–2.5 tons of red mud is generated per ton of alumina produced, depending on the bauxite source and alumina extraction efficiencies. The disposal of red mud is big problem and hazardous [3-5].

1.1. Dumping of Bauxtie Residue

Due to its large volume, high pH, high caustic soda content and high iron oxide content, Red mud disposal remains an issue of great importance with environmental implications in the alumina industry. Red mud till today is disposed off from the plant in two conventional ways depending upon the facilities available and surrounding conditions either in form of slurries (with 15–40% solids) which is disposed off to nearby pools made for this purpose where slurry is left open for sun drying. The other

way is after drying in the form of heaps or impoundment reservoirs in nearby areas. Conventional disposal methods have revolved around the construction of clay-lined dams or dykes, into which the red mud slurry is simply pumped and allowed to dry naturally [6]. The design and construction of such residue impoundments has varied considerably over the years [7], with disposal practices generally dependent upon the nature of the immediate environment. It was noted that the operation of these conventional disposal areas was simple and inexpensive, however the potential impact on the surrounding groundwater and environment, and difficulties associated with surface rehabilitation, forced significant changes in disposal practices. This led to the construction of doubly sealed impoundments, incorporating a polymeric membrane as well as clay lining, and drained lakes, having a drainage network incorporated in the lining material, have subsequently seen widespread use. Drained disposal systems have been found to reduce the threat of the residue to the environment, while also increasing storage capacity as a result of better residue consolidation [8]. The problem associated with the Red mud storage is leakage of alkaline compounds into the ground water, over flow of caustic from red mud pond during rainy season, dusting of dry surfaces during summer season, which contaminate the surrounding environment and interfere in rehabilitation efforts [3-5, 9-12]. Moreover its disposal requires large areas of land which become abandoned and exposed to wind and water erosion. Three major problems are associated with the disposal of red mud that are space, cost of disposal and pollution hazards which has become more acute with increasing amount of red mud. As an alternative, dry disposal of Red mud, involving enhanced dewatering and evaporative drying, has also been found to further decrease environmental risks and lower overall disposal costs [13].

For disposal, initially, the residue is washed, to extract as much valuable caustic soda and dissolved alumina as possible. The caustic soda is recycled back into the digestion process, reducing production costs and in turn lowering the alkalinity of the residue. The pH level of the residue is generally up to 13 or higher in some cases, due to the presence of alkaline sodium compounds, such as sodium carbonate and sodium hydroxide.

Like most ores and soils, bauxite can contain trace quantities of metals such as arsenic, beryllium, cadmium, chromium, lead, manganese, mercury, nickel and naturally-occurring radioactive materials, such as thorium and uranium. Most of these trace elements remain with the Red mud after extraction of the alumina. After washing the Red mud is contained in special facilities known as Bauxite Residue Disposal Areas (BRDA) or Residue Storage Areas (RSA).

1.2. Bauxite Residue Disposal Areas (BRDA)

The type of disposal employed by alumina refineries varies across the world, depending on factors such as land availability, technology availability, climatic & geographic conditions, logistics and regulatory requirements [14]. Companies are

required to ensure that BRDAs comply with the respective environmental standards. Modern BRDA guidelines will include both general and location-specific design criteria such as soil conditions, earthquake risk, long term stability and management of storm events. Careful monitoring ensures structural integrity is maintained.

1.3. Dry Disposal

After being washed, the Red mud is filtered to produce a dry cake (> 65% solids). Drum filters have been used since the 1930s but there is now increasing use of press filters capable of achieving 70 to 75% solids. The dry Red mud material is carried by truck or conveyor to the storage site and stored without further treatment.

This method minimizes the land area required for storage and the risk of leakage to groundwater. Rehabilitation and closure costs are greatly reduced and the material is in a more readily usable form. For sites with a constrained space this approach can often present the best option.

1.4. Mud/Dry Stacking or “Sloped Deposition”

The Red mud is thickened to a high density slurry (48-55% solids or higher), deposited and allowed to consolidate and dry before successive layers deposit. This forms a slope on the deposit, allowing rainwater to run off and minimizing liquid stored in the disposal area; lowering risk of leakage and improving structural integrity.

The water reclaimed from the surface is pumped back to the plant to recover and recycle the soluble sodium salts. Dry stacked red mud is often “under-drained” to improve the consolidation of the residue and recover further water for re-use in the refinery. The combination of dry stacking and a well drained deposits leads to a very stable deposit of red mud.

1.5. Lagooning/Ponding

The red mud is pumped into land based ponds where naturally impervious layers or sealants, minimize seepage. The red mud is typically deposited as dilute slurry, with the solids settling and consolidating over time and the surface water collected for return to the refining process. The design, construction and operation of these storage dams follow guidelines as set out in individual countries and undergo regular maintenance checks.

1.6. Sea Water Discharge

In some countries an early method of bauxite residue (red mud) disposal was to transfer the material via pipeline to deep sea locations following treatment to reduce caustic soda levels. No new refineries have been built using this method since 1970.

1.7. Environmental Risks Associated with Red Mud Disposal and Utilization

The main environmental risks associated with bauxite residue are related to high pH and alkalinity and minor and trace amounts of heavy metals and radionuclides. Establishment of vegetation on these bauxite residue dumping sites is imperative for reducing the environmental risk [15]. Very high pH, very fine in structure, high content of oxides of iron and other metals and deficient in soil nutrients make Bauxite residue (red mud) dumping sites, a poor substrate to re-vegetate [16].

Irrespective to the mode of disposal, red mud is cause of environmental hazards to the surroundings. The environmental chemistry and toxicity of Aluminium in red mud may be significant under such alkaline conditions. Red mud of similar composition may create different types of pollution under different environmental conditions. The conditions are available sunshine, annual rain fall, average temperature, wind velocity, soil permeability and so on for the land disposal while for the sea disposal it depends on specific zone, length of inlet pipe, depth at that point, variety of fish culture and under currents, if any. For utilizing red mud as a soil conditioner, amelioration of red mud disposal sites is essential [17].

1.8. Remediation of Bauxite Residue Pond

A review on uses of red mud was discussed by Ning et al. (2019) [18]. It was stated that based on resource, economic, and environmental benefits, the development of new technologies and new processes with market competitiveness, environmental protection, and ecological balance should be the prerequisite for the low-energy, low-pollution, low-cost, and high-efficiency comprehensive utilization of Red Mud [18]. Three step remediation of Landscape, after the bauxite Residue (Red Mud) disaster in Hungary, was conducted by Gyuricza et al. (2012) [19]. The three-step plan included: (1) the key element of habitat revitalization to recover the soil biological activity and the prevention of the dusting out of the red sludge; (2) after the application of compost-turf mixture to the soil (1st remediation step), annual plants were sown on the area (2nd remediation step), which ensures the quick cover of the soil with vegetation and organic matter replacement; and (3) creating an short rotation coppice plantation (3rd remediation step).

Andrew et al. (2018) [20] stated that Rehabilitation of bauxite residue disposal areas (BRDA) is therefore often costly and resource/infrastructure intensive and associated with its remediation. Data is presented from three neighboring plots of bauxite residue that was deposited 20 years ago. One plot was amended 16 years ago with process sand, organic matter, gypsum, and seeded (fully treated), another plot was amended 16 years ago with process sand, organic matter, and seeded (partially treated), and a third plot was left untreated. These surface treatments lower alkalinity and salinity, and thus produce a substrate more suitable for biological colonisation from seeding. The reduction of pH leads to much lower Al, As and V mobility in the actively treated residue and the beneficial effects of treatment extend passively 20–30 cm below the depth of the original amendment. These positive rehabilitation effects are maintained after 2 decades due to the presence of an active and resilient biological community. This treatment may provide a lower cost solution to BRDA end of use closure plans and orphaned BRDA rehabilitation.

The bio-remediation of red mud seems to be the realistically convenient steps for the disposal of this industrial residue. Bioremediation is a low cost and environmental friendly technique which uses plants and microbes to clean up moderately contaminated areas, lessening metal mobility and bioavailability. The present Chapter is focused on the effect of different Blue green algae/ bioinoculants on the phytotoxicity of the red mud, its bioremediation and selection of promising Blue green algae/bioinoculants for bio-remediation of red mud.

2. METHODOLOGY

2.1. Site Survey and Sample Collection

M/s Hindalco Industries Ltd. (HINDALCo), India, was selected for study as it is the only Aluminium production industry functioning in the State of Uttar Pradesh, India. The Company is situated at Renukoot, Sonbhadra District, and Uttar Pradesh. Hindalco was visited for surveying Red Mud production site with permission of HINDALCo authorities. HINDALCo dumps Red Mud after carrying out a drying process, called Dry Stacking of Red Mud. Triplicate samples of Red mud were collected from HINDALCo and mixed thoroughly for physico chemical analysis. The Red mud sample was analyzed for pH, EC, Organic Carbon and Nitrogen.

2.2. Selection of Promising Cyanobacteria for Bioremediation of Red Mud

Four cyanobacteria viz. *Oscillatoria sp.*, *Lyngbya sp.*, *Phormidium sp.* and *Microcystis sp.* were selected for the study and cultured and propagated on liquid

BG11 medium [21]. These cyanobacteria were reported as dominating species of industrial effluents and tolerant to pollution [21-23].

2.3. To Study the Promising Cyanobacteria on Red Mud Amendments with Different Treatments in Nursery Conditions

Experiment was laid out in trays for studying the effect of Cyanobacteria viz.: *Lyngbya*, *Phormidium*, *Oscillatoria* and *Microcystis* spp on red mud amendments with different treatments in nursery conditions for selection of promising Cyanobacteria for further studies. Effect on red mud was studied with different bio-amendments. Cyanobacterial growth was observed on red mud with different amendments. Treatments were Control 1 (Red mud), Control 2 (Red mud mixed with normal soil in 1:1 amended with Bone Meal bio-source of phosphorus), Red mud mixed with normal soil and Bone Meal inoculated with *Phormidium*, Red mud mixed with normal soil and Bone Meal inoculated with *Oscillatoria*, Red mud mixed with normal soil and Bone Meal inoculated with *Lyngbya*, Red mud mixed with normal soil and Bone Meal inoculated with *Microcystis*. Soil pH, EC, Organic matter and nitrogen was monitored as indicators of bioremediation.

3. RESULTS

3.1. Site Description and Red Mud Characteristics

HINDALCo, India, was selected for the study as it is the only Aluminium production industry functioning in Uttar Pradesh, India. The company was established in 1958, HINDALCo commissioned its aluminium production at Renukoot in Sonbhadra District of Eastern U.P. in 1962. HINDALCo's Alumina Plant employs the conventional Bayer's process for Aluminium extraction. Initially it was commissioned with capacity of 40,000 MTPA which was increased to 700,000 MTPA. The Company has been inducting new technology from time to time and the most recent initiative in this regard is the adoption of Alusuisse Precipitation Technology for energy efficiency and capacity enhancement. The major raw materials for the Alumina Plant are Bauxite, Steam and Caustic Soda. Bauxite is procured from the Company's Mines in Jharkhand and Chhatisgarh, as well as through market purchases and requirement of steam is met through Cogeneration plant at Renukoot. HINDALCo dumps Red Mud after carrying out a drying process, called Dry Stacking of Red Mud [24]. Red mud is dried through Drum Filter Unit and finally disposed to dumping site. In HINDALCo average red mud Disposal is 3200-3500 Dry MT/ Day. Red Mud is highly alkaline in nature having a very high pH in the range of 10.5 – 13 due to the presence of Sodium Hydroxide (NaOH) and Sodium Carbonate (Na₂CO₃). These compounds are expressed in terms of Na₂O. The composition of Red Mud sample, provided by the HINDALCo Industries,

Renukoot, Sonebhadra, Uttar Pradesh, India, has been depicted in (Figure-3.1.1). The pH and EC, Organic carbon and Nitrogen were depicted in Figure 3.1.2 and 3.1.3.

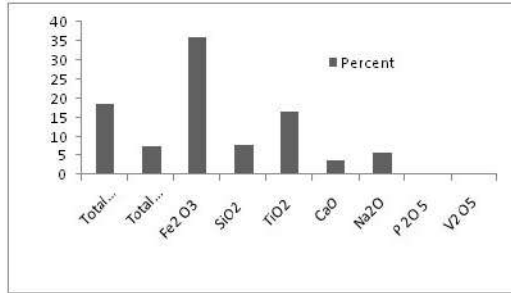


Figure 3.1.1. The composition of Red Mud sample.

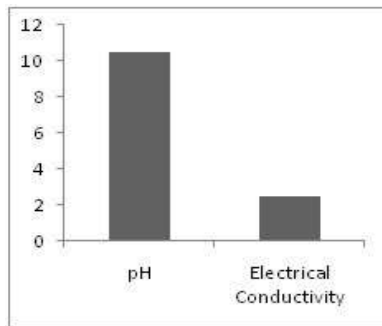


Figure 3.1.2. pH and EC of Red Mud.

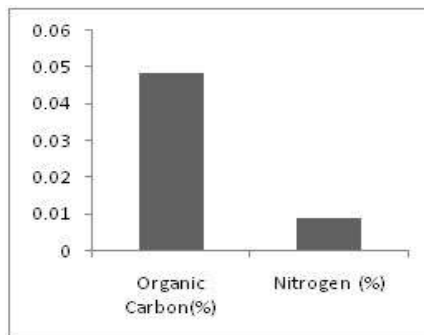


Figure 3.1.3. Organic Carbon and Nitrogen of Red Mud.

3.2. Selection of Promising Cyanobacteria for Bioremediation of Red Mud

Experiment was laid out in trays for studying the effect of Cyanobacteria viz: *Lyngbya*, *Phormidium*, *Oscillatoria* and *Microcystis* *sps* on red mud amendments with different treatments in nursery conditions for selection of promising Cyanobacteria for

further studies. Effect on red mud was studied with different bio-amendments. Cyanobacterial growth was observed on red mud with different amendments with ocular observations. Growth wise the *Phormidium* and *Oscillatoria* had given plus three (+3), *Lyngbya* plus two(+2) and for *Microcystis* plus one (+1). The Soil pH, EC, Organic carbon and nitrogen was observed after 45 days and depicted in following Figure 3.2.1 a, b, c and d:

Based on these, the physical growth of these Cyanobacteria in Red mud amended medium and their effect on physico-chemical characteristics of red mud, the promising cyanobacterial species were selected for bioremediation. Two cyanobacterial species viz. *Phormidium* and *Oscillatoria* were identified promising for bioremediation of red mud. They improve the red mud by reducing its pH, increasing organic carbon, nitrogen content, and reducing its toxicity by reducing its heavy metals.

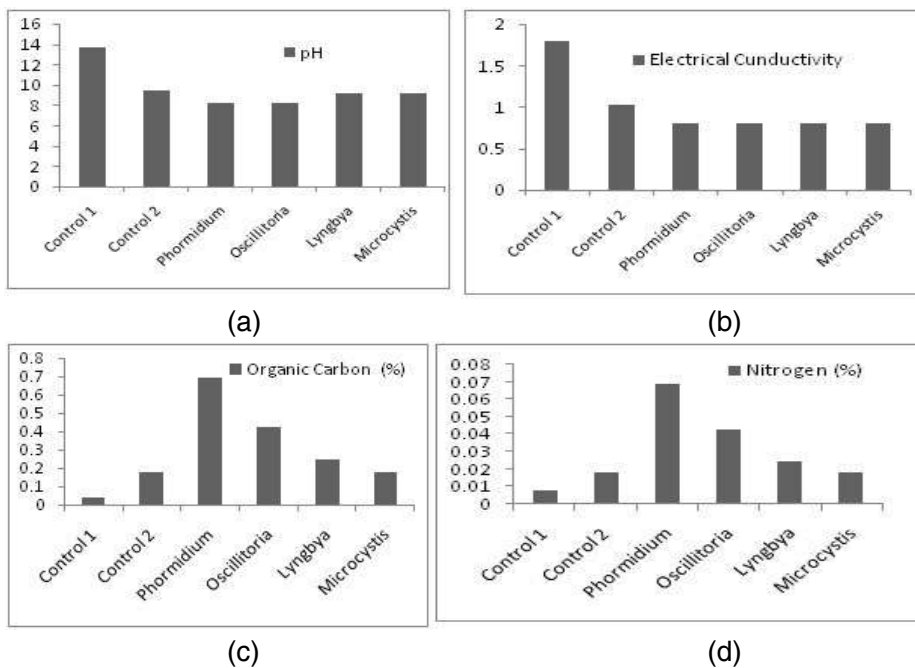


Figure 3.2.1. Effect of Cyanobacterial inoculation on Characteristics of Red mud with different treatments (a) pH, (b) Electrical Conductivity, (c) Organic Carbon and (d) Nitrogen.

As cyanobacteria are considered as an important group of micro-organisms having ability to carry out both photosynthesis as well as nitrogen fixation non-symbiotically, they may be applied to remediate bauxite residue. It has the added bonus of being photosynthesizers, which supply organic carbon at a rapid rate and self propagating, once inoculated. They also act as an important tool for ensuring assimilation of carbon and its sequestration concomitantly [22]. These form a mat or crust like structures on soil surface, which are not only resistant to metals and metalloids but also remove these harmful substances from the environment. These Cyanobacterial mats are an ideal system for bioremediation of mine wastes that are significantly hazardous to

human health [23, 25]. Cyanobacteria have also been reported as agents for bioremediation of alkali soils due to their ability to secrete organic acids and immobilize sodium in the biomass [26-32]. Cyanobacteria have also been found to remove harmful metals from the environment through their biosorption to extracellular polysaccharides and their intracellular accumulation involving metal sequestering metallothionein proteins. This Cyanobacterium remediate by both adsorbing and taking up metal ions [33]. *Phormidium* can adsorb heavy trace metals [34- 35]. Biosorption of Zinc was reported by *Oscillatoria sp.* [36]. The *Phormidium* and *Oscillatoria* cyanobacterial morphotypes have been used for bioremediating the sites contaminated with petroleum products [37]. The cyanobacterial crusts may help in surface soil stabilization, increasing water infiltration and reducing wind and water erosion. These findings too, strongly support the principle that Cyanobacteria may play a major role in detoxifying Red Mud by immobilizing heavy metals, establishment of crust on Red Mud dumps thereby reducing the environmental risks due to water and wind erosion and enriching its nutrient status in an environmentally sustainably way.

3.3. Biomining and Bioleaching for Bioremediation

Biomining is the process of using microorganisms (microbes) to extract metals from rock ores or mine waste. This techniques may also be used to remove toxic metal contaminants from the bauxite residue dumping sites. For example, The Iron may be removed/ recovered from bauxite residue by exploiting the metabolism of iron reducing microorganisms like *Desulfuromonas palmitatis* [38-39]. The green microalgae like *Desmodesmus quadricauda*, *Chlamydomonas reinhardtii*, etc. and fungi like *Penicillium tricolor* and *Aspergillus niger* may be used to remove lanthanides and other metals from Bauxite residue through intracellular accumulation [40]. Bio-mining techniques are generally less energy-intensive and less polluting. Through Biomining or bioleaching, *in situ* bioremediation of bauxite residue storage ponds may be done. Establishment of the microbial ecology of the waste is essential, and acid-forming capabilities of indigenous microorganisms need to be ascertained. Native microorganisms producing organic acids may be used to neutralize red mud alkalinity [41]. Bio-mining/Bioleaching techniques are generally less energy-intensive and less polluting.

3.4. Application of Nanotechnology

Recent days, nanotechnology has also shown promising potential to promote sustainable remediation of contaminated soils. It may play an important role regarding the fate, mobility and toxicity of soil pollutants and are essential part of different biotic and abiotic remediation strategies. Nano material may be applied for bioremediation, which will not only have less toxic effect on microorganisms, but will also improve the

microbial activity of the specific waste and toxic material which will reduce the overall time consumption as well as reduce the overall cost [42]. Plant *Noaea mucronata* belonging to Chenopodiaceae is good accumulator of heavy metals like Pb, Zn, Cu, and Ni. Likewise *Reseda lutea* is good accumulator of Fe. The bioaccumulation ability of nano-particles prepared from these plants may be used for removing these metals from the industrial waste like red mud and reduce its toxicity [43]. These nano-particles not only directly catalyze degradation of waste and toxic materials, but also it also helps enhance the efficiency of microorganisms in degradation of waste and toxic materials [44]. Recent day's nanotechnology is being used for making it suitable for its utilization. For example nano-SiO₂ has been produced for enhancing its strength as binder [45].

4. CONCLUSION

Bauxite residue (Red Mud) is a high volume byproduct of alumina manufacture which is commonly disposed of in purpose-built bauxite residue dumping areas (BRDAs). Bauxite residue is highly alkaline and has elevated concentrations of Na, Al, and other trace and heavy metals. Neutralized red mud from the aluminum plant which after drying and treated with cyanobacteria and covered with soil may provide a medium on which plants may grow. This method provides an environmentally less hazardous and much more acceptable disposal approach with a smaller risk of ecological accidents.

Cyanobacteria in combination with microbes involved in bio-mining, bioleaching removes its toxicity and improve its fertility by increasing organic matter and nitrogen content of Red Mud. The establishment of cyanobacterial crust shall also be helpful in reducing environmental risks due to water and wind erosion. The above mentioned microbes in combination with nanotechnology may provide a sustainable technology for the remediation of red mud. Nanotechnology may also be combined for making its utilization in construction.

ACKNOWLEDGMENTS

Authors acknowledge ICFRE, Dehradun for financial support and Divisional Forest Officers of Renukoot Territorial Forest Division, Uttar Pradesh, India and their associated forest officials for providing the local logistics, staff, infrastructural and field survey support.

REFERENCES

- [1] Das, S. N. & Thakur, R. S. (1995). *International series on environment, Red mud analysis and utilization*. Publication and information Directorate, New Delhi.
- [2] Xue, S., Zhu, F., Kong, X., Wu, C., Huang, L., huang, N. & Hartley, W. (2016). A review of the characterization and revegetation of bauxite residues (Red mud). *Env.. Sci. Pollut. Res.*, 23, 120–1132.
- [3] Newson, T., Dyer, T., Adam, C. & Sharp, S. (2006). Effect of structure on the geotechnical properties of bauxite residue. *J. Geotech. & Geoenviron. Eng.*, 132 (2), 143-151.
- [4] Fois, E., Lallai, A. & Mura, G. (2007). Sulfur dioxide absorption in a bubbling reactor with suspensions of bayer red mud. *Ind. Eng. Chem. Res.*, 46, 6770-6776.
- [5] Collazo, A., Cristobal, M. J., Novoa, X. R., Pena, G. & Perez, M. C. (2006). Electrochemical impedance spectroscopy as a tool for studying steel corrosion inhibition in simulated concrete environments- red mud used as rebar corrosion inhibitor. *J. ASTM. Int.*, 3, 2.
- [6] Hind, A. R., Bhargava, S. K. & Stephen, C. G. (1999). The surface chemistry of Bayer process solids: a review. *Colloids and Surfaces A: Physicochem. Eng. Aspects*, 146, 359–374.
- [7] Strazisar. S. J. (1993). *The influence of red mud impoundments on the environment*. Light Metals (Warrendale, PA, United States), 1993, 41-44.
- [8] Perander, L. M., Metson, J. B. & Klett, C. (2011). Two Perspectives on the Evolution and Future of Alumina. In: Lindsay S.J. (eds) *Light Metals.*, 151-155. https://doi.org/10.1007/978-3-319-48160-9_26.
- [9] Genc, H., Tjell, J. C., Conchle, D. M. & Schuiling, O. (2003). Adsorption of arsenate from water using neutralized red mud. *J. Colloid Interface Sci.*, 264, 327-334.
- [10] Liu, Y., Lin, C. & Wu, Y. (2007). Characterization of red mud derived from a combined Bayer process and bauxite calcinations method. *J. Hazard. Mater.*, 146, 255-261.
- [11] Genc-Fuhrman, H., Tjell, J. C. & McConchie, D. (2004). Adsorption of arsenic from water using activated neutralized red mud. *Env. Sci. Tech.*, 38, 2428-2435.
- [12] Sahu, R., Patel, R. K. & Ray, B. C. (2010). Neutralization of red mud using CO₂ sequestration cycle. *J. Hazar. Mats.*, 179, 28-34.
- [13] Rai, S., Wasewar, K. L. & Agnihotri, A. (2017). Treatment of alumina refinery waste (red mud) through neutralization techniques: A review. *J. Sust. Circ. Economy.*, 35, 563–580.
- [14] Rai, S., Bahadure, S., Chaddha, M. J. & Agnihotri, A. (2020). Disposal Practices and Utilization of Red Mud (Bauxite Residue): A Review in Indian Context and Abroad. *J. Sustain. Metall.*, 6, 1–8. <https://doi.org/10.1007/s40831-019-00247-5>.

- [15] Wehr, J. B., Fulton, I. & Menzies, N. W. (2006). Revegetation strategies for bauxite refinery residue: A case study of Alcan Gove in Northern Territory. *Australia. Environ. Manage.*, 37, 297–306.
- [16] Milačić, R., Zuliani, T. & Ščančar, J. (2012). Environmental impact of toxic elements in red mud studied by fractionation and speciation procedures. *Sci. of the Total Env.*, 426, 359-65.
- [17] Dubey, Kumud. (2012). Bio-remediation of Bauxite residue (red mud) generated from Aluminium industry by using blue green algae/bio-inoculants” *ICFRE Project Report.*, pp. 95.
- [18] Ning, L. W., Sun, Honghu Tang, S. H. & Wei, S. (2019). A Review on Comprehensive Utilization of Red Mud and Prospect Analysis. *Minerals*, 9(6), 362, <https://doi.org/10.3390/min9060362>.
- [19] Gyuricza, C., Junek, N. & Csuzi, S. (2012). Landscape remediation after the red mud disaster in Hungary with short rotation coppice. *Hung. Agr. Res.*, 21, 10-13.
- [20] Andrew, W., Bray, A. W., Stewart, D. I., Courtney, R., Rout, S. P., Humphreys, P. N., Mayes, W. N. & Burke, I. T. (2018). Sustained Bauxite Residue Rehabilitation with Gypsum and Organic Matter 16 years after Initial Treatment. *Env. Sci. Technol.*, 52, 152–161.
- [21] Dubey, K. & Dubey, K. P. (2011). A Study of the Effect of Red Mud Amendments on the Growth of Cyanobacterial Species. *Bioremediation J.*, 15, 133-139.
- [22] Singh, J. S., Kumar, A. & Singh, M. (2019). Cyanobacteria: A sustainable and commercial bio-resource in production of bio-fertilizer and bio-fuel from waste waters. *Env. Sust. Indicators.*, Volumes 3–4, 100008.
- [23] Dubey, S. K., Dubey, J., Mehra, S., Tiwari, P. & Bishwas, A. J. (2011). Potential use of cyanobacterial species in bioremediation of industrial effluents. *African J. of Biotech.*, 10, 1125-1132.
- [24] Agrawal, A., Sahu, K. K. & Pandey, B. D. (2004). Solid waste management in non-ferrous industries in India. *Res. Conserv. and Recycling.*, 42, 99–120.
- [25] SubbaRao, N. S. (2017). *Bio-fertilizers in Agriculture and Forestry*. 4th edition. Oxford & IBH Publishing Co. Pvt. Ltd., New Delhi.
- [26] Jeganathan, K. (2006). *Bioremediation studies on oil refinery industry effluent using Oscillatoriaearli Gartner*. M. Phil. dissertation. Bharathidasan University. Tiruchirapalli, India.
- [27] Kaushik, B. D. (1989). Reclamative potential of cyanobacteria in salt-affected soils. *Phykos.*, 28, 101–109.
- [28] Kaushik, B. D. & Krishnamurti, G. S. R. (1981). Effect of blue-green algae and gypsum application on physico-chemical properties of alkali soils. *Phykos.*, 20, 91–94.
- [29] Kaushik, B. D. & Subhashini, D. (1985). Amelioration of salt-affected soils with blue-green algae. II Improvement in soil properties. *Proc. Indian Na. I Sci. Acad. Part B.*, 51, 386–389.

- [30] Singh, R. N. (1950). Reclamation of Usar lands in India through blue green algae. *Nature.*, 165, 325-326.
- [31] Subhashini, D. & Kaushik, B. D. (1981). Amelioration of sodic soils with blue green algae." *Australian J. Soil Res.*, 19, 361-367.
- [32] Ueda, S., Kawamura, Y. & Iijima, H. (2016). Anionic metabolite biosynthesis enhanced by potassium under dark, anaerobic conditions in cyanobacteria. *Sci. Reports.*, 6, 32354.
- [33] Bender, J., Gould, J. P., Vatcharapijarn, Y., Young, J. S. & Phillips, P. (1994). Removal of Zinc and Manganese from Contaminated Water with *Cyanobacteria* Mats. *Water Env.. Research.*, 66 (5), 679-683.
- [34] Sadettin, S. & Donmez, G. (2006). Simultaneous bioaccumulation of reactive dye and chromium (VI) by using thermophilic *Phormidium* sp. *Enzyme Microbiol Technol.*, 41, 175–180.
- [35] Wang, T., Weissman, J., Ramesh, G., Varadarajan, R. & Benemann, J. R. (1998). Heavy Metal Binding and Removal by *Phormidium*. *Bull. Env. Contam. Toxicol.*, 60, 739–744. <https://doi.org/10.1007/s001289900688>.
- [36] Ahuja, P., Gupta, R. & Saxena, R. K. (1999). Zn⁺biosorption by *Oscillatoriaanguistissima*. *Process Biochem.*, 34, 77–85.
- [37] Cohen, Y. (2002). Bioremediation of oil by marine microbial mats. *Int. Microbiol.*, 5, 189–193.
- [38] Papassiopi, N., Vaxevanidou, K. & Paspaliaris, I. (2010). Effectiveness of iron reducing bacteria for the removal of iron from bauxite ores. *Minerals Engg.*, 23(1), 25-31.
- [39] Krishna, P. (2003). *Bioremediation of bauxite residue (red mud) using microbes*. A Dissertation submitted to Department of Biotechnology and Environmental Sciences Thapar Institute of Engineering and Technology, Patiala, Punjab, India.
- [40] Čížková, M., Mezricky, D., Rucki, M., Tivadar M. Tóth, T. M., Náhlík, V., Lanta, V., Bišová, K., Vilém Zachleder, V. & Milada Vítová, M. (2019). Bio-mining of Lanthanides from Red Mud by Green Microalgae. *Molecules.*, 24(7), 1356. <https://doi.org/10.3390/molecules24071356>.
- [41] K. A. (2018). Microbially induced mineral beneficiation. *Book biotechnology of metals principles, recovery methods, and environmental concerns*, pp-502. publisher elsevier. 243-304.
- [42] Liu, M., Wang, Z. & Zong, S. (2014). SERS detection and removal of mercury(II)/silver(I) using oligonucleotide-functionalized core/shell magnetic silica sphere@Au nanoparticles. *ACS Appl. Mat. & Interfaces.*, 6, 7371–7379.
- [43] Mohsenzadeh, F. & Rad, A. C. (2012). Bioremediation of heavy metal pollution by nano-particles of *noeamucronata*, *Int. J. of Biosci. Biochem. and Bioinform.*, 2, 85–89.
- [44] Rizwan, Md., Singh, M., Mitra, C. K., Roshan, K. & Morve, R. K. (2014). ecofriendly application of nanomaterials: nanobioremediation. *Journal of Nanoparticles.*, 2014. Article ID 43178717 pages.

- [45] Ahmed, S., Meng, T. & Taha, M. (2020). Utilization of red mud for producing a high strength binder by composition optimization and nano strengthening. *Nanotech. Rev.* 9, 396-409.
- [46] WEB REFERENCE: <http://redmud.org/red-mud/production/>.

Complimentary Contributor Copy

Chapter 19**DECONTAMINATION OF WATER WITH METAL
NANOCOMPOSITES AND HYBRID NANOMATERIALS**

***Vijay Pandey, Mahesh Kumar Gupta,
Harendra Singh and P. K. Tandon****

Department of Chemistry, University of Allahabad, Prayagraj, India

ABSTRACT

Now-a-days water pollution has become a serious problem throughout the world. Toxic pollutants coming out from various sources pollute water and deteriorate water quality. Through out the world major part of the population, especially in the developing countries, does not have access to the pure water leading to various life threatening diseases. Researchers are utilizing nanotechnology front line innovation field to create fantastic new items useful in almost every field of life. In recent years, metal nanocomposites and hybrid nanomaterials have attracted the attention of scientists and technologists in water purification due to improved processability, large surface area, stability, tunable properties, and cost effectiveness. These materials show fast decontamination ability with high selectivity to remove various pollutants. Even the traces of contaminants pollute water making it unfit for human consumption. Nanocomposites are solid materials having multiple phases in which at least one of the phases has a nanoscale structure. Nanocomposites have numerous applications. Generally, in nanocomposite the properties of organic and inorganic structural units give a material with composite properties while in hybrid material new properties other than those of the constituent materials may also emerge due to intimate mixing. In the hybrid material an additional degree of freedom is obtained which in the new material may lead to the emergence of new properties like sorption, conductivity, magnetic and catalytic or the mechanical properties. Due to their extremely large surface area and the high potential to combine rapidly with majority of particles, nanocomposites and nanohybrids are the ideal candidates for decontamination of the polluted water having a variety of pollutants.

* Corresponding Author's Email: pktandon1@gmail.com.

Thus these materials may contribute in a big way in modifying the future water related technologies.

Keywords: nanocomposites, nanotechnology, hybrid nanomaterial, adsorbent, water purification

1. INTRODUCTION

Being the need of modern society, the technological advances are growing at a faster rate. On the one hand industrialization of society has fulfilled the demand of human beings but on the other hand it has greatly increased the challenges for environment. Anthropogenic activities, include mining operations, industrialization and the use of metals and metal-containing compounds for domestic and agricultural purposes which are the main sources of water pollution [1]. Release of toxic chemicals by the industries contaminates air, water and the soil. Water pollution is a great environmental concern globally as the concentration of toxic pollutants in the water bodies is many times higher compared to the designated limits established by the world health organization (WHO) and environmental protection agency (EPA) and moreover it is assumed to get worse over coming decades. Many organic and inorganic pollutants are the major contaminants in the aqueous environment [2], and continuous exposure of human beings with polluted water leads to high-risk health problems. Particularly in developing countries, industrial effluents containing pollutants like heavy metals, inorganic anions, and organic pollutants are discharged directly or indirectly into the environment. Heavy metals are non-biodegradable, tend to accumulate in living organisms, and are carcinogenic. Toxic heavy metals that are of particular concern in the treatment of industrial wastewaters include lead, arsenic, chromium, copper, nickel, mercury, cadmium, zinc, and arsenic which are found as anions (i.e., arsenate AsO_4^{3-} , arsenite AsO_3^{3-} , etc.). It has been proven that these heavy metals have detrimental effects on the ecosystem [3-4]. Organic dyes which have become other sources of pollution of surface water are extensively used in industries like leather, textile, paper, printing, etc. More than 15% of the dye used in industries is wasted and released as the untreated effluent. Removal of organic dyes faces a huge challenge due to its aromatic structure and its non-biodegradable origin. The largest class of synthetic dyes include azo dyes which are highly toxic and carcinogenic for human beings as well as aquatic organisms due to the presence of nitrogen double bonds ($-\text{N}=\text{N}$). Removal of toxic azo dyes from the effluent is necessary before their discharge into the water streams [5-6]. Along with these pollutants pathogenic contamination of water resulting in water borne diseases is also a worldwide problem especially in the developing countries. Hence, water is one of the major routes through which these pollutants and radionuclides may enter the human body through the consumption of polluted water.

Revolution in the field of nanotechnology has reached many fields and its applications have great potential to be utilized in wastewater treatment. The unique

properties incorporated in nanomaterials consist of fabrication of nanoparticles of desired shape and size with increased surface area and stability which enable nanotechnologies for removal of contaminations along with better resource recovery [7]. Nanoparticles showing size and shape-dependent properties are interesting for applications in biosensing and catalysts to optics, antimicrobial activity, computer transistors, electrometers, chemical sensors, and wireless electronic logic and memory schemes. Of the various processes available for the synthesis of nanoparticles, the biosynthetic process plays a very important role in nanotechnology as it is cost-effective, eco-friendly, and is a better alternative to chemical and physical methods. Moreover, chemical methods employ toxic chemicals, additives, or capping agents and non-polar solvents in the synthesis procedure and thus are not suitable for their application in clinical and biomedical fields. Therefore, the need for the development of a clean, reliable, biocompatible, benign, and eco-friendly process to synthesize nanoparticles forced many researchers to develop green chemistry and bioprocesses [8-9].

A composite could be a combination of two or more diverse materials having multiple phases in which at least one of the phases has a nanoscale structure. Nanocomposites have numerous applications. Generally, in nanocomposite the properties of organic and inorganic structural units give a material with composite properties. Nanocomposites are now commonly employed to enhance useful properties of the standard polymeric membrane materials employed in water treatment processes. Different materials and methods have been put forward for the developments in the use of polymeric nanocomposite membranes for purifying water; amongst those that show the greatest potential so far are the thin-film nanocomposite (TFN), electrospun polymeric nanofibrous membranes, carbon nanotubes, metal and metal oxides, graphene and graphene oxide, and zwitterionic materials. Effectiveness of metal and metal oxide nanocomposites have been evaluated to offer resistance to fouling and the performance of the membranes. Researchers are interested to understand in a better way that how nanomaterials can be used in a number of ways, such as nanofiltration, micro-filtration, reverse osmosis, and membrane distillation. Bassyouni et al. in a review has covered the preparation, characteristics, and applications of thin-film composite (TFC) and thin film nanocomposite (TFN) membranes, electrospun polymeric nanofibrous membranes, molecular dynamics (MD) simulations of graphene oxide applications in desalination and the interactions of various contaminants with several types of polymeric nanomaterials including metal, metal oxides like Fe, Si, Zr, Al, Ti, Ag etc, based nanocomposite membranes for water desalination technologies [10].

Xingsheng et al. synthesized CuO-ZnO nanocomposite using a bio-templated method from biowaste-eggshell membranes. Results showed that morphology and structure of composite preserved the original structural characteristics of egg shell membrane with interlaced network coated by small inorganic nanoparticles and showed excellent adsorption, catalysis and antibacterial activities [11].

Hybrid nanomaterials have also been widely used for applications in materials science, biomedicine, tissue engineering, sensors, energy, catalysis, and environmental science due to their unique physical, chemical, and electronic properties. Graphene-based hybrid nanomaterials exhibited higher surface area and special porous structure, making them excellent candidates for practical applications in water purification. Sharma et al. described the synthesis of carbon and iron-based nanomaterials, graphene-carbon nanotubes-iron oxides, which can remove pollutants and inactivate viruses and bacteria efficiently in water. Removal of metals (e.g., Cu, Pb, Cr(VI), and As) and organics (e.g., dyes and oil) by graphene-based nanostructures as well as the inactivation of Gram-positive and Gram-negative bacterial species (e.g., *Escherichia coli* and *Staphylococcus aureus*) has been reported [12]. Morshed et al. prepared titania-loaded cellulose-based functional hybrid nanomaterial for photocatalytic degradation of toxic aromatic dye (methylene blue) in water [13]. On the other hand, a new mesoporous hybrid nanomaterial comprising of gelatin/SiO₂/TiO₂ was synthesized via the sol-gel method by Jamwal et al. It has a high surface area of 675.92 m²/g, pore volume 0.795 nm, and average pore size of 4.7 nm. The material was used for the purification of water containing Hg²⁺ [14].

The present chapter focuses on metal nanocomposite and hybrid nanomaterials for the removal of heavy metals, inorganic anions, organic pollutants, and microorganisms from water including tap water, groundwater, and wastewater. Metal nanocomposites include transition metal/oxide/sulfide nanocomposite and hybrid nanomaterials include carbon/silicon-based nanocomposite. There is to some extent an overlap between inorganic nanomaterials and organic polymer-supported nanomaterials i.e., when organic polymers are applied to support inorganic nanoparticles cores as nanocomposites. It can be concluded that the metal nanocomposite and hybrid nanomaterials might be considered as effective materials for the purification of water from industrial wastewater containing heavy metals, inorganic anions organic contaminants, and microorganisms.

2. SYNTHESIS OF NANOCOMPOSITES AND THEIR APPLICATIONS

Incorporation of nanoparticles into the polymer network or the synthesis of nanocomposite can be done in various ways, such as solution intercalation, melt intercalation, and *in-situ* polymerization [15-16]. The processing conditions, such as the alteration of the filler particles and compatibilizer agents used, play an important role in obtaining a nanocomposite with proper dispersion of the nanoparticles in melt intercalation. This method is useful for the synthesis of a polyolefin nanocomposite, but for an adsorption process this method may result in degradation and the side reactions if the polymer possesses functional groups due to the temperature and the shear forces during the mixing phase. Use of support in strengthening the physico-chemical properties of Nanomaterials in wastewater treatment is shown in figure 1. In addition, intercalation in a solution requires the polymer to be solubilized and the nanoparticles to be dispersed in an acceptable solvent. Interaction of the polymer with

nanoparticles increases on agitating the mixture resulting the filler's dispersion and distribution, and then the polymer nanocomposite is obtained by the removal of the solvent. Due to the milder conditions compared to melting intercalation, this strategy seems to be more appropriate to obtain a nanocomposite; however, this technique (together with melt intercalation) does not allow the reticulated polymer to be obtained that provides stabilization in the sorption phase for the composite. Compared to other methods, the *in-situ* polymerization method has many benefits since it facilitates the production of thermoplastics and thermoset polymer nanocomposites. In addition, *in-situ* polymerization offers greater versatility in synthesis, allowing, among other things, the modification of nanoparticles on the surface with compounds that favor the dispersion or functionalization of the surface to start reactions during polymerization. In addition, higher dispersion of the nanoparticles can be achieved through this technique and the formation of a crosslinked polymer hosting the nanoparticles in the polymeric network can be enabled [15]. Organic-inorganic hybrid materials consist of two elements, organic and inorganic, which are combined at the molecular level with each other. These are either homogeneous systems obtained from miscible organic and inorganic components and monomers, or heterogeneous systems generally known as nanocomposites, in which at least one of the components has a dimension in the nanometer range. These can be divided into two categories; In the first category organic and inorganic components are weakly joined by hydrogen bonding, van der Waals, π - π or weak electrostatic forces. In the second category organic and inorganic components are joined by strong covalent or coordinative bonds with each other [17].

Sun et al. [18] reported that the solvothermal synthesis of magnetite/reduced graphene oxide (MRGO) nanocomposites for decontamination of water polluted with dyes. These MRGO nanocomposites show excellent efficiency to remove Rhodamine B and Malachite Green from the industrial waste water and from the lake water. Additional benefit is the rapid separation of nanocomposite from aqueous solution by applying an external magnetic field. Bagheri et al. [19] sonochemically synthesized nanocomposite of Au-Fe₃O₄ loaded on activated carbon (Au-Fe₃O₄NPs-AC). In this firstly the prepared Fe₃O₄ nanoparticles were loaded on activated carbon and the resulting solid was added to the solution containing gold nanoparticles. The prepared Au-Fe₃O₄NPs-AC nanocomposite was used for the removal of Disulfide blue (DSB) and Rhodamine123 (R123) dyes from contaminated wate. Core-shell magnetic hollow Fe₃O₄ nanoparticles (MNPs) coated with polystyrene were fabricated by Chen et al. in a two-step process which can efficiently separate oils from water surface under a magnetic field [20]. Orooji et al. firstly reported a procedure to prepare GZMO/ZnO NCs by a sol-gel auto-combustion method utilizing the grape syrup and coffee as fuel. Prepared nanocomposites (GZMO/ZnO NCs) showed wide applications on photocatalytic behavior of degradation of various pollutants such as Erythrosine, Methyl Violet (MV), Eriochrome black T (EBT), and Methylene Blue (MB) dyes from polluted water [21]. Synthesis of polyvinyl alcohol/polyacrylic acid/MXene fiber membrane nanocomposite (PVA/PAA/MXene@PdNPs) by electrospinning method reported by Yin et al. showed high catalytic potential for waste-water treated nitro

compound degradation. A simple method for the preparation of TiO₂@C core@shell (TC) nanocomposites by a single alkoxide precursor and their application for solar water treatment has been reported [22].

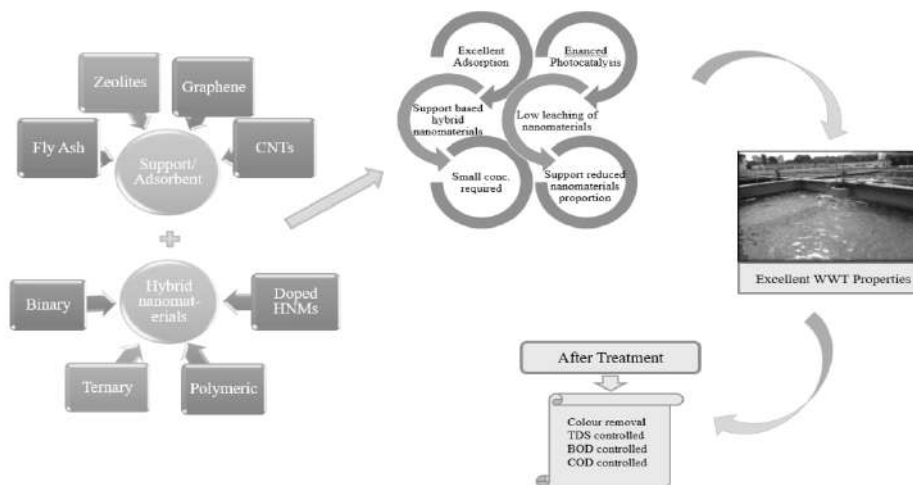


Figure 1. Use of support in strengthening the physico-chemical properties of Nanomaterials (NMs) in wastewater treatment (WWT). CNTs; Carbon Nanotubes, TDS; Total Dissolved Solids, BOD; Biochemical Oxygen Demand, and COD; Chemical Oxygen Demand.

A novel flexible nanocellulose MOF composite material was synthesized by Ashour et al. 2020 in aqueous media by a novel and straightforward *in-situ* one-pot green method. The material consisted of MOF particles immobilized onto bacterial cellulose (BC) nanofibers. This combination produced a shapeable, low-cost, chemically inert and scalable product that was used as an efficient adsorbent for the removal of arsenic As(III), and Rhodamine B from aqueous medium [23]. Saifeldin M. Siddeeq synthesized graphene oxide-based titanium nanocomposite immobilized on 1-ethyl-3-methylimidazolium tetrafluoroborate [EMIM-BF₄] ionic liquid. The synthesized nanocomposite was found to be an efficient active material for the removal of heavy metal ions (Cd²⁺ and Pb²⁺) from the contaminated water [24].

3. HYBRID NANOMATERIALS AND THEIR APPLICATIONS

The unique properties such as particle size, surface area, phase composition of hybrid nanomaterials make them versatile materials which have various applications towards environmental purification.

3.1. Chalcogenide-Based Hybrid Nanomaterials

Metal chalcogenides found in abundance on the earth. Various transition metal chalcogenides (selenides and sulfides) have been used as effective catalysts for the

degradation of hazardous pollutants. Initially the metal chalcogenides of ZnS and CdS were the most studied materials for the efficient degradation of toxic pollutants and for photovoltaic devices. However, later on many shortcomings were noticed like instability and photocorrosion of CdS and wide band gap energy of ZnS hybrid materials with these single sulfides were developed either by coupling or by the incorporation of coating materials. Dichalcogenides of Transition metal and sulfides of other heavy metals like MoS₂, Bi₂S₃, and ZnS have been widely explored for the photocatalytic mineralization of water contaminants [25]. These transition metal dichalcogenides have indicated amazing advancement in the synthesis of hybrid nanocomposite for decontamination of wastewater. Doping of binary dichalcogenides with transition metals increases the degradation efficiency of dyes e.g., doping of ZnS nanopowder with iron showed the best result of photocatalytic degradation of methylene blue (MB) [26].

3.2. Iron Oxide-Based Hybrid Nanomaterials

Separation of catalysts from treated solutions is time consuming and expensive. Thus, scientists tried to find out photocatalysts that can be separated under the influence of an external magnetic field. Iron oxide-based hybrid nanomaterials such as hydroxides, zeolites, and pillared clays have been widely examined for their applications in environment and remediation processes. Generation of hydroxyl radicals by the Fenton-like process and reaction parameters are responsible for the catalytic efficiency of these magnetic hybrids. Performance of hybrid photocatalysts may be retained by incorporating magnetic particles into semiconductor photocatalysts.

3.3. Colloidal-Based Hybrid Nanomaterials

Colloidal nanoparticles are microscopic substances. The properties of these hybrid materials can be controlled by their shape, composition, and size. Enhanced properties of these particles may be used in for getting desired properties in solution chemistry, biology, electrooptics, medical diagnostics etc. Haldar et al. synthesized Au-Cd Sepentapods colloidal-hybrid nanomaterials by chemical method and showed their increased photocatalytic efficiency [27]. Splitting of water and hydrogen production was investigated by Jones et al. with the help of colloidal-based hybrids like CdS-Pt as well as TiO₂-Au and CdS-Au nanomaterials[28].

3.4. Molybdate-Based Ternary Hybrid Nanomaterials

Combinations of molybdates to form ternary hybrid photocatalysts and plasmonic metal-based ternary molybdates, bismuth-based ternary molybdates, and transition

metal-based ternary molybdates have been studied extensively. Doping of plasmonic metals with heterojunctions of ternary tungstates and molybdates enhances photocatalytic degradation of organic compounds. The coupling of silver and bismuth molybdates $\text{Ag}_2\text{MoO}_4/\text{Bi}_2\text{MoO}_6$ heterojunctions show enhanced photocatalytic efficiency. Hybrid composites of molybdates (sulfides and oxides) with supports and cocatalysts such as graphene oxide, reduced graphene oxide, and noncarbon adsorbents have been studied. The improved photocatalytic degradation of dyes has been observed by coupling molybdenum oxide along with reduced graphene oxide and magnetite [29].

3.5. Vanadate-Based Hybrid Nanomaterials

Recent research has shown that noble metal loading, such as silver and copper and cocatalyst binding, can increase the photocatalytic efficiency of the vanadates by constructing a heterojunction structure of vanadates. The development of silver metavanadate ternary hybrids has shown very high absorption in visible light, leading to improved pollutant degradation efficiency [30].

3.6. Ferrite-Based Hybrid Nanomaterials

Various synthesis techniques such as microwave-assisted, hydrothermal, sol-gel, sonochemical, and solid-state reactions are available for the preparation of ferrite-based ternary hybrids nanomaterials. These hybrid photocatalysts have enhanced properties that allow their use in the remediation of the environment. They are conveniently isolated from the suspension of the reaction due to the magnetic properties of ferrites. Hybrid ternary ferrites are prepared either by doping with transition metals or coupling with other binary or ternary metals [31]. In order to form high-performance hybrid photocatalysts, metal ferrites can be mixed with graphitic carbon nitride and multi-walled carbon nanotubes (MWCNTs) [32].

4. ORGANIC/INORGANIC HYBRID NANOMATERIALS

Hybrid nanomaterials for both organic and inorganic nanomaterials combinations are referred to as organic-inorganic HNMs. Organic moieties are carbonaceous and polymeric materials, while antimicrobial agents such as ZnO and AgNPs have potential applications for pathogen removal from water. Human exposure, cost, and environmental toxicity are the problems related with inorganic materials which can be solved by the use of TiO_2 , silica, and Ag organic supports. These organic supports are cost-effective and can provide potential remediation of wastewater, particularly in developing countries.

4.1. Activated Carbon Supported HNMs

TiO₂ supported activated carbon hybrid nanomaterials is another form of HNM with properties of both adsorption and photocatalysis. The high popularity of these supportive hybrid materials is triggered by the synergistic effect of adsorption and photocatalysis. For TiO₂ applications, these hybrid nanomaterials provide the successful mass transfer. The main features of HNMs are improved photocatalytic degradation, simple separation along with low deactivation. Compared to simple TiO₂, these characteristics make these materials durable and flexible HNMs. The comparison of operative conditions between bare TiO₂ and TiO₂ supported by activated carbon results in the removal of methylene blue (MB) by 25 percent and 100 percent in 1h and 3h, respectively [33]. To extend the light response region of photocatalytic materials, sulfur and carbon may be used that can narrow the band gap to less than 3.2 eV. Creation of trap sites between the conduction band gap (CB) and the valence band (VB) results in the narrowing of the band gap. Even at low energy the presence of trap sites results in the generation of electron/hole pairs [34].

4.2. Graphene-Supported HNMs

Just a single atom thick graphite layer is known as grapheme which has potential uses in environmental protection. The chemical oxidation-reduction, mechanical peeling, and conversion of carbon. Because of the large surface area, chemical oxidation-reduction, mechanical peeling, and converting of carbon nanotubes are typical methods of graphene synthesis. For the adsorption of contaminants such as surfactants, dyes, heavy metals, pesticides, etc., graphene (G) and reduced graphene oxide (rGO) have been used. The results show that GO and rGO had optimum adsorption potential for nano ionic surfactants (TX-100) in a comparative analysis between GO, rGO, and other adsorptive materials [35]. Greater adsorption of tetracycline can be achieved by the electrostatic properties of graphene-based hybrid nanomaterials (GHNMs). For instance, the successful adsorptive removal of tetracycline, graphene, and carbon nanotubes (CNTs), both common carbon nanomaterials, were used [36].

4.3. Fly Ash Supported HNMs

Aluminosilicate-rich byproducts known as fly ash (FA) are produced by coal-firing power plants. Fly ash coating with TiO₂ of anatase crystal is capable to remove NO [37]. While by increasing TiO₂ contents to 25% Visa and Duta showed higher adsorption of copper and cadmium ions [38]. Modification of TiO₂-loaded fly ash with H₂O₂ increases efficiency of MB degradation [39].

4.4. Some Other Supports Used

In addition to all the above-mentioned adsorbents used for the synthesis of supported HNMs, the other low-cost adsorbents have been used for wastewater treatment such as biomass and agricultural waste products. Use of activated carbon as adsorbent is costly, forms a lot of sludge and has a long reaction time [40].

Table 1. Hybrid nanomaterials based on various solid support and their applications in WWT

Support	Hybrid nanomaterials	Synthesis approach	Application	Reusability	Ref.
Graphene	GO-CuFe ₂ O ₄	Hydrothermal	Arsenic removal	No change in up to nine cycles	[45]
Sawdust	EDTA-modified sawdust nanocomposites loaded with Fe ₃ O ₄	Synthesis through green biogenic process	Dye adsorption (brilliant green) and methylene blue	64% and 80% adsorption for MB and BG after five cycles	[46]
CNTs	Multilayer CNTs composite membrane		Oily WWT		[47]
	Alumina-CNT membrane		Removal of Cadmium		[48]
Reduced grapheme oxide (rGO)	Bi ₂ Fe ₄ O ₉ /rGO	Facile one-step hydrothermal method	Methyl violet (MV) removal		[49]
	MnFe ₂ O ₄ -reduced graphene Oxide	Chemical deposition	Organic dyes (methylene blue, methyl orange, methyl violet, rhodamine B, and orange II)		[50]
	CoFe ₂ O ₄ /Rgo	One-pot solvothermal	Methylene blue removal	Minor change	[51]
	ZnFe ₂ O ₄ /reduced grapheneoxide (rGO)	Hydrothermal reaction	Methyl orange and rhodamine B		[52]
	GO-NF	Chemical coprecipitation	Removal of U(VI) and Th(IV)	Stable within five cycles	[53]
Fly ash (FA)	FA/NiFe ₂ O ₄	Coprecipitation	Removal of CR (Congo Red) dye	10%–15%	[54]
	Sulfophthalocyanine/TiO ₂ /FAC	Sol-gel	Removal of Methylene blue		[39]
	TiO ₂ /ZnFe ₂ O ₄ /A FAC	Sol-gel	Removal of Rhodamine B dye	Minor decrease after three consecutive uses	[55]

Out of several ashes studied Tandon et al. reported that the ash of *Unio (Lamellidens marginalis)* was the best in decreasing arsenic(V) concentration from 1000 ppb to >10 ppb, TDS from 16.9 ppt to 8.5 ppt and conductivity from 33.8 mS to 17.1 mS from the contaminated water [41]. Iron nanoparticles prepared with the help

of tea extract and supported on MMT K10 have been reported by Tandon et al. to remove up 99% arsenic as As (III) from aqueous solution. It may be mentioned that almost complete removal of arsenic as As(III) directly from aqueous solution has not been reported [42]. Another significant material used as an adsorbent is chitosan. Interaction of functional groups present in chitosan (hydroxyl and amino group) with contaminants such as drugs/pharmaceuticals, pesticides, ions, phenols, metals, dyes, etc. are responsible for the removal [43]. Highly porous and low-cost materials are also acceptable candidates to be used as water purifiers. The use of nanotechnology has also been documented to make nanoadsorbents of bentonite and its hybrids [44]. Nanoadsorbents are commonly used as a sequence of nanomaterials (NMs) with distinct physicochemical properties. For wastewater treatment (WWT), nanomaterials, nanocomposites, hydrogel nanocomposites, boron nitride NMs, and several others materials have been and are being used. For environmental applications, a comparative analysis between them and other conventional adsorbents has been given in Table 1.

CONCLUSION

The necessity to provide clean drinking water, the most important parameter in determining the quality of life of human society, has forced the researchers to develop and optimize potential wastewater treatment approaches to remove both biological as well as chemical contaminations. Modern wastewater treatment technologies should include the removal of bacterial as well as the chemical contaminations both. Although great achievements have been obtained on the fabrication of nanocomposites and hybrid nanomaterials for water purification applications recently, there are still spaces in this field need to be filled in. Considering the threats from the resistant pathogens the preparations of drug molecules with the help of nanotechnology have some advantages over the other methods of preparation. Biological methods are environmentally safe and have clean preparation techniques that do not produce unwanted hazardous materials during the synthesis, as well as yield a high level of chemical composition, high monodispersity, and shape/size. Engineering nanotechnology is being extensively evaluated by researchers to make binary, ternary, polymer, and various support-based nanocomposites.

In this chapter classification, synthetic approaches, effectiveness of various supports and applications of multifunctional hybrid nanomaterials are assessed for their application in wastewater treatment. This chapter can be an input to understand the basics of photocatalyst and disinfectant property of metal oxide/grapheme nanocomposites and usefulness of other hybrid nanomaterials and composites for the water treatment should be further investigated, in which the economic production of these materials for stable, recyclable, and environment-adaptable water purification are highly expected. Chapter contains a brief review of the current literature available on the application of different types of metal nanocomposites and hybrid nanomaterials

for the removal of pollutants in waste water. Matter given in this chapter will help the reader to compare various methods and strategies taken for the synthesis of nanocomposites/hybrid nanomaterials by varying particle size, surface area, and phase composition to enhance removal/degradation efficiency and their outcome in few pages.

REFERENCES

- [1] Lingamdinne, L.P., Koduru, J.R. and Karri, R.R.(2019). A comprehensive review of applications of magnetic graphene oxide based nanocomposites for sustainable water purification. *J. Environ. Manage.*, 231: 622–634.
- [2] Danil de Namor, A.F., El Gamouz, A., Frangie, S., Martinez, V., Valiente, L. and Webb, O.A.(2012). Turning the volume down on heavy metals using tuned diatomite. a review of diatomite and modified diatomite for the extraction of heavy metals from water. *J. Hazard. Mater.*, 241–242: 14–31.
- [3] Fu, F. and Wang, Q.(2011). Removal of heavy metal ions from wastewaters : a review. *J. Environ. Manage.*, 92: 407–418.
- [4] Ihsanullah, Abbas, A., Al-Amer, A.M., Laoui, T., Al-Marri, M.J., Nasser, M.S., Khraisheh, M. and Atieh, M.A.(2016). Heavy metal removal from aqueous solution by advanced carbon nanotubes: critical review of adsorption applications. *Sep. Purif. Technol.*, 157: 141–161.
- [5] Gupta, M.K., Tandon, P.K., Shukla, N., Singh, H. and Srivastava, S.(2020). Efficient removal of methyl orange and rhodamine-b dyes with low cost banana peel activated carbon. *Asian J. Chem.*, 32: 1121–1127.
- [6] Chen, Z., Zhang, J., Fu, J., Wang, M., Wang, X., Han, R. and Xu, Q.(2014). Adsorption of methylene blue onto poly(cyclotriphosphazene-co-4,4'-sulfonyldiphenol) nanotubes: kinetics, isotherm and thermodynamics analysis. *J. Hazard. Mater.*, 273: 263–271.
- [7] El Rouby, W.M.A., El-Dek, S.I., Goher, M.E. and Noaemy, S.G.(2018). Efficient water decontamination using layered double hydroxide beads nanocomposites. *Environ. Sci. Pollut. Res.* <https://doi.org/10.1007/s11356-018-3257-7>.
- [8] Irvani, S.(2011). Green synthesis of metal nanoparticles using plants. *Green Chem.*, 13: 2638–2650.
- [9] Kumar, P.P.N.V., Shameem, U., Kollu, P., Kalyani, R.L. and Pammi, S.V.N.(2015). Green synthesis of copper oxide nanoparticles using aloe vera leaf extract and its antibacterial activity against fish bacterial pathogens. *Bionanoscience.*, 5: 135–139.
- [10] Bassyouni, M., Abdel-Aziz, M.H., Zoromba, M.S., Abdel-Hamid, S.M.S. and Drioli, E.(2019). A review of polymeric nanocomposite membranes for water purification. *J. Ind. Eng. Chem.*, 73: 19–46.
- [11] He, X., Yang, D.P., Zhang, X., Liu, M., Kang, Z., Lin, C., Jia, N. and Luque, R.(2019). Waste eggshell membrane-templated CuO-ZnO nanocomposites with

- enhanced adsorption, catalysis and antibacterial properties for water purification. *Chem. Eng. J.*, 369: 621–633.
- [12] Sharma, V.K., McDonald, T.J., Kim, H. and Garg, V.K.(2015). Magnetic graphene-carbon nanotube iron nanocomposites as adsorbents and antibacterial agents for water purification. *Adv. Colloid Interface Sci.*, 225: 229–240.
- [13] Morshed, M.N., Al Azad, S., Deb, H., Shaun, B.B. and Shen, X.L.(2020). Titania-loaded cellulose-based functional hybrid nanomaterial for photocatalytic degradation of toxic aromatic dye in water. *J. Water Process Eng.*, 33: 101062. <https://doi.org/10.1016/j.jwpe.2019.101062>.
- [14] Jamwal, H.S., Ranote, S., Kumar, D., Chauhan, G.S. and Bansal, M.(2020). Gelatin-based mesoporous hybrid materials for Hg²⁺ ions removal from aqueous solutions. *Sep. Purif. Technol.*, 239: 116513. <https://doi.org/10.1016/j.seppur.2020.116513>.
- [15] Rivas, B.L., Urbano, B.F. and Sánchez, J.(2018). Water-soluble and insoluble polymers, nanoparticles, nanocomposites and hybrids with ability to remove hazardous inorganic pollutants in water. *Front. Chem.*, 6: 1–13.
- [16] Pavlidou, S. and Papaspyrides, C.D.(2008). A review on polymer-layered silicate nanocomposites. *Prog. Polym. Sci.*, 33: 1119–1198.
- [17] Sanchez, C., Julián, B., Belleville, P. and Popall, M.(2005). Applications of hybrid organic-inorganic nanocomposites. *J. Mater. Chem.*, 15: 3559–3592.
- [18] Sun, H., Cao, L. and Lu, L.(2011). Magnetite/reduced graphene oxide nanocomposites: one step solvothermal synthesis and use as a novel platform for removal of dye pollutants. *Nano Res.*, 4: 550–562.
- [19] Bagheri, S., Aghaei, H., Ghaedi, M., Asfaram, A., Monajemi, M. and Bazrafshan, A.A.(2018). Synthesis of nanocomposites of iron oxide/gold (Fe₃O₄/Au) loaded on activated carbon and their application in water treatment by using sonochemistry: optimization study. *Ultrason. Sonochem.*, 41: 279–287.
- [20] Chen, M., Jiang, W., Wang, F., Shen, P., Ma, P., Gu, J., Mao, J. and Li, F.(2013). Synthesis of highly hydrophobic floating magnetic polymer nanocomposites for the removal of oils from water surface. *Appl. Surf. Sci.*, 286: 249–256.
- [21] Orooji, Y., Mohassel, R., Amiri, O., Sobhani, A. and Salavati-Niasari, M.(2020). Gd₂ZnMnO₆/ZnO nanocomposites: green sol-gel auto-combustion synthesis, characterization and photocatalytic degradation of different dye pollutants in water. *J. Alloys Compd.*, 835: 155240. <https://doi.org/10.1016/j.jallcom.2020.155240>.
- [22] Yin, J., Zhan, F., Jiao, T., Deng, H., Zou, G., Bai, Z., Zhang, Q. and Peng, Q. (2019). Highly efficient catalytic performances of nitro compounds via hierarchical PdNPs-loaded MXene/polymer nanocomposites synthesized through electrospinning strategy for wastewater treatment. *Chinese Chem. Lett.*, 31: 992–995.
- [23] Ashour, R.M., Abdel-Magied, A.F., Wu, Q., Olsson, R.T. and Forsberg, K.(2020). Green synthesis of metal-organic framework bacterial cellulose nanocomposites

- for separation applications. *Polymers (Basel)*, 12: 1104. <https://doi.org/10.3390/POLYM12051104>.
- [24] Siddeeg, S.M.(2020). A novel synthesis of TiO₂/GO nanocomposite for the uptake of Pb²⁺ and Cd²⁺ from wastewater. *Mater. Res. Express.*, 7. <https://doi.org/10.1088/2053-1591/ab7407>.
- [25] Bai, W., Cai, L., Wu, C., Xiao, X., Fan, X., Chen, K. and Lin, J.(2014). Alcohothermal synthesis of flower-like ZnS nano-microstructures with high visible light photocatalytic activity. *Mater. Lett.*, 124: 177–180.
- [26] Chauhan, R., Kumar, A. and Chaudhary, R.P.(2013). Photocatalytic degradation of methylene blue with Fe doped ZnS nanoparticles. *Spectrochim. Acta - Part A Mol. Biomol. Spectrosc.*, 113: 250–256.
- [27] Haldar, K.K., Sinha, G., Lahtinen, J. and Patra, A.(2012). Hybrid colloidal Au-CdSe pentapod heterostructures synthesis and their photocatalytic properties. *ACS Appl. Mater. Interfaces.*, 4: 6266–6272.
- [28] Jones, M.R., Osberg, K.D., MacFarlane, R.J., Langille, M.R. and Mirkin, C.A.(2011). Templated techniques for the synthesis and assembly of plasmonic nanostructures. *Chem. Rev.*, 111: 3736–3827.
- [29] Anjaneyulu, R.B., Mohan, B.S., Naidu, G.P. and Muralikrishna, R.(2018). Visible light enhanced photocatalytic degradation of methylene blue by ternary nanocomposite, MoO₃/Fe₂O₃/rGO. *J. Asian Ceram. Soc.*, 6: 183–195.
- [30] Guo, J., Liang, J., Yuan, X., Jiang, L., Zeng, G., Yu, H. and Zhang, J.(2018). Efficient visible-light driven photocatalyst, silver (meta)vanadate: synthesis, morphology and modification. *Chem. Eng. J.*, 352: 782–802.
- [31] Shekofteh-Gohari, M. and Habibi-Yangjeh, A.(2016). Novel magnetically separable ZnO/AgBr/Fe₃O₄/Ag₃VO₄ nanocomposites with tandem n-n heterojunctions as highly efficient visible-light-driven photocatalysts. *RSC Adv.*, 6: 2402–2413.
- [32] Shu, R., Zhang, G., Zhang, J., Wang, X., Wang, M., Gan, Y., Shi, J. and He, J.(2018). Fabrication of reduced graphene oxide/multi-walled carbon nanotubes/zinc ferrite hybrid composites as high-performance microwave absorbers. *J. Alloys Compd.*, 736: 1–11.
- [33] Jian-hua, L., Rong, Y. and Song-mei, L.(2006). Preparation and application of efficient TiO₂/ACFs photocatalyst. *J. Environ. Sci.*, 18: 979–982.
- [34] Ahmad, R., Ahmad, Z., Khan, A.U., Mastoi, N.R., Aslam, M. and Kim, J.(2016). Photocatalytic systems as an advanced environmental remediation: recent developments, limitations and new avenues for applications. *J. Environ. Chem. Eng.*, 4: 4143–4164.
- [35] Prediger, P., Cheminski, T., Neves, T. de F., Nunes, W.B., Sabino, L., Picone, C.S.F., Oliveira, R.L. and Correia, C.R.D.(2018). Graphene oxide nanomaterials for the removal of non-ionic surfactant from water. *J. Environ. Chem. Eng.*, 6: 1536–1545.
- [36] Zheng, S., Shi, J., Zhang, J., Yang, Y., Hu, J. and Shao, B.(2018). Identification of the disinfection byproducts of bisphenol S and the disrupting effect on

- peroxisome proliferator-activated receptor gamma (PPAR γ) induced by chlorination. *Water Res.*, 132: 167–176.
- [37] Asl, S.M.H., Ghadi, A., Baei, M.S., Javadian, H., Maghsudi, M. and Kazemian, H. (2018). Porous catalysts fabricated from coal fly ash as cost-effective alternatives for industrial applications: a review. *Fuel.*, 217: 320–342.
- [38] Visa, M. and Duta, A.(2013). TiO₂/fly ash novel substrate for simultaneous removal of heavy metals and surfactants. *Chem. Eng. J.*, 223: 860–868.
- [39] Huo, P., Yan, Y., Li, S., Li, H. and Huang, W.(2009). Preparation and characterization of cobalt sulfophthalocyanine/TiO₂/fly-ash cenospheres photocatalyst and study on degradation activity under visible light. *Appl. Surf. Sci.*, 255: 6914–6917.
- [40] Danish, M. and Ahmad, T.(2018). A review on utilization of wood biomass as a sustainable precursor for activated carbon production and application. *Renew. Sustain. Energy Rev.*, 87: 1–21.
- [41] Tandon, P.K. and Singh, S.B.(2011). Hexacyanoferrate(III) oxidation of arsenic and its subsequent removal from the spent reaction mixture. *J. Hazard. Mater.*, 185: 930–937.
- [42] Tandon, P.K., Shukla, R.C. and Singh, S.B.(2013). Removal of Arsenic (III) from water with clay-supported zerovalent iron nanoparticles synthesized with the help of tea liquor. *Ind. Eng. Chem. Res.*, 52: 10052–10058.
- [43] Edwards, J., Johnson, C., Santos-Medellín, C., Lurie, E., Podishetty, N.K., Bhatnagar, S., Eisen, J.A. and Sundaresan, V.(2015). Structure, variation, and assembly of the root-associated microbiomes of rice. *Proc. Natl. Acad. Sci.*, 112: E911–E920.
- [44] Bialczyk, J., Natkański, P., Kuśtrowski, P., Czaja-Prokop, U., Bober, B. and Kaminski, A.(2017). Removal of cyanobacterial anatoxin-a from water by natural clay adsorbents. *Appl. Clay Sci.*, 148: 17–24.
- [45] Wu, L.K., Wu, H., Zhang, H. Bin, Cao, H.Z., Hou, G.Y., Tang, Y.P. and Zheng, G.Q.(2018). Graphene oxide/CuFe₂O₄ foam as an efficient absorbent for arsenic removal from water. *Chem. Eng. J.*, 334: 1808–1819.
- [46] Kataria, N. and Garg, V.K.(2019). Application of EDTA modified Fe₃O₄/sawdust carbon nanocomposites to ameliorate methylene blue and brilliant green dye laden water. *Environ. Res.*, 172: 43–54.
- [47] Yan, L., Zhang, G., Zhang, L., Zhang, W., Gu, J., Huang, Y., Zhang, J. and Chen, T.(2018). Robust construction of underwater superoleophobic CNTs/nanoparticles multifunctional hybrid membranes via interception effect for oily wastewater purification. *J. Memb. Sci.* <https://doi.org/10.1016/j.memsci.2018.09.060>.
- [48] Shahzad, H.K., Hussein, M.A., Patel, F., Al-Aqeeli, N., Atieh, M.A. and Laoui, T.(2018). Synthesis and characterization of alumina-CNT membrane for cadmium removal from aqueous solution. *Ceram. Int.*, 44: 17189–17198.
- [49] Sun, H., Liu, Y., Zhang, Y., Lv, L., Zhou, J. and Chen, W.(2014). Synthesis of Bi₂Fe₄O₉/reduced graphene oxide composite by one-step hydrothermal method

- and its high photocatalytic performance. *J. Mater. Sci. Mater. Electron.*, 25: 4212–4218.
- [50] Yao, Y., Cai, Y., Lu, F., Wei, F., Wang, X. and Wang, S.(2014). Magnetic recoverable MnFe_2O_4 and MnFe_2O_4 -graphene hybrid as heterogeneous catalysts of peroxymonosulfate activation for efficient degradation of aqueous organic pollutants. *J. Hazard. Mater.*, 270: 61–70.
- [51] Qu, Y., Zhang, X., Shen, W., Ma, Q., You, S., Pei, X., Li, S., Ma, F. and Zhou, J.(2016). Illumina MiSeq sequencing reveals long-term impacts of single-walled carbon nanotubes on microbial communities of wastewater treatment systems. *Bioresour. Technol.*, 211: 209–215.
- [52] Meidanchi, A. and Akhavan, O.(2014). Superparamagnetic zinc ferrite spinel-graphene nanostructures for fast wastewater purification. *Carbon.*, 69: 230–238.
- [53] Lingamdinne, L.P., Choi, Y.L., Kim, I.S., Yang, J.K., Koduru, J.R. and Chang, Y.Y.(2017). Preparation and characterization of porous reduced graphene oxide based inverse spinel nickel ferrite nanocomposite for adsorption removal of radionuclides. *J. Hazard. Mater.*, 326: 145–156.
- [54] Sonar, S.K., Niphadkar, P.S., Mayadevi, S. and Joshi, P.N.(2014). Preparation and characterization of porous fly ash/ NiFe_2O_4 composite: promising adsorbent for the removal of congo red dye from aqueous solution. *Mater. Chem. Phys.*, 148: 371–379.
- [55] Fan, H., Chen, D., Ai, X., Han, S., Wei, M., Yang, L., Liu, H. and Yang, J.(2018). Mesoporous TiO_2 coated ZnFe_2O_4 nanocomposite loading on activated fly ash cenosphere for visible light photocatalysis. *RSC Adv.*, 8: 1398–1406.

Chapter 20

NANOCONJUGATES FROM CHITOSAN HYDROGEL: A NOVEL DRUG DELIVERY TOOL

Tanvi Jain^{1,*} and P. K. Dutta²

¹Faculty of Biotechnology, Institute of Biosciences and Technology,
Shri Ramswaroop Memorial University, Barabanki, Uttar Pradesh, India

²Department of Chemistry,
Motilal Nehru National Institute of Technology Allahabad,
Prayagraj, Uttar Pradesh, India

ABSTRACT

In today's world, biopolymers which are abundantly available on earth are much more attractive than synthetic polymers because of their excellent characteristics, such as biodegradability, permeability, biocompatibility, renewability and solubility. Chitosan is more fascinating polysaccharide due to the presence of the amino groups, which could appropriately be modified to deliver required characteristics and distinguishing biological roles as well as solubility. Chitin has the ability and multipurpose uses not only in the biomedical field but also in, agricultural, wastewater treatment and industrial areas. In the last few decades, various drug-delivery modalities have been materialized and an alluring part of this branch is the development and designing of nanoscale drug delivery nano devices. Nanoconjugates may also undergo polymerization with various phenols, combine with other polymers, magnetic nanoparticles and thus introduce antimicrobial, antidiabetic and antioxidant activities in it. In this chapter we discussed various nanoconjugates with enhanced antibacterial and effective drug release properties, some recent chitosan hydrogel based nanoconjugates, and some other nanocojugates dealing with drug delivery. It is expected that nanoconjugates from chitosan hydrogel will show a novel path for drug delivery tool in biomedical applications in the service of the mankind.

Keywords: nanoparticles, nanoconjugate, chitosan, hydrogels, drug delivery

* Corresponding Author's Email: tanvijain87@gmail.com.

1. INTRODUCTION

Material plays very important role in our society. Today's development and advancement are mostly depended on materials. From that perspective the role of material science in the service of the society is immense. Materials may be classified in different categories. Out of these, polymer is the youngest member of the material family. Further, polymer also may be classified into natural and synthetic. The first derivative of chitin is chitosan, and it is much more versatile than cellulose. With the help of nanotechnology and modern biomedical application aspect nanoconjugates from chitosan hydrogel will replace conventional drug delivery methods.

1.1. Chitosan

Chitosan (CS) is a well known natural and linear polysaccharide produced from chitin by deacetylation available abundantly on earth in the solid state under alkaline conditions, or by enzymatic hydrolysis of chitin deacetylase. It is the second largest renewable biomaterial after cellulose in terms of distribution and consumption [1-5]. Some of the most unique and important properties of chitosan in the medical field are its non-toxicity, biodegradability, biocompatibility, and immunoenhancing, antitumoral, antibacterial and antimicrobial activity shown in Figure 1.

The biodegradability of chitosan was proven both *in vitro* and *in vivo*, where macromolecules were split into several smaller sections of monomers. CS could help in decreasing the cholesterol absorption [6], disrupt the chain oxidation procedure by shifting the free radicals [7], and act as an antimicrobial agent against many yeasts, fungi and bacteria [8]. In the presence of Laccase, chitosan functionalised with quercetin shows a remarkable anti-microbial activity against various bacterial species.

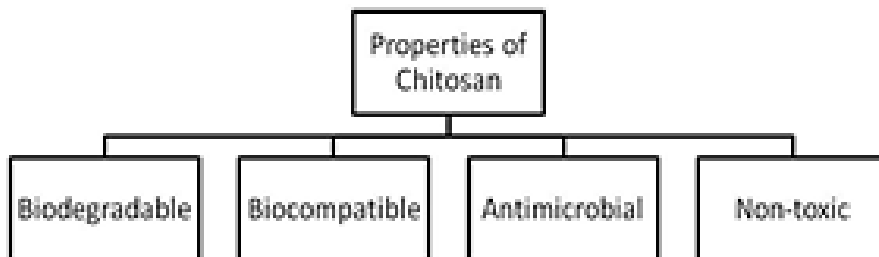


Figure 1. Major properties of Chitosan.

1.2. Fundamental Concept and Vital Properties of Hydrogels

Hydrogels are defined as the 3D polymer matrices created by cross-linking the hydrophilic copolymers or homopolymers that have the capacity to absorb big number

of biological fluids and water [9]. Ample of materials, both natural and synthetic, or composite of them, fit the meaning of hydrogels. The background of hydrogels began in 1950s when Lim and Wichterle fabricated the hydrogels from on 2-hydroxyethyl methacrylate as a copolymer with the compound ethylene dimethacrylate [10] and use them as contact lenses. Consequently, a broad range of research enabled the advancement in the field of hydrogels with various chemical based compounds, morphologies, and characteristics through several techniques. The motivation in the field of hydrogels is the amalgamation of “smart” hydrogels that are able to modify their properties when exposed to various external factors like such as pH, temperature, light, or electric field [11-13].

The utilization of natural biopolymers in the synthesis of hydrogels has fascinated the interest of many scientists both for their natural availability and for their enhanced biocompatibility when utilized as a biomaterials and chitosan being one of them which is mainly frequently used for various biomedical applications [14]. Hydrogels derived from those sources found naturally on earth and thus they are productive because of their intrinsic enormous biological characteristics which are widely studied and analysed for tissue engineering purposes. However, as with other naturally occurring biomaterials, variation in bunch composition indicates an important demerit [15].

1.3. An Overview to Nanocarriers and Nanoconjugates

All the subcellular structures, like cell organelles, biological macromolecules present in this size range which enables them to incorporate into biological system. They are defined as ultrafine particles having one systemic dimension in the range of 1-100 nm [16]. The word “nano” is derived form a Greek word “dwarf.” The main concept behind the foundation of nanotechnology was put in first by Richard Feynman in the lecture, “There’s plenty of room at the bottom.” Various lethal problems can be cured by treatment by using fabricated surgical bots of nano size.

Norio Taniguchi a professor and a researcher at University of Tokyo have proposed a term nanobiotechnology which is a discipline form which tools of nanotechnology are expanded and are used to study phenomenon of biology. It involves all the designing, fabrication and characterization technique of various materials and new devices. The research in the field of nanotechnology has benefitted in various health sectors. Nanotechnology has found its application in the field of Genomics, robotics, medicines etc, Nanoparticles have been characterized as the dispersive solution of colloidal particles of size ranging between 1 nm to 100 nm. NPs can be modified for the use of drug delivery [17]. Using this technology, drug molecules are entrapped or encapsulated to make a nano-particles, nanospheres and nano-capsules of varying size and having different physical and chemical properties. Nano-capsules are such type of arrangement in which drugs are enclosed in a cavity which is surrounded by a polymer membrane. The reason behind this is their biocompatibility. This gave rise to the implementation of methods of biosynthesis for the synthesis of

nanoparticles. Different classes of types of material used for nanoparticles is shown in Figure 2.

Nanoparticles that are made up of living systems are highly active in nature. They act as both stabilizing and reducing agents as well. Purification method is different for different nanoparticles and they control quality as well as quantity of new nanoparticles. Nanoparticles also exhibit high surface to volume ratio because of the decreased size and properties like biological effectiveness as well as magnetic properties has been enhanced [18]. The morphology of nanoparticles also introduced the knowledge of particles' anisotropic nature. The particles of this nature exhibit required properties like time of circulation enhanced, efficient penetration of tumor. Still there is insufficient knowledge of interaction [19].

1.4. Drug Delivery

Drug delivery is an interdisciplinary and autonomous branch of research and is acquiring the attention of theragnostic researchers, biomedical engineering and pharmaceutical industries [20-21]. Nanoparticles and other colloidal drug-delivery methodologies can also modify the drug kinetics and drug release profile pattern of a particular drug [22-23].

Drug delivery approach is aimed at synthesizing and creating nano regime particles to enhance the bioavailability of a drug. Nanocarriers (ncs) have extraordinary features that can be utilized to enhance drug delivery process. The lipid or biopolymer-based nanoparticles had been synthesized which are able to alter the pharmacokinetics and bio distribution of a drug. While larger particles are soon discharged from the body, nanocarriers through the mechanism of drug delivery are capable to cross the cell membrane barrier and get inserted to cell cytoplasm for the mechanism [24-26]. The main features of an effective drug delivery system are shown in Figure 3.

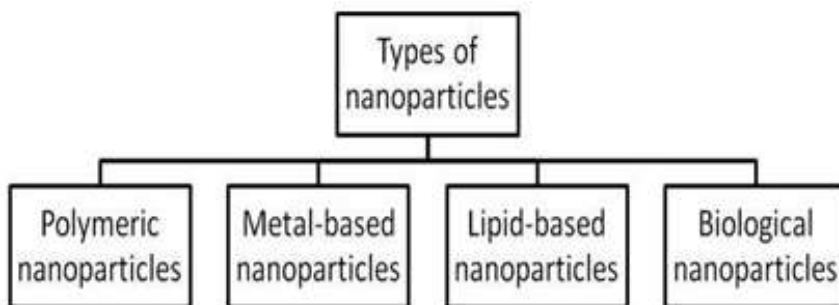


Figure 2. Types of Nanoparticles.

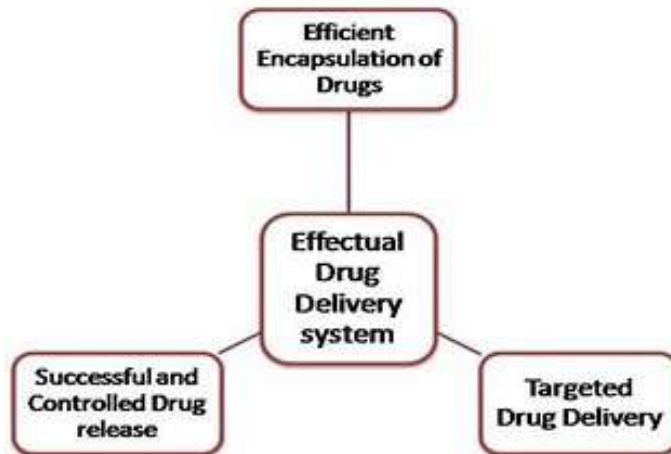


Figure 3. Main Features of Drug Delivery System.

Some merits of various formulations of nanoconjugates as a drug delivery system are given below point wise and its various design parameters are shown in Figure 4.

- Particle size and surface characteristics can be effortlessly altered to accomplish in targeted drug delivery.
- They can easily regulate, categorically type of release required for a particular drug for targeting during the transportation into the system and at the targeted site, altering organ distribution of the drug.
- Site-specific targeting can be accomplished by attributing targeting ligands to the surface of particle or usage of magnetic particles assistance etc.

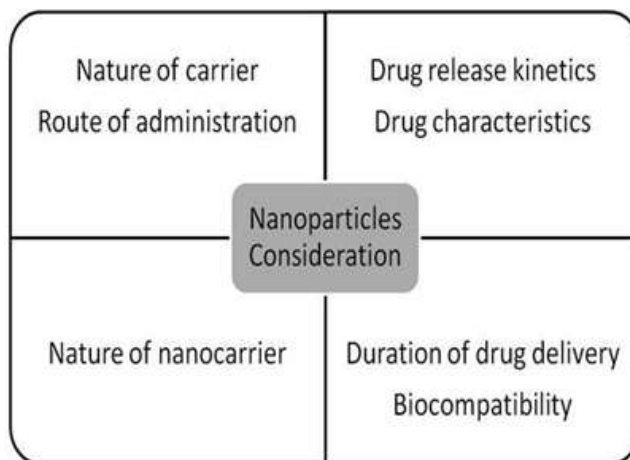


Figure 4. Parameters to design a smart biopolymeric nanoconjugate for drug delivery.

2. CHITOSAN WITH COMPOUNDS IN DRUG DELIVERY

Chitosan combining with other compounds like folic acid and glucose had already been studied as a targeted drug delivery tool, particularly for cancerous cells [27-28].

Jain et al., [29], used butyric anhydride and perchloric acid as a catalyst to produce dibutylchitin nanoparticles. Dibutylchitin nanoparticles loaded with 5-fluorouracil (Fu) showed increased rate of drug release in acidic pH rather than in neutral pH as shown in the drug release profiles.

A biocompatible chitosan-poly(lactide-co-glycolide) nanocomplex was prepared and drug was loaded as a therapeutic loom for the delivery of neuroprotective drug to the brain to treat the epilepsy [30-31], which has been distinct as a impulsive set of chronic neurological disorder in the human brain. L-pGlu-(1-benzyl)-L-His-LProNH₂ (NP-355) and L-pGlu-(2-propyl)-L-His-L-ProNH₂ (NP-647)-loaded PLGA nanoparticles were fabricated, and surface modified with chitosan to provide mucoadhesive properties for successful intranasal delivery of drugs to the brain.

3. CHITOSAN WITH METALLIC NANOCONJUGATES IN DRUG DELIVERY

Nanoconjugates of chitosan indicates to a complex of nanoformulated chitosan which can combine with one or more other component(s) like metals, polymers, compounds etc., Chitosan as a biopolymer has a native characteristics of chelating with metal ions like Cu, Zn, Fe etc [32-34]. Copious studies have proven the fact that chitosan hydrogel-metal nanoconjugates are biologically more valuable as compared to chitosan and metals at individual level which had already proven an excellent tool for drug delivery system [35-38]. An example of this is that chitosan and the metallic nanoparticles such as silver (Ag), copper (Cu), nickel (Ni), and zinc (Zn) displays certain level of disinfection and bactericidal properties, however the synthesis of all such these metal ions into a specific nanoconjugate developed in unusual and enhanced biochemical properties which are specifically suitable for bioengineering and biomedical applications [39-41]. These prepared nanoconjugates were dynamically delivered to liver cancer tissue in rats by static magnetic field to minimise the effect of the stability which was offered by chitosan matrix in intestinal fluids which are also responsible for the local heating of tumor cells on application of external magnetic field and thus accelerated the apoptosis of cancerous cells [42-44]

In a related chitosan-metallic nanoconjugate study, it was spotted that packing of copper (Cu) NPs onto chitosan's matrix enhanced the antimicrobial and antibacterial property and thus the nanocomplexes synthesized are strongly influenced by the solution pH. In a related study conducted by using Cur-loaded carboxymethyl chitosan NPs greatly upgraded the antibacterial property by more than 30% when tested against *S. aureus* and thus increases the efficiency which was credited to the enhanced zeta potential of the prepared nanocomplex [45]. It is already proven that both chitosan and zinc oxide (ZnO) display the properties of disinfection and bactericidal. In one of the

related studies, the existence of very small ZnO NPs (< 2.1 nm) in chitosan-ZnO nanocomplex led to a substantial decrease towards water solubility and increases the antibacterial property. Hence, these chitosan - ZnO nanocomplex are beneficial for various applications [46] Chitosan and metal nanoparticles of platinum (Pt) have possible applications in amperometric sensors and as antimicrobial agents [47-48]. In a study, the amperometric biosensors synthesised by the electrochemical accumulation of Pt NPs on to carbon nanotube-chitosan matrices confirmed to be appropriate as cholesterol biosensors. Chitosan served as stabilizing vehicle for the scattering of carbon nanotubes and later allowed for an enhancement in the exposed surface area [49].

4. CHITOSAN WITH MAGNETIC NANOPARTICLES IN DRUG DELIVERY

The organic-inorganic hybrid nanoconjugates have been inchoate as a novel and exciting tool for biomedical applications specifically in drug delivery [39, 50]. Hybrid magnetic nanocomplexes how tremendously enhanced properties as compared to their parent nanomaterial. The precise targeting of antitumor drugs to the cancerous tissue can be accomplished by utilizing advance methods for the synthesis of nanoconjugates that permits their selective passage to the targeted site through various stimuli or by a specific recognition system [51]. Another important feature of nanoparticle is that it can stimulate malignant tissues death by magnetic fluid hyperthermia [52-53].

Arias L. et al., [51] synthesised magnetite (Fe₃O₄)/chitosan composite for intravenous delivery of anticancer nucleoside analogue “gemcitabine.” The magnetic responsiveness was examined by recording the hysteresis cycle via exposed to a 1.1 T permanent magnet. The entrapment of drug into the polymeric shell gives higher drug loading along with a slower drug release profile. Thus, a new delivery device was synthesized having stimuli-sensitive, magnetically targeted, with high drug loading and slow release along with hyperthermia inducing capability delivery device with potential for effective cancer therapy. In another report, a magnetic nanocomposite based on magnetite and silica (SiO₂) enclosed in chitosan to control the drug release of DOX [54]. This prepared nanocomposite shows decent pH sensitivity and drug release was found to be 86.1% of the total drug loaded in 48 hours at pH 4.0. Lin et al., [55] fabricated a biocompatible and useful polyethylene glycol-chitosan-iron oxide nanoconjugate using a infrared fluorescent cyanin dye (MTX-PEG-CS-IONPs- Cy5.5). In another study, Zinc oxide (ZnO)- chitosan nanocomplex have also been narrated as an excellent drug delivery vehicle [56-57]. The amassed concentration of ZnO nanoparticles in the nanocomposite give better sustained and controlled drug release.

Singh R. et al., [58] synthesised surface functionalized magnetic nanoparticles (Fe₃O₄) and quantum dots (CdTe-ZnS) with carboxymethyl chitosan which were further examined for drug release and cell imaging. The later shows excellent magnetic

and fluorescence characteristics while it was also tested for *in-vitro* cell culture and cell imaging.

5. CHITOSAN WITH OTHER BIOPOLYMERS IN DRUG DELIVERY

To enhance various characteristics of chitosan as drug delivery vehicle, various studies had been reported with other biopolymer for the synthesis of a better and improved drug delivery tool. As reported many times, biopolymers are of different nature (cationic, anionic) and acquired distinctive biological properties [59]. For example, alginate is testified to be used as an adhesive and contains unique tissue compatibility because of its ability to give mechanical strength [38, 60-62], dextran have low protein binding capacity [63], carrageenan has gelling behaviour [64-65] etc.

Graphene oxide modified nanocomplex with chitosan and dextran in a layer-by-layer self-assembly was appraised as a nanocarrier for anticancerous drug Doxorubicin [66]. The prepared nanocomplex was able to be taken up by MCF-7 cells and showed robust cytotoxicity to cancer cells.

In another study [67], Chitosan nanocomplexes gets doped with Ag nanoparticles and then were fabricated. The chitosan NPs were synthesised by desolvation poly(ethylene glycol-di-aldehyde) was used as a crosslinker. These nanocomposites were shown to have excellent anti bacterial property towards *Escherichia coli*. The results in the study showed that the prepared nanoconjugate can be useful in drug delivery applications.

In another study, [68] used rectorite which is a kind of layered silicate and then Chitosan/organic rectorite (chitosan/OREC) nanoconjugate films with different concentration ratios of chitosan to organic rectorite and corresponding drug-loaded films were effectively produced by a solvent evaporation method. This study showed that the prepared chitosan/OREC nanocomplex films offer better properties as antimicrobial agent, water-barrier compounds, controlled release nanocarriers and anti-ultraviolet compounds in food packaging and drug-delivery system.

Geisberger G. et al., [69] utilised polyoxometalates (POMs) as it shows good antiviral property incorporated onto carboxymethyl chitosan (CMC). The prepared nanocapsules were fabricated by ionic gelation method. The results showed their size distribution ranges from 60 to 150 nm. This showcases new doors for designing novel inorganic drug delivery tool from bioactive POM's.

CONCLUSION

Targeted and controlled drug delivery scheme in the biomedical area has attractive and motivating aspects with today's world with escalating availability of vastly precise drug to reduce the side effects. Large number of chitosan based nanocomplexes were fabricated and investigated and thus comes out to be a boon in the field of drug delivery

due to its enhanced properties with modified and stimulus responsive structure for targeted specific drugs. Chitosan and its nanocomplexes with inorganic compounds, organic compounds, other polymers, magnetic nanoparticles enhance the solubility of immiscible drugs, numerous properties and forms stable complex and their safe delivery to the specific site. Finally we conclude that chitosan hydrogel based nanoconjugates for drug delivery will emerge as an important tool in biomedical applications in the service of the society.

REFERENCES

- [1] Elgadir, M. A., Uddin, M. S., Ferdosh, S., Adam, A., Chowdhury, A. J. K., Sarker. (2015). Impact of chitosan composites and chitosan nanoparticle composites on various drug delivery systems: A review. *J. Food Drug Anal*, 23 (4): 619-629.
- [2] Pang, Y., Qin, A., Lin, X., Yang, L., Wang, Q., Wang, Z., Shan, Z., Li, S., Wang, J., Fan, S. (2017). Biodegradable and biocompatible high elastic chitosan scaffold is cell-friendly both *in vitro* and *in vivo*. *Oncotarget*. 8; 22:35583-35591.
- [3] Allaher, C. M., Munion, J., Hesslink, Jr. R., Wise J., Gallaher D. D. (2000) Cholesterol reduction by glucomannan and chitosan is mediated by changes in cholesterol absorption and bile acid and fat excretion in rats. *J. Nutr.*, 130 (11): 2753-2759.
- [4] Dutta, P. K., Ravikumar, M. N. V., Dutta, J. (2002) Chitin and chitosan for versatile applications, *Journal of Macromolecular Science, Part C*, 42: 307-354.
- [5] Dutta, P. K., Dutta, J., Tripathi, V. S. (2004) Chitin and chitosan: Chemistry, properties and applications, *Journal of Scientific and Industrial Research*, 63:20-31.
- [6] Chen, Z., Zhang, L., Song, Y., He, J., Wu, L., Zhao, C., Xiao, Y., Li, W., Cai, B., Cheng, H., Li, W. (2015). Hierarchical targeted hepatocyte mitochondrial multifunctional chitosan nanoparticles for anticancer drug delivery, *Biomaterials*; 52:240-250.
- [7] Liu, J., Meng, C. G., Liu, S., Kan, J., Jin, CH., (2017). Preparation and characterization of protocatechuic acid grafted chitosan films with antioxidant activity. *Food Hydrocoll*; 63: 457-466.
- [8] Goy, R. C., Britto, D. D., Assis, O. B. (2009). A review of the antimicrobial activity of chitosan. *Polímeros*, 19(3): 241-247.
- [9] Pakdel, P. M., Peighambari, S. D. (2018). A review on acrylic based hydrogels and their applications in wastewater treatment. *Journal of Environmental Management*, 217; 123-143. 5-148.
- [10] Singh, B., Sharma, V., Pal, L. (2011). Formation of sterculia polysaccharide networks by gamma rays induced graft copolymerization for biomedical applications. *Carbohydr. Polym*, 86: 1371-1380.

- [11] Tsai, Y. C., Chen, S. Y., Lee, C. A., (2008). Amperometric cholesterol biosensors based on carbon nanotube-chitosan-platinum-cholesterol oxidase nanobiocomposite. *Sens. Actuators, B.*; 135; 1: 96-101.
- [12] Vittorio, O., Brandl, M., Cirillo, G., Kimpton, K., Hinde, E., Gaus, K., Yee, E., Kumar, N., Duong, H., Fleming, C., Haber, M., Norris, M., Boyer, C., Kavallaris, M., (2016). Dextran-Catechin: An anticancer chemically-modified natural compound targeting copper that attenuates neuroblastoma growth. *Oncotarget*, 7; 30: 47479-47493.
- [13] Zhang, N., Shen, Y., Li, X., Cai, S., Liu, M., (2012). Synthesis and characterization of thermo- and pH-sensitive poly (vinyl alcohol)/poly(N, N-diethylacrylamide-co-itaconic acid) semi-IPN hydrogels. *Biomedical Materials*, 7: 035014.
- [14] Bhattarai, N., Li, Z., Edmondson, D., Zhang, M., (2006). Alginate-Based Nanofibrous Scaffolds: Structural, Mechanical, and Biological Properties, *Adv. Mater.* 18; 1463-1467.
- [15] Nilasaroya, A., Poole-Warren, L. A., Whitelock, J. M., Jo Martens, P. (2008). Structural and functional characterisation of poly (vinyl alcohol) and heparin hydrogels. *Biomaterials*. 29:4658-4664.
- [16] Oliver, S., Thomas, D. S., Kavallaris, M., Vittorio, O., Boyer, C. (2016). Efficient Functionalisation of Dextran-Aldehyde with Catechin: Potential Applications in the treatment of Cancer. *Pol Chem.* 7: 2542-2552.
- [17] Gallaher, C. M., Munion, J., Hesslink, Jr. R., Wise J., Gallaher D. D. (2000) Cholesterol reduction by glucomannan and chitosan is mediated by changes in cholesterol absorption and bile acid and fat excretion in rats. *J. Nutr.*, 130 (11): 2753-2759.
- [18] Jain, T., Kumar S., Dutta P. K. (2016). Dibutylchitin nanoparticles as novel drug carrier. *Int. J. Bio. Mac.*, 82: 1011-1017.
- [19] Singh, A., Dutta, P. K., Kumar, H., Kureel, A. K., Rai, A. K., (2018) Synthesis of chitin-glucan-aldehyde-querceetin conjugate and evaluation of anticancer and antioxidant activities, *Carbohydrate polymers* 193; 99-107.
- [20] Dutta, P. K., Dutta, J., Tripathi, V. S. (2004) Chitin and chitosan: Chemistry, properties and applications, *Journal of Scientific and Industrial Research*, 63:20-31.
- [21] Dajas, F., (2012) Life or death: Neuroprotective and anticancer effects of quercetin. *J Ethnopharmacol.*, 143: 383-396.
- [22] Marimuthu, M, Bennet, D, Kim, S. (2013) Self-assembled Nanoparticles of PLGA-Conjugated Glucosamine as a Sustained Transdermal Drug Delivery Vehicle. *Polymer Journal*, 45: 202-209.
- [23] Yoo, H. S., Oh, J. E., Lee, K. H., Park, T. G., (1999). Biodegradable nanoparticles containing PLGA conjugate for sustained release. *Pharmaceutical Research*, 16:1114-8.

- [24] Jain, T., Kumar, S., Dutta, P. K. (2019), Carboxymethylchitin Nanocarrier (CMCNC): A Novel Therapeutic Formulation for Drug Release. *Polymer-Plastics Technology and Materials*. 58(1): 55-69.
- [25] Wang, J., Liu, C., Chi, P. (2008) *In situ* preparation of glycoconjugate hollow microspheres mimics the extracellular matrix via interfacial polymerization, *International Journal of Biological Macromolecules*; 42;5: 450-4.
- [26] Madhumathi, K., Sudheesh Kumar, P. T., Kavya, K. C., Furuike, T., Tamura, H., Nair, S. V., Jayakumar, R. (2009). Novel chitin/nanosilica composite scaffolds for bone tissue engineering applications, *International Journal of Biological Macromolecules*, 45; 3: 289-92.
- [27] Liu, F., Sun, C., Yang, W., Yuan, F., Gao, Y. (2015). Structural characterization and functional evaluation of lactoferrin-polyphenol conjugates formed by free-radical graft copolymerization. *RSC Adv.*, 5: 15641-15651.
- [28] Laquintana, V., Denora N., Lopalco, Lopodota A., Cutrignelli A., Lasorsa F. M., Agostino G., Franco M. (2014). Translocator protein ligand-PLGA conjugated nanoparticles for 5-fluorouracil delivery to glioma cancer cells, *Molecular Pharmacology*; 11(3):859-71.
- [29] Jain, T., Kumar S., Dutta P. K. (2016). Dibutylchitin nanoparticles as novel drug carrier. *Int. J. Bio. Mac.*, 82: 1011-1017.
- [30] Li, J. F. K. Ma, Q. F. Dang, X. G. Liang, X. G. (2014). Chen, Glucose-conjugated chitosan nanoparticles for targeted drug delivery and their specific interaction with tumor cells, *Front. Mater. Sci.*, 8; 363-372.
- [31] Kaur, S., Manhas, P., Swami, A., Bhandari, R., Sharma, K. K., Jain R., Kumar, R., Pandey, S. K., Kuhad, A., Sharma, R. K., Wangoo, N. (2018). Bioengineered PLGA-chitosan nanoparticles for brain targeted intranasal delivery of antiepileptic TRH analogues. *Chemical Engineering Journal*, 346: 630-639.
- [32] Esmaeili, F., Ghahremani, M. H., Ostad, S. N., Atyabi, F., Seyedabadi M., Malekshahi M. R., Amini M., Dinarvand R. (2008). Folate-receptor-targeted delivery of docetaxel nanoparticles prepared by PLGA-PEG-folate conjugate. *Journal of Drug Targeting*. 16(5):415-423.
- [33] Motwani, S. K., Chopra, S., Talegaonkar, S., Kohli, K., Ahmad, F. J., Khar, R. K., (2008). Chitosan-sodium alginate nanoparticles as submicroscopic reservoirs for ocular delivery: Formulation, optimisation and *in vitro* characterisation, *European Journal of Pharmaceutics and Biopharmaceutics*; 68:513-525.
- [34] Shu, X. Z., Zhu, K. J., The influence of multivalent phosphate structure on the properties of ionically cross-linked chitosan films for controlled drug release. (2002). *Eur. J. Pharm. Biopharm.*, 54; 2; 235-243.
- [35] Wang, X., Du, Y., Luo, J., Lin, B., Kennedy, J. F. (2007). Chitosan/organic rectorite nanocomposite films: Structure, characteristic and drug delivery behaviour. *Carbohydr. Polym*, 69; 1: 41-49.
- [36] Saharan, V., Mehrotra, A., Khatik, R., Rawal, P., Sharma, S. S., Pal, A., (2013). Synthesis of chitosan-based nanoparticles and their *in vitro* evaluation against phytopathogenic fungi. *Int. J. Biol. Macromol.*, 62: 677-683.

- [37] Duong, H., Fleming C., Haber M., Norris M., Boyer C., Kavallaris M., (2016). Dextran-Catechin: An anticancer chemically-modified natural compound targeting copper that attenuates neuroblastoma growth. *Oncotarget*, 7; 30: 47479-47493.
- [38] Wang, X., Du, Y., Luo, J., Lin, B., Kennedy, J. F., (2007). Chitosan/Organic Rectorite Nanocomposite Films: Structure, Characteristic and Drug Delivery Behaviour, *Carbohydr. Polym* 69; 1: 41-49.
- [39] Muzzarelli, R. A. A., Ubertini, O. T., (1969). Chitin and chitosan as chromatographic supports and adsorbents for collection of metal ions from organic and aqueous solutions and sea-water. *Talanta*, 16: 1571-1577.
- [40] Muzzarelli, C., Muzzarelli, R. A. A. (2002). Natural and Artificial Chitosan-Inorganic Composites. *J. Inorg. Biochem.* 92; 2:89-94.
- [41] Wei, D., Sun, W., Qian, W., Ye, Y., Ma, X., (2009). The Synthesis of Chitosan-Based Silver Nanoparticles and Their Antibacterial Activity. *Carbohydr. Res.*, 344; 17; 2375-82.
- [42] Sreeram, K. J., Nidhin, M., Nair, B. U., (2009). Synthesis of aligned hematite nanoparticles on chitosan-alginate films. *Colloid. Surf. B.*, 71; 2; 260-267.
- [43] Li, F., R., Yan, W. H., Guo, Y. H., Qi H., Zhou, H. X., (2009). Preparation of carboplatin-Fe@C-loaded Chitosan Nanoparticles and Study on Hyperthermia Combined with Pharmacotherapy for Liver Cancer., *Int. J. Hypertherm.* 25; 5; 383-91.
- [44] Li, L. H., Deng, J. C., Deng, H. R., Liu, Z. L., Xin, L. (2010). Synthesis and characterization of chitosan/ZnO nanoparticle composite membranes. *Carbohydrate Research*; 345: 994-998.
- [45] Gu, C., Sun, B., Wu, W., Wang, F., Zhu, M., (2007) Synthesis, Characterization of Copper Loaded Carboxymethyl Chitosan Nanoparticles with Effective Antibacterial Activity. *Macromol. Symp.* 254 (1): 160-166.
- [46] Perelshtein, I., Ruderman, E., Perkas, N., Tzanov, T., (2013), Chitosan and chitosan-ZnO-based complex nanoparticles: formation, characterization, and antibacterial activity. *J. Mater. Chem. B.*, 1: 1968-1976.
- [47] Tsai, Y. C., Chen, S. Y., Lee, C. A., (2008). Amperometric cholesterol biosensors based on carbon nanotube-chitosan-platinum-cholesterol oxidase nanobiocomposite. *Sens. Actuators, B.*; 135; 1: 96-101.
- [48] Vittorio, O., Cirillo, G., Lemma, F., Turi, G. D., Jacchetti, E., Curcio, M., Barbuti, S., Funel N., Parisi, O. I., Puoci, F., Picci, N., (2012). Dextran-Catechin Conjugate: A Potential Treatment against the Pancreatic Ductal Adenocarcinoma. *Pharm Res.*, 29:2601-2614.
- [49] Zhu, X., Ding, A., (2013). One-step Construction of Sensor Based on Nanocomposite of Platinum and Chitosan Formed by Electrodeposition and Its Application for Determination of Nitrite. *Int. J. Electrochem. Sci.*, 8: 135-148.
- [50] Goy, R. C., Britto, D. D., Assis, O. B. (2009). A review of the antimicrobial activity of chitosan. *Polímeros*, 19(3): 241-247.

- [51] Reddy, L. H. and P. C. Jose L. Arias (2012), Fe₃O₄/chitosan nanocomposite for magnetic drugtargeting to cancer, *J. Mater. Chem.*, 22: 7622-7632.
- [52] Gutiérrez, V. A., Alvarez, T. J., Nanoparticles for hyperthermia applications, in: C. M. Hussain (Ed.), *Handb. Nanomater. Ind. Appl.*, Elsevier, 2018.
- [53] Wichterle, O., Lím, D. (1960) Hydrophilic gels for biological use. *Nature*. 1: 185: 117-118.
- [54] Queiroz, M. F., Sabry, D. A., Sasaki, G. L., Rocha, H. A. O., Costa, L. S., (2019). Gallic Acid-Dextran Conjugate: Green Synthesis of a Novel Antioxidant Molecule. *Antioxidants*, 8; 1: 478.
- [55] Lin, J., Li, Y. Li, H. Wu, F. Yu, S. Zhou, L. Xie, F. Luo, C. Lin, Z. Hou. (2015). Drug/Dye-Loaded, Multifunctional PEG-Chitosan-Iron Oxide Nanocomposites for Methotrexate Synergistically Self-Targeted Cancer Therapy and Dual Model Imaging, *ACS Appl. Mater. Interfaces*. 7: 11908-11920.
- [56] Liu, M., Zhou, Z., Wang, X., Xu, J., Yang, K., Cui, Q., Chen, X., Cao, M., Weng, J., Zhang, Q. (2007). Formation of poly (l,d lactide) spheres with controlled size by direct dialysis, *Polymer*; 48: 5767-79.
- [57] Bharathi, D., Rajamani, R. K., Bellan, C. S., Veluswamy, B. (2019). Preparation of chitosan coated zinc oxide nanocomposite for enhanced antibacterial and photocatalytic activity: As a bionanocomposite. *Int J Bio Mac*, 129: 989-996.
- [58] Singh, R., Lillard, J. W. (2009). Nanoparticle-based targeted drug delivery. *ExpMolPathol*. 86; 3: 215-223.
- [59] Mangalathillam, S., Sanoj, R. N., Nair, A., Lakshmanan, V. K., Shantikumar, V. N., Rangasamy, J. (2012). Curcumin loaded chitin nanogels for skin cancer treatment via the transdermal Route. *The Royal Society of Chemistry Nanoscale*, 4; 1: 239-250.
- [60] Abolhasani, A., Biria, D., Abolhasani, H., Zarrabi, A., Komelli T. (2019). Investigation of the Role of Glucose Decorated Chitosan and PLGA Nanoparticles as Blocking Agents to Glucose Transporters of Tumor Cells. *Int J Nanomedicine*, 14: 9535-9546.
- [61] Badel, D. A. P., Urbano, P., Rivas, B. L. (2018). Hydrogels based on alkylated chitosan and polyelectrolyte copolymers. *Journal of Applied Polymer Science*, 135: 46556.
- [62] Bhattarai, N., Li, Z., Edmondson, D., Zhang, M. (2006). Alginate-Based Nanofibrous Scaffolds: Structural, Mechanical, and Biological Properties. *Adv. Mater*, 18(11):1463-1467.
- [63] Miyazaki, S., Nakayama, A., Masako, O. D. A., Takada, M., Attwood, D. (1994). Chitosan and sodium alginate based bioadhesive tablets for intraoral drug delivery. *Biol. Pharm. Bull*, 17; 5: 745-7.
- [64] Bhattarai, N., Li, Z., Edmondson, D., Zhang, M., (2006). Alginate-Based Nanofibrous Scaffolds: Structural, Mechanical, and Biological Properties, *Adv. Mater*. 18; 1463-1467.

- [65] Elgadir, M. A., Uddin, M. S., Ferdosh, S., Adam, A., Chowdhury, A. J. K., Sarker. (2015). Impact of chitosan composites and chitosan nanoparticle composites on various drug delivery systems: A review. *J. Food Drug Anal*, 23 (4): 619-629.
- [66] Massia, S. P., Stark, J., Letbetter, D. S. (2000). Surface-immobilized dextran limits cell adhesion and spreading. *Biomaterials*, 21; 22: 2253-2261.
- [67] Krishna, K. S. V., Ramasubba, R., Lee, Y. III., Kim, C., (2012). Synthesis and characterization of chitosan-PEG-Ag nanocomposites for antimicrobial application, *Carbohydr. Polym*, 87(1): 920-925.
- [68] Wu, Y., Wang, X., (2017). Binding, Stability, and Antioxidant Activity of Curcumin with Self-assembled Casein-Dextran Conjugate Micelles. *International Journal of Food Properties*, 20: 12: 3295-3307.
- [69] Geisberger, G., Paulus, S., Carraro, M., Bonchio, M., Patzke, G. R. (2011) *Synthesis, Characterisation and Cytotoxicity of Polyoxometalate/Carboxymethyl Chitosan Nanocomposites*, 17(16): 4619-4625.

ABOUT THE EDITORS

Dr. Mridula Tripathi

Associate Professor

Department of Chemistry, CMP Degree College, Prayagraj, India



Dr. Mridula Tripathi is Associate Professor of Chemistry, CMP, PG College, University of Allahabad, Praygaraj. She is having more than Twenty years of teaching experiences and has received many Awards in different fields. Dr Tripathi has published more than 80 research papers /bookchapters / popular articles in International and national reputed journals, Periodicals and Books. She was awarded Research Associateship by CSIR New Delhi, Ministry of Renewable Energy, New Delhi, All india council of Technical education and university Grant Commission New Delhi. She has experience of handling three major projects by Department of Science and technology, New Delhi, Council of Science and technology, UP Lucknow, and Board of Research in Nuclear Sciences, Mumbai. She Visited *Abdus Salam, International Centre for Theoretical Physics. Trieste, Italy, University of Ontario, Canada and University of Kingston, London.* She guided three Ph.D. students. She received DST-International travel fellowship, UGC- International travel fellowship, CICS- International travel fellowship. She has organized three National Conference sponsored by DST, new Delhi, UGC New Delhi, BRNS Mumbai. CST, UP Lucknow and CSTT, member of various New Delhi. She is life academic societies.

Dr. Arti Srivastava

Assistant Professor

Department of Chemistry, Guru Ghasidas Vishwavidyalaya, Bilaspur, India



At present Dr Arti Srivastava working as senior Assistant Professor in Department of Chemistry, Guru Ghasidas vishwavidyala, Bilaspur, India since 2011. She did her degrees from University of Allahabad, Allahabad, India. Dr Arti Srivastava did her Ph. D on topic related to material science. She received research Associatship from CSIR, India and she has been also awarded with young scientist from DST, India. Dr Srivastava have also learned german language. She has completed two research projects and two stuedents have got their Ph. D. under her guidance. Dr. Arti published over 30 scientific research papers and more than 12 book chapters in national and international repute. Dr Srivastava also patented one of her research work as Indian Patent.

Dr. Kalpana AwasthiAssistant Professor, Department of Physics
K.N. Govt. P.G. College, Gyanpur, Bhadohi, India

Dr. Kalpana Awasthi post graduated in Condensed Matter Physics from Banaras Hindu University, Varanasi, India. She completed her doctoral degree (Ph.D.) and post -doctorate under supervision of Prof. Padamshri Onkar Nath Srivastava from Banaras Hindu University, Varanasi, India. She has expertise in synthesis of carbon nanomaterials (carbon nanotubes, graphene) and its application in polymer composite. She has also expertise in functionalization of carbon nanomaterials and its application in agriculture and medical fields. She has received prestigious young scientist award from the Indian Science Congress Association, Kolkata and certificate of merit for the R&D efforts on Carbon Nanotubes and its Applications from Nanoscience center, Department of Physics, B.H.U., Varanasi. She has published more than thirty research papers including review articles in reputed international journals and contributed eight chapters in various international and national edited books. Presently, she is working as Assistant Professor in Department of Physics, Kashi Naresh Government Post Graduate College, Gyanpur, Bhadohi, India.

INDEX

#

20th century, 52, 53, 54
2D hetero-structured QDs, 82
2D nanomaterials, 235, 236, 237, 240, 241, 242

A

AC impedance spectroscopy, 62
access, 258, 265, 283
acetaminophen, 201, 210, 211
acid, 48, 55, 56, 113, 121, 123, 134, 164, 180, 195, 197, 200, 201, 204, 206, 207, 209, 212, 214, 220, 221, 224, 226, 232, 238, 249, 253, 257, 258, 265, 276, 287, 304, 307, 308
acidic, 64, 84, 102, 122, 178, 224, 225, 226, 228, 230, 240, 243, 259, 263, 304
activated carbon, 96, 155, 156, 157, 159, 160, 169, 170, 229, 243, 287, 291, 292, 294, 295, 297
activation energy, 61, 69, 70, 72
active site(s), 31, 87, 89, 101, 104, 105, 107, 110, 173, 174, 176, 185, 186, 188, 198, 223, 229, 241
additives, 62, 64, 71, 162, 164, 285
adenine, 200, 202, 210
adhesion, 21, 240, 252, 312
adsorbent, 25, 173, 176, 177, 179, 180, 185, 284, 288, 292, 293, 298
adsorption, 1, 9, 20, 22, 24, 29, 89, 117, 145, 152, 159, 165, 166, 171, 174, 178, 179, 180, 181, 182, 184, 188, 189, 190, 193, 195, 197, 206, 221, 225, 228, 230, 242, 250, 285, 286, 291, 292, 294, 295, 298

adsorption capacity, 24, 117, 166, 174, 178, 179, 180, 181, 184, 197, 242
advancement(s), viii, 1, 5, 26, 45, 58, 81, 99, 100, 101, 106, 160, 169, 194, 289, 300, 301
aerogels, 170, 223, 232
aggregation, 19, 23, 85, 89, 92, 102, 198
agriculture, 5, 32, 249, 314
alcohols, 222, 249, 262, 266
aldehydes, 260, 261, 262, 263
alkaline media, 223, 224, 225, 226, 228, 233
alkalinity, 269, 271, 272, 276
aluminium, 2, 21, 24, 273
amine(s), 32, 199, 201, 202, 211, 261
amino, 64, 100, 110, 207, 237, 249, 293, 299
ammonia, 15, 25, 120
anatase, 93, 94, 291
anchoring, 119, 176, 178, 179
annealing, 23, 142, 143, 144, 150, 151, 229, 244
anticancer, 51, 54, 57, 259, 305, 307, 308, 310
antioxidant, 57, 259, 265, 299, 307, 308
antitumor, 55, 265, 305
apoptosis, 107, 265, 304
aqueous solutions, 30, 188, 295, 310
argon, 93, 120, 146
arsenic, 179, 269, 278, 284, 288, 292, 297
ascorbic acid, 25, 200, 205, 207, 208, 212, 213, 214
aspartic acid, 200, 206, 208, 213
atmosphere, 3, 10, 93, 120, 252
atoms, 3, 5, 20, 25, 32, 37, 46, 66, 87, 116, 157, 159, 160, 165, 175, 196, 223, 228, 230, 237

B

bacteria, 9, 14, 24, 26, 42, 48, 113, 280, 286, 300

band gap, 23, 82, 86, 87, 93, 95, 103, 118, 124, 131, 132, 134, 160, 163, 174, 177, 178, 181, 183, 185, 198, 238, 241, 258, 291

base, 23, 36, 55, 110, 118, 121, 127, 128, 129, 137, 162, 163, 168, 170, 179, 180, 231, 232, 249, 257, 258, 286

batteries, viii, 5, 6, 61, 70, 72, 81, 87, 89, 91, 155, 157, 158, 159, 160, 162, 163, 164, 166, 170, 171, 175, 196, 219, 220, 231, 240, 251

bauxite, 268, 269, 271, 272, 275, 276, 277, 278, 279, 280

bauxite residue, 267, 268, 271, 272, 275, 276, 277, 278, 279, 280

behaviors, 35, 36, 191, 254

benefits, 9, 10, 13, 38, 42, 44, 58, 83, 271, 287

binding energy, 37, 134, 166

bioavailability, 39, 106, 272, 302

biocatalysts, 100, 106, 249

biocompatibility, 38, 48, 95, 164, 194, 299, 300, 301

biological systems, 26, 100, 118

biomass, 276, 292, 297

biomaterials, viii, 58, 301

biomedical applications, 19, 23, 27, 32, 33, 43, 45, 46, 102, 208, 299, 301, 304, 305, 307

biomolecules, 53, 100, 197, 258

biopolymer(s), 62, 64, 71, 73, 250, 254, 299, 301, 302, 304, 306

bioremediation, vi, ix, 267, 268, 272, 273, 274, 275, 276, 279, 280

biosensing, viii, 26, 99, 100, 101, 103, 110, 111, 112, 113, 189, 209, 210, 285

biosensors, 1, 11, 25, 31, 43, 45, 111, 197, 198, 207, 231, 232, 251, 305, 308, 310

biotechnology, 1, 48, 99, 196, 280

bismuth, 53, 56, 57, 110, 289

blood, 7, 39, 53, 111, 207, 213

bonding, 6, 31, 55, 62, 64, 66, 71, 117, 118, 121, 204, 287

bonds, 87, 119, 160, 180, 194, 287

bone, 7, 64, 68, 249, 252, 309

bottom-up, 83, 84, 237

brain, 7, 39, 304, 309

bulk materials, 21, 36, 83

C

cadmium, 38, 206, 269, 284, 291, 297

cancer, 7, 10, 13, 26, 36, 38, 39, 40, 44, 45, 46, 47, 48, 54, 55, 305, 306, 309, 311

cancer cells, 7, 26, 39, 48, 306, 309

cancer therapy, 38, 45, 305

candidates, 5, 22, 88, 101, 118, 155, 157, 160, 164, 241, 249, 283, 286, 293

capillary, 22, 194, 254

carbon, viii, 3, 4, 6, 9, 10, 11, 15, 17, 18, 21, 22, 25, 26, 29, 32, 35, 37, 39, 42, 49, 81, 83, 87, 93, 94, 96, 99, 100, 103, 105, 112, 115, 116, 120, 126, 127, 129, 130, 132, 139, 141, 146, 153, 155, 156, 157, 158, 159, 160, 163, 164, 165, 166, 167, 168, 169, 170, 171, 176, 178, 179, 180, 183, 185, 188, 189, 190, 191, 192, 193, 194, 195, 196, 197, 198, 199, 200, 201, 202, 203, 205, 206, 207, 208, 209, 210, 211, 212, 213, 214, 215, 218, 219, 220, 223, 224, 229, 230, 236, 243, 244, 245, 250, 251, 254, 255, 258, 274, 275, 285, 286, 287, 290, 291, 292, 294, 295, 296, 297, 298, 305, 308, 310, 314

carbon atoms, 37, 115, 116, 157, 158, 159, 160, 193, 195, 196, 197, 220, 230, 236

carbon based nanomaterials, 156

carbon film, 96, 127, 244

carbon materials, 126, 160, 166, 167, 176, 179, 185, 193, 199, 201, 208, 210, 230

carbon nanotubes, 4, 9, 10, 15, 22, 25, 26, 29, 32, 35, 49, 83, 99, 103, 116, 127, 130, 141, 155, 156, 157, 158, 168, 169, 170, 171, 178, 180, 185, 189, 190, 191, 193, 194, 197, 206, 209, 210, 211, 212, 214, 223, 243, 251, 254, 285, 286, 290, 291, 294, 296, 298, 305, 314

carbon-based materials, viii, 193, 194, 195, 196, 198, 205, 207, 209

carboxyl, 103, 118, 166, 197, 199, 200, 202

carboxylic acid, 108, 195, 201, 202, 206, 213

catalysis, vii, viii, 1, 17, 18, 22, 23, 24, 26, 27, 31, 82, 97, 99, 100, 102, 105, 107, 108, 110, 230, 233, 240, 253, 257, 258, 264, 285, 286, 295

catalyst, 6, 10, 25, 31, 93, 97, 99, 100, 101, 110, 113, 119, 120, 149, 175, 176, 182, 184, 198, 203, 211, 220, 222, 223, 225, 227, 228, 229, 230, 231, 232, 234, 241, 253, 258, 259, 261, 263, 265, 266, 304

- catalytic activity, 39, 99, 100, 101, 102, 103, 104, 105, 106, 110, 111, 112, 113, 175, 176, 183, 223, 229, 244, 265, 266
- catalytic properties, 24, 81, 87, 93, 111
- cathode materials, 91, 164, 169, 220, 229
- cation, 62, 71, 90, 181
- cellulose, 11, 64, 286, 288, 295, 300
- chalcogenides, 99, 244, 288
- challenges, 1, 11, 31, 44, 47, 81, 99, 100, 101, 107, 155, 160, 167, 208, 242, 284
- chemical(s), 1, 2, 3, 8, 10, 11, 18, 19, 22, 24, 25, 26, 35, 36, 37, 38, 39, 51, 62, 64, 65, 66, 69, 70, 71, 77, 83, 84, 86, 88, 93, 95, 96, 97, 102, 103, 104, 106, 107, 108, 112, 115, 117, 119, 120, 126, 129, 133, 136, 137, 142, 145, 149, 150, 155, 156, 157, 159, 160, 163, 165, 166, 171, 174, 176, 178, 180, 183, 186, 188, 191, 194, 195, 196, 197, 198, 218, 225, 230, 236, 237, 238, 242, 248, 252, 267, 272, 275, 279, 284, 285, 286, 288, 289, 291, 293, 301
- chemical properties, 22, 26, 36, 63, 64, 71, 103, 115, 117, 157, 175, 196, 236, 279, 286, 288, 301
- chemical reactions, 10, 22, 102, 225, 237
- chemical stability, 24, 66, 69, 70, 72, 77, 156, 163, 194, 196
- chemical vapor deposition, 83, 129, 195, 197
- chemotherapy, 7, 53, 55
- chitin, 64, 300, 308, 309, 311
- chitosan, vi, ix, 64, 66, 71, 73, 78, 79, 80, 102, 110, 208, 209, 250, 293, 299, 300, 301, 304, 305, 306, 307, 308, 309, 310, 311, 312
- cholesterol, 25, 300, 305, 307, 308, 310
- chromium, 269, 280, 284
- CIS, viii, 62, 67
- classes, 9, 22, 82, 142, 197, 247, 248, 302
- classification, 2, 27, 293
- clean energy, 17, 140, 156, 165, 166, 174, 219, 235
- cleaning, 4, 6, 8, 42, 118, 123, 134
- cleavage, 83, 85, 108, 119
- clusters, 96, 101, 110, 111, 196
- CO₂, 24, 25, 31, 32, 91, 132, 159, 174, 177, 181, 218, 220, 221, 227, 250, 254, 278
- coal, 10, 131, 156, 291, 297
- coatings, viii, 6, 17, 51, 250, 251, 252, 258
- cobalt, 9, 20, 26, 32, 104, 204, 232, 234, 297
- color, 95, 120, 174, 264
- combustion, 28, 140, 265, 287, 295
- commercial, 13, 24, 162, 219, 223, 224, 229, 279
- community, 2, 5, 9, 81, 155, 156, 157, 160, 272
- compatibility, 64, 77, 94, 140, 190, 306
- composites, 4, 22, 23, 29, 32, 94, 96, 117, 118, 123, 163, 190, 219, 226, 228, 229, 230, 233, 240, 242, 248, 290, 293, 296, 307, 312
- composition, 10, 11, 20, 88, 101, 142, 143, 144, 145, 147, 150, 180, 194, 268, 271, 273, 274, 281, 288, 289, 293, 294, 301
- compounds, viii, 21, 23, 51, 56, 59, 99, 106, 107, 144, 147, 151, 153, 245, 263, 266, 268, 269, 273, 284, 287, 295, 301, 304, 306, 307
- compression, 140, 143, 149, 151, 194
- computer, 4, 21, 107, 285
- condensation, 84, 263, 266
- conduction, 62, 76, 87, 88, 95, 117, 147, 173, 177, 181, 182, 185, 241, 291
- conductivity, viii, 1, 4, 61, 62, 69, 70, 71, 72, 73, 74, 75, 76, 77, 79, 80, 88, 92, 117, 119, 128, 147, 148, 155, 156, 157, 158, 159, 162, 164, 178, 195, 197, 220, 224, 231, 236, 283, 292
- conductor(s), 69, 117, 164, 192
- confinement, 5, 6, 37, 82, 86, 87, 174, 183
- Congo, 180, 181, 182, 188, 292
- conjugation, 164, 183, 187, 204
- consolidation, 3, 269, 270
- constituents, 1, 36, 37, 65, 163
- construction, 18, 35, 84, 95, 111, 132, 194, 257, 269, 270, 277, 297
- consumption, 117, 121, 132, 277, 283, 284, 300
- contaminant, 7, 177, 188
- contaminated water, 8, 288, 292
- contamination, 101, 147, 267, 284
- COOH, 178, 179, 196, 253
- coordination, 45, 53, 104
- copolymer(s), 300, 301, 311
- copper, 2, 4, 9, 21, 52, 54, 117, 129, 148, 163, 202, 206, 284, 290, 291, 294, 304, 308, 310
- coronavirus, 11, 15, 42, 48
- correlation, 29, 145, 147, 168
- corrosion, 83, 144, 146, 174, 186, 278
- cosmetics, 1, 35, 248
- cost, 5, 6, 11, 13, 14, 25, 35, 41, 42, 43, 64, 70, 83, 84, 86, 89, 91, 92, 99, 103, 106, 118, 121, 122, 126, 140, 141, 142, 143, 148, 164, 166, 175, 194, 217, 219, 220, 222, 231, 233, 235, 236, 241, 258, 269, 271, 272, 277, 283, 285, 288, 290, 292, 293, 294, 297
- cost effectiveness, 118, 122, 283
- covalent bond, 63, 65, 193, 195, 199, 202
- covalent functionalization, 194, 199, 202, 204, 210, 211, 212

Covid-19, 1, 2, 11, 15, 42, 48, 242
 crystalline, viii, 21, 22, 39, 61, 66, 67, 69, 134,
 160, 244, 258, 261
 crystallinity, 18, 22, 125
 crystals, 82, 168, 236, 238
 CVD, 83, 120, 195, 197
 cyanobacteria, 267, 268, 272, 273, 274, 275,
 277, 279, 280
 cycles, 90, 91, 92, 93, 144, 145, 224, 241, 261,
 292
 cycling, 90, 91, 93, 96, 130, 144, 145, 151, 229
 cytochrome, 113, 204, 206, 212, 214
 cytotoxicity, 41, 44, 47, 48, 306

D

decomposition, 18, 86, 88, 148, 174, 187, 264
 decontamination, 191, 283, 287, 289, 294
 defects, 85, 86, 87, 95, 119, 121, 130, 138, 142,
 145, 179, 184
 degradation, 11, 23, 24, 30, 31, 131, 132, 135,
 136, 137, 138, 153, 174, 177, 178, 179, 180,
 181, 182, 183, 184, 186, 187, 188, 190, 191,
 192, 277, 286, 287, 289, 290, 291, 294, 295,
 296, 297, 298
 degradation rate, 178, 180, 181, 184, 187
 deposition, 3, 88, 91, 120, 134, 137, 138, 153,
 236, 245, 292
 depth, 21, 107, 132, 271, 272
 derivatives, 62, 100, 107, 119, 121, 126, 155,
 157, 160, 163, 164, 169, 212, 259, 260, 261,
 262, 265, 266
 desorption, 9, 90, 142, 143, 144, 146, 147, 148,
 151, 225, 241
 destruction, 18, 42, 90
 detection, 6, 11, 25, 29, 32, 39, 40, 41, 45, 46,
 48, 57, 102, 106, 109, 110, 111, 112, 113,
 194, 195, 200, 201, 202, 204, 207, 210, 211,
 212, 213, 214, 250, 255, 280
 developing countries, 283, 284, 290
 diabetes, 36, 58, 59
 diagnostics, 14, 25, 35, 36, 38, 44, 46, 101, 289
 dielectric constant, 68, 75, 76, 80
 dielectric permittivity, 61, 68, 75, 80
 dielectric properties, viii, 61, 62, 66, 77, 132
 diffusion, viii, 77, 90, 92, 119, 131, 132, 134,
 174, 178, 226, 227, 230
 diffusion length, 119, 131, 132, 134, 174, 178
 direct methanol fuel cell, 168, 217, 218, 220,
 233

diseases, 10, 15, 26, 35, 36, 38, 42, 51, 52,
 106, 242, 283, 284
 disinfection, 4, 8, 9, 14, 22, 175, 296, 304
 dispersion, 80, 90, 124, 167, 176, 180, 187,
 197, 204, 231, 245, 286
 dissociation, 69, 71, 74, 75, 146, 148, 221
 distribution, 2, 11, 20, 82, 125, 126, 147, 156,
 159, 166, 198, 287, 300, 302, 303, 306
 DNA, 2, 7, 31, 38, 46, 53, 54, 62, 102, 107, 108,
 110, 111, 113, 114
 dopamine, 197, 204, 207, 209, 210, 212, 213,
 214
 dopants, 86, 87, 183
 doping, 4, 20, 28, 92, 145, 165, 174, 184, 194,
 223, 229, 230, 289, 290
 drawing, 100, 104, 156
 drinking water, 8, 176, 293
 drug delivery, ix, 1, 3, 6, 7, 13, 23, 27, 29, 30,
 36, 43, 44, 46, 95, 104, 127, 195, 196, 199,
 208, 249, 251, 299, 300, 301, 302, 303, 304,
 305, 306, 307, 309, 311, 312
 drug release, ix, 38, 299, 302, 304, 305, 309
 drug-delivery, 2, 299, 302, 306
 drugs, 1, 7, 36, 39, 53, 54, 55, 293, 301, 304,
 305, 307
 drying, 85, 196, 268, 272, 273, 277
 dumping, 267, 271, 273, 276, 277
 durability, 70, 89, 198, 222, 230
 dyes, 7, 17, 23, 24, 93, 180, 181, 186, 188, 190,
 191, 192, 204, 284, 286, 287, 289, 290, 291,
 292, 293, 294

E

economics, 132, 141, 151
 efficiency, 5, 6, 9, 13, 30, 89, 91, 92, 104, 113,
 118, 131, 132, 137, 138, 140, 141, 142, 157,
 163, 164, 173, 174, 177, 178, 179, 180, 181,
 183, 185, 186, 187, 188, 189, 217, 219, 220,
 230, 271, 273, 277, 287, 289, 290, 291, 294,
 304
 effluent(s), 175, 273, 279, 284
 electric field, 66, 67, 74, 75, 76, 135, 301
 electrical conductivity, 4, 61, 72, 79, 90, 118,
 156, 160, 178, 185, 196
 electrical properties, 4, 62, 80, 95, 97, 130, 159,
 257, 258
 electricity, 5, 13, 131, 166, 175
 electrocatalysis, 22, 25, 31, 230, 247

- electrocatalyst, 31, 88, 183, 217, 218, 219, 223, 224, 231, 232, 233
 electrochemical impedance, viii, 61, 77
 electrochemical sensor, 62, 95, 193, 194, 197, 198, 200, 201, 204, 207, 209, 211, 212, 213, 214, 232, 251
 electrochemistry, 47, 241, 247
 electrode surface, 161, 193, 196, 200, 221, 226, 230
 electrodes, 3, 5, 28, 67, 72, 77, 88, 90, 92, 120, 122, 123, 149, 158, 160, 161, 162, 163, 164, 167, 170, 201, 206, 207, 208, 209, 213, 224, 240, 251
 electrolyte, viii, 61, 62, 64, 66, 69, 70, 71, 72, 73, 74, 75, 76, 77, 79, 80, 88, 90, 122, 123, 125, 158, 161, 162, 164, 165, 175, 183, 218, 224, 225, 227, 230, 241
 electromagnetic, 22, 42, 119
 electron(s), 5, 20, 21, 37, 53, 62, 66, 76, 82, 86, 88, 89, 90, 93, 94, 103, 105, 111, 117, 121, 122, 124, 125, 126, 128, 129, 132, 133, 134, 138, 157, 159, 160, 163, 167, 169, 175, 176, 177, 179, 180, 181, 182, 184, 185, 186, 187, 191, 193, 194, 196, 204, 212, 218, 223, 224, 225, 226, 227, 229, 230, 241, 291
 electron microscopy, 21, 121, 124
 electron pairs, 89, 95, 177
 electronic structure, 18, 142, 153, 175, 194
 electroreduction, 31, 228, 232, 233
 emission, 6, 38, 39, 41, 82, 87, 94, 95, 134, 167, 217, 219, 251
 emitters, 159, 168, 250
 energy, vii, viii, ix, 1, 5, 6, 8, 10, 14, 17, 18, 20, 21, 22, 23, 24, 25, 29, 48, 62, 68, 69, 70, 74, 75, 76, 77, 78, 82, 87, 88, 89, 90, 91, 92, 93, 95, 97, 105, 118, 119, 120, 126, 128, 131, 133, 134, 137, 139, 140, 141, 142, 143, 145, 147, 148, 149, 150, 155, 156, 157, 159, 160, 161, 162, 163, 164, 165, 166, 167, 168, 169, 170, 171, 174, 175, 177, 181, 182, 185, 186, 187, 189, 195, 217, 218, 219, 230, 231, 232, 235, 236, 239, 240, 242, 247, 251, 271, 273, 276, 286, 289, 291
 energy band gap, 131, 134
 energy consumption, 132, 137, 140, 177
 energy density, 69, 70, 90, 91, 92, 141, 147, 162, 164, 219, 230
 energy efficiency, 6, 89, 273
 energy harvesting, viii, ix, 132, 134, 137, 155, 156, 157, 159, 162, 166, 167, 182, 235, 242
 energy storage, vii, 1, 17, 22, 23, 24, 62, 78, 82, 92, 118, 126, 128, 132, 156, 157, 160, 161, 162, 163, 164, 166, 169, 170, 171, 175, 195, 231, 240, 247, 251
 engineering, 8, 107, 134, 149, 154, 192, 236, 245, 258, 302
 environment(s), vii, viii, 4, 5, 14, 17, 18, 25, 27, 83, 84, 88, 132, 144, 155, 156, 157, 163, 174, 179, 181, 190, 222, 231, 249, 251, 269, 275, 278, 284, 289, 290, 293
 environmental conditions, 100, 106, 271
 environmental protection, 271, 284, 291
 enzyme(s), viii, 7, 53, 99, 100, 101, 102, 103, 104, 105, 106, 107, 108, 109, 110, 112, 113, 114, 200, 237, 249
 equilibrium, 116, 142, 147
 erosion, 269, 276, 277
 ethanol, 134, 218, 232, 259
 ethylene, 64, 78, 79, 199, 301, 306
 ethylene oxide, 64, 78, 79
 evolution, 30, 31, 81, 88, 97, 144, 185, 191, 192, 241, 243, 245
 excitation, 7, 40, 48, 82, 86, 87, 95, 167, 181
 exploitation, viii, 24, 25, 26, 37, 117, 194
 exposure, 10, 18, 284, 290
 extraction, 133, 184, 268, 269, 273, 294

F

- fabrication, 18, 28, 29, 69, 81, 83, 84, 92, 127, 132, 134, 138, 143, 157, 159, 161, 169, 174, 190, 194, 197, 199, 203, 213, 243, 285, 293, 296, 301
 fat, 56, 307, 308
 ferrite, 20, 28, 194, 208, 290, 296, 298
 ferromagnetic, 20, 100, 107, 109, 113
 fiber(s), 36, 40, 140, 159, 165, 169, 287
 films, viii, 15, 29, 64, 66, 70, 71, 77, 79, 83, 91, 130, 134, 163, 233, 252, 306, 307, 309, 310
 filters, 9, 11, 159, 270
 filtration, 8, 22, 285
 financial, 27, 44, 78, 188, 277
 financial support, 27, 44, 277
 flexibility, 63, 66, 67, 69, 70, 71, 76, 77, 117, 163, 164, 217, 235, 248
 flocculation, 248, 250, 254
 fluid, 20, 26, 33, 252, 305
 fluorescence, 38, 39, 41, 96, 97, 102, 198, 211, 306
 fluorine, 133, 134, 183, 187

food, 10, 12, 25, 32, 66, 79, 100, 248, 249, 306
 force, 84, 117, 222, 238
 formation, 54, 56, 83, 84, 85, 86, 109, 110, 111,
 112, 120, 124, 139, 143, 145, 146, 147, 148,
 161, 162, 176, 193, 220, 222, 236, 258, 287,
 310
 fossil fuel, 10, 25, 32, 88, 91, 131, 140, 156,
 166, 174, 218
 free radicals, 177, 181, 187, 300
 fuel cell, 5, 6, 25, 61, 62, 70, 72, 89, 157, 158,
 164, 166, 168, 198, 204, 210, 217, 218, 220,
 230, 231, 232, 233, 258
 fullerene(s), 3, 22, 84, 100, 103, 108, 116, 120,
 137, 139, 141, 155, 156, 157, 158, 160, 163,
 164, 165, 167, 168, 193, 194, 195, 196, 199,
 200, 204, 205, 206, 207, 209, 211, 213, 214,
 236
 functionalization, vii, viii, 92, 95, 102, 128, 174,
 178, 179, 180, 181, 188, 189, 190, 193, 194,
 195, 196, 197, 198, 199, 200, 201, 202, 204,
 206, 207, 208, 210, 211, 212, 249, 250, 251,
 287, 314
 fungi, 276, 300, 309

G

gas sensors, 11, 15, 26, 32, 157, 159, 160, 168,
 249
 gel, 19, 190, 252, 254, 292
 geometry, 86, 147, 153, 158, 165
 glucose, 7, 11, 25, 32, 56, 102, 109, 110, 111,
 112, 113, 196, 197, 208, 210, 255, 304
 gold nanoparticles, 1, 11, 27, 29, 32, 43, 45, 48,
 100, 102, 108, 110, 113, 189, 204, 209, 214,
 287
 GQD, 83, 84, 86, 90
 graphene, v, 13, 19, 22, 23, 25, 28, 29, 30, 31,
 32, 39, 42, 47, 48, 81, 82, 83, 84, 86, 92, 94,
 95, 96, 97, 98, 103, 105, 110, 112, 114, 115,
 116, 117, 118, 119, 120, 121, 123, 124, 125,
 126, 127, 128, 129, 130, 139, 141, 155, 156,
 157, 158, 160, 162, 163, 164, 165, 166, 167,
 168, 169, 170, 171, 179, 180, 183, 189, 190,
 193, 194, 195, 196, 197, 199, 201, 204, 205,
 206, 207, 209, 210, 212, 214, 218, 231, 232,
 233, 234, 236, 238, 240, 241, 243, 244, 245,
 285, 286, 287, 288, 290, 291, 292, 294, 295,
 296, 297, 298, 306, 314
 graphene nanosheet, 25, 32, 119, 218, 233

graphene sheet, 84, 96, 119, 120, 121, 122,
 123, 125, 126, 130, 158, 160, 162, 164, 165,
 171, 196, 197, 206, 209
 graphite, 4, 18, 82, 83, 85, 91, 92, 115, 116,
 119, 120, 121, 122, 123, 124, 125, 126, 129,
 130, 151, 155, 156, 159, 160, 170, 179, 196,
 206, 207, 208, 209, 212, 238, 240, 251, 291
 green alga, 272, 279, 280
 greenhouse gas, 10, 218, 219
 groundwater, ix, 8, 269, 270, 286
 growth, vii, 11, 86, 88, 101, 120, 131, 166, 174,
 201, 223, 258, 267, 273, 275, 308, 310
 guanine, 202, 210, 222, 232
 guidelines, 233, 234, 270

H

hardness, 21, 66, 195
 harvesting, viii, ix, 132, 134, 137, 155, 156, 157,
 159, 162, 166, 167, 177, 180, 182, 185, 189,
 190, 191, 235, 242
 hazards, 4, 6, 217, 269, 271
 healing, 55, 118, 128
 health, vii, 4, 6, 13, 35, 36, 39, 44, 53, 54, 284,
 301
 healthcare, vii, 35, 36, 37, 43
 heat transfer, 20, 147, 148
 heavy metals, ix, 29, 93, 174, 271, 275, 276,
 277, 284, 286, 289, 291, 294, 297
 heterocyclic molecules, 257
 heterogeneous catalysis, 31, 258, 264
 high strength, 160, 164, 241, 281
 HIV, 10, 39, 54, 58, 259
 host, 42, 43, 53, 62, 64, 70, 71, 77
 human, vii, 1, 4, 5, 8, 10, 11, 12, 13, 36, 37, 38,
 39, 43, 51, 52, 54, 58, 107, 111, 131, 140,
 155, 176, 214, 276, 283, 284, 293, 304
 human body, 37, 38, 39, 51, 284
 human health, 4, 8, 10, 58, 155, 176, 276
 humidity, viii, 11, 15, 135, 136, 137, 138, 210,
 250
 hybrid, ix, 33, 35, 92, 93, 94, 113, 116, 137,
 157, 158, 162, 163, 165, 166, 171, 187, 213,
 223, 228, 229, 230, 233, 234, 247, 248, 249,
 250, 251, 252, 253, 254, 255, 283, 284, 286,
 287, 288, 289, 290, 291, 293, 295, 296, 297,
 298, 305
 hybrid materials, ix, 165, 166, 171, 187, 233,
 247, 248, 249, 250, 251, 252, 253, 254, 287,
 289, 291, 295

- hybrid nanomaterial, ix, 33, 35, 283, 284, 286, 288, 289, 290, 291, 292, 293, 295
- hybridization, 193, 195, 196
- hydrazine, 25, 204, 212, 259
- hydrides, 139, 140, 141, 144, 145, 146, 147, 148, 149, 151, 152, 153, 154, 165
- hydrogels, 299, 301, 307, 308
- hydrogen, 6, 23, 29, 30, 31, 32, 64, 66, 86, 88, 97, 102, 105, 110, 113, 120, 122, 139, 140, 141, 142, 143, 144, 145, 146, 147, 148, 149, 150, 151, 152, 153, 154, 155, 156, 159, 160, 162, 164, 165, 166, 167, 169, 171, 180, 191, 192, 194, 197, 201, 204, 208, 209, 211, 214, 218, 219, 233, 235, 241, 243, 244, 245, 287, 289
- hydrogen energy, 140, 235
- hydrogen peroxide, 86, 102, 105, 110, 113, 194, 197, 201, 208, 209, 211, 214
- hydrogenation, viii, 139, 140, 142, 143, 144, 146, 150, 151, 152
- hydrophilicity, 53, 195, 197
- hydroxide, 32, 57, 104, 112, 113, 181, 294
- hydroxyl, 64, 66, 83, 86, 90, 103, 118, 166, 180, 181, 195, 197, 199, 200, 202, 238, 258, 289, 293
- hyperthermia, 26, 33, 305, 311
- hysteresis, 132, 135, 136, 137, 138, 144, 148, 305
- inorganic material, viii, 21, 26, 51, 52, 53, 54, 55, 56, 58, 186, 247, 248, 290
- insulin mimetic, 51
- integration, 10, 118, 168, 183, 199
- interface, 67, 69, 73, 75, 88, 90, 92, 95, 119, 128, 175, 177, 187, 194, 248
- intermetallics, 116, 127, 143, 151
- ionic conductivity, viii, 62, 70, 71, 72, 77, 79, 80
- ions, 28, 30, 52, 53, 54, 56, 62, 69, 70, 72, 74, 76, 90, 91, 95, 105, 161, 162, 181, 212, 225, 240, 265, 291, 293, 295, 304
- iron, 8, 14, 24, 26, 27, 33, 41, 52, 54, 105, 144, 146, 179, 206, 209, 233, 236, 255, 268, 271, 276, 280, 286, 289, 295, 297, 305
- irradiation, 24, 88, 93, 94, 174, 178, 182, 187
- isotherms, 139, 142, 143, 144, 147, 148, 153
- issues, 3, 4, 32, 37, 44, 70, 100, 163, 175, 217, 218, 222

K

- kinetics, 101, 102, 139, 142, 143, 144, 145, 146, 148, 151, 152, 174, 179, 184, 194, 217, 221, 222, 226, 241, 294, 302
- KOH, 226, 227, 229

L

- I
- ideal, 4, 90, 157, 159, 249, 275, 283
- identification, 42, 97, 112
- illumination, 88, 93, 95, 178, 181, 184, 192
- image(s), 6, 21, 40, 45, 124, 125
- impurities, 4, 255, 268
- in vitro, 36, 43, 48, 300, 307, 309
- in vivo, 30, 36, 38, 41, 43, 44, 45, 47, 48, 49, 208, 300, 307
- India, 1, 51, 61, 78, 81, 131, 139, 155, 173, 193, 235, 247, 257, 267, 272, 273, 277, 279, 280, 283, 299, 313, 314
- induction, 46, 142, 144
- industrialization, viii, 137, 284
- industry/industries, vii, 5, 7, 94, 117, 131, 155, 156, 157, 160, 176, 236, 248, 267, 268, 272, 273, 279, 284, 302
- infection, 12, 26, 39
- inflammation, 26, 36, 55
- inhibition, 53, 54, 55, 56, 185, 278
- lakes, 123, 129, 269
- laser ablation, 3, 18, 197
- lead, 25, 32, 36, 51, 52, 108, 115, 116, 117, 123, 164, 166, 193, 198, 201, 207, 209, 269, 283, 284
- leakage, 69, 269, 270
- lifetime, 39, 47, 187
- ligand, 53, 180, 309
- light, 6, 7, 20, 24, 30, 31, 38, 41, 88, 93, 94, 131, 132, 134, 137, 148, 160, 163, 165, 174, 177, 178, 180, 181, 185, 186, 187, 189, 190, 191, 192, 212, 241, 244, 290, 291, 296, 297, 298, 301
- liposomes, 26, 35, 42, 106
- lithium, 55, 71, 98, 128, 158, 159, 164, 168, 169, 219, 231, 232, 241, 251
- lithium ion batteries, 128, 159, 169, 219, 232
- liver, 26, 33, 40, 56, 304
- liver cancer, 26, 33, 304
- luminescence, 38, 86, 94
- lung cancer, 6, 33, 55

Luo, 30, 31, 97, 113, 130, 151, 192, 212, 309, 310, 311

M

macromolecules, 62, 300, 301
 magnetic field, 12, 287, 289, 304
 magnetic properties, 27, 28, 290, 302
 magnetic resonance, 6, 37, 39, 48
 magnetic resonance imaging, 6, 37, 39, 48
 magnitude, 3, 117, 219
 majority, 100, 198, 283
 management, 8, 147, 161, 240, 270
 manganese, 9, 10, 120, 194, 207, 209, 210, 234, 269
 manipulation, 12, 53, 107
 manufacturing, vii, 3, 5, 10, 13, 24, 25, 157, 175
 mass, 11, 26, 92, 143, 147, 165, 219, 224, 226, 227, 228, 291
 materials, vii, viii, ix, 1, 2, 3, 5, 8, 12, 13, 17, 18, 20, 22, 23, 24, 26, 27, 36, 39, 41, 43, 44, 45, 51, 52, 54, 55, 56, 58, 61, 62, 64, 66, 67, 70, 71, 77, 79, 82, 85, 87, 89, 92, 94, 96, 97, 98, 100, 101, 103, 104, 106, 115, 116, 117, 118, 119, 121, 124, 125, 126, 127, 128, 129, 130, 132, 134, 139, 141, 143, 144, 146, 151, 154, 155, 156, 157, 158, 159, 160, 162, 163, 164, 165, 166, 167, 168, 170, 171, 173, 175, 178, 180, 184, 186, 187, 193, 194, 195, 196, 198, 199, 201, 205, 207, 208, 209, 228, 231, 233, 235, 236, 237, 238, 239, 241, 242, 243, 245, 247, 248, 249, 250, 251, 252, 253, 254, 257, 258, 264, 268, 269, 277, 283, 285, 286, 287, 288, 289, 290, 291, 293, 295, 300, 301
 materials science, 44, 115, 116, 248, 286
 matrix, 23, 28, 30, 62, 71, 77, 118, 129, 208, 247, 304
 matter, 2, 3, 12, 116, 272, 273
 measurement(s), viii, 2, 26, 47, 68, 72, 77, 145, 152, 230, 250
 mechanical properties, 4, 18, 21, 29, 117, 118, 119, 166, 217, 220, 235, 238, 283
 media, 30, 84, 148, 178, 186, 224, 228, 288
 medical, vii, 1, 13, 18, 20, 25, 26, 36, 38, 43, 47, 66, 106, 117, 196, 289, 300, 314
 medicinal inorganic, 51
 medicine, vii, viii, 5, 12, 26, 35, 39, 44, 46, 47, 48, 51, 54, 208, 251
 medicines, 23, 25, 35, 51, 52, 54, 159, 301
 melting, 37, 72, 84, 142, 144, 146, 287

membranes, 8, 10, 53, 168, 285, 294, 297, 310
 memory, 12, 95, 161, 242, 285
 mercury, 29, 52, 269, 280, 284
 metal complexes, viii, 51, 53, 54
 metal hydrides, 139, 140, 141, 144, 145, 147, 149, 151, 152, 154, 165
 metal ion, 8, 22, 24, 52, 53, 54, 58, 71, 79, 104, 105, 176, 230, 276, 288, 294, 304, 310
 metal nanoparticles, 24, 99, 100, 165, 244, 254, 264, 294, 305
 metal oxide nanoparticles, 24, 257, 258
 metal oxides, 20, 23, 26, 35, 99, 175, 180, 239, 240, 254, 267, 285
 metalloenzymes, viii, 51, 53, 54
 metals, viii, 6, 9, 20, 22, 23, 26, 31, 51, 52, 53, 116, 144, 174, 228, 231, 232, 269, 271, 275, 276, 277, 280, 284, 286, 289, 290, 293, 294, 304
 methanol, 110, 168, 217, 218, 219, 220, 221, 222, 223, 229, 230, 231, 232, 233, 243
 methanol oxidation reaction, 218, 219, 223, 232, 233
 methylene blue, 30, 93, 180, 185, 186, 190, 191, 286, 289, 291, 292, 294, 296, 297
 microorganisms, ix, 9, 22, 26, 53, 276, 286
 microstructure(s), 115, 116, 127, 143, 150, 247, 296
 migration, 77, 174, 177
 mixing, 56, 223, 283, 286
 models, 3, 55, 107, 152
 modern society, 18, 24, 61, 62, 284
 modifications, 38, 139, 197
 modulus, viii, 4, 21, 62, 69, 76, 77, 79, 117, 119, 159, 220
 molecules, ix, 2, 3, 11, 18, 23, 52, 53, 62, 64, 65, 66, 86, 93, 119, 145, 158, 159, 160, 165, 166, 167, 174, 177, 181, 186, 187, 188, 193, 195, 197, 198, 199, 204, 230, 237, 239, 257, 259, 293, 301
 molybdenum, 97, 206, 236, 290
 monolayer, 85, 87, 94, 95, 97, 98, 128, 147, 236, 238, 242
 monomers, 62, 64, 287, 300
 morphology, 18, 21, 22, 29, 74, 83, 97, 110, 111, 124, 126, 178, 194, 261, 285, 296, 302
 MRI, 6, 37, 39, 40, 42, 44, 47, 57

N

NADH, 200, 201, 205

- nanocomposites, vi, ix, 15, 17, 23, 24, 29, 30, 31, 93, 99, 104, 113, 114, 127, 128, 160, 175, 185, 191, 197, 206, 207, 231, 241, 243, 247, 249, 252, 253, 254, 265, 283, 284, 285, 286, 287, 292, 293, 294, 295, 296, 297, 306, 311, 312
- nanocrystals, 35, 38, 48, 103, 111, 209, 234
- nanodots, 45, 190, 193, 195
- nanofibers, 11, 151, 175, 187, 189, 192, 193, 195, 205, 288
- nanomaterials, v, vi, vii, viii, ix, 1, 2, 3, 4, 5, 6, 7, 8, 11, 12, 13, 14, 15, 17, 18, 24, 25, 26, 27, 28, 29, 30, 32, 33, 35, 36, 37, 38, 39, 40, 42, 43, 44, 46, 47, 48, 51, 89, 99, 100, 101, 102, 103, 106, 109, 110, 111, 112, 113, 116, 117, 120, 126, 127, 155, 156, 157, 161, 163, 164, 165, 167, 168, 170, 173, 174, 177, 178, 179, 180, 181, 182, 183, 185, 187, 188, 189, 190, 191, 192, 194, 195, 199, 207, 208, 209, 211, 214, 231, 235, 236, 237, 240, 241, 242, 243, 244, 245, 257, 258, 280, 283, 285, 286, 288, 289, 290, 291, 292, 293, 296, 314
- nanomedicine, 17, 18, 26, 27, 32, 33, 38, 39, 44, 46, 242
- nanometer, 39, 82, 116, 237, 287
- nanoparticles, vii, 1, 2, 4, 6, 7, 8, 11, 17, 18, 19, 20, 22, 23, 24, 25, 26, 27, 28, 29, 30, 31, 32, 33, 35, 37, 38, 39, 40, 41, 42, 43, 44, 45, 46, 47, 48, 49, 88, 94, 99, 100, 102, 103, 105, 106, 107, 108, 109, 110, 111, 112, 113, 114, 118, 127, 146, 165, 169, 170, 174, 178, 180, 181, 182, 186, 188, 189, 190, 191, 192, 197, 201, 204, 206, 208, 209, 211, 212, 213, 214, 223, 229, 231, 232, 233, 234, 244, 254, 255, 258, 259, 260, 261, 262, 264, 265, 266, 280, 285, 286, 287, 289, 292, 294, 295, 296, 297, 299, 301, 302, 304, 305, 306, 307, 308, 309, 310, 311
- nanoribbons, 19, 28, 163
- nanorods, 6, 7, 12, 109, 175, 213
- nanostructured materials, 6, 45, 116, 177, 197
- nanostructures, 2, 6, 11, 26, 32, 37, 90, 103, 104, 109, 110, 111, 157, 163, 165, 167, 168, 184, 185, 192, 207, 208, 209, 237, 250, 286, 296, 298
- nanotechnology, vii, 1, 2, 3, 4, 5, 6, 8, 9, 10, 11, 12, 13, 14, 15, 19, 24, 26, 27, 28, 32, 36, 42, 44, 46, 48, 99, 100, 106, 167, 170, 189, 194, 208, 236, 252, 268, 276, 277, 283, 284, 293, 300, 301
- nanotube, 3, 4, 11, 32, 88, 97, 112, 129, 167, 168, 176, 178, 179, 183, 185, 191, 206, 211, 214, 231, 236, 244, 245, 251, 254, 255, 258, 295, 305, 308, 310
- nanowires, 6, 9, 14, 31, 46, 90, 103, 111, 175
- nanozymes, viii, 99, 101, 104, 105, 106, 108, 109, 112, 113
- natural compound, 106, 308, 310
- natural gas, 131, 140, 156, 218, 219
- natural polymers, 63, 64, 249
- NH₂, 64, 178, 179, 201, 209
- nickel, 20, 26, 32, 53, 144, 146, 164, 206, 223, 269, 284, 298, 304
- NIR, 45, 88, 94
- nitrides, 194, 198, 203, 207, 235
- nitrite, 25, 200, 211
- nitrogen, 30, 94, 166, 185, 198, 205, 206, 214, 223, 229, 232, 233, 234, 273, 275, 277, 284
- Nobel Prize, 63, 78, 116, 160, 236
- noble metals, 222, 224, 228
- non-covalent functionalization, 194, 195, 198, 204, 206, 212
- nucleation, 84, 86, 88, 102, 208
- nucleus/nuclei, 40, 65, 259
- nucleic acid, 44, 100, 102
- nutrient(s), 95, 176, 271, 276

O

- oil, 9, 131, 156, 240, 264, 279, 280, 286
- one dimension, 116, 117, 236, 237, 238
- opportunities, 28, 47, 208, 247
- optical properties, 2, 20, 23, 25, 39, 66, 95, 127, 156
- optimization, 143, 153, 281, 295
- optoelectronics, 82, 87, 94, 96, 112, 117, 156, 160
- ores, 52, 268, 269, 276, 280, 286
- organ(s), viii, 6, 40, 51, 53, 132, 238, 303
- organic compounds, 21, 116, 177, 181, 232, 290, 307
- organic matter, 95, 271, 272, 277
- organic polymers, 23, 252, 286
- organic solvents, 64, 65, 158, 164, 198, 257
- ox, 84, 87, 103, 179, 257, 258
- oxidation, 1, 25, 56, 83, 84, 86, 87, 89, 91, 96, 102, 104, 105, 109, 110, 120, 122, 130, 142, 145, 152, 159, 177, 179, 180, 183, 185, 187, 192, 200, 201, 210, 214, 217, 218, 219, 220,

221, 222, 223, 224, 230, 231, 232, 233, 238,
291, 297, 300
oxide nanoparticles, 24, 26, 33, 49, 114, 206,
214, 257, 258, 266, 294
oxygen, 54, 83, 87, 88, 97, 102, 120, 126, 131,
148, 166, 175, 177, 178, 179, 181, 183, 185,
189, 196, 206, 208, 210, 217, 218, 219, 221,
224, 226, 228, 231, 233, 234, 241, 258
oxygen reduction reaction, 181, 189, 208, 210,
217, 218, 219, 224, 233, 234

P

PAA, 47, 251, 287
paints, 25, 61, 62
palladium, 153, 232, 233
passivation, 94, 97, 186, 191
pathogens, 10, 42, 293
pathway(s), 55, 175, 220, 224, 225, 226, 229
peptide(s), 1, 2, 11, 23
permeability, 38, 271, 299
permission, 125, 179, 180, 182, 184, 200, 201,
202, 203, 272
permittivity, 69, 74, 75, 76
perovskite solar cell, viii, 131, 132, 133, 134,
135, 136, 137, 138, 190
peroxide, 105, 197, 200, 204, 206, 225
PET, 9, 41, 123
petroleum, 131, 140, 249, 276
pH, 100, 102, 106, 179, 181, 221, 223, 268,
269, 271, 272, 273, 274, 275, 301, 304, 305,
308
pharmaceutical(s), 5, 26, 35, 156, 196, 214,
248, 257, 293, 302
phosphate(s), 24, 47, 55, 309
phosphorus, 52, 166, 235, 273
photo activity, 174
photo degradation, 174, 176, 178, 179, 181,
185, 186
photocatalysis, 9, 22, 23, 31, 87, 97, 98, 178,
185, 265, 291, 298
photodegradation, 24, 93, 190
photodetectors, viii, 82, 87, 94
photovoltaic devices, 97, 157, 162, 163, 289
physical properties, 26, 39, 63, 65, 66, 118,
174, 178
physicochemical properties, 49, 95, 194, 293
physics, 3, 5, 116, 132, 147, 152, 154, 236, 237
pipeline, 2, 11, 12, 271
plants, 10, 26, 53, 64, 271, 272, 277, 294

platelets, 160, 162, 163, 164
platform, 96, 99, 106, 112, 209, 210, 211, 214,
295
platinum, 55, 102, 107, 109, 111, 122, 124, 206,
213, 217, 222, 229, 232, 233, 243, 305, 308,
310
PMMA, 63, 64, 66, 79, 163
polar, 62, 63, 66, 180, 185, 196, 198
polarity, 53, 63, 66, 95
polarization, 67, 69, 73, 74, 75, 228
pollutant(s), ix, 4, 8, 14, 24, 25, 93, 160, 174,
177, 180, 185, 186, 188, 189, 192, 244, 250,
276, 283, 284, 286, 287, 289, 290, 294, 295,
298
pollution, 10, 11, 26, 131, 164, 174, 217, 269,
271, 273, 280, 283, 284
polymer(s), viii, 6, 10, 20, 23, 25, 26, 30, 37, 42,
44, 45, 57, 61, 62, 63, 64, 65, 66, 67, 69, 70,
71, 72, 74, 75, 76, 77, 78, 79, 80, 100, 102,
108, 118, 119, 120, 127, 128, 129, 160, 171,
174, 176, 177, 178, 186, 187, 189, 190, 192,
197, 209, 218, 239, 240, 249, 252, 254, 286,
293, 295, 296, 299, 300, 301, 304, 307, 308,
314
polymer chain, 62, 64, 65, 66, 67, 71, 76, 178,
187
polymer composites, 118, 128, 129
polymer electrolytes, 62, 64, 69, 70, 71, 74, 77,
78, 79
polymer nanocomposites, 127, 128, 287, 295
polymeric chains, 63, 65, 67
polymeric materials, 62, 64, 65, 290
polymerization, 62, 200, 286, 299, 309
polysaccharide(s), 250, 254, 276, 299, 300, 307
population, 91, 131, 156, 283
porosity, 104, 156, 159, 198
potassium, 121, 238, 280
precipitation, 3, 27, 28, 146, 258, 264
preparation, 27, 64, 71, 77, 85, 91, 97, 98, 103,
106, 130, 188, 197, 201, 202, 203, 204, 212,
236, 237, 252, 285, 288, 290, 293, 309
prevention, 15, 37, 271
principles, 3, 8, 18, 53, 153, 157, 228, 233, 280
protection, 12, 109, 262, 266
proteins, 1, 2, 23, 26, 38, 41, 42, 43, 44, 48, 53,
56, 100, 211, 249, 276
protons, 218, 225, 226, 240, 241
purification, 1, 8, 9, 84, 139, 149, 159, 257, 258,
283, 284, 286, 288, 293, 294, 295, 297, 298
PVA, 66, 79, 287
PVP, 66, 71, 79, 186, 191

pyrolysis, 3, 258, 264
 pyrolytic graphite, 122, 124, 206

Q

quantification, 11, 210, 212
 quantum confinement, 6, 37, 82, 86, 87, 174, 183
 quantum dot(s), 5, 14, 26, 31, 35, 37, 38, 41, 44, 46, 81, 82, 83, 92, 93, 96, 97, 98, 99, 101, 103, 105, 112, 163, 183, 189, 190, 191, 192, 237, 243, 305

R

radiation, 41, 42, 53, 109, 132, 144, 238
 radicals, 83, 86, 181, 289
 Raman spectroscopy, 40, 124, 125, 126
 raw materials, 121, 142, 273
 reaction mechanism, viii, 99, 101, 102, 104, 105, 225, 226, 233
 reaction time, 86, 186, 260, 261, 292
 reactions, 10, 25, 31, 88, 90, 91, 121, 142, 161, 176, 181, 187, 204, 210, 223, 230, 232, 233, 241, 251, 258, 259, 260, 261, 262, 263, 265, 286, 290
 reactive oxygen, 9, 39, 200
 reactivity, 1, 9, 18, 24, 26, 27, 142, 160, 174, 188, 195, 197, 229, 258
 receptor(s), 54, 145, 204, 297, 309
 reclamation, 268, 280
 recognition, 38, 106, 247, 305
 recombination, 15, 89, 95, 134, 176, 177, 183, 184, 187
 recovery, 9, 44, 136, 137, 175, 177, 280, 285
 recycling, 8, 55, 92, 177
 red mud, ix, 267, 268, 269, 270, 271, 272, 273, 274, 275, 276, 277, 278, 279, 280, 281
 redox activity, 174, 185
 relaxation, 40, 66, 67, 69, 74, 76, 79, 80
 remediation, vii, 7, 9, 23, 25, 27, 35, 174, 190, 271, 272, 276, 277, 279, 289, 290, 296
 renewable energy, vii, 5, 91, 93, 140, 166, 176, 218, 241
 repellent, 3, 9, 252
 requirement(s), 90, 92, 104, 131, 159, 160, 163, 165, 166, 273
 researchers, 9, 10, 24, 25, 26, 36, 42, 51, 102, 103, 120, 157, 196, 247, 249, 285, 293, 302

residue(s), 64, 267, 268, 269, 270, 271, 272, 275, 276, 277, 278, 279, 280
 resistance, 1, 4, 39, 62, 72, 89, 90, 142, 145, 146, 147, 148, 163, 184, 248, 252, 285
 resolution, 21, 40, 41, 81, 82, 125
 resources, 8, 25, 132, 218, 230, 268
 response, 46, 74, 90, 95, 160, 196, 198, 200, 201, 204, 209, 238, 291
 risk(s), ix, 4, 8, 13, 36, 41, 268, 269, 270, 271, 276, 277, 284
 RNA, 2, 11, 53, 108, 109
 rods, 36, 83, 120, 122, 233
 room temperature, 66, 70, 71, 77, 118, 119, 134, 148, 155, 157, 158, 181, 259, 261
 rotations, 69, 226, 227
 routes, 37, 120, 198, 207, 284
 Royal Society, 58, 59, 78, 107, 311
 rubber, 61, 62, 120
 rutile, 93, 94, 137

S

safety, 6, 37, 38, 41, 70, 91, 164
 salts, 56, 62, 71, 120, 254, 268, 270
 SARS, 1, 11, 15
 scattering, 20, 38, 243, 305
 science, vii, 2, 6, 14, 24, 35, 51, 99, 100, 106, 115, 116, 248, 257, 258, 286, 300, 314
 scope, 99, 100, 103, 106, 188
 selectivity, 24, 25, 31, 38, 95, 99, 100, 104, 176, 188, 207, 230, 257, 283
 self-assembly, 11, 108, 223, 306
 semiconductor(s), 5, 17, 18, 20, 23, 27, 38, 80, 82, 87, 93, 117, 132, 149, 160, 167, 169, 175, 177, 183, 190, 289
 sensing, vii, viii, 6, 15, 22, 25, 32, 48, 82, 104, 112, 113, 130, 149, 160, 167, 169, 193, 194, 195, 197, 198, 200, 201, 202, 203, 204, 205, 206, 207, 208, 209, 210, 211, 212, 213, 214, 215, 249
 sensitivity, 24, 25, 35, 36, 38, 40, 41, 106, 201, 207, 240, 254, 305
 sensor(s), vii, 1, 3, 4, 6, 10, 11, 15, 17, 18, 24, 27, 31, 32, 39, 62, 81, 82, 95, 96, 97, 102, 111, 112, 119, 129, 149, 168, 175, 189, 193, 194, 195, 196, 197, 198, 200, 201, 202, 204, 207, 209, 210, 211, 212, 213, 214, 220, 232, 240, 250, 251, 258, 285, 286, 305

- shape, 5, 17, 18, 19, 20, 21, 22, 23, 37, 43, 69, 72, 101, 103, 116, 175, 194, 195, 197, 285, 289, 293
- showing, 37, 103, 133, 203, 228, 285
- side chain, 64, 66, 67, 74, 118, 180, 187
- silica, 12, 24, 48, 174, 249, 252, 253, 268, 280, 290, 305
- silicon, 5, 6, 14, 38, 46, 94, 117, 120, 133, 160, 163, 164, 170, 286
- silver, 9, 29, 30, 31, 38, 43, 102, 110, 111, 170, 175, 236, 280, 290, 296, 304
- SiO₂, 21, 28, 29, 37, 254, 265, 277, 286
- sludge, 169, 248, 271, 292
- societal applications, 17
- society, vii, viii, 1, 4, 5, 13, 17, 51, 52, 58, 77, 139, 140, 150, 173, 176, 235, 284, 293, 300, 307
- sodium, 56, 71, 79, 86, 92, 130, 206, 269, 270, 276, 309, 311
- solar cell(s), 5, 6, 14, 17, 25, 72, 130, 131, 132, 133, 134, 136, 137, 138, 155, 156, 159, 160, 163, 167, 170, 175, 179, 183, 184, 188, 189, 190, 191, 192, 217, 240
- solar energy, 5, 14, 131, 132, 137, 140, 163, 174, 181, 183, 185, 186, 189, 241
- sol-gel, 3, 15, 252, 254, 258, 259, 263, 286, 287, 290, 295
- solid state, 51, 70, 141, 249, 264, 300
- solubility, vii, 43, 65, 87, 95, 162, 196, 226, 299, 305, 307
- solution, 28, 51, 64, 71, 84, 88, 90, 95, 122, 134, 162, 165, 174, 181, 204, 218, 223, 228, 229, 238, 241, 272, 286, 287, 289, 293, 294, 297, 298, 301, 304
- solvents, 65, 71, 85, 87, 90, 121, 122, 126, 162, 196, 236, 258, 285
- sorption, 142, 145, 147, 151, 152, 153, 154, 242, 244, 245, 283, 287
- sorption kinetics, 145, 152, 245
- species, 9, 24, 29, 39, 95, 110, 120, 123, 188, 194, 195, 198, 200, 202, 204, 206, 217, 219, 221, 223, 224, 229, 230, 240, 267, 273, 275, 279, 286, 300
- specific surface, 39, 87, 88, 103, 126, 130, 156, 159, 160, 175, 178, 194, 198, 220
- spectroscopy, viii, 20, 61, 62, 67, 68, 72, 76, 77, 79, 125, 130, 144, 278
- spin, 87, 119, 134
- stability, viii, 26, 29, 38, 55, 69, 70, 72, 79, 90, 91, 92, 93, 94, 96, 97, 99, 100, 102, 106, 111, 112, 135, 136, 137, 138, 139, 142, 143, 144, 145, 146, 147, 148, 150, 154, 155, 167, 174, 177, 178, 179, 186, 194, 195, 197, 201, 206, 222, 224, 228, 229, 230, 241, 248, 261, 270, 283, 285, 304
- stabilization, 19, 146, 276, 287
- state(s), 4, 15, 49, 52, 56, 66, 70, 71, 87, 90, 133, 137, 139, 141, 142, 145, 147, 151, 159, 162, 165, 181, 186, 249, 290
- steel, 4, 67, 120, 278
- storage, vii, viii, ix, 1, 5, 6, 10, 17, 22, 23, 24, 25, 32, 62, 68, 78, 82, 87, 90, 91, 92, 98, 100, 118, 126, 128, 132, 139, 140, 141, 142, 143, 144, 145, 146, 147, 148, 149, 150, 151, 152, 153, 154, 155, 156, 157, 159, 160, 161, 162, 163, 164, 165, 166, 167, 168, 169, 170, 171, 175, 185, 188, 195, 219, 230, 231, 232, 235, 240, 241, 243, 245, 247, 250, 251, 269, 270, 276
- structure, 2, 4, 21, 31, 39, 42, 43, 49, 53, 54, 61, 62, 63, 65, 85, 87, 89, 90, 93, 95, 100, 103, 116, 117, 120, 121, 124, 125, 126, 131, 133, 143, 144, 146, 148, 151, 152, 158, 159, 160, 161, 164, 165, 166, 168, 176, 178, 179, 180, 181, 183, 185, 191, 193, 194, 195, 196, 197, 198, 220, 224, 230, 237, 243, 271, 278, 283, 284, 285, 286, 290, 307, 309
- substitution, 28, 140, 143, 144, 145, 146, 147, 150, 152, 202
- substrate(s), 81, 82, 91, 97, 102, 104, 105, 106, 108, 112, 113, 120, 123, 134, 162, 177, 222, 228, 271, 272, 297
- sulphur/sulfur, 30, 63, 92, 166, 203, 206, 211, 232, 291
- Sun, 5, 28, 29, 45, 47, 48, 78, 96, 97, 112, 113, 128, 130, 189, 212, 234, 279, 287, 295, 297, 309, 310
- super capacitors, 6, 62
- surface area, 9, 10, 18, 20, 25, 26, 43, 84, 88, 90, 92, 93, 102, 104, 117, 118, 126, 156, 158, 162, 165, 166, 169, 175, 176, 180, 193, 195, 196, 197, 198, 217, 219, 220, 223, 230, 235, 236, 238, 240, 241, 257, 283, 285, 286, 288, 291, 294, 305
- surface chemistry, 38, 43, 86, 124, 193, 195, 198, 278
- surface functionalization, 95, 174, 178, 180, 198, 199
- surface modification, 20, 202, 206
- surfactant(s), viii, 51, 121, 123, 129, 130, 239, 245, 291, 296, 297
- sustainable development, viii, 3, 118, 173, 176

- sustainable energy, 190, 235, 241
 symptoms, 12, 35, 39
 synergistic effect, 103, 185, 223, 229, 291
 synthesis, viii, ix, 2, 3, 17, 18, 19, 22, 27, 28, 30, 31, 45, 47, 51, 56, 81, 83, 84, 96, 97, 99, 100, 102, 106, 109, 112, 113, 115, 116, 118, 120, 121, 123, 124, 125, 127, 130, 139, 140, 142, 143, 144, 150, 151, 153, 168, 194, 197, 201, 203, 214, 218, 223, 232, 235, 236, 241, 242, 243, 245, 249, 250, 251, 253, 257, 258, 259, 261, 262, 263, 264, 265, 266, 285, 286, 289, 290, 291, 292, 293, 294, 295, 296, 301, 304, 305, 306, 314
 synthetic polymers, 63, 64, 249, 299
- T**
- tanks, 141, 151, 219
 target, 7, 174, 181, 194, 198, 199, 201, 242
 techniques, viii, 8, 9, 12, 14, 19, 27, 39, 41, 81, 82, 92, 95, 100, 102, 106, 120, 124, 125, 130, 132, 145, 195, 197, 198, 276, 278, 290, 293, 296, 301
 technology/technologies, 1, 2, 3, 4, 5, 6, 8, 9, 10, 11, 13, 14, 17, 18, 19, 24, 25, 38, 39, 42, 51, 100, 101, 106, 115, 116, 127, 131, 140, 141, 143, 169, 174, 217, 231, 235, 236, 242, 258, 269, 271, 273, 277, 284, 285, 293, 301, 313
 TEM, 17, 18, 21, 22, 125
 temperature, 8, 9, 11, 25, 26, 31, 32, 66, 67, 69, 71, 72, 73, 74, 75, 76, 100, 102, 106, 121, 137, 139, 141, 142, 143, 144, 145, 146, 147, 148, 149, 152, 165, 168, 175, 177, 195, 200, 217, 229, 245, 264, 268, 271, 286, 301
 tensile strength, 4, 158, 159
 testing, 1, 11, 12, 46, 135
 therapeutics, vii, 15, 36, 43, 44, 99
 therapy, 26, 38, 39, 42, 44, 45
 thermal properties, 18, 20, 29, 117, 163
 thermal stability, 46, 79, 104, 156, 159
 thermodynamic properties, 144, 145, 152
 thermodynamics, 147, 241, 294
 thin films, 163, 180, 191, 249, 253, 264
 tin, 133, 134, 163, 183, 206, 232
 tin oxide, 133, 134, 163
 tissue, 7, 23, 36, 39, 40, 41, 95, 119, 128, 238, 249, 250, 252, 286, 301, 304, 305, 306, 309
 tissue engineering, 23, 119, 128, 250, 252, 286, 301, 309
 titania, 15, 30, 286
 titanium, 7, 9, 24, 27, 175, 184, 191, 206, 209, 268, 288
 top-down, 83, 238, 243
 toxicity, 8, 13, 24, 30, 32, 36, 37, 38, 39, 43, 44, 46, 48, 49, 87, 93, 94, 195, 271, 275, 276, 277, 290, 300
 trace elements, 54, 267, 268, 269
 transformation(s), 8, 25, 131, 166, 257, 258
 transition metal, viii, 18, 28, 41, 53, 54, 81, 82, 87, 91, 92, 96, 164, 228, 231, 235, 238, 239, 240, 241, 245, 286, 288, 290
 transition metal dichalcogenide, 18, 28, 81, 82, 96, 235, 238, 239, 240, 241, 245, 289
 transmission, 17, 18, 124, 125
 transmission electron microscopy (TEM), 17, 18, 21, 124
 transparency, 155, 157, 163, 236, 248
 transport, viii, 28, 61, 75, 77, 90, 132, 138, 141, 143, 155, 157, 158, 160, 163, 174, 175, 178, 179, 183, 184, 187, 193, 217, 226, 227, 228
 transportation, 5, 69, 139, 146, 153, 219, 303
 treatment, vii, viii, 1, 4, 8, 13, 14, 15, 17, 18, 24, 26, 30, 33, 36, 37, 38, 39, 44, 45, 48, 53, 54, 55, 57, 59, 82, 84, 101, 121, 150, 159, 175, 178, 190, 201, 202, 230, 240, 248, 250, 251, 252, 270, 271, 272, 284, 285, 286, 288, 292, 293, 295, 298, 299, 301, 307, 308, 311
 tumor(s), 7, 38, 39, 42, 47, 55, 265, 302, 304, 309
 tumor cells, 39, 42, 265, 304, 309
- U**
- ultrasound, 39, 41, 47, 245
 uniform, 84, 86, 102, 104, 138
 United States (USA), 14, 47, 107, 108, 109, 242, 278
 urea, 25, 196, 200, 208
 uric acid, 197, 204, 205, 207, 212, 213
 UV light, 132, 135, 136, 182, 184
- V**
- valence, 20, 87, 88, 90, 177, 181, 185, 224, 291
 vanadium, 55, 56, 109, 112
 varieties, 54, 143, 202
 vegetation, 10, 267, 271
 vehicles, 63, 139, 141, 149, 157, 162, 219
 versatility, 115, 149, 287

vinylidene fluoride, 25, 32, 79
viruses, vii, 2, 4, 9, 11, 26, 42, 43, 286

World Health Organization (WHO), 10, 11, 284
worldwide, 8, 64, 116, 126, 132, 156, 194, 284

W

waste, 8, 10, 25, 148, 150, 162, 170, 175, 248, 250, 251, 252, 267, 268, 276, 277, 278, 279, 287, 292, 294
wastewater, viii, ix, 1, 8, 14, 24, 30, 82, 150, 175, 180, 248, 250, 251, 252, 254, 279, 284, 286, 287, 288, 289, 290, 292, 293, 294, 295, 296, 297, 298, 299, 307
water, vii, ix, 1, 4, 8, 9, 14, 17, 18, 22, 23, 24, 25, 29, 30, 31, 48, 64, 66, 85, 87, 88, 95, 120, 121, 129, 134, 140, 159, 173, 174, 177, 178, 181, 183, 186, 187, 188, 189, 190, 191, 197, 198, 200, 207, 212, 214, 217, 218, 221, 226, 238, 241, 250, 252, 260, 265, 266, 269, 270, 276, 277, 278, 283, 284, 285, 286, 287, 289, 290, 293, 294, 295, 296, 297, 301, 305, 306, 310
water purification, 8, 283, 284, 286, 293, 294, 295
water quality, 8, 14, 283
wavelengths, 20, 43, 86, 95

X

XPS, 126, 142
X-ray diffraction (XRD), 17, 18, 22, 125, 142, 143, 144

Y

yield, 6, 83, 86, 87, 93, 119, 121, 122, 130, 163, 229, 230, 238, 242, 245, 293

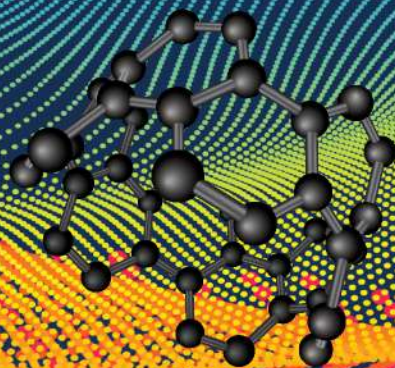
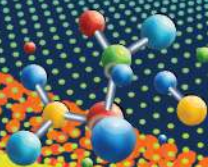
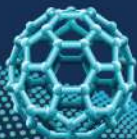
Z

zeolites, 9, 141, 289
zinc, 27, 206, 211, 214, 243, 284, 296, 298, 304, 311
zinc oxide, 27, 206, 243, 304, 311
zirconia, 258, 262, 264, 266
ZnO, 15, 23, 31, 32, 48, 94, 134, 175, 185, 187, 188, 190, 191, 192, 205, 206, 214, 255, 287, 290, 294, 295, 296, 304, 305, 310

Complimentary Contributor Copy

Versatile Solicitations of Materials Science in Diverse Science Fields

Mridula Tripathi
Arti Srivastava
Kalpana Awasthi
Editors



**nova**
science publishers

www.novapublishers.com

ISBN 978-1-53619-763-1



9 781536 197631

Complimentary Contributor Copy